THE CITY UNIVERSITY

DEPARTMENT OF MECHANICAL ENGINEERING

"THE SOUND AND VIBRATION RESULTING FROM THE IMPACT OF SPHERES"

by

Shahrokh Hosseini-Hashemi

This Thesis is submitted
for the degree of Doctor
of Philosophy

DECEMBER 1985.

CONTENTS

	Page No.
List of Figures	iv
List of Tables	ix
NOMENCLATURE	x
SUMMARY	xxv
ACKNOWLEDGEMENTS	xxvi
1. INTRODUCTION	1
1.1. General Introduction	1
1.2. Review of Literature	3
1.2.1. Rigid body radiation	3
1.2.2. Pseudo steady state radiation	9
2. FUNDAMENTAL CONCEPTS USED IN THE SUBSEQUENT CHAPTERS	13
2.1. The Cartesian form of the three dimensional acoustic wave equation	14
2.2. General solution of acoustic wave equation in spherical co-ordinates	17
2.3. Monopole and simple sources.	23
2.4. The dipole source	27
2.5. Impact of elastic bodies	28
2.6. Numerical solution of force-time history	32
2.7. Equation of motion in an elastic medium	33
2.8. Solution of equations of motion for solid spheres	36
3. RIGID BODY RADIATION DUE TO ELASTIC COLLISIONS OF SPHERES	49
3.1. Sound radiation from an impulsively accelerated sphere	50
3.2. The impulsive monopole source	53
3.3. Velocity potential of an impulsively accelerated sphere (Laplace transform method)	54
3.4. Sound radiated by a sphere undergoing a Hertzian acceleration (Laplace transform method)	58
3.5. Sound radiated by a sphere undergoing a Hertzian acceleration (Approximate method)	66

		Page No.
3.6.	Sound radiated by a pair of colliding spheres (Convolution method)	70
3.7.	Sound radiated by a pair of colliding spheres (Numerical method)	78
3.8.	Sound radiated due to change of volume of sphere undergoing an elastic collision	79
3.9.	Acoustic energy of an impulsively accelerated sphere	82
3.10.	Acoustic energy of sphere undergoing a Hertzian acceleration	86
4.	RADIATION DUE TO INELASTIC COLLISION OF SPHERES	110
4.1.	Elastic-plastic contact deformation	110
4.2.	Numerical solution of sound pressure	117
4.3.	Sound radiation from a sphere subjected to inelastic collision by a sphere (Analytical solution)	125
4.4.	Fourier transform of pressure-time history	131
5.	SOUND PRESSURE RADIATED BY A VISCO-ELASTIC SPHERE	142
5.1.	Impact solution	142
5.2.	Numerical solution of sound pressure	144
5.3.	Discrete finite transform for evaluating the Fourier transform of pressure-time history	148
6.	SOUND RADIATION FROM TRANSIENT VIBRATION OF SOLID SPHERE	157
6.1.	Vibrations of elastic sphere	157
6.2.	Solution of equations of motion (Alternative approach)	163
6.3.	Frequency equation	170
6.4.	Orthogonality and normalisation of torsional modes	174
6.5.	Modal shapes of torsional vibrations	179
6.6.	Orthogonality and normalisation of spheroidal modes	184
6.7.	Modal shapes of spheroidal vibrations	193
6.8.	Response of a sphere to a radial concentrated force	198
6.9.	Response due to collision	210
6.10.	Sound generated by transient vibration of solid spheres	216

Page No.

7. SOUND RADIATION FROM TRANSIENT VIBRATION OF HOLLOW SPHERE 247

7.1. Vibrations of hollow sphere 247

7.2. Frequency equation 249

7.3. Orthogonality and normalisation of torsional modes 253

7.4. Orthogonality and normalisation of spheroidal modes 256

7.5. Sound generated by transient vibration of hollow sphere 263

8. EXPERIMENT 287

8.1. Specimens and suspension 287

8.2. Design of the test rig 288

8.3. Fourier Analyzer 289

8.4. Anechoic chamber 290

8.5. Acoustic measurements 291

8.6. Acceleration measurements 292

9. DISCUSSION AND CONCLUSIONS 298

9.1. Force-time history 298

9.2. Impulsively accelerated and pulsating sphere 298

9.3. Sphere undergoing a Hertzian acceleration 299

9.4. Radiation due to change of volume of sphere 308

9.5. Acoustic energy 308

9.6. Radiation of sound due to inelastic collision of spheres 311

9.7. Radiation of sound due to collision of visco-elastic spheres 312

9.8. Vibration of solid and hollow spheres 312

9.9. Experimental results 314

9.10. Conclusions 316

REFERENCES 343

LIST OF FIGURES

Figure No.		Page No.
2.1.	Illustration of elements $dS = r^2 \sin\theta d\theta d\psi$	47
2.2.	Force-time history for 1.27 cm diameter steel spheres with an initial impact velocity of 1.52 m/s	47
2.3.	Stresses acting on a small rectangular parallelepiped	48
3.1.	Pressure-time curves of impulsively accelerated sphere	90
3.2.	Pressure-time curves of impulsively pulsating sphere	90
3.3.	Dimensionless peak pressure against dimensionless contact time	91
3.4.	Variations of $\hat{n}_{max}$ with β	91
3.5.	Dimensionless peak of transform against β	92
3.6.	Variations of n^{*}_{max} with β	92
3.7.	A Comparison of the exact solution for the sound radiated by an impulsively accelerated sphere and approximate evaluation of that sound obtained by aerodynamic approach	93
3.8.	A Comparison of the exact solution for the sound radiated by a sphere undergoing a Hertzian acceleration and approximate evaluation of that sound obtained by aeroacoustic approach	93
3.9.	Model of colliding spheres	94
3.10.	Model of wave path from impactor to measuring microphone located at $\theta = 0^{o}$	94
3.11.	Dimensionless pressure-time curve for a pair of similar spheres of equal sizes ($\theta = 0^{o}$)	95
3.12.	Dimensionless pressure-time curve for a pair of similar spheres of unequal sizes ($\theta = 0^{o}$)	96
3.13.	Dimensionless pressure-time curve for a pair of dissimilar spheres of equal sizes ($\theta = 0^{o}$)	97
3.14.	Dimensionless pressure-time curve for a pair of dissimilar spheres of unequal sizes ($\theta = 0^{o}$)	98
3.15.	Directional distribution of maximum pressure radiated by a pair of similar spheres of equal sizes.	99

Figure No.		Page No.
3.16.	Directional distribution of maximum pressure radiated by a pair of similar spheres of unequal sizes.	99
3.17.	Directional distribution of maximum pressure radiated by a pair of dissimilar spheres of equal sizes.	100
3.18.	Directional distribution of maximum pressure radiated by a pair of dissimilar spheres of unequal sizes.	100
3.19.	Dimensionless rarefractive peak pressure against β.	101
3.20.	Variation of $\hat{n}_{max}$ with β.	101
3.21.	Fourier transform of pressure for a pair of similar spheres of equal sizes.	102
3.22.	Fourier transform of pressure for a pair of similar spheres of unequal sizes.	103
3.23.	Fourier transform of pressure for a pair of dissimilar spheres of equal sizes,	104
3.24.	Fourier transform of pressure for a pair of dissimilar spheres of unequal sizes.	105
3.25.	Variation of n^*_{max} with β.	106
3.26.	Sound pressure time history for 2.54 cm diameter steel sphere with an initial impact velocity of 2.5 m/s.	106
3.27.	Illustration of element dS for evaluating the shaded volume.	107
3.28.	Dimensionless pressure time curve due to change of volume of sphere undergoing an elastic collision.	108
3.29.	Variation of dimensionless energy with β (Impactee only).	109
3.30.	Variation of total dimensionless energy with β.	109
4.1.	Force versus time for 2.54 cm diameter lead spheres with an initial impact velocity of 0.55 m/s.	136
4.2.	Comparison of analytical and numerical solution of pressure time histories for 2.54 cm diameter lead spheres with an initial velocity of 0.55 m/s. (Impactee only).	137
4.3.	Sound pressure-time history for 2.54 cm diameter lead spheres with an initial impact velocity of 0.55 m/s.	138

Figure No.		Page No.
4.4.	Fourier transform of pressure for 2.54 cm diameter lead sphere with an initial impact velocity 0,55 m/s.	139
4.5.	Fourier transform of dimensionless pressure, (Impactee only)	140
4.6.	Fourier transform of dimensionless acceleration.	141
5.1.	Sound pressure time history for 2.54 cm diameter sphere with the same properties described in Case 1.	152
5.2.	Sound pressure time history for 2.54 cm diameter sphere with the same properties described in Case 2.	153
5.3.	Sound pressure time history for 2.54 cm diameter sphere with the same properties described in Case 3.	154
5.4.	Force-time curves due to collision of steel sphere and visco-elastic sphere described in Table 5.1.	155
5.5.	Fourier transform of pressure for sphere with the pressure time history as given in Figure 5.3.	156
6.1.	Variation of normalised displacement of torsional vibration of sphere along the radius (n = 2).	223
6.2.	Diagrams of the surface mode spheres of torsional vibration.	227
6.3.	Variation of normalised displacement (u_r) of spheroidal vibration along the radius.	232
6.4.	Variation of normalised displacement (u_θ) of spheroidal vibration along the radius.	237
6.5.	Diagrams of the surface mode shapes of spheroidal vibration.	241
6.6.	Force-time curves for a pair of colliding spheres of radii 1.27 cm and 7.112 cm (Eq.(6.161), n = 0 and ℓ =1,5).	246
7.1.	Variation of normalised displacement of torsional vibration of hollow sphere along the thickness.	274
7.2.	Variation of normalised displacement (u_r) of spheroidal vibration of hollow sphere along the thickness.	278
7.3.	Variation of normalised displacement (u_θ) of spheroidal vibration of hollow sphere along the thickness.	283
8.1.	Schematic of Ball Suspension.	294

Figure No.		Page No
8.2.	Schematic diagram of test rig.	295
8.3.	General arrangement of acoustic measurements.	296
8.4.	General arrangement of acceleration measurements and apparatus used in calibration.	297
9.1.	Comparison of measured pressure time result and calculated result for 2.54 cm diameter spheres.	321
9.2.	Comparison of measured pressure time result and calculated result for 2.54 cm diameter spheres.	322
9.3.	Comparison of measured pressure time result and calculated result for 2.54 cm diameter spheres.	323
9.4.	Comparison of measured pressure time result and calculated result for 2.54 cm diameter spheres.	324
9.5.	Comparison of measured Fourier transform pressure result and calculated result for 2.54 cm diameter spheres.	325
9.6.	Comparison of measured Fourier transform pressure result and calculated result for 2.54 cm diameter spheres.	326
9.7.	Comparison of measured Fourier transform pressure result and calculated result for 2.54 cm diameter spheres.	327
9.8.	Comparison of measured Fourier transform pressure result and calculated result for 2.54 cm diameter spheres.	328
9.9.	Fourier transforms for various size spheres.	329
9.10.	Fourier transform comparison for 2.54 cm diameter sphere as a function of the angle for v_o =2.5 m/s.	330
9.11.	Measured Fourier transform pressure for 5.08 cm diameter spheres.	331
9.12.	Polar distribution of positive peak pressure for 2.54 cm diameter spheres.	332
9.13.	Polar distribution of negative peak pressure for 2.54 cm diameter spheres.	332

Figure No.		Page No.
9.14.	Comparison of measured energy integration result and calculated result for 2.54 cm diameter spheres.	333
9.15.	Positive peak pressure vs impact velocity for 2.54 cm diameter spheres.	334
9.16.	Negative peak pressure vs impact velocity for 2.54 cm diameter spheres.	334
9.17.	Energy integration vs impact velocity for 2.54 cm diameter spheres.	335
9.18.	Energy integration vs impact velocity for 2.54 cm diameter spheres.	335
9.19.	Distribution of Energy Integration for 2.54 cm diameter spheres.	336
9.20.	Comparison of measured Fourier transform acceleration result and calculated result for Impactee of radius 7.1 cm at position r = 7.1 cm and $\theta = 0^{o}$.	337
9.21.	Comparison of measured Fourier transform acceleration result and calculated result for Impactee of radius 7.1 cm at position r = 7.1 cm and $\theta = 0^{o}$.	338
9.22.	Comparison of measured Fourier transform acceleration result and calculated result for Impactee of radius 7.1 cm at position r = 7.1 cm, and $\theta = 0^{o}$.	339
9.23.	Comparison of measured Fourier transform acceleration result and calculated result for Impactee of radius 7.1 cm at position r = 7.1 cm and $\theta = 0^{o}$.	340
9.24.	Comparison of measured Fourier transform pressure result and calculated result for 7.1 cm radius spheres.	341
9.25.	Comparison of measured Fourier transform pressure result and calculated result for 7.1 cm radius spheres.	342

LIST OF TABLES

Table No.		Page No.
5.1.	Material properties and assumed relaxation times of three visco-elastic spheres.	151
6.1.	Non-dimensional frequency of torsional vibration of spheres.	221
6.2.	Non-dimensional frequency of spheroidal vibration of spheres.	222
7.1.	Non-dimensional frequency of torsional vibration of hollow sphere. (b/a = 0.2)	226
7.2.	Non-dimensional frequency of torsional vibration of hollow sphere (b/a = 0.4).	267
7.3.	Non-dimensional frequency of torsional vibration of hollow sphere (b/a = 0.6).	268
7.4.	Non-dimensional frequency of torsional vibration of hollow sphere (b/a = 0.8).	269
7.5.	Non-dimensional frequency of spheroidal vibration of hollow sphere (b/a = 0.2).	270
7.6.	Non-dimensional frequency of spheroidal vibration of hollow sphere (b/a = 0.4).	271
7.7.	Non-dimensional frequency of spheroidal vibration of hollow sphere (b/a = 0.6).	272
7.8.	Non-dimensional frequency of spheroidal vibration of hollow sphere (b/a = 0.8).	273
8.1.	Characteristic of the balls used for the tests.	294

NOMENCLATURE

a, a_1, a_2, a_x	radius of sphere
a_M, a_{M1}, a_{M2}	maximum value of the acceleration in the elastic collision
a^*	inner radius of hollow sphere
$\hat{a}_0, \hat{a}_1, \hat{a}_2$, etc.	coefficient of zero and even powers of k_2 in expansion of $\bar{\alpha}_n$
$\bar{a}_{kj}$	elements of matrix 4 by 4 defined in (7.9a) to (7.9h)
A	integral function in Hertz's theory of contact
A_n	arbitrary constant in the equation (6.6)
A^*	real part of the Fourier transform of acceleration in inelastic collision
A^*_n	coefficients of component waves in equation (2.23)
$\hat{A}$	acceleration function
$\hat{A}_1$	acceleration function during elastic loading period
$\hat{A}_2$	acceleration function during elastic-plastic period
$\hat{A}_3$	acceleration function during unloading period
$\lvert\hat{A}\rvert$	absolute value of acceleration
$\bar{A}$	coefficient of periodic function in equation (2.23)
$\bar{A}_n$	arbitrary constant in the equation (6.18a)
$\bar{A}_{nm}$	coefficient of component waves in equation (2.37)
$\bar{A}_{nm\ell}$	arbitrary constant in the equation (6.42b)
$\bar{A}_{nmq}$	arbitrary constant in the solution of equation (6.49b)
$\bar{A}_{psq}$	arbitrary constant in equation (6.44b)
$\bar{\bar{A}}_n$	arbitrary constant in equation (6.18a)
$\bar{\bar{A}}_{nm\ell}$	arbitrary constant in equation (7.12b)
$\bar{\bar{A}}_{psq}$	arbitrary constant in equation (7.14b)

b	$= \frac{\pi}{d}$
b^*	$= \frac{\pi}{2t_3}$
b_0, b_1, b_2, etc.	coefficients of zero and even powers of k_2 in expansion of $\bar{\beta}_n$
$\bar{b}$	a position along the length of beam
B	integral function in Hertz's theory of contact
B_n	arbitrary constant in equation (6.9a)
B^*	imaginary part of the Fourier transform of acceleration in inelastic collision
B^*_n	$= \frac{\alpha^*}{M}$
$\hat{B}_1, \hat{B}_2, \hat{B}_3$	time independent coefficients in expressions of sound pressure due to inelastic collision
$\bar{B}$	coefficient of periodic function in equation (2.23)
$\bar{B}_n$	arbitrary constant in equation (6.23a)
$\bar{B}_{nm}$	coefficients of component waves in equation (2.37)
$\bar{B}_{nm\ell}$	arbitrary constant in R_1
$\bar{B}_{nmq}$	arbitrary constant in R_2
$\bar{\bar{B}}_n$	arbitrary constant in equation (6.23a)
$\bar{\bar{B}}_{nm\ell}$	arbitrary constant in R_1
$\bar{\bar{B}}_{nmq}$	arbitrary constant in R_2
c	sound velocity
$\bar{c}$	$= \frac{3}{4} \frac{(A+B)^{\frac{1}{2}}}{q_k}$
C_1	velocity of dilatation waves $= \frac{(\lambda+2\mu)^{\frac{1}{2}}}{\rho}$
C_2	velocity of distortion waves $= (\frac{\mu}{\rho})^{\frac{1}{2}}$
$\hat{C}_1, \hat{C}_2, \hat{C}_3$	time independent coefficients in expressions of sound pressure due to inelastic collision
$\bar{C}_1, \bar{C}_2$	coefficients of modified Bessel functions of the first and second kind in equation (3.25)

d	duration of contact
$\hat{d}_0, \hat{d}_1, \hat{d}_2$	coefficients of zero and even powers of k_2 in expansion of $\bar{\gamma}_n$
$\bar{d}$	duration of contact in inelastic collision
D	integral domain
D_n	arbitrary constant in equation (6.9b)
D^*_n	coefficients of Legendre polynomial in equation (2.42)
$\hat{D}_1, \hat{D}_2, \hat{D}_3$	time independent coefficients in expressions of sound pressure due to inelastic collision
$\bar{D}$	coefficients of cylindrical Bessel function of the first kind in equation (2.31)
$\bar{D}_n$	arbitrary constant in equation (6.23c)
$\bar{D}_{nm\ell}$	arbitrary constant in Y_1
$\bar{D}_{nmq}$	arbitrary constant in Y_2
$\bar{\bar{D}}_n$	arbitrary constant in equation (6.23c)
$\bar{\bar{D}}_{nm\ell}$	arbitrary constant in Y_1
$\bar{\bar{D}}_{nmq}$	arbitrary constant in Y_2
E, E_1, E_2, E_x	Young's modulus
E_K	kinetic energy
E_P	potential energy
E^*	$= \frac{2\bar{M}^2}{(1+\bar{M})^2} \frac{=}{m} v_o^2$
$\hat{E}$	energy
$\hat{E}_1, \hat{E}_2, \hat{E}_3$	time independent coefficients in expressions of sound pressure due to inelastic collision
$\hat{E}_T$	energy for a pair of colliding spheres
$\bar{E}$	coefficient of cylindrical Bessel function of the second kind in equation (2.31)

f	frequency
f_θ	radial dependent function in solution in U_θ
f_ψ	radial dependent function in solution of U_ψ
f_{max}	maximum frequency in D.F.T. method
f'_θ, f'_ψ	first derivatives of f_θ and f_ψ with respect to r
f''_θ, f''_ψ	second derivatives of f_θ and f_ψ with respect to r
Δf	frequency resolution
$f^*_{nm\ell}$	time independent part of F*
$\bar{f}$	function dependent on α in equation (4.38)
$\bar{\bar{f}}$	function dependent on $\bar{Z}$ in equation (4.43)
F	force function
F_j, F_k	force at instants $t = j\Delta t$ and $t = k\Delta t$
F_x, F_y, F_z	resultant force in direction x, y and z
F_E	force in the elastic annulus
F_P	force in the plastic circle
F_S	magnitude of force in the form of a step function
F_{EP}	total force in the elastic-plastic loading period
F_{EU}	total force in the elastic unloading period
F_{max}	$= \hat{K}_2\left(\frac{5v_o^2}{4\hat{K}_1\hat{K}_2}\right)^{0.6}$
$F_{nm\ell}, F_{nmq}, F_{psq}$	function defined in (6.80a) and (7.21a)
F^*	left-hand side of equation (6.125a)
$\bar{F}$	coefficient of spherical Bessel function of the first kind in equation (2.33)

g	function dependent on α in equation (4.24)
g_1, g_2, g_3	separation functions for solving equation (2.16)
g_G	gravitational acceleration
g'_1, g'_2, g'_3	first derivatives of separation functions with respect to their arguments used for solving equation (2.16)
g''_1, g''_2, g''_3	second derivatives of separation functions with respect to their arguments used for solving equation (2.16)
$g^*_{nm\ell}$	time independent part of G*
$G_{nm\ell}, G_{nmq}, G_{psq}$	function defined in (6.80b) and (7.21b)
G^*	left-hand side of equation (6.125b)
G^*_n	expression defined in (6.175c)
$\hat{G}_1, \hat{G}_2, \hat{G}_3$	time independent coefficients in expression of sound pressure due to inelastic collision
$\bar{G}$	coefficient of spherical Bessel function of the second kind in equation (2.33)
h	$= \frac{\alpha_1}{n}$
$h_n^{(1)}, h_n^{(2)}$	spherical Hankel functions of the n^{th} order of the first and second kind respectively
h_D	drop height of the ball
$\bar{h}$	$= \frac{\alpha_{max} - \alpha_1}{\bar{n}}$
$\bar{\bar{h}}$	$= \frac{1}{\bar{\bar{n}}}$
H	heavyside function
H_r, H_θ, H_ψ	components of vector potential in the r, θ, ψ directions
$\underline{H}$	vector potential
i	positive root of minus one
$\underline{i}$	unit vector in x direction
I	acoustic intensity
$I_{\bar{\nu}}$	modified Bessel function of the first kind
$\bar{I}$	shortened for integration in equation (5.6)

j	any integer
j_n	spherical Bessel function of the n^{th} order of the first kind
$\underline{j}$	unit vector in y direction
$J_{\bar{v}}$	cylindrical Bessel function of the n^{th} order of the first kind
k	any integer
$\underline{k}$	unit vector in z direction
K	wave number, $= \frac{\omega}{c}$
K_1	circular frequency divided by velocity of dilatation waves, $= \frac{\omega}{C_1}$
K_2	circular frequency divided by velocity of distortion waves, $= \frac{\omega}{C_2}$
$K_{\bar{v}}$	modified Bessel function of the second kind
K^*	$= \frac{2}{3}\,\eta\,\frac{\alpha_1}{\alpha_{max}}$
$\hat{K}_1, \hat{K}_2$	constants in the Hertz's theory of contact
$\bar{K}_1, \bar{K}_2, \bar{K}_3$	bulk modulus
ℓ, ℓ_1, ℓ_2	ratio of velocity of sound to the radius of sphere
m	any integer
$m_1, m_2, \bar{m}$	mass
$\bar{\bar{m}}$	mass of air displaced by the sphere
M	mass of solid or hollow sphere
$\bar{M}$	$= \frac{m_2}{m_1}$
n	any integer
n_1	$= \frac{t_1}{\bar{d}}$
n_2	$= \frac{t_2}{\bar{d}}$

n'	dimensionless time delay
$\underline{n}$	unit normal vector
n^*	dimensionless frequency
n^*_d	$= d/\Delta t$
n^*_{max}	dimensionless frequency at which peak of transform occurs
$\hat{n}$	dimensionless time
$\hat{n}_{max}$	dimensionless time at which peak pressure occurs
$\bar{n}, \bar{\bar{n}}$	any integer
N	number of samples in D.F.T. method
$N_{nm\ell}$	generalized force
p, p_0, p_1, p_2, p_3	sound pressure
p_{RE}	real part of sound pressure
p_{UI}	pressure due to unit impulse acceleration
p_{max}	peak pressure amplitude
$\|p\|$	absolute value of sound pressure
p'	static pressure and acoustic pressure
$\bar{p}$	static pressure
P	pressure distribution across the circular contact area
P_n	Legendre polynomial of the n^{th} order
P_n^m	associated Legendre function
P_D	$= 0.142\rho_o v_o^2 \frac{a_1}{r}$
P_L	$= 2.34 \frac{\bar{M}}{1+\bar{M}} \rho_o v_o^2 \frac{a_2}{r}$
P_M	$= \rho_o c v_o \frac{a}{r}$
P_N	$= \frac{1.17\bar{M}}{1+\bar{M}} \rho_o c v_o \frac{a}{r}$
P_{rms}	root of mean square pressure
$\bar{P}_o$	dynamic flow pressure

q_a, q_k	elliptic integral in the Hertz's theory of contact
$q_{nm\ell}$	associated generalized coordinate
$\dot{q}_{nm\ell}$	differentiation of $q_{nm\ell}$ with respect to time
$\ddot{q}_{nm\ell}$	second differentiation of $q_{nm\ell}$ with respect to time
$\underline{q}$	velocity vector
r	radial coordinate
r_o	arbitrary radial coordinate
r_1, r_2	distance from the centre of sphere to the microphone position
$\underline{r}$, $\underline{r_o}$	position vector
$\bar{r}$	distance from the centre of the circular contact area
$\bar{r}_1$	radius of the circle of the plastic region
$\bar{r}_2$	radius of the circle of the plastic region at the end of elastic-plastic period
R	radial dependent function in equation (6.22a)
R_1	$= \bar{B}_{nm\ell} \cdot j_n(\omega_{n\ell} \frac{r}{c_1}) + \bar{\bar{B}}_{nm\ell} y_n(\omega_{n\ell} \frac{r}{c_1}), \begin{cases} \bar{\bar{B}}_{nm\ell} = 0 \\ \bar{\bar{B}}_{nm\ell} \neq 0 \end{cases}$
R_2	$= \bar{B}_{nmq} \cdot j_n(\omega_{nq} \frac{r}{c_1}) + \bar{\bar{B}}_{nmq} y_n(\omega_{nq} \frac{r}{c_1}), \begin{cases} \bar{\bar{B}}_{nmq} = 0 \\ \bar{\bar{B}}_{nmq} \neq 0 \end{cases}$
R'	differentiation of R with respect to r
R'_1, R'_2	differentiation of R_1 and R_2 with respect to r
R''	second differentiation of R with respect to r
$\hat{R}_1, \hat{R}_2$	dimensionless coefficients in expressions (2.122) and (2.123)
$\bar{R}$	radius of contact area
$\bar{R}_1$	radius of the contact area at the end of elastic loading period.

s	$= i\omega$
s^*	condensation
S	surface area
$S_{n\ell}$	quantity defined in (6.156a)
$\underline{S}$	displacement vector
$\bar{S}_n$	spherical surface harmonic of degree n
$\bar{S}_{n\ell}$	quantity defined in (6.156b)
t	time
t_1	termination time of the elastic loading period
t_2	duration of the elastic-plastic loading period
t_3	duration of the elastic unloading period
$\Delta t, \bar{\Delta} t, \bar{\bar{\Delta}} t$	time step size
t^*	$= t-(t_1+t_2)$
$\hat{t}$	$= t-t_1$
$\bar{t}$	$= t-t_1$
T	period
T_d	time delay
u_r, u_θ, u_ψ	time independent displacement components in the r,θ,ψ directions
$u_{r,nm\ell}$	ℓ-th natural mode of degree m and order n in the r direction
$u_{r,psq}$	q-th natural mode of degree S and order p in the r direction
$u_{\theta,nm\ell}$	ℓ-th natural mode of degree m and order n in the θ direction
$u_{\theta,psq}$	q-th natural mode of degree S and order p in the θ direction

$u_{\psi,nm\ell}$	ℓ-th natural mode of degree m and order n in the ψ direction
$u_{\psi,psq}$	q-th natural mode of degree S and order p in the ψ direction
$u^*_{r,n\ell}$	ℓ-th normal mode of degree zero and order n in the r direction
$u^*_{r,nm\ell}$	ℓ-th normal mode of degree m and order n in the r direction
$u^*_{\theta,nm\ell}$	ℓ-th normal mode of degree m and order n in the θ direction
$u^*_{\psi,nm\ell}$	ℓ-th normal mode of degree m and order n in the ψ direction
$\hat{u}$	time independent displacement in the x direction
$\hat{u}_n$	n^{th} component of $\hat{u}$
U_1, U_2	displacement
U_r, U_θ, U_ψ	displacement components in the r,θ,ψ directions
U_{RIG}	rigid body displacement
$\dot{U}_r$	differentiation of U_r with respect to time
$\ddot{U}_r$	second differentiation of U_r with respect to time
$\hat{U}$	displacement in the x direction
v	velocity amplitude
v_o	constant velocity
v_1, v_2, v_r	radial velocity
v_x, v_y, v_z	velocity components
$v(\mathcal{T})$	Fourier transform of impulsive velocity $v_o H(\tau)$
v^*_r	complex conjugate of Fourier transform of radial velocity
$\hat{v}$	time independent displacement in the y direction
$\hat{v}_n$	n^{th} component of $\hat{v}$

V	volume
$\hat{V}$	displacement in y direction
$w^*_{nm\ell}$	time independent part of W*
$\hat{w}$	time independent displacement in the z direction
$\hat{w}_n$	n^{th} component of $\hat{w}$
W	function dependent on r and t
W^*	left-hand side of equation (6.125c)
$\hat{W}$	displacement in z direction
$\bar{W}$	Laplace transform of W
x	Cartesian coordinate
δx	infinitesimal length in x direction
X	transformation variable for solving equation (2.21)
$\bar{X}$	function dependent on r and s
$\bar{X}_n$	spherical solid harmonic of degree n
y	Cartesian coordinate
y_n	spherical Bessel function of the n^{th} order of the second kind
δy	infinitesimal length in y direction
y^*	$= \frac{S_r}{c}$
Y	$= \frac{d^m}{dX^m} P_n(X)$
Y_1	$= \bar{D}_{nm\ell} \cdot j_n(\omega_{n\ell} \frac{r}{c_2}) + \bar{\bar{D}}_{nm\ell} y_n(\omega_{n\ell} \frac{r}{c_2})$, $\bar{\bar{D}}_{nm\ell} = 0$ / $\bar{\bar{D}}_{nm\ell} \neq 0$
Y_2	$= \bar{D}_{nmq} \cdot j_n(\omega_{nq} \frac{r}{c_2}) + \bar{\bar{D}}_{nmq} y_n(\omega_{nq} \frac{r}{c_2})$, $\bar{\bar{D}}_{nmq} = 0$ / $\bar{\bar{D}}_{nmq} \neq 0$
$Y_{\bar{v}}$	cylindrical Bessel function of the second kind
Y^e_{mn}, Y^o_{mn}	spherical surface harmonic of degree n

Y'_1, Y'_2	differentiations of Y_1 and Y_2 with respect to r
Y''_1, Y''_2	second differentiations of Y_1 and Y_2 with respect to r
z	Cartesian coordinate
z_1	$= \bar{A}_{nm\ell} \cdot j_n(\omega_{n\ell} \frac{r}{c_2}) + \bar{\bar{A}}_{nm\ell} y_n(\omega_{n\ell} \frac{r}{c_2}), \begin{cases} \bar{\bar{A}}_{nm\ell} = 0 \\ \bar{\bar{A}}_{nm\ell} \neq 0 \end{cases}$
z_2	$= \bar{A}_{psq} \cdot j_p(\omega_{pq} \frac{r}{c_2}) + \bar{\bar{A}}_{psq} y_p(\omega_{pq} \frac{r}{c_2}), \begin{cases} \bar{\bar{A}}_{psq} = 0 \\ \bar{\bar{A}}_{psq} \neq 0 \end{cases}$
z'_1, z'_2	differentiations of z_1 and z_2 with respect to r
z''_1, z''_2	second differentiations of z_1 and z_2 with respect to r
δz	infinitesimal length in z direction
Z	$= (Kr)^{\frac{1}{2}} g_1$
$Z_{\bar{\nu}}$	$= \bar{c}_1 K_{\bar{\nu}}(\ ) + \bar{c}_2 I_{\bar{\nu}}(\ )$
Z^*	$= \frac{\alpha}{\bar{\alpha}_{max}}$
$\hat{Z}$	specific acoustic impedance
$\bar{Z}$	$= \frac{\alpha + \alpha_1 - \alpha_{max}}{\alpha_1}$
$\dot{\bar{Z}}$	derivative of $\bar{Z}$ with respect to time
α	approach
α_1	approach at the end of elastic loading period
α_F	permanent deformation
α_{max}	$= (\frac{5 v_o^2}{4 \hat{K}_1 \hat{K}_2})^{2/5}$
$\dot{\alpha}$	first derivative of α with respect to time
$\dot{\alpha}_1$	first derivative of α_1 with respect to time
$\ddot{\alpha}$	second derivative of α with respect to time
$\dddot{\alpha}$	third derivative of α with respect to time

α^*	expression defined in equation (6.175b)
$\hat{\alpha}$	coefficient of viscous damping
$\bar{\alpha}$	series solution of equation (2.90)
$\bar{\alpha}_n$	n^{th} term in expansion of $\bar{\alpha}$
$\bar{\alpha}_{max}$	$= \frac{1}{3}\alpha_1 + (\frac{4}{9}\alpha_1^2 + \frac{\alpha_1^2}{\eta^2})^{\frac{1}{2}}$
$\beta, \beta_1, \beta_2, \beta_x$	dimensionless contact time
$\beta_{n\ell}$	viscous damping factor
β^*	$= \frac{8E\sqrt{a_1}}{3(1-\nu^2)m_1}^{\frac{1}{2}}$
$\hat{\beta}$	dimensionless contact time in inelastic collision
$\hat{\beta}_2$	$= \frac{\ell}{\eta}$
$\hat{\beta}_3$	$= \frac{\ell}{b^*}$
$\bar{\beta}$	series solution of equation (2.91)
$\bar{\beta}_n$	n^{th} term in expansion of $\bar{\beta}$
$\bar{\gamma}$	series solution of equation (2.92)
$\bar{\gamma}_n$	n^{th} term in expansion of $\bar{\gamma}$
δ_1, δ_2	material property in Hertz's theory of contact
$\delta_{\ell q}, \delta_{ms}, \delta_{np}$	Kronecker delta
δ^*	$= \frac{2}{3}\eta \frac{\alpha_1}{\alpha_2}$
$\hat{\delta}$	Dirac delta function
$\bar{\delta}$	dilatation divided by $e^{i\omega t}$
$\bar{\delta}_n$	n^{th} component of $\bar{\delta}$
Δ	dilatation = $\varepsilon_{xx}+\varepsilon_{yy}+\varepsilon_{zz}$
ε_m	= 1 (for m = 0), = 2 (for m ≠ 0)
$\varepsilon_{xx}, \varepsilon_{xy}, \varepsilon_{xz}$, etc.	components of strain in Cartesian coordinates

ζ	integration variable in the convolution integral
η	$= \frac{\pi \bar{P}_o a_1}{m_1}$
η_n	quantity defined in equation (6.27b)
θ	angular coordinate
θ_o	arbitrary angular coordinate
θ_1, θ_2	angular coordinates of impactee and impactor
λ	Lame's constant
μ, μ_1, μ_2	rigidity modulus
$\bar{\mu}_1$	i-th modulus of rigidity in summation form of presentation of $\mu\psi$
ν, ν_1, ν_2	Poisson's ratio
$\bar{\nu}$	fractionals of half orders, = n+ ½
ξ, ξ_1, ξ_2	ratio of radial coordinate to the radius of sphere
$\xi_{n\ell}$	quantity defined in equation (6.99b)
$\bar{\xi}_{n\ell}$	quantity defined in equation (7.31)
π_6	Koss's dimensionless pressure time
π_q	Koss's dimensionless pressure frequency
Π	acoustic power
ρ, ρ_1, ρ_x	density
ρ_o	original density, density of air
ρ'	density of medium
$\sigma_{rr}, \sigma_{r\theta}, \sigma_{r\psi}$, etc.	components of stress in spherical coordinates
$\sigma_{xx}, \sigma_{xy}, \sigma_{xz}, \sigma_{yz}$, etc.	components of stress in Cartesian coordinates
τ	$= t - \frac{r-a}{c}$
τ^*	$= -2a/c$
$\bar{\tau}_i$	relaxation or retardation time of viscoelasticity

ϕ	velocity potential function
$\phi_{n\ell}$	$= \tan^{-1} \frac{\beta_{n\ell}}{(1-\beta_{n\ell})^{\frac{1}{2}}}$
$\bar{\phi}_n$	spherical solid harmonic of degree n
χ	function dependent on θ only ($\chi(\theta) = \cos\theta$p 6)
ψ	angular coordinate
ψ_n	series in the form of, $1 - \frac{K_2^2 r^2}{2(2n+3)} + \frac{K_2^4 r^4}{2x4(2n+3)(2n+5)}$
Ψ	relaxation function of viscoelasticity
$\dot{\Psi}$	rate of relaxation
ω	circular frequency
$\omega_{n\ell}, \omega_{nq}, \omega_{pq}$	ℓ-th and q-th circular frequencies of orders n and p
$\omega^*_{n\ell}$	$= \omega_{n\ell}(1-\beta_{n\ell})^{\frac{1}{2}}$
$\bar{\omega}_n$	spherical solid harmonic of degree n
$\bar{\omega}_x, \bar{\omega}_y, \bar{\omega}_z$	components of rotation in Cartesian coordinates
$\bar{\omega}_{n\ell}$	ℓ-th circular frequency of order n of impactor
$\Omega_{n\ell}$	ℓ-th dimensionless frequency of order n
∇^2	Laplacian operator
	Laplace transform operator

SUMMARY

In this research project the rigid body (or acceleration) noise together with the sound due to transient vibration has been studied for colliding spheres. In the investigation of the rigid body sound radiated by colliding spheres the three cases considered cover elastic,plastic and visco-elastic impact.

For elastic impact the Hertz law of contact was used for predicting the force time history during the contact period. The velocity potential for an oscillating sphere is also obtained and from this can be derived the sound pressure in the far field for a unit acceleration impulse. Convolution of this pressure term with the acceleration from the Hertz theory enables the computation of the pressure as a function of time.

For the case of radiation due to inelastic collision the Andrews theory is used in which the contact period is divided into three stages, an initial elastic loading period, secondly an elastic-plastic loading and finally an elastic loading period. Knowledge of the accelerations during each period enabled prediction of sound pressure with the aid of the convolution method.

The sound pressure radiated by a visco-elastic sphere in collision with a metallic sphere is also analysed. The model was based upon the use of the force-time relationship developed by Pao.

Finally, the transient vibrations of solid and hollow spheres are studied and the sound caused by transient vibration for both types of sphere are computed.

ACKNOWLEDGEMENTS

The author would like to express his sincere appreciation to his supervisor, Dr.J.S.Anderson, for many valuable discussions and the continuous advice and encouragement offered during this work.

Especial thanks are also due to [redacted] for his assistance in the preparation of the test rig, to [redacted] for typing t he manuscript and to [redacted] for her partial help in proof reading of manuscript.

1. INTRODUCTION

1.1. General introduction

Many of us have experienced pleasant feelings whilst listening to our favourite music during the evenings after a hard working day at the office or factory. This delicate instrument (i.e. the human ear) through which such comfort and relaxation is achievable may easily be annoyed by unpleasant noise. Continuous and discontinuous exposure to the hostile noise will effect man both physically, psychologically and socially.

The development of industry in modern societies has lead to more and more sound sources giving higher and higher noise levels. In most of the industrial machinery such as punch presses, gear boxes and computer print-out mechanisms, the impact noise is the dominant source of noise. Thus, work is required to be carried out in the field of impact noise in order to provide methods of acoustical prediction of impact machinery noise in a form which can be used at the design stage.

Five mechanisms of impact noise have been introduced by Akay [1]. These are rigid body radiation, pseudo-steady-state radiation, air-ejection, radiation due to rapid surface deformations, and sound radiation due to fracture of materials following impact.

The first two of the above mechanisms are subjects which have received attention in this report.

A review of rigid body radiation and pseudo-steady-state radiation is given in this Chapter. Following that, some principles of sound wave theory together with concepts required for analysing the sound radiated by elastic collision of spheres are discussed in Chapter 2.

In Chapter 3 the rigid body sound caused by elastic collision of spheres is considered. The Hertz law of contact is used for predicting the force time history during the contact period. The resultant sound pressure for a pair of colliding spheres is obtained according to the ray theory.

The rigid body sound due to inelastic collision of spheres is dealt with in Chapter 4. A numerical method as well as analytical one is introduced for predicting the sound pressure.

Chapter 5 considers the sound caused by the impact of viscoelastic spheres. The discrete finite transform method is given for evaluation of Fourier transform of pressure-time history.

Torsional and spheroidal vibrations of solid and hollow spheres are investigated in Chapter 6 and 7. The response of a sphere to a radial concentrated force is obtained and sound due to transient vibrations is calculated.

In Chapter 8 the experimental results concerning elastic collision are given.

Finally, in Chapter 9, both theoretical and experimental results are discussed and conclusions drawn.

1.2. Review of Literature

1.2.1. Rigid body radiation

The rigid body radiation can be described as a pressure disturbance generated in an acoustic medium by the acceleration of an object. The study of this type of radiation goes back to the nineteenth century when Kirchhoff [2] calculated the velocity potential generated by an impulsively accelerated sphere. Later Taylor [3] studied the motion of a sphere in a compressible fluid subjected to a sudden impulse. He used a special case of the more general solution given by Love [4] and included the effect of the relative ratio of the densities of the sphere and the fluid in which it is immersed. Taylor showed that the final velocity of a sphere given an initial velocity U_o becomes $U_o/(1+\beta)$, where β is the ratio of the virtual mass m' (half the mass of fluid displaced) to the mass of the sphere m and gave an expression for energy lost as $\frac{1}{2}mU_o^2\beta/(1+\beta)$. He argued that this energy is propagated away as a sound wave.

A similar study was carried out by Miles [5] for a cylinder in a compressible flow at low Mach number. By a simple analysis he explained the mechanism of sound radiation from an accelerating body in the following way: When a body immersed in an inviscid compressible fluid is brought to its final uniform velocity U_o impulsively and kept at this constant velocity by a force F(t), the final momentum of the associated flow will be $m'U_o$, where m' is the virtual mass. Hence the total impulse delivered by F(t) to the body is equal to $I=\int_o^\infty F(t)dt=m'U_o$. Since the force F(t)

acts on a constant velocity the total work done is $W_T = \int_0^\infty F(t)U_o dt = \dot{m}U_o^2$. After the steady state is reached no resultant force acts on the body and the flow becomes potential; therefore, the energy of the associated flow is $\frac{1}{2}\dot{m}U_o^2$. Miles attributed the dissipation of the remaining $\frac{1}{2}\dot{m}U_o^2$ to sound radiation. When Miles result is compared to that of Taylor's since $\dot{m}/m=\beta$ and for air $\beta \ll 1$, it follows that the amount of energy dissipated is the same in both analyses to first order in β. He also computed the indicial admittance, the velocity response to a suddenly applied unit force, and the indicial impedance, which is the force response to a suddenly imposed unit velocity. He obtained series solutions for these quantities and plotted them in graphical form. Later Miles extended these results in two papers [6,7] to compute the indicial impedance of either a piston or strip in a baffle.

Longhorn [8] investigated the effect of the compressibility on the work required to accelerate a rigid sphere when it was immersed in a fluid. He also calculated the work done on the sphere to maintain its velocity constant and the energy of the fluid from the potential field for both impulsive and arbitrary acceleration.

Chen and Schweikert [9] developed a method of analysis for predicting sound radiation from an arbitrary body vibrating in an infinite fluid medium. In their analysis the acoustic field was described by a distribution of surface sources of unknown strength at the body-fluid boundaries.

Junger and Thompson [10] by using the standard dipole formula in the frequency domain and then by Fourier transforming into the time domain, obtained an expression for sound pressure radiated by an impulsively accelerated sphere. In their analysis the velocity was assumed to decay exponentially in time, which gives rise to a forced exponentially decaying pressure field. However, in the limiting case of a velocity step function, the forced solution vanished and the pressure obtained was the same as Kirchhoff's [2] velocity potential solution after differentiating with respect to time. Later, Junger [11], by analysis in the time domain, treated the cases of an impulsively expanding sphere and a circular baffle subjected to a velocity step. He found that in both cases half of the work done on the fluid is radiated as sound during acceleration, and the other half is radiated when the source boundaries are suddenly stopped.

Farm and Huang [12] used the source density method developed by Chen and Schweikert [9] to find the acoustic field generated by the arbitrarily time dependent motion of a rigid circular baffled piston in a rigid infinite plane. They also developed a numerical method and solved the sound pressure induced by the sudden start of a rigid sphere in an infinite fluid. The surface of the sphere was divided into 648 triangles and each element was considered as a rigid piston. They compared their numerical results for a sphere with Kirchhoff's results. An asymptotic description of the sound pulse front for the case of arbitrary shaped bodies was given by Junger [13] with similar numerical

results for the sphere as were obtained by Farm and Huang [12]. Farassat and Sears [14] also treated the present problem as a special case of the far field sound radiation for rigid bodies in arbitrary motion.

Ffowcs Williams and Lovely [15] gave an approximate method for evaluating the sound of impulsively accelerated bodies. In their approximation method they used the local ray theory to evaluate the surface pressure fluctuation in the Kirchhoff integral to give a simple estimate of the sound field radiated by the impulsive motion of solid bodies. The method was tested by comparing the approximate calculations with exact results for an impulsively accelerated rigid sphere. The outcome of this comparison showed a good degree of agreement.

Akay and Hodgson [16] calculated the potential velocity of an impulsively accelerated sphere in an arbitrary fluid medium and showed that as the relative density ratio of the fluid to the sphere is increased the amplitude of pressure increases too. They also investigated the effect of the rate of change of velocity by solving the sound pressure radiated by a sphere subjected to a ramp step velocity and found out that as the velocity changes become smaller, the sound radiation decreases. Finally, they calculated the energy in both time and frequency domains and concluded that the energy lost in the acceleration or deceleration is dissipated as sound.

Banerji [17,18] was the first to investigate the radiation of sound generated by collision of two spheres. He employed

an apparatus which was based on a ballistic principle and measured intensity in different directions for pairs of spheres of various materials. These measurements showed that the maximum intensity was along the direction of impact and minimum intensity occurred at an angle of about 67^{o} with the same direction. He also gave an expression for the velocity potential but did not take the Hertzian acceleration into account.

Nishimura and Takahashi [19,20] studied the characteristics of impact sound generated by both normal and oblique collision of two steel balls of different radii. The duration of contact was measured electrically and the form of stress wave was observed by using a piezoelectric transducer and a synchroscope. A condenser microphone was also employed to investigate the wave forms of sound pressure due to the collision of the balls. They showed that the peak sound pressure was proportional to the 6/5th power of the impact velocity which was also in good agreement with the Hertz contact stress theory.

Further studies of this problem were made by Koss and Alfredson [21] who extended the work of Nishimura and Takahashi [19,20] by combining acoustic theory with the Hertz theory of contact stresses. They showed both analytically and experimentally that the sound radiation from the colliding spheres is solely due to their acceleration-time history. In separate studies Koss [22,23] reported results for sound radiation from the impact of elastic spheres in normalised forms and extended these results to inelastic collisions.

Hudson and Copley [24] investigated the sound generated by a pair of colliding spheres in a similar way as carried out by Koss and Alfredson [21].

Anderson [25] studied the noise produced by the impact of a pile and a hammer in pile driving experimentally. For this purpose he first considered collision of two spheres and then investigated the impact of a hammer and a rod which was partially burried in sand. He found that for objects with small dimensions the impulsive acceleration and deceleration of the objects were the main source for generating the noise, whereas for objects with relatively large size the major part of the noise was due to transient vibration of the objects at their natural frequencies.

Hodgson [26] employed the finite difference method to calculate the sound pulse radiated by a platen in the form of a solid cylinder undergoing Hertzian deceleration. The results were presented in dimensionless form in order to enable the pulse to be calculated for a wide range of platen sizes and impact times.

Holmes [27] developed an analysis for the acoustic energy of impact sounds. He showed that the maximum acoustic energy that can be radiated due to sudden acceleration is related to the kinetic energy of the fluid flow near the bodies before and after the impact. He then applied his theory to impact of spheres and concluded that only a small fraction of this maximum energy was actually radiated as sound.

A.T. Holmes et al [28] later showed that sound energy due to rigid body radiation in industrial machinery can reach considerable levels and proved that rigid body type radiation can be an important factor in impact sound generation.

Richards et al [29] studied the noise generated by impacting bodies due to the high surface acceleration during the contact period. They produced theoretical and empirical formulae together with curves for the initial peak pressures and the total acceleration noise energy associated with simple impact processes.

1.2.2. Pseudo-steady-state radiation

Another fundamental mechanism of impact noise is the pseudo-steady-state radiation. Richards [30] argued that an impact process is generally employed to convert a vast amount of energy into useful work in a very short time span. The time span is often too short for the applied energy to be wholly converted into work. The excess energy is absorbed by the mechanical structural which subsequently undergoes transient vibrations for a limited period. It is useful here to consider the role of elastic vibrations on sound radiated from an impacted sphere. Lord Rayleigh [31] showed that except for spheres with very large diameters or very high impact velocities energy absorbed by the elastic vibrations of an impacted sphere is a fraction of its initial kinetic energy on the order of $1/50(v_o/C_o)$, where v_o is the relative impact

velocity and C_o is the material elastic wave velocity. Also, Lamb's analytical results [32] demonstrate that the natural frequencies of vibrations of small spheres are so high that they can not contribute to the audible sound field.

Sound radiation due to pseudo-steady-state radiation from impactively excited structures have been investigated analytically and experimentally for simple cases of an impacted plate and an impacted rod by several workers.

The first investigation of sound radiation from impacted plates was performed by Tokita [33-35], who found the empirical relationship between either the peak sound pressure or the peak acceleration level of the plate and the momentum of the impacting hammer to be $A_o=C_1(mv)^{C}2$, where A_o is the peak value of either acceleration or sound pressure, m is the mass and v is the impact velocity of the hammer. C_1 and C_2 are frequency dependent coefficients. Tokita [33] described C_1 as a reduction factor indicating the momentum converted into plate vibrations but found this coefficient too complex to be analysed quantitatively. Tokita found the coefficient C_2 to be unity in the low frequency region and less than unity in the high frequency region and interpreted this result as inefficient transfer of momentum into plate vibrations at higher frequencies. Tokita further examined the relationship between vibrational characteristics of the plate and the radiated sound pressure and found that at low frequencies the sound pressure was almost proportional to plate vibrational velocity, while at high frequencies sound pressure

was almost proportional to acceleration. Similar studies were carried out by Magrab and Reader [36] who analytically investigated the far field radiation from an infinite elastic plate excited by a transient point loading. Their investigation led to the conclusion that only the radiation from flexural waves with frequencies above the critical frequency would reach the acoustic far field.

Akay et al [37] made an experimental study of the sound generated by the impact of small spheres and steel plates of different thicknesses. They found the peak sound pressure level to be linearly dependent on the peak plate acceleration level at impact.

Matsumoto and Simpson [38] determined by modal analysis the longitudinal response of an unrestrained elastic cylinder subjected to a contact force at its end, where radiation from the radial surface was considered negligible. Matsumoto and Simpson's experimental results show agreement with their prediction for the rigid body radiation followed by the lower amplitude structural ringing corresponding to the modal acceleration terms of the bar.

Akay and Hodgson [39] examined both theoretically and experimentally radiation of sound due to collision of a small sphere and a thick plate. In this study radiation from the flexural vibrations of the thick plate were found to be negligible.

Richards et al [40] in their comprehensive studies regarding noise arising from the subsequent free vibration have drawn attention to the radiation efficiency of simple components having various modes of vibration, and have presented this information in the form of charts.

Benedetto et al [41] investigated radiation of sound resultant from the central impact of a sphere on a thin plate supported along all edges. The observed acoustic phenomenon consists of an initial sound pressure peak followed by vibrations at the natural frequencies of the plate.

The pseudo-steady-state radiation from a steel cylinder impacted by a steel sphere from the longitudinal or the transverse direction was investigated by Endo et al [42]. They examined both theoretically and experimentally the influence of impact speed and the aspect ratio of the impactee on the radiated sound. They concluded that whether the dispersion of the elastic waves is significant as in the transverse impact, or not as in the longitudinal one, the product of the fundamental natural radian frequency ω_1 of the cylinder and the contact time T, i.e. ωT_1, is a suitable parameter for characterising the generation conditions under which rigid body radiation or pseudo-steady-state radiation is the predominant source of sound. The pseudo-steady-state becomes predominant for comparatively small $\omega_1 T$, while the rigid body sound is predominant for large values of $\omega_1 T$.

2. FUNDAMENTAL CONCEPTS USED IN THE SUBSEQUENT CHAPTERS

In this Chapter some principles of acoustics together with those concepts later used in the following Chapters are reviewed. The reviews are divided into three parts as follows:

1. Acoustic wave equation and its solution together with some characteristics of simple, monopole, and dipole sources of sound are given. The potential functions of monopole and dipole sources of sound are later used in Chapter 3 to find their impulsive solution.
2. The impact of elastic bodies is investigated by means of the Hertz law of contact. The original work is in German but an outline of which is given by Goldsmith [43]. The Hertz law of contact is used later for studying the sound radiated by colliding spheres. The author also employed a numerical method in order to calculate the differential equation relating the force and time which has not been examined anywhere else. The results of this examination are compared in Figure (2.2) with the half sine pulse approximation.
3. Equations of motion for an isotropic elastic solid and its solution for a sphere are given. These solutions are based on the remarkable work of Lamb [32, 44] given in the series of two papers. Later in Chapter 6 these solutions will be used in order to study the vibration of spheres, and results will be compared with those given by the author.

2.1. The Cartesian form of the three dimensional acoustic wave equation

The derivation of the acoustic wave equation is given in many classical acoustic's text books (e.g. Malecki [45], Junger [46], James [47], and Hunter [48]). Following procedures may be found similar to one or another. To produce the acoustic wave equation one should use both the continuity equation and the dynamic equation. These equations may be written as:

$$\frac{\partial}{\partial x}(\rho' v_x)+\frac{\partial}{\partial y}(\rho' v_y)+\frac{\partial}{\partial z}(\rho' v_z) = -\frac{\partial \rho'}{\partial t}\ , \qquad (2.1)$$

$$\frac{\partial}{\partial t}(\rho' v_x)= -\frac{\partial p'}{\partial x},\ \frac{\partial}{\partial t}(\rho' v_y) = -\frac{\partial p'}{\partial y}\ , \text{ and } \frac{\partial}{\partial t}(\rho' v_z) = -\frac{\partial p'}{\partial z} \qquad (2.2)$$

where ρ' is the density of medium, v_x, v_y and v_z are the components of particle velocity, and p' is the sum of static pressure $\bar{p}$ and excess or sound pressure p. The details concerning derivation of the above equations may be found in [47, 48].

The dynamic equations given in the above are based on assumptions that the particle velocities are small and the forces due to viscous stresses are negligible. Another assumption which is essential for derivation of the acoustic wave equation is the conservation of heat energy. This means that the adiabatic law holds. As a result of this assumption

one obtains:

$$p = \rho_o c^2 \overset{*}{s} \tag{2.3}$$

where ρ_o, c, and $\overset{*}{s}$ are original density, velocity of sound, and condensation respectively. The condensation of a gas may be defined as the ratio of the increment of density change to the original density, and can be expressed as:

$$\overset{*}{s} = \frac{\rho' - \rho_o}{\rho_o} \tag{2.4}$$

Using equation (2.4) and substituting for ρ' in both equation of continuity and the dynamic equation gives:

$$\frac{\partial \overset{*}{s}}{\partial t} = -\text{div } \underline{q} \tag{2.5}$$

and

$$-\text{gradp} = \rho_o \frac{\partial}{\partial t} \underline{q} \tag{2.6}$$

where $\text{div}\underline{q} = \frac{\partial}{\partial x} v_x + \frac{\partial}{\partial y} v_y + \frac{\partial}{\partial z} v_z$ and $\text{gradp} = \frac{\partial p}{\partial x}\underline{i} + \frac{\partial p}{\partial y}\underline{j} + \frac{\partial p}{\partial z}\underline{k}$.

But from (2.3):

$$\frac{\partial p}{\partial t} = \rho_o c^2 \frac{\partial \overset{*}{s}}{\partial t} \tag{2.7}$$

Substituting for $\frac{\partial \overset{*}{s}}{\partial t}$ from (2.5) gives:

$$\frac{\partial p}{\partial t} = -\rho_o c^2 \text{div}\underline{q} \tag{2.8}$$

Eliminating $\underline{q}$ between (2.6) and (2.8) yields:

$$\frac{\partial^2 p}{\partial t^2} = c^2 \nabla^2 p \qquad (2.9)$$

where $\nabla^2 p$ is a shortened form of $(\frac{\partial^2}{\partial x^2} + \frac{\partial^2}{\partial y^2} + \frac{\partial^2}{\partial z^2})p$.

It is called the Laplacian of p.

The sound field is considered to be irrotational, i.e.

$$\text{curl}\underline{q} = 0 \qquad (2.10.a)$$

or

$$\nabla^2 \underline{q} = \text{graddiv}\underline{q} \qquad (2.10.b)$$

Thus one may define the potential function such that:

$$\underline{q} = -\text{grad}\phi \qquad (2.11)$$

where ϕ is the velocity potential function. Using equation (2.6) and substituting for $\underline{q}$ from (2.11) gives:

$$p = \rho_o \frac{\partial \phi}{\partial t} \qquad (2.12)$$

From (2.11) and (2.12) one may write:

$$\text{div}\underline{q} = -\text{divgrad}\phi = -\nabla^2 \phi \qquad (2.13)$$

and

$$\frac{\partial p}{\partial t} = \rho_o \frac{\partial^2 \phi}{\partial t^2} \qquad (2.14)$$

Substituting in (2.8) for $\text{div}\underline{q}$ and $\frac{\partial p}{\partial t}$ gives:

$$\frac{\partial^2 \phi}{\partial t^2} = c^2 \nabla^2 \phi \tag{2.15}$$

Equation (2.15) is called the acoustic wave equation.

2.2. General solution of acoustic wave equation in spherical co-ordinates

The acoustic wave equation given by (2.15) can be written in spherical co-ordinates r, θ, and ψ (Figure 2.1) as:

$$\frac{1}{c^2} \frac{\partial^2 \phi}{\partial t^2} = \frac{1}{r^2} \frac{\partial}{\partial r}\left(r^2 \frac{\partial \phi}{\partial r}\right) + \frac{1}{r^2 \sin\theta} \frac{\partial}{\partial \theta}\left(\sin\theta \frac{\partial \phi}{\partial \theta}\right) + \frac{1}{r^2 \sin^2\theta} \frac{\partial^2 \phi}{\partial \psi^2} \tag{2.16}$$

The proof of it is given by Skudrzyk [49].

The solution of (2.16) may be represented in the form:

$$\phi = g_1(r) g_2(\theta) g_3(\psi) e^{i\omega t} \tag{2.17}$$

where $g_1(r)$, $g_2(\theta)$ and $g_3(\psi)$ are the individual functions of one of the space co-ordinates. Substituting the above solution into the wave equation yields:

$$r^2 \frac{g_1''}{g_1} + 2r \frac{g_1'}{g_1} + \frac{\omega^2}{c^2} r^2 = -\left(\frac{g_2''}{g_2} + \text{cotg}\theta \frac{g_2'}{g_2} + \frac{1}{\sin^2\theta} \frac{g_3''}{g_3}\right) \tag{2.18}$$

where $g_1' = \frac{dg_1}{dr}$, $g_1'' = \frac{d^2 g_1}{dr}$, $g_2' = \frac{dg_2}{d\theta}$, $g_2'' = \frac{d^2 g_2}{d\theta^2}$, and so forth.

Since g_1 is a function of r only, the left hand side of equation (2.18) is independent of θ and ψ. Similarly the right hand side is independent of r, so each side must be equal to a constant. Let this constant be $n(n+1)$, where n is an integer. Thus one may write:

$$r^2 g_1'' + 2r g_1' + [\frac{\omega^2}{c^2} r^2 - n(n+1)] g_1 = 0 \qquad (2.19)$$

and

$$\sin^2\theta \, [\frac{g_2''}{g_2} + \cot g\theta \, \frac{g_2'}{g_2} + n(n+1)] = - \frac{g_3''}{g_3} = m^2 \qquad (2.20)$$

Using (2.20) and following similar procedure for the separation of variables gives:

$$g_2'' + \cot g\theta \, g_2' + [n(n+1) - \frac{m^2}{\sin^2\theta}] g_2 = 0 \qquad (2.21)$$

and

$$g_3'' + m^2 g_3 = 0 \qquad (2.22)$$

where m^2 is the constant of separation. In order that the potential ϕ be single valued, m should be an integer. Thus $g_3(\psi)$ may be expressed in terms of periodic function as:

$$g_3(\psi) = \bar{A}\cos(m\psi) + \bar{B}\sin(m\psi) \qquad (2.23)$$

The transformation $\cos\theta = X$ transforms (2.21) to the so-called Legendre's associated differential equation:

$$(1-X^2)\frac{d^2}{dX^2}g_2 - 2X\frac{d}{dX}g_2 + [n(n+1) - \frac{m^2}{1-X^2}]g_2 = 0 \quad (2.24)$$

where $\frac{d}{dX}g_2 = -g_2'/\sin\theta$ and $\frac{d^2}{dX^2}g_2 = \frac{1}{\sin^2\theta}(g_2'' - g_2'\cot g\theta)$.
Equation (2.24) is the same as Skudrzyk [49] except $X = \mu$.

To find the solution of (2.24) one may first consider the Legendre's equation derivable from (2.24) by letting m = 0. Thus:

$$(1-X^2)\frac{d^2g_2}{dX^2} - 2X\frac{dg_2}{dX} + n(n+1)g_2 = 0 \quad (2.25)$$

The general solution of (2.25) may be expressed in terms of Legendre polynominals and Legendre functions of the second kind. Since the desired solution should be finite at the poles $X = \pm 1$, one may choose a solution as:

$$g_2 = P_n(X) = P_n(\cos\theta) \quad (2.26)$$

where $P_n(X)$ is the Legendre polynomial of the nth order.

The first few Legendre polynomials are:

$$P_0(X) = 1, \quad P_1(X) = x, \quad P_2(X) = \tfrac{1}{2}(3X^2 - 1)$$

$$P_3(X) = \tfrac{1}{2}(5X^3 - 3X), \quad P_4(X) = \tfrac{1}{8}(35X^4 - 30X^2 + 3),$$

$$P_5(X) = \tfrac{1}{8}(63X^5 - 70X^3 + 15X). \quad (2.27)$$

Using equation (2.25) and differentiating it m times with respect to X gives:

$$(1-X^2)\frac{dY^2}{dX^2} - 2(m+1)X\frac{dY}{dX} + [n(n+1) - m(m+1)]Y = 0 \quad (2.28)$$

where $Y = \frac{d^m}{dX^m}g_2 = \frac{d^m}{dX^m}P_n(X)$.

A similar equation to (2.28) can be obtained from (2.24) by substituting

$$g_2 = Y(1-X^2)^{m/2}$$

Thus the solution to the equation (2.24) may be given by:

$$g_2 = (1-X^2)^{m/2} \frac{d^m}{dX^m} P_n(X) = P_n^m(X) \qquad (2.29)$$

where functions $P_n^m(X)$ are called associated Legendre functions of the first kind, and these functions in turn are related to the Legendre polynomials listed in (2.27).

To solve the equation (2.19) one may write:

$$r^2 \frac{d^2Z}{dr^2} + r \frac{dZ}{dr} + [K^2r^2 - (n+\tfrac{1}{2})^2]Z = 0 \qquad (2.30)$$

where $Z = (Kr)^{\frac{1}{2}} g_1$ and $K = \frac{\omega}{c}$. Equation (2.30) is Bessel's differential equation and its solution may be expressed in terms of Bessel functions as:

$$Z = \bar{D} J_{n+\frac{1}{2}}(Kr) + \bar{E} Y_{n+\frac{1}{2}}(Kr) \qquad (2.31)$$

Rewriting (2.31) in terms of spherical Bessel functions gives:

$$Z = \bar{D}\left(\frac{2Kr}{\pi}\right)^{\frac{1}{2}} j_n(Kr) + \bar{E}\left(\frac{2Kr}{\pi}\right)^{\frac{1}{2}} y_n(Kr) \qquad (2.32)$$

Thus the solution for g_1 may be written as:

$$g_1 = \left(\frac{2}{\pi}\right)^{\frac{1}{2}} [\bar{D} j_n(Kr) + \bar{E} y_n(Kr)] = \bar{F} j_n(Kr) + \bar{G} y_n(Kr) \qquad (2.33)$$

The above radial dependent function together with time dependent function should be representable in forms of functions with arguments ct-r and ct+r. Thus coefficients $\bar{F}$ and $\bar{G}$ should be related to each other as:

$$\bar{G} = -i\bar{F} \qquad \text{(diverging)}$$

and

$$\bar{G} = i\bar{F} \qquad \text{(converging)}$$

Substituting for $\bar{G}$ into (2.33) and representing the result in terms of Hankel functions gives

$$g_1(r) = \bar{F} h_n^{(1,2)}(Kr) \tag{2.34}$$

where $h_n^{(1,2)}(Kr)$ are spherical Hankel functions of the first and second kind, and may be related to the spherical Bessel functions through relations $h_n^{(1,2)}(Kr) = j_n(Kr) \pm i y_n(Kr)$. The first few spherical Bessel and Hankel functions may be expressed as:

$$j_0(Kr) = \frac{\sin Kr}{Kr}, \quad y_0(Kr) = -\frac{\cos Kr}{Kr}, \quad h_0^{(1)}(Kr) = \frac{e^{iKr}}{iKr},$$

$$h_0^{(2)}(Kr) = -\frac{e^{-iKr}}{iKr}, \quad h_1^{(1)}(Kr) = -\frac{e^{iKr}}{Kr}\left(1+\frac{i}{Kr}\right), \quad h_1^{(2)}(Kr) = -\frac{e^{-iKr}}{Kr}\left(1-\frac{i}{Kr}\right)$$

$$j_1(Kr) = \frac{\sin Kr}{K^2r^2} - \frac{\cos Kr}{Kr}, \quad y_1(Kr) = -\frac{\cos Kr}{K^2r^2} - \frac{\sin Kr}{Kr},$$

$$j_2(Kr) = \left(\frac{3}{K^3r^3} - \frac{1}{Kr}\right)\sin Kr - \frac{3}{K^2r^2}\cos Kr,$$

$$y_2(Kr) = -\left(\frac{3}{K^3r^3} - \frac{1}{Kr}\right)\cos Kr - \frac{3}{K^2r^2}\sin Kr,$$

$$h_2^{(1)}(Kr) = \frac{ie^{iKr}}{Kr}\left(1 + \frac{3i}{Kr} - \frac{3}{K^2r^2}\right), \quad h_2^{(2)}(Kr) = -\frac{ie^{-iKr}}{Kr}\left(1 - \frac{3i}{Kr} - \frac{3}{K^2r^2}\right.$$

(2.35)

It should be emphasised that different notations have been used to represent spherical Bessel functions. The above notations are the same as those employed by Junger [46] , whereas Skudnzyk [49] , Morse [50], and Stratton [51] used $n_n(Kr)$ instead of $y_n(Kr)$. Skudrzyk [49] also considered the Stokes-Rayleigh solution of the radial part which has the advantage of giving the solution in terms of a near field component and a far field one.

Substituting for g_1, g_2 and g_3 into the expression (2.17) gives:

$$\phi = \bar{F} h_n^{(1,2)}(Kr) p_n^m(\cos\theta)[\bar{A}\cos(m\psi)+\bar{B}\sin(m\psi)]e^{i\omega t} \tag{2.36}$$

or by summing over both n and m

$$\phi = e^{i\omega t} \sum_{n=0}^{\infty} \sum_{m=0}^{\infty} h_n^{(1,2)}(Kr) p_n^m(\cos\theta)[\bar{A}_{nm}\cos(m\psi) + \bar{B}_{nm}\sin(m\psi)] \tag{2.37}$$

Equation (2.37) may now be used for obtaining the sound radiated by a general spherical source. The procedure is as follows:

1. Expressing the radial velocity at the surface of a spherical source which is in general a function of θ, ψ and t in terms of a series of Legendre functions.

2. Finding the radial velocity at the vicinity of the source by simply differentiating the potential field ϕ with respect to r and substituting for r the radius of the source.

3. Equating both radial velocities to deduce $\bar{A}_{nm}$'s and $\bar{B}_{nm}$'s.

4. Using equation (2.12) to obtain the radiated sound pressure.

As far as the purposes of this study is concerned attention has been given to those spherical sources that are symmetric about the polar axis and consequently ψ independent. The sound radiated from the semicircular array on the equator of a spherical baffle which has been considered by Junger [46] may be given as an example of the sound radiated by a nonaxisymmetrical source. Equation (2.37) for a spherical symmetric field reduces to:

$$\phi = e^{i\omega t} \sum_{n=0}^{\infty} \bar{A}_n h_n^{(1,2)}(\mathbb{k}r) p_n(\cos\theta) \qquad (2.38)$$

2.3. Monopole and Simple Source

Suppose that a sphere of radius a is located at the centre of the field and behaves as a source by vibrating uniformly in the radial direction. Such a sphere is also called pulsating sphere or monopole and the radial velocity of its surface can be given by:

$$v_r = ve^{i\omega t} \qquad (2.39)$$

Differentiating (2.38) with respect to r and substituting r = a gives:

$$v_r\Big|_{r=a} = -\frac{\partial \phi}{\partial r}\Big|_{r=a} = -e^{i\omega t} \sum_{n=0}^{\infty} \bar{A}_n \frac{\partial}{\partial r} h_n^{(1,2)}(\mathbb{k}r)\Big|_{r=a} P_n(\cos\theta) \qquad (2.40)$$

For a free field situation, i.e. in the absence of reflecting surfaces (2.40) can be written as:

$$v_r|_{r=a} = -e^{i\omega t} \sum_{n=0}^{\infty} \bar{A}_n \frac{\partial}{\partial r} h_n^{(2)}(Kr)|_{r=a} \cdot P_n(\cos\theta) \tag{2.41}$$

Rewriting (2.39) in terms of a series of Legendre functions and equating to (2.41) gives:

$$\sum_{n=0}^{\infty} \bar{D}_n P_n(\cos\theta) = -\sum_{n=0}^{\infty} \bar{A}_n \frac{\partial}{\partial r} h_n^{(2)}(Kr)|_{r=a} \cdot P_n(\cos\theta) \tag{2.42}$$

where $\bar{D}_o = v$ and $\bar{D}_n = 0$ for $n = 1, 2, \ldots .$ Expanding both sides of equation (2.42) and equating the constants yields:

$$\bar{A}_o \frac{\partial}{\partial r} h_o^{(2)}(Kr)|_{r=a} = -i \frac{\bar{A}_o}{ka^2}(1+iKa)e^{-iKa} = -v \tag{2.43}$$

and $\bar{A}_n = 0$ for $n = 1,2, \ldots .$ Substituting for $\bar{A}_n$'s into equation (2.38) gives:

$$\phi = \frac{va^2}{(1+iKa)} \cdot \frac{e^{i(\omega t - Kr + Ka)}}{r} \tag{2.44}$$

The sound pressure and the radial velocity of the pulsating sphere or monopole sound source can now be given by:

$$p = \rho_o \frac{\partial \phi}{\partial t} = \frac{i\rho_o Kcva^2}{(1+iKa)} \cdot \frac{e^{i(\omega t - Kr + Ka)}}{r} \tag{2.45}$$

$$v_r = -\frac{\partial \phi}{\partial r} = \frac{va^2}{(1+ika)} \cdot \frac{1+ikr}{r^2} \cdot e^{i(\omega t-kr-ka)} \qquad (2.46)$$

The specific acoustic impedance which is defined as the ratio of the sound pressure to the velocity may be expressed as:

$$\hat{Z} = \frac{p}{v_r} = \rho_o c\left(\frac{k^2r^2}{1+k^2r^2} + \frac{ikr}{1+k^2r^2}\right) \qquad (2.47)$$

where $\rho_o C$ is called the characteristic impedance or radiation resistance for a plane wave. The mean square pressure which is directly related to the amount of energy in the sound signal and its root, which can be measured by a sound level meter, is given by:

$$p^2_{rms} = \tfrac{1}{2}|p|^2 = \frac{1}{T}\int_0^T [p_{RE}]^2 dt \qquad (2.48)$$

where $|p|$ is the pressure amplitude. Thus multiplying (2.45) by its complex conjugate and dividing by two gives:

$$p^2_{rms} = \tfrac{1}{2}\rho_o{}^2 c^2 \frac{k^2a^2}{1+k^2a^2} \cdot v^2 \frac{a^2}{r^2} \qquad (2.49)$$

The acoustic power radiated from the source may now be expressed as:

$$\Pi = \int_S I dS \qquad (2.50)$$

where $I = \frac{p^2_{rms}}{\rho_o c}$ is called the acoustic intensity and $dS = r^2 \sin\theta d\theta d\psi$ is the element of the surface area as shown in Figure (2.1). Thus the acoustic intensity and the acoustic power for the pulsating sphere or monopole sound sources, respectively are:

$$I = \tfrac{1}{2}\rho_o c \frac{K^2a^2}{1+K^2a^2} \cdot v^2 \frac{a^2}{r^2} \tag{2.51}$$

$$\Pi = \tfrac{1}{2}\rho_o c \frac{K^2a^2}{1+K^2a^2} .4\pi a^2 v^2 \tag{2.52}$$

An example of a monopole source of sound is pulsations at the intake of an internal combustion engine. The potential function of pulsating sphere may also be used for derivation of potential function of a simple source. Thus from (2.44)

$$\phi = \frac{va^2}{(1+iKa)}(\cos Ka + i \sin Ka). \frac{e^{i(\omega t-Kr)}}{r} \tag{2.53}$$

If Ka is small $\cos Ka \to 1$ and $\sin Ka \to Ka$, so that (2.53) reduces to:

$$\phi = \frac{va^2}{r} e^{i(\omega t-Kr)} \tag{2.54}$$

The sound pressure, radial velocity and other acoustical parameters of a simple source may now be easily given by following expressions.

$$p = \frac{i\rho_o K c v a^2}{r} e^{i(\omega t-Kr)} ,$$

$$v_r = va^2 \frac{(1+iKr)}{r^2} e^{i(\omega t-Kr)} ,$$

$$\hat{Z} = \rho_o c \left(\frac{K^2r^2}{1+K^2r^2} + \frac{iKr}{1+K^2r^2}\right) ,$$

$$p^2_{rms} = \tfrac{1}{2}\rho_o{}^2 c^2 K^2 a^2 . v^2 \frac{a^2}{r^2} ,$$

$$\Pi = \tfrac{1}{2}\rho_o K^2 a^2 . 4\pi a^2 v^2 . \tag{2.55}$$

2.4. The dipole source

Another example of a spherical source is the oscillating sphere, that is a sphere of radius a oscillating back and forth as a rigid body in the direction of the principal axis. This is also called dipole source of the sound. The radial velocity at the surface of the source may be expressed as:

$$v_r|_{r=a} = ve^{i\omega t}P_1(\cos\theta) \qquad (2.56)$$

Expressing (2.56) in terms of a series of Legendre functions and repeating the same procedure as given for the derivation of the potential function of a monopole source, gives:

$$\phi = \frac{va^3(1+iKr)}{2(1+iKa)-K^2a^2}\cdot\frac{e^{i(\omega t-Kr+Ka)}}{r^2}\cos\theta, \qquad (2.57.a)$$

$$p = \frac{i\rho_o K c va^3}{2(1+iKa)-K^2a^2}(1+iKr)\cdot\frac{e^{i(\omega t-Kr+Ka)}}{r^2}\cos\theta \qquad (2.57.b)$$

$$v_r = \frac{2(1+iKr)-K^2r^2}{2(1+iKa)-K^2a^2}\cdot\frac{va^3}{r^3}\cdot e^{i(\omega t-Kr+Ka)}\cos\theta \cdot \qquad (2.57.c)$$

Oscillations of the whole body of the diesel engine, cavitation in liquids, exhaust emissions and organ pipes are all examples of dipole sources of the sound.

From Equation (2.57) the radial specific acoustic impedance for the dipole source can be written as:

$$\hat{Z} = \rho_o c\left(\frac{K^4r^4}{4+K^4r^4} + iKr\,\frac{2+K^2r^2}{4+K^4r^4}\right) \qquad (2.58)$$

The mean square pressure, the acoustic intensity, and the radiated power may now be obtained by following similar process as given for the monopole source. Thus:

$$P^2_{rms} = \tfrac{1}{2}\rho_o{}^2c^2.\frac{K^4a^4}{4+K^4a^4}.\frac{v^2a^2}{r^2}\left(\frac{1+K^2r^2}{K^2r^2}\right)\cos^2\theta$$

$$I = \tfrac{1}{2}\rho_o c.\frac{K^4a^4}{4+K^4a^4}.\frac{v^2a^2}{r^2}\frac{(1+K^2r^2)}{K^2r^2}\cos^2\theta$$

$$\Pi = \frac{1}{6}\rho_o c.\frac{K^4a^4}{4+K^4a^4}.4\pi a^2v^2.\frac{(1+K^2r^2)}{K^2r^2} \qquad (2.59)$$

2.5. Impact of elastic bodies

According to the Hertz law of contact the force-deformation relation for collision of elastic bodies may be expressed in the form:

$$F = \hat{K}_2\alpha^{3/2} \qquad (2.60)$$

where

$$\hat{K}_2 = \frac{4}{3}\frac{q_K}{(\delta_1+\delta_2)\sqrt{A+B}} \qquad (2.61)$$

and α is called the approach. The values of A, B and q_K are tabulated by Goldsmith [43] for different types of contact. He has also given the following expressions for δ_1 and δ_2:

$$\delta_1 = \frac{1-\nu_1^2}{\pi E_1} \quad , \tag{2.62.a}$$

$$\delta_2 = \frac{1-\nu_2^2}{\pi E_2} \quad , \tag{2.62.b}$$

where ν_1 and ν_2 are the Poisson's ratio for the bodies 1 and 2 respectively and E is the Young's modulus. Goldsmith [43] investigated several impact problems involving vibrational phenomena by use of equation (2.60) and concluded that good correlation with experimental results can be achieved. Consider now two elastic bodies colliding into each other with an initial relative velocity v_o. Thus the initial conditions can be written as:

$$\dot{\alpha} = v_o \tag{2.63.a}$$

and

$$\alpha = 0 \tag{2.63.b}$$

The displacements of these bodies under action of a contact force F and in absence of any vibrational phenomena may be given by:

$$U_1 = v_o t - \frac{1}{m_1} \int_o^t dt \int_o^t F dt \tag{2.64.a}$$

and

$$U_2 = \frac{1}{m_2} \int_o^t dt \int_o^t F dt \tag{2.64.b}$$

where m_1 and m_2 are the masses of the bodies. The approach α may now be written as:

$$\alpha = U_1 - U_2 = v_o t - \hat{K}_1 \int_o^t dt \int_o^t F dt \qquad (2.65)$$

where

$$\hat{K}_1 = \frac{m_1+m_2}{m_1 m_2} \qquad (2.66)$$

Differentiating (2.65) twice with respect to t and using equation (2.60) gives:

$$\ddot{\alpha} = \dot{\alpha} \frac{d\dot{\alpha}}{d\alpha} = -\hat{K}_1 \hat{K}_2 \alpha^{3/2} \qquad (2.67)$$

Integrating both sides and inserting the initial conditions yields:

$$\dot{\alpha}^2 - v_o^2 = -\frac{4}{5} \hat{K}_1 \hat{K}_2 \alpha^{5/2} \qquad (2.68)$$

When the approach is maximum the relative velocity $\dot{\alpha}$ is equal to zero. Thus by making use of (2.68) one may find that:

$$\alpha_{max} = \left(\frac{5v_o^2}{4\hat{K}_1 \hat{K}_2}\right)^{2/5} \qquad (2.69)$$

which can also be used for evaluating F_{max}:

$$F_{max} = \hat{K}_2 \left(\frac{5v_o^2}{4\hat{K}_1 \hat{K}_2}\right)^{0.6} \qquad (2.70)$$

TO find the approach-time relation one may rewrite equation (2.68) in the form:

$$t = \int_o^\alpha \frac{d\alpha}{v_o \sqrt{1-\left(\frac{\alpha}{\alpha_{max}}\right)^{5/2}}} \qquad (2.71)$$

the approximate solution of which is given by Hunter [52] in the following form:

$$\alpha = \alpha_{max} \sin \frac{\pi t}{d} \tag{2.72}$$

where

$$d = 2 \int_0^{\frac{1}{2}d} dt = \frac{2}{v_o} \int_0^{\alpha_{max}} \frac{d\alpha}{\sqrt{1-(\frac{\alpha}{\alpha_{max}})^{5/2}}} = 2.9432 \frac{\alpha_{max}}{v_o} \tag{2.73}$$

is called the duration of contact. By making use of (2.72) and (2.65) the force-time relation can be approximated as:

$$F = F_{max} \sin \frac{\pi t}{d} \tag{2.74}$$

Thus the acceleration of each body is given by:

$$\hat{A} = \frac{F}{\bar{m}} = \frac{F_{max}}{\bar{m}} \sin \frac{\pi t}{d} \tag{2.75}$$

where $\bar{m}$ is either equal to m_1 or m_2.

In the above analysis no attention has been given towards the vibration of the bodies, or in other words, vibration produced by the collision is assumed to be negligible. This is true for the bodies with dimensions that permit a duration of contact much longer than the period of lowest mode of vibration. To study the impact problems involving vibrational phenomena responses of the bodies to contact force F=F(t) should be taken into account. As an example consider the transverse collision

of a sphere of mass m_1 with a simply supported beam. If the vibration of the sphere can be neglected one may write:

$$\alpha = v_o t - \frac{1}{m_1} \int_o^t dt \int_o^t F(t)dt - U_2(x=\bar{b},t) \qquad (2.76)$$

where v_o is the impact velocity and $U_2(x=\bar{b},t)$ is the deflection of the beam due to applied force $F=F(t)$ at position $x = \bar{b}$. Equation (2.76) may now be represented in terms of $F(t)$ by simply substituting a suitable force approach relation. The resultant equation which includes the unknown function $F(t)$ should be solved numerically.

2.6. Numerical solution of force-time history

To solve the equation (2.67) numerically one may use the initial conditions at instant $t = 0$ to predict the value of α at time $t = \Delta t$. This can be done easily by use of Taylor's formula. Thus:

$$\alpha|_{t=\Delta t} = \alpha|_{t=0} + \Delta t\, \dot{\alpha}|_{t=0} + \frac{(\Delta t)^2}{2!} \ddot{\alpha}|_{t=0} + \ldots . \qquad (2.77)$$

where Δt is a suitable time step size, $\alpha|_{t=0} = 0$, $\dot{\alpha}|_{t=0} = v_o$, and $\ddot{\alpha}|_{t=0} = \dddot{\alpha}|_{t=0} = \ldots\ldots\ldots = 0$. To estimate the value of α at time $t = 2\Delta t$ one needs to know the value of $\dot{\alpha}|_{t=\Delta t}$, $\ddot{\alpha}|_{t=\Delta t}$ and etc. These values can be easily determined by use of equations (2.68) and (2.67). By repeating the same process α and corresponding force can be calculated at any instant $t = n\Delta t$, $n = 0, 1, 2\ldots\ldots$. The force-time history calculated numerically is compared with the half sine pulse approximation in Figure (2.2).

2.7. Equation of motion in an elastic medium

To derive the equation of motion in an elastic medium Kolsky [53] used a cubic element with its sides parallel to a set of rectangular axes as shown in Figure (2.3). The resultant force in each direction, x, y and z due to variations of components of normal and shear stresses are:

$$F_x = \left(\frac{\partial \sigma_{xx}}{\partial x} + \frac{\partial \sigma_{xy}}{\partial y} + \frac{\partial \sigma_{xz}}{\partial z}\right)\delta x \delta y \delta z$$

$$F_y = \left(\frac{\partial \sigma_{yx}}{\partial x} + \frac{\partial \sigma_{yy}}{\partial y} + \frac{\partial \sigma_{yz}}{\partial z}\right)\delta x \delta y \delta z$$

$$F_z = \left(\frac{\partial \sigma_{zx}}{\partial x} + \frac{\partial \sigma_{zy}}{\partial y} + \frac{\partial \sigma_{zz}}{\partial z}\right)\delta x \delta y \delta z \qquad (2.78)$$

where δx, δy and δz are dimensions of cubic element in directions x, y and z respectively. Assume that $\hat{U}$, $\hat{V}$ and $\hat{W}$ are displacements in directions x, y and z respectively. Thus by Newton's second law:

$$\rho \frac{\partial^2 \hat{U}}{\partial t^2} = \frac{\partial \sigma_{xx}}{\partial x} + \frac{\partial \sigma_{xy}}{\partial y} + \frac{\partial \sigma_{xz}}{\partial z}$$

$$\rho \frac{\partial^2 \hat{V}}{\partial t^2} = \frac{\partial \sigma_{yx}}{\partial x} + \frac{\partial \sigma_{yy}}{\partial y} + \frac{\partial \sigma_{yz}}{\partial z}$$

$$\rho \frac{\partial^2 \hat{W}}{\partial t^2} = \frac{\partial \sigma_{zx}}{\partial x} + \frac{\partial \sigma_{zy}}{\partial y} + \frac{\partial \sigma_{zz}}{\partial z} \qquad (2.79)$$

where ρ is the density of the element. Equations (2.79) are known as equations of motion in an elastic medium. For an isotropic medium the stress-strain behaviour of the medium in terms of dilatation, Δ and Lame's constants, λ and μ where μ

is also the modulus of rigidity as given by Kolsky [53] are:

$$\sigma_{xx} = \lambda\Delta + 2\mu\varepsilon_{xx}, \quad \sigma_{yy} = \lambda\Delta + 2\mu\varepsilon_{yy}, \quad \sigma_{zz} = \lambda\Delta + 2\mu\varepsilon_{zz}$$

$$\sigma_{xy} = \sigma_{yx} = \mu\varepsilon_{xy}, \quad \sigma_{xz} = \sigma_{zx} = \mu\varepsilon_{xz}, \quad \sigma_{yz} = \sigma_{zy} = \mu\varepsilon_{yz} \tag{2.80}$$

where $\Delta = \varepsilon_{xx} + \varepsilon_{yy} + \varepsilon_{zz} = \frac{\partial \hat{U}}{\partial x} + \frac{\partial \hat{V}}{\partial y} + \frac{\partial \hat{W}}{\partial z}$. The above stress-strain relations may also been expressed in terms of Young's modulus E, and Poisson's ratio ν, through relations $E = \frac{\mu(3\lambda+2\mu)}{\lambda + \mu}$ and $\nu = \frac{\lambda}{2(\lambda+\mu)}$.

Substituting from (2.80) for the stress components in (2.79) and rewriting the result in terms of displacements gives:

$$\rho \frac{\partial^2 \hat{U}}{\partial t^2} = (\lambda+\mu) \frac{\partial \Delta}{\partial x} + \mu\nabla^2\hat{U} \tag{2.81.a}$$

$$\rho \frac{\partial^2 \hat{V}}{\partial t^2} = (\lambda+\mu) \frac{\partial \Delta}{\partial y} + \mu\nabla^2\hat{V} \tag{2.81.b}$$

$$\rho \frac{\partial^2 \hat{W}}{\partial t^2} = (\lambda+\mu) \frac{\partial \Delta}{\partial z} + \mu\nabla^2\hat{W} \tag{2.81.c}$$

Equations (2.81.a) to (2.81.c) are known as equations of motion of an isotropic elastic solid and may be represented in vector form as:

$$\rho \frac{\partial^2 \underline{S}}{\partial t^2} = (\lambda+\mu)\text{grad div } \underline{S} + \mu\nabla^2\underline{S} \tag{2.82}$$

where $\underline{S} = \hat{U}\underline{i} + \hat{V}\underline{j} + \hat{W}\underline{k}$. Differentiating both sides of (2.81.a) with respect to x, both sides of (2.81.b) with respect to y, and both sides of (2.81.c) with respect to z and adding them together gives:

$$\frac{\partial^2 \Delta}{\partial t^2} = C_1{}^2 \nabla^2 \Delta \tag{2.83}$$

where $C_1 = \frac{(\lambda+2\mu)^{\frac{1}{2}}}{\rho}$ is the velocity of the dilatation wave. Equations (2.81.a) to (2.81.c) can also be used for derivation of equations in terms of rotation. This can be achieved by eliminating Δ between any selected pair of equations. Thus:

$$\frac{\partial^2 \bar{\omega}_x}{\partial t^2} = C_2{}^2 \nabla^2 \bar{\omega}_x$$

$$\frac{\partial^2 \bar{\omega}_y}{\partial t^2} = C_2{}^2 \nabla^2 \bar{\omega}_y$$

$$\frac{\partial^2 \bar{\omega}_z}{\partial t^2} = C_2{}^2 \nabla^2 \bar{\omega}_z \tag{2.84}$$

where

$$\bar{\omega}_x = \tfrac{1}{2}\left(\frac{\partial \hat{W}}{\partial y} - \frac{\partial \hat{V}}{\partial z}\right), \quad \bar{\omega}_y = \tfrac{1}{2}\left(\frac{\partial \hat{U}}{\partial z} - \frac{\partial \hat{W}}{\partial x}\right), \quad \bar{\omega}_z = \tfrac{1}{2}\left(\frac{\partial \hat{V}}{\partial x} - \frac{\partial \hat{U}}{\partial y}\right)$$

and

$C_2 = \left(\frac{\mu}{\rho}\right)^{\frac{1}{2}}$ is the velocity of the distortion waves.

2.8. Solution of equations of motion for solid sphere

In the case of simple harmonic motion, the solution of equations of motion can be represented as:

$$\hat{U} = \hat{u}(x,y,z)e^{i\omega t}, \quad \hat{V} = \hat{v}(x,y,z)e^{i\omega t}, \text{ and}$$

$$\hat{W} = \hat{w}(x,y,z)e^{i\omega t} \tag{2.85}$$

Substituting these solutions into equations (2.81.a) to (2.81.c) gives:

$$\nabla^2\hat{u} + K_2^2\,\hat{u} = \left(1 - \frac{K_2^2}{K_1^2}\right)\frac{\partial\bar{\delta}}{\partial x} \tag{2.86.a}$$

$$\nabla^2\hat{v} + K_2^2\,\hat{v} = \left(1 - \frac{K_2^2}{K_1^2}\right)\frac{\partial\bar{\delta}}{\partial y} \tag{2.86.b}$$

$$\nabla^2\hat{w} + K_2^2\,\hat{w} = \left(1 - \frac{K_2^2}{K_1^2}\right)\frac{\partial\bar{\delta}}{\partial z} \tag{2.86.c}$$

where $K_1 = \frac{\omega}{C_1}$, $K_2 = \frac{\omega}{C_2}$ and $\bar{\delta} = \Delta e^{-i\omega t} = \frac{\partial\hat{u}}{\partial x} + \frac{\partial\hat{v}}{\partial y} + \frac{\partial\hat{w}}{\partial z}$. Let us assume now $\hat{u}$, $\hat{v}$ and $\hat{w}$ can be expressed as

$$\hat{u} = -\frac{1}{K_1^2}\frac{\partial\bar{\delta}}{\partial x} + \bar{\alpha}, \quad \hat{v} = -\frac{1}{K_1^2}\frac{\partial\bar{\delta}}{\partial y} + \bar{\beta}, \text{ and } \hat{w} = -\frac{1}{K_1^2}\frac{\partial\bar{\delta}}{\partial z} + \bar{\gamma} \tag{2.87}$$

where $\bar{\alpha}$, $\bar{\beta}$ and $\bar{\gamma}$ each are functions of x, y and z. Substituting for $\hat{u}$ into equation (2.86.a) gives:

$$\nabla^2\bar{\alpha} + K_2^2\,\bar{\alpha} = \frac{1}{K_1^2}\nabla^2\left(\frac{\partial\bar{\delta}}{\partial x}\right) + \frac{\partial\bar{\delta}}{\partial x} \tag{2.88}$$

Using a set of solutions given by (2.85) and substituting them into equation (2.83) yields:

$$\nabla^2\bar{\delta} + K_1^2\bar{\delta} = 0 \tag{2.89}$$

Inspection of (2.89) suggests that the right hand side of equation (2.88) should be equal to zero. Thus (2.88) reduces to:

$$\nabla^2\bar{\alpha} + K_2^2\bar{\alpha} = 0 \tag{2.90}$$

By following similar procedure one obtains:

$$\nabla^2\bar{\beta} + K_2^2\bar{\beta} = 0 \tag{2.91}$$

$$\nabla^2\bar{\gamma} + K_2^2\bar{\gamma} = 0 \tag{2.92}$$

In order that equation (2.89) be satisfied by the set of assumed solutions (2.87) one requires:

$$\frac{\partial\bar{\alpha}}{\partial x} + \frac{\partial\bar{\beta}}{\partial y} + \frac{\partial\bar{\gamma}}{\partial z} = 0 \tag{2.93}$$

The general solution of the system of equations given by (2.90) to (2.93) has been investigated by Lamb [44] . In his method of solution he assumed that the functions $\bar{\alpha}$, $\bar{\beta}$, and $\bar{\gamma}$ can be expanded in series of solid harmonics, and employed the notation $\bar{\alpha}_n$, $\bar{\beta}_n$ and $\bar{\gamma}_n$ to express the terms of degree n in these expansions.

Before going any further some explanation regarding functions called solid harmonics may be useful. Lamb [54] remarks that

amongst the methods available for solving $\nabla^2\phi = 0$ in three dimensions, the most important is that of spherical harmonics. This is especially suitable when the boundary conditions have relation to spherical or nearly spherical surfaces. He further states that if $\bar{\phi}_n$ is a spherical solid harmonic of degree n it may be expressed as $\bar{\phi}_n = r^n\bar{S}_n$, where functions $\bar{S}_n$ are called spherical surface harmonics. Morse's representations [55] of spherical surface harmonics are given as:

$$Y_{mn}^{e} = \cos(m\psi)P_n^m(\cos\theta), \quad \text{and} \quad Y_{mn}^{o} = \sin(m\psi)P_n^m(\cos\theta)$$

where the ones for m = 0 being zonal harmonics, the ones for m = n being sectoral harmonics, and the rest, for $0<m<n$, being tesseral harmonics.

Substituting $\bar{\alpha}_n$, $\bar{\beta}_n$ and $\bar{\gamma}_n$ into equations (2.90) to (2.93) and rewriting them without K_2 (i.e. $K_2 = 0$) gives:

$$\nabla^2\bar{\alpha}_n = 0, \qquad \nabla^2\bar{\beta}_n = 0, \qquad \nabla^2\bar{\gamma}_n = 0 \tag{2.94}$$

$$\frac{\partial\bar{\alpha}_n}{\partial x} + \frac{\partial\bar{\beta}_n}{\partial y} + \frac{\partial\bar{\gamma}_n}{\partial z} = 0 \tag{2.95}$$

Differentiating (2.95) with respect to x and substituting for $\frac{\partial^2\bar{\alpha}_n}{\partial x^2}$ into the first equation of (2.94) yields:

$$\frac{\partial}{\partial y}\left(\frac{\partial\bar{\beta}_n}{\partial x} - \frac{\partial\bar{\alpha}_n}{\partial y}\right) = \frac{\partial}{\partial z}\left(\frac{\partial\bar{\alpha}_n}{\partial z} - \frac{\partial\bar{\gamma}_n}{\partial x}\right) \tag{2.96}$$

By following the similar procedures one finds:

$$\frac{\partial}{\partial x}\left(\frac{\partial \bar{\beta}_n}{\partial x} - \frac{\partial \bar{\alpha}_n}{\partial y}\right) = \frac{\partial}{\partial z}\left(\frac{\partial \bar{\gamma}_n}{\partial y} - \frac{\partial \bar{\beta}_n}{\partial z}\right) \tag{2.97}$$

$$\frac{\partial}{\partial y}\left(\frac{\partial \bar{\gamma}_n}{\partial y} - \frac{\partial \bar{\beta}_n}{\partial z}\right) = \frac{\partial}{\partial x}\left(\frac{\partial \bar{\alpha}_n}{\partial z} - \frac{\partial \bar{\gamma}_n}{\partial x}\right) \tag{2.98}$$

From (2.96) to (2.98) one finds that there must be a function, say $\bar{X}_n$, such that its derivatives with respect to x, y and z can be expressed as:

$$\frac{\partial \bar{X}_n}{\partial x} = \frac{\partial \bar{\gamma}_n}{\partial y} - \frac{\partial \bar{\beta}_n}{\partial z}$$

$$\frac{\partial \bar{X}_n}{\partial y} = \frac{\partial \bar{\alpha}_n}{\partial z} - \frac{\partial \bar{\gamma}_n}{\partial x}$$

$$\frac{\partial \bar{X}_n}{\partial z} = \frac{\partial \bar{\beta}_n}{\partial x} - \frac{\partial \bar{\alpha}_n}{\partial y} \tag{2.99}$$

Multiplying both sides of the last two equations of (2.99) by z and y respectively, and subtracting from each other gives:

$$z\frac{\partial \bar{X}_n}{\partial y} - y\frac{\partial \bar{X}_n}{\partial z} = z\frac{\partial \bar{\alpha}_n}{\partial z} - z\frac{\partial \bar{\gamma}_n}{\partial x} - y\frac{\partial \bar{\beta}_n}{\partial x} + y\frac{\partial \bar{\alpha}_n}{\partial y}$$

$$= x\frac{\partial \bar{\alpha}_n}{\partial x} + y\frac{\partial \bar{\alpha}_n}{\partial y} + z\frac{\partial \bar{\alpha}_n}{\partial z} + \bar{\alpha}_n - \frac{\partial}{\partial x}(x\bar{\alpha}_n + y\bar{\beta}_n + z\bar{\gamma}_n) \tag{2.100.a}$$

Similarly,

$$x\frac{\partial \bar{X}_n}{\partial z} - z\frac{\partial \bar{X}_n}{\partial x} = x\frac{\partial \bar{\beta}_n}{\partial x} + y\frac{\partial \bar{\beta}_n}{\partial y} + z\frac{\partial \bar{\beta}_n}{\partial z} + \bar{\beta}_n$$

$$- \frac{\partial}{\partial y}(x\bar{\alpha}_n + y\bar{\beta}_n + z\bar{\gamma}_n) \tag{2.100.b}$$

and

$$y\frac{\partial \bar{X}_n}{\partial x} - x\frac{\partial \bar{X}_n}{\partial y} = x\frac{\partial \bar{\gamma}_n}{\partial x} + y\frac{\partial \bar{\gamma}_n}{\partial y} + z\frac{\partial \bar{\gamma}_n}{\partial z} + \bar{\gamma}_n$$

$$- \frac{\partial}{\partial z}(x\bar{\alpha}_n + y\bar{\beta}_n + z\bar{\gamma}_n) \qquad (2.100.c)$$

It can be shown from (2.94) and (2.95) that:

$$\nabla^2(x\bar{\alpha}_n + y\bar{\beta}_n + z\bar{\gamma}_n) = 0 \qquad (2.101)$$

Thus:

$$x\bar{\alpha}_n + y\bar{\beta}_n + z\bar{\gamma}_n = \bar{\phi}_{n+1} \qquad (2.102)$$

where $\bar{\phi}_{n+1}$ is a solid harmonic of degree n+1.

Equation (2.100.a) can now be written as:

$$(n+1)\bar{\alpha}_n = \frac{\partial \bar{\phi}_{n+1}}{\partial x} + z\frac{\partial \bar{X}_n}{\partial y} - y\frac{\partial \bar{X}_n}{\partial z} \qquad (2.103)$$

Dropping the factor n+1 causes no loss of generality. Thus the complete solution of the system of equations given by (2.90) to (2.93) in the absence of K_2 may be written as:

$$\bar{\alpha} = \Sigma\left(\frac{\partial \bar{\phi}_{n+1}}{\partial x} + z\frac{\partial \bar{X}_n}{\partial y} - y\frac{\partial \bar{X}_n}{\partial z}\right) \qquad (2.104.a)$$

$$\bar{\beta} = \Sigma\left(\frac{\partial \bar{\phi}_{n+1}}{\partial y} + x\frac{\partial \bar{X}_n}{\partial z} - z\frac{\partial \bar{X}_n}{\partial x}\right) \qquad (2.104.b)$$

$$\bar{\gamma} = \Sigma\left(\frac{\partial \bar{\phi}_{n+1}}{\partial z} + y\frac{\partial \bar{X}_n}{\partial x} - x\frac{\partial \bar{X}_n}{\partial y}\right) \qquad (2.104.c)$$

To find the solution of the system of equations in the case of $K_2 \neq 0$, one may assume a solution in the form of:

$$\bar{\alpha}_n = \hat{a}_o - K_2^2\hat{a}_1 + K_2^4\hat{a}_2 - K_2^6\hat{a}_3 + \ldots\ldots \qquad (2.105)$$

Substituting this solution into equation (2.90) gives:

$$\nabla^2\hat{a}_o - K_2^2(\nabla^2\hat{a}_1 - \hat{a}_o) + K_2^4(\nabla^2\hat{a}_2 - \hat{a}_1) - K_2^6(\nabla^2\hat{a}_3 - \hat{a}_2) + \ldots = 0 \qquad (2.106)$$

In order to satisfy (2.106) the coefficients of the various powers of K_2^2 should be equated to zero. Thus:

$$\nabla^2\hat{a}_o = 0,\ \nabla^2\hat{a}_1 = \hat{a}_o,\ \nabla^2\hat{a}_2 = \hat{a}_1 \ldots\ldots \qquad (2.107)$$

The solution of the first equation has already been proved to be:

$$\hat{a}_o = \frac{\partial\bar{\phi}_{n+1}}{\partial x} + z\frac{\partial\bar{\chi}_n}{\partial y} - y\frac{\partial\bar{\chi}_n}{\partial z} \qquad (2.108)$$

To obtain the solution of the remaining equations one may write:

$$\nabla^2(r^m\hat{a}_o) = r^m\nabla^2\hat{a}_o + 2mr^{m-2}\left(x\frac{\partial\hat{a}_o}{\partial x} + y\frac{\partial\hat{a}_o}{\partial y} + z\frac{\partial\hat{a}_o}{\partial z}\right) + \hat{a}_o\nabla^2(r^m) \qquad (2.109)$$

But by the definition of a solid harmonic:

$$x\frac{\partial\hat{a}_o}{\partial x} + y\frac{\partial\hat{a}_o}{\partial y} + z\frac{\partial\hat{a}_o}{\partial z} = n\hat{a}_o \qquad (2.110)$$

Thus (2.109) reduces to:

$$\nabla^2(r^m \hat{a}_o) = m(2n+m+1)r^{m-2}\hat{a}_o \qquad (2.111)$$

Using the second equation of (2.107) and substituting for a_o in the right hand side of equation (2.111) gives:

$$\nabla^2(r^m \hat{a}_o) = m(2n+m+1)r^{m-2}\nabla^2\hat{a}_1 \qquad (2.112)$$

Upon letting m = 2 yields,

$$\hat{a}_1 = \frac{r^2}{2(2n+3)}\hat{a}_o \qquad (2.113)$$

Similarly,

$$\hat{a}_2 = \frac{r^4}{2\cdot4(2n+3)(2n+5)}\hat{a}_o \qquad (2.114)$$

and so on. Substituting for $\hat{a}_o$, $\hat{a}_1$, $\hat{a}_2$ and etc. into equation (2.105) gives:

$$\bar{\alpha}_n = \psi_n\left(\frac{\partial\bar{\phi}_{n+1}}{\partial x} + z\frac{\partial\bar{\chi}_n}{\partial y} - y\frac{\partial\bar{\chi}_n}{\partial z}\right) \qquad (2.115)$$

where

$$\psi_n = 1 - \frac{K_2^2r^2}{2(2n+3)} + \frac{K_2^4r^4}{2\cdot4(2n+3)(2n+5)} - \cdots \qquad (2.116)$$

By following similar procedures one obtains:

$$\bar{\beta}_n = \psi_n\hat{b}_o = \psi_n\left(\frac{\partial\bar{\phi}_{n+1}}{\partial y} + x\frac{\partial\bar{\chi}_n}{\partial z} - z\frac{\partial\bar{\chi}_n}{\partial x}\right) \qquad (2.117)$$

$$\bar{\gamma}_n = \psi_n\hat{d}_o = \psi_n\left(\frac{\partial\bar{\phi}_{n+1}}{\partial z} + y\frac{\partial\bar{\chi}_n}{\partial x} - x\frac{\partial\bar{\chi}_n}{\partial y}\right) \qquad (2.118)$$

where $\hat{b}_o$, $\hat{b}_1$.... and $\hat{d}_o$, $\hat{d}_1$.... are coefficients of the various powers of K_2^2 in expansion of $\bar{\beta}_n$ and $\bar{\gamma}_n$ in forms of series similar to that shown for $\bar{\alpha}_n$. In order to satisfy (2.93) one should examine the following equations:

$$\frac{\partial \hat{a}_o}{\partial x} + \frac{\partial \hat{b}_o}{\partial y} + \frac{\partial \hat{d}_o}{\partial z} = 0 \tag{2.119}$$

$$\frac{\partial \hat{a}_1}{\partial x} + \frac{\partial \hat{b}_1}{\partial y} + \frac{\partial \hat{d}_1}{\partial z} = 0 \tag{2.120}$$

etc. It can be easily found that the solution given for $\hat{a}_o$, $\hat{b}_o$ and $\hat{d}_o$ satisfy equation (2.119) whereas solutions for $\hat{a}_1$, $\hat{b}_1$ and $\hat{d}_1$ need to be modified to satisfy (2.120). Substituting for $\hat{a}_1$, $\hat{b}_1$ and $\hat{d}_1$ into equation (2.120) gives:

$$\frac{\partial \hat{a}_1}{\partial x} + \frac{\partial \hat{b}_1}{\partial y} + \frac{\partial \hat{d}_1}{\partial z} = \frac{\hat{a}_o x + \hat{b}_o y + \hat{d}_o z}{2n+3} = \frac{n+1}{2n+3} \bar{\phi}_{n+1} \tag{2.121}$$

The form of (2.121) suggest a new solution as follows:

$$\hat{a}_1 = \frac{r^2}{2(2n+3)} \hat{a}_o + \hat{R}_1 r^{2n+5} \frac{\partial}{\partial x} \frac{\bar{\phi}_{n+1}}{r^{2n+3}}$$

$$\hat{b}_1 = \frac{r^2}{2(2n+3)} \hat{b}_o + \hat{R}_1 r^{2n+5} \frac{\partial}{\partial y} \frac{\bar{\phi}_{n+1}}{r^{2n+3}}$$

$$\hat{d}_1 = \frac{r^2}{2(2n+3)} \hat{d}_o + \hat{R}_1 r^{2n+5} \frac{\partial}{\partial z} \frac{\bar{\phi}_{n+1}}{r^{2n+3}} \tag{2.122}$$

where

$$\hat{R}_1 = \frac{n+1}{n+2} \cdot \frac{1}{(2n+3)(2n+5)}$$

Similarly,

$$\hat{a}_2 = \frac{r^4}{2.4(2n+3)(2n+5)}\,\hat{a}_o + \hat{R}_2 r^{2n+7}\,\frac{\partial}{\partial x}\,\frac{\bar{\phi}_{n+1}}{r^{2n+3}}$$

$$\hat{b}_2 = \frac{r^4}{2.4(2n+3)(2n+5)}\,\hat{b}_o + \hat{R}_2 r^{2n+7}\,\frac{\partial}{\partial y}\,\frac{\bar{\phi}_{n+1}}{r^{2n+3}}$$

$$\hat{d}_2 = \frac{r^4}{2.4(2n+3)(2n+5)}\,\hat{d}_o + \hat{R}_2 r^{2n+7}\,\frac{\partial}{\partial z}\,\frac{\bar{\phi}_{n+1}}{r^{2n+3}} \qquad (2.123)$$

where $\hat{R}_2 = \frac{n+1}{n+2} \cdot \frac{1}{2(2n+3)(2n+5)(2n+7)}$

Substituting for $\hat{a}_o$, $\hat{a}_1$ $\hat{a}_2$ and etc. into equation (2.105) gives:

$$\bar{\alpha}_n = \psi_n\left(\frac{\partial\bar{\phi}_{n+1}}{\partial x} + z\frac{\partial\bar{X}_n}{\partial y} - y\,\frac{\partial\bar{X}_n}{\partial z}\right) - \frac{n+1}{n+2} \cdot \frac{K_2^2 r^{2n+5}}{(2n+3)(2n+5)}$$

$$\cdot\,\psi_{n+2}\,\frac{\partial}{\partial x}\,\frac{\bar{\phi}_{n+1}}{r^{2n+3}} \qquad (2.124)$$

where ψ_{n+2} can be deduced from (2.116). The solution for $\bar{\beta}_n$ and $\bar{\gamma}_n$ can also be found by following similar procedure.

Thus the complete solution of the equations (2.90) to (2.93) which are also finite at the origin, may be expressed as:

$$\bar{\alpha} = \Sigma\{\psi_n\left(\frac{\partial\bar{\phi}_{n+1}}{\partial x} + z\frac{\partial\bar{X}_n}{\partial y} - y\frac{\partial\bar{X}_n}{\partial z}\right) - \frac{n+1}{n+2} \cdot \frac{K_2^2 r^{2n+5}}{(2n+3)(2n+5)}$$

$$\cdot\psi_{n+2}\,\frac{\partial}{\partial x}\,\frac{\bar{\phi}_{n+1}}{r^{2n+3}}\}$$

$$\bar{\beta} = \Sigma\{\psi_n(\frac{\partial\bar{\phi}_{n+1}}{\partial y} + x\frac{\partial\bar{X}_n}{\partial z} - z\frac{\partial\bar{X}_n}{\partial x}) - \frac{n+1}{n+2}\cdot\frac{K_2^2 r^{2n+5}}{(2n+3)(2n+5)}$$

$$\cdot\psi_{n+2}\cdot\frac{\partial}{\partial y}\frac{\bar{\phi}_{n+1}}{r^{2n+3}}\}$$

$$\bar{\gamma} = \Sigma\{\psi_n(\frac{\partial\bar{\phi}_{n+1}}{\partial z} + y\frac{\partial\bar{X}_n}{\partial x} - x\frac{\partial\bar{X}_n}{\partial y}) - \frac{n+1}{n+2}\cdot\frac{K_2^2 r^{2n+5}}{(2n+3)(2n+5)}$$

$$\cdot\psi_{n+2}\cdot\frac{\partial}{\partial z}\frac{\bar{\phi}_{n+1}}{r^{2n+3}}\} \qquad (2.125)$$

Inspection of (2.125) suggests that the solutions of the system of equations are of two distinct types. Thus one may write:

$$\bar{\alpha} = \Sigma\{\psi_n(z\frac{\partial\bar{X}_n}{\partial y} - y\frac{\partial\bar{X}_n}{\partial z})\} \qquad (2.126)$$

and

$$\bar{\alpha} = \Sigma\{\psi_n\frac{\partial\bar{\phi}_{n+1}}{\partial x} - \frac{n+1}{n+2}\cdot\frac{K_2^2 r^{2n+5}}{(2n+3)(2n+5)}\cdot\psi_{n+2}\cdot\frac{\partial}{\partial x}\frac{\bar{\phi}_{n+1}}{r^{2n+3}}\} \qquad (2.127)$$

The solution of the second type can also be written in the form:

$$\bar{\alpha} = \Sigma\{\psi_{n-1}\frac{\partial\bar{\phi}_n}{\partial x} - \frac{n}{n+1}\cdot\frac{K_2^2 r^{2n+3}}{(2n+1)(2n+3)}\cdot\psi_{n+1}\cdot\frac{\partial}{\partial x}\frac{\bar{\phi}_n}{r^{2n+1}}\} \qquad (2.128)$$

In order to represent the solutions of the equations (2.86.a) to (2.86.c) by expressions (2.87) one must also find $\bar{\delta}$. Thus the solution to the differential equation (2.89) should be determined. This solution has been given by Lamb [32] as follows:

$$\bar{\delta} = \Sigma \psi_n(K_1 r).\bar{\omega}_n \qquad (2.129)$$

where $\bar{\omega}_n$ is a solid harmonic of degree n.

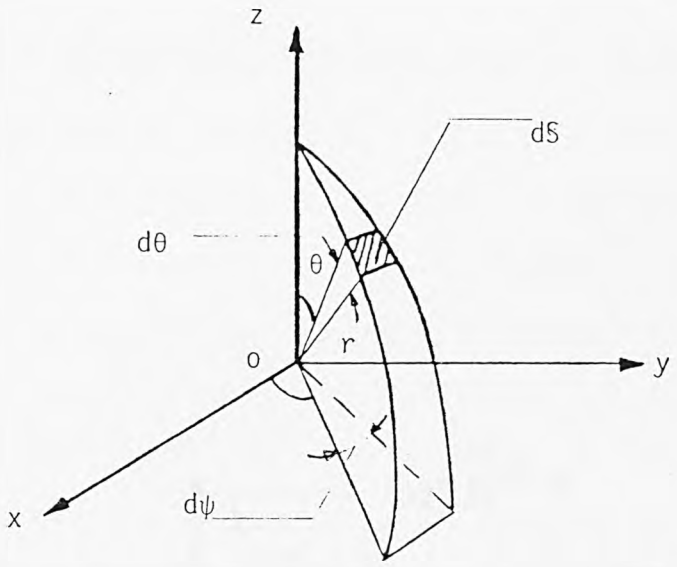

Fig.2.1. Illustration of element $dS = r^2 \sin\theta d\theta d\psi$

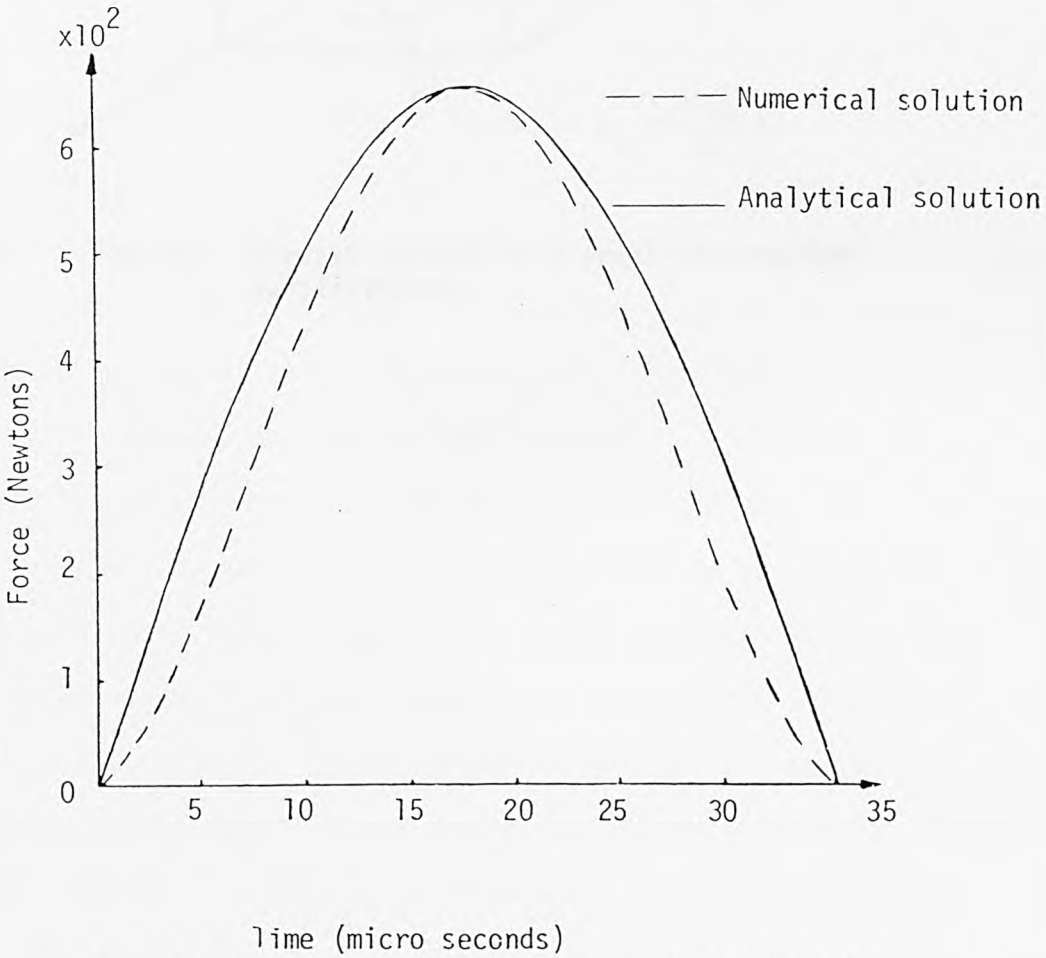

Fig. 2.2. Force-time history for 1.27 cm diameter steel spheres with an initial impact velocity of 1.52 m/s.

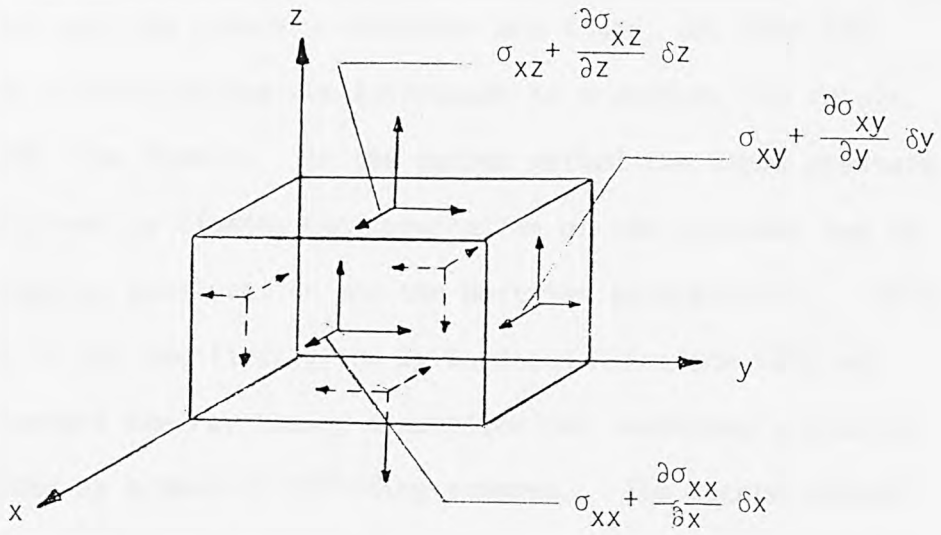

Fig.2.3. Stresses acting on a small rectangular parallelepiped.

3. RIGID BODY RADIATION DUE TO ELASTIC COLLISION OF SPHERES

The sound pressure radiated by elastic collision of spheres is dealt with in this chapter. Two methods of derivation of sound as such are introduced. These are the Laplace transform and the convolution methods. In the first method the Laplace transform of the potential function satisfying both the wave equation and the boundary condition was found, and then the inverse transformation was introduced to transform the result into the time domain. In the second method the sound pressure was obtained by finding the convolution of the response due to unit impulse acceleration and the Hertzian acceleration. This method is the one first given by Koss and Alfredson [21] who also suggest the ray theory assumption for combining pressures generated by a pair of colliding spheres. The second method was also used for the derivation of the approximate formula for sound pressure. The response due to unit impulse acceleration for derivation of these formulae is the one given by Ffowcs Williams and Lovely [13]. A brief introduction to a numerical method for calculating the pressure is given. This numerical method is useful when an analytical solution is either complicated or cannot be achieved. This method is discussed in detail in chapter 5. Attention is also paid to the sound radiated by the change of volume of a sphere undergoing a Hertzian acceleration. In this investigation the sphere was assumed to be a monopole source of sound expanding and contracting impulsively in its radial direction. Finally, an expression for evaluating energy

in the far field is given. The results obtained in this chapter are also expressed in dimensionless form. Graphical presentation of some of the dimensionless results later will be used in chapter 9 for evaluation of empirical formulae.

3.1. Sound radiation from an impulsively accelerated sphere

It is shown earlier that an oscillating sphere moving back and forth as a rigid body in the direction of the principal axis behaves as a dipole source of the sound. The corresponding field can be deduced by substituting $m \neq 0$ and $n = 1$ in equation (2.37) which upon satisfying the radial velocity at the surface of sphere yields to the result given by the equation (2.57a). This velocity potential may also be written as:

$$\phi = \phi(r,\theta,\omega)e^{i\omega\tau} \tag{3.1}$$

where

$$\phi(r,\theta,\omega) = \frac{va^3(1+iKr)}{2(1+iKa)-K^2a^2}\frac{\cos\theta}{r^2} \tag{3.2a}$$

and

$$\tau = t\,\frac{r-a}{c} \tag{3.2b}$$

Consider now a sphere of radius a which is subjected to an impulsive velocity $v_oH(\tau)$ in the direction of one of the principal axes. The impulsive velocity $v_oH(\tau)$ may be defined as:

$$v_o H(\tau) = \begin{cases} v_o, & \tau > 0 \\ 0, & \text{otherwise} \end{cases} \tag{3.3}$$

where $H(\tau)$ is a unit step function and also may be referred to as the unit Heaviside function. The Fourier transform of this velocity, as given by Champeney [56] is:

$$v^{(T)} = \int_{-\infty}^{\infty} v_o H(\tau) e^{-i\omega\tau}\, d\tau = v_o\{\pi\hat{\delta}(\omega) - \frac{i}{\omega}\} \tag{3.4}$$

where $\hat{\delta}(\omega)$ is the Dirac delta function. The velocity potential of an impulsively accelerated sphere can now be obtained by finding the inverse of the Fourier transform of (3.2a) after substituting $v = v^{(T)}$. Thus:

$$\phi(r,\theta,\tau) = \frac{v_o a^3 \cos\theta}{2\pi r^2} \int_{-\infty}^{\infty} \frac{[\pi\hat{\delta}(\omega) - \frac{i}{\omega}](1+iKr)}{2(1+iKa)-K^2a^2}\, e^{i\omega\tau} d\omega \tag{3.5}$$

which by evaluating the residues of function at its poles yields the solution:

$$\phi(r,\theta,\tau) = \frac{v_o a^3 \cos\theta}{2\, r^2} \{1 + e^{-\ell\tau}[(\frac{2r}{a} - 1)\sin\ell\tau - \cos\ell\tau]\} \tag{3.6}$$

where $\ell = \frac{c}{a}$. Equation (3.6) is the same as one given by Koss and Alfredson [21]. By making use of equations(2.12) and (2.11) the pressure $p(r,\theta,\tau)$ and the radial velocity $v_r(r,\theta,\tau)$ are found to be:

$$p(r,\theta,\tau) = \rho_o \frac{\partial\phi}{\partial t} = \rho_o c\, \frac{v_o a^2}{r^2} \cos\theta e^{-\ell\tau}[\frac{r}{a}\cos\ell\tau + (1-\frac{r}{a})\sin\ell\tau] \tag{3.7}$$

and

$$v_r(r,\theta,\tau) = -\frac{\partial\phi}{\partial r} = \frac{v_o a^3}{r^2}\cos\theta e^{-\ell\tau}\left[\left(\frac{2}{a} - \frac{r}{a^2} - \frac{1}{r}\right)\sin\ell\tau + \left(\frac{r}{a^2} - \frac{1}{r}\right)\cos\ell\tau\right] + \frac{v_o a^3}{r^3}\cos\theta \qquad (3.8)$$

The Fourier transforms of equation (3.7) is:

$$p(r,\theta,\omega) = \rho_o \frac{v_o a^3}{r^2}\cos\theta \frac{(1+iKr)}{2(1+iKa)-K^2a^2} \qquad (3.9)$$

The sound pressure caused by a unit impulse of acceleration can be simply found by substituting $v_o = 1$ into equation (3.7). The sound pressure due to the other forms of acceleration may be given by convolution of the response to a unit impulse acceleration with any arbitrary acceleration, $\hat{A}$. Thus:

$$p(r,\theta,\tau) = \int_0^\tau p_{UI}(r,\theta,\tau-\zeta)\hat{A}(\zeta)\,d\zeta \qquad \tau > 0$$

$$= 0 \qquad \tau < 0 \qquad (3.10)$$

where p_{UI} is the pressure due to the unit impulse acceleration and ζ is the integration variable. The sound pressure in the far field which is radiated by an impulsively accelerated sphere may be chosen as that part of the pressure which decays like r^{-1} as $r \to \infty$. Thus from equation (3.7) one obtains:

$$p(r,\theta,\tau) = P_M e^{-\ell\tau}(\cos\ell\tau - \sin\ell\tau)\cos\theta \qquad (3.11)$$

where $P_M = \frac{\rho_o c v_o a}{r}$. Graphs showing variations of $\frac{p}{P_M}$ against τ for $\theta = 0^o$ and 60^o are given in Figure (3.1).

3.2. The impulsive monopole source

The potential function ϕ given by equation (2.44) for a pulsating sphere may be used to evaluate the sound pressure radiated by an impulsively pulsating sphere. This is a sphere subjected to a uniform impulsive velocity $v_o H(\tau)$ in its radial direction. By following a similar process as given above for the oscillating sphere one obtains:

$$\phi(r,\tau) = \frac{v_o a^2}{2\pi r} \int_{-\infty}^{\infty} \frac{[\pi\hat{\delta}(\omega) - \frac{i}{\omega}]}{(1 + iKa)} e^{i\omega\tau} d\omega \qquad (3.12)$$

Finding the residues of the function at its poles ($\omega = 0$ and $\omega = i\ell$), yields the solution:

$$\phi(r,\tau) = \frac{v_o a^2}{r}(1 - e^{-\ell\tau}) \qquad (3.13)$$

The sound pressure and the radial velocity may now be given by:

$$p(r,\tau) = \rho_o c \frac{v_o a}{r} e^{-\ell\tau} \qquad (3.14)$$

and

$$v_r(r,\tau) = \frac{v_o a^2}{r^2} [1 - e^{-\ell\tau}(1 - \frac{r}{a})] \qquad (3.15)$$

The Fourier transforms of equation (3.14) is:

$$p(r,\omega) = \rho_o \frac{v_o a^2}{r(1 + iKa)} \qquad (3.16)$$

Graph showing variations of $\frac{p}{P_M}$ against τ is given in Fig.(3.2).

3.3. Velocity potential of an impulsively accelerated sphere (Laplace Transform method)

The Laplace transform method as shown by Langhorn [8] may also be used to evaluate the velocity potential of an impulsively accelerated sphere. Consider a rigid sphere of radius a subjected to an impulsive velocity $v_o H(\tau)$ in direction of one of the principal axes. The velocity potential ϕ at any observation point p with co-ordinates (r,θ,ψ) must satisfy the wave equation:

$$\nabla^2\phi = \frac{1}{c^2}\frac{\partial^2\phi}{\partial t^2} \tag{3.17}$$

where $\phi = \phi(r,\theta,\psi, t)$. Equation (3.17) can be written in terms of spherical polar co-ordinates as given by equation (2.16) in section (2.2). For a potential function independent of ψ equation (2.16) reduces to:

$$\frac{\partial^2\phi}{\partial r^2} + \frac{2}{r}\frac{\partial\phi}{\partial r} + \frac{1}{r^2}\frac{\partial^2\phi}{\partial\theta^2} + \frac{\cot g\theta}{r^2}\frac{\partial\phi}{\partial\theta} = \frac{1}{c^2}\frac{\partial^2\phi}{\partial t^2} \tag{3.18}$$

where $\phi = \phi(r,\theta, t)$. The boundary condition on the surface of the sphere at $r = a$ is:

$$\frac{\partial\phi}{\partial r} = -v_o\cos\theta H(t) \tag{3.19a}$$

Also at $t = 0$,

$$\phi = \frac{\partial\phi}{\partial t} = 0 \tag{3.19b}$$

Let us assume now the solution of the differential equation (3.18) can be represented in the form of $\phi(r,\theta, t) = W(r,t).\chi(\theta)$ Inspection of the boundary condition on the surface of the sphere suggests that $\chi(\theta) = \cos\theta$. Thus the potential function may be represented in the following form:

$$\phi(r,\theta,t) = \cos\theta.W(r,t) \tag{3.20}$$

Substituting this solution into the equation (3.18) yields:

$$\frac{\partial^2 W}{\partial r^2} + \frac{2}{r}\frac{\partial W}{\partial r} - \frac{2W}{r^2} = \frac{1}{c^2}\frac{\partial^2 W}{\partial t^2} \tag{3.21}$$

Multiplying both sides of the above differential equation by e^{-st} and integrating over t gives:

$$\frac{d^2\bar{W}}{dr^2} + \frac{2}{r}\frac{d\bar{W}}{dr} - \frac{2}{r^2}\bar{W} = \frac{s^2}{c^2}\bar{W} \tag{3.22}$$

where

$$\bar{W} = \bar{W}(r,s) = \int_0^\infty W(r,t)e^{-st}dt \tag{3.23a}$$

$$\int_0^\infty \frac{\partial^n W(r,t)}{\partial r^n} e^{-st}dt = \frac{\partial^n}{\partial r^n}\int_0^\infty W(r,t)e^{-st}dt = \frac{d^n\bar{W}(r,s)}{dr^n} \tag{3.23b}$$

and

$$\int_0^\infty \frac{\partial^2 W(r,t)}{\partial t^2} e^{-st}dt = s^2\bar{W}(r,s) - sW(r,t)e^{-st}\Big|_{t=0} - \frac{\partial W(r,t)}{\partial t}e^{-st}\Big|_{t=0} \tag{3.23c}$$

The conditions given by expression (3.19b) require that the last two terms in (3.23c) be zero. Thus (3.22) can be easily derived. The transformation $\bar{W} = \frac{\bar{X}(r,s)}{\sqrt{r}}$ transforms (3.22) to the equation:

$$r^2 \frac{d^2\bar{X}}{dr^2} + r \frac{d\bar{X}}{dr} - (\frac{9}{4} + \frac{s^2r^2}{c^2})\bar{X} = 0 \qquad (3.24)$$

The solution of this type of Bessel's equation as suggested by McLachlan [57] can be represented in terms of Bessel's functions of imaginary argument. Thus, the general solution of (3.24) is:

$$\bar{X} = Z_{3/2}(is\frac{r}{c}) = \bar{C}_1 K_{3/2}(\frac{sr}{c}) + \bar{C}_2 I_{3/2}(\frac{sr}{c}) \qquad (3.25)$$

The function in general form $I_{\bar{\nu}}(y^*)$ and $K_{\bar{\nu}}(y^*)$ are known as the modified Bessel functions of the first and second kind, respectively. The asymptotic expansions of these functions are:

$$I_{\bar{\nu}}(y^*) \simeq \frac{e^{y^*}}{\sqrt{2\pi y^*}} W_{\bar{\nu}}(y^*) \qquad (3.26a)$$

$$K_{\bar{\nu}}(y^*) \simeq -\frac{e^{-y^*}}{\sqrt{\frac{2y^*}{\pi}}} W_{\bar{\nu}}(-y^*) \qquad (3.26b)$$

where

$$W_{\bar{\nu}}(y^*) = 1 - \frac{4\bar{\nu}^2 - 1^2}{1!8y^*} + \frac{(4\bar{\nu}^2 - 1^2)(4\bar{\nu}^2 - 3^2)}{2!(8y^*)^2} \cdots\cdots \qquad (3.26c)$$

Using the asymptotic expansion of $K_{\nu}(y^*)$ as a solution of (3.24) for the +ve going wave only, gives:

$$\bar{W} = \bar{C}_1 \left(\frac{2s}{\pi c}\right)^{-\frac{1}{2}} \left(\frac{1}{r} + \frac{c}{sr^2}\right) e^{-s\frac{r}{c}} \tag{3.27}$$

The constant $\bar{C}_1$ can be evaluated by using the transformation of boundary condition given by expression (3.19a). Thus at $r = a$,

$$\left.\frac{d\bar{W}}{dr}\right|_{r=0} = \int_0^\infty \frac{\partial W(r,t)}{\partial r} e^{-st} dt = -v_o \int_0^\infty H(t) e^{-st} dt = -\frac{v_o}{s} \tag{3.28a}$$

and

$$\bar{C}_1 = \frac{v_o a^3 c}{s^2a^2 + 2sac + 2c^2} \left(\frac{2s}{\pi c}\right)^{\frac{1}{2}} e^{s\frac{a}{c}} \tag{3.28b}$$

Using $\bar{C}_1$ given by (3.28b) and substituting in (3.27) gives:

$$\bar{W} = \frac{v_o a^3 c(rs + c)}{r^2 s(s^2a^2 + 2sac + 2c^2)} e^{-\frac{s}{c}(r-a)} \tag{3.29}$$

To find $W(r,t)$ defined by (3.23a) one should obtain the inverse Laplace transform of expression (3.29). This may be carried out by finding the residues of function $\bar{W}(r,s)e^{st}$ at its poles. Thus, the velocity potential given by (3.20) can be derived to be:

$$\phi(r,\theta,\tau) = \frac{v_o a^3 \cos\theta}{2r^2} \{1 + e^{-\ell\tau}[(\frac{2r}{a} - 1)\sin\ell\tau - \cos\ell\tau]\} \tag{3.30}$$

where $\tau = t - \frac{r-a}{c}$ and $\ell = \frac{c}{a}$. Note that equation (3.30) is exactly the same as equation (3.6), but has been derived by a different approach. The result also agrees with Kirchhoff's solution [2].

3.4. Sound radiated by a sphere undergoing a Hertzian acceleration (Laplace Transform method)

In the study of impact of elastic bodies the Hertz law of contact was used for the derivation of the acceleration of each body. Thus from equation (2.75) the acceleration of a sphere undergoing an elastic collision can be given by:

$$\hat{A}(t) = a_M \sin bt \qquad 0 < t < d$$

$$= 0 \qquad \text{otherwise} \tag{3.31}$$

where $a_M = \frac{F_{max}}{\bar{m}}$ and $b = \frac{\pi}{d}$. The boundary condition on the surface of the sphere at r = a may now be written as:

$$-\frac{1}{\rho_o}\frac{\partial p}{\partial r}\Big|_{r=a} = \frac{\partial v_r}{\partial t}\Big|_{r=a} = -\frac{\partial^2 \phi}{\partial r \partial t}\Big|_{r=a} = a_M \sin bt \cos\theta \tag{3.32a}$$

Also at t = 0,

$$\phi = \frac{\partial \phi}{\partial t} = 0 \tag{3.32b}$$

The Laplace transform of the potential function ϕ satisfying the wave equation, and the conditions given by expression (3.32b) can be found by following similar procedures as given in section (3.3) to be:

$$\bar{W} = \bar{C}_1 \left(\frac{2s}{c}\right)^{-\frac{1}{2}} \left(\frac{1}{r} + \frac{c}{sr^2}\right) e^{-s\frac{r}{c}} \tag{3.33}$$

where $\bar{W}$ is the Laplace transform of $W(r,t)$ related to the potential function ϕ through the expression (3.20) and $\bar{C}_1$ is a constant to be determined. The constant $\bar{C}_1$ can be evaluated by using the transformation of boundary condition given by equation (3.32a). Thus at $r = a$.

$$s \left.\frac{d\bar{W}}{dr}\right|_{r=a} = \frac{\partial}{\partial r} \int_0^\infty \frac{\partial W(r,t)}{\partial t} e^{-st} dt = -a_M \int_0^\infty \sin bt e^{-st} dt$$

$$= -\frac{a_M b}{(s^2+b^2)} (1 + e^{-sd}) \tag{3.34a}$$

and

$$\bar{C}_1 = \frac{a_M bca^3}{(s^2+b^2)} \left(\frac{2s}{\pi c}\right)^{\frac{1}{2}} \cdot \frac{e^{\frac{s}{c}a}}{s^2a^2+2sac+2c^2} (1+ e^{-sd}) \tag{3.34b}$$

Using $\bar{C}_1$ given by (3.79b) and substituting in (3.33) gives:

$$\bar{W} = \frac{a_M bca^3}{s^2+b^2} \frac{(sr+c)}{sr^2} \cdot \frac{e^{-\frac{s}{c}r-a}}{s^2a^2+2sac+2c^2} (1 +e^{-sd}) \tag{3.35}$$

The inverse Laplace transform of equation (3.35) may now be obtained by simply finding the residues of function $\bar{W}e^{st}$ at its poles. Thus the velocity potential ϕ related to $W(r,t)$ through the expression (3.20) can be derived to be:

$$\phi(r,\theta,\tau) = \frac{a_M a^3 \cos\theta}{8(b^4+4\ell^4)r^2}\{(\frac{2r}{a}-1)(4b^3\sin\ell\tau+8b\ell^2\cos\ell\tau)e^{-\ell\tau}$$

$$-(4b^3\cos\ell\tau-8b\ell^2\sin\ell\tau)e^{-\ell\tau}$$

$$+(\frac{2r}{a}-1)[4b^3\sin\ell(\tau-d)+8b\ell^2\cos\ell(\tau-d)]e^{-\ell(\tau-d)}$$

$$-[4b^3\cos\ell(\tau-d)-8b\ell^2\sin\ell(\tau-d)]e^{-\ell(\tau-d)}\}$$

$$+\frac{a_M a^3}{r^2 b}\cos\theta \qquad (3.36a)$$

$$\tau > d$$

where $\tau = t - \frac{r-a}{c}$ and $\ell = \frac{c}{a}$.

The sound pressure and the radial velocity may now be expressed as:

$$p(r,\theta,\tau) = \rho_o \frac{\partial\phi}{\partial t} = \frac{\rho_o a_M a^3 \cos\theta}{8(b^4+4\ell^4)r^2}\{(\frac{2r}{a}-1)[(4b^3\ell-8b\ell^3)\cos\ell\tau$$

$$-(4b^3\ell+8b\ell^3)\sin\ell\tau]e^{-\ell\tau}+[(4b^3\ell+8b\ell^3)\cos\ell\tau$$

$$+(4b^3\ell-8b\ell^3)\sin\ell\tau]e^{-\ell\tau}+(\frac{2r}{a}-1)[(4b^3\ell-8b\ell^3)\cos\ell(\tau-d)$$

$$-(4b^3\ell+8b\ell^3)\sin\ell(\tau-d)]e^{-\ell(\tau-d)}$$

$$+[(4b^3\ell+8b\ell^3)\cos\ell(\tau-d)+(4b^3\ell-8b\ell^3)\sin\ell(\tau-d)]e^{-\ell(\tau-d)}\}$$

$$\tau > d \qquad (3.36b)$$

and

$$v_r = -\frac{\partial\phi}{\partial r} = \frac{a_M a^3 \cos\theta}{4(b^4+4\ell^4)r^2}\{(\frac{r}{a^2}-\frac{1}{r})(4b^3\cos\ell\tau-8b\ell^2\sin\ell\tau)e^{-\ell\tau}$$

$$-(\frac{r}{a^2}-\frac{2}{a}+\frac{1}{r})(4b^3\sin\ell\tau+8b\ell^2\cos\ell\tau)e^{-\ell\tau}$$

$$+(\frac{r}{a^2}-\frac{1}{r})[4b^3\cos\ell(\tau-d)-8b\ell^2\sin\ell(\tau-d)]e^{-\ell(\tau-d)}$$

$$-(\frac{r}{a^2}-\frac{2}{a}+\frac{1}{r})[4b^3\sin\ell(\tau-d)+8b\ell^2\cos\ell(\tau-d)]e^{-\ell(\tau-d)}\}$$

$$+\frac{2a_M a^3}{r^3 b}\cos\theta$$

$$\tau > d \qquad (3.36c)$$

To find the potential function for $\tau < d$ one may similarly write:

$$\bar{W} = \frac{a_M bca^3}{s^2+b^2} \frac{(sr+c)}{sr^2} \cdot \frac{e^{-\frac{s}{c}(r-a)}}{s^2a^2+2sac+2a^2} \qquad (3.37)$$

By repeating the process as before the velocity potential can be found to be:

$$\begin{aligned}\phi(r,\theta,\tau) = {} & \frac{a_M a^3\cos\theta}{8(b^4+4\ell^4)r^2}\{(\frac{2r}{a}-1)(4b^3\sin\ell\tau+8b\ell^2\cos\ell\tau)e^{-\ell\tau} \\ & -(4b^3\cos\ell\tau-8b\ell^2\sin\ell\tau)e^{-\ell\tau} \\ & -(\frac{2r}{a}-1)(4\ell b^2\sin b\tau-8\ell^3\sin b\tau+8b\ell^2\cos b\tau) \\ & +(4b^3\cos b\tau-4\ell b^2\sin b\tau-8\ell^3\sin b\tau)\} \\ & + \frac{a_M a^3\cos\theta}{2r^2 b}(1-\cos b\tau) \qquad 0<\tau<d \end{aligned} \qquad (3.38a)$$

The sound pressure and the radial velocity are:

$$\begin{aligned}p(r,\theta,\tau) = {} & \frac{\rho_o a_M a^3\cos\theta}{8(b^4+4\ell^4)r^2}\{(\frac{2r}{a}-1)(4b^3\ell\cos\ell\tau-8b\ell^3\sin\ell\tau-4b^3\ell\sin\ell\tau \\ & -8b\ell^3\cos\ell\tau)e^{-\ell\tau}+(4b^3\ell\sin\ell\tau+8b\ell^3\cos\ell\tau+4b^3\ell\cos\ell\tau \\ & -8b\ell^3\sin\ell\tau)e^{-\ell\tau}+(\frac{2r}{a}-1)(8\ell^3 b\cos b\tau-4\ell b^3\cos b\tau+8b^2\ell^2\sin b\tau) \\ & -(4b^4\sin b\tau+4\ell b^3\cos b\tau+8\ell^3 b\cos b\tau)\} \\ & + \frac{\rho_o a_M a^3\cos\theta}{2r^2}\sin b\tau \qquad 0<\tau<d \end{aligned} \qquad (3.38b)$$

and

$$v_r = \frac{a_M a^3 \cos\theta}{4(b^4+4\ell^4)r^2}\{(\frac{r}{a^2} - \frac{1}{r})(4b^3\cos\ell\tau - 8b\ell^2\sin\ell\tau)e^{-\ell\tau}$$

$$-(\frac{r}{a^2} - \frac{2}{a} + \frac{1}{r})(4b^3\sin\ell\tau + 8b\ell^2\cos\ell\tau)e^{-\ell\tau}$$

$$-(\frac{1}{a} - \frac{1}{r})(4\ell b^2\sin b\tau - 8\ell^3\sin b\tau + 8b\ell^2\cos b\tau) - (\frac{r}{a^2} - \frac{1}{r})(4b^3\cos b\tau)$$

$$-(\frac{1}{a} - \frac{r}{a^2})(8\ell^2 b\cos b\tau) + (2\frac{r}{a^2} - \frac{1}{a} - \frac{1}{r})(4\ell b^2\sin b\tau)$$

$$-(\frac{1}{r} - \frac{1}{a})(8\ell^3\sin b\tau)\} + \frac{a_M a^3\cos\theta}{br^3}(1 - \cos b\tau)$$

$$\tau < d \qquad (3.38c)$$

It can be easily deduced from equation (3.38c) and (3.36c) that at the surface of the sphere

$$v_r\Big|_{r=a} = \frac{a_M}{b}(1 - \cos b\tau)\cos\theta \qquad \tau < d \qquad (3.39a)$$

$$v_r\Big|_{r=a} = \frac{2a_M}{b}\cos\theta \qquad \tau > d \qquad (3.39b)$$

Similarly,

$$\frac{\partial v_r}{\partial t}\Big|_{r=a} = a_M \sin b\tau\cos\theta \qquad \tau < d \qquad (3.39c)$$

$$\frac{\partial v_r}{\partial t}\Big|_{r=a} = 0 \qquad \tau > d \qquad (3.39d)$$

The sound pressure in the far field may be given by that part of pressure which decays like r^{-1} as $r \to \infty$. Thus from equations (3.38b) and (3.36b) one obtains:

$$p(r,\theta,\tau) = \frac{\rho_o a_M a^2 \ell b \cos\theta}{(b^4+4\ell^4)r}\{[(b^2-2\ell^2)\cos\ell\tau-(b^2+2\ell^2)\sin\ell\tau]e^{-\ell\tau}$$

$$-(b^2-2\ell^2)\cos b\tau+2\ell b\sin b\tau\} \qquad (3.40a)$$

$$\tau < d$$

and

$$p(r,\theta,\tau) = \frac{\rho_o a_M a^2 \ell b \cos\theta}{(b^4+4\ell^4)r}\{[(b^2-2\ell^2)\cos\ell\tau-(b^2+2\ell^2)\sin\ell\tau]e^{-\ell\tau}$$

$$+[(b^2-2\ell^2)\cos\ell(\tau-d)-(b^2+2\ell^2)\sin\ell(\tau-d)]e^{-\ell(\tau-d)}\}$$

$$\tau > d \qquad (3.40b)$$

By employing equation (2.70) the amplitude of acceleration can be written as:

$$a_{M1} = \frac{F_{max}}{m_1} = \frac{\bar{M}}{1+\bar{M}}\left(\frac{5}{4}\right)^{0.6}(\hat{K}_1\hat{K}_2)^{0.4}.v_o^{1.2} \qquad (3.41a)$$

where $\bar{M} = \frac{m_2}{m_1}$ is the ratio of mass of striker to the mass of the sphere under consideration. The duration of contact given by equation (2.73) can also be expressed in terms of impact velocity and coefficients $\hat{K}_1$ and $\hat{K}_2$ as:

$$d = 2.9432\left(\frac{5}{4}\right)^{0.4}.\frac{v_o^{-0.2}}{(\hat{K}_1\hat{K}_2)^{0.4}} \qquad (3.41b)$$

Substituting (3.41b) into (3.41a) gives:

$$a_{M1} = 3.68 \frac{\bar{M}}{1+\bar{M}} \frac{v_o}{d} = 1.17 \frac{\bar{M}}{1+\bar{M}} b\, v_o \qquad (3.42)$$

The sound pressure in the far field may now be given by:

$$p = \frac{P_N \cos\theta}{(1+4\beta^4)} \{[(1-2\beta^2)\cos(\hat{n}\pi\beta)-(1+2\beta^2)\sin(\hat{n}\pi\beta)]e^{-\hat{n}\pi\beta}$$

$$-(1-2\beta^2)\cos(\hat{n}\pi)+2\beta\sin(\hat{n}\pi)\} \qquad (3.43a)$$

$$\hat{n} < 1$$

and

$$p = \frac{P_N \cos\theta}{(1+4\beta^4)} \{[(1-2\beta^2)\cos(\hat{n}\pi\beta)-(1+2\beta^2)\sin(\hat{n}\pi\beta)]e^{-\hat{n}\pi\beta}$$

$$+[(1-2\beta^2)\cos[(\hat{n}-1)\pi\beta]-(1+2\beta^2)\sin[(\hat{n}-1)\pi\beta]]e^{-(\hat{n}-1)\pi\beta}\}$$

$$\hat{n} > 1 \qquad (3.43b)$$

where $P_N = \frac{1.17\bar{M}}{1+\bar{M}} \cdot \frac{\rho_o c v_o a}{r}$, $\beta = \frac{\ell}{b}$ and $\hat{n} = \frac{\tau}{d}$.

Graph showing variations of dimensionless peak pressure against β is given in Figure (3.3). Variations of $\hat{n}_{max}$ at which the peak occurs is also plotted against β, and is given in Figure (3.4).

In order to study the frequency spectrum one should establish the Fourier transform of the sound pressure. This can be done simply either by multiplying equation (3.35) by $\rho_o s \cos\theta e^{\frac{s}{c}(r-a)}$

and then substituting $s = i\omega$, or by finding the product of the Fourier transform of the pressure due to unit impulse acceleration given by equation (3.9) and the Fourier transform of half sine pulse represented by expression (3.31). Thus.

$$p(r,\theta,\omega) = \frac{\rho_o a_M bca^3}{b^2-\omega^2} \frac{(i\omega r+c)}{r^2} \frac{\cos\theta}{2c^2+2i\omega ac-\omega^2 a^2}(1+e^{-i\omega d}) \tag{3.44}$$

Multiplying equation (3.44) by its complex conjugate and using (3.42) gives:

$$|p|^2 = \frac{4(1.17)^2\bar{M}^2}{(1+\bar{M})^2} \frac{\rho_o^2 v_o^2 a^2 \cos^2\theta n^{*2}\beta^2}{\xi^2(1-4n^{*2})^2} \left(1+\frac{\beta^2}{4n^{*2}\xi^2}\right) \frac{\cos^2(n^*\pi)}{(\beta^4+4n^{*4})} \tag{3.45a}$$

or

$$|p| = \frac{2.34\bar{M}}{1+\bar{M}} \frac{\rho_o v_o a\cos\theta n^*\beta}{\xi|(1-4n^{*2})|}\left(1+\frac{\beta^2}{4n^{*2}\xi^2}\right)^{\frac{1}{2}} \frac{|\cos(n^*\pi)|}{(\beta^4+4n^{*4})^{\frac{1}{2}}} \tag{3.45b}$$

where $n^* = fd$ and $\xi = \frac{r}{a}$.

At a large distance r, $\frac{\beta^2}{4n^{*2}\xi^2} \ll 1$ and (3.45b) reduces to:

$$|p| = P_L \cos\theta \left[\frac{n^*\beta}{(\beta^4+4n^{*4})^{\frac{1}{2}}} \times \frac{|\cos(n^*\pi)|}{|(1+4n^{*2})|}\right] \tag{3.45c}$$

where $P_L = 2.34 \frac{\bar{M}}{1+\bar{M}} \frac{\rho_o v_o a^2}{r}$.

It may be noted that if $\bar{M}$ is small (i.e. mass of striker is small compared with mass of sphere), the radiated sound pressure is negligible.

Graph representing variations of dimensionless peak of transform against β is given in Figure (3.5). Variations of n^*_{max} at which the peak of transform occurs is also plotted against β and is shown in Figure (3.6).

3.5. Sound radiated by a sphere undergoing a Hertzian acceleration (Approximate method)

An approximate method based on aero acoustic theory is given by Ffowcs Williams and Lovely [15] for evaluating the sound pressure generated by an impulsively accelerated sphere. This sound pressure can be written as:

$$p = \frac{P_M}{2}\{[5e^{-\ell\tau}+(\ell\tau-3)]H(2a-c\tau)+[5e^{-\ell\tau}-e^{-\ell\tau+2}]H(\tau-2\tfrac{a}{c})\}\cos\theta \qquad (3.46)$$

where $P_M = \frac{\rho_o c v_o a}{r}$, $\tau = t - \frac{r-a}{c}$,

$$H(2a - c\tau) = 1 \quad \tau < \frac{2a}{c} \qquad (3.47a)$$
$$= 0 \text{ otherwise}$$

and

$$H(\tau - \frac{2a}{c}) = 1 \quad \tau > \frac{2a}{c} \qquad (3.47b)$$
$$= 0 \text{ otherwise}$$

Equation (3.46) gives an approximate evaluation of the sound pressure in the far field and may be compared with the exact solution (Equation 3.11) as shown in Figure (3.7). Using the

response to unit impulse deduced from (3.46) together with Hertzian acceleration given by Equation (3.31) and substituting in (3.10) gives:

$$p(r,\theta,\tau) = \frac{\rho_o c a_M a \cos\theta}{2r}\{ \int_o^{\tau}[5e^{-\ell(\tau-\zeta)}+\ell(\tau-\zeta)-3]$$

$$H[2a-c(\tau-\zeta)]\sin b\zeta d\zeta - (2.389)\int_o^{\tau} e^{-\ell(\tau-\zeta)} H(\tau-\zeta-\frac{2a}{c})$$

$$\sin b\zeta d\zeta\} \qquad (3.48a)$$

and

$$p(r,\theta,\tau) = \frac{\rho_o c a_M a \cos\theta}{2r}\{ \int_o^{d}[5e^{-\ell(\tau-\zeta)}+\ell(\tau-\zeta)-3]$$

$$H[2a-c(\tau-\zeta)]\sin b\zeta d\zeta - (2.389)\int_o^{d} e^{-\ell(\tau-\zeta)} H(\tau-\zeta-\frac{2a}{c})$$

$$\sin b\zeta d\zeta\} \qquad (3.48b)$$

The sound pressure radiated by one sphere undergoing a Hertzian acceleration may now be written as:

$$p(r,\theta,\tau) = \frac{\rho_o c a_M a}{2r}\cos\theta\{\frac{5b}{\ell^2+b^2}(e^{-\ell\tau}-\cos b\tau+\frac{\ell}{b}\sin b\tau)$$

$$+\frac{1}{b}(\ell\tau-\frac{\ell}{b}\sin b\tau+3\cos b\tau-3)\} \qquad (3.49a)$$

$$\tau < \frac{2a}{c} < d$$

$$p(r,\theta,\tau) = \frac{\rho_o c a_M a}{2r}\cos\theta\{\frac{b}{\ell^2+b^2}[\cos b\tau^* - \frac{\ell}{b}\sin b\tau^* - 5\cos b\tau + 5\frac{\ell}{b}\sin b\tau$$

$$-0.323e^{-\ell\tau^*}] - \frac{1}{b}(\cos b\tau^* - \frac{\ell}{b}\sin b\tau^* - 3\cos b\tau + \frac{\ell}{b}\sin b\tau)\}$$

$$\frac{2a}{c} < \tau < d \quad (3.49b)$$

$$p(r,\theta,\tau) = \frac{\rho_o c a_M a}{2r}\cos\theta\{\frac{b}{\ell^2+b^2}[\cos b\tau^* - \frac{\ell}{b}\sin b\tau^* + 0.676e^{-\ell(\tau^*-d)}$$

$$-0.323e^{-\ell\tau^*}] - \frac{1}{b}(\cos b\tau^* - \frac{\ell}{b}\sin b\tau^* - \ell\tau^* + \ell d + 1)\}$$

$$\frac{2a}{c} < d < \tau \ , \ \tau^* < d$$

$$(3.49c)$$

$$p(r,\theta,\tau) = -\frac{\rho_o c a_M a}{2r}\cos\theta\{\frac{0.323b}{\ell^2+b^2}[e^{-\ell(\tau^*-d)} + e^{-\ell\tau^*}]\}$$

$$\frac{2a}{c} < d < \tau, \ \tau^* > d$$

$$(3.49d)$$

where $\tau^* = \tau - \frac{2a}{c}$. It should be emphasised that the above equations, except (3.49b) are also applicable to the case $\frac{2a}{c} > d$. In this case equation (3.49b) should be replaced by:

$$p(r,\theta,\tau) = \frac{\rho_o c a_M a}{2r}\cos\theta\{\frac{5b}{\ell^2+b^2}[e^{-\ell(\tau-d)} + e^{-\ell\tau}] + \frac{1}{b}(2\ell\tau - \ell d - 6)\}$$

$$d < \tau < \frac{2a}{c} \qquad (3.49e)$$

Substituting for a_M from equation (3.42) and rewriting the results in non-dimensional form gives;

$$\frac{p}{P_N} = \frac{\cos\theta}{2}\left\{\frac{5}{1+\beta^2}\left[e^{-\hat{n}\pi\beta}-\cos(\hat{n}\pi)+\beta\sin(\hat{n}\pi)\right]+\hat{n}\pi\beta-\beta\sin(\hat{n}\pi)\right.$$

$$\left.-3\cos(\hat{n}\pi)-3\right\}$$

$$\hat{n} < \frac{2}{\pi\beta} < 1 \qquad (3.50a)$$

$$\frac{p}{P_N} = \frac{\cos\theta}{2}\left\{\frac{1}{1+\beta^2}\left[\cos(\hat{n}\pi-\frac{2}{\beta})-\beta\sin(\hat{n}\pi-\frac{2}{\beta})-5\cos(\hat{n}\pi)+5\beta\sin(\hat{n}\pi)\right.\right.$$

$$\left.-2.389e^{-\hat{n}\pi\beta}\right]$$

$$\left.-\left[\cos(\hat{n}\pi-\frac{2}{\beta})-\beta\sin(\hat{n}\pi-\frac{2}{\beta})-3\cos(\hat{n}\pi)+\beta\sin(\hat{n}\pi)\right]\right\}$$

$$\frac{2}{\pi\beta} < \hat{n} < 1 \qquad (3.50b)$$

$$\frac{p}{P_N} = \frac{\cos\theta}{2}\left\{\frac{1}{1+\beta^2}\left[\cos(\hat{n}\pi-\frac{2}{\beta})-\beta\sin(\hat{n}\pi-\frac{2}{\beta})+5e^{-(\hat{n}-1)\pi\beta}-2.389e^{-\hat{n}\pi\beta}\right]\right.$$

$$\left.+\left[(\hat{n}-1)\pi\beta-3-\cos(\hat{n}\pi-\frac{2}{\beta})+\beta\sin(\hat{n}\pi-\frac{2}{\beta})\right]\right\}$$

$$\frac{2}{\pi\beta} < 1 < \hat{n}, \quad \hat{n}-\frac{2}{\pi\beta} < 1 \qquad (3.50c)$$

$$\frac{p}{P_N} = -\frac{\cos\theta}{2}\left\{\frac{2.389}{1+\beta^2}\left[e^{-(\hat{n}-1)\pi\beta}+e^{-\hat{n}\pi\beta}\right]\right\}$$

$$\frac{2}{\pi\beta} < 1 < \hat{n}, \ \hat{n}-\frac{2}{\pi\beta} > 1 \qquad (3.50d)$$

$$\frac{p}{P_N} = \frac{\cos\theta}{2}\left\{\frac{5}{1+\beta^2}\left[e^{-(\hat{n}-1)\pi\beta}+e^{-\hat{n}\pi\beta}\right]+(2\hat{n}-1)\pi\beta-6\right\}$$

$$1 < \hat{n} < \frac{2}{\pi\beta} \qquad (3.50e)$$

where $P_N = \frac{1.17\bar{M}}{1+\bar{M}} \frac{\rho_o c v_o a}{r}$, $\beta = \frac{\ell}{b}$ and $\hat{n} = \frac{\tau}{d}$. Figure (3.8) shows a comparison of this approximate approach with the exact method for a single sphere undergoing a Hertzian acceleration.

3.6. Sound radiated by a pair of colliding spheres (Convolution method)

The convolution method may as well as the Laplace transforms method, be used in the derivation of the sound generated by a sphere undergoing an elastic collision. This is the method used by Koss and Alfredson [21] for studying the sound radiated by a pair of colliding spheres.

It is mentioned in section (3.1) that the sound pressure due to any arbitrary acceleration may be given by a convolution integral, which was given previously as equation (3.10). Using the Hertzian acceleration given by equation (3.31) together with response to unit impulse expressed by (3.7) and substituting in (3.10) gives:

$$p(r,\theta,\tau) = \frac{\rho_o c a_M a^2 \cos\theta}{r^2} \int_o^\tau [\frac{r}{a}\cos\ell(\tau-\zeta)+(1 - \frac{r}{a})\sin\ell(\tau-\zeta)]$$

$$e^{-\ell(\tau-\zeta)}\sin b\zeta d\zeta \qquad 0 < \tau < d \qquad (3.51a)$$

and

$$p(r,\theta,\tau) = \frac{\rho_o c a_M a^2 \cos\theta}{r^2} \int_o^d [\frac{r}{a}\cos\ell(\tau-\zeta)+(1 - \frac{r}{a})\sin\ell(\tau-\zeta)]$$

$$e^{-\ell(\tau-\zeta)}\sin b\zeta d\zeta \qquad \tau > d \qquad (3.51b)$$

Solving (3.51a) and (3.51b) leads to exactly the same results as given in Equations (3.38b) and (3.36b) respectively.

Consider now a pair of colliding spheres modelled as shown in Figure (3.9) and assume that the sphere 1, which is initially at rest, is called the impactee and the other one the impactor. For a microphone positioned at $\theta<90^{o}$ (θ anti-clockwise, see Figure (3.9)) the sound radiated by the impactor arrives with a delay in time in comparison with the sound arriving from the impactee; the process would be the reverse if the microphone were positioned at $\theta>90^{o}$. The sound pressure at any microphone position can be simply given by the sum of the pressures radiated by the impactee and impactor. Thus at a position defined by the polar co-ordinate (r,θ) (see Figure (3.9)), the pressure is:

$$p(r,\theta,\tau) = H(-\tau+d)p(r_1,\theta_1,\tau)+H(\tau-d)p(r_1,\theta_1,\tau)+H(\tau-T_d)$$

$$xH(-\tau+T_d+d)p(r_2,\theta_2,\tau-T_d)+H(\tau-T_d-d)p(r_2,\theta_2,\tau-T_d)$$

$$-90^{o} < \theta < 90^{o} \qquad (3.52a)$$

where

$$H(-\tau+d) = \begin{cases} 1 & \tau < d \\ 0 & \text{Otherwise} \end{cases}, \quad H(\tau-d) = \begin{cases} 1 & \tau > d \\ 0 & \text{Otherwise} \end{cases},$$

$$H(\tau-T_d) = \begin{cases} 1 & \tau > T_d \\ 0 & \text{Otherwise} \end{cases}, \quad H(-\tau+T_d+d) = \begin{cases} 1 & \tau < T_d+d \\ 0 & \text{Otherwise} \end{cases}$$

$$H(\tau-T_d-d) = \begin{cases} 1 & \tau > T_d+d \\ 0 & \text{Otherwise} \end{cases} \qquad (3.52b)$$

and T_d is the time delay between the arrival of the sound to the microphone from each sphere. The time delay T_d may be approximated according to the ray theory and given by:

$$T_d = \frac{|r_2 - r_1|}{c} \tag{3.53}$$

for a suitable range of θ depending upon the size of spheres. An approximate time delay for $\theta = 0^o$ and equal radii spheres is given in reference [21] as follows:

$$T_d = \frac{2.57a + (r_1^2 + a^2)^{\frac{1}{2}} - r_1}{c} \tag{3.54}$$

For $\theta = 0^o$ and unequal radii spheres one may similarly write:

$$T_d = \frac{a_2 + 1.57a_1 + (r_1^2 + a_1^2)^{\frac{1}{2}} - r_1}{c} \tag{3.55}$$

where $r_2 = a_2 + \frac{\pi}{2}a_1 + (r_1^2 + a_1^2)^{\frac{1}{2}}$ is the path of a-b-c-d as shown in Figure (3.10). By following the similar procedures as given in section (3.4) for the impactee the amplitude of deceleration of the impactor can be found to be:

$$a_{M2} = -\frac{1.17}{1+\bar{M}} bv_o \tag{3.56}$$

where $\bar{M} = \frac{m_2}{m_1}$ is the ratio of mass of impactor to the mass of impactee. For a pair of colliding spheres as shown in Figure (3.9) one may write:

$$r_1 \simeq r - a_1\cos\theta \tag{3.57a}$$

$$r_2 \simeq r + a_2\cos\theta \tag{3.57b}$$

$$\cos\theta_1 = \frac{r}{r_1}\cos\theta - \frac{a_1}{r_1} \tag{3.58a}$$

and

$$\cos\theta_2 = \frac{r}{r_2}\cos\theta + \frac{a_2}{r_2} \tag{3.58b}$$

Substituting for r from (3.57a) and (3.57b) into equations (3.58a) and (3.58b) respectively gives:

$$\cos\theta_1 \simeq \cos\theta - \frac{1}{\xi_1}\sin^2\theta \tag{3.59a}$$

$$\cos\theta_2 \simeq \cos\theta + \frac{1}{\xi_2}\sin^2\theta \tag{3.59b}$$

where $\xi_1 = \frac{r_1}{a_1}$ and $\xi_2 = \frac{r_2}{a_2}$.

The sound pressure in the far field radiated by the impactee may now be written as:

$$p_1 = \frac{1.17\bar{M}}{1+\bar{M}}\frac{\rho_o c v_o}{(1+4\beta_1^4)} \times \frac{1}{\xi_1}\left(\cos\theta - \frac{1}{\xi_1}\sin^2\theta\right)$$

$$\{[(1-2\beta_1^2)\cos(\hat{n}\pi\beta_1)-(1+2\beta_1^2)\sin(\hat{n}\pi\beta_1)]e^{-\hat{n}\pi\beta_1}$$

$$-(1-2\beta_1^2)\cos(\hat{n}\pi)+2\beta_1\sin(\hat{n}\pi)\} \tag{3.60a}$$

$$\hat{n} < 1$$

and

$$p_1 = \frac{1.17\bar{M}}{1+\bar{M}} \frac{\rho_o c v_o}{(1+4\beta_1^4)} \frac{1}{\xi_1}(\cos\theta - \frac{1}{\xi_1}\sin^2\theta)$$

$$\{[(1-2\beta_1^2)\cos(\hat{n}\pi\beta_1)-(1+2\beta_1^2)\sin(\hat{n}\pi\beta_1)]e^{-\hat{n}\pi\beta_1}$$

$$+[(1-2\beta_1^2)\cos[(\hat{n}-1)\pi\beta_1]-(1+2\beta_1^2)\sin[(\hat{n}-1)\pi\beta_1]]e^{-(n-1)\pi\beta_1}\}$$

$$\hat{n} > 1 \qquad (3.60b)$$

where $\beta_1 = \frac{\ell_1}{b}$.

Similarly the sound pressure radiated by the impactor can be found to be:

$$p_2 = -\frac{1.17}{1+\bar{M}} \frac{\rho_o c v_o}{(1+4\beta_2^4)} x \frac{1}{\xi_2}(\cos\theta + \frac{1}{\xi_2}\sin^2\theta)$$

$$\{[(1-2\beta_2^2)x\cos[(\hat{n}-n')\pi\beta_2]-(1+2\beta_2^2)\sin[(\hat{n}-n')\pi\beta_2]]$$

$$e^{-(\hat{n}-n')\pi\beta_2} -(1-2\beta_2^2)\cos[(\hat{n}-n')\pi]+2\beta_2\sin[(\hat{n}-n')\pi]\}$$

$$0 < \hat{n} - n' < 1 \qquad (3.60c)$$

and

$$p_2 = -\frac{1.17}{1+\bar{M}} \frac{\rho_o c v_o}{(1+4\beta_2^4)} x \frac{1}{\xi_2}(\cos\theta + \frac{1}{\xi_2}\sin^2\theta)$$

$$\{[(1-2\beta_2^2)x\cos[(\hat{n}-n')\pi\beta_2] -(1+2\beta_2^2)\sin[(\hat{n}-n')\pi\beta_2]]$$

$$e^{-(\hat{n}-n')\pi\beta_2}+[(1-2\beta_2^2)\cos[(\hat{n}-n'-1)\pi\beta_2]$$

$$-(1+2\beta_2^2)\sin[(\hat{n}-n'-1)\pi\beta_2]]e^{-(\hat{n}-n'-1)\pi\beta_2}\}$$

$$\hat{n} > n'+1 \qquad (3.60d)$$

where $\beta_2 = \frac{\ell_2}{b}$ and $n' = \frac{T_d}{d}$.

The total sound pressure may now be written as:

$$p = H(-\hat{n}+1)p_1+H(\hat{n}-1)p_1+H(\hat{n}-n')xH(-\hat{n}+n'+1)p_2+H(\hat{n}-n'-1)p_2$$

$$-90^o < \theta < 90^o \qquad (3.61)$$

The total sound pressure for $90^o < \theta < 270^o$ can be obtained by changing the role of the impactee and impactor. Graphs representing variations of dimensionless pressure against $\hat{n}$ for a pair of similar spheres of equal and unequal sizes are given in Figure (3.11) and (3.12) respectively. The dimensionless pressure versus $\hat{n}$ for a pair of dissimilar spheres of equal and unequal sizes are also given in Figures (3.13) and (3.14). The directional distribution of sound for all above cases are presented in Figures (3.15) to (3.18).

Equations (3.60a) to (3.60d) make also possible that the variations of dimensionless rarefactive peak against β be studied for the case of similar spheres of equal radii and $\theta = 0^o$. Graphical presentation as such is given in Figure (3.19). Variations of $\hat{n}_{max}$ at which the rarefactive peak occurs is also shown in Figure (3.20).

In order to study the frequency spectrum of a pair of colliding spheres equation (3.44) may be written as:

$$p_1(r_1,\theta_1,\omega) = 1.17\,\frac{\bar{M}}{1+\bar{M}}\,\frac{\rho_o b^2 c v_o a_1^3}{b^2-\omega^2}\,\frac{(i\omega r_1+c)}{r_1^2}\,\frac{\cos\theta_1(1+e^{-i\omega d})}{2c^2+2i\omega a_1 c-\omega^2 a_1^2}$$

(3.62a)

Similarly for the impactor arriving with a time delay T_d one obtains:

$$p_2(r_2,\theta_2,\omega) = -\frac{1.17}{1+\bar{M}}\frac{\rho_o b^2 c v_o a_2^3}{b^2-\omega^2}\frac{(i\omega r_2+c)}{r_2^2}\frac{\cos\theta_2(1+e^{-i\omega d})e^{-i\omega T_d}}{2c^2+2i\omega a_2 c-\omega^2 a_2^2} \tag{3.62b}$$

Adding (3.62a) and (3.62b) and then multiplying the results by its complex conjugate gives:

$$|p|^2 = \frac{4(1.17)^2\rho_o^2 v_o^2 a_1^2\beta_1^2 n^{*2}\cos^2(n^*\pi)}{(1+\bar{M})^2(1-4n^{*2})^2(\beta_1^4+4n^{*4})(\beta_2^4+4n^{*4})}$$

$$\{\frac{\bar{M}^2}{\xi_1^4}(\beta_2^4+4n^{*4})(1+\frac{\beta_1^2}{4n^{*2}\xi_1^2})(\xi_1\cos\theta-\sin^2\theta)^2+\frac{(\beta_1^4+4n^{*4})}{\xi_2^4}$$

$$(1+\frac{\beta_2^2}{4n^{*2}\xi_2^2})(\xi_2\cos\theta+\sin^2\theta)^2-\frac{\bar{M}}{\xi_1^3\xi_2^3 n^*}[4n^{*4}-2n^{*2}(\beta_1-\beta_2)^2$$

$$+\beta_1^2\beta_2^2]x[2n^*\xi_1\xi_2(1+\frac{\beta_1\beta_2}{4n^{*2}\xi_1\xi_2})\cos(2\pi n^*n')+(\xi_2\beta_1-\xi_1\beta_2)$$

$$\sin(2\pi n^*n')](\xi_1\cos\theta-\sin^2\theta)x(\xi_2\cos\theta+\sin^2\theta)-\frac{2\bar{M}}{\xi_1^3\xi_2^3}$$

$$(2n^{*2}+\beta_1\beta_2)(\beta_1-\beta_2)[(\xi_2\beta_1-\xi_1\beta_2)\cos(2\pi n^*n')-2n^*\xi_1\xi_2$$

$$(1+\frac{\beta_1\beta_2}{4n^{*2}\xi_1\xi_2})\sin(2\pi n^*n')](\xi_1\cos\theta-\sin^2\theta)(\xi_2\cos\theta+\sin^2\theta)\} \tag{3.63}$$

At a large distance r, $\frac{\beta_1\beta_2}{4n^{*2}\xi_1\xi_2}$, $\frac{\beta_1^2}{4n^{*2}\xi_1^2}$ and $\frac{\beta_2^2}{4n^{*2}\xi_2^2}$

are all much less than unity and one may write:

$$|p| = \frac{2.34\rho_o v_o a_1 \beta_1 n^* \cos(n^*\pi)}{(1+M)(1-4n^{*2})(\beta_1^4+4n^{*4})^{\frac{1}{2}}(\beta_2^4+4n^{*4})^{\frac{1}{2}}}$$

$$\left\{ \frac{\bar{M}^2}{\xi_1^4}(\beta_2^4+4n^{*4})(\xi_1\cos\theta-\sin^2\theta)^2 + \frac{(\beta_1^4+4n^{*4})}{\xi_2^4}\right.$$

$$(\xi_2\cos\theta+\sin^2\theta)^2 - \frac{\bar{M}}{\xi_1^3\xi_2^3 n^*}[4n^{*4}-2n^{*2}(\beta_1-\beta_2)^2+\beta_1^2\beta_2^2]$$

$$x[2n^*\xi_1\xi_2\cos(2\pi n^* n')+(\xi_2\beta_1-\xi_1\beta_2)\sin(2\pi n^* n')]$$

$$(\xi_1\cos\theta-\sin^2\theta)(\xi_2\cos\theta+\sin^2\theta) - \frac{2\bar{M}}{\xi_1^3\xi_2^3}(2n^{*2}+\beta_1\beta_2)(\beta_1-\beta_2)$$

$$[(\xi_2\beta_1-\xi_1\beta_2)\cos(2\pi n^* n')-2n^*\xi_1\xi_2\sin(2\pi n^* n')]$$

$$\left. x(\xi_1\cos\theta-\sin^2\theta)(\xi_2\cos\theta+\sin^2\theta)\right\}^{\frac{1}{2}} \qquad (3.64)$$

Graphs showing variations of $|p|$ versus n^* for a pair of similar spheres of equal and unequal radii are given in Figures (3.21) and (3.22) respectively. Similar graphs for a pair of dissimilar spheres of equal and unequal sizes are also given in Figures (3.23) and (3.24). Variations of n^*_{max} at which the peak of transform occurs is also plotted against β in Figure (3.25) for a pair of similar spheres of equal radii and $\theta = 0^o$.

It should be emphasised that the dimensionless forms of pressure-time and pressure-frequency introduced in this section

may be easily related to those given by Koss [22] through the relations:

$$\frac{p(r,\theta,\tau)/\rho_o c v_o}{\pi_6} = \frac{1.17}{\beta_1} \times \frac{\bar{M}}{1+\bar{M}}$$

and

$$\frac{p(r,\theta,\omega)/\rho_o v_o a_1}{\pi_9} = 4.68\pi^2\beta_1 \times \frac{\bar{M}}{1+\bar{M}}$$

where $\pi_6 = \frac{p(r,\theta,\tau)}{\rho_o a_{M1} a_1}$ and $\pi_9 = \frac{|p(r,\theta,\omega)|}{4\rho_o c a_{M1} d^2}$ are Koss's normalised pressure-time and pressure-frequency respectively. The difference between the results is due to use of equation (2.42) which is not being used by Koss [22]. His dimensionless result in the frequency domain is also limited to case of pair of similar and dissimilar spheres of equal radii.

3.7. Sound radiated by a pair of colliding spheres (Numerical Method)

In section (2.6) a numerical method was given for calculating the force at any instant of time by solving equation (2.67) numerically. The method can be developed for predicting the sound radiated by a pair of colliding spheres if the instantaneous values of acceleration are being employed for calculating (3.51a) and (3.51b) numerically. The method will be explained in detail later on in chapter 5 because of its common use in predicting the sound radiated by a pair of viscoelastic spheres. Typical sound

pressure time history calculated both numerically and analytically (equation (3.52a) are compared in Figure (3.26).

3.8. Sound radiated due to change of volume of sphere undergoing an elastic collision

The change of volume at any instant of time for a sphere of radius a_1 subjected to an elastic collision by another sphere of radius a_2 as shown by shaded region in Figure (3.27a) can be written as:

$$V = \int_{x}^{a_1} dx \int_{0}^{\sqrt{a_1^2-x^2}} \bar{r}\, d\,\bar{r} \int_{0}^{2\pi} d\theta = \frac{\pi}{3}(2a_1^3-3a_1^2x+x^3) \tag{3.65}$$

where x, $\bar{r}$ and θ are illustrated in Figure (3.27b). The change of volume may also be expressed in terms of instantaneous radius of surface of contact by substituting $x = \sqrt{a_1^2-R^2}$ into equation (3.65). Thus:

$$V = \frac{\pi}{3}(2a_1^3-2a_1^2\sqrt{a_1^2-R^2} - R^2\sqrt{a_1^2-R^2}) \tag{3.66}$$

where R is the instantaneous radius of the surface of contact and is given by Goldsmith [43] as:

$$R = q_o\left[\frac{3}{4}\frac{F(\delta_1+\delta_2)}{A+B}\right]^{1/3} \tag{3.67}$$

Using the relationship between force and approach given by equation (2.60) together with equation (2.61) and substituting into equation (3.67) gives:

$$R^2 = q_a{}^2 . q_K^{2/3} \left(\frac{\alpha}{A+B}\right) = \frac{a_1 a_2}{a_1+a_2}\alpha \qquad (3.68)$$

where $q_a = 3\sqrt{\pi}$, $q_K = \frac{1}{\pi}$ and $A = B = \frac{1}{2}\left(\frac{1}{a_1} + \frac{1}{a_2}\right)$ for a pair of colliding spheres of radii a_1 and a_2. Rewriting equation (3.68) in terms of t by using the approach-time relation given in equation (2.72) yields:

$$R^2 = \frac{a_1 a_2}{a_1+a_2} . \alpha_{max} \sin bt \qquad (3.69)$$

Substituting (3.69) into (3.66) and finding the rate of change of volume, one obtains:

$$\frac{\partial V}{\partial t} = \frac{\pi}{4} b \frac{\alpha^2_{max}}{(a_1+a_2)^2} a_1 a_2{}^2 \sin 2bt \left[1 - \frac{a_2}{a_1} x \frac{\alpha_{max}}{(a_1+a_2)} \sin bt\right]^{-\frac{1}{2}} \qquad (3.70a)$$

Neglecting the term $\frac{a_2}{a_1} x \frac{\alpha_{max}}{(a_1+a_2)} \sin bt$ in comparison with unity gives:

$$\frac{\partial V}{\partial t} \simeq \frac{\pi}{4} b \frac{\alpha^2_{max}}{(a_1+a_2)^2} a_1 a_2{}^2 \sin 2bt \qquad (3.70b)$$

The radial velocity of a sphere of radius a_1 at its surface may now be expressed in terms of the volume velocity as:

$$v_r\Big|_{r=a_1} = \frac{1}{4\pi a_1{}^2} \frac{\partial V}{\partial t} = \frac{1}{16} x \frac{b a_2{}^2 \alpha^2_{max}}{a_1 (a_1+a_2)^2} \sin 2bt \qquad (3.71)$$

Using differential of (3.71) with respect to t together with the impulse potential function of a pulsating sphere given by equation (3.13) and substituting into the convolution integral produces:

$$\phi(r,\tau) = \frac{1}{8}\frac{b^2 a_1 a_2^2 \alpha^2_{max}}{(a_1+a_2)^2 r}\int_o^\tau (1-e^{-\ell(\tau-\zeta)})\sin 2b\zeta d\zeta$$

$$0 < \tau < d \qquad (3.72a)$$

and

$$\phi(r,\tau) = \frac{1}{8}\frac{b^2 a_1 a_2^2 \alpha^2_{max}}{(a_1+a_2)^2 r}\int_o^d (1-e^{-\ell(\tau-\zeta)})\sin 2b\zeta d\zeta$$

$$\tau > d \qquad (3.72b)$$

The solutions to the equations (3.72a) and (3.72b) are:

$$\phi(r,\tau) = \frac{1}{8}\frac{cb^2\alpha^2_{max}}{(\ell^2+4b^2)}\frac{a_2^2}{(a_1+a_2)^2 r}\left[\frac{\ell}{2b}\sin 2b\tau - \cos 2b\tau + e^{-\ell\tau}\right]$$

$$0 < \tau < d \qquad (3.73a)$$

and

$$\phi(r,\tau) = \frac{1}{8}\frac{cb^2\alpha^2_{max}}{(\ell^2+4b^2)}\frac{a_2^2}{(a_1+a_2)^2 r}\left[e^{-\ell\tau} - e^{-\ell(\tau-d)}\right]$$

$$\tau > d \qquad (3.73b)$$

The sound pressure may now be found to be:

$$p(r,\tau) = \frac{1}{8}\frac{\rho_o cb^2\alpha^2_{max}}{(\ell^2+4b^2)}\frac{a_2^2\ell}{(a_1+a_2)^2 r}\left[\cos 2b\tau + \frac{2b}{\ell}\sin 2b\tau - e^{-\ell\tau}\right]$$

$$0 < \tau < d \qquad (3.74a)$$

and

$$p(r,\tau) = \frac{1}{8}\frac{\rho_o cb^2\alpha^2_{max}}{(\ell^2+4b^2)}\frac{a_2^2\ell}{(a_1+a_2)^2 r}\left[e^{-\ell(\tau-d)} - e^{-\ell\tau}\right]$$

$$\tau > d \qquad (3.74b)$$

Substituting in equations (3.74a) and (3.74b) for α_{max} from (2.69) and rewriting the results in terms of non-dimensional variables gives:

$$p = \frac{P_D}{(4+\beta_1^2)} \frac{\beta_1}{(1+\frac{\beta_2}{\beta_1})^2}[2\sin(2\hat{n}\pi)+\beta_1\cos(2\hat{n}\pi)-\beta_1 e^{-\hat{n}\pi\beta_1}]$$

$$0 < n < 1 \qquad (3.75a)$$

and

$$p = \frac{P_D}{(4+\beta_1^2)} \frac{\beta_1^2}{(1+\frac{\beta_2}{\beta_1})^2}[e^{-(\hat{n}-1)\pi\beta_1} - e^{-\hat{n}\pi\beta_1}]$$

$$\hat{n} > 1 \qquad (3.75b)$$

where $P_D = 0.142\ \rho_o v_o^2 \frac{a_1}{r}$.

Figure (3.28) shows variations of p/P_D versus $\hat{n}$ for a single sphere.

3.9. Acoustic energy of an impulsively accelerated sphere

Consider a volume V of a fluid surrounded by inner and outer spherical boundaries at r = a and r = r, respectively. Further assume that the sphere of radius a is subjected to an impulsive velocity $v_o H(t)$ and is surrounded by inner boundary of this fluid. The kinetic energy of the element of this fluid having the volume dV and the mass ρdV is:

$$dE_K = \frac{1}{2} \rho'(\underline{q})^2 dV \tag{3.76}$$

where $\underline{q}$ is the velocity vector.

The condensation of the medium which is given by equation (2.4) confirms that for small condensation $\rho' = \rho_o$. Thus,

$$E_K = \frac{1}{2} \rho_o \int_V (\underline{q})^2 dV \tag{3.77}$$

The change in the volume of the element generates the potential energy which by assuming an adiabatic relationship between pressure and volume, can be written as:

$$E_P = \frac{1}{2\rho_o c^2} \int_V p^2 dV \tag{3.78}$$

So the total energy at any given instant of time is:

$$\hat{E} = E_K + E_P = \frac{1}{2} \rho_o \int_V (\underline{q})^2 dV + \frac{1}{2\rho_o c^2} \int_V p^2 dV \tag{3.79}$$

The flux of energy propagating out of the volume V may now be obtained by differentiating (3.79) with respect to time. Thus:

$$\frac{\partial \hat{E}}{\partial t} = \rho_o \int_V (\underline{q}) \frac{\partial}{\partial t} \underline{q} \, dV + \frac{1}{\rho_o c^2} \int_V p \frac{\partial p}{\partial t} dV \tag{3.80}$$

Using equations (2.6) and (2.8) gives:

$$\frac{\partial \hat{E}}{\partial t} = -\int_V \underline{q} (\text{grad } p) dV - \int_V p (\text{div } \underline{q}) dV \tag{3.81}$$

By using Green's theorem equation (3.81) can be reduced to the surface integral of the density of energy flow in a direction normal to the surface S which bounds the volume V of the fluid. Thus:

$$\frac{\partial \hat{E}}{\partial t} = -\int_V \text{div}\,(p\underline{q})dV = \int_S p\underline{q}\underline{n}dS \qquad (3.82)$$

where $\underline{n}$ is the outward unit normal.

Representing the element of dS as shown in Figure (2.1) gives:

$$\frac{\partial \hat{E}}{\partial t} = 2\pi r^2 \int_0^{\pi} p v_r \sin\theta\, d\theta \qquad (3.83)$$

where $v_r = \underline{q}\,\underline{n}$.

Using expressions (3.7) and (3.8) given for pressure and raidal velocity, substituting them into (3.83) and integrating over the interval of θ gives:

$$\frac{\partial \hat{E}}{\partial t} = \frac{4\pi\rho_o c v_o^2 a^5}{3r^2} e^{-2\frac{c}{a}\tau}\left[\left(\frac{4}{a} - \frac{3r}{a^2} - \frac{1}{r}\right)\sin^2\frac{c}{a}\tau + \left(\frac{3r}{2a^2} - \frac{r^2}{a^3} - \frac{1}{2r}\right)\sin 2\frac{c}{a}\tau + \left(\frac{r^2}{a^3} - \frac{1}{a}\right)\right]$$

$$+ \frac{4\pi\rho_o c v_o^2 a^5}{3r^3} e^{-\frac{c}{a}\tau}\left[\left(1 - \frac{r}{a}\right)\sin\frac{c}{a}\tau + \frac{r}{a}\cos\frac{c}{a}\tau\right] \qquad (3.84)$$

where $\tau = t - \frac{r-a}{c}$.

Equation (3.84) shows that the flux of energy propagating in direction normal to the surface S which is positioned at a distance r from the centre of the sphere decreases by increasing the time, and has a maximum amount at $\tau = 0$. Thus:

$$\frac{\partial \hat{E}}{\partial t} = \frac{4}{3}\pi\rho_o c v_o^2 a^2 \tag{3.85}$$

which is independent of r.

To evaluate the energy equation (3.82) can be written as:

$$\hat{E} = \int_t \int_S p v_r \, dS dt \tag{3.86}$$

which by carrying out the similar process as given before and integrating over the interval of τ from zero to infinity yields to the following result:

$$\hat{E} = \frac{\pi\rho_o a^3 v_o^2}{3}\left(1 + \frac{a^3}{r^3}\right) \tag{3.87}$$

To find the energy radiated in the far field one may use the fact that

$$-\frac{\partial \phi}{\partial r} = \frac{1}{c}\frac{\partial \phi}{\partial t} \tag{3.88a}$$

or, in other words,

$$v_r = \frac{p}{\rho_o c} \tag{3.88b}$$

Thus from equation (3.86)

$$\hat{E} = \frac{1}{\rho_o c} \int_t \int_S p^2 dS dt \tag{3.89}$$

By making use of equation (3.89) the energy radiated in the far field can be evaluated to be:

$$\hat{E} = \frac{1}{3} \pi \rho_o a^3 v_o^2 \tag{3.90}$$

The same result may also be obtained from (3.87) by estimating limit of $\hat{E}$ as $r \to \infty$. The result given by (3.87) is similar to that given by Akay and Hodgson [16] who have also given an expression in the form of:

$$\hat{E} = \frac{1}{2\pi} \int_S \int_{-\infty}^{\infty} p(\omega) v_r^*(\omega) d\omega dS \tag{3.91}$$

for evaluating energy in frequency domain, where $v_r^*(\omega)$ is the complex conjugate of $v_r(\omega)$.

3.10. Acoustic energy of sphere undergoing a Hertzian acceleration

As shown in section (3.4) the sound pressure generated by a sphere undergoing a Hertzian acceleration can be represented by two expressions, each for a certain interval of time. Let $p_1(r,\theta,\tau)$ and $p_2(r,\theta,\tau)$ denote the sound pressures in intervals $0 < \tau < d$ and $\tau > d$ respectively. Thus the intensity of energy per unit area of any spherical surface positioned at a distance

r from the centre of sphere can be given by:

$$\frac{1}{\cos^2\theta}\frac{\partial\hat{E}}{\partial S} = \int_0^d p_1(r,\tau).v_1(r,\tau)d\tau + \int_d^\infty p_2(r,\tau).v_2(r,\tau)d\tau \qquad (3.92)$$

where $v_1(r,\theta,\tau)$ and $v_2(r,\theta,\tau)$ correspond to radial velocities in each interval. To solve the above equation one may use Simpson's rule which is a well known method for solving an integral numerically. So the integrals on the right hand side of equation (3.92) can be evaluated approximately as:

$$\frac{1}{\cos^2\theta}\frac{\partial\hat{E}}{\partial S} \simeq \frac{\Delta t}{3}\left[(pv_r)|_{\tau=0} + (4pv_r)|_{\tau=\Delta t} + (2pv_r)|_{\tau=2\Delta t} + (4pv_r)|_{\tau=3\Delta t} + \right.$$

$$\left. \ldots\ldots + (2pv_r)|_{\tau=(n-2)\Delta t} + (4pv_r)|_{\tau=(n-1)\Delta t} + (pv_r)_{\tau=n\Delta t}\right] \qquad (3.93)$$

where Δt is a constant increment of time, pv_r is either equal to p_1v_1 for $0 < \tau < d$ or p_2v_2 for $\tau > d$, and n is an even number. Since the pressure decays with increasing time, n may be chosen as a suitable large number to give a negligible value of pv for $\tau > n\Delta t$. The result obtained from (3.93) gives the amount of the intensity of energy in a certain direction. Thus, to find the energy one should multiply this result by $\frac{4}{3}\pi r^2$.

By taking the far field condition into account one may reduce (3.92) to:

$$\frac{1}{\cos^2\theta}\frac{\partial\hat{E}}{\partial S} = \frac{1}{\rho_o c}\int_o^d p_1^2 d\tau + \frac{1}{\rho_o c}\int_d^\infty p_2^2 d\tau \qquad (3.94)$$

which can be solved either numerically or analytically. It should be emphasised that representing an analytical expression as a solution to (3.92) required a long calculation. Therefore, a numerical solution is preferable, but in the far field case the operations are shorter and analytical solution may be achieved. Thus, by substituting for p from equations (3.40a) and (3.40b) the intensity of energy per unit area can be found from (3.94) to be:

$$\frac{\partial\hat{E}}{\partial S} = \frac{a_M^2 a^3 \rho_o b^2 \cos^2\theta}{2(b^4+4\ell^4)^2 r^2}\left[(4\ell^4-b^4-4b^2\ell^2)\sin\ell d e^{-\ell d} - (4\ell^4-b^4+4b^2\ell^2)(\cos\ell d e^{-\ell d}+1)+(4\ell^4+b^4)\ell d\right] \qquad (3.95)$$

By making use of equation (3.95) the radiation energy can be obtained as:

$$\hat{E} = \frac{2a_M^2 a^3 \rho_o b^2 \pi}{3(b^4+4\ell^4)^2}\left[(4\ell^4-b^4-4b^2\ell^2)\sin\ell d e^{-\ell d} - (4\ell^4-b^4+4b^2\ell^2)(\cos\ell d e^{-\ell d}+1)+(4\ell^4+b^4)\ell d\right] \qquad (3.96)$$

or in terms of β

$$\frac{\hat{E}}{E^*} = \frac{0.342}{(1+4\beta^4)^2}\left[(4\beta^4-4\beta^2-1)\sin\beta\pi e^{-\pi\beta} - (4\beta^4+4\beta^2-1)(\cos\pi\beta e^{-\pi\beta}+1) + \pi\beta(4\beta^4+1)\right] \qquad (3.97)$$

where $E^* = \frac{2\bar{M}^2}{(1+\bar{M})^2} \bar{\bar{m}} v_o^2$ and $\bar{\bar{m}}$ is the mass of air displaced by the sphere.

Figure (3.29) shows variations of $\hat{E}/0.342E^*$ against β for a single sphere. Variations of total dimensionless energy, $\hat{E}_T/0.5E^*$ versus β for a pair of similar and equal radii spheres is also given in Figure (3.30).

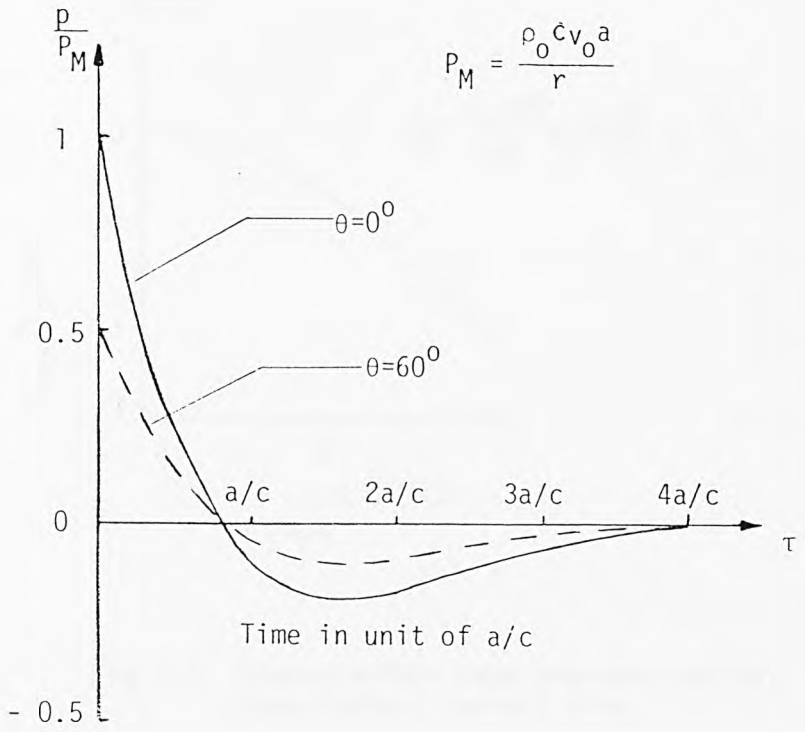

Fig.3.1. Pressure-time curves of impulsively accelerated sphere.

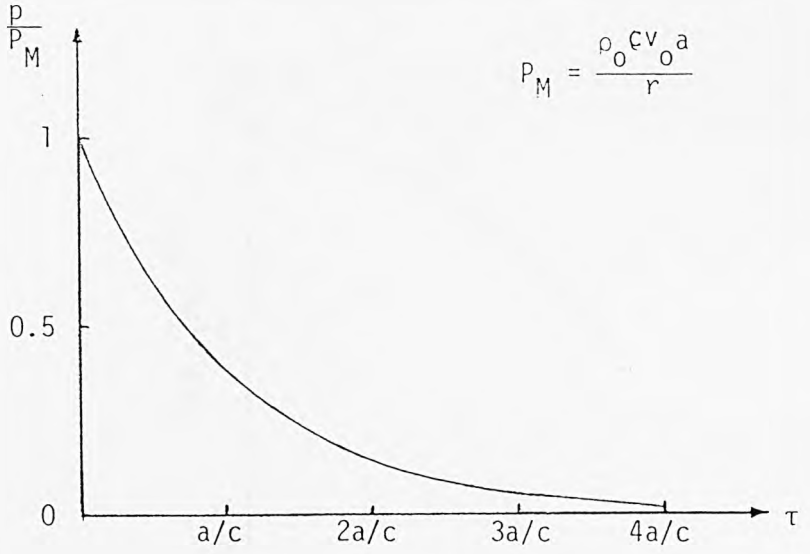

Fig.3.2. Pressure-time curve of impulsively pulsating sphere.

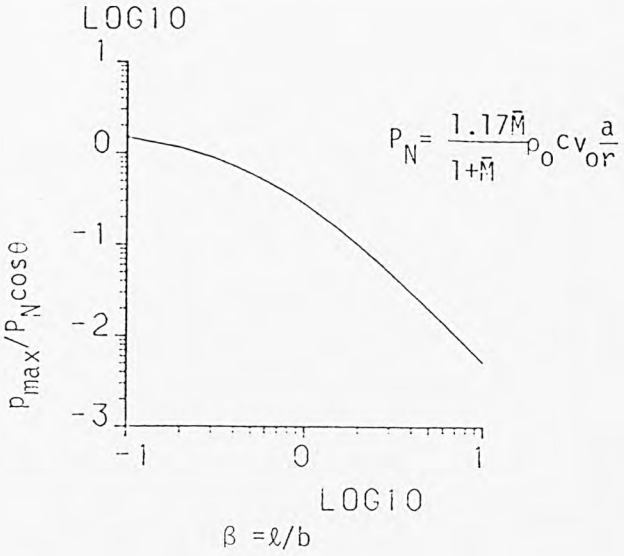

Fig.3.3. Dimensionless peak pressure against dimensionless contact time.

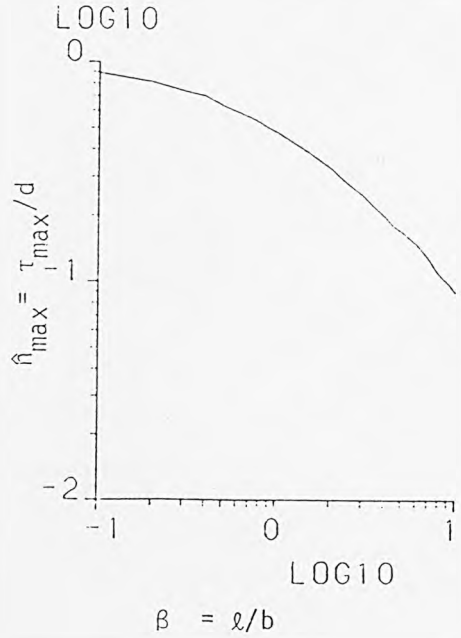

Fig.3.4. Variation of $\hat{n}_{max}$ with β.

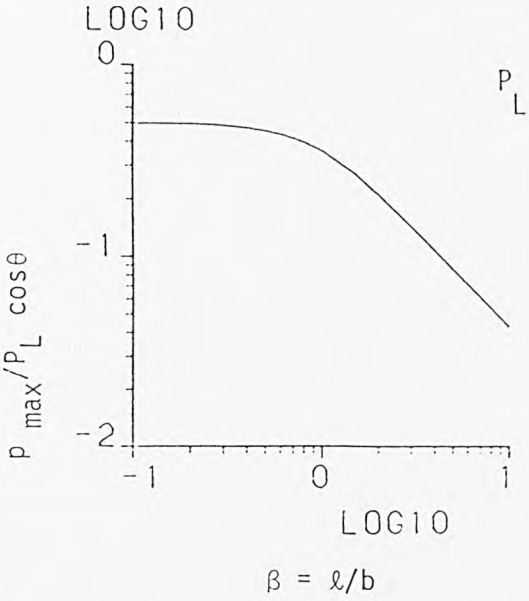

$$P_L = 2.34 \frac{\bar{M}}{1+\bar{M}} \rho_o v_o \frac{a^2}{r}$$

Fig.3.5. Dimensionless peak of transform against β.

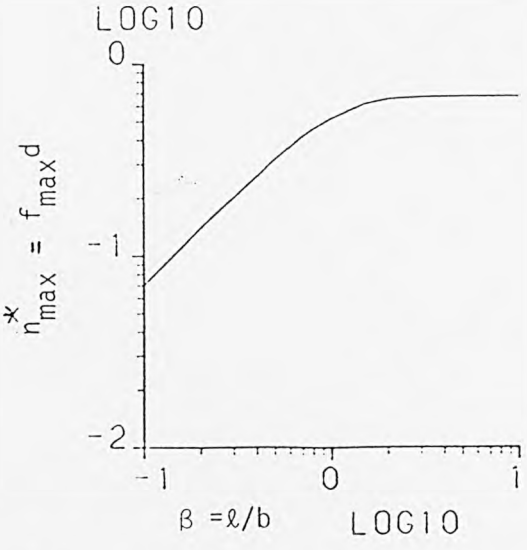

Fig.3.6. Variation of n^*_{max} with β

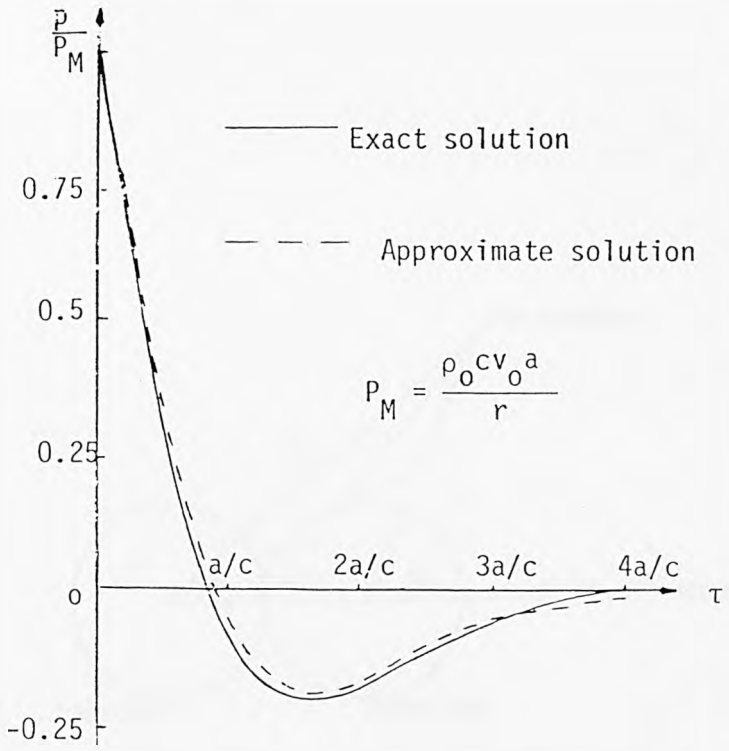

Fig.3.7. A Comparison of the exact solution for the sound radiated by an impulsively accelerated sphere and approximate solution of that sound obtained by aerodynamic approach.

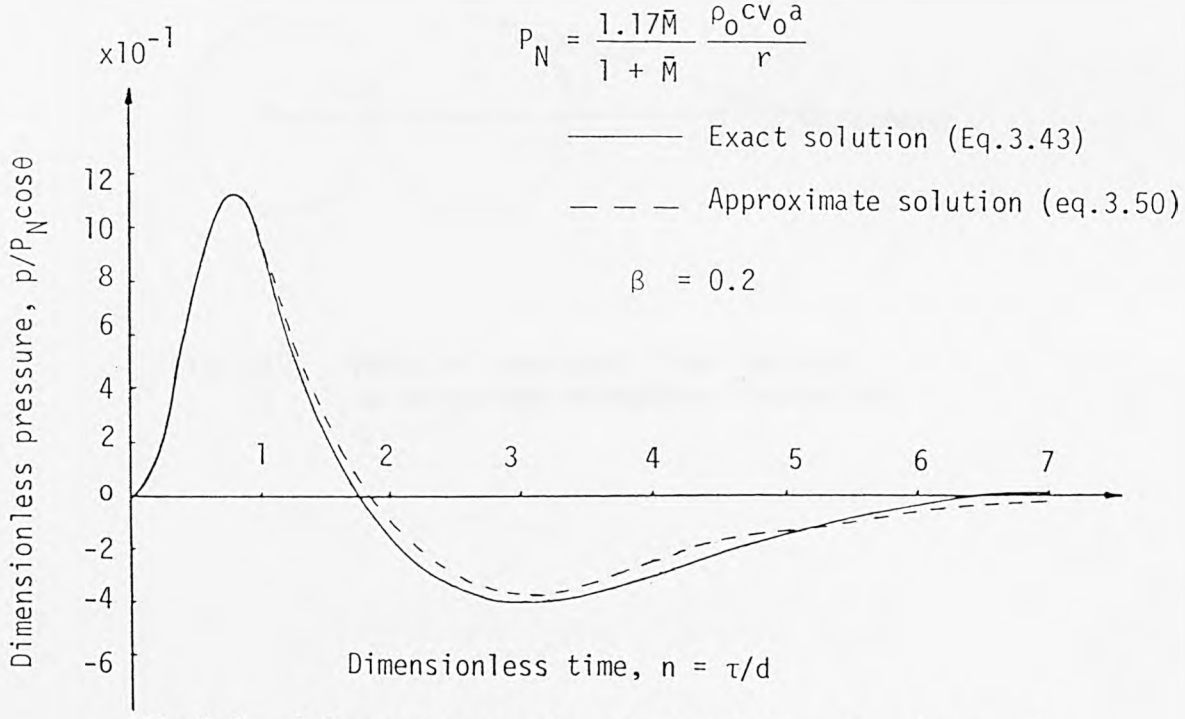

Fig.3.8. A Comparison of the exact solution for the sound radiated by a sphere undergoing a Hertzian acceleration and approximate evaluation of that sound obtained by aeroacoustic approach.

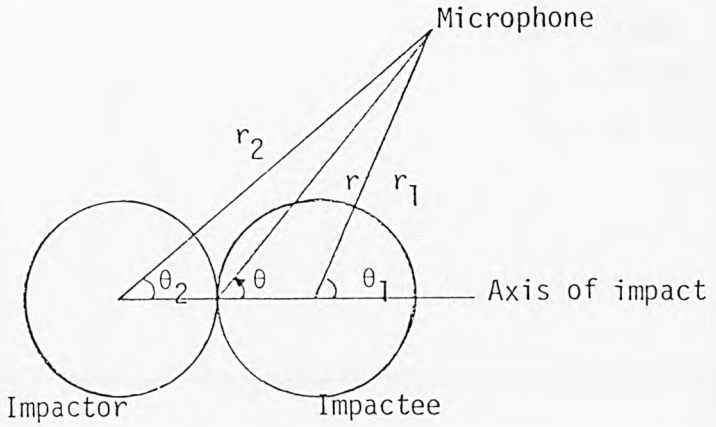

Fig.3.9. Model of colliding spheres.

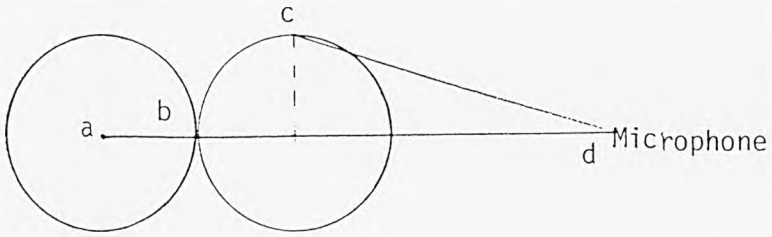

Fig.3.10. Model of wave path from impactor to measuring microphone located at $\theta = 0^{o}$.

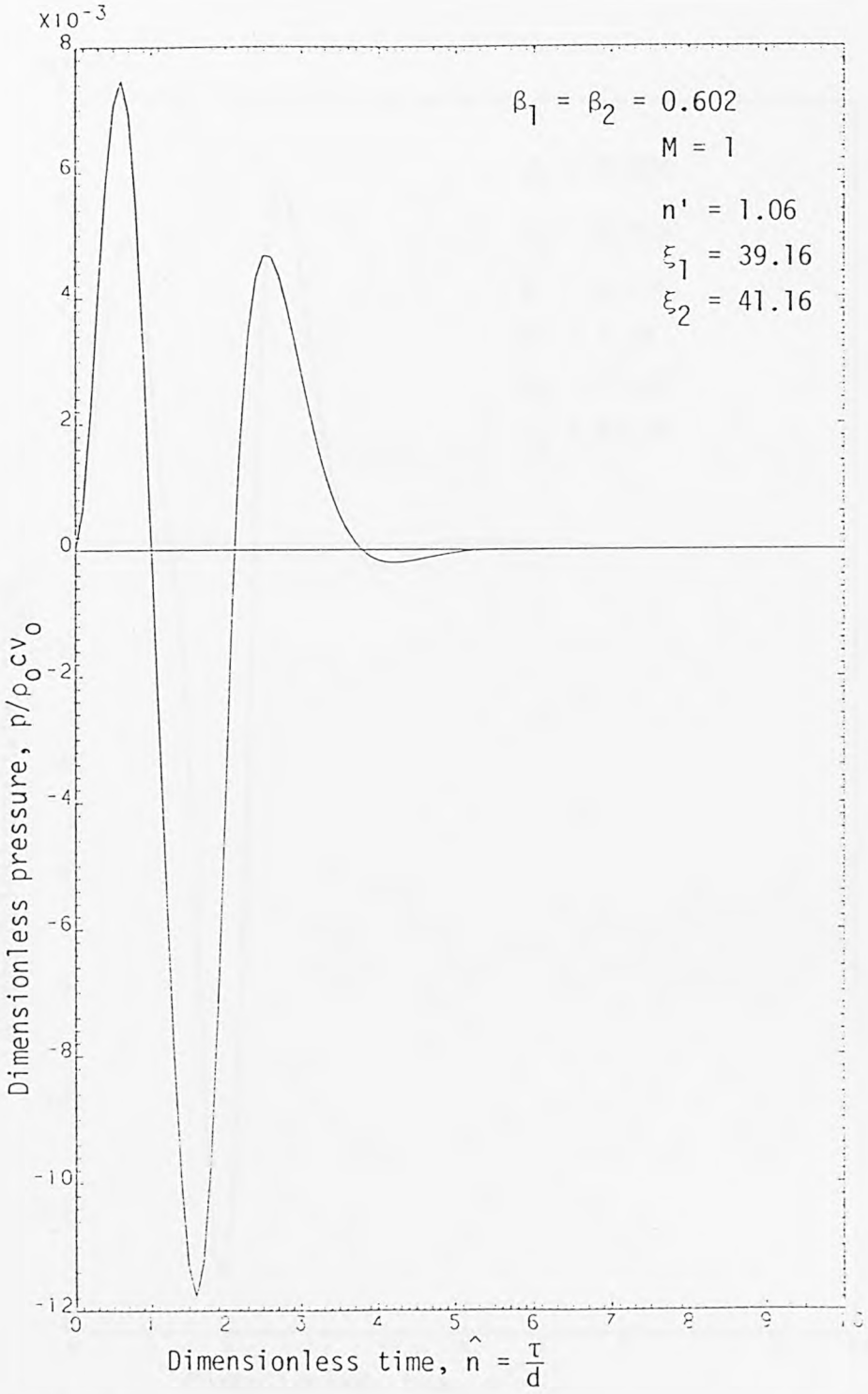

Fig.3.11. Dimensionless pressure-time curve for a pair of similar spheres of equal sizes. ($\theta = 0^o$).

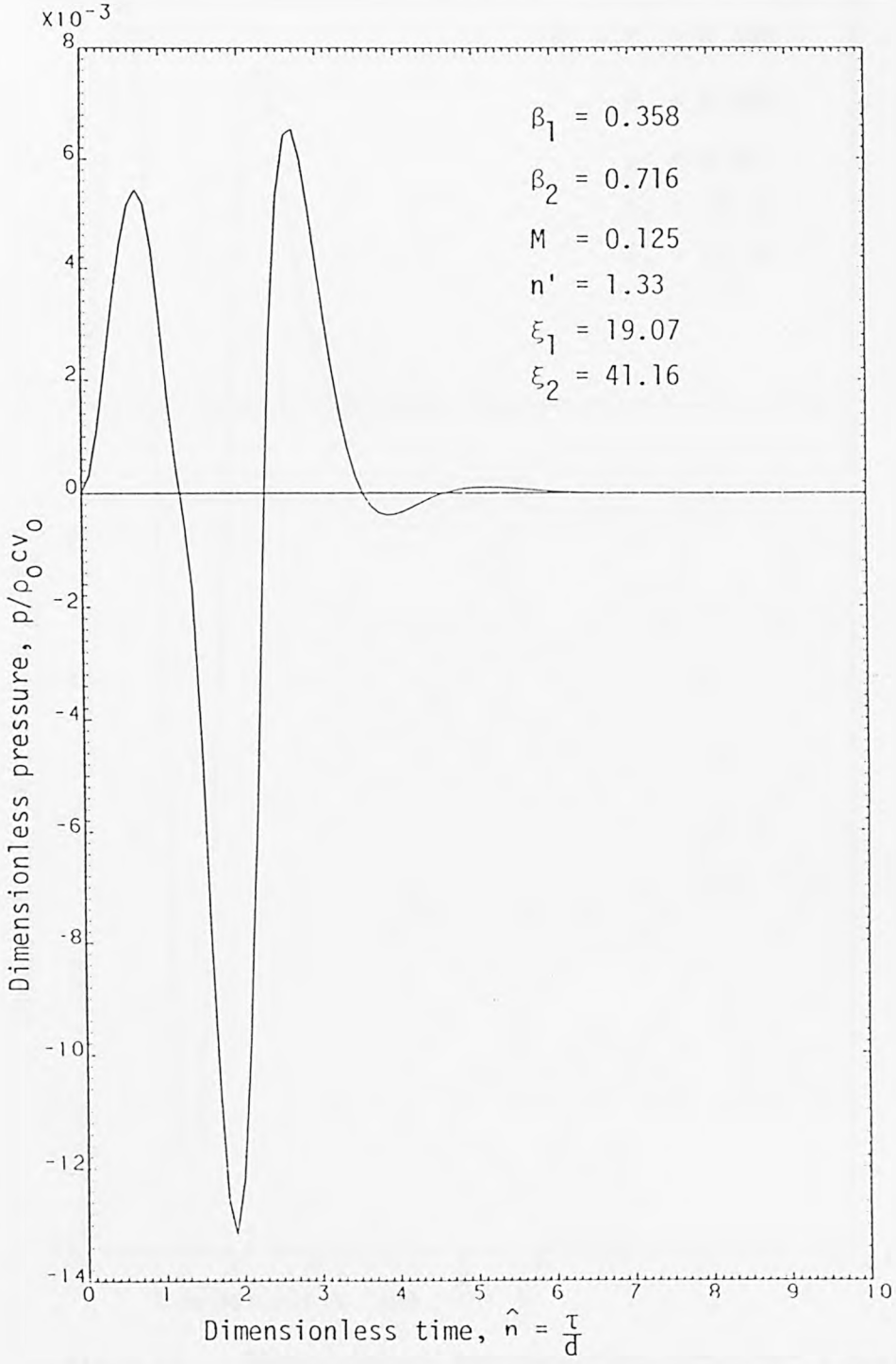

Fig.3.12. Dimensionless pressure-time curve for a pair of similar spheres of unequal sizes ($\theta = 0^{0}$).

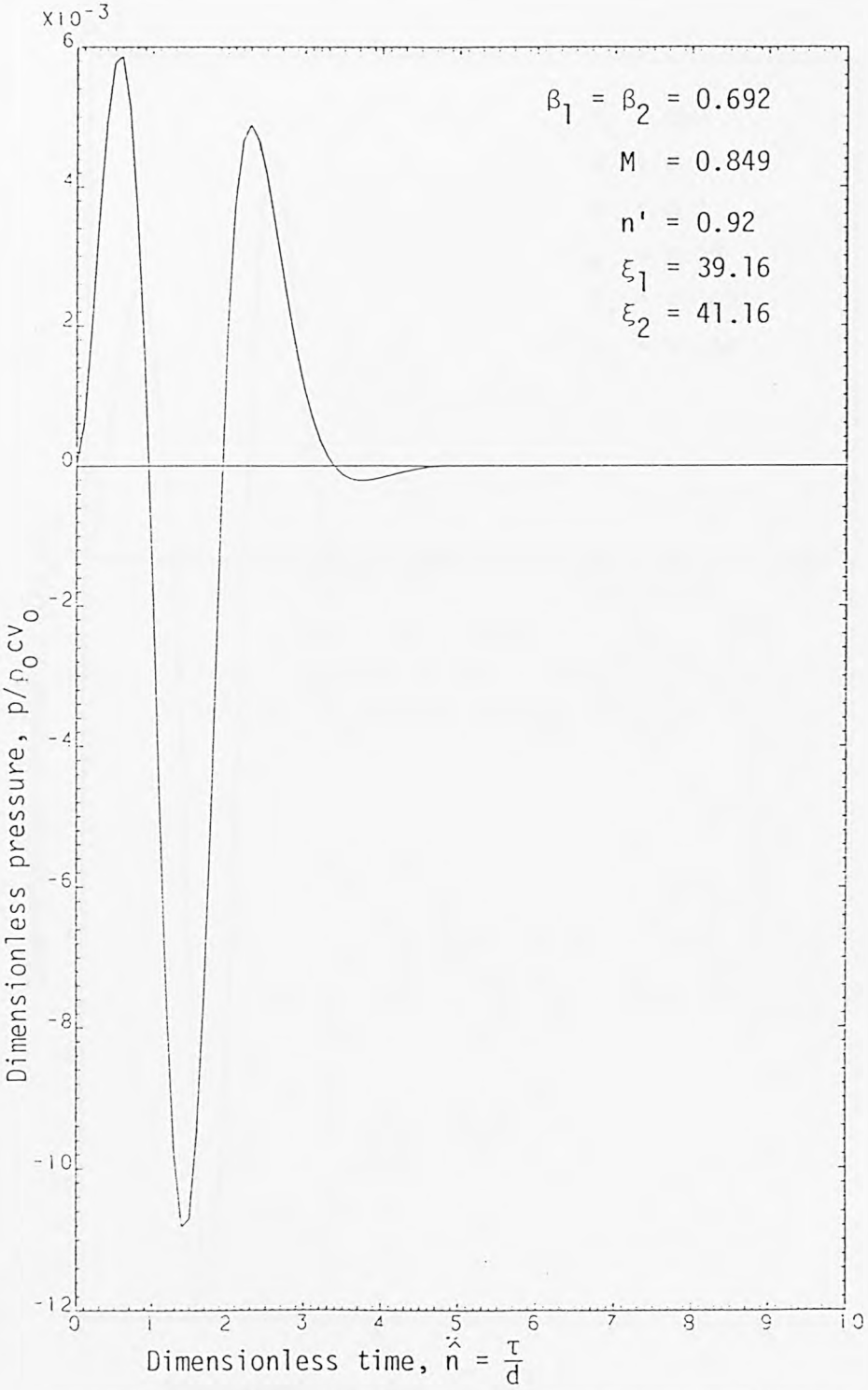

Fig.3.13. Dimensionless pressure-time curve for a pair of dissimilar spheres of equal sizes ($\theta = 0^0$).

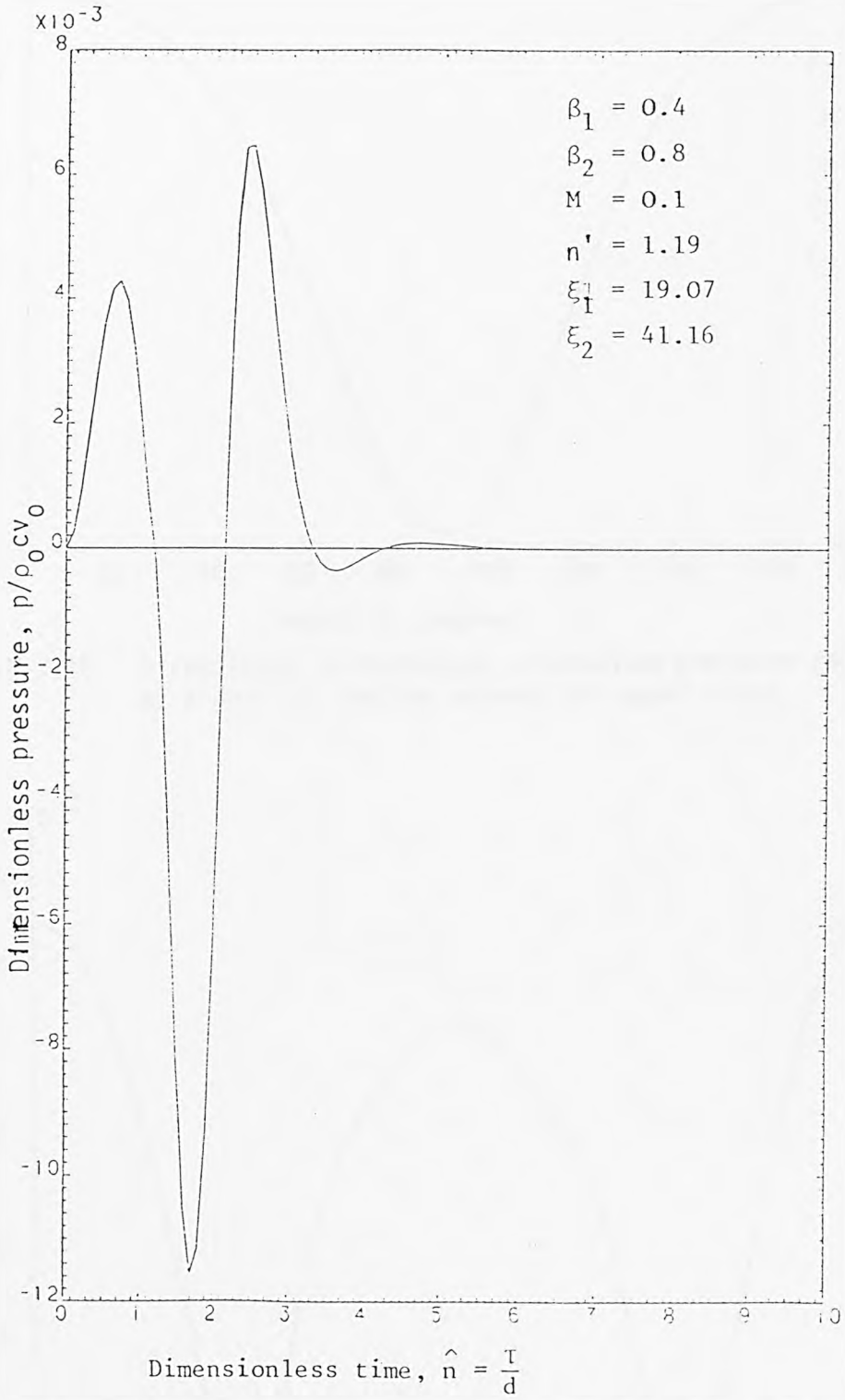

Fig.3.14. Dimensionless pressure-time curve for a pair of dissimilar spheres of unequal sizes.

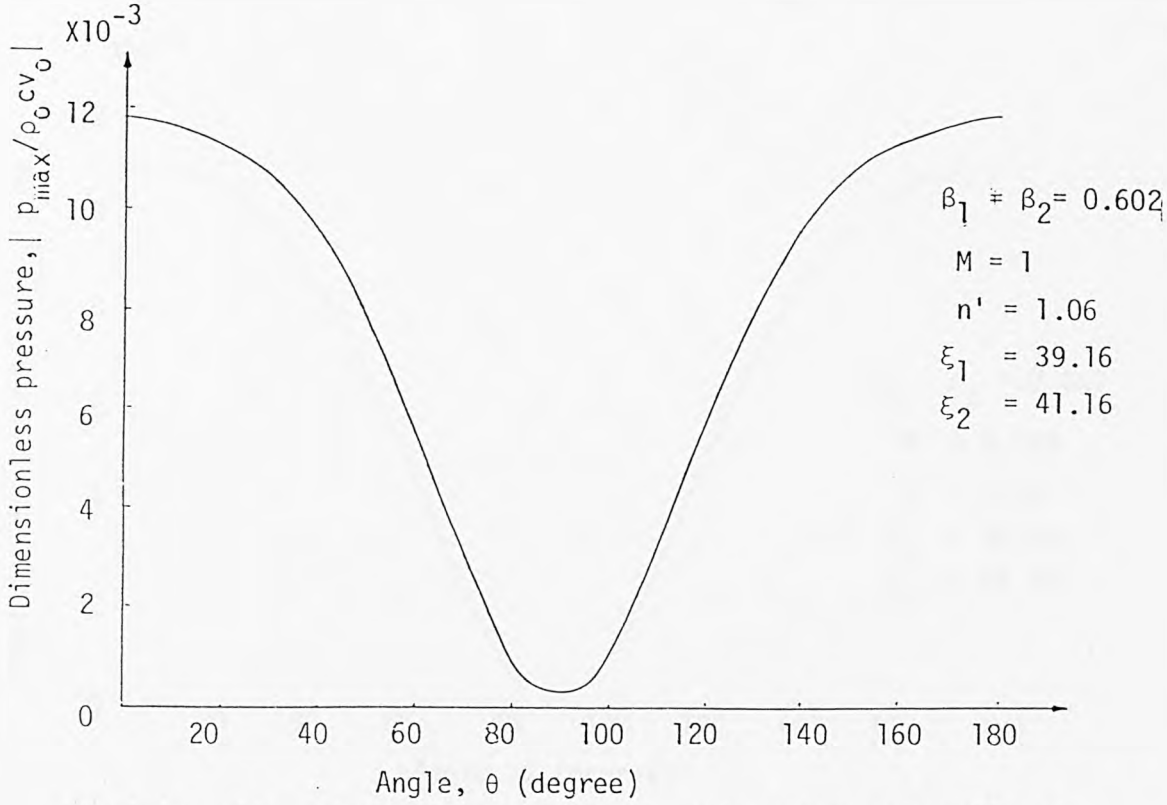

Fig.3.15. Directional distribution of maximum pressure radiated by a pair of similar spheres of equal sizes.

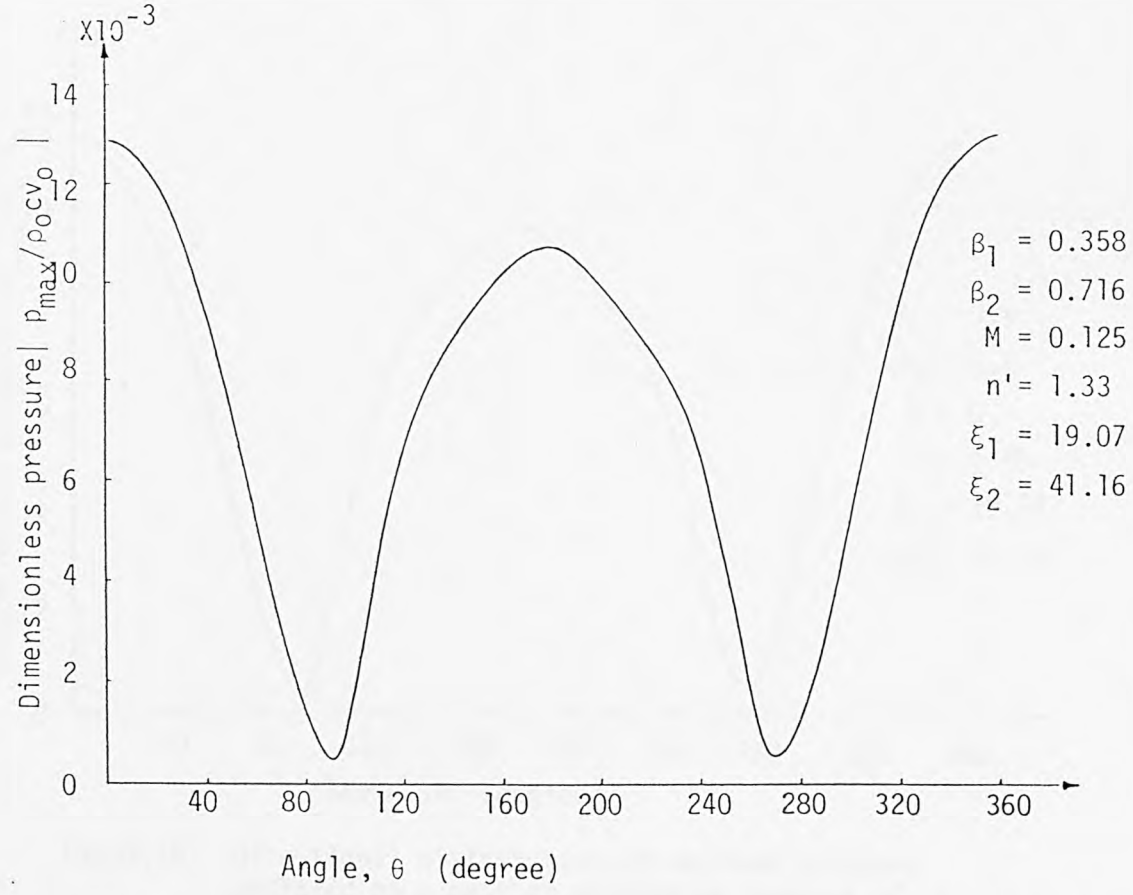

Fig.3.16. Directional distribution of maximum pressure radiated by a pair of similar spheres of unequal sizes.

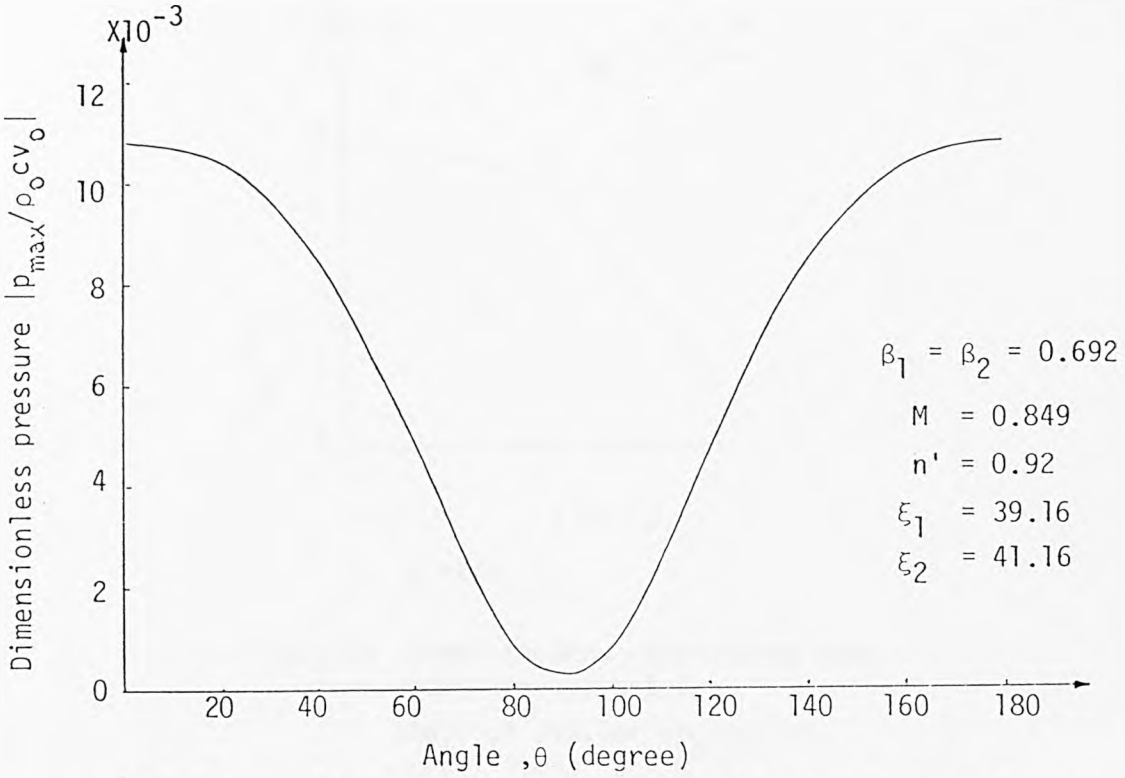

Fig.3.17. Directional distribution of maximum pressure radiated by a pair of dissimilar spheres of equal sizes.

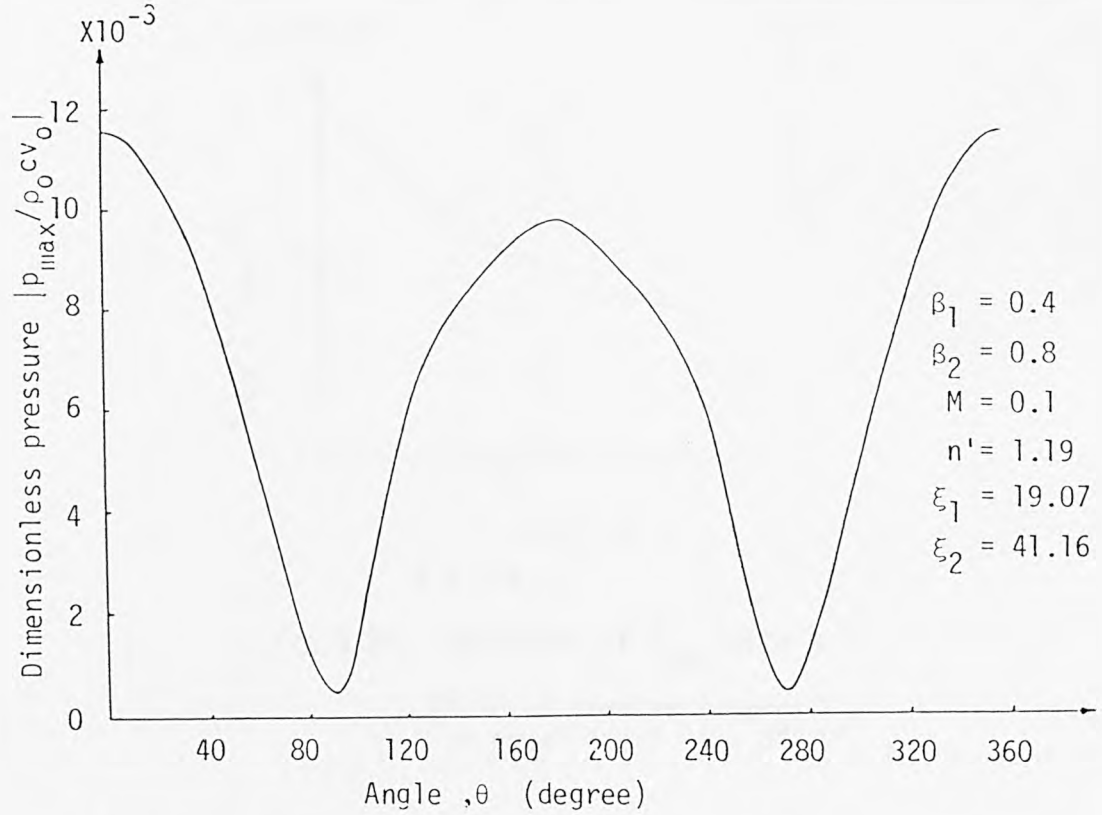

Fig.3.18. Directional distribution of maximum pressure radiated by a pair of dissimilar spheres of unequal sizes.

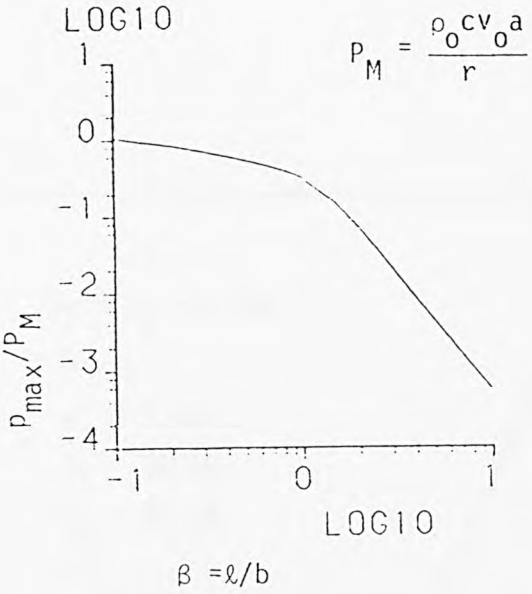

Fig.3.19 Dimensionless rarefactive peak pressure against β.

(Pair of similar spheres of equal radii $\theta = 0^o$.)

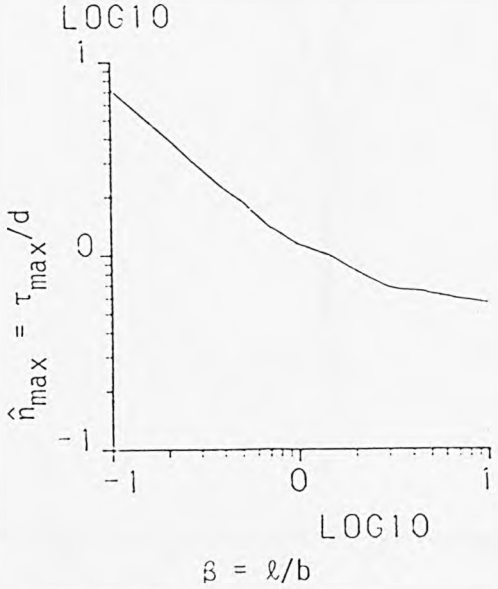

Fig.3.20. Variation of $\hat{n}_{max}$ with β

(Pair of similar spheres of equal radii $\theta = 0^o$)

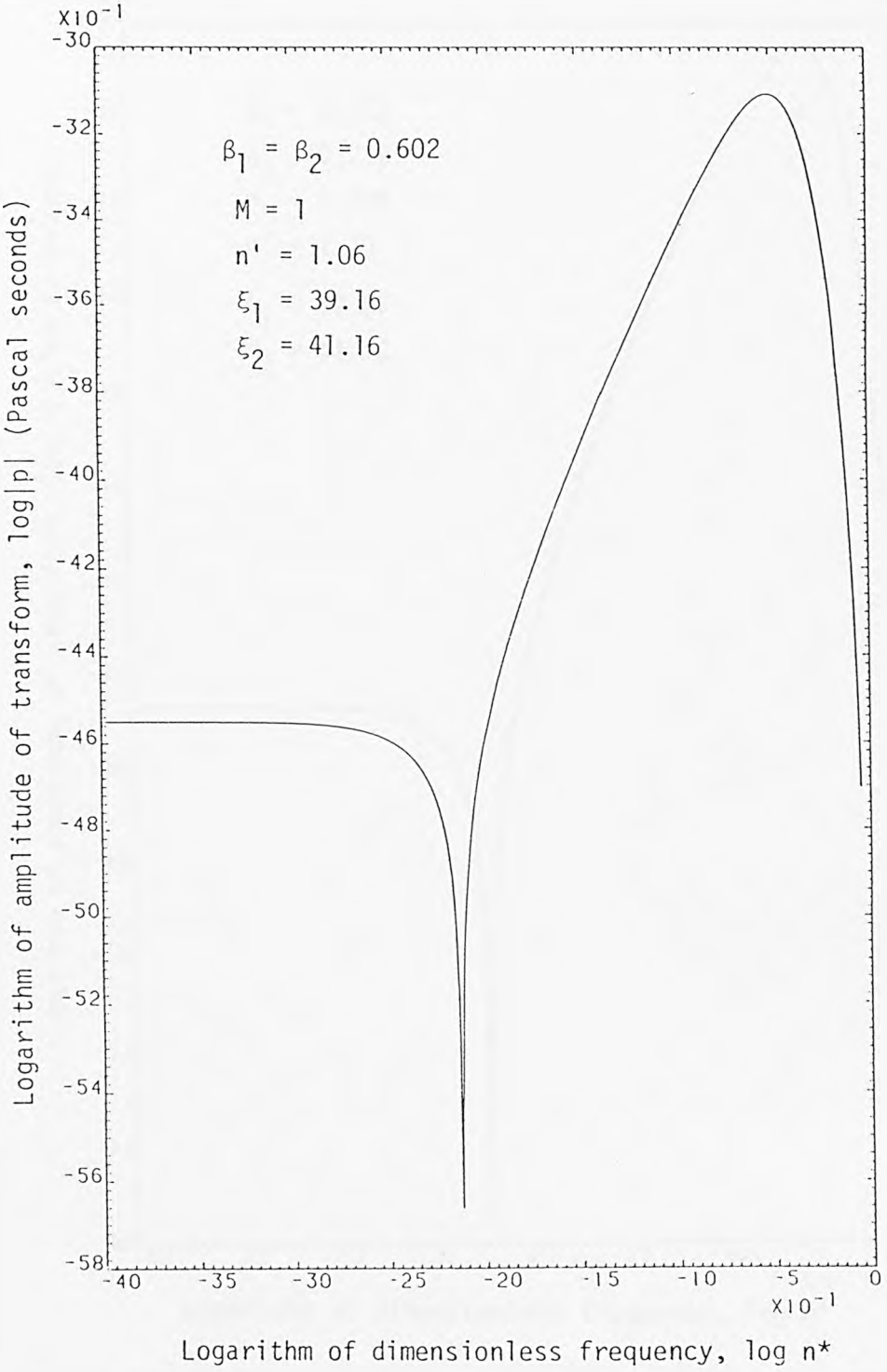

Fig.3.21. Fourier transform of pressure for a pair of similar spheres of equal sizes. (v_o = 1.52 m/s, r = 0.255 m, $\theta = 0^o$)

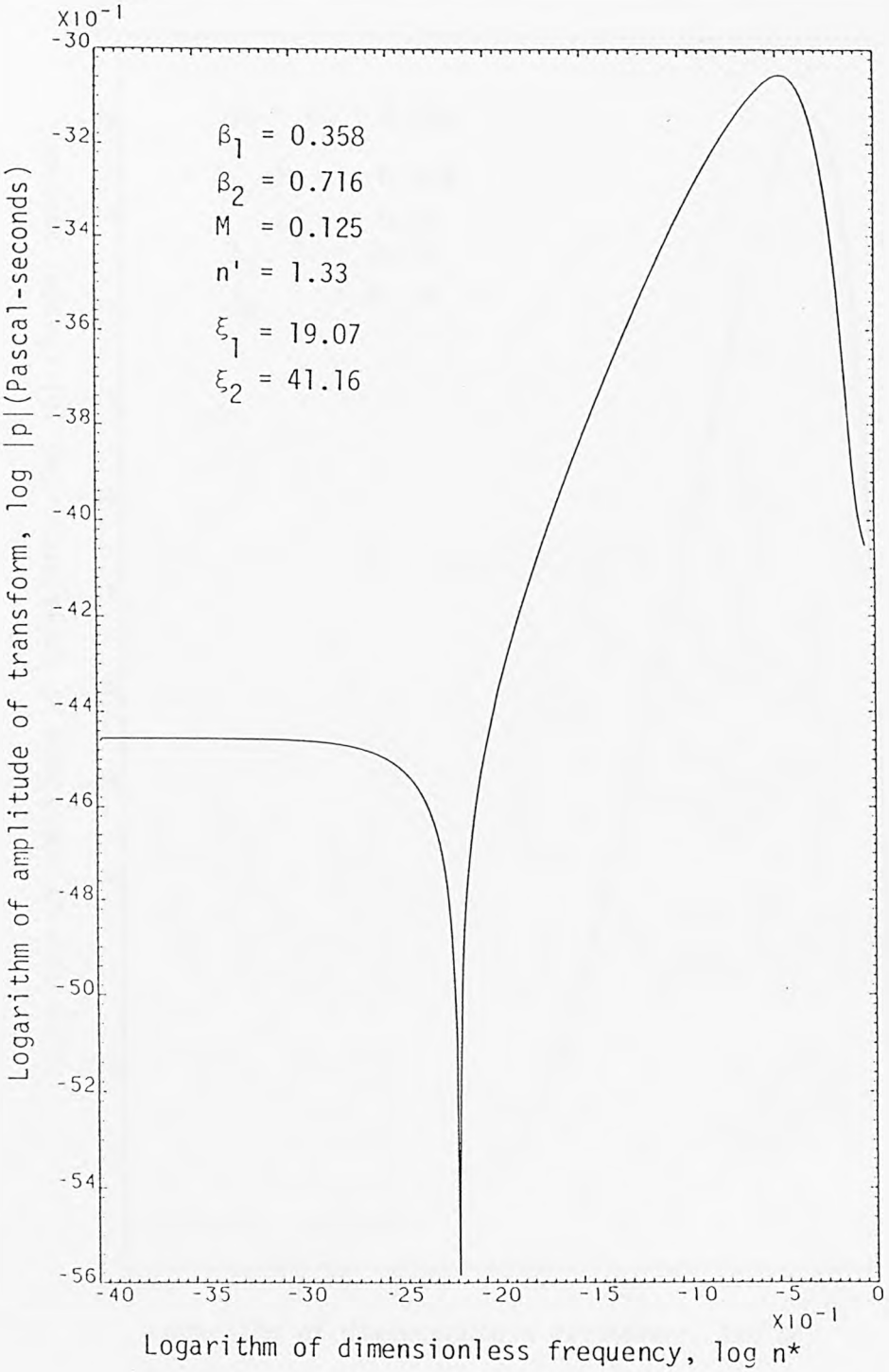

Fig.3.22. Fourier transform of pressure for a pair of similar spheres of unequal sizes, (v_o = 1.52 m/s, r = 0.255 m, $\theta = 0^o$.)

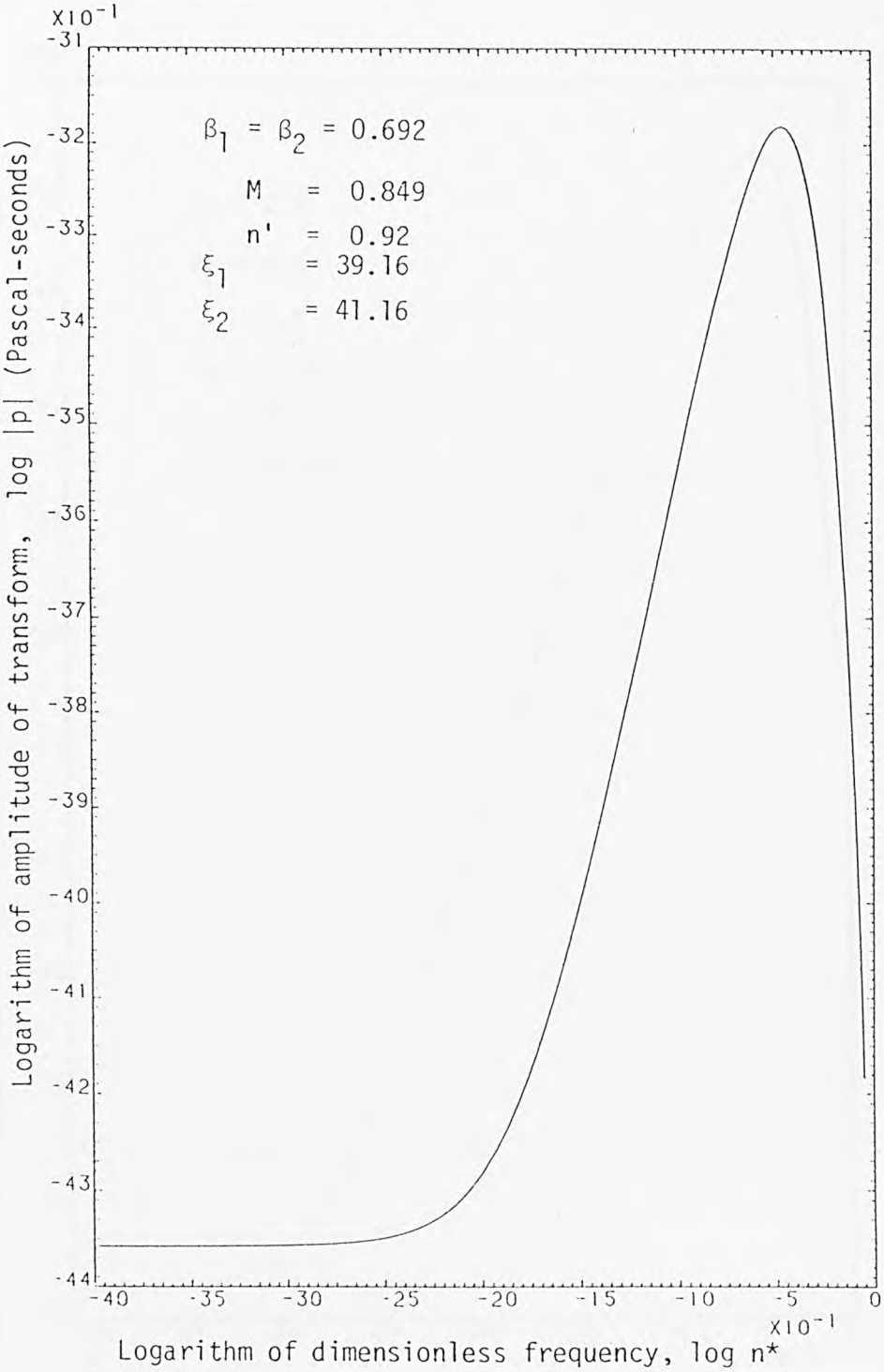

Fig.3.23. Fourier transform of pressure for a pair of dissimilar spheres of equal sizes. (v_o = 1.52 m/s, r = 0.255 m, $\theta = 0^o$.)

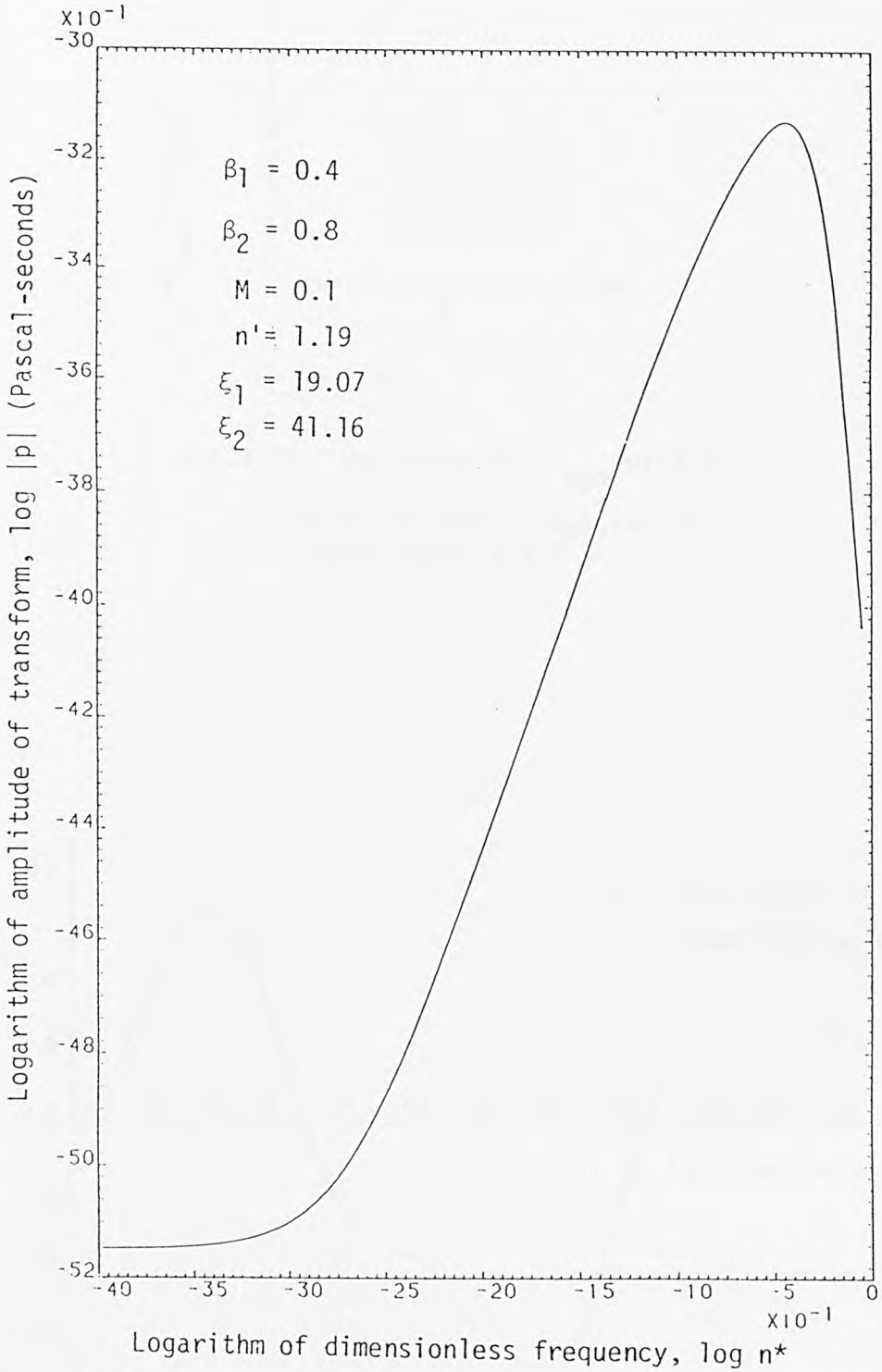

Fig.3.24. Fourier transform of pressure for a pair of dissimilar spheres of unequal sizes. (v_o = 1.52 m/s, r = 0.255 m, $\theta = 0^0$.)

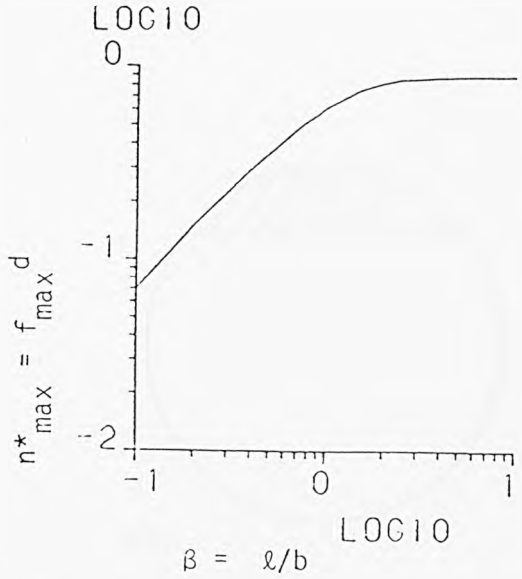

Fig.3.25. Variation of n^*_{max} with β

(Pair of similar spheres of equal radii θ = 0^0)

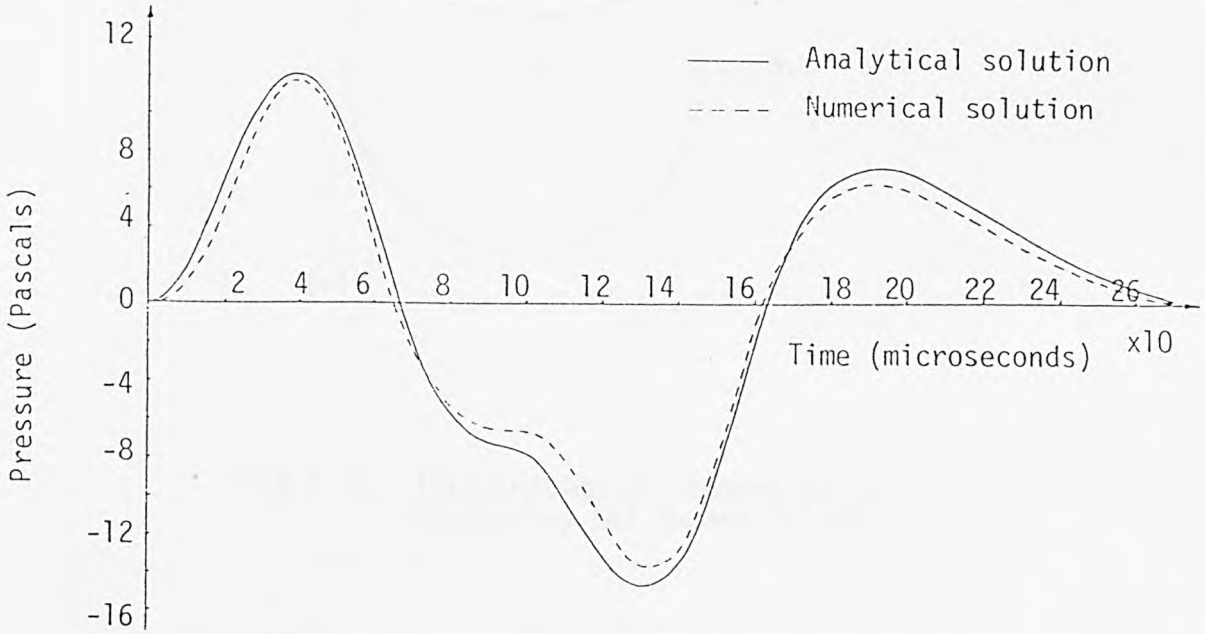

Fig.3.26. Sound pressure time history for 2.54 cm diameter steel sphere with an initial impact velocity 2.5 m/s.

(θ = 0^0, r = 0.375 m)

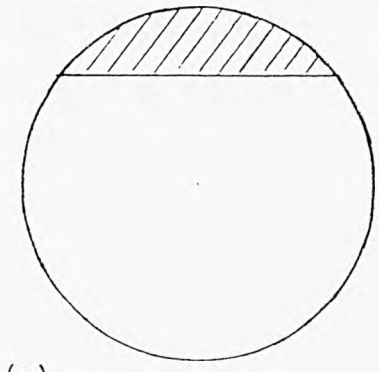

(a)

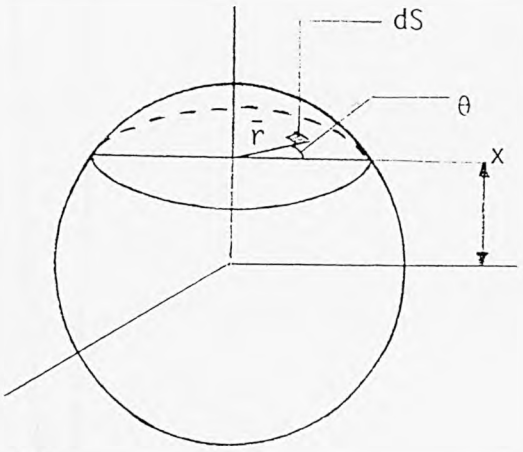

(b)

Fig.3.27. Illustration of element dS for evaluating the shaded volume.

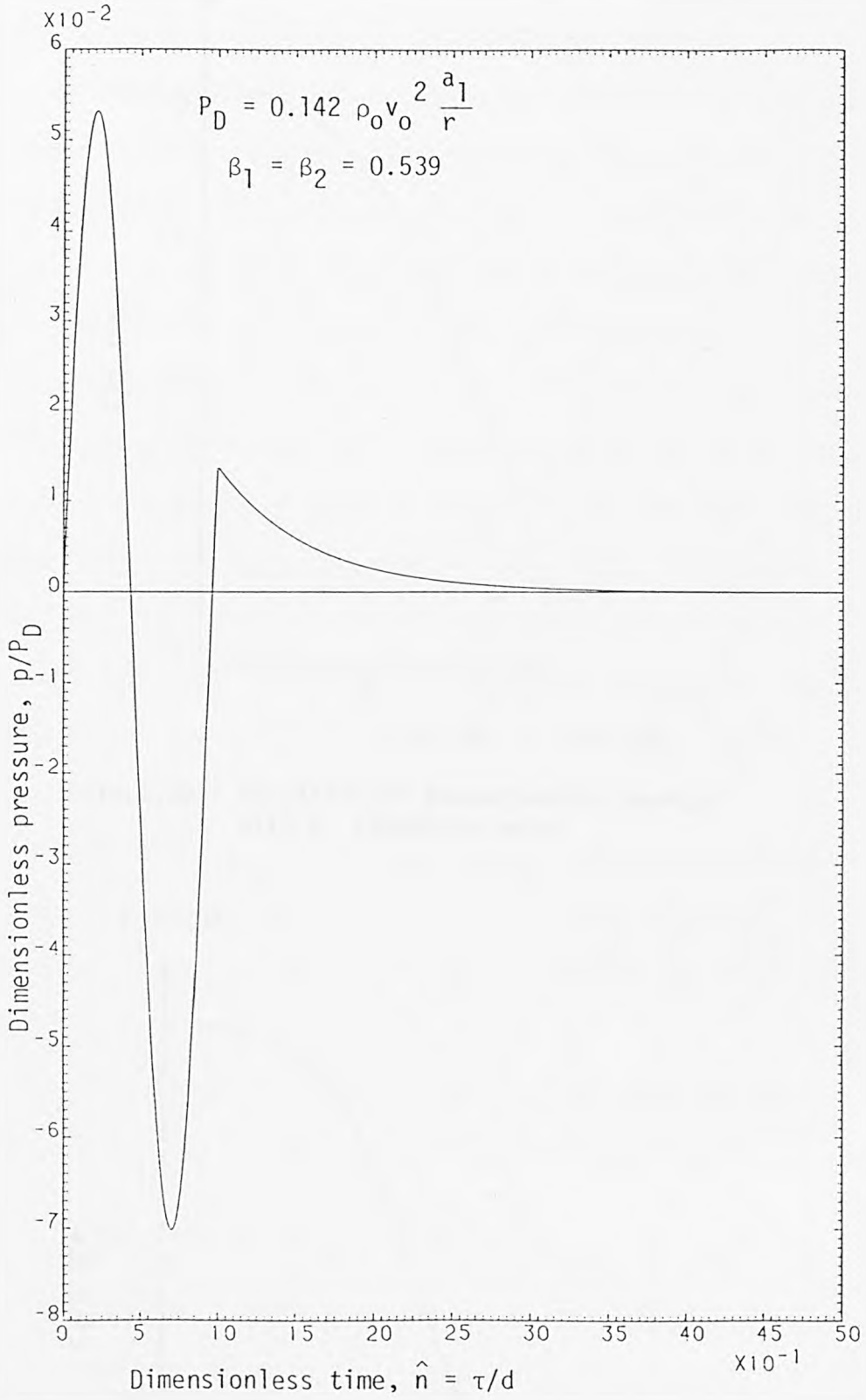

Fig.3.28. Dimensionless pressure time curve due to change of volume of sphere undergoing an elastic collision.

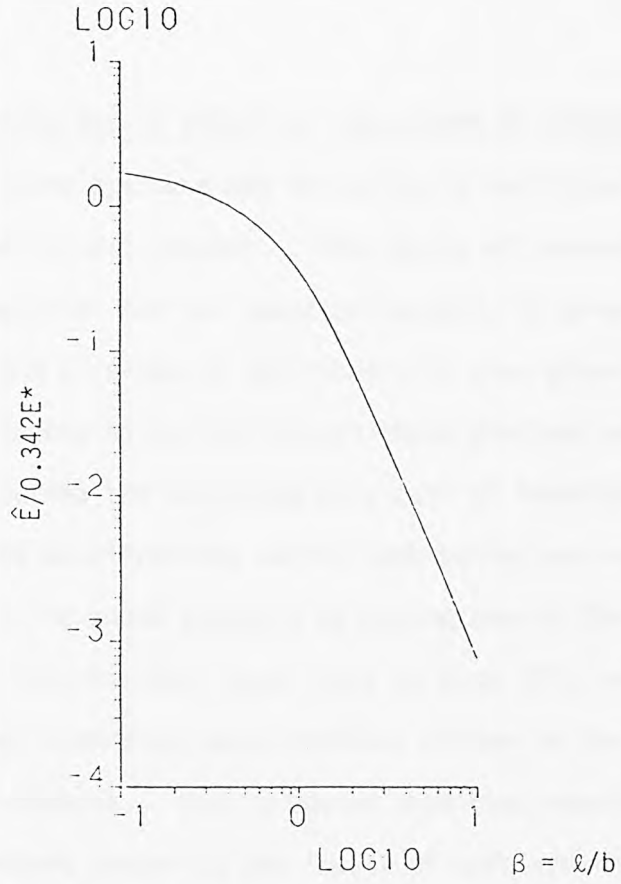

Fig.3.29. Variation of dimensionless energy with β (Impactee only)

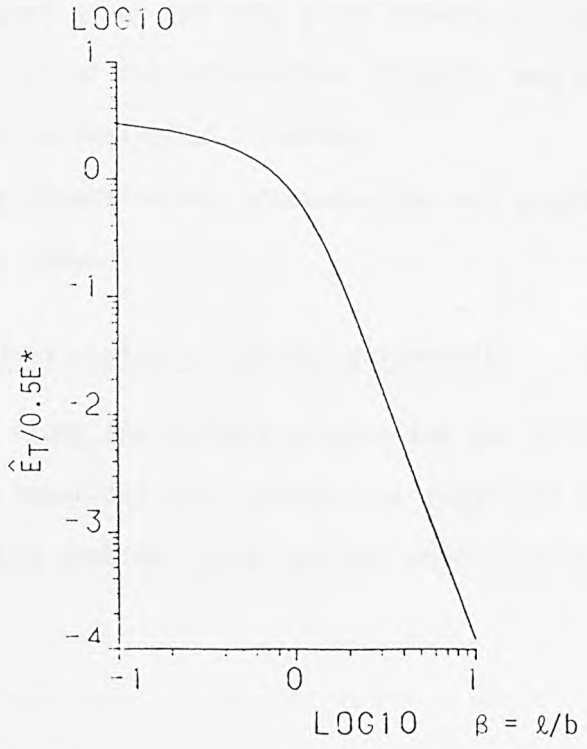

Fig.3.30 Variation of total dimensionless energy with β

(Pair of similar spheres of equal radii)

4. RADIATION DUE TO INELASTIC COLLISIONS OF SPHERES

The sound pressure due to inelastic collision of spheres is studied in this chapter. The theory of inelastic collision of soft material for two identical spheres is given by Andrews [58, 59] and a review of this theory is also given by Goldsmith [43]. According to this theory three distinct periods are existing during the collision of a pair of identical soft spheres. Knowing the accelerations during each period one would be able to predict the sound pressure by making use of the convolution method. This has been done first by Koss [23], who gave no expressions regarding sound pressure either in the time or frequency domains. Koss produced predicted results for the sound pressure caused by the impact of soft spheres, but he gave no information on how these results were derived. It is likely that he calculated the convolution integral numerically. The present study not only gives details of the numerical calculation of the convolution integral, but also provides in addition an analytical solution.

The dimensionless pressure-time and pressure-frequency are also given.

4.1. Elastic-plastic contact deformation

To study the contact deformation due to collision of a pair of identical soft spheres, as suggested by Andrews [58, 59] one should consider three periods which are as follows:

1. an elastic loading period., 2. an elastic-plastic loading period., 3. an elastic unloading period. Each sphere may also be considered as impacting a completely rigid massive plane surface ($E_2 = \infty$ and $m_2 = \infty$) with an initial relative velocity equal to half the relative velocity of the spheres. During the first period the Hertz law of contact is valid, and the following expressions:

$$\delta_1 = \frac{1-\nu^2}{\pi E},\quad \delta_2 = 0,\quad \hat{K}_1 = \frac{1}{m_1},\quad \hat{K}_2 = \frac{4}{3\pi}\frac{\sqrt{a_1}}{\delta_1},$$

$$F_{max} = \hat{K}_2\left(\frac{5}{16}\, v_o^{\,2}\, \frac{m_1}{\hat{K}_2}\right)^{0.6},\quad \alpha_{max} = \left(\frac{5}{16}\, v_o^{\,2}\, \frac{m_1}{\hat{K}_2}\right)^{0.4},$$

$$d = 5.886\, \frac{\alpha_{max}}{v_o},$$

and $$\hat{A}_1(t) = \frac{F_{max}}{m_1} \sin\frac{\pi t}{d} = a_{M1}\sin bt \quad 0< t< t_1 \qquad (4.1)$$

may be found by using equations given in section 2.5, and assuming ($A=B = \frac{1}{2a_1}$ and $q_K = \frac{1}{\pi}$) as shown in reference [43]. The pressure distribution within the contact area of radius $\bar{R}$ may be expressed as:

$$P = \frac{2E[(\bar{R}^2-\bar{r}^2)]^{\frac{1}{2}}}{\pi a_1(1-\nu^2)} \qquad (4.2)$$

where $\bar{r}$ is a distance from the centre of the circle of the contact area. It should be emphasised that an area of contact, in general, has an elliptical shape, but in special cases such as the collision of a sphere and a massive plane or collision of a pair of spheres a contact area of circular shape exists. The first period terminates when the maximum pressure which occurs at the centre

of contact area ($\bar{r}$=0) reaches a critical amount like $\bar{P}_o$. Thus at this instant the radius of the contact area and deformation can be given as:

$$\bar{R}_1 = \frac{\pi \bar{P}_o a_1 (1-\nu^2)}{2E} \tag{4.3a}$$

and

$$\alpha_1 = \frac{\bar{R}_1^2}{a_1} = a_1 \left[\frac{\pi \bar{P}_o (1-\nu^2)}{2E} \right]^2 \tag{4.3b}$$

By making use of equation (2.71) the termination time of the first period may be evaluated to be:

$$t_1 = \int_o^{\alpha_1} \frac{d\alpha}{\dot{\alpha}} = \frac{2}{v_o} \int_o^{\alpha_1} \left[1 - \left(\frac{\alpha}{\alpha_{max}} \right)^{5/2} \right]^{-\frac{1}{2}} d\alpha \tag{4.4}$$

The contact area during the second period consists of two regions: a plastic region which is a circle of radius $\bar{r}_1$, with a constant pressure distribution $\bar{P}_o$ and an elastic region which is an annulus of thickness $\bar{R}-\bar{r}_1$ with a pressure distribution given by equation (4.2). Thus the force in the plastic circle and in the elastic annulus are respectively:

$$F_P = \pi \bar{r}_1^2 \bar{P}_o \tag{4.5a}$$

and

$$F_E = \int_{\bar{r}_1}^{R} 2\pi \bar{r} P d\bar{r} = \int_{\bar{r}_1}^{R} \frac{4E\bar{r}[(\bar{R}^2-\bar{r}^2)]^{\frac{1}{2}}}{a_1(1-\mu^2)} d\bar{r} = \frac{4}{3} \frac{E(\bar{R}^2-\bar{r}_1^2)^{3/2}}{a_1(1-\nu^2)} \tag{4.5b}$$

Inserting the conditions $P = \bar{P}_o$ at $\bar{r} = \bar{r}_1$ into the equation (4.2) gives:

$$\bar{R}^2 - \bar{r}_1^2 = \frac{\pi^2 a_1^2 \bar{P}_o^2 (1-\nu^2)^2}{4E^2} \tag{4.6}$$

By making use of the above expression, F_P and F_E may be written as:

$$F_P = \pi \bar{P}_o \left[\bar{R}^2 - \frac{\pi^2 a_1^2 \bar{P}_o^2 (1-\nu^2)^2}{4E^2} \right] \tag{4.7a}$$

and

$$F_E = \frac{\pi^3 \bar{P}_o^3 a_1^2 (1-\nu^2)^2}{6E^2} \tag{4.7b}$$

Thus the total force in the second period is:

$$F_{EP} = \pi \bar{P}_o \alpha a_1 - \frac{1}{12} \frac{\pi^3 \bar{P}_o^3 a_1^2 (1-\nu^2)^2}{E^2} \tag{4.8}$$

where $\alpha = \frac{\bar{R}^2}{a_1}$. The equation of motion may now be written as:

$$F_{EP} = -m_1 \ddot{\alpha} = m_1 \eta^2 \alpha - \frac{1}{3} m_1 \eta^2 \alpha_1 \tag{4.9}$$

where $\eta^2 = \frac{\pi \bar{P}_o a_1}{m_1}$. By making use of equation (2.68) the initial velocity at the beginning of the second period may be expressed as:

$$\dot{\alpha}_1 = \left(\frac{1}{4} v_o^2 - \frac{4}{5} \frac{\hat{K}_2}{m_1} \alpha_1^{5/2} \right)^{1/2} \tag{4.10}$$

Thus the solution to the differential equation (4.9) is:

$$\dot{\alpha}^2 = -\eta^2 \alpha^2 + \frac{2}{3} \eta^2 \alpha_1 \alpha + \frac{1}{3} \eta^2 \alpha_1^2 + \dot{\alpha}_1^2 \tag{4.11}$$

When α is maximum the relative velocity $\dot{\alpha}$ is equal to zero. Thus from equation (4.11):

$$\bar{\alpha}_{max} = \frac{1}{3}\alpha_1 + \left(\frac{4}{9}\alpha_1^2 + \frac{\dot{\alpha}_1^2}{\eta^2}\right)^{\frac{1}{2}} \tag{4.12}$$

To evaluate the approach-time relation, one may write equation (4.11) in the form:

$$\hat{t} = \frac{1}{\eta}\int_{\alpha_1/\bar{\alpha}_{max}}^{\alpha/\bar{\alpha}_{max}} \frac{dZ^*}{\sqrt{(1-Z^*)(1+Z^*-K^*)}} \tag{4.13}$$

where $Z^* = \frac{\alpha}{\bar{\alpha}_{max}}$, $K^* = \frac{2}{3}\frac{\alpha_1}{\bar{\alpha}_{max}}$, and $\hat{t} = t - t_1$. The solution to equation (4.13) may be expressed as:

$$\alpha = \frac{1}{3}\alpha_1 + (\bar{\alpha}_{max} - \frac{1}{3}\alpha_1)\sin(\eta\hat{t} + \delta^*) \tag{4.14}$$

where $\tan\delta^* = \frac{2}{3}\eta\frac{\alpha_1}{\dot{\alpha}_1}$. By making use of equation (4.14) the acceleration and duration of the second period may be written as:

$$\hat{A}_2(t) = (\bar{\alpha}_{max} - \frac{1}{3}\alpha_1)\eta^2\sin(\eta\hat{t} + \delta^*) \quad t_1 < t < t_1 + t_2 \tag{4.15a}$$

$$t_2 = \frac{1}{\eta}\left(\frac{\pi}{2} - \delta^*\right) \tag{4.15b}$$

Consider now the final period which is an elastic unloading from $\bar{\alpha}_{max}$ given by equation (4.12) to the permanent deformation like α_F. During this period it may be assumed that the plastic

region which is created during the second period returns elastically to the original surface of the sphere, so that at the end of the period the permanent deformation can be given by $\alpha_F = \frac{\bar{r}_2^2}{a_1}$, where $\bar{r}_2$ is the radius of the circle of the plastic region at the end of the second period. The total force as given in reference [43] is:

$$F_{EU} = \frac{2E}{a_1(1-\nu^2)}\left[\frac{2}{3}(\bar{R}^2 - \bar{r}_2^2)^{3/2} + \bar{r}_2^2(\bar{R}^2 - \bar{r}_2^2)^{1/2}\right] \tag{4.16}$$

Substituting $\bar{R}^2 = a_1\alpha$ into the above equation and using Newton's second law gives:

$$\ddot{\alpha} = \frac{-2E}{a_1(1-\nu^2)m_1}\left[\frac{2}{3}(a_1\alpha - \bar{r}_2^2)^{3/2} + \bar{r}_2^2(a_1\alpha - \bar{r}_2^2)^{1/2}\right] \tag{4.17}$$

By making use of equation (4.6) the radius of the plastic circle at the end of the second period may be written as:

$$\bar{r}_2 = \left[a_1(\bar{\alpha}_{max} - \alpha_1)\right]^{1/2} = (a_1\alpha_F)^{1/2} \tag{4.18}$$

where $\bar{\alpha}_{max}$ is given by equation (4.12). By introducing the initial conditions ($\alpha = \bar{\alpha}_{max}$ and $\dot{\alpha} = 0$) the solution to the non-linear differential equation (4.17) may be expressed as:

$$\dot{\bar{Z}}^2 = \beta^{*2}\alpha_1^{-1/2}\left[\frac{2}{5}\alpha_1(1 - \bar{Z}^{5/2}) + (\bar{\alpha}_{max} - \alpha_1)(1 - \bar{Z}^{3/2})\right] \tag{4.19}$$

where $\beta^{*2} = \dfrac{8E\sqrt{a_1}}{3(1-\nu^2)m_1}$ and $\bar{Z} = \dfrac{\alpha + \alpha_1 - \bar{\alpha}_{max}}{\alpha_1}$

The duration and acceleration of the third period may now be given by:

$$t_3 = -\frac{\alpha_1^{\frac{1}{4}}}{\beta^*} \int_0^1 \left[\frac{2}{5}\alpha_1(1-\bar{Z}^{5/2}) + (\bar{\alpha}_{max} - \alpha_1)(1-\bar{Z}^{3/2})\right]^{-\frac{1}{2}} d\bar{Z} \tag{4.20}$$

and

$$\hat{A}_3(t) = \eta^2(\bar{\alpha}_{max} - \frac{1}{3}\alpha_1)\cos b^* t^* \qquad t_1+t_2 < t < t_1+t_2+t_3 \tag{4.21}$$

where $b^* = \dfrac{\pi}{2t_3}$,

and $t^* = t-(t_1 + t_2)$. Equations given in this section as shown by Koss [23] may be used for evaluating the sound pressure generated by the collision of soft spheres. Thus by using equation (3.10) one may find that:

$$p(r,\theta,\tau) = \int_0^{\tau} p_{UI}(r,\theta,\tau-\zeta)\left[\hat{A}_1(\zeta) + \hat{A}_2(\zeta) + \hat{A}_3(\zeta)\right] d\zeta$$

$$t_1 + t_2 < \tau \leq t_1 + t_2 + t_3 \tag{4.22}$$

where $p(r,\theta,\tau)$ is the sound pressure generated by each sphere. The total sound pressure can be expressed in the similar form as given by equation (3.52a).

4.2. Numerical Solution of Sound Pressure

The sound pressure due to inelastic collision of spheres may be calculated numerically by employing steps as follows:

1. Calculation of termination time of each period.
2. Numerical estimation of force or acceleration at different instants during each period.
3. Evaluation of sound pressure at different instants during each period and after termination of last period.

To make the above steps more clear, let us consider an instant τ defined by $0 < \tau < t_1$, where t_1 is the termination time of the first period given by equation (4.4). Equation (4.4.) is a function of α and may be written as:

$$t_1 = \int_0^{\alpha_1} g(\alpha)\, d\alpha \qquad (4.23)$$

where $g(\alpha) = \frac{2}{v_o}[1 - (\frac{\alpha}{\alpha_{max}})^{5/2}]^{-\frac{1}{2}}$. To solve (4.23) one may use the trapezoidal rule which is a well known method as well as Simpson's rule for solving an integral numerically. So the integral on the right hand side of equation (4.23) may be found approximately to be:

$$t_1 \simeq \frac{h}{2}[g(\alpha)\Big|_{\alpha=0} + 2g(\alpha)\Big|_{\alpha=h} + \ldots + 2g(\alpha)\Big|_{\alpha=(n-1)h} + g(\alpha)\Big|_{\alpha=nh}] \qquad (4.24)$$

where $h = \frac{\alpha_1}{n}$ and n is an integer. By making use of equation (2.67) the differential form of acceleration during the first period may be written as:

$$\hat{A}_1(t) = \frac{F}{m_1} = \frac{\hat{K}_2 \alpha^{3/2}}{m_1} = \hat{K}_1 \hat{K}_2 \alpha^{3/2} = -\ddot{\alpha} \qquad (4.25)$$

Thus to find the acceleration at different instants during the first period one must solve a differential equation in the form of:

$$\ddot{\alpha} = - \hat{K}_1 \hat{K}_2 \alpha^{3/2} \qquad (4.26)$$

Many methods, such as Runge-Kutta, Numerov's and Taylor's expansion are suggested in references [60 and 61] for solving the differential equation. Let us now use the Taylor's expansion method for solving equation (4.26). According to the Taylor's expansion formula the value of α at instant $t = \Delta t$ may be expressed in terms of successive derivative of α with respect to t at instant t= 0 as:

$$\alpha\Big|_{t=\Delta t} = \alpha\Big|_{t=0} + \Delta t \dot{\alpha}\Big|_{t=0} + \frac{(\Delta t)^2}{2!}\ddot{\alpha}\Big|_{t=0} + \ldots \qquad (4.27)$$

where $\Delta t = \frac{t_1}{n}$ and n is an integer.

The initial conditions at instant t = 0 are:

$$\alpha\Big|_{t=0} = 0 \ , \quad \dot{\alpha}\Big|_{t=0} = \frac{v_o}{2} \qquad (4.28)$$

and the higher order derivatives at the same instant may be

found to be zero by the use of equation (4.26). The value of α at $t = \Delta t$ may now be simply estimated by substituting the initial conditions into equation (4.27). Thus the corresponding $\ddot{\alpha}$ can be evaluated from (4.26). To repeat the process one needs to estimate the first derivative. It can be easily shown graphically that:

$$\dot{\alpha}\Big|_{t=n\Delta t} \simeq \frac{\alpha\Big|_{t=(n+1)\Delta t} - \alpha\Big|_{t=(n-1)\Delta t}}{2\Delta t} \tag{4.29}$$

Using now the Taylor's formula to estimate the value of α at $t = 2\Delta t$ and ignoring the derivatives of higher than second gives:

$$\alpha\Big|_{t=2\Delta t} \simeq \alpha\Big|_{t=\Delta t} + \Delta t\dot{\alpha}\Big|_{t=\Delta t} + \frac{(\Delta t)^2}{2!}\ddot{\alpha}\Big|_{t=\Delta t} \tag{4.30}$$

Estimating the value of $\dot{\alpha}$ at $t = \Delta t$ by making use of equation (4.29) and substituting into equation (4.30) yields:

$$\alpha\Big|_{t=2\Delta t} \simeq 2\alpha\Big|_{t=\Delta t} - \alpha\Big|_{t=0} + (\Delta t)^2\ddot{\alpha}\Big|_{t=\Delta t} \tag{4.31}$$

or more generally,

$$\alpha\Big|_{t=n\Delta t} \simeq 2\alpha\Big|_{t=(n-1)\Delta t} - \alpha\Big|_{t=(n-2)\Delta t} + (\Delta t)^2\ddot{\alpha}\Big|_{t=(n-1)\Delta t}$$

$$n \geqslant 2 \tag{4.32}$$

Thus, at each iteration one would be able to calculate α and consequently $\ddot{\alpha}$. Having calculated $\ddot{\alpha}$ both force and acceleration may be found from (4.25) to be:

$$F\Big|_{t=n\Delta t} = -m_1\ddot{\alpha}\Big|_{t=n\Delta t} \qquad n \geqslant 0 \qquad (4.33a)$$

and

$$\hat{A}_1\Big|_{t=n\Delta t} = -\ddot{\alpha}\Big|_{t=n\Delta t} \qquad n \geqslant 0 \qquad (4.33b)$$

To estimate the sound pressure the convolution integral (4.22) may be written as:

$$p(r,\theta,\tau) = \int_{\zeta=0}^{\zeta=\tau} p_{UI}(r,\theta,\tau-\zeta)\hat{A}_1(\zeta)d\zeta$$

$$0 \leqslant \tau \leqslant t_1 \qquad (4.34)$$

where p_{UI} can be given by equation (3.7) after substituting v_o equal to unity. By making use of equation (4.34) the sound pressure at $\tau = n\Delta t$ can be expressed as:

$$p(r,\theta, n\Delta t) = \int_{\zeta=0}^{\zeta=n\Delta t} p_{UI}(r,\theta,n\Delta t-\zeta)\hat{A}_1(\zeta)d\zeta$$

$$0 \leqslant n\Delta t \leqslant t_1 \qquad (4.35)$$

Using now the trapezoidal rule to calculate (4.35) numerically gives:

$$p(r,\theta,n\Delta t) = \frac{\Delta t}{2}\Big[p_{UI}(r,\theta,n\Delta t-0)\hat{A}_1(0)+2p_{UI}(r,\theta,n\Delta t-\Delta t)\hat{A}_1(\Delta t)$$

$$+....+2p_{UI}[r,\theta,n\Delta t-(n-1)\Delta t]\hat{A}_1[(n-1)\Delta t]$$

$$+\ p_{UI}(r,\theta,n\Delta t-n\Delta t)\hat{A}_1(n\Delta t)\Big]$$

$$0 \leqslant n\Delta t \leqslant t_1 \qquad (4.36)$$

By making use of (4.36) the sound pressure at different instants of the first period can be evaluated. Consider now instant τ defined by $t_1<\tau< t_1+t_2$, where t_2 is the duration of the second period given by equation (4.15b). The duration of the second period can also be given by equation (4.13) as:

$$t_2 = \frac{1}{\eta} \int_{\alpha_1}^{\bar{\alpha}_{max}} [(\bar{\alpha}_{max}-\alpha)(\alpha- \tfrac{2}{3}\alpha_1 + \bar{\alpha}_{max})]^{-\frac{1}{2}} d\alpha \quad (4.37)$$

Using the trapezoidal rule to evaluate (4.37) numerically gives:

$$t_2 \simeq \frac{\bar{h}}{2}[\bar{f}(\alpha)\Big|_{\alpha=0} + 2\bar{f}(\alpha)\Big|_{\alpha=\bar{h}} + \ldots 2\bar{f}(\alpha)\Big|_{\alpha=(\bar{n}-1)\bar{h}} + \bar{f}(\alpha)\Big|_{\alpha=\bar{n}\bar{h}}] \quad (4.38)$$

where $\bar{f}(\alpha) = \frac{1}{\eta}[(\bar{\alpha}_{max}-\alpha)(\alpha- \frac{2}{3}\alpha_1 + \bar{\alpha}_{max})]^{-\frac{1}{2}}$, $\bar{h} = \frac{\bar{\alpha}_{max} - \alpha_1}{\bar{n}}$, and $\bar{n}$ is an integer. In order to find the acceleration at different instants during the second period one must solve a differential equation in the form of:

$$\ddot{\alpha} = -\eta^2\alpha + \frac{1}{3}\eta^2\alpha_1 \quad (4.39)$$

with initial conditions:

$$\left.\begin{aligned} \alpha &= \alpha_1 \\ \dot{\alpha} &= \dot{\alpha}_1 \end{aligned}\right| \quad \text{at } t = t_1 \quad (4.40)$$

This can be done easily by using Taylor's expansion method and following similar procedures as given previously for solving

equation (4.26). Thus at any instant during the second period the force and acceleration can be given by:

$$F\Big|_{t=t_1+\bar{n}\overline{\Delta t}} = -m_1\ddot{\alpha}\Big|_{t=t_1+\bar{n}\overline{\Delta t}} \qquad \bar{n} > 0 \qquad (4.41a)$$

$$\hat{A}_2\Big|_{t=t_1+\bar{n}\overline{\Delta t}} = -\ddot{\alpha}\Big|_{t=t_1+\bar{n}\overline{\Delta t}} \qquad \bar{n} > 0 \qquad (4.41b)$$

where $\overline{\Delta t} = \dfrac{t_2}{\bar{n}}$. The sound pressure at $\tau = t_1+\bar{n}\overline{\Delta t}$ may now be found by use of the trapezoidal rule to be:

$$\begin{aligned} p(r,\theta,t_1+\bar{n}\overline{\Delta t}) = \frac{\Delta t}{2}\Big[& p_{UI}(r,\theta,t_1+\bar{n}\overline{\Delta t}-0)\hat{A}_1(0) \\ & +2p_{UI}(r,\theta,t_1+\bar{n}\overline{\Delta t}-\Delta t)\hat{A}_1(\Delta t)+.... \\ & +2p_{UI}[r,\theta,t_1+\bar{n}\overline{\Delta t}-(n-1)\Delta t]\,\hat{A}_1[(n-1)\Delta t] \\ & +p_{UI}(r,\theta,t_1+\bar{n}\overline{\Delta t}-n\Delta t)\hat{A}_1(n\Delta t)\Big] \\ & + \frac{\overline{\Delta t}}{2}\Big[p_{UI}(r,\theta,t_1+\bar{n}\overline{\Delta t}-t_1)\hat{A}_2(t_1) \\ & +2p_{UI}[r,\theta,t_1+\bar{n}\overline{\Delta t}-(t_1+\overline{\Delta t})]\,\hat{A}_2(t_1+\overline{\Delta t}) \\ & +..... \\ & +2p_{UI}[r,\theta,t_1+\bar{n}\overline{\Delta t}-[t_1+(\bar{n}-1)\overline{\Delta t}]]\hat{A}_2[t_1+(\bar{n}-1)\overline{\Delta t}] \\ & +p_{UI}[r,\theta,t_1+\bar{n}\overline{\Delta t}-(t_1+\bar{n}\overline{\Delta t})]\hat{A}_2(t_1+\bar{n}\overline{\Delta t})\Big] \end{aligned}$$

$$t_1 < t_1 + \bar{n}\overline{\Delta t} \leq t_1+t_2 \qquad (4.42)$$

Let us now apply the trapezoidal rule to calculate the integral on the right hand side of equation (4.20). One can obtain:

$$t_3 \simeq \frac{\bar{\bar{h}}}{2}\left[\bar{\bar{f}}(\bar{z})\Big|_{\bar{z}=0} + 2\bar{\bar{f}}(\bar{z})\Big|_{\bar{z}=\bar{\bar{h}}} + \ldots 2\bar{\bar{f}}(\bar{z})\Big|_{\bar{z}=(\bar{\bar{n}}-1)\bar{\bar{h}}} + \bar{\bar{f}}(\bar{z})\Big|_{\bar{z}=\bar{\bar{n}}\bar{\bar{h}}}\right] \tag{4.43}$$

where $\bar{\bar{f}}(\bar{z}) = -\frac{\alpha_1}{\beta^*}^{\frac{1}{4}}\left[\frac{2}{5}\alpha_1(1-\bar{z}^{5/2}) + (\bar{\alpha}_{max}-\alpha_1)(1-\bar{z}^{3/2})\right]^{-\frac{1}{2}}$, $\bar{\bar{h}} = \frac{1}{\bar{\bar{n}}}$ and $\bar{\bar{n}}$ is an integer. The differential equation needs to be solved numerically is equation (4.17) with initial conditions:

$$\alpha\Big|_{t=t_1+t_2} = \bar{\alpha}_{max} \tag{4.44a}$$

and

$$\dot{\alpha}\Big|_{t=t_1+t_2} = 0 \tag{4.44b}$$

By following a similar process as before the force, acceleration and the sound pressure at $t_1 + t_2 < \tau < t_1+t_2+t_3$ can be determined. It is clear that the acceleration at any instant $\tau > t_1+t_2+t_3$ is equal to zero. Thus the sound pressure at instant $\tau = \bar{d}+\bar{\bar{n}}\bar{\bar{\Delta t}}$ can be given by:

$$
\begin{aligned}
p(r,\theta,\bar{d}+\bar{\bar{n}}\bar{\bar{\Delta t}}) = \frac{\Delta t}{2}\Big[& p_{UI}(r,\theta,\bar{d}+\bar{\bar{n}}\bar{\bar{\Delta t}}-0)\hat{A}_1(0)+2p_{UI}(r,\theta,\bar{d}+\bar{\bar{n}}\bar{\bar{\Delta t}}-\Delta t)\hat{A}_1(\Delta t) \\
& +\cdots\cdots+2p_{UI}[r,\theta,\bar{d}+\bar{\bar{n}}\bar{\bar{\Delta t}}-(n-1)\Delta t]\hat{A}_1 \\
& [(n-1)\Delta t]+ p_{UI}(r,\theta,\bar{d}+\bar{\bar{n}}\bar{\bar{\Delta t}}-n\Delta t)\hat{A}_1(n\Delta t)\Big] \\
+ \frac{\bar{\Delta t}}{2}\Big[& p_{UI}(r,\theta,\bar{d}+\bar{\bar{n}}\bar{\bar{\Delta t}}-t_1)\hat{A}_2(t_1)+\cdots\cdots \\
& +2p_{UI}[r,\theta,\bar{d}+\bar{\bar{n}}\bar{\bar{\Delta t}}-(t_1+\bar{\Delta t})]\hat{A}_2(t_1+\bar{\Delta t})+\cdots \\
& +2p_{UI}[r,\theta,\bar{d}+\bar{\bar{n}}\bar{\bar{\Delta t}}-[t_1+(\bar{n}-1)\bar{\Delta t}]]\hat{A}_2[t_1+(\bar{n}-1)\bar{\Delta t}] \\
& +p_{UI}[r,\theta,\bar{d}+\bar{\bar{n}}\bar{\bar{\Delta t}}-(t_1+\bar{n}\bar{\Delta t})]\hat{A}_2(t_1+\bar{n}\bar{\Delta t})\Big] \\
+ \frac{\bar{\bar{\Delta t}}}{2}\Big[& p_{UI}[r,\theta,\bar{d}+\bar{\bar{n}}\bar{\bar{\Delta t}}-(t_1+t_2)]\hat{A}_3(t_1+t_2) \\
& +2p_{UI}[r,\theta,\bar{d}+\bar{\bar{n}}\bar{\bar{\Delta t}}-(t_1+t_2+\bar{\bar{\Delta t}})]\hat{A}_3(t_1+t_2+\bar{\bar{\Delta t}})+\cdots \\
& +2p_{UI}[r,\theta,\bar{d}+\bar{\bar{n}}\bar{\bar{\Delta t}}-[t_1+t_2+(\bar{\bar{n}}-1)\bar{\bar{\Delta t}}]]\hat{A}_3 \\
& [t_1+t_2+(\bar{\bar{n}}-1)\bar{\bar{\Delta t}}]+p_{UI}[r,\theta,\bar{d}+\bar{\bar{n}}\bar{\bar{\Delta t}}-(t_1+t_2+\bar{\bar{n}}\bar{\bar{\Delta t}})] \\
& A_3(t_1+t_2+\bar{\bar{n}}\bar{\bar{\Delta t}})\Big]
\end{aligned}
$$

$$\tau > \bar{d} \qquad (4.45)$$

where $\bar{d} = t_1+t_2+t_3$ is the total contact duration, $\bar{\bar{\Delta t}} = \frac{t_3}{\bar{\bar{n}}}$, and $\bar{\bar{n}}$ is an integer. It should be emphasised that the numerical method described in this section is not necessarily the best method but it is the simplest one. The accuracy of the results may be increased if, instead of using equation (4.29) for estimating the first derivative, the actual equation such as (4.11) and (4.19) are used. More accurate results can also be obtained by taking derivatives higher than second into account. Graphs showing variations of force versus time for 2.54 cm diameter lead spheres

with an initial impact velocity of 0.55 m/s is given in Fig.(4.1).

4.3. Sound radiation from a sphere subjected to inelastic collision by a sphere (Analytical Solution)

The sound pressure due to inelastic collision of spheres can also be given analytically by using the convolution integral. Using acceleration given by equation (4.1) together with response to unit impulse expressed by (3.7) and substituting in (3.10) gives:

$$p_1(r,\theta,\tau) = \frac{\rho_o c a^2 a_M}{r^2}\cos\theta \int_0^{\tau}[\frac{r}{a}\cos\ell(\tau-\zeta)+(1-\frac{r}{a})\sin\ell(\tau-\zeta)]\, e^{-\ell(\tau-\zeta)}\sin b\zeta\, d\zeta$$

$$0 < \tau < t_1 \qquad (4.46)$$

The solution to the equation (4.46) is:

$$p_1(r,\theta,\tau) = \hat{G}_1\left[(\hat{B}_1+\hat{D}_1)\sin b\tau+(\hat{C}_1-\hat{E}_1)\cos b\tau-e^{-\ell\tau}[(\hat{B}_1-\hat{D}_1)\sin\ell\tau+(\hat{C}_1-\hat{E}_1)\cos\ell\tau]\right] \qquad (4.47)$$

$$0 < \tau < t_1$$

where $\hat{G}_1 = \frac{\rho_o c a^2 a_M \cos\theta}{2(4\ell^4+b^4)r^2}$, $\hat{B}_1 = (2\ell^2+b^2+2b\ell)[\ell-b(1-\frac{r}{a})]$, $\hat{C}_1 = (2\ell^2+b^2+2b\ell)[\frac{r}{a}(2\ell-b)-\ell]$, $\hat{D}_1=(2\ell^2+b^2-2b\ell)[\ell+b(1-\frac{r}{a})]$, and $\hat{E}_1 = (2\ell^2+b^2-2b\ell)[\frac{r}{a}(2\ell+b)-\ell]$. The contribution of the first period to the sound pressure at instant $\tau > t_1$ can be obtained from (4.46) by replacing the upper limit of integral by t_1.

Thus one may find:

$$p_1(r,\theta,\tau) = \hat{G}_1 \Bigg[[\hat{B}_1 \sin\ell(\tau-t_1+\frac{bt_1}{\ell})+\hat{C}_1\cos\ell(\tau-t_1+\frac{bt_1}{\ell}) - \hat{D}_1\sin\ell(\tau-t_1-\frac{bt_1}{\ell})-\hat{E}_1\cos\ell(\tau-t_1-\frac{bt_1}{\ell})]e^{-\ell(\tau-t_1)} - [(\hat{B}_1-\hat{D}_1)\sin\ell\tau+(\hat{C}_1-\hat{E}_1)\cos\ell\tau]e^{-\ell\tau} \Bigg]$$

$$\tau > t_1 \qquad (4.48)$$

During the second period one must use acceleration given by equation (4.15b) and establish a new convolution integral as:

$$p_2(r,\theta,\tau) = \frac{\rho_o c a^2 \eta^2}{r^2}(\bar{\alpha}_{max} - \frac{1}{3}\alpha_1)\cos\theta \int_{t_1}^{\tau} [\frac{r}{a}\cos\ell(\tau-\zeta)+(1-\frac{r}{a}) \sin\ell(\tau-\zeta)].\bar{e}^{\ell(\tau-\zeta)}\sin[\eta(\zeta-t_1)+\delta]d\zeta$$

$$t_1 < \tau < t_1+t_2 \qquad (4.49)$$

The solution to the equation (4.49) can be given by:

$$p_2(r,\theta,\tau) = \hat{G}_2\Bigg[(\hat{B}_2+\hat{D}_2)\sin[\eta(\tau-t_1)+\delta^*]+(\hat{C}_2-\hat{E}_2)\cos[\eta(\tau-t_1)+\delta^*] -\Big[\hat{B}_2\sin[\ell(\tau-t_1)+\delta^*]+\hat{C}_2\cos[\ell(\tau-t_1)+\delta^*] -\hat{D}_2\sin[\ell(\tau-t_1)-\delta^*]-\hat{E}_2\cos[\ell(\tau-t_1)-\delta^*]\Big]e^{-\ell(\tau-t_1)} \Bigg]$$

$$t_1 < \tau < t_1+t_2 \qquad (4.50)$$

where $\hat{G}_2 = \frac{\rho_o c a^2 \eta^2}{2(4\ell^4+\eta^4)r^2}(\bar{\alpha}_{max} - \frac{1}{3}\alpha_1)\cos\theta$, $\hat{B}_2 = (2\ell^2+\eta^2+2\eta\ell)[\ell-\eta(1-\frac{r}{a})]$, $\hat{C}_2 = (2\ell^2+\eta^2+2\eta\ell)[\frac{r}{a}(2\ell-\eta)-\ell]$, $\hat{D}_2 = (2\ell^2+\eta^2-2\eta\ell)[\ell+\eta(1-\frac{r}{a})]$, and

$\hat{E}_2 = (2\ell^2+\eta^2-2\eta\ell)[\frac{r}{a}(2\ell+\eta)-\ell]$. The sound pressure at instant $t_1 < \tau < t_1+t_2$ may now be written as:

$$p(r,\theta,\tau) = p_1(r,\theta,\tau)\Big|_{\tau>t_1} + p_2(r,\theta,\tau)\Big|_{t_1<\tau<\bar{t}} \qquad (4.51)$$

where $\bar{t} = t_1+t_2$. The contribution of the second period to the sound pressure at instant $\tau > \bar{t}$ may be deduced from (4.49) by replacing the upper limit of integral by $\bar{t}$. Thus:

$$p_2(r,\theta,\tau) = \hat{G}_\zeta \Big\{ \Big[\hat{B}_2 \sin[\ell(\tau-\bar{t})+\eta t_2+\delta^*] + \hat{C}_2 \cos[\ell(\tau-\bar{t})+\eta t_2+\delta^*] - \hat{D}_2 \sin[\ell(\tau-\bar{t})-\eta t_2-\delta^*] - \hat{E}_2 \cos[\ell(\tau-\bar{t})-\eta t_2-\delta^*] \Big] e^{-\ell(\tau-\bar{t})} - \Big[\hat{B}_2 \sin[\ell(\tau-t_1)+\delta^*] + \hat{C}_2 \cos[\ell(\tau-t_1)+\delta^*] - \hat{D}_2 \sin[\ell(\tau-t_1)-\delta^*] - \hat{E}_2 \cos[\ell(\tau-t_1)-\delta^*] \Big] e^{-\ell(\tau-t_1)} \Big\}_{\tau>\bar{t}} \qquad (4.52)$$

Finally the convolution integral requires to evaluate the sound pressure during the third period which its acceleration is given by equation (4.21) can be expressed as:

$$p_3(r,\theta,\tau) = \frac{\rho_o c a^2 \eta^2}{r^2}(\bar{\alpha}_{max} - \frac{1}{3}\alpha_1)\cos\theta \int_{\bar{t}}^{\tau} [\frac{r}{a}\cos\ell(\tau-\zeta)+(1-\frac{r}{a}) \sin\ell(\tau-\zeta)]\, e^{-\ell(\tau-\zeta)} \cdot \cos\bar{b}(\zeta-\bar{t})\, d\zeta$$

$$\bar{t} < \tau < \bar{d} \qquad (4.53)$$

where $\bar{d} = t_1+t_2+t_3$. The solution to the equation (4.53) may be written as:

$$p_3(r,\theta,\tau) = \hat{G}_3\Big[(\hat{B}_3+\hat{D}_3)\cos b^*(\tau-\bar{t})-(\hat{C}_3-\hat{E}_3)\sin b^*(\tau-\bar{t}) - \Big[(\hat{B}_3+\hat{D}_3)\cos\ell(\tau-\bar{t})-(\hat{C}_3+\hat{E}_3)\sin\ell(\tau-\bar{t})\Big]e^{-\ell(\tau-\bar{t})}\Big]$$

$$\bar{t} < \tau < \bar{d} \qquad (4.54)$$

where $\hat{G}_3 = \frac{\rho_o c a^2 \eta^2}{2(4\ell^4+b^{*4})r^2}(\bar{\alpha}_{max} - \frac{1}{3}\alpha_1)\cos\theta$, $\hat{B}_3 = (2\ell^2+b^{*2}+2\ell b^*)[\ell-b^*(1-\frac{r}{a})]$

$\hat{C}_3 = (2\ell^2+b^{*2}+2\ell b^*)[\frac{r}{a}(2\ell-b^*)-\ell]$, $\hat{D}_3 = (2\ell^2+b^{*2}-2\ell b^*)[\ell+b^*(1-\frac{r}{a})]$, and $\hat{E}_3 = (2\ell^2+b^{*2}-2\ell b^*)[\frac{r}{a}(2\ell+b^*)-\ell]$. The sound pressure at instant $\bar{t} < \tau < \bar{d}$ may now be found to be:

$$p(r,\theta,\tau) = p_1(r,\theta,\tau)\Big|_{\tau>t_1} + p_2(r,\theta,\tau)\Big|_{\tau>\bar{t}} + p_3(r,\theta,\tau)\Big|_{\bar{t}<\tau<\bar{d}} \qquad (4.55)$$

Replacing the upper limit of convolution integral (4.53) by $\bar{d}$ and evaluating the integral gives:

$$p_3(r,\theta,\tau) = \hat{G}_3\Big[[-(\hat{B}_3-\hat{D}_3)\sin\ell(\tau-\bar{d})-(\hat{C}_3-\hat{E}_3)\cos\ell(\tau-\bar{d})]e^{-\ell(\tau-\bar{d})} - [(\hat{B}_3+\hat{D}_3)\cos\ell(\tau-\bar{t})-(\hat{C}_3+\hat{E}_3)\sin\ell(\tau-\bar{t})]e^{-\ell(\tau-\bar{t})}\Big]$$

$$\tau > \bar{d} \qquad (4.56)$$

Thus the sound pressure at instant $\tau > \bar{d}$ may be expressed as:

$$p(r,\theta,\tau) = p_1(r,\theta,\tau)\Big|_{\tau>t_1} + p_2(r,\theta,\tau)\Big|_{\tau>\bar{t}} + p_3(r,\theta,\tau)\Big|_{\tau>\bar{d}} \qquad (4.57)$$

Analytical and numerical solutions of sound pressure for impactee are compared in Fig.(4.2). The sound pressure-time history for a pair of lead spheres is also given in Fig.(4.3).

The non-dimensional form of sound pressure in the far field can also be easily represented by following a similar process as given for elastic collision. Thus equation (4.47) and (4.48) reduce to:

$$p_1 = 0.58 \frac{\rho_o c v_o a \cos\theta}{r(1+4\beta_1^4)} \left[\begin{array}{l} 2\beta_1 \sin\hat{n}\pi \frac{\hat{\beta}}{\beta_1} - (1-2\beta_1^2)\cos\hat{n}\pi \frac{\hat{\beta}}{\beta_1} \\ -[(1+2\beta_1^2)\sin\hat{n}\pi\hat{\beta} - (1-2\beta_1^2)\cos\hat{n}\pi\hat{\beta}]e^{-\hat{n}\pi\hat{\beta}} \end{array} \right]$$

$$0 \leq \hat{n} \leq n_1 \qquad (4.58)$$

and

$$p_1 = \frac{0.58\rho_o c v_o a \cos\theta}{2(1+4\beta_1^4)r} \left[\begin{array}{l} (1+2\beta_1^2+2\beta_1)[\sin\pi\hat{\beta}(\hat{n}-n_1+\frac{n_1}{\beta_1}) \\ -(1-2\beta_1)\cos\pi\hat{\beta}(\hat{n}-n_1+\frac{n_1}{\beta_1})]e^{-\pi\hat{\beta}(\hat{n}-n_1)} \\ +(1+2\beta_1^2-2\beta_1)[\sin\pi\hat{\beta}(\hat{n}-n_1-\frac{n_1}{\beta_1}) \\ -(1+2\beta_1)\cos\pi\hat{\beta}(\hat{n}-n_1-\frac{n_1}{\beta_1})]e^{-\pi\hat{\beta}(\hat{n}-n_1)} \\ -2[(1+2\beta_1^2)\sin\hat{n}\pi\hat{\beta} - (1-2\beta_1^2)\cos\hat{n}\pi\hat{\beta}]e^{-\hat{n}\pi\hat{\beta}} \end{array} \right]$$

$$\hat{n} > n_1 \qquad (4.59)$$

where $\beta_1 = \frac{\ell}{b}$, $\hat{\beta} = \frac{\ell d}{\pi}$, $\hat{n} = \frac{\tau}{d}$, and $n_1 = \frac{t_1}{d}$. Similarly (4.50) and (4.52) may be written as:

$$p_2 = \frac{\rho_o c \dot{\alpha}_1 a \cos\theta}{2(1+4\hat{\beta}_2^4) r \cos\delta^*} \left[\begin{array}{l} 4\hat{\beta}_2 \sin\pi \frac{\hat{\beta}}{\hat{\beta}_2}(\hat{n}-n_1+\frac{\hat{\beta}_2}{\hat{\beta}}\frac{\delta^*}{\pi}) \\ -2(1-2\hat{\beta}_2^2)\cos\pi\frac{\hat{\beta}}{\hat{\beta}_2}(\hat{n}-n_1+\frac{\hat{\beta}_2}{\hat{\beta}}\frac{\delta^*}{\pi}) \\ -(1+2\hat{\beta}_2^2+2\hat{\beta}_2)[\sin\pi\hat{\beta}(\hat{n}-n_1+\frac{\delta^*}{\pi\hat{\beta}}) \\ -(1-2\hat{\beta}_2)\cos\pi\hat{\beta}(\hat{n}-n_1+\frac{\delta^*}{\pi\hat{\beta}})] \cdot e^{-\pi\hat{\beta}(\hat{n}-n_1)} \\ -(1+2\hat{\beta}_2^2-2\hat{\beta}_2)[\sin\pi\hat{\beta}(\hat{n}-n_1-\frac{\delta^*}{\pi\hat{\beta}}) \\ -(1+2\hat{\beta}_2)\cos\pi\hat{\beta}(\hat{n}-n_1-\frac{\delta^*}{\pi\hat{\beta}})] e^{-\pi\hat{\beta}(\hat{n}-n_1)} \end{array} \right]$$

$$n_1 < \tau \leq n_1+n_2 \qquad (4.60)$$

and

$$p_2 = \frac{\rho_o c \dot{\alpha}_1 a \cos\theta}{2(1+4\hat{\beta}_2^4) r \cos\delta^*} \left[\begin{array}{l} (1+2\hat{\beta}_2^2+2\hat{\beta}_2)[\sin\pi\hat{\beta}(\hat{n}-n_1-n_2+\frac{n_2}{\hat{\beta}_2}+\frac{\delta^*}{\pi\hat{\beta}}) \\ -(1-2\hat{\beta}_2)\cos\pi\hat{\beta}(\hat{n}-n_1-n_2+\frac{n_2}{\hat{\beta}_2}+\frac{\delta^*}{\pi\hat{\beta}})] e^{-\pi\hat{\beta}(\hat{n}-n_1-n_2)} \\ +(1+2\hat{\beta}_2^2-2\hat{\beta}_2)[\sin\pi\hat{\beta}(\hat{n}-n_1-n_2-\frac{n_2}{\hat{\beta}2}-\frac{\delta^*}{\pi\hat{\beta}}) \\ -(1+2\hat{\beta}_2)\cos\pi\hat{\beta}(\hat{n}-n_1-n_2-\frac{n_2}{\hat{\beta}_2}-\frac{\delta^*}{\pi\hat{\beta}})] e^{\pi\hat{\beta}(\hat{n}-n_1-n_2)} \\ -(1+2\hat{\beta}_2^2+2\hat{\beta}_2)[\sin\pi\hat{\beta}(\hat{n}-n_1+\frac{\delta^*}{\pi\hat{\beta}}) \\ -(1-2\hat{\beta}_2)\cos\pi\hat{\beta}(\hat{n}-n_1+\frac{\delta^*}{\pi\hat{\beta}})] e^{-\pi\hat{\beta}(\hat{n}-n_1)} \\ -(1+2\hat{\beta}_2^2-2\hat{\beta}_2)[\sin\pi\hat{\beta}(\hat{n}-n_1-\frac{\delta^*}{\pi\hat{\beta}}) \\ -(1+2\hat{\beta}_2)\cos\pi\hat{\beta}(\hat{n}-n_1-\frac{\delta^*}{\pi\hat{\beta}})] e^{-\pi\hat{\beta}(\hat{n}-n_1)} \end{array} \right]$$

$$\hat{n} > n_1+n_2 \qquad (4.61)$$

where $\hat{\beta}_2 = \frac{\ell}{\eta}$, and $n_2 = \frac{t_2}{d}$. Finally equation (4.54) and (4.56) can be expressed as:

$$p_3 = \frac{\rho_o c \dot{\alpha}_1 a \cos\theta}{(1+4\hat{\beta}_3^4) r \cos\delta^*} \frac{\hat{\beta}_3}{\hat{\beta}_2} \left[\begin{array}{l} 2\hat{\beta}_3 \cos \frac{\pi\hat{\beta}}{\hat{\beta}_3}(\hat{n}-n_1-n_2)+(1-2\hat{\beta}_3^2)\sin\frac{\pi\hat{\beta}}{\hat{\beta}_3}(\hat{n}-n_1-n_2) \\ -[2\hat{\beta}_3 \cos\pi\hat{\beta}(\hat{n}-n_1-n_2)-4\hat{\beta}_3^3 \sin\pi\hat{\beta}(\hat{n}-n_1-n_2)] \\ e^{-\pi\hat{\beta}(\hat{n}-n_1-n_2)} \end{array} \right]$$

$$n_1+n_2 \leqslant \hat{n} < 1 \qquad (4.62)$$

and

$$p_3 = \frac{\rho_o c \dot{\alpha}_1 a}{r(1+4\hat{\beta}_3^4)} \frac{\cos\theta}{\cos\delta^*} \frac{\hat{\beta}_3}{\hat{\beta}_2} \left[\begin{array}{l} [-(1+2\hat{\beta}_3^2)\sin\pi\hat{\beta}(\hat{n}-1)+(1-2\hat{\beta}_3^2)\cos\pi\hat{\beta}(\hat{n}-1)] \\ e^{-\pi\hat{\beta}(\hat{n}-1)} \\ -[2\hat{\beta}_3 \cos\pi\hat{\beta}(\hat{n}-n_1-n_2)-4\hat{\beta}_3^3 \sin\pi\hat{\beta}(\hat{n}-n_1-n_2)] \\ e^{-\pi\hat{\beta}(\hat{n}-n_1-n_2)} \end{array} \right]$$

$$\hat{n} > 1 \qquad (4.63)$$

where $\hat{\beta}_3 = \frac{\ell}{b^*}$.

4.4. Fourier Transform of pressure-time history

The Fourier transform of acceleration may be written as:

$$\hat{A}(\omega) = \int_{-\infty}^{\infty} \hat{A}(t) e^{-i\omega t}\, dt = \int_{o}^{\bar{d}} \hat{A}(t) e^{-i\omega t}\, dt \qquad (4.64)$$

where $\hat{A}(t) = a_{M1} \sin bt \qquad 0 < t < t_1 \qquad (4.65a)$

$$\hat{A}(t) = (\bar{\alpha}_{max} - \tfrac{1}{3}\alpha_1)\eta^2 \sin[\eta(t-t_1)+\delta^*] \quad t_1 < t \leqslant t_1+t_2 \qquad (4.65b)$$

$$\hat{A}(t) = (\bar{\alpha}_{max} - \frac{1}{3}\alpha_1)\eta^2 \cos b^*(t-t_1-t_2) \quad t_1+t_2 < t \leq \bar{d} \qquad (4.65c)$$

Substituting (4.65a) to (4.65c) into equation (4.64) gives:

$$\hat{A}(\omega) = a_{M1} \int_0^{t_1} \sin bt\, e^{-i\omega t} dt + \frac{\dot{\alpha}_1 \eta}{\cos\delta^*} \int_{t_1}^{t_1+t_2} \sin\left[\eta(t-t_1)+\delta^*\right] e^{i\omega t}\, dt + \frac{\dot{\alpha}_1 \eta}{\cos\delta^*} \int_{t_1+t_2}^{\bar{d}} \cos b^*(t-t_1-t_2) e^{i\omega t}\, dt \qquad (4.66)$$

where $\frac{\dot{\alpha}_1 \eta}{\cos\delta^*} = \eta^2(\bar{\alpha}_{max} - \frac{1}{3}\alpha_1)$. Solving the integrals on the right hand side of equation (4.66) and making some simplifications yields:

$$\hat{A}(\omega) = A^* + iB^* \qquad (4.67)$$

where

$$A^* = \frac{a_{M1}}{\omega^2-b^2}(\omega \sin bt_1 \sin\omega t_1 + b\cos bt_1 \cos\omega t_1 - b) - \frac{\eta\dot{\alpha}_1}{\cos\delta^*(\omega^2-\eta^2)(\omega^2-b^{*2})}\left[\omega(\omega^2-b^{*2})\sin\delta^* \sin\omega t_1 + \eta(\omega^2-b^{*2})\cos\delta^* \cos\omega t_1 - \omega(\eta^2-b^{*2})\sin\omega\bar{t} + b^*(\omega^2-\eta^2)\cos\omega\bar{d}\right] \qquad (4.68a)$$

and

$$B^* = \frac{a_{M1}}{\omega^2-b^2}(\omega \sin bt_1 \cos\omega t_1 - b\cos bt_1 \sin\omega t_1) - \frac{\eta\dot{\alpha}_1}{\cos\delta^*(\omega^2-\eta^2)(\omega^2-b^{*2})}\left[\omega(\omega^2-b^{*2})\sin\delta^* \cos\omega t_1 - \eta(\omega^2-b^{*2})\cos\delta^* \sin\omega t_1 - \omega(\eta^2-b^{*2})\cos\omega\bar{t} - b^*(\omega^2-\eta^2)\sin\omega\bar{d}\right] \qquad (4.68b)$$

The Fourier transform of the pressure due to unit impulse acceleration may also be given by:

$$p_{UI}(r,\theta,\omega) = \frac{\rho_o a c \cos\theta}{(\omega^4+4\ell^4)r^2}\left[\ell(2a\ell^2-\omega^2 a+2\omega^2 r)+i\omega(2\ell^2 r-\omega^2 r-2a\ell^2)\right] \tag{4.69}$$

Using now (4.69) together with (4.67) the transform of the pressure for a sphere subjected to inelastic collision by a sphere can be obtained to be:

$$p(r,\theta,\omega) = p_{UI}(r,\theta,\omega)(A^*+B^*i) \tag{4.70}$$

where A* and B* are given by equations (4.68a) and (4.68b) respectively. Multiplying (4.70) by its complex conjugate gives:

$$|p(r,\theta,\omega)|^2 = \frac{\rho_o^2 a^2 c^2 \cos^2\theta}{(\omega^4+4\ell^4)r^4}(a^2\ell^2+\omega^2 r^2)(A^{*2}+B^{*2}) \tag{4.71a}$$

or

$$|p(r,\theta,\omega)| = \frac{\rho_o a c \cos\theta}{(\omega^4+4\ell^4)^{\frac{1}{2}}r^2}(a^2\ell^2+\omega^2 r^2)^{\frac{1}{2}}(A^{*2}+B^{*2})^{\frac{1}{2}} \tag{4.71b}$$

A graph representing variations of $|p|$ against frequency for a pair of lead spheres is given in Fig.(4.4). In order to represent $|p(r,\theta,\omega)|$ in terms of non-dimensional variables A*,B*, and pressure due to unit impulse may be written respectively as:

$$A^* = \frac{0.58v_o\hat{\beta}^2}{(4n^{*2}\beta_1^2-\hat{\beta}^2)}\left[2n^*\frac{\beta_1}{\hat{\beta}}\sin(n_1\pi\frac{\hat{\beta}}{\beta_1})\sin(2n_1n^*\pi)+\cos(n_1\pi\frac{\hat{\beta}}{\beta_1})\cos(2n_1n^*\pi)-1\right]$$

$$-\frac{\dot{\alpha}_1\hat{\beta}^2}{\cos\delta^*(4n^{*2}\hat{\beta}_2^2-\hat{\beta}^2)}\left\{2n^*\frac{\hat{\beta}_2}{\hat{\beta}}\sin\delta^*\sin(2n_1n^*\pi)+\cos\delta^*\cos(2n_1n^*\pi)-\frac{2\hat{\beta}(\hat{\beta}_3^2-\hat{\beta}_2^2)n^*}{\hat{\beta}_2(4n^{*2}\hat{\beta}_3^2-\hat{\beta}^2)}\sin[2(n_1+n_2)n^*\pi]+\frac{\hat{\beta}_3(4n^{*2}\hat{\beta}_2^2-\hat{\beta}^2)}{\hat{\beta}_2(4n^{*2}\hat{\beta}_3^2-\hat{\beta}^2)}\cos(2n^*\pi)\right\}$$

(4.72a)

$$B^* = \frac{0.58v_o\hat{\beta}^2}{(4n^{*2}\beta_1^2-\hat{\beta}^2)}\left[2n^*\frac{\beta_1}{\hat{\beta}}\sin(n_1\frac{\hat{\beta}}{\beta_1}\pi)\cos(2n_1n^*\pi)-\cos(n_1\frac{\hat{\beta}}{\beta_1}\pi)\sin(2n_1n^*\pi)\right]$$

$$-\frac{\dot{\alpha}_1\hat{\beta}^2}{\cos\delta^*(4n^{*2}\hat{\beta}_2^2-\hat{\beta}^2)}\left\{2n^*\frac{\hat{\beta}_2}{\hat{\beta}}\sin\delta^*\cos(2n_1n^*\pi)-\cos\delta^*\sin(2n_1n^*\pi)-\frac{2\hat{\beta}(\hat{\beta}_3^2-\hat{\beta}_2^2)n^*}{\hat{\beta}_2(4n^{*2}\hat{\beta}_3^2-\hat{\beta}^2)}\cos[2(n_1+n_2)n^*\pi]-\frac{\beta_3(4n^{*2}\hat{\beta}_2^2-\hat{\beta}^2)}{\hat{\beta}_2(4n^{*2}\hat{\beta}_3^2-\hat{\beta}^2)}\sin(2\pi n^*)\right\}$$

(4.72b)

$$p_{UI} = \frac{\rho_o a\cos\theta}{2(4n^{*4}+\hat{\beta}^4)}\frac{\hat{\beta}^2}{\xi^2}\left[(\hat{\beta}^2-2n^{*2}+4n^{*2}\xi)-i\frac{2n^*}{\hat{\beta}}(\hat{\beta}^2+2n^{*2}\xi-\hat{\beta}^2\xi)\right]$$

(4.73)

where $n^* = f\bar{d}$ and $\xi = \frac{r}{a}$. The non-dimensional form of pressure may now be given by substituting A^*, B^* and p_{UI} in equation (4.70) and multiplying the result by its complex conjugate as already carried out for establishing $|p(r,\theta,\omega)|$. A plot of pressure against n^* is given in Fig.(4.5). Graph showing variations of $|\hat{A}(\omega)|$ versus n^* is also given in Fig.(4.6).

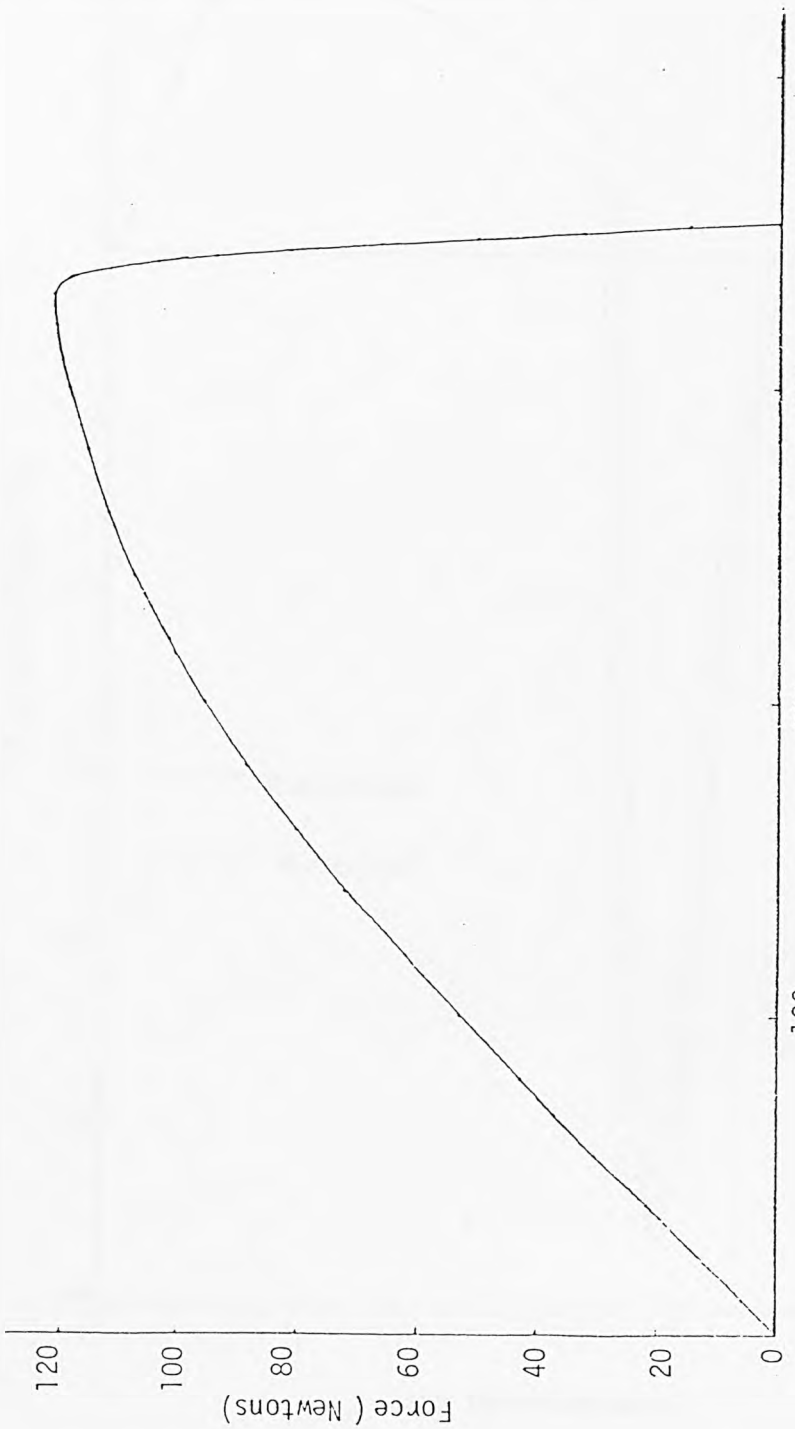

FIG.4.1. Force versus time for 2.54 cm diameter lead spheres with an initial impact velocity of 0.55 m/s.

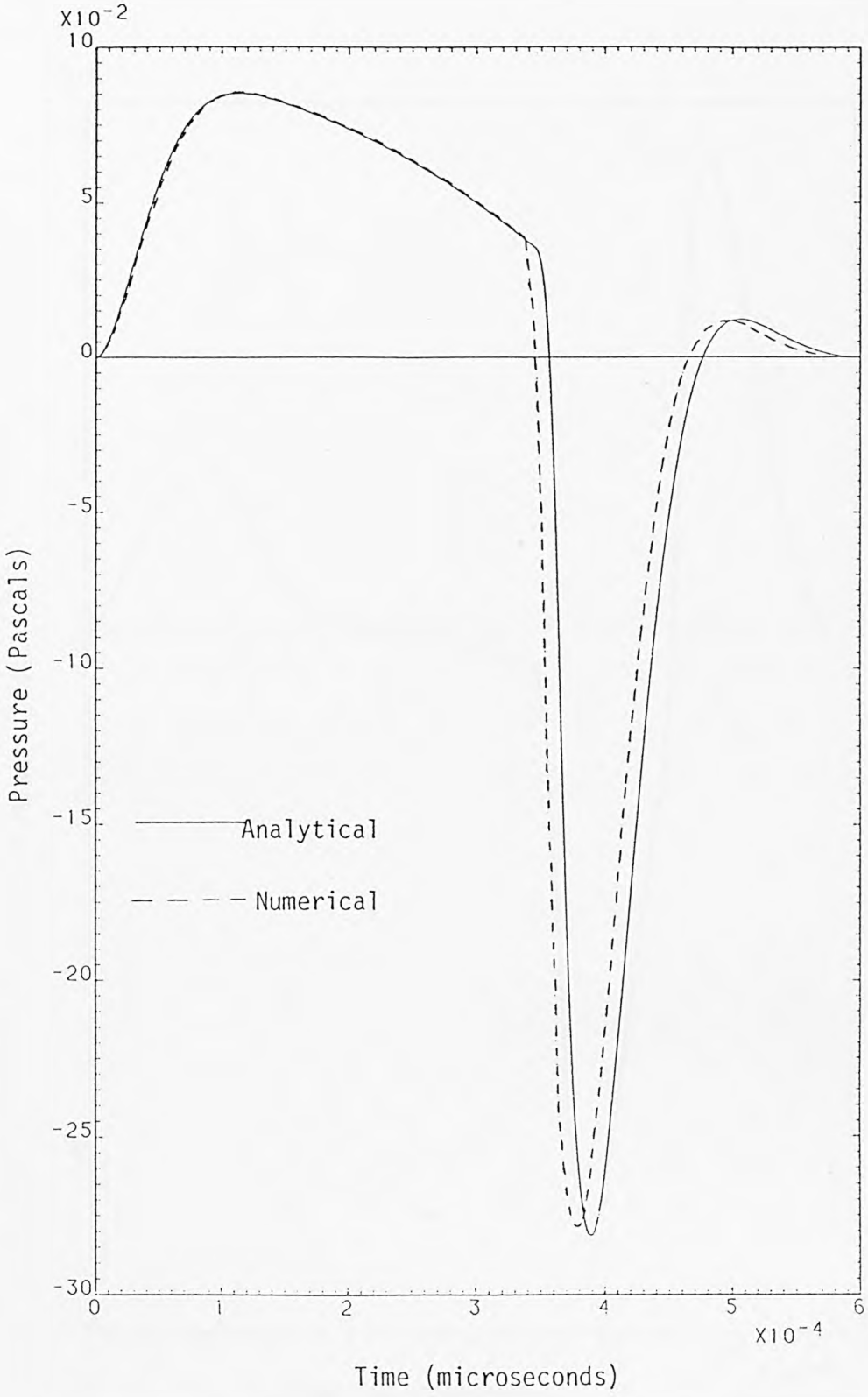

FIG.4.2. Comparison of analytical and numerical solution of pressure time histories for 2.54 cm diameter lead spheres with an initial impact velocity 0.55 m/s, impactee only.
($\theta = 0^{o}$, r = 0.26 m, $\bar{P}_{o} = 5 \times 10^{7}$ Pascals)

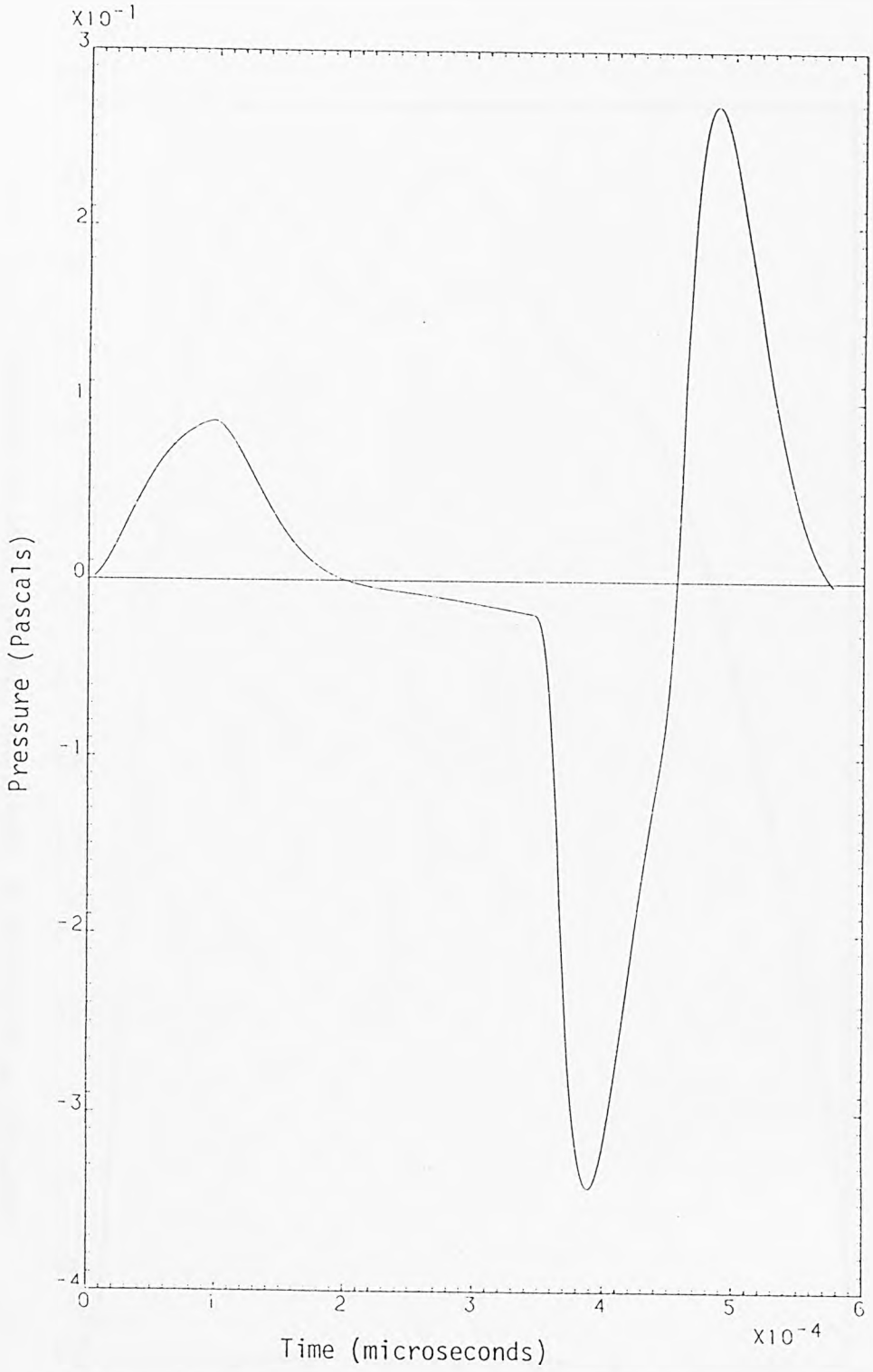

FIG.4.3. Sound pressure time history for 2.54 cm diameter lead spheres with an initial impact velocity 0.55 m/s.

($\theta = 0^{o}$, r = 0.26 m, $\bar{P}_{o} = 5 \times 10^{7}$ Pascals)

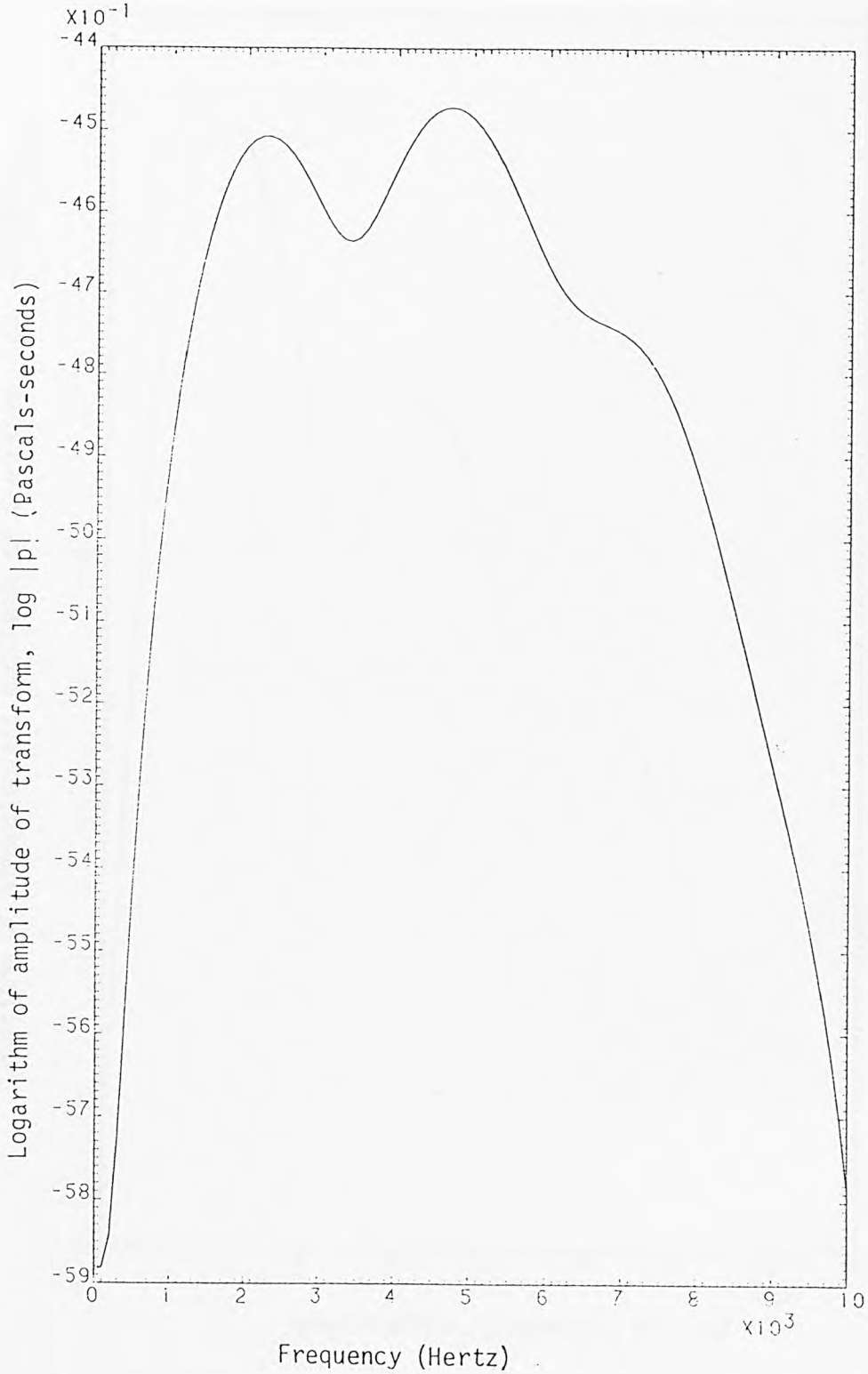

FIG.4.4. Fourier transform of pressure for 2.54 cm diameter lead spheres with an initial impact velocity 0.55 m/s. ($\theta = 0^{o}$, r = 0.26 m, $\bar{P}_{o} = 5 \times 10^{7}$ Pascals)

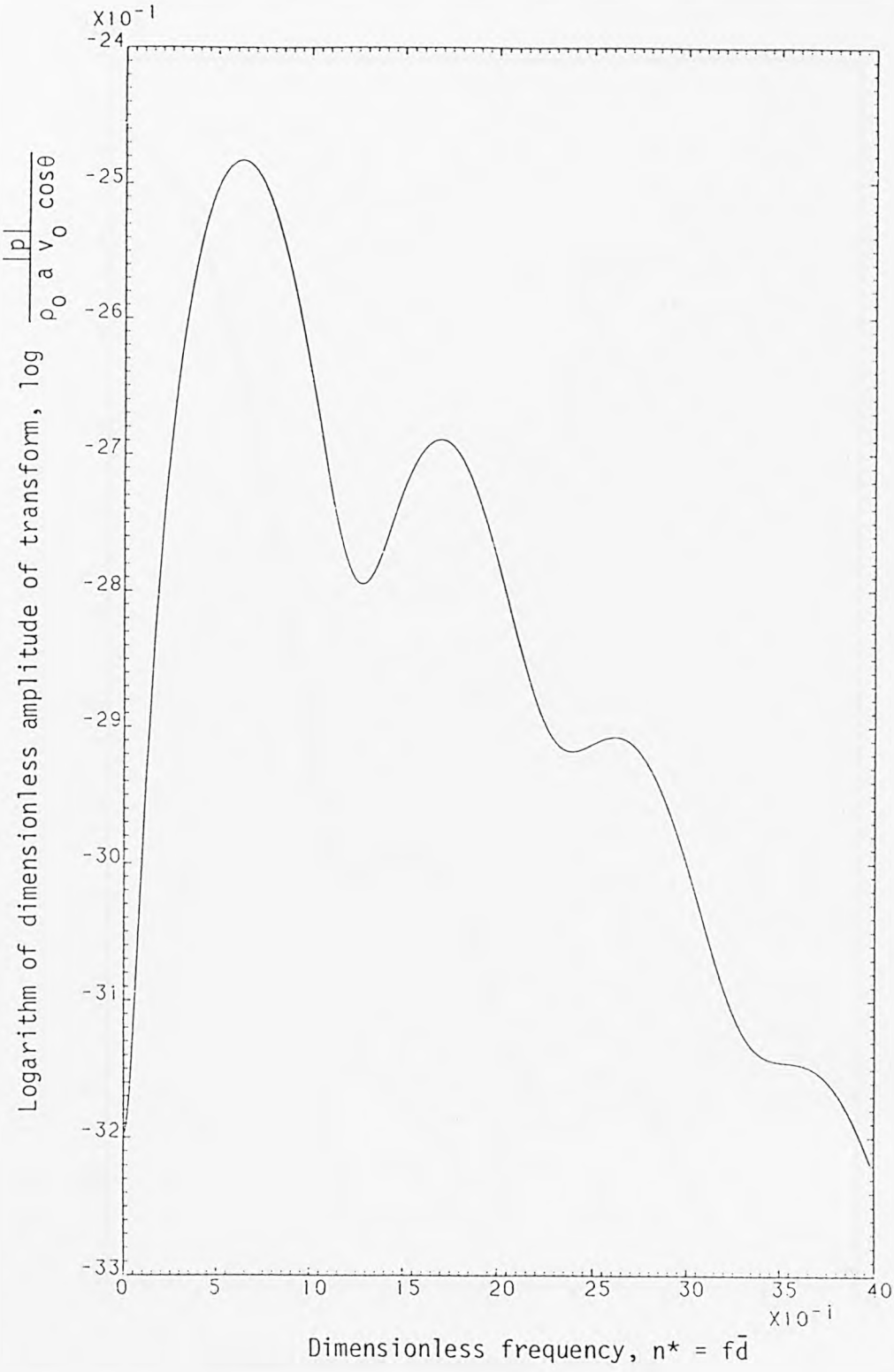

FIG. 4.5. Fourier transform of dimensionless pressure, impactee only.

(r = 0.26 m, $\bar{P}_o = 5 \times 10^7$ Pascals, v_o = 0.55 m/s, a = 1.27 cm)

FIG.4.6. Fourier transform of dimensionless acceleration.
(r = 0.26 m, $\bar{P}_o = 5 \times 10^7$ Pascals, v_o = 0.55 m/s, a = 1.27 cm)

5. SOUND PRESSURE RADIATED BY A VISCOELASTIC SPHERE

In this chapter the sound radiated by a viscoelastic sphere in collision with a metallic sphere is investigated. The Hertz law of contact provides a useful approximation in the case of elastic objects. To deal with collisions in which one or both of the impinging bodies are of viscoelastic material the Hertz law of contact should be extended. This has been done by Pao [62] who used the Laplace transform method to obtain the viscoelastic expression for the force developed between two surfaces.

Having a knowledge of force-approach relation a numerical method is developed for solving the sound pressure. In order to study the sound pressure in the frequency domain a method involving the discrete finite transform is introduced.

5.1. Impact Solution

The force-approach relation given by equation (2.60) may be written in terms of the bulk modulus $\bar{K} = \lambda + \frac{2}{3}\mu$ and rigidity modulus μ in the form:

$$F = \frac{4}{3}\frac{q_K}{(A+B)^{1/2}}\left[\frac{\bar{K}_1 + \frac{4}{3}\mu_1}{4\pi\mu_1(\bar{K}_1+\frac{1}{3}\mu_1)} + \frac{\bar{K}_2 + \frac{4}{3}\mu_2}{4\pi\mu_2(\bar{K}_2+\frac{1}{3}\mu_2)}\right]^{-1}\alpha^{3/2} \tag{5.1}$$

where

$$\frac{\bar{K}_1 + \frac{4}{3}\mu_1}{4\pi\mu_1(\bar{K}_1 + \frac{1}{3}\mu_1)} = \frac{1-\nu_1^2}{\pi E_1} = \delta_1 \tag{5.2a}$$

and

$$\frac{\bar{K}_2 + \frac{4}{3}\mu_2}{4\pi\mu_2(\bar{K}_2 + \frac{1}{3}\mu_2)} = \frac{1-\nu_2^2}{\pi E_2} = \delta_2 \qquad (5.2b)$$

In the collison of a metallic body with a material constant δ_2 and a viscoelastic body with a material constant δ_1, δ_2 is much less than δ_1 and can be neglected. Thus the Laplace transform of equation (5.1) in absence of δ_2 can be given as:

$$(\bar{K}_1 + \frac{1}{3}\mu_1)\mathcal{L}(\alpha^{3/2}) = \frac{3\sqrt{A+B}}{4q_K}\left(\frac{\bar{K}_1}{4\pi\mu_1} + \frac{1}{3\pi}\right)\mathcal{L}(F) \qquad (5.3)$$

It has been shown by Pao [62] that the solution to the viscoelastic case is obtainable from the solution to the elastic case by simply replacing μ_1 by $\mu_1[1 - \mathcal{L}(\dot{\Psi})]$ in the Laplace transform of the elastic equation. Thus from (5.3)

$$\mathcal{L}(\alpha^{3/2}) = \frac{3\sqrt{A+B}}{4q_K}\left[\frac{\bar{K}_1}{4\pi\mu_1[1-\mathcal{L}<\dot{\Psi}>][\bar{K}_1 + \frac{1}{3}\mu_1(1-\mathcal{L}<\dot{\Psi}>)]} + \frac{1}{3\pi[\bar{K}_1 + \frac{1}{3}\mu_1(1-\mathcal{L}<\dot{\Psi}>)]}\right]\mathcal{L}(F) \qquad (5.4)$$

where Ψ is called the relaxation function, $\dot{\Psi} = \frac{d\Psi}{dt}$, $\Psi(0) = 0$, and $\Psi(\infty) = 1$.

Neglecting the second term on the right hand side of equation (5.4) in comparison with the first one, using the inequality $\mu_1(1-\mathcal{L}<\dot{\Psi}>) << 3\bar{K}_1$, and finding the inverse transform gives:

$$F = \frac{16\pi}{3}\frac{q_K}{\sqrt{A+B}}\mu_1\left[\alpha^{3/2} - \int_0^t \Psi<t-\zeta>\alpha^{3/2}<\zeta>d\zeta\right] \qquad (5.5)$$

The equation of motion may now be written as:

$$\frac{m_1 m_2}{m_1+m_2}\ddot{\alpha} = -\frac{16\pi}{3}\frac{q_K}{\sqrt{A+B}}\left[\mu_1\,\alpha^{3/2} - \int_0^t \frac{\bar{\mu}_k}{\bar{\tau}_k} e^{-\frac{t-\zeta}{\bar{\tau}_k}} \alpha^{3/2}_{<\zeta>}\, d\zeta\right] \tag{5.6}$$

where $\mu_1 \Psi\,<t> = \Sigma\bar{\mu}_k(1-e^{-t/\bar{\tau}_k})$.

5.2. Numerical solution of sound pressure

The sound pressure due to collison of a metallic sphere upon a viscoelastic sphere can be obtained by solving the corresponding convolution integral numerically. To carry out this one must first calculate the acceleration at different instants $t = n\Delta t$, $(n=0,1,2....)$. The acceleration of a viscoelastic sphere of mass m_1 may be given by:

$$\hat{A}(t) = \frac{F}{m_1} = -\frac{\ddot{\alpha}}{m_1\hat{K}_1} \tag{5.7}$$

where $\hat{K}_1 = \frac{m_1+m_2}{m_1 m_2}$ and m_2 is the mass of the metallic sphere. Thus to find the acceleration one needs to solve the differential equation (5.6) numerically, which can also be written as:

$$\ddot{\alpha} = -\frac{4\pi\mu_1}{\bar{c}}\hat{K}_1\,\alpha^{3/2} + \frac{4\pi}{\bar{c}}\hat{K}_1 \int_0^t \frac{\bar{\mu}_k}{\bar{\tau}_k} e^{-\frac{t-\zeta}{\bar{\tau}_k}} \alpha^{3/2}_{<\zeta>}\, d\zeta \tag{5.8}$$

where $\bar{c} = \frac{3}{4}\frac{(A+B)^{1/2}}{q_K}$. The initial conditions at instant $t = 0$ are:

$$\alpha\big|_{t=0} = 0, \quad \dot{\alpha}\big|_{t=0} = v_o \tag{5.9}$$

and the higher order derivatives at the same instant may be found to be zero. Thus by using Taylor's expansion formula the value of α at instant $t = \Delta t$ can be given by:

$$\alpha\Big|_{t=\Delta t} = \alpha\Big|_{t=0} + \Delta t\dot{\alpha}\Big|_{t=0} + \frac{(\Delta t)^2}{2!}\ddot{\alpha}\Big|_{t=0} + \ldots. \qquad (5.10)$$

In the next iteration the new value of α may be estimated from (4.32) to be:

$$\alpha\Big|_{t=2\Delta t} = 2\alpha\Big|_{t=\Delta t} - \alpha\Big|_{t=0} + (\Delta t)^2\ddot{\alpha}\Big|_{t=\Delta t} \qquad (5.11)$$

The only unknown on the right hand side of equation (5.11) is the value of $\ddot{\alpha}$ at instant $t = \Delta t$ which can be easily determined by writing equation (5.8) as:

$$\ddot{\alpha}\Big|_{t=\Delta t} = -\frac{4\pi\mu_1}{\bar{c}}\hat{K}_1\alpha^{3/2}\Big|_{t=\Delta t} + \frac{4\pi}{\bar{c}}\hat{K}_1\bar{I}\Big|_{\zeta=0}^{\zeta=\Delta t} \qquad (5.12)$$

where

$$\bar{I}\Big|_{\zeta=0}^{\zeta=\Delta t} = \int_0^{\Delta t}\Sigma\frac{\bar{\mu}_k}{\bar{\tau}_k}e^{-\frac{\Delta t-\zeta}{\bar{\tau}_k}}\alpha^{3/2}<\zeta>d\zeta \qquad (5.13)$$

By making use of the trapezoidal rule, equation (5.13) can be expressed as:

$$\bar{I}\Big|_{\zeta=0}^{\zeta=\Delta t} = \frac{\Delta t}{2}\left[\Sigma\frac{\bar{\mu}_k}{\bar{\tau}_k}e^{-\frac{\Delta t-0}{\bar{\tau}_k}}\alpha^{3/2}\Big|_{\zeta=0} + \Sigma\frac{\bar{\mu}_k}{\bar{\tau}_k}e^{-\frac{\Delta t-\Delta t}{\bar{\tau}_k}}\alpha^{3/2}\Big|_{\zeta=\Delta t}\right] \qquad (5.14)$$

Thus the value of $\ddot{\alpha}$ at instant $t = \Delta t$ and consequently the value of α at $t = 2\Delta t$ can be determined. The general form of equation (5.11), (5.12) and (5.14) are respectively:

$$\alpha\Big|_{t=(n+1)\Delta t} = 2\alpha\Big|_{t=n\Delta t} - \alpha\Big|_{t(n-1)\Delta t} + (\Delta t)^2 \ddot{\alpha}\Big|_{t=n\Delta t} \tag{5.15a}$$

$$\ddot{\alpha}\Big|_{t=n\Delta t} = \frac{4\pi\mu_1}{\bar{c}}\hat{K}_1 \alpha^{3/2}\Big|_{t=n\Delta t} + \frac{4\pi}{\bar{c}}\hat{K}_1 \bar{I}\Big|_{\zeta=0}^{\zeta=n\Delta t} \tag{5.15b}$$

$$\begin{aligned}\bar{I}\Big|_{\zeta=0}^{\zeta=n\Delta t} = \frac{\Delta t}{2}\Bigg[& \Sigma \frac{\bar{\mu}_k}{\bar{\tau}_k} e^{-\frac{n\Delta t-0}{\bar{\tau}_k}} \alpha^{3/2}\Big|_{\zeta=0} + 2\Sigma \frac{\bar{\mu}_k}{\bar{\tau}_k} e^{-\frac{n\Delta t-\Delta t}{\bar{\tau}_k}} \alpha^{3/2}\Big|_{\zeta=n\Delta t} + \cdots \\ & 2\Sigma \frac{\bar{\mu}_k}{\bar{\tau}_k} e^{-\frac{n\Delta t-(n-1)\Delta t}{\bar{\tau}_k}} \alpha^{3/2}\Big|_{\zeta=(n-1)\Delta t} \\ & + \Sigma \frac{\bar{\mu}_k}{\bar{\tau}_k} e^{-\frac{n\Delta t-n\Delta t}{\bar{\tau}_k}} \alpha^{3/2}\Big|_{\zeta=n\Delta t} \Bigg]\end{aligned} \tag{5.15c}$$

where n is an integer. The force and acceleration can also be found from (5.7) to be:

$$F\Big|_{t=n\Delta t} = -\frac{1}{\hat{K}_1}\ddot{\alpha}\Big|_{t=n\Delta t} \tag{5.16a}$$

and

$$\hat{A}\Big|_{t=n\Delta t} = -\frac{1}{m_1\hat{K}_1}\ddot{\alpha}\Big|_{t=n\Delta t} \tag{5.16b}$$

The duration of contact may be given at instant $t = d$ in which the calculated force changes its sign. The sound pressure at instant $\tau = n\Delta t$ may now be given by:

$$p(r,\theta,n\Delta t) = \frac{\Delta t}{2}[p_{UI}(r,\theta,n\Delta t-0)\hat{A}(0)+2p_{UI}(r,\theta,n\Delta t-\Delta t)\hat{A}(\Delta t)$$

$$+....+2p_{UI}[r,\theta,n\Delta t-(n-1)\Delta t]\hat{A}[(n-1)\Delta t]$$

$$+p_{UI}(r,\theta,n\Delta t-n\Delta t)\hat{A}(n\Delta t)] \qquad (5.17a)$$

$$0 < n\Delta t < d$$

or

$$p(r,\theta,\ n\Delta t) = \frac{\Delta t}{2}\ p_{UI}(r,\theta,\ n\Delta t-0)\hat{A}(0)+2p_{UI}(r,\theta,n\Delta t-\Delta t)\hat{A}(\Delta t)$$

$$+...+2p_{UI}[r,\theta,n\Delta t-(n_d^*-1)\Delta t]\hat{A}[(n_d^*-1)\Delta t]$$

$$+p_{UI}(r,\theta,n\Delta t - n_d^*\Delta t)\hat{A}(n_d^*\Delta t)$$

$$n\Delta t > d \qquad (5.17b)$$

where $n_d^* = \frac{d}{\Delta t}$ and p_{UI} is the pressure due to unit impulse given by equation (3.7). The sound pressure time histories produced by the collision of a steel sphere and a viscoelastic sphere with material properties given in Table (5.1) are illustrated in Figs. (5.1) to (5.3). The corresponding force-time histories are also given in Fig.(5.4). The numerical method described in this section may also be used for calculating the sound pressure produced by collision of elastic spheres. The differential equation required to be solved numerically is given by equation (2.67) which can be deduced from (5.8) by substituting $\bar{\tau}_k = \infty$ and $\mu = \frac{1}{4\pi(\delta_1+\delta_2)}$

5.3. Discrete finite transform for evaluating the Fourier transform of pressure-time history

Consider the sound pressure defined by:

$$p = p(r,\theta,\tau) \qquad 0 < \tau < \infty \qquad \tau < 0 \tag{5.18}$$

The Fourier transform of the above sound pressure-time history may be written as:

$$p(r,\theta,\omega) = \int_{-\infty}^{\infty} p(r,\theta,\tau)e^{-i\omega\tau}d\tau = \int_{0}^{\infty} p(r,\theta,\tau)e^{-i\omega\tau}d\tau \tag{5.19}$$

The integral on the right hand side of equation (5.19) may be expressed approximately as a summation of an infinite number of discrete data each separated by an interval of Δt. Thus:

$$p(r,\theta,\omega) = \Delta t \sum_{n=0}^{n=\infty} p(r,\theta,n\Delta t)e^{-i\omega n\Delta t} \tag{5.20}$$

Because of selection of finite interval of time Δt the Fourier transform calculated by (5.20) no longer contains accurate magnitude and phase information at all frequencies contained in $p(r,\theta,\omega)$, but it accurately describes the spectrum of $p(r,\theta,\tau)$ up to some maximum frequency f_{max} which is dependent upon the sample interval Δt. To calculate (5.20) one must find the summation of infinite discrete data and this is not practical. Therefore it is necessary to select finite number of samples in the range of $\tau=0$ to $\tau=T$. Thus one may write:

$$p(r,\theta,m\Delta f) = \Delta t \sum_{n=0}^{n=N-1} p(r,\theta,n\Delta t)e^{-i2\pi m\Delta f n\Delta t} \tag{5.21}$$

where $N = \frac{T}{\Delta t}$ and N is the number of samples. Equation (5.21) does not give a continuous spectrum it means that making use of (5.21) only predicts the magnitude and phase information at certain frequencies such as $m\Delta f$ in the range of $f = 0$ to $f = f_{max}$. To use equation (5.21) one must assume that the function $p(r,\theta,\tau)$ is a periodic function with period T for all time. This assumption is made whether or not $p(r,\theta,\tau)$ is actually periodic. The number of points in the frequency domain is $\frac{N}{2}$, because the frequency information is broken into two real and imaginary parts. Thus the maximum frequency f_{max} can be related to the number of samples in time domain through the relation:

$$f_{max} = \frac{N}{2}\Delta f \tag{5.22}$$

where $\Delta f = \frac{1}{T}$ is called the frequency resolution. To find the magnitude of transform pressure equation (5.21) may be written as:

$$p(r,\theta,m\Delta f) = \Delta t \sum_{n=0}^{n=N-1} p(r,\theta,n\Delta\tau)[\cos(2\pi m\Delta f n\Delta\tau) - i\sin(2\pi m\Delta f n\Delta\tau)] \tag{5.23}$$

Multiplying (5.23) by its complex conjugate gives:

$$|p(r,\theta,m\Delta f)|^2 = (\Delta t)^2\left[\left[\sum_{n=0}^{n=N-1} f(r,\theta,n\Delta t)\cos(2\pi m\Delta f n\Delta t)\right]^2 + \left[\sum_{n=0}^{n=N-1} f(r,\theta,n\Delta t)\sin(2\pi m\Delta f n\Delta t)\right]^2\right] \tag{5.24}$$

or

$$|p(r,\theta,m\Delta f)| = \Delta t\left\{\left[\sum_{n=0}^{n=N-1} f(r,\theta,n\Delta t)\cos(2\pi m\Delta f n\Delta t)\right]^2 \left[\sum_{n+o}^{n=N-1} f(r,\theta,n\Delta t)\sin(2\pi m\Delta f n\Delta t)\right]^2\right\}^{\frac{1}{2}} \quad (5.25)$$

Graph representing variations of transform pressure versus frequency is given in Fig.(5.5). The time domain samples for establishing Fig.(5.5) are taken from Fig.(5.3).

CASE 1. Sphere of rigidity similar to polyethylene.

$\mu_1 = 1.03 \times 10^8$ N/m^2	$\tau_1 = 10^{-6}$ sec
$\mu_2 = 5.51 \times 10^8$	$\tau_2 = 10^{-5}$
$\mu_3 = 1.1 \times 10^8$	$\tau_3 = 10^{-4}$
$\mu_4 = 0.41 \times 10^8$	$\tau_4 = 1$

$\bar{c} = 29.57$ m$^{-½}$

==========

CASE 2. Sphere of rigidity similar to nylon.

$\mu_1 = 5.72 \times 10^8$ N/m^2	$\tau_1 = 10^{-7}$ sec
$\mu_2 = 2.89 \times 10^8$	$\tau_2 = 5 \times 10^{-6}$
$\mu_3 = 4.55 \times 10^8$	$\tau_3 = 10^{-5}$
$\mu_4 = 6.89 \times 10^8$	$\tau_4 = 1$

$\bar{c} = 29.57$ m$^{-½}$

==========

CASE 3. Sphere of same static rigidity as the nylon described in Case 2.

$\mu_1 = 5.72 \times 10^8$ N/m^2	$\tau_1 = 10^{-7}$ sec
$\mu_2 = 2.89 \times 10^8$	$\tau_2 = 10^{-3}$
$\mu_3 = 4.55 \times 10^8$	$\tau_3 = 10$
$\mu_4 = 6.89 \times 10^8$	$\tau_4 = 1$

$\bar{c} = 29.57$ m$^{-½}$

TABLE 5.1. Material properties and assumed relaxation times of three visco-elastic spheres.

FIG.5.1. Sound pressure time history for 2.54 cm diameter sphere with the same properties described in Case 1. (v_o = 4.87 m/s, $\theta = 0^o$, r = 0.36 m)

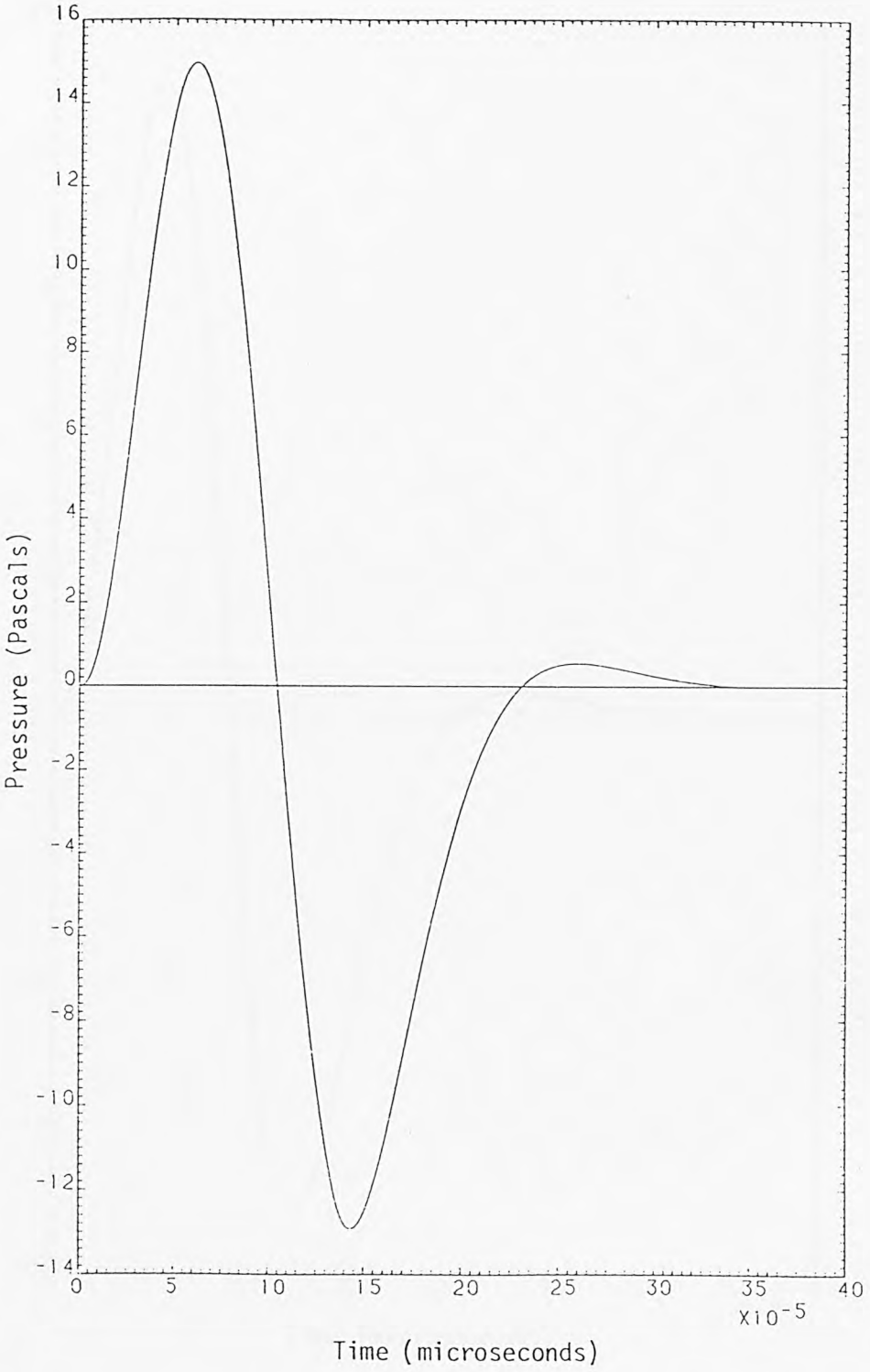

FIG.5.2. Sound pressure time history for 2.54 cm diameter sphere with the same properties described in Case 2. (v_o = 4.87 m/s, $\theta = 0^o$, r = 0.36 m)

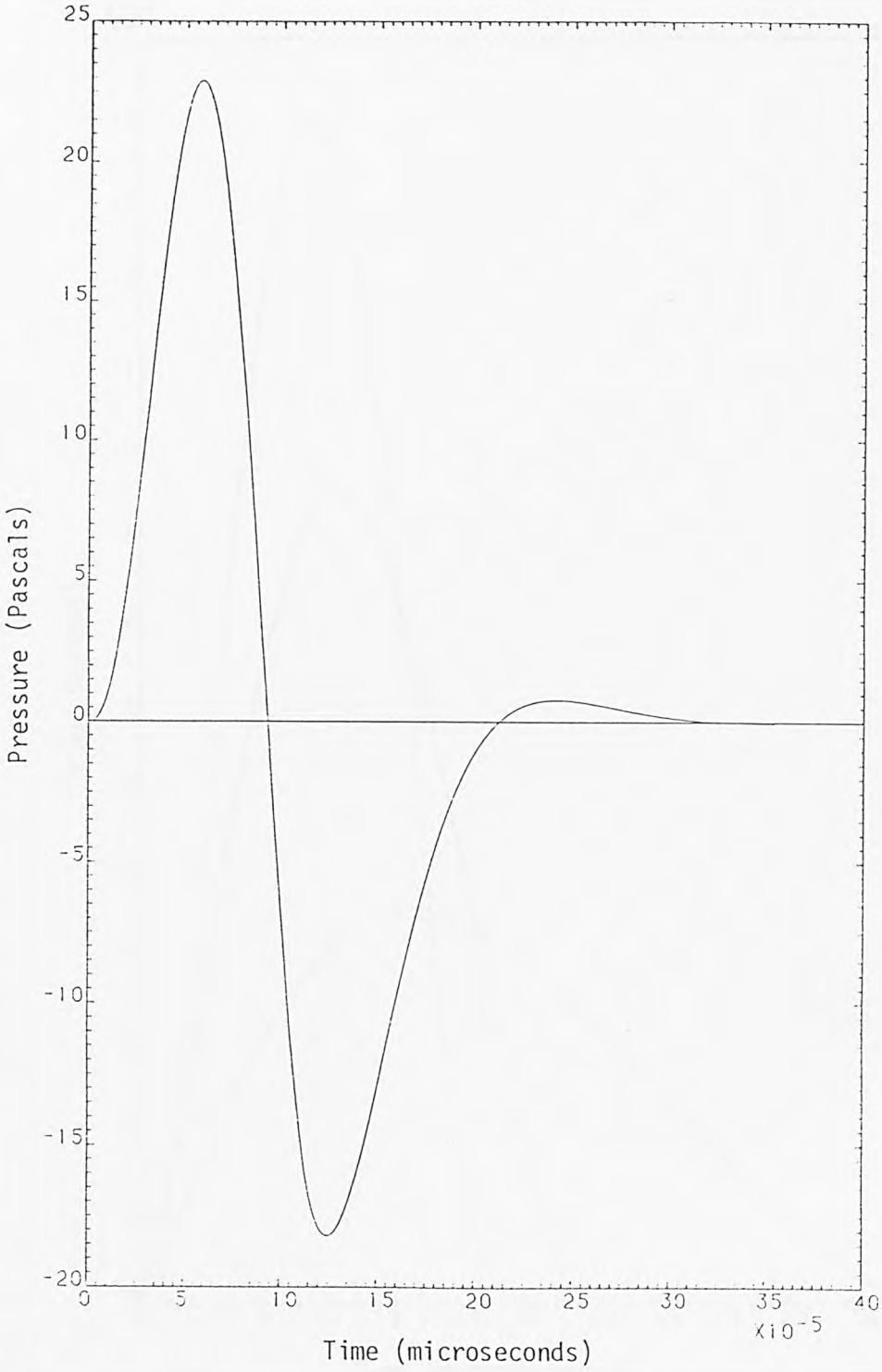

FIG.5.3. Sound pressure time history for 2.54 cm diameter sphere with the same properties described in Case 3. (v_o = 4.87 m/s, $\theta = 0^o$, r = 0.36 m)

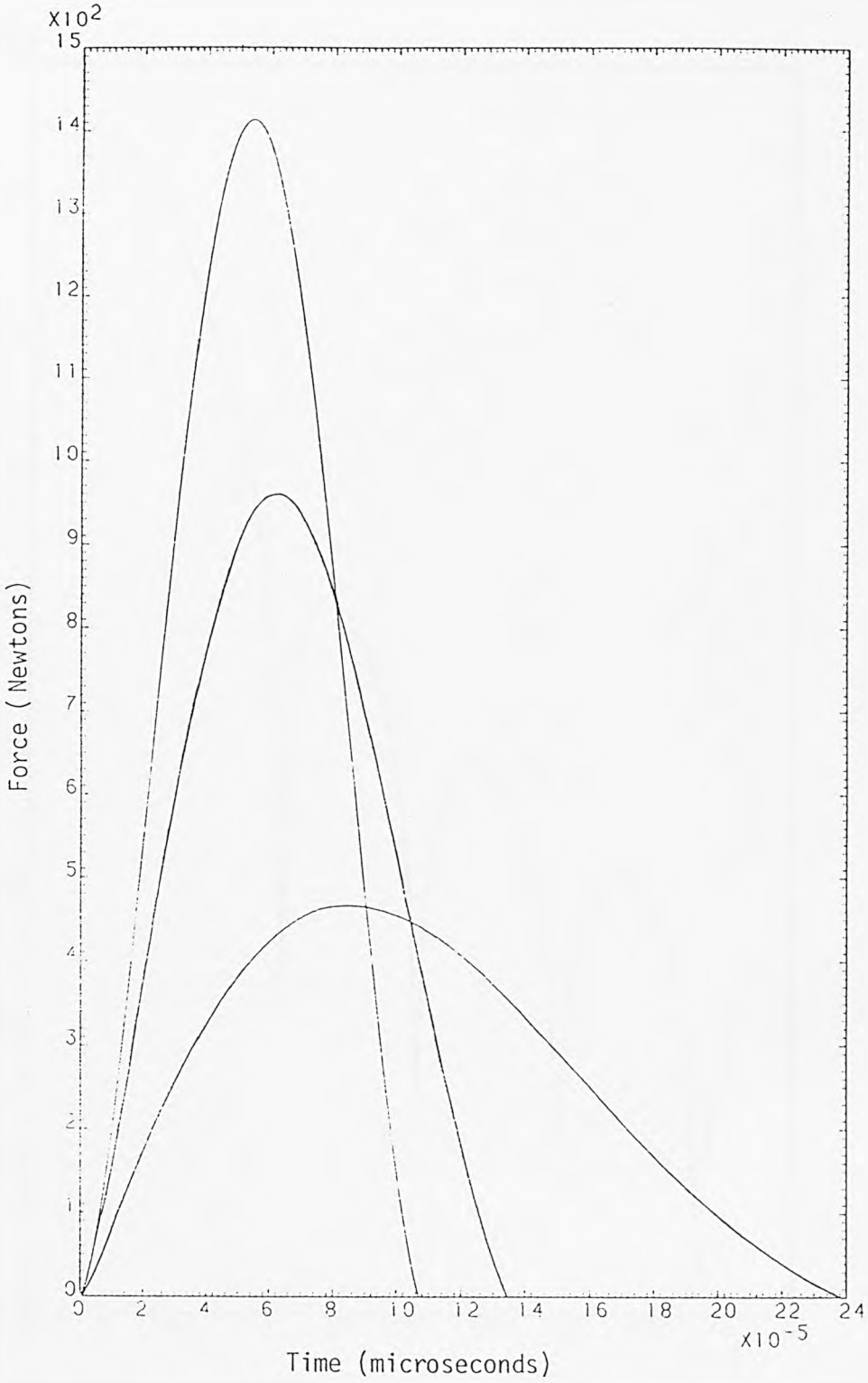

FIG.5.4. Force-time curves due to collision of steel sphere and visco-elastic sphere described in Table 5.1.

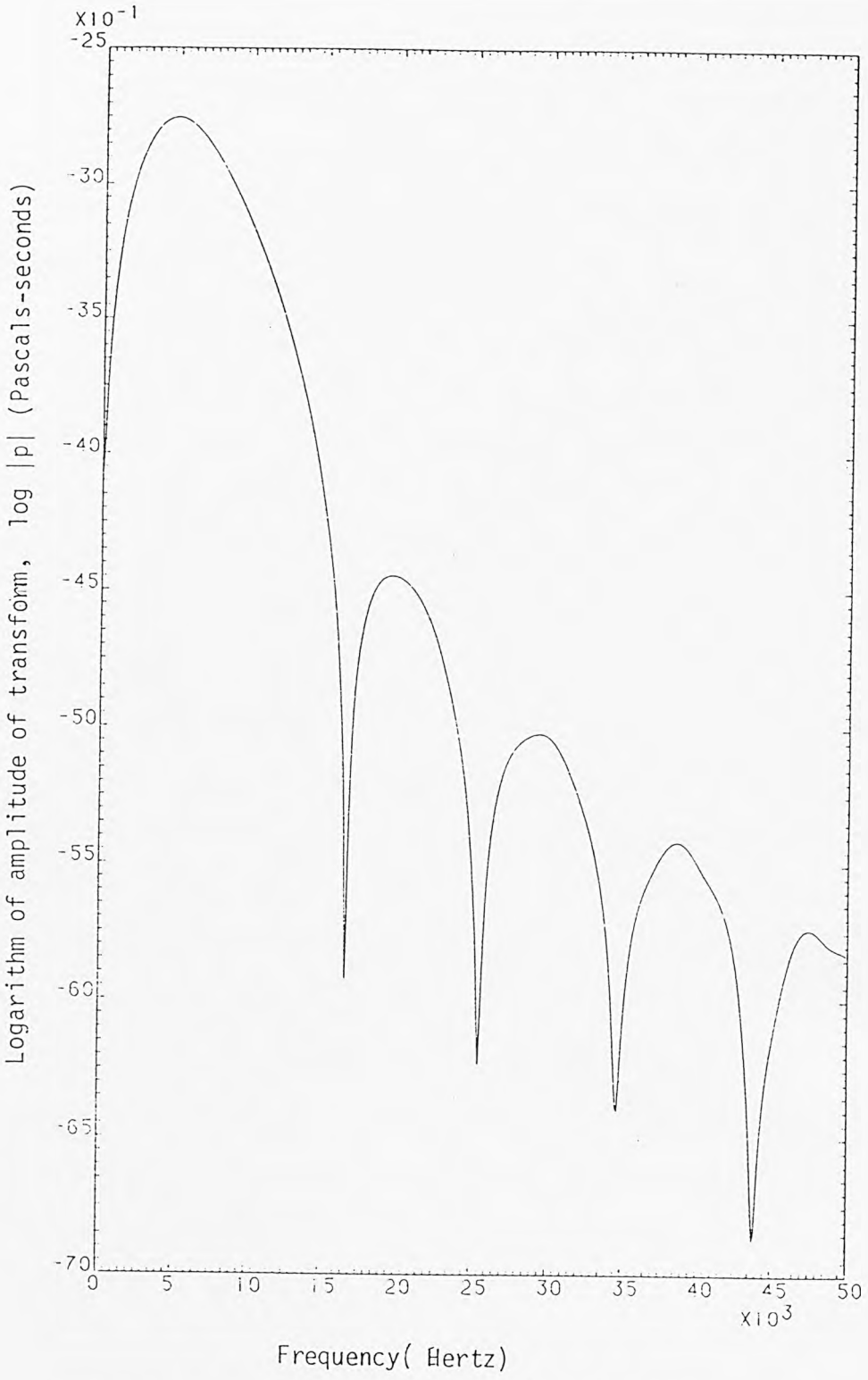

FIG.5.5. Fourier transform of pressure for sphere with the pressure time history as given in Fig.5.3.

6. SOUND RADIATION FROM TRANSIENT VIBRATION OF SOLID SPHERE

In Chapter Two Lamb's solution to the equations of motion for a sphere were introduced. These solutions are transferred to the spherical polar co-ordinates in this chapter and the results are compared with those developed through an alternative method. The results obtained by this new and more complete approach can also be used for studying the vibration of a hollow sphere.

Frequency equations for both torsional and spheroidal vibrations are derived and their successive roots for different orders are tabulated.

The orthogonality in both types of vibration have been established for the first time.

The orthogonality conditions allow the normalised modes to be calculated and enable the possibility of determining the responses to different excitation functions.

The modal shapes of torsional and spheroidal vibrations are studied and three dimensional diagrams of the surface mode shapes are provided.

Finally the response due to collision of a pair of spheres is obtained and used for the derivation of sound radiation by the transient vibration of spheres.

6.1. Vibration of elastic spheres

It has been shown in section (2.8) that the solution of the system of equations (2.86a) to (2.86c) are of two distinct

types, The first type may be given by the expression in the form of (2.126) as:

$$\hat{u}_n = (y \frac{\partial \bar{X}_n}{\partial z} - z \frac{\partial \bar{X}_n}{\partial y}) \psi_n(K_2 r) \tag{6.1a}$$

$$\hat{v}_n = (z \frac{\partial \bar{X}_n}{\partial x} - x \frac{\partial \bar{X}_n}{\partial z}) \psi_n(K_2 r) \tag{6.1b}$$

$$\hat{w}_n = (x \frac{\partial \bar{X}_n}{\partial y} - y \frac{\partial \bar{X}_n}{\partial x}) \psi_n(K_2 r) \tag{6.1c}$$

where $K_2 = \frac{\omega}{C_2}$ and $C_2 = (\frac{\mu}{\rho})^{\frac{1}{2}}$ is the velocity of distortional wave. Since the above modes of vibration make no change of volume (dilatation equal to zero), the vibrations of the first class are purely transversal.

The modes of vibrations of the second class can be represented in terms of expressions in the form of (2.128) as:

$$\hat{u}_n = - \frac{1}{K_1^2} \frac{\partial \bar{\delta}_n}{\partial x} + \psi_{n-1}(K_2 r) \frac{\partial \bar{\phi}_n}{\partial x} - \frac{n}{n+1} \cdot \frac{K_2^2 r^{2n+3}}{(2n+1)(2n+3)} \psi_{n+1}(K_2 r) \frac{\partial}{\partial x} \frac{\bar{\phi}_n}{r^{2n+1}} \tag{6.2a}$$

$$\hat{v}_n = - \frac{1}{K_1^2} \frac{\partial \bar{\delta}_n}{\partial y} + \psi_{n-1}(K_2 r) \frac{\partial \bar{\phi}_n}{\partial y} - \frac{n}{n+1} \cdot \frac{K_2^2 r^{2n+3}}{(2n+1)(2n+3)} \psi_{n+1}(K_2 r) \frac{\partial}{\partial y} \frac{\bar{\phi}_n}{r^{2n+1}} \tag{6.2b}$$

$$\hat{w}_n = - \frac{1}{K_1^2} \frac{\partial \bar{\delta}_n}{\partial z} + \psi_{n-1}(K_2 r) \frac{\partial \bar{\phi}_n}{\partial z} - \frac{n}{n+1} \cdot \frac{K_2^2 r^{2n+3}}{(2n+1)(2n+3)} \psi_{n+1}(K_2 r) \frac{\partial}{\partial z} \frac{\bar{\phi}_n}{r^{2n+1}} \tag{6.2c}$$

where $\delta_n = \omega_n \psi_n(K_1 r)$, $K_1 = \frac{\omega}{C_1}$, and $C_1 = (\frac{\lambda+2\mu}{\rho})^{\frac{1}{2}}$ is the velocity of dilatational waves. Consider now spherical coordinates (r,θ,ψ) in which

$$x = r\sin\theta\cos\psi, \quad y = r\sin\theta\sin\psi, \quad z = r\cos\theta \tag{6.3}$$

The components of displacement in directions, r,θ,ψ can be related to $\hat{u}_n$, $\hat{v}_n$ and $\hat{w}_n$ through the matrix relation

$$\begin{bmatrix} u_r \\ u_\theta \\ u_\psi \end{bmatrix} = \begin{bmatrix} \sin\theta\cos\psi & \sin\theta\sin\psi & \cos\theta \\ \cos\theta\cos\psi & \cos\theta\sin\psi & -\sin\theta \\ -\sin\psi & \cos\psi & 0 \end{bmatrix} \begin{bmatrix} \hat{u}_n \\ \hat{v}_n \\ \hat{w}_n \end{bmatrix} \tag{6.4}$$

Also by representing the gradient in both coordinates one obtains:

$$\begin{bmatrix} \frac{\partial}{\partial x} \\ \frac{\partial}{\partial y} \\ \frac{\partial}{\partial z} \end{bmatrix} = \begin{bmatrix} \sin\theta\cos\psi & \cos\theta\cos\psi & -\sin\psi \\ \sin\theta\sin\psi & \cos\theta\sin\psi & \cos\psi \\ \cos\theta & -\sin\theta & 0 \end{bmatrix} \begin{bmatrix} \frac{\partial}{\partial r} \\ \frac{1}{r}\frac{\partial}{\partial\theta} \\ \frac{1}{r\sin\theta}\frac{\partial}{\partial\psi} \end{bmatrix} \tag{6.5}$$

In equation (6.1a) to (6.1c) $\bar{X}_n$ is a solid harmonic of degree n and may be written as:

$$\bar{X}_n = A_n r^n P_n^m(\cos\theta) \begin{matrix} \sin m\psi \\ \cos m\psi \end{matrix} \tag{6.6}$$

where $P_n^m(\cos\theta)$ is the associated Legendre function. Substituting for solid harmonic $\bar{X}_n$ into equation (6.1a) to (6.1c) and using the matrix transformation (6.5) gives:

$$\hat{u}_n = -A_n r^n \{\frac{d}{d\theta} P_n^m(\cos\theta) \begin{matrix}\sin m\psi \\ \cos m\psi\end{matrix} \sin\psi \pm \frac{m}{\sin\theta} P_n^m(\cos\theta) \begin{matrix}\cos m\psi \\ \sin m\psi\end{matrix} \cos\theta\cos\psi\}$$

$$\psi_n(K_2 r) \qquad (6.7a)$$

$$\hat{v}_n = A_n r^n \frac{d}{d\theta} P_n^m(\cos\theta) \begin{matrix}\sin m\psi \\ \cos m\psi\end{matrix} \cos\psi \mp \frac{m}{\sin\theta} P_n^m(\cos\theta) \begin{matrix}\cos m\psi \\ \sin m\psi\end{matrix} \cos\theta\sin\psi\}$$

$$\psi_n(K_2 r) \qquad (6.7b)$$

$$\hat{w}_n = \pm A_n r^n m P_n^m(\cos\theta) \begin{matrix}\cos m\psi \\ \sin m\psi\end{matrix} \psi_n(K_2 r) \qquad (6.7c)$$

Using now (6.7a) to (6.7c) together with matrix transformation (6.4) yields:

$$u_r = 0 \qquad (6.8a)$$

$$u_\theta = \mp A_n \frac{m}{\sin\theta} r^n P_n^m(\cos\theta)\psi_n(K_2 r) \begin{matrix}\cos m\psi \\ \sin m\psi\end{matrix} \qquad (6.8b)$$

$$u_\psi = A_n r^n \frac{d}{d\theta} P_n^m(\cos\theta)\psi_n(K_2 r) \begin{matrix}\sin m\psi \\ \cos m\psi\end{matrix} \qquad (6.8c)$$

Thus for transversal vibrations of a solid sphere the component of displacement in directions r,θ,ψ may be given by equations (6.8a) to (6.8c) respectively. In this type of vibrations there is neither dilatational nor radial displacement.

In order to find u_r, u_θ and u_ψ for the set of equations (6.2a) to (6.2c) one may similarly introduce the solid harmonics $\bar{\omega}_n$ and $\bar{\phi}_n$ as:

$$\bar{\omega}_n = B_n r^n P_n^m(\cos\theta) \begin{matrix}\sin m\psi \\ \cos m\psi\end{matrix} \qquad (6.9a)$$

$$\bar{\Phi}_n = D_n r^n P_n^m(\cos\theta) \begin{matrix}\sin m\psi \\ \cos m\psi\end{matrix} \qquad (6.9b)$$

Substituting for $\bar{\omega}_n$ and $\bar{\phi}_n$ into equations (6.2a) to (6.2c) and using the matrix transformation (6.5) gives:

$$\hat{u}_n = r^{n-1}\left[\frac{B_n}{K_1^2}\left[(n+1)\psi_n(K_1r)\ (2n+1)\psi_{n-1}(K_1r)\right]\right.$$

$$\left.+nD_n\ _n(K_2r)\right]P_n^m(\cos\theta)\begin{matrix}\sin m\psi\\ \cos m\psi\end{matrix}\ \sin\theta\cos\psi$$

$$-\frac{r^{n-1}}{n+1}\left[\frac{B_n}{K_1^2}(n+1)\psi_n(K_1r)+D_n\left[n\psi_n(K_2r)-(2n+1)\psi_{n-1}(K_2r)\right]\right]$$

$$\frac{d}{d\theta}P_n^m(\cos\theta)\begin{matrix}\sin m\psi\\ \cos m\psi\end{matrix}\ \cos\theta\cos\psi$$

$$\mp\frac{r^{n-1}}{n+1}\left[\frac{B_n}{K_1^2}(n+1)\psi_n(K_1r)+D_n\left[n\psi_n(K_2r)-(2n+1)\psi_{n-1}(K_2r)\right]\right]$$

$$\frac{m}{\sin\theta}P_n^m(\cos\theta)\begin{matrix}\cos m\psi\\ \sin m\psi\end{matrix}\ \sin\psi \qquad (6.10a)$$

$$\hat{v}_n = r^{n-1}\left[\frac{B_n}{K_1^2}\left[(n+1)\psi_n(K_1r)-(2n+1)\psi_{n-1}(K_1r)\right]+nD_n\psi_n(K_2r)\right]$$

$$P_n^m(\cos\theta)\begin{matrix}\sin m\psi\\ \cos m\psi\end{matrix}\ \sin\theta\sin\psi$$

$$-\frac{r^{n-1}}{n+1}\left[\frac{B_n}{K_1^2}(n+1)\psi_n(K_1r)+D_n\left[n\psi_n(K_2r)-(2n+1)\psi_{n-1}(K_2r)\right]\right]$$

$$\frac{d}{d\theta}P_n^m(\cos\theta)\begin{matrix}\sin m\psi\\ \cos m\psi\end{matrix}\cos\theta\sin\psi$$

$$\mp\frac{r^{n-1}}{n+1}\left[\frac{B_n}{K_1^2}(n+1)\psi_n(K_1r)+D_n\left[n\psi_n(K_2r)-(2n+1)\psi_{n-1}(K_2r)\right]\right]$$

$$\frac{m}{\sin\theta}P_n^m(\cos\theta)\begin{matrix}\cos m\psi\\ \sin m\psi\end{matrix}\ \cos\psi \qquad (6.10b)$$

$$\hat{w}_n = r^{n-1}\left[\frac{B_n}{K_1^2}\left[(n+1)\psi_n(K_1r)-(2n+1)\psi_{n-1}(K_1r)\right]+nD_n\psi_n(K_2r)\right]$$

$$P_n^m(\cos\theta)\begin{matrix}\sin m\psi\\ \cos m\psi\end{matrix}\cos\theta$$

$$+\frac{r^{n-1}}{n+1}\left[\frac{B_n}{K_1^2}(n+1)\psi_n(K_1r)+D_n\left[n\psi_n(K_2r)-(2n+1)\psi_{n-1}(K_2r)\right]\right]$$

$$\frac{d}{d\theta}P_n^m(\cos\theta)\begin{matrix}\sin m\psi\\ \cos m\psi\end{matrix}\sin\theta \qquad (6.10c)$$

The components u_r, u_θ and u_ψ may now be found from (6.4) to be:

$$u_r = r^{n-1}\left[\frac{B_n}{K_1^2}\left[(n+1)\psi_n(K_1r)-(2n+1)\psi_{n-1}(K_1r)\right]+nD_n\psi_n(K_2r)\right]$$

$$P_n^m(\cos\theta)\begin{matrix}\sin m\psi\\ \cos m\psi\end{matrix} \qquad (6.11a)$$

$$u_\theta = -\frac{r^{n-1}}{n+1}\left[\frac{B_n}{K_1^2}(n+1)\psi_n(K_1r)+D_n\left[n\psi_n(K_2r)-(2n+1)\psi_{n-1}(K_2r)\right]\right]$$

$$\frac{d}{d\theta}P_n^m(\cos\theta)\begin{matrix}\sin m\psi\\ \cos m\psi\end{matrix} \qquad (6.11b)$$

$$u_\psi = \mp\frac{r^{n-1}}{n+1}\left[\frac{B_n}{K_1^2}(n+1)\psi_n(K_1r)+D_n\left[n\psi_n(K_2r)-(2n+1)\psi_{n-1}(K_2r)\right]\right]$$

$$\frac{m}{\sin\theta}P_n^m(\cos\theta)\begin{matrix}\cos m\psi\\ \sin m\psi\end{matrix} \qquad (6.11c)$$

It can be seen from equations (6.11a) to (6.11c) that except for the case n=m=0 the vibration of what is called second class are accompanied by both distortional and dilatational waves.

The terms torsional and spheroidal vibrations are also used by some writers such as Schreiber et al [63] to distinguish both types of vibrations which are referred in this section as vibrations of the first and the second class respectively.

6.2. Solution of equations of motion (Alternative approach)

The equations of motion of an isotropic elastic solid, given by equations (2.81a) to (2.81c) may be written in vector form as:

$$\rho \frac{\partial^2 \underline{S}}{\partial t^2} = (1+\mu)\,\text{grad div } \underline{S} + \mu \nabla^2 \underline{S} \qquad (6.12)$$

where $\underline{S}$ is the displacement vector. For purely torsional vibrations dilatation (div $\underline{S}$=0) and equation (6.12) reduces to:

$$\frac{\partial^2 U_r}{\partial r^2} + \frac{2}{r}\frac{\partial U_r}{\partial r} + \frac{1}{r^2}\frac{\partial^2 U_r}{\partial \theta^2} + \frac{1}{r^2}\cot g\theta \frac{\partial U_r}{\partial \theta} + \frac{1}{r^2 \sin^2\theta}\frac{\partial^2 U_r}{\partial \psi^2}$$

$$- \frac{2}{r^2}\left(U_r + U_\theta \cot g\theta + \frac{\partial U_\theta}{\partial \theta} + \frac{1}{\sin\theta}\frac{\partial U_\psi}{\partial \psi}\right) = \frac{1}{C_2^2}\frac{\partial^2 U_r}{\partial t^2} \qquad (6.13a)$$

$$\frac{\partial^2 U_\theta}{\partial r^2} + \frac{2}{r}\frac{\partial U_\theta}{\partial r} + \frac{1}{r^2}\frac{\partial^2 U_\theta}{\partial \theta^2} + \frac{1}{r^2}\cot g\theta \frac{\partial U_\theta}{\partial \theta} + \frac{1}{r^2 \sin^2\theta}\frac{\partial^2 U_\theta}{\partial \psi^2}$$

$$+ \frac{1}{r^2}\left(2\frac{\partial U_r}{\partial \theta} - \frac{U_\theta}{\sin^2\theta} - 2\frac{\cot g\theta}{\sin\theta}\frac{\partial U_\psi}{\partial \psi}\right) = \frac{1}{C_2^2}\frac{\partial^2 U_\theta}{\partial t^2} \qquad (6.13b)$$

$$\frac{\partial^2 U_\psi}{\partial r^2} + \frac{2}{r}\frac{\partial U_\psi}{\partial r} + \frac{1}{r^2}\frac{\partial^2 U_\psi}{\partial \theta^2} + \frac{1}{r^2}\cot g\theta \frac{\partial U_\psi}{\partial \theta} + \frac{1}{r^2 \sin^2\theta}\frac{\partial^2 U_\psi}{\partial \psi^2}$$

$$+ \frac{1}{r^2}\left(\frac{2}{\sin\theta}\frac{\partial U_r}{\partial \psi} + 2\frac{\cot g\theta}{\sin\theta}\frac{\partial U_\theta}{\partial \psi} - \frac{U_\psi}{\sin^2\theta}\right) = \frac{1}{C_2^2}\frac{\partial^2 U_\psi}{\partial t^2} \qquad (6.13c)$$

where U_r, U_θ and U_ψ are components of displacement vector in directions r,θ, and ψ respectively. Consider now a solution in the form:

$$u_r = 0 \qquad (6.14a)$$

$$U_\theta = u_\theta(r,\theta,\psi)e^{i\omega t} = f_\theta(r)\frac{m}{\sin\theta} P_n^m(\cos\theta)\begin{matrix}\cos m\psi \\ \sin m\psi\end{matrix} e^{-i\omega t} \qquad (6.14b)$$

$$U_\psi = u_\psi(r,\theta,\psi)e^{i\omega t} = f_\psi(r)\frac{d}{d\theta} P_n^m(\cos\theta)\begin{matrix}\sin m\psi \\ \cos m\psi\end{matrix} e^{i\omega t} \qquad (6.14c)$$

Substituting these solutions into equations (6.13a) to (6.13c) gives:

$$f_\theta(r) \pm f_\psi(r) = 0 \qquad (6.15a)$$

$$\left[f_\theta''(r) + \frac{2}{r} f_\theta'(r)\right] P_n^m(\cos\theta) + \frac{1}{r^2} f_\theta(r)\left[\frac{d^2}{d\theta^2} P_n^m(\cos\theta) - \cot g\theta \frac{d}{d\theta} P_n^m(\cos\theta) - \frac{m^2}{\sin^2\theta} P_n^m(\cos\theta)\right]$$

$$\mp \frac{2}{r^2} f_\psi(r)\cot g\theta \frac{d}{d\theta} P_n^m(\cos\theta) = -K_2^2 f_\theta(r) P_n^m(\cos\theta) \qquad (6.15b)$$

$$\left[f''_\psi(r) + \frac{2}{r} f'_\psi(r)\right]\frac{d}{d\theta} P_n^m(\cos\theta) + \frac{1}{r^2} f_\psi(r)$$

$$\left[\frac{d^3}{d\theta^3}P_n^m(\cos\theta) + \cot g\theta\frac{d^2}{d\theta^2} P_n^m(\cos\theta)\right.$$

$$\left. - \frac{m^2}{\sin^2\theta}\frac{d}{d\theta} P_n^m(\cos\theta) - \frac{1}{\sin^2\theta}\frac{d}{d\theta} P_n^m(\cos\theta)\right]$$

$$\mp \frac{2}{r^2}\frac{\cot g\theta}{\sin^2\theta} m^2 f_\theta(r) P_n^m(\cos\theta) = -K_2^2 f_\psi(r)\frac{d}{d\theta} P_n^m(\cos\theta) \qquad (6.15c)$$

By making use of equation (6.15a), (6.15b) and (6.15c) can be written as:

$$r^2 f''_\theta(r) + 2rf'_\theta(r) + \left[K_2^2 r^2 - n(n+1)\right] f_\theta(r) = 0 \qquad (6.16a)$$

$$r^2 f''_\psi(r) + 2rf'_\psi(r) + \left[K_2^2 r^2 - n(n+1)\right] f_\psi(r) = 0 \qquad (6.16b)$$

In order to deduce (6.16a) and (6.16b) from equation (6.15b) and (6.15c) one should notice that:

$$\frac{d^2}{d\theta^2} P_n^m(\cos\theta) + \cot g\theta \frac{d}{d\theta} P_n^m(\cos\theta) - \frac{m^2}{\sin^2\theta} P_n^m(\cos\theta)$$

$$= -n(n+1) P_n^m(\cos\theta) \qquad (6.17a)$$

and

$$\frac{d^3}{d\theta^3} P_n^m(\cos\theta) + \cot g\theta \frac{d^2}{d\theta^2} P_n^m(\cos\theta) - \frac{1}{\sin^2\theta}\frac{d}{d\theta} P_n^m(\cos\theta)$$

$$- \frac{m^2}{\sin^2\theta}\frac{d}{d\theta} P_n^m(\cos\theta) + \frac{2\cot g\theta}{\sin^2\theta} m^2 P_n^m(\cos\theta)$$

$$= -n(n+1)\frac{d}{d\theta} P_n^m(\cos\theta) \qquad (6.17b)$$

It has been shown in section (2.2) that the solution to the equation such as (6.16a) and (6.16b) can be expressed in terms of spherical Bessel functions. Thus:

$$f_\psi = \bar{A}_n j_n(K_2 r) + \bar{\bar{A}}_n y_n(K_2 r) \tag{6.18a}$$

and

$$f_\theta = \mp f_\psi \tag{6.18b}$$

where $j_n(K_2 r)$ and $y_n(K_2 r)$ are spherical Bessel functions of the first and second kind respectively. For a solid sphere one should seek a solution which is finite at the origin. Thus upon making $\bar{\bar{A}}_n = 0$ the displacements due to torsional vibrations can be written as:

$$u_r = 0 \tag{6.19a}$$

$$u_\theta = \mp \bar{A}_n \frac{m}{\sin\theta} P_n^m(\cos\theta) j_n(K_2 r) \begin{matrix}\cos m\psi \\ \sin m\psi\end{matrix} \tag{6.19b}$$

$$u_\psi = \bar{A}_n \frac{d}{d\theta} P_n^m(\cos\theta) j_n(K_2 r) \begin{matrix}\sin m\psi \\ \cos m\psi\end{matrix} \tag{6.19c}$$

Consider now a second type of solution in the form:

$$\underline{S} = \text{grad}\phi + \text{curl } \underline{H} \tag{6.20}$$

where ϕ and $\underline{H}$ are scalar and vector potentials respectively. Substituting the above solution into equation (6.12) gives:

$$\nabla^2\phi = \frac{1}{C_1^2} \frac{\partial^2 \phi}{\partial t^2} \tag{6.21a}$$

and

$$\nabla^2 \underline{H} = \frac{1}{C_2^2} \frac{\partial^2 \underline{H}}{\partial t^2} \tag{6.21b}$$

To satisfy equations (6.21a) and (6.21b) one may assume solutions in the form:

$$\phi = -R(r) P_n^m(\cos\theta) \begin{matrix} \sin m\psi \\ \cos m\psi \end{matrix} e^{i\omega t} \tag{6.22a}$$

$$H_r = 0 \tag{6.22b}$$

$$H_\theta = f_\theta(r) \frac{m}{\sin\theta} P_n^m(\cos\theta) \begin{matrix} \cos m\psi \\ \sin m\psi \end{matrix} e^{i\omega t} \tag{6.22c}$$

$$H_\psi = -f_\psi(r) \frac{d}{d\theta} P_n^m(\cos\theta) \begin{matrix} \sin m\psi \\ \cos m\psi \end{matrix} e^{i\omega t} \tag{6.22d}$$

where H_r, H_θ and H_ψ are components of vector potential $\underline{H}$ in directions r,θ and ψ respectively. Substitution of the above assumed solutions into equations (6.21a) and (6.21b) suggests that the radial dependent functions should be expressed in terms of spherical Bessel functions of the first and second kind. Thus one may write:

$$R = \bar{B}_n j_n(K_1 r) + \bar{\bar{B}}_n y_n(K_1 r) \tag{6.23a}$$

$$f_\theta = \pm f_\psi \tag{6.23b}$$

$$f_\psi = \bar{D}_n j_n(K_2 r) + \bar{\bar{D}}_n y_n(K_2 r) \tag{6.23c}$$

Using now equation (6.2a) together with the assumed solution (6.22a) to (6.22d) and finding the components of the displacement vector in directions r,θ and ψ gives:

$$U_r = -\left[R' - \frac{n(n+1)}{r} f_\psi\right] P_n^m(\cos\theta) \begin{matrix}\sin m\psi \\ \cos m\psi\end{matrix} e^{i\omega t} \qquad (6.24a)$$

$$U_\theta = -\left[\frac{1}{r} R - \frac{1}{r} f_\psi - f'_\psi \frac{d}{d\theta} P_n^m(\cos\theta) \begin{matrix}\sin m\psi \\ \cos m\psi\end{matrix} e^{i\omega t} \right. \qquad (6.24b)$$

$$U_\psi = \left[\mp \frac{1}{r} R + \frac{1}{r} f_\theta + f'_\theta \frac{m}{\sin\theta} P_n^m(\cos\theta) \begin{matrix}\cos m\psi \\ \sin m\psi\end{matrix} e^{i\omega t} \right. \qquad (6.24c)$$

where primes denote differentiation with respect to r. Substituting from (6.23a) to (6.23c) into equation (6.24a) to (6.24c) yields:

$$\begin{aligned} u_r = -\Bigg[& \bar{B}_n \left[n j_{n-1}(K_1 r) - (n+1) j_{n+1}(K_1 r)\right] \frac{K_1}{2n+1} \\ & + \bar{\bar{B}}_n \left[n y_{n-1}(K_1 r) - (n+1) y_{n+1}(K_1 r)\right] \frac{K_1}{2n+1} \\ & - \frac{n(n+1)}{r} \left[\bar{D}_n j_n(K_2 r) + \bar{\bar{D}}_n y_n(K_2 r)\right] \Bigg] P_n^m(\cos\theta) \begin{matrix}\sin m\psi \\ \cos m\psi\end{matrix} \end{aligned} \qquad (6.25a)$$

$$\begin{aligned} u_\theta = & \left[\frac{1}{r}\left[\bar{B}_n j_n(K_1 r) + \bar{\bar{B}}_n y_n(K_1 r)\right] - \frac{1}{r}\left[\bar{D}_n j_n(K_2 r) + \bar{\bar{D}}_n y_n(K_2 r)\right]\right. \\ & + \Bigg[- \bar{D}_n \left[n j_{n-1}(K_2 r) - (n+1) j_{n+1}(K_2 r)\right] - \bar{\bar{D}}_n \left[n y_{n-1}(K_2 r)\right. \\ & \left. \left. - (n+1) y_{n+1}(K_2 r)\right]\right] \frac{K_2}{2n+1} \Bigg] \times \frac{d}{d\theta} P_n^m(\cos\theta) \begin{matrix}\sin m\psi \\ \cos m\psi\end{matrix} \end{aligned} \qquad (6.25b)$$

$$\begin{aligned} u_\psi = \mp \Bigg[& \frac{1}{r}\left[\bar{B}_n j_n(K_1 r) + \bar{\bar{B}}_n y_n(K_1 r)\right] - \frac{1}{r}\left[\bar{D}_n j_n(K_2 r) + \bar{\bar{D}}_n y_n(K_2 r)\right] \\ & - \bar{D}_n \left[n j_{n-1}(K_2 r) - (n+1) j_{n+1}(K_2 r)\right] \frac{K_2}{2n+1} \\ & - \bar{\bar{D}} \left[n y_{n-1}(K_2 r) - (n+1) y_{n+1}(K_2 r)\right] \frac{K_2}{2n+1} \Bigg] \\ & \times \frac{m}{\sin\theta} P_n^m(\cos\theta) \begin{matrix}\cos m\psi \\ \sin m\psi\end{matrix} \end{aligned} \qquad (6.25c)$$

Requirement that these solutions be finite at $r = 0$ may be accomplished by selecting $\bar{\bar{B}} = \bar{\bar{D}} = 0$. Thus for a solid sphere the modes of the second class or spheroidal modes can be given by:

$$u_r = -\left[\bar{B}_n K_1 \left[j_{n-1}(K_1 r) - \frac{(n+1)}{K_1 r} j_n(K_1 r)\right] - \frac{n(n+1)}{r} \bar{D}_n j_n(K_2 r)\right] P_n^m(\cos\theta) \begin{matrix}\sin m\psi \\ \cos m\psi\end{matrix} \tag{6.26a}$$

$$u_\theta = -\left[\frac{\bar{B}_n}{r} j_n(K_1 r) - \bar{D}_n K_2 \left[j_{n-1}(K_2 r) - \frac{n}{K_2 r} j_n(K_2 r)\right]\right] \frac{d}{d\theta} P_n^m(\cos\theta) \begin{matrix}\sin m\psi \\ \cos m\psi\end{matrix} \tag{6.26b}$$

$$u_\psi = \mp\left[\frac{\bar{B}_n}{r} j_n(K_1 r) - \bar{D}_n K_2 \left[j_{n-1}(K_2 r) - \frac{n}{K_2 r} j_n(K_2 r)\right]\right] \frac{m}{\sin\theta} P_n^m(\cos\theta) \begin{matrix}\cos m\psi \\ \sin m\psi\end{matrix} \tag{6.26c}$$

To express the solutions given in this section in terms of function ψ_n one may simply write:

$$\psi_n(K_1 r) = \eta_n (K_1 r)^{-n} j_n(K_1 r)$$

and

$$\psi_n(K_2 r) = \eta_n (K_2 r)^{-n} j_n(K_2 r) \tag{6.27a}$$

where

$$\eta_n = 1x3x5x.....x(2n+1) \tag{6.27b}$$

It can also be easily shown that the results obtained in this section lead to the same results as given in section (6.1), by

substituting (6.27a) into corresponding equations and taking

$$\bar{A}_n = A_n \eta_n K_2^{-n} \tag{6.28a}$$

$$\bar{B}_n = B_n \eta_n K_1^{-n-2} \tag{6.28b}$$

$$\bar{D}_n = D_n \frac{\eta_n}{n+1} K_2^{-n} \tag{6.28c}$$

6.3. Frequency equation

The stress-strain relations in spherical coordinates may be written as:

$$\sigma_{rr} = \lambda\Delta + 2\mu \frac{\partial U_r}{\partial r} \tag{6.29a}$$

$$\sigma_{r\theta} = \mu\left(\frac{1}{r}\frac{\partial U_r}{\partial \theta} + \frac{\partial U_\theta}{\partial r} - \frac{U_\theta}{r}\right) \tag{6.29b}$$

$$\sigma_{r\psi} = \mu\left(\frac{1}{r\sin\theta}\frac{\partial U_r}{\partial \psi} + \frac{\partial U_\psi}{\partial r} - \frac{U_\psi}{r}\right) \tag{6.29c}$$

where $\Delta = \mathrm{div}\underline{S}$ is the dilatation. For torsional vibrations of the sphere the above stress-strain relations may be given by:

$$\sigma_{rr} = 0 \tag{6.30a}$$

$$\sigma_{r\theta} = \mu\left(f'_\theta - \frac{1}{r} f_\theta\right) \frac{m}{\sin\theta} P_n^m(\cos\theta) \begin{matrix}\cos m\psi \\ \sin m\psi\end{matrix} e^{i\omega t} \tag{6.30b}$$

$$\sigma_{r\psi} = \mu\left(f'_\psi - \frac{1}{r} f_\psi\right) \frac{d}{d\theta} P_n^m(\cos\theta) \begin{matrix}\sin m\psi \\ \cos m\psi\end{matrix} e^{i\omega t} \tag{6.30c}$$

Similarly, for spheroidal vibrations one may obtain:

$$\sigma_{rr} = \left[\lambda K_1^2 R - 2\mu\left[R'' - \frac{n(n+1)}{r}\left(f'_\psi - \frac{1}{r} f_\psi\right)\right]\right] P_n^m(\cos\theta) \begin{matrix}\sin m\psi \\ \cos m\psi\end{matrix} e^{i\omega t} \tag{6.31a}$$

$$\sigma_{r\theta} = -\mu\left[\frac{2}{r}\left(R' - \frac{1}{r} R\right) + \frac{2}{r^2} f_\psi - \frac{n(n+1)}{r^2} f_\psi - f''_\psi\right]$$

$$\frac{d}{d\theta} P_n^m(\cos\theta) \begin{matrix}\sin m\psi \\ \cos m\psi\end{matrix} e^{i\omega t} \tag{6.31b}$$

$$\sigma_{r\psi} = \mu\left[\mp\frac{2}{r}\left(R' - \frac{1}{r}R\right) - \frac{2}{r^2} f_\theta \pm \frac{n(n+1)}{r^2} f_\psi + f''_\theta\right]$$

$$\frac{m}{\sin\theta} P_n^m(\cos\theta) \begin{matrix}\cos m\psi \\ \sin m\psi\end{matrix} e^{i\omega t} \tag{6,31c}$$

The boundary conditions at the surface of the solid sphere (r=a) are:

$$\sigma_{rr} = \sigma_{r\theta} = \sigma_{r\psi} = 0 \tag{6.32}$$

It can be easily found that for torsional vibrations of spheres the above boundary conditions can be satisfied if

$$f'_\theta\Big|_{r=a} - \frac{1}{a} f_\theta\Big|_{r=a} = 0 \tag{6.33}$$

Thus the frequency equation of torsional vibrations of solid spheres may be written as:

$$(n-1) j_n(K_2 a) - K_2 a j_{n+1}(K_2 a) = 0 \tag{6.34}$$

For a certain n there is an unlimited number of roots which can be expressed in the form $\Omega_{n\ell}$, (ℓ=1,2,3,....). The successive roots of equation (6.34) for a different value of n are tabulated

in Table (6.1). To satisfy the boundary conditions on the surface of sphere subjected to spheroidal vibrations equation (6.31a) to (6.31c) may be written as:

$$-\lambda K_1^2 R\Big|_{r=a} + 2\mu\left[R''\Big|_{r=a} - \frac{n(n+1)}{a}\left(f'_\psi\Big|_{r=a} - \frac{1}{a}f_\psi\Big|_{r=a}\right)\right] = 0 \tag{6.35a}$$

$$\frac{2}{a}\left(R'\Big|_{r=a} - \frac{1}{a}R\Big|_{r=a}\right) + \frac{2}{a^2}f_\psi\Big|_{r=a} - \frac{n(n+1)}{a^2}f_\psi\Big|_{r=a} - f''_\psi\Big|_{r=a} = 0 \tag{6.35b}$$

$$\pm\frac{2}{a}\left(R'\Big|_{r=a} - \frac{1}{a}R\Big|_{r=a}\right) + \frac{2}{a^2}f_\theta\Big|_{r=a} \mp \frac{n(n+1)}{a^2}f_\psi\Big|_{r=a} - f''_\theta\Big|_{r=a} = 0 \tag{6.35c}$$

provided the first two of these equations are satisfied, the third one automatically would be satisfied because of ($f_\theta = \pm f_\psi$). Substituting for R and f_ψ into equations (6.35a) and (6.35b) gives:

$$\left[K_2^2a^2j_n(K_1a) - 2n(n-1)j_n(K_1a) - 4K_1aj_{n+1}(K_1a)\right]\bar{B}_n + 2n(n+1)\left[(n-1)j_n(K_2a) - K_2aj_{n+1}(K_2a)\right]\bar{D}_n = 0 \tag{6.36a}$$

$$\left[2(n-1)j_n(K_1a) - 2K_1aj_{n+1}(K_1a)\right]\bar{B}_n + \left[2(1-n^2)j_n(K_2a) - 2K_2aj_{n+1}(K_2a) + K_2^2a^2j_n(K_2a)\right]\bar{D}_n = 0 \tag{6.36b}$$

It is more convenient for our analysis to form new equations by simply mulitiplying equation (6.36b) by n and -(n+1) separately and adding with equation (6.36a). Thus.

$$\left[K_2^2a^2j_n(K_1a)-2(n+2)K_1aj_{n+1}(K_1a)\right]\bar{B}_n+\left[nK_2^2a^2j_n(K_2a)\right.$$

$$\left.-2n(n+2)K_2aj_{n+1}(K_2a)\right]\bar{D}_n \quad =0 \qquad (6.37a)$$

$$\left[K_2^2a^2j_n(K_1a)-2(n-1)K_1aj_{n-1}(K_1a)\right]\bar{B}_n-\left[(n+1)K_2^2a^2j_n(K_2a)\right.$$

$$\left.-2(n^2-1)K_2aj_{n-1}(K_2a)\right]\bar{D}_n = 0 \qquad (6.37b)$$

The ratio $\bar{D}_n/\bar{B}_n$ and the frequency equation may now be given by:

$$\frac{\bar{D}_n}{\bar{B}_n} = \frac{K_2^2a^2j_n(K_1a)-2(n-1)K_1aj_{n-1}(K_1a)}{(n+1)\left[K_2^2a^2j_n(K_2a)-2(n-1)K_2aj_{n-1}(K_2a)\right]} \qquad (6.38)$$

$$\left[nK_2^2a^2j_n(K_2a)-2n(n+2)K_2aj_{n+1}(K_2a)\right]\left[K_2^2a^2j_n(K_1a)\right.$$

$$\left.-2(n-1)K_1aj_{n-1}(K_1a)\right] \quad =$$

$$\left[2(n+2)K_1aj_{n+1}(K_1a)-K_2^2a^2j_n(K_1a)\right](n+1)\left[K_2^2a^2j_n(K_2a)\right.$$

$$\left.-2(n-1)K_2aj_{n-1}(K_2a)\right] \qquad (6.39)$$

In order to solve the frequency equation (6.39) numerically one needed to know the ratio K_1/K_2. This ratio can be expressed in terms of Poisson's ratio ν as:

$$\frac{K_1}{K_2} = \left[\frac{1-2\nu}{2(1-\nu)}\right]^{\frac{1}{2}} \qquad (6.40)$$

The successive roots of equation (6.39) for different values of n and the Poisson's ratio $\nu = 0.29$ are tabulated in Table 6.2.

6.4. Orthogonality and normalisation of torsional modes

The natural modes of torsional vibrations of solid spheres can be given by equations (6.19a) to (6.19c) in the form:

$$u_{r,nm\ell} = 0 \tag{6.42a}$$

$$u_{\theta,nm\ell} = \mp \bar{A}_{nm\ell} \cdot \frac{m}{\sin\theta} P_n^m(\cos\theta) j_n(\omega_{n\ell}\frac{r}{C_2}) \begin{matrix}\cos m\psi \\ \sin m\psi\end{matrix} \tag{6.42b}$$

$$u_{\psi,nm\ell} = \bar{A}_{nm\ell} \frac{d}{d\theta} P_n^m(\cos\theta) j_n(\omega_{n\ell}\frac{r}{C_2}) \begin{matrix}\sin m\psi \\ \cos m\psi\end{matrix} \tag{6.42c}$$

where $\omega_{n\ell}\frac{r}{C_2} = K_2 a \frac{r}{a}$, and $K_2 a$ are successive roots of the characteristic equation given by expression (6.34). Multiplying equations (6.42b) and (6.42c) by $u_{\theta,psq}$ and $u_{\psi,psq}$ respectively and integrating over the volume of the sphere gives:

$$\int_D u_{\theta,nm\ell} \cdot u_{\theta,psq} \cdot dD = \frac{2\pi}{\varepsilon_m} \delta_{ms} \int_0^a z_1 z_2 r^2 dr \int_0^\pi \frac{m.s}{\sin^2\theta} P_n^m(\cos\theta) P_p^s(\cos\theta) \sin\theta d\theta \tag{6.43a}$$

$$\int_D u_{\psi,nm\ell} \cdot u_{\psi,psq} \cdot dD = \frac{2\pi}{\varepsilon_m} \delta_{ms} \int_0^a z_1 z_2 r^2 dr \int_0^\pi \frac{d}{d\theta} P_n^m(\cos\theta) \frac{d}{d\theta} P_p^s(\cos\theta) \sin\theta d\theta \tag{6.43b}$$

where δ_{ms} is the Kronecker delta, $\varepsilon_o = 1$, $\varepsilon_m = 2$, (m=1,2,....),

$$z_1 = \bar{A}_{nm\ell} j_n(\omega_{n\ell}\frac{r}{C_2}) \tag{6.44a}$$

and

$$z_2 = \bar{A}_{psq} j_p(\omega_{pq}\frac{r}{C_2}) \tag{6.44b}$$

Consider now the Legendre's associated differential equation which can be written as:

$$(1-X^2)\frac{d^2}{dX^2}P_n^m(X) - 2X\frac{d}{dX}P_n^m(X) + \left[n(n+1) - \frac{m^2}{1-X^2}\right]P_n^m(X) = 0 \tag{6.45}$$

Multiplying (6.45) by $P_p^m(X)$ gives:

$$(1-X^2)P_p^m(X)\frac{d^2}{dX^2}P_n^m(X) - 2XP_p^m(X)\frac{d}{dX}P_n^m(X)$$

$$= \frac{m^2}{1-X^2}P_p^m(X)P_n^m(X) - n(n+1)P_p^m(X)P_n^m(X) \tag{6.46a}$$

$$\frac{d}{dX}\left[(1-X^2)P_p^m(X)\frac{d}{dX}P_n^m(X)\right] = \frac{m^2}{1-X^2}P_p^m(X)P_n^m(X) + (1-X^2)$$

$$\frac{d}{dX}P_p^m(X)\frac{d}{dX}P_n^m(X) - n(n+1)P_p^m(X)P_n^m(X) \tag{6.46b}$$

Integrating both sides yields:

$$\int_{-1}^{1}\left[\frac{m^2}{1-X^2}P_p^m(X)P_n^m(X) + (1-X^2)\frac{d}{dX}P_p^m(X)\frac{d}{dX}P_n^m(X)\right]dX$$

$$= \frac{2n(n+1)}{2n+1}\cdot\frac{(n+m)!}{(n-m)!}\delta_{np} \tag{6.47}$$

By making use of (6.47) equations (6.43a) and (6.43b) can be represented in the form of a single expression as:

$$\int_D \left[u_{\theta,nm\ell} \cdot u_{\theta,psq} + u_{\psi,nm\ell} \cdot u_{\psi,psq} \right] dD =$$

$$\frac{4\pi n(n+1)(n+m)!}{\varepsilon_m (2n+1)(n-m)!} \delta_{ms} \delta_{np} \int_0^a z_1 z_2 . r^2 dr \qquad (6.48)$$

To solve the integral on the right hand side of equation (6.48) one may consider the following differential equation:

$$r^2 z''_1 + 2rz'_1 + \left[\omega^2_{n\ell} \frac{r^2}{C_2^2} - n(n+1) \right] z_1 = 0 \qquad (6.49a)$$

$$r^2 z''_2 + 2rz'_2 + \left[\omega^2_{nq} \frac{r^2}{C_2^2} - n(n+1) \right] z_2 = 0 \qquad (6.49b)$$

which have as their solutions $z_1 = \bar{A}_{nm\ell} j_n(\omega_{n\ell} \frac{r}{C_2})$ and $z_2 = \bar{A}_{nmq} j_n(\omega_{nq} \frac{r}{C_2})$ respectively. Multiplying the first equation by z_2, the second by z_1 and subtracting gives:

$$\frac{d}{dr}\{r^2 \left[z_2 z'_1 - z_1 z'_2 \right]\} = \frac{r^2}{C_2^2} (\omega^2_{nq} - \omega^2_{n\ell}) z_1 z_2 \qquad (6.50a)$$

or

$$\frac{\omega^2_{nq} - \omega^2_{n\ell}}{C_2^2} \int_0^a r^2 z_1 z_2 dr = r^2 \left[z_2 z'_1 - z_1 z'_2 \right]_0^a \qquad (6.50b)$$

In order to find the value of the right hand side of equation (6.50b) at r=a the characteristic equation of torsional vibrations of spheres, given by expression (6.33) can be written as:

$$z'_1\Big|_{r=a} - \frac{1}{a} z_1\Big|_{r=a} = 0 \qquad (6.51a)$$

and

$$z'_2\Big|_{r=a} - \frac{1}{a} z_2\Big|_{r=a} = 0 \qquad (6.51b)$$

Multiplying the first equation by z_2, the second by z_1 and subtracting, gives:

$$\left[z_2 z'_1 - z_1 z'_2\right]_{r=a} = 0 \qquad (6.52)$$

Thus:

$$\int_0^a r^2 j_n(\omega_{n\ell}\frac{r}{C_2}) j_n(\omega_{nq}\frac{r}{C_2})\,dr = 0, \quad \ell \neq q \qquad (6.53a)$$

Also from (6.50b)

$$\int_0^a r^2 j^2{}_n(\omega_{n\ell}\frac{r}{C_2})\,dr =$$

$$= \lim_{\omega_{nq}\to\omega_{n\ell}} \frac{a^2 C_2{}^2\left[j_n(\omega_{nq}\frac{r}{C_2})\frac{d}{dr}j_n(\omega_{n\ell}\frac{r}{C_2}) - j_n(\omega_{n\ell}\frac{r}{C_2})\frac{d}{dr}j_n(\omega_{nq}\frac{r}{C_2})\right]}{\omega^2_{nq} - \omega^2_{n\ell}}$$

$$= \frac{a^3}{2}\left[j_n{}^2(\omega_{n\ell}\frac{a}{C_2}) - j_{n-1}(\omega_{n\ell}\frac{a}{C_2}) j_{n+1}(\omega_{n\ell}\frac{a}{C_2})\right] \qquad (6.53b)$$

Upon using expression (6.53a) and (6.53b) equation (6.48) can be written as:

$$\int_D \left[u_{\theta,nm\ell}\cdot u_{\theta,psq} + u_{\psi,nm\ell}\cdot u_{\psi,psq}\right] dD$$

$$= \frac{2\pi n(n+1)(n+m)!}{\varepsilon_m (2n+1)(n-m)!}\bar{A}^2_{nm\ell}\cdot a^3\left[j_n{}^2(\omega_{n\ell}\frac{a}{C_2}) - j_{n-1}(\omega_{n\ell}\frac{a}{C_2})\right.$$

$$\left. j_{n+1}(\omega_{n\ell}\frac{a}{C_2})\right]\delta_{ms}\delta_{np}\delta_{\ell q} \qquad (6.54)$$

The orthogonality of the torsional modes may now be given by:

$$\int_D \left[u_{\theta,nm\ell} \cdot u_{\theta,psq} + u_{\psi,nm\ell} \cdot u_{\psi,psq} \right] dD = 0 \qquad (6.55)$$

which is true whenever inequality between any pair of corresponding indices exist. The natural modes of torsional vibrations can also be normalised by mutliplying both sides of equation (6.54) by the density and equating the result to unity. Thus:

$$\int_D \rho \left[u^2_{\theta,nm\ell} + u^2_{\psi,nm\ell} \right] dD = \frac{2\rho\pi n(n+1)(n+m)!}{\varepsilon_m (2n+1)(n-m)!} \bar{A}^2_{nm\ell} a^3$$

$$\left[j_n{}^2(\omega_{n\ell}\frac{a}{C_2}) - j_{n-1}(\omega_{n\ell}\frac{a}{C_2}) j_{n+1}(\omega_{n\ell}\frac{a}{C_2}) \right] = 1 \qquad (6.56a)$$

or

$$\bar{A}^2_{nm\ell} = \frac{\varepsilon_m (2n+1)(n-m)!}{2\pi\rho n(n+1)(n+m)!} \times \frac{1}{a^3 \left[j_n{}^2(\omega_{n\ell}\frac{a}{C_2}) - j_{n-1}(\omega_{n\ell}\frac{a}{C_2}) j_{n+1}(\omega_{n\ell}\frac{a}{C_2}) \right]} \qquad (6.56b)$$

where ρ is the density of the homogeneous sphere under consideration. The spherical Bessel functions of order n-1 and n+1 in equation (6,56b) can be written in terms of spherical Bessel function of order n by using the characteristic equation given by expression (6.34) and noting that:

$$j_{n-1}(\omega_{n\ell}\frac{a}{C_2}) = \frac{(2n+1)C_2}{\omega_{n\ell} a} j_n(\omega_{n\ell}\frac{a}{C_2}) - j_{n+1}(\omega_{n\ell}\frac{a}{C_2}), \qquad (6.57)$$

which is derivable based on the properties of the spherical Bessel function, Thus:

$$\bar{A}^2_{nm\ell} = \frac{2\varepsilon_m(2n+1)(n-m)!}{3Mn(n+1)(n+m)!} \times \frac{\omega^2_{n\ell}a^2}{C_2^2 j_n^2(\omega_{n\ell}\frac{a}{C_2})\left[\frac{\omega^2_{n\ell}a^2}{C_2^2} - (n-1)(n+2)\right]} \tag{6.58}$$

where $M = \frac{4}{3}\rho\pi a^3$ is the mass of sphere. The normal modes of torsional vibrations may now be given by:

$$u^*_{\theta,nm\ell} = \mp \left[\frac{2\varepsilon_m(2n+1)(n-m)!}{3Mn(n+1)(n+m)!}\right]^{\frac{1}{2}} \frac{\omega_{n\ell}amj_n(\omega_{n\ell}\frac{r}{C_2})}{C_2 j_n(\omega_{n\ell}\frac{a}{C_2})\left[\frac{\omega^2_{n\ell}a^2}{C_2^2} - (n-1)(n+2)\right]^{\frac{1}{2}}}$$

$$\frac{P_n^m(\cos\theta)}{\sin\theta} \times \begin{matrix}\cos m\psi \\ \sin m\psi\end{matrix} \tag{6.59a}$$

$$u^*_{\psi,nm\ell} = \left[\frac{2\varepsilon_m(2n+1)(n-m)!}{3Mn(n+1)(n+m)!}\right]^{\frac{1}{2}} \frac{\omega_{n\ell}aj_n(\omega_{n\ell}\frac{r}{C_2})}{C_2 j_n(\omega_{n\ell}\frac{a}{C_2})\left[\frac{\omega^2_{n\ell}a^2}{C_2^2} - (n-1)(n+2)\right]^{\frac{1}{2}}}$$

$$\frac{d}{d\theta}P_n^m(\cos\theta) \times \begin{matrix}\sin m\psi \\ \cos m\psi\end{matrix} \tag{6.59b}$$

6.5. Modal shapes of torsional vibrations

The normal modes of torsional vibrations given by equations (6.59a) and (6.59b) in case n=1 may be expressed as:

$$u_{\theta,1m\ell} = \mp\left[\frac{\varepsilon_m(1-m)!}{M(1+m)!}\right]^{\frac{1}{2}} \frac{j_1(K_2r)}{j_1(K_2a)} \times \frac{m}{\sin\theta} P_1^m(\cos\theta) \times \begin{matrix}\cos m\psi \\ \sin m\psi\end{matrix} \tag{6.60a}$$

$$u_{\psi,1m\ell} = \left[\frac{\varepsilon_m(1-m)!}{M(1+m)!}\right]^{\frac{1}{2}} \frac{j_1(K_2r)}{j_1(K_2a)} \times \frac{d}{d\theta} P_1^m(\cos\theta) \times \begin{matrix}\sin m\psi \\ \cos m\psi\end{matrix} \tag{6.60b}$$

where m is either zero or one. In case of zonal harmonic (m=0) equations (6.60a) and (6.60b) reduce to:

$$u_{\theta,10\ell} = 0 \tag{6.61a}$$

$$u_{\psi,10\ell} = -\frac{1}{\sqrt{M}} \frac{j_1(K_2 r)}{j_1(K_2 a)} \sin\theta \tag{6.61b}$$

Thus each of the thin concentric spherical layers oscillate as a whole about the z axis. The characteristic equation given by expression (6.34) can be written as:

$$j_2(K_2 a) = 0 \tag{6.62}$$

The roots of equation (6.62) from Table 6.1 are:

$$K_2 a = 5.763, 9.095, 12.322, \ldots\ldots \tag{6.63}$$

To find the positions of the spherical nodes, i.e.surfaces across which there is no displacement one may write:

$$j_1(K_2 r) = 0 \tag{6.64}$$

The roots of equation (6.64) are:

$$K_2 r = 4.493, 7.725, 10.904 \tag{6.65}$$

Thus the positions of the spherical nodes for the first three modes whose non-dimensional frequencies are given by expression (6,34) may be found to be:

$$\frac{r}{a} = 0.78 \quad \text{(1st mode)} \tag{6.66a}$$

$$\frac{r}{a} = 0.49,\ 0.85 \qquad \text{(2nd mode)} \qquad (6.66b)$$

$$\frac{r}{a} = 0.365,\ 0.627,\ 0.885 \qquad \text{(3rd mode)} \qquad (6.66c)$$

There are also internal spherical surfaces across which no stress exists. Upon equating equation (6.30b) to zero one obtains:

$$j_2(K_2 r) = 0 \qquad (6.67)$$

or

$$K_2 r = 5.763, 9.095, 12.322..... \qquad (6.68)$$

Thus the positions of these surfaces for the second and third modes are respectively.

$$\frac{r}{a} = 0.63 \qquad \text{(2nd mode)} \qquad (6.69a)$$

$$\frac{r}{a} = 0.467, 0.738 \qquad \text{(3rd mode)} \qquad (6.69b)$$

Consider now the case of sectorial harmonic (m=n=1). The normalised displacements given by equations (6.60a) and (6.60b) can be written as:

$$u_{\theta,11\ell} = \mp \frac{1}{\sqrt{M}} \frac{j_1(K_2 r)}{j_1(K_2 a)} \times \begin{matrix} \cos\psi \\ \sin\psi \end{matrix} \qquad (6.70a)$$

$$u_{\psi,11\ell} = \frac{1}{\sqrt{M}} \frac{j_1(K_2 r)}{j_1(K_2 a)} \cos\theta \times \begin{matrix} \sin\psi \\ \cos\psi \end{matrix} \qquad (6.70b)$$

There are two distinct groups of displacements depending upon whether the upper or lower functions of are selected. It can also be easily verified that the position of spherical nodes and zero stress surfaces remain unchanged. Let us now investigate the second harmonic (n=2). The normalised displacements given by equations (6.59a) and (6.59b) may be written as:

$$u_{\theta,2m\ell} = \mp\left[\frac{5\varepsilon_m(2-m)!}{9M(2+m)!}\right]^{\frac{1}{2}} \frac{K_2 a j_2(K_2 r)}{\left[(K_2 a)^2-4\right]^{\frac{1}{2}} j_2(K_2 a)} \times \frac{m}{\sin\theta} P_2^m(\cos\theta) \times \begin{matrix}\cos m\psi \\ \sin m\psi\end{matrix} \tag{6.71a}$$

$$u_{\psi,2m\ell} = \left[\frac{5\varepsilon_m(2-m)!}{9M(2+m)!}\right]^{\frac{1}{2}} \frac{K_2 a j_2(K_2 r)}{\left[(K_2 a)^2-4\right]^{\frac{1}{2}} j_2(K_2 a)} \times \frac{d}{d\theta} P_2^m(\cos\theta) \times \begin{matrix}\sin m\psi \\ \cos m\psi\end{matrix} \tag{6.71b}$$

where m = 0,1,2. Substituting the values of m into equations (6.71a) and (6.71b) gives:

$$u_{\theta,20\ell} = 0$$

$$u_{\psi,20\ell} = -\frac{\sqrt{5}}{2} \times \frac{1}{\sqrt{M}} \times \frac{K_2 a j_2(K_2 r)}{\left[(K_2 a)^2-4\right]^{\frac{1}{2}} j_2(K_2 a)} \sin 2\theta \quad \text{(Zonal harmonic m=0)} \tag{6.72a}$$

$$u_{\theta,21\ell} = \mp\frac{\sqrt{5}}{\sqrt{3}} \times \frac{1}{\sqrt{M}} \times \frac{K_2 a j_2(K_2 r)}{\left[(K_2 a)^2-4\right]^{\frac{1}{2}} j_2(K_2 a)} \cos\theta \times \begin{matrix}\cos\psi \\ \sin\psi\end{matrix}$$

$$u_{\psi,21\ell} = \frac{\sqrt{5}}{\sqrt{3}} \times \frac{1}{\sqrt{M}} \times \frac{K_2 a j_2(K_2 r)}{\left[(K_2 a)^2-4\right]^{\frac{1}{2}} j_2(K_2 a)} \cos 2\theta \times \begin{matrix}\sin\psi \\ \cos\psi\end{matrix} \quad \text{(Tesseral harmonic m=1)} \tag{6.72b}$$

$$u_{\theta,22\ell} = \mp \frac{\sqrt{5}}{\sqrt{3}} \times \frac{1}{\sqrt{M}} \times \frac{K_2 a j_2(K_2 r)}{\left[(K_2 a)^2 - 4\right]^{\frac{1}{2}} j_2(K_2 a)} \sin\theta \times \begin{matrix}\cos 2\psi \\ \sin 2\psi\end{matrix}$$

(Sectoral harmonic m=2)

$$u_{\psi,22\ell} = \frac{\sqrt{5}}{2\sqrt{3}} \times \frac{1}{\sqrt{M}} \times \frac{K_2 a j_2(K_2 r)}{\left[(K_2 a)^2 - 4\right]^{\frac{1}{2}} j_2(K_2 a)} \sin 2\theta \times \begin{matrix}\sin 2\psi \\ \cos 2\psi\end{matrix} \qquad (6.72c)$$

The characteristic equation may be found from expression (6.34) to be:

$$j_2(K_2 a) - K_2 a j_3(K_2 a) = 0 \qquad (6.73)$$

The roots of (6.73) from Table 6.1 are:

$$K_2 a = 2.501,\ 7.136, 10.514 \ldots\ldots \qquad (6.74)$$

To find the positions of the spherical nodes one may write:

$$j_2(K_2 r) = 0 \qquad (6.75)$$

or

$$K_2 r = 5.763, 9.095, 12.322 \ldots\ldots \qquad (6.76)$$

Thus the positions of the spherical nodes are given by:

$$\frac{r}{a} = 0.807 \qquad \text{(2nd mode)} \qquad (6.77a)$$

$$\frac{r}{a} = 0.548, 0.865 \qquad \text{(3rd mode)} \qquad (6.77b)$$

The positions of the zero stress surfaces may also be written as:

$$\frac{r}{a} = 0.35 \qquad \text{(2nd mode)} \qquad (6.78a)$$

$$\frac{r}{a} = 0.238, 0.679 \qquad \text{(3rd mode)} \tag{6.78b}$$

Plots showing variations of the normalised displacement along the radius of sphere are shown in Fig.(6.1). The three dimensional diagrams of the surface mode shapes are also given in Fig.(6.2).

6.6. Orthogonality and normalisation of spheroidal modes

The natural modes of spheroidal vibration of solid spheres can be derived from equations (6.24a) to (6.24c) to be:

$$u_{r,nm\ell} = -F_{nm\ell}(r).P_n^m(\cos\theta)\begin{matrix}\sin m\psi \\ \cos m\psi\end{matrix} \tag{6.79a}$$

$$u_{\theta,nm\ell} = -G_{nm\ell}(r).\frac{d}{d\theta}P_n^m(\cos\theta)\begin{matrix}\sin m\psi \\ \cos m\psi\end{matrix} \tag{6.79b}$$

$$u_{\psi,nm\ell} = \mp G_{nm\ell}(r).\frac{m}{\sin\theta}P_n^m(\cos\theta)\begin{matrix}\cos m\psi \\ \sin m\psi\end{matrix} \tag{6.79c}$$

where

$$F_{nm\ell}(r) = \bar{B}_{nm\ell}j'_n(\omega_{n\ell}\frac{r}{C_1}) - \frac{n(n+1)}{r}\bar{D}_{nm\ell}j_n(\omega_{n\ell}\frac{r}{C_2}) \tag{6.80a}$$

$$G_{nm\ell}(r) = \frac{1}{r}\bar{B}_{nm\ell}j_n(\omega_{n\ell}\frac{r}{C_1}) - \frac{1}{r}\bar{D}_{nm\ell}j_n(\omega_{n\ell}\frac{r}{C_2}) - \bar{D}_{nm\ell}j'_n(\omega_{n\ell}\frac{r}{C_2}) \tag{6.80b}$$

Multiplying equations (6.79a) to (6.79c) by $u_{r,psq}$, $u_{\theta,psq}$ and $u_{\psi,psq}$ respectively and integrating over the volume of sphere gives:

$$\int_D \rho u_{r,nm\ell}.u_{r,psq}dD = \frac{2\pi\rho}{\varepsilon_m}\delta_{ms}\int_o^a F_{nm\ell}(r).F_{psq}(r).r^2dr$$

$$\int_o^\pi P_n^m(\cos\theta).P_p^s(\cos\theta)\sin\theta d\theta \tag{6.81a}$$

$$\int_D \rho u_{\theta,nm\ell} \cdot u_{\theta,psq}\, dD = \frac{2\pi\rho}{\varepsilon_m}\delta_{ms}\int_o^a G_{nm\ell}(r).G_{psq}(r).r^2dr$$

$$\int_o^\pi \frac{d}{d\theta}P_n^m(\cos\theta)\,\frac{d}{d\theta}P_p^s(\cos\theta)\sin\theta d\theta \qquad (6.81b)$$

$$\int_D \rho u_{\psi,nm\ell} \cdot u_{\psi,psq}\, dD = \frac{2\pi\rho}{\varepsilon_m}\delta_{ms}\int_o^a G_{nm\ell}(r).G_{psq}(r).r^2dr$$

$$\int_o^\pi \frac{ms}{\sin^2\theta} P_n^m(\cos\theta)P_p^s(\cos\theta)\sin\theta d\theta \qquad (6.81c)$$

where ρ is the density, $\varepsilon_o = 1$, and $\varepsilon_m = 2$ (m=1,2,...). Using now (6.47) gives:

$$\int_D \rho\left[u_{\theta,nm\ell}\cdot u_{\theta,psq} + u_{\psi,nm\ell}\cdot u_{\psi,psq}\right]dD$$

$$= \frac{4\pi\rho n(n+1(n+m)!}{\varepsilon_m(2n+1)(n-m)!}\delta_{ms}\delta_{np}\int_o^a G_{nm\ell}(r).G_{psq}(r).r^2dr \qquad (6.82)$$

Also

$$\int_o^\pi P_n^m(\cos\theta).P_p^m(\cos\theta)\sin\theta d\theta = \frac{2}{2n+1}\frac{(n+m)!}{(n-m)!}\delta_{np} \qquad (6.83)$$

Thus (6.81a) can be written as:

$$\int_D \rho u_{r,nm\ell}\cdot u_{r,psq}\, dD = \frac{4\pi\rho(n+m)!}{\varepsilon_m(2n+1)(n-m)!}\delta_{ms}\delta_{np}\int_o^a F_{nm\ell}(r).F_{psq}(r).r^2dr \qquad (6.84)$$

Adding (6.82) and (6.84) yields:

$$\int_D \rho\left[u_{r,nm\ell}\cdot u_{r.psq} + U_{\theta,nm\ell}\cdot u_{\theta,psq} + u_{\psi,nm\ell}\cdot u_{\psi,psq}\right]dD$$

$$= \frac{4\pi\rho(n+m)!}{\varepsilon_m(2n+1(n-m)!}\delta_{ms}\delta_{np}\times\int_o^a\Big[F_{nm\ell}(r).F_{psq}(r)+n(n+1)$$

$$G_{nm\ell}(r).G_{psq}(r)\Big]r^2dr \qquad (6.85)$$

The integral on the right hand side of equation (6.85) when m=s and n=p can be found to be:

$$\int_0^a \left[F_{nm\ell}(r).F_{nmq}(r)+n(n+1)G_{nm\ell}(r).G_{nmq}(r)\right]r^2dr$$

$$= \int_0^a \left[r^2R'_1R'_2+n(n+1)R_1R_2\right]dr - n(n+1)\int_0^a (R_2Y_1+rR'_2Y_1+rR_2Y'_1)dr$$

$$-n(n+1)\int_0^a R_1Y_2+rR'_1Y_2+rR_1Y'_2)dr+ n(n+1)$$

$$+ n(n+1)\int_0^a Y_1Y_2+rY'_1Y_2)dr + n(n+1)\int_0^a (r^2Y'_1Y'_2+n(n+1)Y_1Y_2)dr$$

(6.86)

where

$$R_1 = \bar{B}_{nm\ell}j_n(\omega_{n\ell}\frac{r}{C_1}), \quad Y_1 = \bar{D}_{nm\ell}j_n(\omega_{n\ell}\frac{r}{C_2})$$

$$R_2 = \bar{B}_{nmq}\ j_n(\omega_{nq}\ \frac{r}{C_1}) \text{ and } \ Y_2 = \bar{D}_{nmq}j_n(\omega_{nq}\frac{r}{C_2})$$

It can be easily shown that $Y_1 = \bar{D}_{nm\ell}j_n(\omega_{n\ell}\frac{r}{C_2})$ and $Y_2=\bar{D}_{nmq}j_n(\omega_{nq}\frac{r}{C_2})$ are solutions of the equations:

$$r^2Y''_1+2rY'_1+\left[\omega^2_{n\ell}\frac{r^2}{C_2^2}-n(n+1)\right]Y_1 = 0 \qquad (6.87a)$$

$$r^2Y''_2+2rY'_2+\left[\omega^2_{nq}\frac{r^2}{C_2^2}-n(n+1)\right]Y_2 = 0 \qquad (6.87b)$$

Multiplying the first equation by $\omega^2_{nq}Y_2$, the second by $\omega^2_{n\ell}Y_1$ and subtracting gives:

$$\omega^2_{nq}\frac{d}{dr}(r^2Y'_1Y_2)-\omega^2_{n\ell}\frac{d}{dr}(r^2Y'_2Y_1)=(\omega^2_{nq}-\omega^2_{n\ell})$$

$$\left[r^2Y'_1Y'_2+n(n+1)Y_1Y_2\right] \qquad (6.88a)$$

or

$$(\omega^2_{nq} - \omega^2_{n\ell}) \int_0^a \left[r^2 Y'_1 Y'_2 + n(n+1) Y_1 Y_2\right] dr$$

$$= \omega^2_{nq} \left[r^2 Y'_1 Y_2\right]_0^a - \omega^2_{n\ell} \left[r^2 Y'_2 Y_1\right]_0^a \qquad (6.88b)$$

Thus (6.86) can be written as:

$$\int_0^a \left[F_{nm\ell}(r).F_{nmq}(r) + n(n+1) G_{nm\ell}(r).G_{nmq}(r)\right] r^2 dr$$

$$= \frac{1}{\omega^2_{nq} - \omega^2_{n\ell}} \{\omega^2_{nq} \left[r^2 R'_1 R_2\right]_0^a$$

$$- \omega^2_{n\ell} \left[r^2 R'_2 R_1\right]_0^a - n(n+1)(\omega^2_{nq} - \omega^2_{n\ell}) \left[r R_1 Y_2\right]_0^a$$

$$- n(n+1)(\omega^2_{nq} - \omega^2_{n\ell}) \left[r R_2 Y_1\right]_0^a + n(n+1)(\omega^2_{nq} - \omega^2_{n\ell})$$

$$\left[r Y_1 Y_2\right]_0^a + n(n+1)\omega^2_{nq} \left[r^2 Y'_1 Y_2\right]_0^a - n(n+1)\omega^2_{n\ell} \left[r^2 Y'_2 Y_1\right]_0^a \}$$

(6.89)

Equations (6.35a) and (6.35b) may now be used for estimating the value of the above integral at r=a. Thus by substituting R_1 and Y_1 for R and f_ψ one may obtain:

$$\frac{\omega^2_{n\ell}}{C_2^2} a^2 R_1|_{r=a} - 2n(n+1) R_1|_{r=a} + 4a R'_1|_{r=a} - 2n(n+1)(Y_1|_{r=a} - a Y'_1|_{r=a}) = 0$$

(6.90a)

$$-2(R_1|_{r=a} - aR'_1|_{r=a}) + \left[2Y_1|_{r=a} - 2n(n+1)Y_1|_{r=a} + 2aY'_1|_{r=a} + \frac{\omega^2}{C_2^2} n\ell a^2 Y_1|_{r=a}\right] = 0 \qquad (6.90b)$$

The new set of equations may be furnished by combining both equations after multiplying the second one once by n and then by -(n+1). Thus:

$$\left[\frac{\omega^2}{C_2^2} n\ell a^2 - 2n(n+2)\right](R_1|_{r=a} + nY_1|_{r=a}) + 2(n+2)a(R'_1|_{r=a} + nY'_1|_{r=a}) = 0 \qquad (6.91a)$$

$$\left[\frac{\omega^2}{C_2^2} n\ell a^2 - 2(n^2-1)\right]\left[R_1|_{r=a} - (n+1)Y_1|_{r=a}\right] - 2(n-1)a\left[R'_1|_{r=a} - (n+1)Y'_1|_{r=a}\right] = 0 \qquad (6.91b)$$

Similarly,

$$\left[\frac{\omega^2}{C_2^2} nq a^2 - 2n(n+2)\right](R_2|_{r=a} + nY_2|_{r=a}) + 2(n+2)a(R'_2|_{r=a} + nY'_2|_{r=a}) = 0 \qquad (6.92a)$$

$$\left[\frac{\omega^2}{C_2^2} nq a^2 - 2(n^2-1)\right]\left[R_2|_{r=a} - (n+1)Y_2|_{r=a}\right] - 2(n-1)a\left[R'_2|_{r=a} - (n+1)Y'_2|_{r=a}\right] = 0 \qquad (6.92b)$$

Multiplying (6.91a) by $\omega^2_{nq}(R_2|_{r=a}+nY_2|_{r=a})$, (6.92a) by $\omega^2_{n\ell}(R_1|_{r=a}+nY_1|_{r=a})$ and subtracting gives:

$$n(\omega^2_{n\ell}-\omega^2_{nq})\left[R_1R_2+n(R_2Y_1+R_1Y_2)+n^2Y_1Y_2\right]_{r=a}$$

$$-a\left[\omega^2_{n\ell}\left[R_1R'_2+n(R_1Y'_2+R'_2Y_1)+n^2Y_1Y'_2\right]_{r=a}\right.$$

$$\left.-\omega^2_{nq}\left[R_2R'_1+n(R_2Y'_1+R'_1Y_2)+n^2Y_2Y'_1\right]_{r=a}\right]=0 \qquad (6.93a)$$

Applying the same procedure on equations (6.91b) and (6.92b) yields:

$$(n+1)(\omega^2_{n\ell}-\omega^2_{nq})\left[R_1R_2-(n+1)(R_2Y_1+R_1Y_2)+(n+1)^2Y_1Y_2\right]_{r=a}$$

$$+a\left[\omega^2_{n\ell}\left[R_1R'_2-(n+1)(R_1Y'_2+Y_1R'_2)+(n+1)^2Y_1Y'_2\right]_{r=a}\right.$$

$$\left.-\omega^2_{nq}\left[R_2R'_1-(n+1)(R_2Y'_1+Y_2R'_1)+(n+1)^2Y'_1Y_2\right]\right]=0 \qquad (6.93b)$$

Multiplying (6.93a) by (n+1), (6.93b) by (-n) and adding gives:

$$\omega^2_{nq}a\left[R'_1R_2\right]_{r=a}-\omega^2_{n\ell}a\left[R'_2R_1\right]_{r=a}-n(n+1)(\omega^2_{nq}-\omega^2_{n\ell})\left[R_1Y_2+R_2Y_1\right]_{r=a}$$

$$+n(n+1)(\omega^2_{nq}-\omega^2_{n\ell})\left[Y_1Y_2\right]_{r=a}+n(n+1)\omega^2_{nq}a\left[Y'Y_2\right]_{r=a}$$

$$-n(n+1)\omega^2_{n\ell}a\left[Y_1Y'_2\right]_{r=a}=0 \qquad (6.94)$$

By making use of (6.94) expression (6.89) can be written as:

$$\int_0^a \left[F_{nm\ell}(r).F_{nmq}(r)+n(n+1)G_{nm\ell}(r).G_{nmq}(r)\right]r^2dr = 0 \qquad \ell\neq q \tag{6.95}$$

Also from (6.86)

$$\int_0^a \left[F^2_{nm\ell}(r)+n(n+1)G^2_{nm\ell}(r)\right]r^2dr = \int_0^a \left[r^2R'^2_1 +n(n+1)R_1^2\right]dr$$

$$-2n(n+1)\left[rR_1Y_1\right]_0^a + n(n+1)\left[rY_1^2\right]_0^a$$

$$+n(n+1)\int_0^a \left[r^2Y'^2_1 +n(n+1)Y_1^2\right]dr \tag{6.96}$$

To simplify the integrals on the right hand side of equation (6.96) equation (6.87a) may be multiplied by Y_1 to give:

$$\int_0^a \left[r^2Y'^2_1+n(n+1)Y_1^2\right]dr = \frac{\omega^2_{n\ell}}{C_2^2}\int_0^a r^2Y_1^2dr+\left[r^2Y'_1Y_1\right] \tag{6.97a}$$

Similarly,

$$\int_0^a \left[r^2R'^2_1+n(n+1)R_1^2\right]dr = \frac{\omega^2_{n\ell}}{C_1^2}\int_0^a r^2R_1^2dr+\left[r^2R'_1R_1\right]_0^a \tag{6.97b}$$

Thus (6,96) can be written as:

$$\int_0^a \left[F^2_{nm\ell}(r) + n(n+1)G^2_{nm\ell}(r)\right]r^2dr = \frac{\omega^2_{n\ell}}{C_1^2}\int_0^a r^2R_1^2dr$$

$$+\left[r^2R'_1R_1\right]_0^a -2n(n+1)\left[rR_1Y_1\right]_0^a + n(n+1)\left[rY_1^2\right]_0^a$$

$$+n(n+1)\frac{\omega^2_{n\ell}}{C_2^2}\int r^2Y_1^2dr +\left[r^2Y'_1Y_1\right]_0^a \tag{6,98}$$

Substituting for R_1 and Y_1 into equation (6.98) and using (6.53b) gives:

$$\int_0^a \left[F^2_{nm\ell}(r)+n(n+1)G^2_{nm\ell}(r)\right]r^2dr = \frac{1}{2}\bar{D}^2_{nm\ell}a\ \xi_{n\ell} \quad (6.99a)$$

where

$$\xi_{n\ell} = 2n\left[\frac{\bar{B}_{nm\ell}}{\bar{D}_{nm\ell}}\ j_n(\omega_{n\ell}\frac{a}{C_1}) - (n+1)j_n(\omega_{n\ell}\frac{a}{C_2})\right]^2$$

$$- (2n+3)\omega_{n\ell}\frac{a}{C_1}\left[\frac{\bar{B}^2_{nm\ell}}{\bar{D}^2_{nm\ell}}j_n(\omega_{n\ell}\frac{a}{C_1})j_{n+1}(\omega_{n\ell}\frac{a}{C_1})\right.$$

$$\left. + n(n+1)\frac{C_1}{C_2}\ j_n(\omega_{n\ell}\frac{a}{C_2})j_{n+1}(\omega_{n\ell}\frac{a}{C_2})\right] + \omega^2_{n\ell}\frac{a^2}{C_1^2}\left[\frac{\bar{B}^2_{nm\ell}}{\bar{D}^2_{nm\ell}}\right.$$

$$\left[j^2_n(\omega_{n\ell}\frac{a}{C_1}) + j^2_{n+1}(\omega_{n\ell}\frac{a}{C_1})\right] + n(n+1)\ \frac{C_1^2}{C_2^2}\left[j^2_n(\omega_{n\ell}\frac{a}{C_2})\right.$$

$$\left.\left. + j^2_{n+1}(\omega_{n\ell}\frac{a}{C_2})\right]\right] \quad (6.99b)$$

Upon using (6.95) and (6.99a) equation (6.85) can be written as:

$$\int_D \rho\left[u_{r,nm\ell}\cdot u_{r,psq} + u_{\theta,nm\ell}\cdot u_{\theta,psq} + u_{\psi,nm\ell}\cdot u_{\psi,psq}\right]dD$$

$$= \frac{2\pi\rho(n+m)!}{\varepsilon_m(2n+1)(n-m)!}\ \bar{D}^2_{nm\ell}a.\xi_{n\ell}\ \delta_{ms}\delta_{np}\delta_{\ell q} \quad (6.100)$$

The orthogonality of the spheroidal modes may now be represented by:

$$\int_D \rho\left[u_{r,nm\ell}\cdot u_{r,psq} + u_{\theta,nm\ell}\cdot u_{\theta,psq} + u_{\psi,nm\ell}\cdot u_{\psi,psq}\right]dD = 0 \quad (6.101)$$

which is true whenever inequality between any pair of corresponding indices exist. In order to normalise the natural modes of spheroidal equations (6.100) should be equated to unity. Thus:

$$\bar{D}^2_{nm\ell} = \frac{2\varepsilon_m(2n+1)(n-m)!}{3M(n+m)!} \cdot \frac{a^2}{\xi_{n\ell}} \tag{6.102}$$

where $M = \frac{4}{3}\rho\pi a^3$ is the mass of sphere. The normal modes of spheroidal vibrations may now be given by:

$$u^*_{r,nm\ell} = -\left[\frac{2\varepsilon_m(2n+1)(n-m)!}{3M\xi_{n\ell}(n+m)!}\right]^{\frac{1}{2}} a\left[\frac{\bar{B}_{nm\ell}}{\bar{D}_{nm\ell}}\left[\frac{\omega_{n\ell}}{C_1} j_{n-1}(\omega_{n\ell}\frac{r}{C_1}) - \frac{(n+1)}{r} j_n(\omega_{n\ell}\frac{r}{C_1})\right] - \frac{n(n+1)}{r} j_n(\omega_{n\ell}\frac{r}{C_2})\right] P_n^m(\cos\theta)\begin{matrix}\sin m\psi \\ \cos m\psi\end{matrix} \tag{6.103a}$$

$$u^*_{\theta,nm\ell} = -\left[\frac{2\varepsilon_m(2n+1)(n-m)!}{3M\xi_{n\ell}(n+m)!}\right]^{\frac{1}{2}} a\left[\frac{\bar{B}_{nm\ell}}{\bar{D}_{nm\ell}} \frac{1}{r} j_n(\omega_{n\ell}\frac{r}{C_1}) - \left[\frac{\omega_{n\ell}}{C_2} j_{n-1}(\omega_{n\ell}\frac{r}{C_2}) - \frac{n}{r} j_n(\omega_{n\ell}\frac{r}{C_2})\right]\right] x \frac{d}{d\theta} P_n^m(\cos\theta)\begin{matrix}\sin m\psi \\ \cos m\psi\end{matrix} \tag{6.103b}$$

$$u^*_{\psi,nm\ell} = \mp\left[\frac{2\varepsilon_m(2n+1)(n-m)!}{3M\xi_{n\ell}(n+m)!}\right]^{\frac{1}{2}} a\left[\frac{\bar{B}_{nm\ell}}{\bar{D}_{nm\ell}} \frac{1}{r} j_n(\omega_{n\ell}\frac{r}{C_1}) - \left[\frac{\omega_{n\ell}}{C_2} j_{n-1}(\omega_{n\ell}\frac{r}{C_2}) - \frac{n}{r} j_n(\omega_{n\ell}\frac{r}{C_2})\right]\right] x \frac{m}{\sin\theta} P_n^m(\cos\theta)\begin{matrix}\cos m\psi \\ \sin m\psi\end{matrix} \tag{6.103c}$$

6.7. Modal shapes of spheroidal vibrations

The normal modes of spheroidal vibrations given by equations (6.103a) to (6.103c) in case n=0 may be written as:

$$u_{r,00\ell} = \left(\frac{2}{3M\xi_{0\ell}}\right)^{\frac{1}{2}} K_1 a \, \frac{\bar{B}_{00\ell}}{\bar{D}_{00\ell}} \, j_1(K_1 r) \tag{6.104a}$$

$$u_{\theta,00\ell} = 0, \qquad u_{\psi,00\ell} = 0 \tag{6.104b}$$

where

$$\xi_{0\ell} = \left[-\frac{3}{K_1 a} j_0(K_1 a) j_1(K_1 a) + j_0^2(K_1 a) + j_1^2(K_1 a)\right] \times K_1^2 a^2 \, \frac{\bar{B}^2_{00\ell}}{\bar{D}^2_{00\ell}} \tag{6.105}$$

The characteristic equation given by expression (6.39) reduces to:

$$4K_1 a j_1(K_1 a) - K_2^2 a^2 j_0(K_1 a) = 0 \tag{6.106}$$

Substituting for $j_1(K_1 a)$ from (6.106) into equation (6.105) gives:

$$\xi_{0\ell} = (K_2^4 a^4 + 16K_1^2 a^2 - 12K_2^2 a^2) \, \frac{\bar{B}^2_{00\ell}}{\bar{D}^2_{00\ell}} \, j_0^2(K_1 a) \tag{6.107}$$

Thus (6.104a) can be simplified as:

$$u_{r,00\ell} = \left[\frac{32}{3M(K_2^4 a^4 + 16K_1^2 a^2 - 12K_2^2 a^2}\right]^{\frac{1}{2}} \frac{K_1 a j_1(K_1 r)}{j_0(K_1 a)} \tag{6.108}$$

Since the only non zero component of vector displacement is the radial one, therefore the motion everywhere is in the direction

of the radius vector. The roots of equation (6.106) for the Poisson's ratio $\nu = 0.29$ from Table 6.2 are:

$$K_1 a = 2.6528, 6.086, 9.2974..... \tag{6.109}$$

By examining the roots of the characteristic equations for different Poisson's ratios, one can easily find that for any particular mode the value of $K_1 a$ increases as Poisson's ratio increases, and vice versa. As an example, the roots of equation (6.106) for $\nu = 0.25$ are:

$$K_1 a = 2.563, 6.058, 9.279 \tag{6.110}$$

To find the position of the spherical nodes one may write:

$$j_1(K_1 r) = 0 \tag{6.111}$$

whose roots are:

$$K_1 r = 4.493, 7.725, 10.904 \tag{6.112}$$

Thus the positions of the spherical nodes for the second and third modes are respectively,

$$\begin{aligned} \frac{r}{a} &= 0.739 \quad \text{(2nd mode)} \\ \frac{r}{a} &= 0.483, 0.83 \quad \text{(3rd mode)} \end{aligned} \qquad \nu = 0.29 \tag{6.113}$$

Similarly, for $\nu = 0.25$

$$\begin{aligned} \frac{r}{a} &= 0.741 \quad \text{(2nd mode)} \\ \frac{r}{a} &= 0.484, 0.832 \quad \text{(3rd mode)} \end{aligned} \tag{6.114}$$

Thus for the ℓth mode of the harmonic n=0, there are ℓ-1 spherical surfaces across which there is no displacement. To investigate the position of the zero stress surfaces equation (6.31a) may be written as:

$$4K_1 r j_1(K_1 r) - K_2^2 r^2 j_0(K_1 r) = 0 \qquad (6.115)$$

The roots of equation (6.115) for $\nu = 0.29$ are given by (6.109). Thus the position of the zero stress surfaces can be found to be:

$$\begin{aligned} \frac{r}{a} &= 0.436 \qquad \text{(2nd mode)} \\ \frac{r}{a} &= 0.285, 0.6546 \quad \text{(3rd mode)} \end{aligned} \qquad (6.116)$$

Consider now the harmonic n=1. The normalised displacement may be written as:

$$u_{r,1m\ell} = -\left[\frac{2\varepsilon_m (1-m)!}{M\xi_{1\ell}(1+m)!}\right]^{\frac{1}{2}} a\left[\frac{\bar{B}_{1m\ell}}{\bar{D}_{1m\ell}}\left[K_1 j_0(K_1 r) - \frac{2}{r} j_1(K_1 r)\right] - \frac{2}{r} j_1(K_2 r)\right] P_1^m(\cos\theta) \begin{matrix}\sin m\psi \\ \cos m\psi\end{matrix} \qquad (6.117a)$$

$$u_{\theta,1m\ell} = -\left[\frac{2\varepsilon_m (1-m)!}{M\xi_{1\ell}(1+m)!}\right]^{\frac{1}{2}} a\left[\frac{\bar{B}_{1m\ell}}{\bar{D}_{1m\ell}} \frac{1}{r} j_1(K_1 r) - \left[K_2 j_0(K_2 r) - \frac{1}{r} j_1(K_2 r)\right]\right] \frac{d}{d\theta} P_1^m(\cos\theta) \begin{matrix}\sin m\psi \\ \cos m\psi\end{matrix} \qquad (6.117b)$$

$$u_{\psi,1m\ell} = \mp\left[\frac{2\varepsilon_m(1-m)!}{M\xi_{i\ell}(1+m)!}\right]^{\frac{1}{2}} a\left[\frac{\bar{B}_{1m\ell}}{\bar{D}_{1m\ell}}\frac{1}{r}j_1(K_1r) - \left[K_2 j_0(K_2r) - \frac{1}{r}j_1(K_2r)\right]\right]\frac{m}{\sin\theta}P_1^m(\cos\theta)\begin{matrix}\cos m\psi \\ \sin m\psi\end{matrix} \qquad (6.117c)$$

where m is either zero or one,

$$\frac{\bar{B}_{1m\ell}}{\bar{D}_{1m\ell}} = \frac{2j_1(K_2a)}{j_1(K_1a)} \qquad (6.118)$$

and

$$\xi_{1\ell} = j_1^2(K_2a)\left[-10K_1a\left[2\frac{j_2(K_1a)}{j_1(K_1a)} + \frac{K_2}{K_1}\frac{j_2(K_2a)}{j_1(K_2a)}\right] + 2K_1^2a^2\left[2\frac{j_2^2(K_1a)}{j_1^2(K_1a)} + \frac{K_2^2}{K_1^2}\frac{j_2^2(K_2a)}{j_1^2(K_2a)}\right] + 4K_1^2a^2 + 2K_2^2a^2\right] \qquad (6.119)$$

The characteristic equation may be found from expression (6.39) to be:

$$\left[K_2^2a^2j_1(K_2a) - 6K_2aj_2(K_2a)\right]j_1(K_1a) = 2\left[6K_1aj_2(K_1a) - K_2^2a^2j_1(K_1a)\right]j_1(K_2a) \qquad (6.120)$$

Using (6.120) and substituting for $\frac{j_2(K_2a)}{j_1(K_2a)}$ into equation (6.119) gives:

$$\xi_{1\ell} = \frac{j_1^2(K_2a)}{2}\left[K_2^4a^4 - 6K_2^2a^2 + 8K_1^2a^2 + 24K_1^2a^2\frac{j_2^2(K_1a)}{j_1^2(K_1a)} - 8K_1aK_2^2a^2\frac{j_2(K_1a)}{j_1(K_1a)}\right] \qquad (6.121)$$

The roots of characteristic equation from Table 6.2 are:

$$K_2 a = 3.5132,\ 7.057, 7.9992..... \qquad (6.122)$$

The positions of the spherical surfaces across which the only non-zero component of vector displacement is the radial one are:

$$\frac{r}{a} = 0.625 \quad \text{(1st mode)}$$

$$\frac{r}{a} = 0.47, 0.81 \quad \text{(2nd mode)} \qquad \nu = 0.29 \qquad (6.123)$$

$$\frac{r}{a} = 0.22,\ 0.82 \quad \text{(3rd mode)}$$

The positions of the zero stress surfaces are given by:

$$\frac{r}{a} = 0.498 \quad \text{(2nd mode)}$$

$$\nu = 0.29 \qquad (6.124)$$

$$\frac{r}{a} = 0.439, 0.882 \quad \text{(3rd mode)}$$

Graphs showing variations of the normalised u_r and u_θ along the radius of sphere are given in Figs.(6.3) and (6.4) respectively. The three dimensional diagrams of the surface mode shapes are also given in Fig.(6.5).

6.8. Response of a sphere to a radial concentrated force

Consider a solid sphere of radius a subjected to a radial concentrated force of amplitude F(t) as shown in Fig.6.6. The equations of motion in terms of stresses may be written as:

$$\frac{\partial\sigma_{rr}}{\partial r}+\frac{1}{r}\frac{\partial\sigma_{r\theta}}{\partial\theta}+\frac{1}{r\sin\theta}\frac{\partial\sigma_{r\psi}}{\partial\psi}+\frac{1}{r}(2\sigma_{rr}-\sigma_{\theta\theta}-\sigma_{\psi\psi}+\sigma_{r\theta}\cot g\theta)$$
$$=\rho\frac{\partial^2 U_r}{\partial t^2}-F(t)\hat{\delta}(\underline{r}-\underline{r_o}) \qquad (6.125a)$$

$$\frac{\partial\sigma_{r\theta}}{\partial r}+\frac{1}{r}\frac{\partial\sigma_{\theta\theta}}{\partial\theta}+\frac{1}{r\sin\theta}\frac{\partial\sigma_{\theta\psi}}{\partial\psi}+\frac{1}{r}\left[(\sigma_{\theta\theta}-\sigma_{\psi\psi})\cot g\theta+3\sigma_{r\theta}\right]$$
$$=\rho\frac{\partial^2 U_\theta}{\partial t^2} \qquad (6.125b)$$

$$\frac{\partial\sigma_{r\psi}}{\partial r}+\frac{1}{r}\frac{\partial\sigma_{\theta\psi}}{\partial\theta}+\frac{1}{r\sin\theta}\frac{\partial\sigma_{\psi\psi}}{\partial\psi}+\frac{1}{r}(3\sigma_{r\psi}+2\sigma_{\theta\psi}\cot g\theta)$$
$$=\rho\frac{\partial^2 U_\psi}{\partial t^2} \qquad (6.125c)$$

where $\hat{\delta}(\underline{r}-\underline{r_o})$ is the three dimensional Dirac delta function and may be represented in spherical polar coordinates as:

$$\hat{\delta}(\underline{r}-\underline{r_o})=\frac{\hat{\delta}(r-r_o)\hat{\delta}(\theta-\theta_o)\hat{\delta}(\psi-\psi_o)}{r_o^2\sin\theta} \qquad (6.126)$$

The left hand side of equation (6.125a) to (6.125c) may be represented in terms of components of displacement and their derivatives with respect to spherical polar coordinates. The new set of equations have many terms, therefore to avoid representing these lengthy equations one may write:

$$F^* = \rho \frac{\partial^2 U_r}{\partial t^2} - F(t)\hat{\delta}(\underline{r} - \underline{r_o}) \tag{6.127a}$$

$$G^* = \rho \frac{\partial^2 U_\theta}{\partial t^2} \tag{6.127b}$$

$$W^* = \rho \frac{\partial^2 U_\psi}{\partial t^2} \tag{6.127c}$$

where F*, G* and W* are the left hand side of new set of equations as described above. Let us assume now a solution in the form:

$$U_r(r,\theta,\psi,t) = \sum_{n=0}^{\infty} \sum_{m=0}^{n} \sum_{\ell=1}^{\infty} u_{r,nm\ell}\, q_{nm\ell}(t) \tag{6.128a}$$

$$U_\theta(r,\theta,\psi,t) = \sum_{n=0}^{\infty} \sum_{m=0}^{n} \sum_{\ell=1}^{\infty} u_{\theta,nm\ell}\, q_{nm\ell}(t) \tag{6.128b}$$

$$U_\psi(r,\theta,\psi,t) = \sum_{n=0}^{\infty} \sum_{m=0}^{n} \sum_{\ell=1}^{\infty} u_{\psi,nm\ell}\, q_{nm\ell}(t)$$

where $u_{r,nm\ell}$, $u_{\theta,nm\ell}$, $u_{\psi,nm\ell}$ are the eigenfunctions given by expression (6.79a) to (6.79c) and $q_{nm\ell}(t)$ are associated generalised coordinates.

Substituting the above solutions into equations (6.127a) to (6.127c) gives:

$$\sum_{n=0}^{\infty} \sum_{m=0}^{n} \sum_{\ell=1}^{\infty} f^*_{nm\ell}\, q_{nm\ell} - \rho \sum_{n=0}^{\infty} \sum_{m=0}^{n} \sum_{\ell=1}^{\infty} u_{r,nm\ell}\, \ddot{q}_{nm\ell}$$

$$= -F(t)\hat{\delta}(\underline{r} - \underline{r_o}) \tag{6.129a}$$

$$\sum_{n=0}^{\infty} \sum_{m=0}^{n} \sum_{\ell=1}^{\infty} g^*_{nm\ell}\, q_{nm\ell} - \rho \sum_{n=0}^{\infty} \sum_{m=0}^{n} \sum_{\ell=1}^{\infty} u_{\theta,nm\ell}\, \ddot{q}_{nm\ell} = 0 \tag{6.129b}$$

$$\sum_{n=0}^{\infty} \sum_{m=0}^{n} \sum_{\ell=1}^{\infty} w^*_{nm\ell}\, q_{nm\ell} - \rho \sum_{n=0}^{\infty} \sum_{m=0}^{n} \sum_{\ell=1}^{\infty} u_{\psi,nm\ell}\, \ddot{q}_{nm\ell} = 0 \tag{6.129c}$$

Multiplying equations (6.129a) to (6.129c) by $u_{r,psq}$, $u_{\theta,psq}$ $u_{\psi,psq}$ respectively, adding them together and integrating over the volume of the sphere yields:

$$\int_D \sum_{n=0}^{\infty} \sum_{m=0}^{n} \sum_{\ell=1}^{\infty} \left[u_{r,psq} f^*_{nm\ell} + u_{\theta,psq} g^*_{nm\ell} + u_{\psi,psq} w^*_{nm\ell} \right] q_{nm\ell} \, dD$$

$$-\rho \int_D \sum_{n=0}^{\infty} \sum_{m=0}^{n} \sum_{\ell=1}^{\infty} \left[u_{r,nm\ell} u_{r,psq} + u_{\theta,nm\ell} u_{\theta,psq} + u_{\psi,nm\ell} u_{\psi,psq} \right]$$

$$\ddot{q}_{nm\ell} \, dD = -F(t) \int_D u_{r,psq} \hat{\delta} (\underline{r}-\underline{r}_o) \, dD \qquad (6.130)$$

In order to simplify equation (6.130) one may consider the free vibration problem. Since the eigenfunctions must satisfy the equations of motion in the absence of external forces one may write:

$$f^*_{nm\ell} = -\rho\omega^2_{n\ell} u_{r,nm\ell} \qquad (6.131a)$$

$$g^*_{nm\ell} = -\rho\omega^2_{n\ell} u_{\theta,nm\ell} \qquad (6.131b)$$

$$w^*_{nm\ell} = -\rho\omega^2_{n\ell} u_{\psi,nm\ell} \qquad (6.131c)$$

Multiplying equations (6.131a) to (6.131c) by $u_{r,psq}$, $u_{\theta,psq}$, $u_{\psi,psq}$ respectively and adding them together gives:

$$u_{r,psq} f^*_{nm\ell} + u_{\theta,psq} g^*_{nm\ell} + u_{\psi,psq} w^*_{nm\ell}$$
$$= -\rho\omega^2_{n\ell} \left[u_{r,nm\ell} u_{r,psq} + u_{\theta,nm\ell} u_{\theta,psq} + u_{\psi,nm\ell} u_{\psi,psq} \right] \qquad (6.132)$$

By making use of (6.132) equation (6.130) may be written as:

$$-\rho \int_D \sum_{n=0}^{\infty} \sum_{m=0}^{n} \sum_{\ell=1}^{\infty} \omega_{n\ell}^2 \Big[u_{r,nm\ell}\, u_{r,psq} + u_{\theta,nm\ell}\, u_{\theta,psq} + u_{\psi,nm\ell}\, u_{\psi,psq} \Big] q_{nm\ell}\, dD$$

$$-\rho \int_D \sum_{n=0}^{\infty} \sum_{m=0}^{n} \sum_{\ell=1}^{\infty} \Big[u_{r,nm\ell}\, u_{r,psq} + u_{\theta,nm\ell}\, u_{\theta,psq} + u_{\psi,nm\ell}\, u_{\psi,psq} \Big] \ddot{q}_{nm\ell}\, dD$$

$$= -F(t) \int_D u_{r,psq}\, \hat{\delta}(\underline{r}-\underline{r}_o)\, dD \qquad (6.133)$$

Using now the orthogonality of the eigenfunctions given by expression (6.101) equation (6.133) reduces to:

$$\rho \int_D \omega_{pq}^2 \Big[u_{r,psq}^2 + u_{\theta,psq}^2 + u_{\psi,psq}^2 \Big] q_{psq}\, dD$$

$$+\rho \int_D \Big[u_{r,psq}^2 + u_{\theta,psq}^2 + u_{\psi,psq}^2 \Big] \ddot{q}_{psq}\, dD$$

$$= F(t) \int_D u_{r,psq}\, \hat{\delta}(\underline{r}-\underline{r}_o)\, dD \qquad (6.134)$$

or

$$\ddot{q}_{nm\ell} + \omega_{n\ell}^2 q_{nm\ell} = \frac{F(t) \int_D u_{r,nm\ell}\, \hat{\delta}(\underline{r}-\underline{r}_o)\, dD}{\rho \int_D \Big[u_{r,nm\ell}^2 + u_{\theta,nm\ell}^2 + u_{\psi,nm\ell}^2 \Big] dD} \qquad (6.135)$$

The solution to equation (6.135) can be easily obtained through standard techniques, and it appears as:

$$q_{nm\ell}(t) = q_{nm\ell}(0)\cos\omega_{n\ell}t + \dot{q}_{nm\ell}(0)\frac{\sin\omega_{n\ell}t}{\omega_{n\ell}} + \frac{1}{\omega_{n\ell}}\frac{\int_0^t N_{nm\ell}(\zeta)\sin\omega_{n\ell}(t-\zeta)d\zeta}{\rho\int_D\left[u^2_{r,nm\ell}+u^2_{\theta,nm\ell}+u^2_{\psi,nm\ell}\right]dD} \qquad (6.136)$$

where $q_{nm\ell}(0)$ and $\dot{q}_{nm\ell}(0)$ are the initial generalised displacement and initial generalised velocity respectively, and

$$N_{nm\ell}(t) = F(t)\int_D u_{r,nm\ell}\hat{\delta}(\underline{r}-\underline{r_o})\,dD \qquad (6.137)$$

For any form of radial concentrated force acting at the position $r=r_o, \theta = \theta_o$ and $\psi = \psi_o$ equation (6.137) reduces to:

$$N_{nm\ell}(t) = F(t)\,u_{r,nm\ell}(r_o,\theta_o,\psi_o) \qquad (6.138)$$

Substituting (6.138) into equation (6.136) and assuming $q_{nm\ell}(0) = \dot{q}_{nm\ell}(0) = 0$ gives:

$$q_{nm\ell}(t) = \frac{u_{r,nm\ell}(r_o,\theta_o,\psi_o)}{\omega_{n\ell}} \times \frac{\int_0^t F(\zeta)\sin\omega_{n\ell}(t-\zeta)d\zeta}{\rho\int_D\left[u^2_{r,nm\ell}+u^2_{\theta,nm\ell}+u^2_{\psi,nm\ell}\right]dD} \qquad (6.139)$$

The response may now be obtained by substituting (6.139) for $q_{nm\ell}(t)$ into equation (6.128a) to (6.128c). Thus:

$$U_r(r,\theta,\psi,t) = \sum_{n=0}^{\infty}\sum_{m=0}^{n}\sum_{\ell=1}^{\infty} \frac{u_{r,nm\ell}(r,\theta,\psi).u_{r,nm\ell}(r_o,\theta_o,\psi_o)}{\rho\omega_{n\ell}} \times \frac{\int_0^t F(\zeta)\sin\omega_{n\ell}(t-\zeta)d\zeta}{\int_D\left[u^2_{r,nm\ell}+u^2_{\theta,nm\ell}+u^2_{\psi,nm\ell}\right]dD} \qquad (6.140a)$$

$$U_\theta(r,\theta,\psi,t) = \sum_{n=0}^{\infty}\sum_{m=0}^{n}\sum_{\ell=1}^{\infty} \frac{u_{\theta,nm\ell}(r,\theta,\psi).u_{r,nm\ell}(r_o,\theta_o,\psi_o)}{\rho\omega_{n\ell}} \times \frac{\int_0^t F(\zeta)\sin\omega_{n\ell}(t-\zeta)d\zeta}{\int_D\left[u^2_{r,nm\ell}+u^2_{\theta,nm\ell}+u^2_{\psi,nm\ell}\right]dD} \qquad (6.140b)$$

$$U_\psi(r,\theta,\psi,t) = \sum_{n=0}^{\infty}\sum_{m=0}^{n}\sum_{\ell=1}^{\infty} \frac{u_{\psi,nm\ell}(r,\theta,\psi).u_{r,nm\ell}(r_o,\theta_o,\psi_o)}{\rho\omega_{n\ell}} \times \frac{\int_0^t F(\zeta)\sin\omega_{n\ell}(t-\zeta)d\zeta}{\int_D\left[u^2_{r,nm\ell}+u^2_{\theta,nm\ell}+u^2_{\psi,nm\ell}\right]dD} \qquad (6.140c)$$

or in terms of normalised modes:

$$U_r(r,\theta,\psi,t) = \sum_{n=0}^{\infty}\sum_{m=0}^{n}\sum_{\ell=1}^{\infty} \frac{u^*_{r,nm\ell}(r,\theta,\psi).u^*_{r,nm\ell}(r_o,\theta_o,\psi_o)}{\omega_{n\ell}} \times \int_0^t F(\zeta)\sin\omega_{n\ell}(t-\zeta)d\zeta \qquad (6.141a)$$

$$U_\theta(r,\theta,\psi,t)= \sum_{n=0}^{\infty} \sum_{m=0}^{n} \sum_{\ell=1}^{\infty} \frac{u^*_{\theta,nm\ell}(r,\theta,\psi).u^*_{r,nm\ell}(r_o,\theta_o,\psi_o)}{\omega_{n\ell}}$$

$$\times \int_0^t F(\zeta)\sin\omega_{n\ell}(t-\zeta)d\zeta \qquad (6.141b)$$

$$U_\psi(r,\theta,\psi,t)= \sum_{n=0}^{\infty} \sum_{m=0}^{n} \sum_{\ell=1}^{\infty} \frac{u^*_{\psi,nm\ell}(r,\theta,\psi).u^*_{r,nm\ell}(r_o,\theta_o,\psi_o)}{\omega_{n\ell}}$$

$$\times \int_0^t F(\zeta)\sin\omega_{n\ell}(t-\zeta)d\zeta \qquad (6.141c)$$

where $u^*_{r,nm\ell}$, $u^*_{\theta,nm\ell}$, and $u^*_{\psi,nm\ell}$ are given by equations (6.103a) to (6.103c) respectively. As an illustration let the applied force be in the form of a step function of magnitude F_S,

$$F(t) = F_S H(t) \qquad (6.142)$$

and evaluate the integral:

$$\int_0^t F_S H(\tau)\sin\omega_{n\ell}(t-\tau)d\tau = \frac{F_S}{\omega_{n\ell}}(1 - \cos\omega_{n\ell}t) \qquad (6.143)$$

Upon assuming $r_o = a$, and $\theta_o = \pi$ the response may be represented as:

$$U_r(r,\theta,t) = \sum_{n=0}^{\infty} \sum_{\ell=1}^{\infty} \frac{2(2n+1)(-1)^n a^2 F_S}{3M\xi_{n\ell}\omega^2_{n\ell}}$$

$$\left\{ \frac{\bar{B}_{n\ell}}{\bar{D}_{n\ell}} \left[\frac{\omega_{n\ell}}{C_1} j_{n-1}(\omega_{n\ell}\frac{a}{C_1}) - \frac{(n+1)}{a} j_n(\omega_{n\ell}\frac{a}{C_1})\right] \right.$$

$$\left. - \frac{n(n+1)}{a} j_n(\omega_{n\ell}\frac{a}{C_2})\right\} \times \left\{\frac{\bar{B}_{n\ell}}{\bar{D}_{n\ell}} \left[\frac{\omega_{n\ell}}{C_1} j_{n-1}(\omega_{n\ell}\frac{r}{C_1}) - \frac{(n+1)}{r} j_n(\omega_{n\ell}\frac{r}{C_1})\right]\right.$$

$$\left. - \frac{n(n+1)}{r} j_n(\omega_{n\ell}\frac{a}{C_1})\right\} \times (1 - \cos\omega_{n\ell}\tau)\frac{d}{d\theta} P_n(\cos\theta)$$

(6.144a)

$$U_\theta(r,\theta,t) = \sum_{n=0}^{\infty}\sum_{\ell=1}^{\infty} \frac{2(2n+1)(-1)^n a^2 F_S}{3M\xi_{n\ell}\omega_{n\ell}^2}$$

$$\left\{\frac{\bar{B}_{n\ell}}{\bar{D}_{n\ell}}\left[\frac{\omega_{n\ell}}{C_1} j_{n-1}(\omega_{n\ell}\frac{a}{C_1}) - \frac{(n+1)}{a} j_n(\omega_{n\ell}\frac{a}{C_1})\right]\right.$$

$$\left. - \frac{n(n+1)}{a} j_n(\omega_{n\ell}\frac{a}{C_2})\right\} \times \left\{-\frac{\bar{B}_{n\ell}}{\bar{D}_{n\ell}} \frac{1}{r} j_n(\omega_{n\ell}\frac{r}{C_1})\right.$$

$$\left. -\left[\frac{\omega_{n\ell}}{C_2} j_{n-1}(\omega_{n\ell}\frac{r}{C_2}) - \frac{n}{r} j_n(\omega_{n\ell}\frac{r}{C_2})\right]\right\} \times (1-\cos\omega_{n\ell}t)\frac{d}{d\theta}\left[P_n(\cos\theta)\right]$$

(6.144b)

$$u_\psi(r,\theta,t) = 0 \tag{6.144c}$$

Note that: $$P_n^m(-1) = \begin{cases} (-1)^n, & m=0 \\ 0, & \text{otherwise} \end{cases} \tag{6.145}$$

To represent the response in frequency domain one may simply evaluate the Fourier transforms of equations (6.144a) and (6.144b) Thus.

$$U_r(r,\theta,\omega) = -\sum_{n=0}^{\infty}\sum_{\ell=1}^{\infty} \frac{2(2n+1)(-1)^n a^2 F_S i}{3M\xi_{n\ell}\omega(\omega_{n\ell}^2-\omega^2)}$$

$$\left\{\frac{\bar{B}_{n\ell}}{\bar{D}_{n\ell}}\left[\frac{\omega_{n\ell}}{C_1} j_{n-1}(\omega_{n\ell}\frac{a}{C_1}) - \frac{(n+1)}{a} j_n(\omega_{n\ell}\frac{a}{C_1})\right]\right.$$

$$\left. - \frac{n(n+1)}{a} j_n(\omega_{n\ell}\frac{a}{C_2})\right\} \times \left\{\frac{\bar{B}_{n\ell}}{\bar{D}_{n\ell}}\left[\frac{\omega_{n\ell}}{C_1} j_{n-1}(\omega_{n\ell}\frac{r}{C_1})\right.\right.$$

$$\left.\left. - \frac{(n+1)}{r} j_n(\omega_{n\ell}\frac{r}{C_1})\right] - \frac{n(n+1)}{r} j_n(\omega_{n\ell}\frac{r}{C_2})\right\} P_n(\cos\theta)$$

(6.146a)

and

$$U_\theta(r,\theta,\omega) = -\sum_{n=0}^{\infty}\sum_{\ell=1}^{\infty} \frac{2(2n+1)(-1)^n a^2 F_S i}{3M\xi_{n\ell}\omega(\omega^2_{n\ell}-\omega^2)}$$

$$\left\{\frac{\bar{B}_{n\ell}}{\bar{D}_{n\ell}}\left[\frac{\omega_{n\ell}}{C_1}j_{n-1}(\omega_{n\ell}\frac{a}{C_1})-\frac{(n+1)}{a}j_n(\omega_{n\ell}\frac{a}{C_1})\right]\right.$$

$$\left.-\frac{n(n+1)}{a}j_n(\omega_{n\ell}\frac{a}{C_2})\right\}\times\left\{\frac{\bar{B}_{n\ell}}{\bar{D}_{n\ell}}\frac{1}{r}\,j_n(\omega_{n\ell}\frac{r}{C_1})\right.$$

$$\left.-\left[\frac{\omega_{n\ell}}{C_2}j_{n-1}(\omega_{n\ell}\frac{r}{C_2})-\frac{n}{r}\,j_n(\omega_{n\ell}\frac{r}{C_2})\right]\right\}\frac{d}{d\theta}\left[P_n(\cos\theta)\right] \tag{6.146b}$$

In order to take into account the effect of viscous damping equations (6.127a) to (6.127c) can be modified as:

$$F^* = \rho\frac{\partial^2 U_r}{\partial t^2} + \hat{\alpha}\frac{\partial U_r}{\partial t} - F(t)\hat{\delta}(\underline{r}-\underline{r}_o) \tag{6.147a}$$

$$G^* = \rho\frac{\partial^2 U_\theta}{\partial t^2} + \hat{\alpha}\frac{\partial U_\theta}{\partial t} \tag{6.147b}$$

$$W^* = \rho\frac{\partial^2 U_\psi}{\partial t^2} + \hat{\alpha}\frac{\partial U_\psi}{\partial t} \tag{6.147c}$$

where $\hat{\alpha}$ is the coefficient of viscous damping. By repeating the similar procedure as given for undamped problems, one obtains:

$$\ddot{q}_{nm\ell} + 2\beta_{n\ell}\omega_{n\ell}\dot{q}_{nm\ell} + \omega^2_{n\ell}q_{nm\ell} = \frac{N_{nm\ell}(t)}{\rho\int_D\left[u^2_{r,nm\ell}+u^2_{\theta,nm\ell}+u^2_{\psi,nm\ell}\right]dD} \tag{6.148}$$

where $\beta_{n\ell}$'s are the viscous damping factors. The solution of

(6.148) can be easily obtained by means of the Laplace transformation (see for example Meirovitch 64). Thus:

$$q_{nm\ell}(t) = \frac{u_{r,nm\ell}(r_o,\theta_o,\psi_o)}{\omega^*_{n\ell}} \times \frac{\int_0^t F(\zeta)e^{-\beta_{n\ell}\omega_{n\ell}(t-\zeta)} \sin\omega^*_{n\ell}(t-\zeta)d\zeta}{\rho\int_D \left[u^2_{r,nm\ell}+u^2_{\theta,nm\ell}+u^2_{\psi,nm\ell}\right]dD} \tag{6.149}$$

where $\omega^*_{n\ell} = \omega_{n\ell}\sqrt{1-\beta^2_{n\ell}}$. Substituting (6.149) into equations (6.128a) to (6.128c) gives:

$$U_r(r,\theta,\psi,t) = \sum_{n=0}^{\infty}\sum_{m=0}^{n}\sum_{\ell=1}^{\infty} \frac{u_{r,nm\ell}(r,\theta,\psi).u_{r,nm\ell}(r_o,\theta_o,\psi_o)}{\omega^*_{n\ell}} \times \frac{\int_0^t F(\zeta)e^{-\beta_{n\ell}\omega_{n\ell}(t-\zeta)} \sin\omega^*_{n\ell}(t-\zeta)d\zeta}{\int_D \left[u^2_{r,nm\ell}+u^2_{\theta,nm\ell}+u^2_{\psi,nm\ell}\right]dD} \tag{6.150a}$$

$$U_\theta(r,\theta,\psi,t) = \sum_{n=0}^{\infty}\sum_{m=0}^{n}\sum_{\ell=1}^{\infty} \frac{u_{\theta,nm\ell}(r,\theta,\psi).u_{r,nm\ell}(r_o,\theta_o,\psi_o)}{\rho\omega^*_{n\ell}} \times \frac{\int_0^t F(\zeta)e^{-\beta_{n\ell}\omega_{n\ell}(t-\zeta)} \sin\omega^*_{n\ell}(t-\zeta)d\zeta}{\int_D \left[u^2_{r,nm\ell}+u^2_{\theta,nm\ell}+u^2_{\psi,nm\ell}\right]dD} \tag{6.150b}$$

$$U_\psi(r,\theta,\psi,t) = \sum_{n=0}^{\infty}\sum_{m=0}^{n}\sum_{\ell=1}^{\infty} \frac{u_{\psi,nm\ell}(r,\theta,\psi).u_{r,nm\ell}(r_o,\theta_o,\psi_o)}{\rho\omega^*_{n\ell}} \times \frac{\int_0^t F(\zeta)e^{-\beta_{n\ell}\omega_{n\ell}(t-\zeta)} \sin\omega^*_{n\ell}(t-\zeta)d\zeta}{\int_D \left[u^2_{r,nm\ell}+u^2_{\theta,nm\ell}+u^2_{\psi,nm\ell}\right]dD} \tag{6.150c}$$

or in terms of normalised modes:

$$U_r(r,\theta,\psi,t) = \sum_{n=0}^{\infty} \sum_{m=0}^{n} \sum_{\ell=1}^{\infty} \frac{u^*_{r,nm\ell}(r,\theta,\psi).u^*_{r,nm\ell}(r_o,\theta_o,\psi_o)}{\omega^*_{n\ell}}$$

$$\int_o^t F(\zeta)e^{-\beta_{n\ell}\omega_{n\ell}(t-\zeta)} \sin\omega^*_{n\ell}(t-\zeta)d\zeta \qquad (6.151a)$$

$$U_\theta(r,\theta,\psi,t) = \sum_{n=0}^{\infty} \sum_{m=0}^{n} \sum_{\ell=1}^{\infty} \frac{u^*_{\theta,nm\ell}(r,\theta,\psi).u^*_{r,nm\ell}(r_o,\theta_o,\psi_o)}{\omega^*_{n\ell}}$$

$$\int_o^t F(\zeta)e^{-\beta_{n\ell}\omega_{n\ell}(t-\zeta)} \sin\omega^*_{n\ell}(t-\zeta)d\zeta \qquad (6.151b)$$

$$U_\psi(r,\theta,\psi,t) = \sum_{n=0}^{\infty} \sum_{m=0}^{n} \sum_{\ell=1}^{\infty} \frac{u^*_{\psi,nm\ell}(r,\theta,\psi).u^*_{r,nm\ell}(r_o,\theta_o,\psi_o)}{\omega^*_{n\ell}}$$

$$\int_o^t F(\zeta)e^{-\beta_{n\ell}\omega_{n\ell}(t-\zeta)} \sin\omega^*_{n\ell}(t-\zeta)d\zeta \qquad (6.151c)$$

Assume now a forcing function given by equation (6.142) being applied at position $r_o = a$, and $\theta_o = \pi$. The response can be easily found to be:

$$U_r(r,\theta,t) = \sum_{n=0}^{\infty} \sum_{\ell=1}^{\infty} \frac{2(2n+1)(-1)^n a^2 F_S}{3M\xi_{n\ell}\omega^2_{n\ell}}$$

$$\left\{\frac{\bar{B}_{n\ell}}{\bar{D}_{n\ell}}\left[\frac{\omega_{n\ell}}{C_1}j_{n-1}(\omega_{n\ell}\frac{a}{C_1}) - \frac{(n+1)}{a}j_n(\omega_{n\ell}\frac{a}{C_1})\right]\right.$$

$$\left. - \frac{n(n+1)}{a}j_n(\omega_{n\ell}\frac{a}{C_2})\right\} x \left\{\frac{\bar{B}_{n\ell}}{\bar{D}_{n\ell}}\left[\frac{\omega_{n\ell}}{C_1}j_{n-1}(\omega_{n\ell}\frac{r}{C_1})\right.\right.$$

$$\left.\left. - \frac{(n+1)}{r}j_n(\omega_{n\ell}\frac{r}{C_1})\right] - \frac{n(n+1)}{r}j_n(\omega_{n\ell}\frac{r}{C_2})\right\}$$

$$x\left[1 - \frac{1}{(1-\beta^2_{n\ell})^{\frac{1}{2}}}e^{-\beta_{n\ell}\omega_{n\ell}t}\cos(\omega^*_{n\ell}t-\phi_{n\ell})\right]P_n(\cos\theta) \qquad (6.152a)$$

$$U_\theta(r,\theta,t) = \sum_{n=0}^{\infty}\sum_{\ell=1}^{\infty} \frac{2(2n+1)(-1)^n a^2 F_S}{3M\xi_{n\ell}\omega^2_{n\ell}}$$

$$\left\{ \frac{\bar{B}_{n\ell}}{\bar{D}_{n\ell}} \left[\frac{\omega_{n\ell}}{C_1} j_{n-1}(\omega_{n\ell}\frac{a}{C_1}) - \frac{(n+1)}{a} j_n(\omega_{n\ell}\frac{a}{C_1}) \right] \right.$$

$$\left. - \frac{n(n+1)}{a} j_n(\omega_{n\ell}\frac{a}{C_2}) \right\} x \left\{ \frac{\bar{B}_{n\ell}}{\bar{D}_{n\ell}} \frac{1}{r} j_n(\omega_{n\ell}\frac{r}{C_1}) \right.$$

$$\left. - \left[\frac{\omega_{n\ell}}{C_2} j_{n-1}(\omega_{n\ell}\frac{r}{C_2}) - \frac{n}{r} j_n(\omega_{n\ell}\frac{r}{C_2}) \right] \right\}$$

$$x \left[1 - \frac{1}{(1-\beta^2_{n\ell})^{\frac{1}{2}}} e^{-\beta_{n\ell}\omega_{n\ell}t} \cos(\omega^*_{n\ell}t - \phi_{n\ell}) \right] \frac{d}{d\theta}\left[P_n(\cos\theta) \right] \tag{6.152b}$$

where

$$T_{an}\phi_{n\ell} = \frac{\beta_{n\ell}}{(1-\beta^2_{n\ell})^{\frac{1}{2}}} \tag{6.153}$$

The Fourier transforms of equations (6.152a) and (6.152b) are respectively:

$$U_r(r,\theta,\omega) = - \sum_{n=0}^{\infty}\sum_{\ell=1}^{\infty} \frac{2(2n+1)(-1)^n a^2 F_S i}{3M\xi_{n\ell}\omega(\omega^2_{n\ell} - \omega^2 + 2\beta_{n\ell}\omega_{n\ell} i\omega)}$$

$$\left\{ \frac{\bar{B}_{n\ell}}{\bar{D}_{n\ell}} \left[\frac{\omega_{n\ell}}{C_1} j_{n-1}(\omega_{n\ell}\frac{a}{C_1}) - \frac{(n+1)}{a} j_n(\omega_{n\ell}\frac{a}{C_1}) \right] \right.$$

$$\left. - \frac{n(n+1)}{a} j_n(\omega_{n\ell}\frac{a}{C_2}) \right\} x \left\{ \frac{\bar{B}_{n\ell}}{\bar{D}_{n\ell}} \left[\frac{\omega_{n\ell}}{C_1} j_{n-1}(\omega_{n\ell}\frac{r}{C_1}) \right. \right.$$

$$\left. \left. - \frac{(n+1)}{r} j_n(\omega_{n\ell}\frac{r}{C_1}) \right] - \frac{n(n+1)}{r} j_n(\omega_{n\ell}\frac{r}{C_2}) \right\} P_n(\cos\theta)$$

(6.154a)

$$U_\theta(r,\theta,\omega) = - \sum_{n=0}^{\infty} \sum_{\ell=1}^{\infty} \frac{2(2n+1)(-1)^n a^2 F_S i}{3M\xi_{n\ell}\omega(\omega^2_{n\ell} - \omega^2 + 2\beta_{n\ell}\omega_{n\ell} i\omega)}$$

$$\left\{\frac{\bar{B}_{n\ell}}{\bar{D}_{n\ell}}\left[\frac{\omega_{n\ell}}{C_1} j_{n-1}(\omega_{n\ell}\frac{a}{C_1}) - \frac{(n+1)}{a} j_n(\omega_{n\ell}\frac{a}{C_1})\right]\right.$$

$$\left. - \frac{n(n+1)}{a} j_n(\omega_{n\ell}\frac{a}{C_2})\right\} \times \left\{\frac{\bar{B}_{n\ell}}{\bar{D}_{n\ell}} \frac{1}{r} j_n(\omega_{n\ell}\frac{r}{C_1})\right.$$

$$\left. - \left[\frac{\omega_{n\ell}}{C_2} j_{n-1}(\omega_{n\ell}\frac{r}{C_2}) - \frac{n}{r} j_n(\omega_{n\ell}\frac{r}{C_2})\right]\right\} \frac{d}{d\theta}\left[P_n(\cos\theta)\right] \tag{6.154b}$$

6.9. Response due to collision

Consider a pair of colliding spheres as shown in Fig.(3.9) Displacement of each sphere at the contact point can be easily written as:

$$U_1 = \frac{1}{m_1} \int_o^t dt \int_o^t F(t)dt + \sum_{n=0}^{\infty} \sum_{\ell=1}^{\infty} \frac{S_{n\ell}}{\omega_{n\ell}} \int_o^t F(\zeta)\sin\omega_{n\ell}(t-\zeta)d\zeta \tag{6.155a}$$

$$U_2 = v_o t - \frac{1}{m_2} \int_o^t dt \int_o^t F(t)dt - \sum_{n=0}^{\infty} \sum_{\ell=1}^{\infty} \frac{\bar{S}_{n\ell}}{\bar{\omega}_{n\ell}} \int_o^t F(\zeta)\sin\bar{\omega}_{n\ell}(t-\zeta)d\zeta \tag{6.155b}$$

where v_o is the initial relative velocity,

$$S_{n\ell} = u^{*2}_{r,n\ell}(r=a_1, \theta=\pi) \tag{6.156a}$$

$$\bar{S}_{n\ell} = u^{*2}_{r,n\ell}(r=a_2, \theta=0) \tag{6.156b}$$

and m_1 and m_2 are the masses of the spheres. The approach α may now be given by:

$$\alpha = U_2 - U_1 = \left(\frac{F}{\hat{K}_2}\right)^{2/3} = v_o t - \hat{K}_1 \int_o^t dt \int_o^t F(t)dt$$

$$- \sum_{n=0}^{\infty} \sum_{\ell=1}^{\infty} \frac{S_{n\ell}}{\omega_{n\ell}} \int_o^t F(\zeta)\sin\omega_{n\ell}(t-\zeta)d\zeta$$

$$- \sum_{n=0}^{\infty} \sum_{\ell=1}^{\infty} \frac{\bar{S}_{n\ell}}{\bar{\omega}_{n\ell}} \int_o^t F(\zeta)\sin\bar{\omega}_{n\ell}(t-\zeta)d\zeta \qquad (6.157)$$

where $\hat{K}_1$ and $\hat{K}_2$ are given by equations (2.66) and (2.61) respectively. It can be easily shown by means of Laplace transformation that the displacement of rigid body of mass M under action of a force F(t) is:

$$U_{RIG} = \frac{1}{M} \int_o^t (t-\zeta)f(\zeta)d\zeta \qquad (6.158)$$

Thus equation (6.157) may be written as:

$$\alpha = \left(\frac{F}{\hat{K}_2}\right)^{2/3} = v_o t - \hat{K}_1 \int_o^t (t-\zeta)f(\zeta)d\zeta$$

$$- \sum_{n=0}^{\infty} \sum_{\ell=1}^{\infty} \frac{S_{n\ell}}{\omega_{n\ell}} \int_o^t F(\zeta)\sin\omega_{n\ell}(t-\zeta)d\zeta$$

$$- \sum_{n=0}^{\infty} \sum_{\ell=1}^{\infty} \frac{\bar{S}_{n\ell}}{\bar{\omega}_{n\ell}} \int_o^t F(\zeta)\sin\bar{\omega}_{n\ell}(t-\zeta)d\zeta \qquad (6.159)$$

To solve the equation (6.159) the contact force may be assumed to be constant during any time interval Δt. The time interval Δt may be chosen as some small fraction of the fundamental period of vibration of the small sphere. Thus the value of approach at $t=2\Delta t$ may be given by:

$$\alpha\Big|_{t=2\Delta t} = \left(\frac{F_2}{\hat{K}_2}\right)^{2/3} = 2v_o\Delta t - F_1\left[(2\Delta t-\tfrac{1}{2}\Delta t)\Delta t-(2\Delta t-\tfrac{1}{2}x0)0\right]$$

$$-F_2\left[(2\Delta t-\tfrac{1}{2}x2\Delta t)(2\Delta t)-(2\Delta t-\tfrac{1}{2}\Delta t)\Delta t\right]$$

$$-\sum_{n=0}^{\infty}\sum_{\ell=1}^{\infty}\frac{S_{n\ell}}{\omega_{n\ell}}\left[\frac{F_1}{\omega_{n\ell}}\left[\cos\omega_{n\ell}(2\Delta t-\Delta t)-\cos\omega_{n\ell}(2\Delta t-0)\right]\right.$$

$$\left.+\frac{F_2}{\omega_{n\ell}}\left[\cos\omega_{n\ell}(2\Delta t-2\Delta t)-\cos\omega_{n\ell}(2\Delta t-\Delta t)\right]\right]$$

$$-\sum_{n=0}^{\infty}\sum_{\ell=1}^{\infty}\frac{\bar{S}_{n\ell}}{\bar{\omega}_{n\ell}}\left[\frac{F_1}{\bar{\omega}_{n\ell}}\left[\cos\bar{\omega}_{n\ell}(2\Delta t-\Delta t)-\cos\bar{\omega}_{n\ell}(2\Delta t-0)\right]\right.$$

$$\left.+\frac{F_2}{\bar{\omega}_{n\ell}}\left[\cos\bar{\omega}_{n\ell}(2\Delta t-2\Delta t)-\cos\bar{\omega}_{n\ell}(2\Delta t-\Delta t)\right]\right] \qquad (6.160)$$

By repeating the process one obtains:

$$\alpha\Big|_{t=k\Delta t} = \left(\frac{F_k}{\hat{K}_2}\right)^{2/3} = v_o k\Delta t - \hat{K}_1(\Delta t)^2\sum_{j=1}^{k}F_j(k-j+\tfrac{1}{2})$$

$$-\sum_{j=1}^{k}F_j\sum_{n=0}^{\infty}\sum_{\ell=1}^{\infty}\frac{S_{n\ell}}{\omega_{n\ell}^2}\left[\cos\omega_{n\ell}(k-j)\Delta t-\cos\omega_{n\ell}(k-j+1)\Delta t\right]$$

$$-\sum_{j=1}^{k}F_j\sum_{n=0}^{\infty}\sum_{\ell=1}^{\infty}\frac{\bar{S}_{n\ell}}{\bar{\omega}_{n\ell}^2}\left[\cos\bar{\omega}_{n\ell}(k-j)\Delta t-\cos\bar{\omega}_{n\ell}(k-j+1)\Delta t\right] \qquad (6.161)$$

Graphs representing force-time history for a pair of colliding spheres is given in Fig.(6.6).

Consideration of this graph verifies that for the size of spheres being investigated the force-time history may be approximated as a half sine pulse. Thus:

$$F(t) = F_{max}\sin bt \qquad (6.162)$$

and

$$\int_0^t F_{max}\ \sin b\zeta \sin\omega_{n\ell}(t-\zeta)\,d\zeta = \frac{F_{max}}{b^2-\omega_{n\ell}^2}(b\sin\omega_{n\ell}t-\omega_{n\ell}\sin bt)$$

$$t< d \qquad (6.163a)$$

$$\int_0^d F_{max}\sin b\zeta \sin\omega_{n\ell}(t-\zeta)\,d\zeta = \frac{F_{max}}{b^2-\omega_{n\ell}^2}\ b\sin\omega_{n\ell}(t-d)+b\sin\omega_{n\ell}t$$

$$t> d \qquad (6.163b)$$

where d is the duration of contact. The response at position r=a, θ= 0 of sphere (1) may now be given by:

$$U_r(r=a,\theta=0,t) = \sum_{n=0}^{\infty}\ \sum_{\ell=1}^{\infty}\ \frac{(-1)^n F_{max} S_{n\ell}}{\omega_{n\ell}(b^2-\omega_{n\ell}^2)}\ (b\sin\omega_{n\ell}t-\omega_{n\ell}\sin bt)$$

$$t\ < d \qquad (6.164a)$$

$$U_r(r=a,\theta=0,t) = \sum_{n=0}^{\infty}\ \sum_{\ell=1}^{\infty}\ \frac{(-1)^n F_{max} S_{n\ell}}{\omega_{n\ell}(b^2-\omega_{n\ell}^2)}\ b\sin\omega_{n\ell}(t-d)+b\sin\omega_{n\ell}t \qquad (6.164b)$$

$$t \geq d$$

Differentiating twice with respect to t to obtain the acceleration gives:

$$\frac{\partial^2 U_r}{\partial t^2}\Big|_{r=a,\theta=0} = \sum_{n=0}^{\infty}\ \sum_{\ell=1}^{\infty}\ \frac{(-1)^n b F_{max} S_{n\ell}}{(b^2-\omega_{n\ell}^2)}(b\sin bt-\omega_{n\ell}\sin\omega_{n\ell}t)$$

$$t < d \qquad (6.165a)$$

$$\left.\frac{\partial^2 U_r}{\partial t^2}\right|_{r=a,\theta=0} = \sum_{n=0}^{\infty}\sum_{\ell=1}^{\infty} \frac{(-1)^n b F_{max}\omega_{n\ell}S_{n\ell}}{(b^2-\omega^2_{n\ell})} -\sin\omega_{n\ell}(t-d)-\sin\omega_{n\ell}t$$

$$t > d \qquad (6.165b)$$

The effect of viscous damping may be taken into account by following similar procedures as given in section (6.8). Thus:

$$U_r(r=a,\theta=0,t) = \sum_{n=0}^{\infty}\sum_{\ell=1}^{\infty} \frac{(-1)^n F_{max}S_{n\ell}}{\omega^*_{n\ell}} \int_0^t \sin b\zeta \sin\omega^*_{n\ell}(t-\zeta)\, e^{-\beta_{n\ell}\omega_{n\ell}(t-\zeta)}\, d\zeta$$

$$t < d \qquad (6.166a)$$

$$U_r(r=a,\theta=0,t) = \sum_{n=0}^{\infty}\sum_{\ell=1}^{\infty} \frac{(-1)^n F_{max}S_{n\ell}}{\omega^*_{n\ell}} \int_0^d \sin b\zeta \sin\omega^*_{n\ell}(t-\zeta)\, e^{-\beta_{n\ell}\omega_{n\ell}(t-\zeta)}\, d\zeta$$

$$t > d \qquad (6.166b)$$

where

$$\int_0^t \sin b\zeta \sin\omega^*_{n\ell}(t-\zeta) e^{-\beta_{n\ell}(t-\zeta)}\, d\zeta$$

$$= \tfrac{1}{2}\left[\frac{\beta_{n\ell}\omega_{n\ell}\cos bt+(b+\omega^*_{n\ell})\sin bt-\left[\beta_{n\ell}\omega_{n\ell}\cos\omega^*_{n\ell}t-(b+\omega^*_{n\ell})\sin\omega^*_{n\ell}t\right]}{\beta^2_{n\ell}\,\omega^2_{n\ell}+(b+\omega^*_{n\ell})^2} \times e^{-\beta_{n\ell}\omega_{n\ell}t}\right.$$

$$\left. - \frac{\beta_{n\ell}\omega_{n\ell}\cos bt+(b-\omega^*_{n\ell})\sin bt-\left[\beta_{n\ell}\omega_{n\ell}\cos\omega^*_{n\ell}t+(b-\omega^*_{n\ell})\sin\omega^*_{n\ell}t\right]}{\beta^2_{n\ell}\,\omega^2_{n\ell}+(b-\omega^*_{n\ell})^2} \times e^{-\beta_{n\ell}\omega_{n\ell}t}\right] \qquad (6.167a)$$

$$t < d$$

and

$$\int_0^d \sin b\zeta \sin\omega^*_{n\ell}(t-\zeta) e^{-\beta_{n\ell}(t-\zeta)} d\zeta$$

$$= \tfrac{1}{2}\left[\frac{\left[-\beta_{n\ell}\omega_{n\ell}\cos\omega^*_{n\ell}(t-d)+(b+\omega^*_{n\ell})\sin\omega^*_{n\ell}(t-d)\right]e^{-\beta_{n\ell}\omega_{n\ell}(t-d)}}{\beta^2_{n\ell}\omega^2_{n\ell}+(b+\omega^*_{n\ell})^2}\right.$$

$$\left. - \frac{\left[\beta_{n\ell}\omega_{n\ell}\cos\omega^*_{n\ell}t - (b+\omega^*_{n\ell})\sin\omega^*_{n\ell}t\right]e^{-\beta_{n\ell}\omega_{n\ell}t}}{\beta^2_{n\ell}\omega^2_{n\ell}+(b+\omega^*_{n\ell})^2}\right]$$

$$+\tfrac{1}{2}\left[\frac{\left[\beta_{n\ell}\omega_{n\ell}\cos\omega^*_{n\ell}t + (b-\omega^*_{n\ell})\sin\omega^*_{n\ell}t)\right]e^{-\beta_{n\ell}\omega_{n\ell}t}}{\beta^2_{n\ell}\omega^2_{n\ell}+(b-\omega^*_{n\ell})^2}\right.$$

$$\left. - \frac{\left[-\beta_{n\ell}\omega_{n\ell}\cos\omega^*_{n\ell}(t-d)-(b-\omega^*_{n\ell})\sin\omega^*_{n\ell}(t-d)\right]e^{-\beta_{n\ell}\omega_{n\ell}(t-d)}}{\beta^2_{n\ell}\omega^2_{n\ell}+(b-\omega^*_{n\ell})^2}\right]$$

$$t > d \qquad (6.167b)$$

The response and acceleration in frequency domain may now be represented as:

$$U_r(r=a,\theta=0,\omega) = \frac{bF_{max}}{(b^2-\omega^2)}(1+e^{-i\omega d})\sum_{n=0}^{\infty}\sum_{\ell=1}^{\infty}\frac{(-1)^n S_{n\ell}}{\omega^2_{n\ell}-\omega^2+2i\beta_{n\ell}\omega_{n\ell}\omega} \qquad (6.168a)$$

$$\ddot{U}_r(r=a,\theta=0,\omega) = -\frac{\omega^2 bF_{max}}{(b^2-\omega^2)}(1+e^{-i\omega d})\sum_{n=0}^{\infty}\sum_{\ell=1}^{\infty}\frac{(-1)^n S_{n\ell}}{\omega^2_{n\ell}-\omega^2+2i\beta_{n\ell}\omega_{n\ell}\omega} \qquad (6.168b)$$

6.10. Sound generated by transient vibration of solid spheres

Consider a solid sphere of radius a subjected to force-time history given by expression (6.162) at position r=a, and $\theta = \pi$. The acceleration of the sphere at its surface may be assumed to be the sum of both rigid body and vibratory acceleration. Thus the Fourier transform of the total acceleration at the surface of sphere can be written as:

$$\ddot{U}_r(r=a,\theta,\omega) = \frac{bF_{max}}{b^2-\omega^2}(1+e^{-i\omega d})\left[\frac{1}{M}\cos\theta-\omega^2 \sum_{n=0}^{\infty}\sum_{\ell=1}^{\infty} \frac{(-1)^n S_{n\ell} P_n(\cos\theta)}{\omega^2_{n\ell}-\omega^2 + 2i\beta_{n\ell}\omega_{n\ell}\omega}\right] \tag{6.169}$$

where M is the mass of the sphere. The velocity potential ϕ satisfying the acoustic wave equation for a spherical symmetric field is given by equation (2.38) and may reappear here as:

$$\phi = \phi(r,\theta,\omega)e^{i\omega t} \tag{6.170}$$

where

$$\phi(r,\theta,\omega) = \sum_{n=0}^{\infty} A^*_n h_n^{(2)}(Kr)P_n(\cos\theta) \tag{6.171}$$

Suppose now sphere being located at the centre of the field and behaves as a source of sound. The boundary condition which must be satisfied is:

$$\dot{U}_r(r=a,\theta,t) = -\left[\frac{\partial}{\partial r}\phi(r,\theta,t)\right]_{r=a} \tag{6.172}$$

where $\dot{U}_r$ is the radial velocity at the surface of sphere. By the properties of the Fourier transform it can be easily shown that:

$$\dot{U}_r(r=a,\theta,\omega) = \frac{\ddot{U}_r(r=a,\theta,\omega)}{i\omega} = -\left[\frac{\partial}{\partial r}\phi(r,\theta,\omega)\right]_{r=a} \qquad (6.173)$$

Substituting for $\ddot{U}_r$ and $\phi(r,\theta,\omega)$ into equation (6.173) gives:

$$\sum_{n=0}^{\infty}\left[B^*_n-(-1)^n G^*_n\right]P_n(\cos\theta) = -\sum_{n=0}^{\infty} A^*_n\left[\frac{\partial}{\partial r}\, h_n^{(2)}(Kr)\right]_{r=a} P_n(\cos\theta) \qquad (6.174)$$

where

$$B^*_n = \frac{\alpha^*}{M} \qquad n=1 \qquad (6.175a)$$

$$= 0 \quad \text{otherwise,}$$

$$\alpha^* = \frac{bF_{max}}{i\omega(b^2-\omega^2)}(1+e^{-i\omega d}) \qquad (6.175b)$$

and

$$G^*_n = \sum_{\ell=1}^{\infty} \frac{\alpha^* S_{n\ell}\omega^2}{\omega^2_{n\ell}-\omega^2+2i\beta_{n\ell}\omega_{n\ell}\omega} \qquad (6.175c)$$

The spherical Hankel function in equation (6.174) may be expressed in terms of spherical Bessel functions of the first and second kinds, and then differentiated. The result can be reproduced in terms of Hankel function and written as:

$$\left[\frac{\partial}{\partial r} h_n^{(2)}(Kr)\right]_{r=a} = \frac{n}{a}\, h_n^{(2)}(Ka) - K h_{n+1}^{(2)}(Ka) \qquad (6.176)$$

Substituting (6.176) into equation (6.174) gives:

$$A^*_n = - \frac{B^*_n - (-1)^n G^*_n}{\frac{n}{a} h_n^{(2)}(Ka) - K h_{n+1}^{(2)}(Ka)} \tag{6.177}$$

The potential $\phi(r,\theta,\omega)$ given by equation (6.171) may now be written as:

$$\phi(r,\theta,\omega) = \sum_{n=0}^{\infty} \frac{\left[(-1)^n G^*_n - B^*_n\right] h_n^{(2)}(Kr)}{\frac{n}{a} h_n^{(2)}(Ka) - K h_{n+1}^{(2)}(Ka)} P_n(\cos\theta) \tag{6.178}$$

In order to find the relation between pressure and potential function in the frequency domain one may simply transform both sides of equation (2.12) to obtain:

$$p(r,\theta,\omega) = \rho_o \, i\omega \phi(r,\theta,\omega) \tag{6.179}$$

where ρ_o is the density of the air. Substituting (6.178) into equation (6.179) gives:

$$p(r,\theta,\omega) = \rho_o i\omega \sum_{n=0}^{\infty} \frac{\left[(-1)^n G^*_n - B^*_n\right] h_n^{(2)}(Kr)}{\frac{n}{a} h_n^{(2)}(Ka) - K h_{n+1}^{(2)}(Ka)} P_n(\cos\theta)$$

$$= \sum_{n=0}^{\infty} p_n(r,\theta,\omega) \tag{6.180}$$

As an illustration of the result let us examine the case n=0. Thus:

$$p_0(r,\omega) = - \frac{\rho_o C b a^2 F_{max} \omega^2 (1+e^{-i\omega d}) e^{-i\omega\left(\frac{r-a}{C}\right)}}{r(b^2 - \omega^2)(C+i\omega a)}$$

$$\sum_{\ell=1}^{\infty} \frac{S_{0\ell}}{\omega_{0\ell}^2 - \omega^2 + 2i\beta_{0\ell}\omega_{0\ell}\omega} \tag{6.181}$$

where $C = \frac{\omega}{K}$ is the velocity of the sound in the air. To represent the sound pressure in time domain one must find the inverse transform. This can be done easily by finding the residues of function $p_o e^{i\omega t}$ at its poles. Thus:

$$p_o(r,\tau) = \frac{\rho_o C a^2 b F_{max}}{r} \sum_{\ell=1}^{\infty} S_{0\ell} \Bigg[\frac{C^2 a e^{-\frac{c}{a}\tau}}{(C^2+a^2b^2)(C^2+a^2\omega^2_{0\ell}-2aC\beta_{0\ell}\omega_{0\ell})}$$

$$+ \frac{b^2\left[(\omega^2_{0\ell}-b^2)a+2C\beta_{0\ell}\omega_{0\ell}\right]\cos b\tau - b\left[(\omega^2_{0\ell}-b^2)C-2b^2a\beta_{0\ell}\omega_{0\ell}\right]\sin b\tau}{(C^2+b^2a^2)\left[(b^2-\omega^2_{0\ell})^2+4b^2\beta^2_{0\ell}\omega^2_{0\ell}\right]}$$

$$- \frac{\omega_{0\ell}\left[(\omega^2_{0\ell}-b^2)a\omega_{0\ell}+2b^2C\beta_{0\ell}\right]e^{-\beta_{0\ell}\omega_{0\ell}\tau}\cos\omega^*_{0\ell}\tau}{(\omega^2_{0\ell}a^2+C^2-2aC\beta_{0\ell}\omega_{0\ell})\left[(\omega^{*2}_{0\ell}-b^2-\beta^2_{0\ell}\omega^2_{0\ell})^2+4\beta^2_{0\ell}\omega^2_{0\ell}\omega^{*2}_{0\ell}\right]}$$

$$- \frac{\omega^2_{0\ell}\left[(\omega^2_{0\ell}+b^2)a\beta_{0\ell}\omega_{0\ell}-C\omega^2_{0\ell}-Cb^2(2\beta^2_{0\ell}-1)\right]e^{-\beta_{0\ell}\omega_{0\ell}\tau}\sin\omega^*_{0\ell}\tau}{\omega^*_{0\ell}(\omega^2_{0\ell}a^2+C^2-2aC\beta_{0\ell}\omega_{0\ell})\left[(\omega^{*2}_{0\ell}-b^2-\beta^2_{0\ell}\omega^2_{0\ell})^2+4\beta^2_{0\ell}\omega^2_{0\ell}\omega^{*2}_{0\ell}\right]}\Bigg]$$

$$t < d \qquad (6.182a)$$

and

$$p_o(r,\tau) = \frac{\rho_o C a^2 b F_{max}}{r} \sum_{\ell=1}^{\infty} S_{0\ell} \Bigg[\frac{C^2 a\left(e^{-\frac{c}{a}\tau}+e^{-\frac{c}{a}(\tau-d)}\right)}{(C^2+a^2b^2)(C^2+a^2\omega^2_{0\ell}-2aC\beta_{0\ell}\omega_{0\ell}}$$

$$- \frac{\omega_{0\ell}\left[(\omega^2_{0\ell}-b^2)a\omega_{0\ell}+2b^2C\beta_{0\ell}\right]\left[\cos\omega^*_{0\ell}\tau+\cos\omega^*_{0\ell}(\tau-d)e^{\beta_{0\ell}\omega_{0\ell}d}\right]e^{-\beta_{0\ell}\omega_{0\ell}\tau}}{(\omega^2_{0\ell}+C^2-2aC\beta_{0\ell}\omega_{0\ell})\left[(\omega^{*2}_{0\ell}-b^2-\beta^2_{0\ell}\omega^2_{0\ell})^2+4\beta^2_{0\ell}\omega^2_{0\ell}\omega^{*2}_{0\ell}\right]}$$

$$- \frac{\omega^2_{0\ell}\left[(\omega^2_{0\ell}+b^2)a\beta_{0\ell}\omega_{0\ell}-C\omega^2_{0\ell}-Cb^2(2\beta^2_{0\ell}-1)\right]}{\omega^*_{0\ell}(\omega^2_{0\ell}a^2+C^2-2aC\beta_{0\ell}\omega_{0\ell})\left[(\omega^{*2}_{0\ell}-b^2-\beta^2_{0\ell}\omega^2_{0\ell})^2+4\beta^2_{0\ell}\omega^2_{0\ell}\omega^{*2}_{0\ell}\right]}$$

$$\left[\sin\omega^*_{0\ell}\tau+\sin\omega^*_{0\ell}(\tau-d)e^{\beta_{0\ell}\omega_{0\ell}d}\right]e^{-\beta_{0\ell}\omega_{0\ell}\tau}\Bigg]$$

$$\tau > d \qquad (6.182b)$$

where $\tau = t - \frac{r-a}{C}$. Calculations of sound pressure in time domain can be carried out by means of inverse discrete Fourier transform. The method is similar to forward transform given in section (5.3.).

Value of n	ℓ=1	ℓ=2	ℓ=3	ℓ=4	ℓ=5
1	*	5.763	9.095	12.322	15.514
2	2.501	7.136	10.514	13.771	16.983
3	3.865	8.444	11.881	15.175	18.412
4	5.095	9.712	13.210	16.544	19.809
5	6.266	10.950	14.510	17.885	21.180
6	7.404	12.166	15.787	19.204	22.529
7	8.520	13.364	17.045	20.503	23.860
8	9.621	14.548	18.287	21.786	25.174
9	10.711	15.720	19.515	23.054	26.473
10	11.792	16.882	20.731	24.310	27.760

TABLE 6.1. Non-dimensional frequency of torsional vibration of spheres

Value of n	ℓ=1	ℓ=2	ℓ=3	ℓ=4	ℓ=5
0	4.894	11.229	17.153	23.01	28.842
1	*	3.513	7.056	7.999	10.711
2	2.645	4.985	8.499	10.257	12.202
3	3.934	6.584	9.856	12.303	13.762
4	5.04	8.191	11.197	14.066	15.479
5	6.075	9.756	12.543	15.593	17.319
6	7.076	11.259	13.905	17.004	19.156
7	8.058	12.696	15.289	18.366	20.9
8	9.028	14.066	16.69	19.709	22.51
9	9.99	15.379	18.099	21.046	24.002
10	10.946	16.645	19.505	22.385	25.415

TABLE 6.2. Non-dimensional frequency of spheroidal vibration of sphere. (Poisson ratio = 0.29)

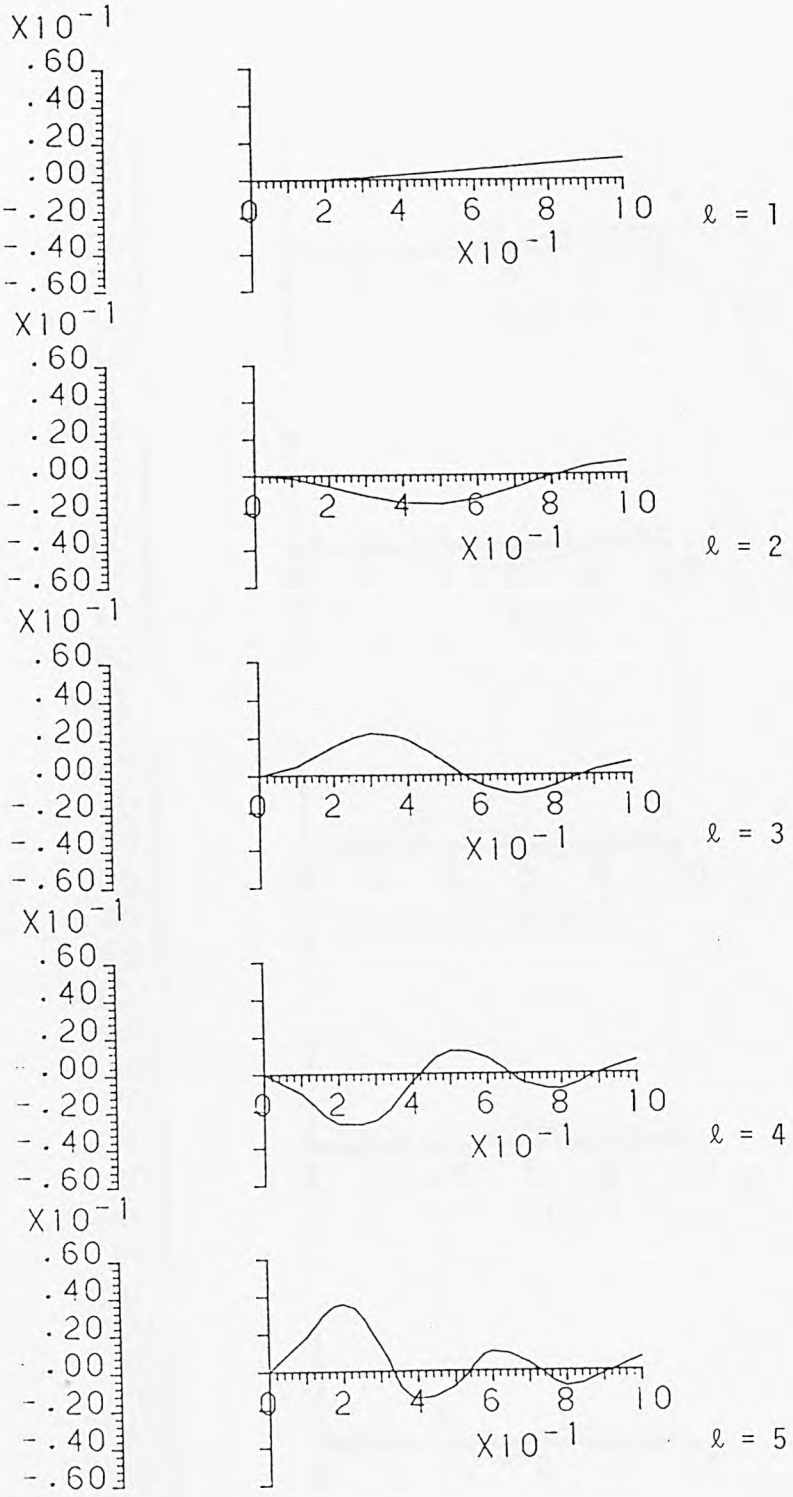

FIG.6.1. Variation of normalised displacement of torsional vibration of sphere along the radius (n = 2)

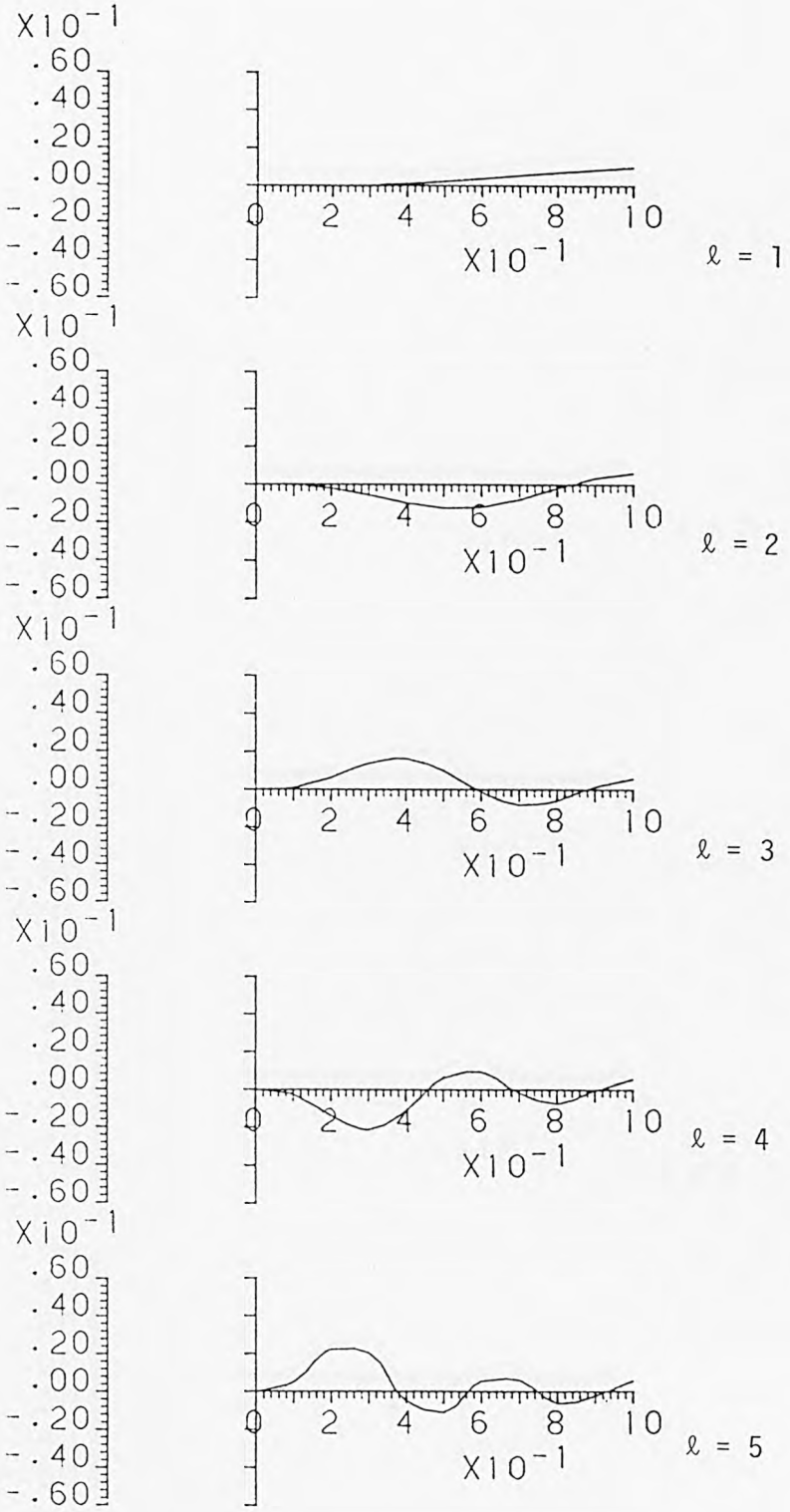

Distance along the radius = r/a

FIG. 6.1 (Continued) n = 3

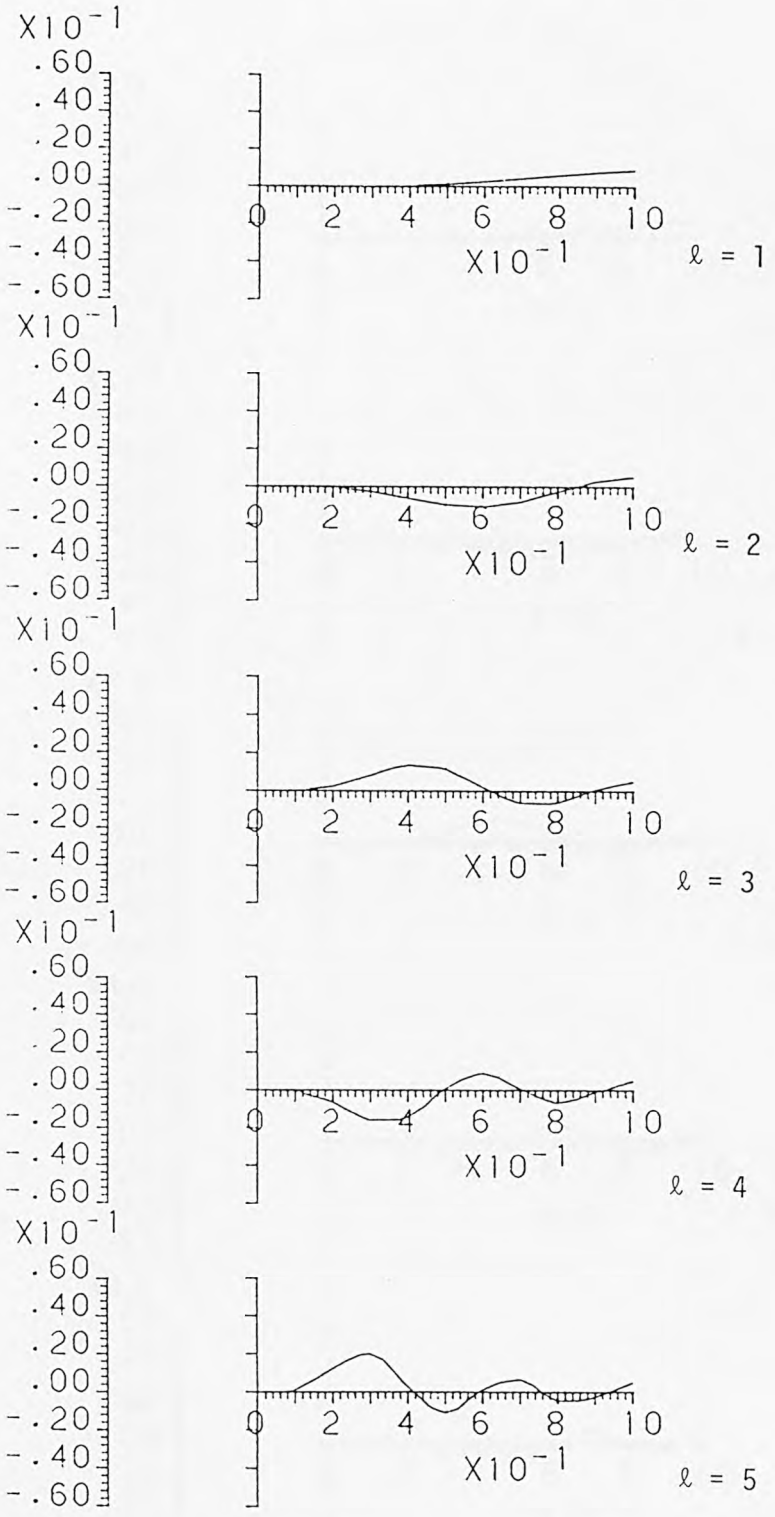

FIG. 6.1. (Continued) n = 4

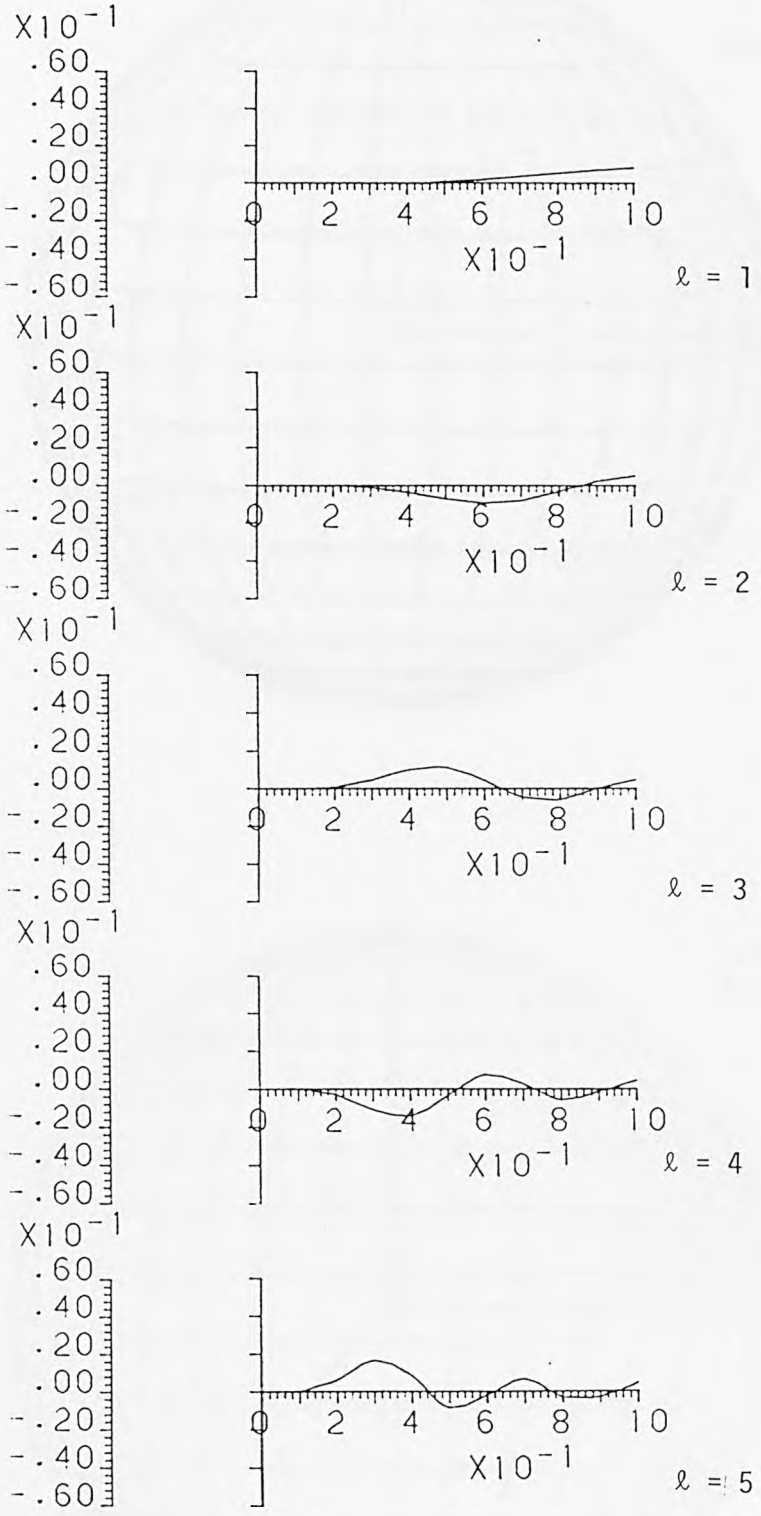

FIG. 6.1.(Continued) n = 5.

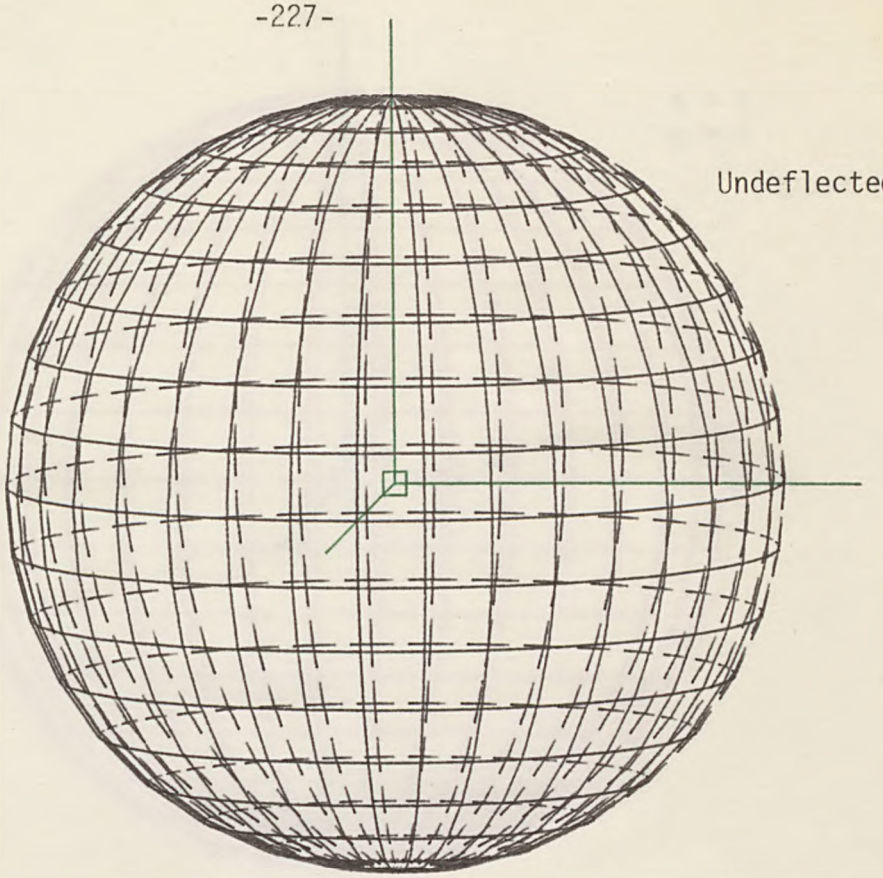

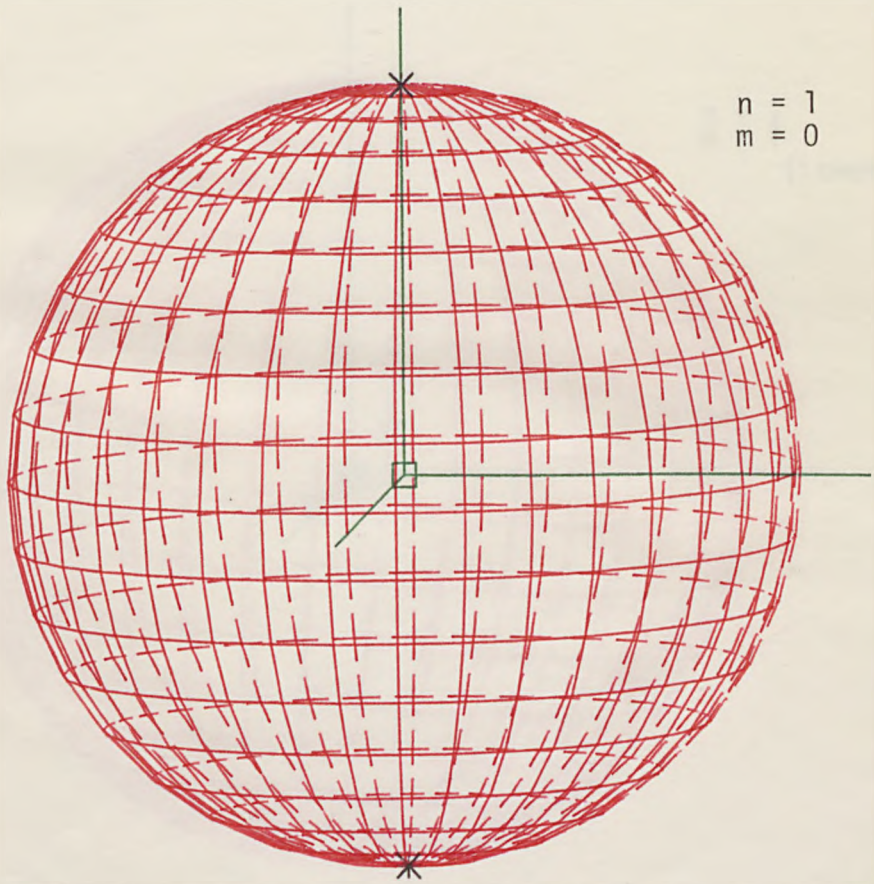

FIG.6.2. Diagrams of the surface mode shapes of torsional vibration
(* Nodal point)

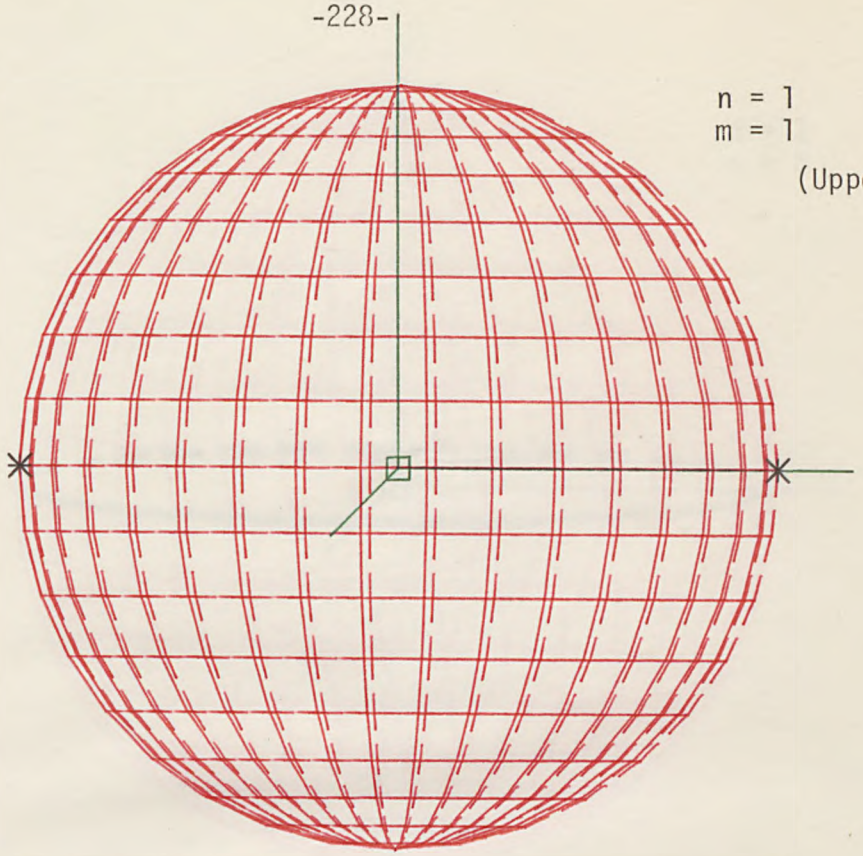

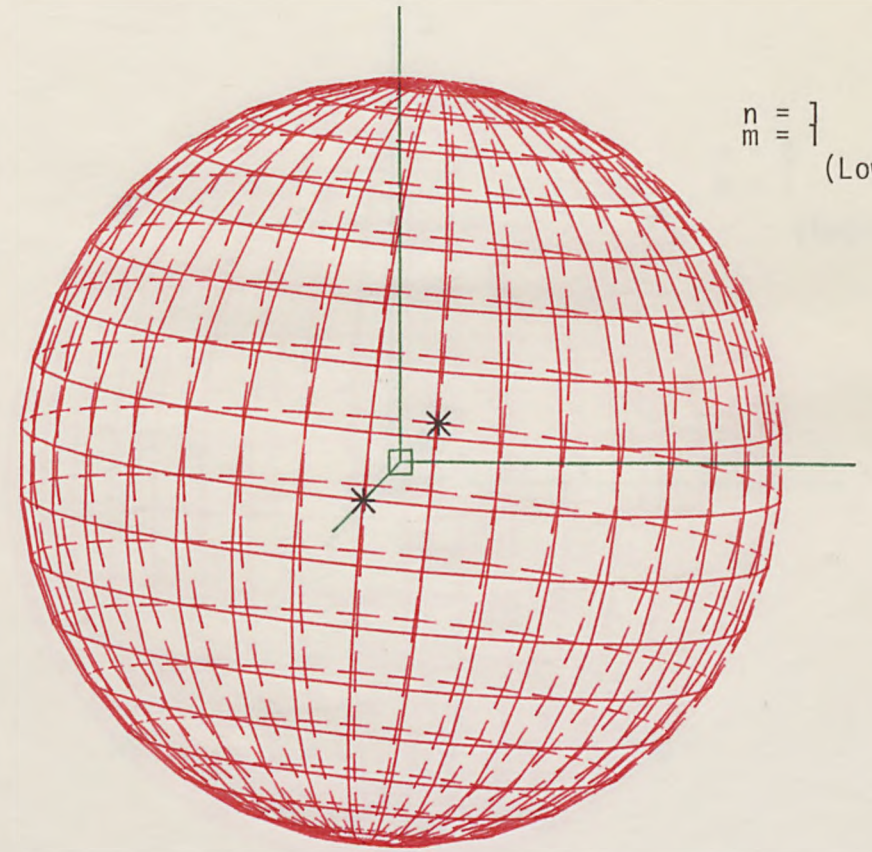

FIG.6.2. (Continued)

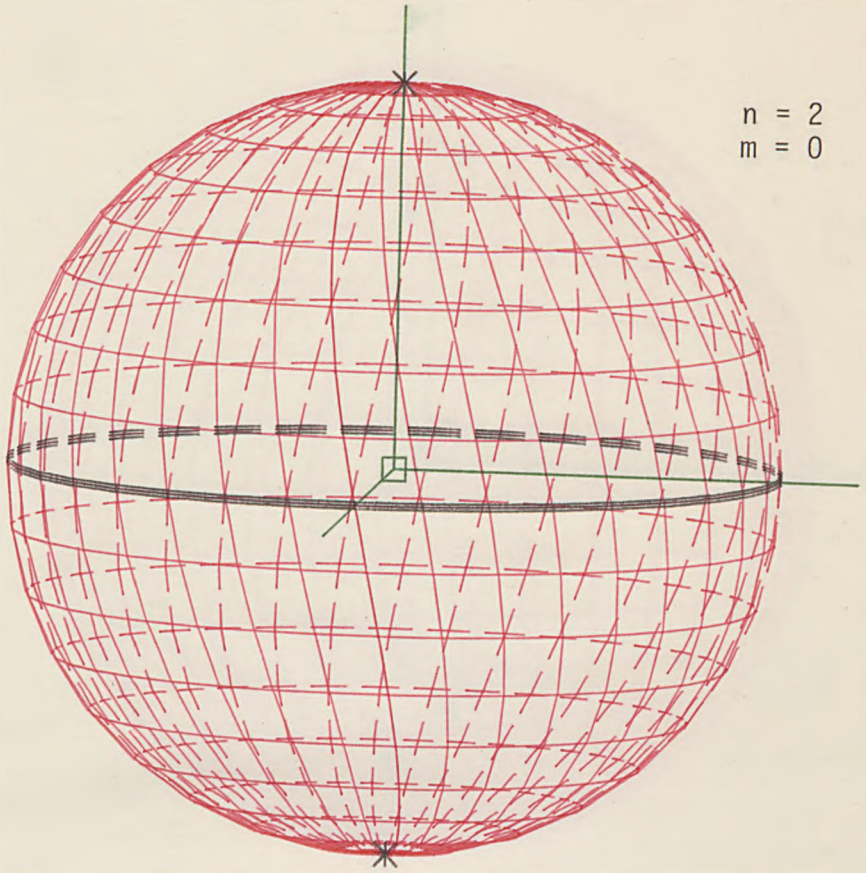

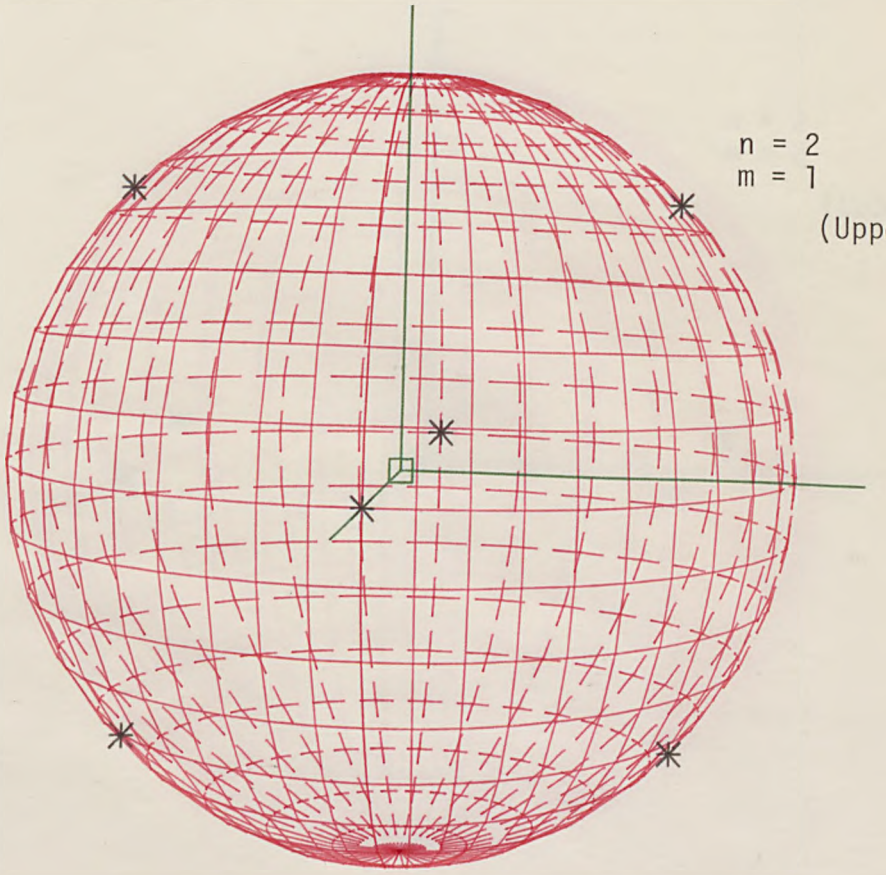

FIG.6.2. (Continued)

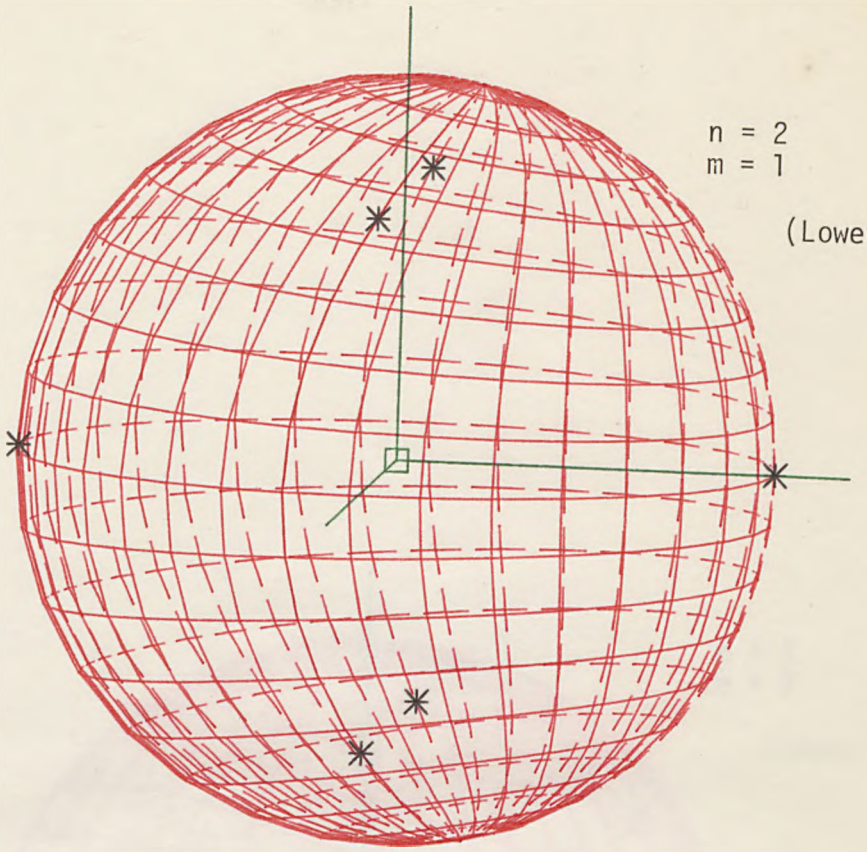

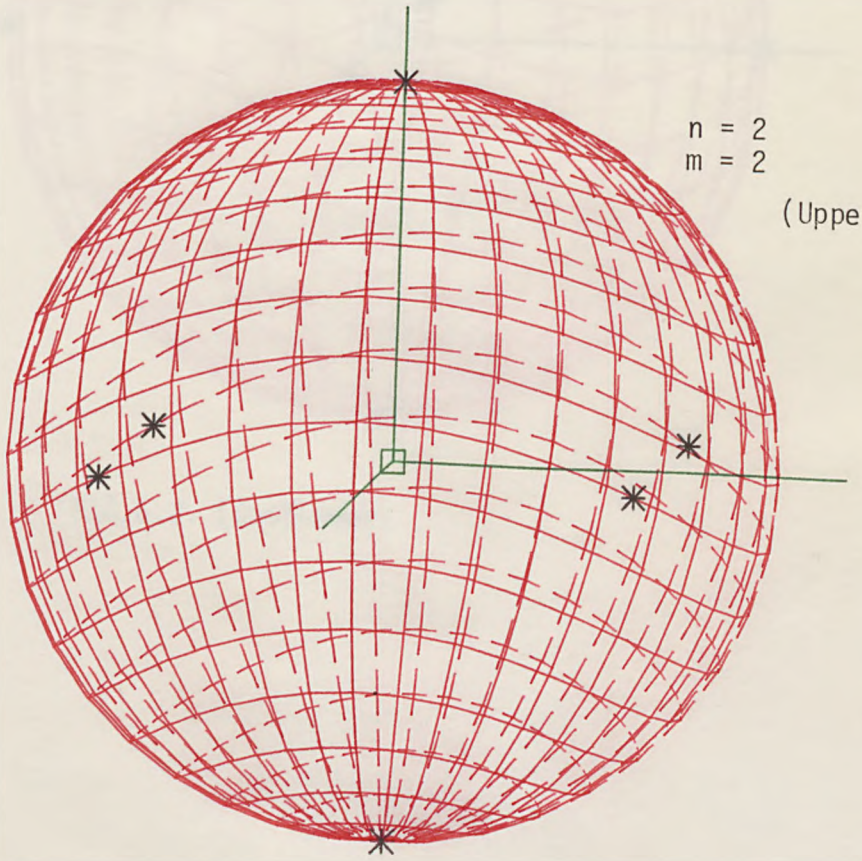

FIG.6.2. (Continued)

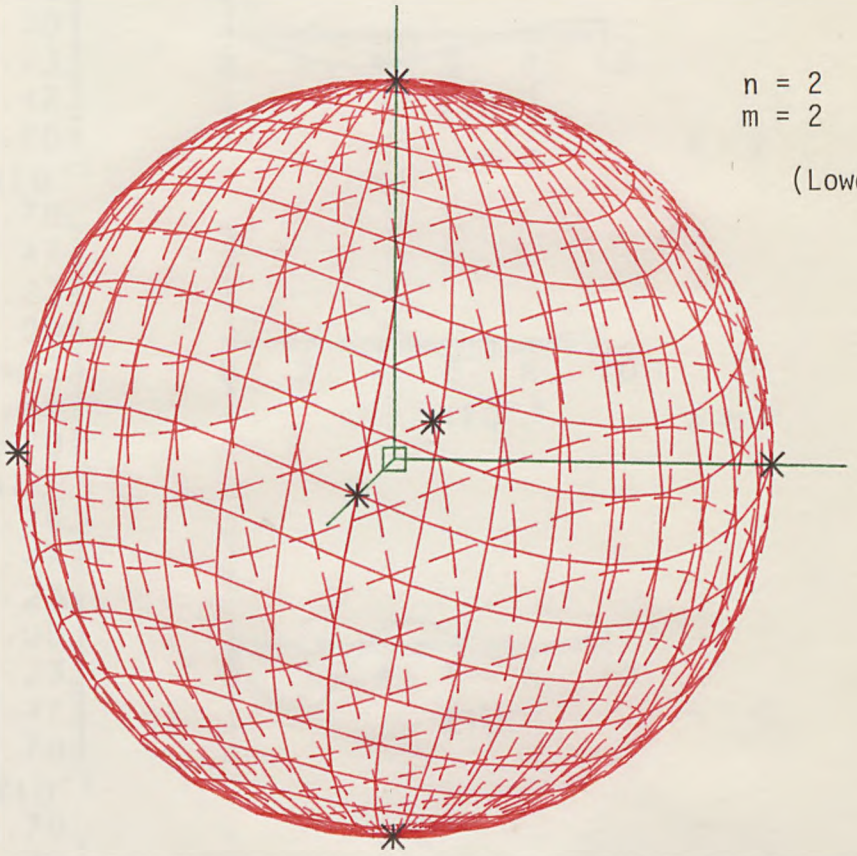

FIG.6.2. (Continued)

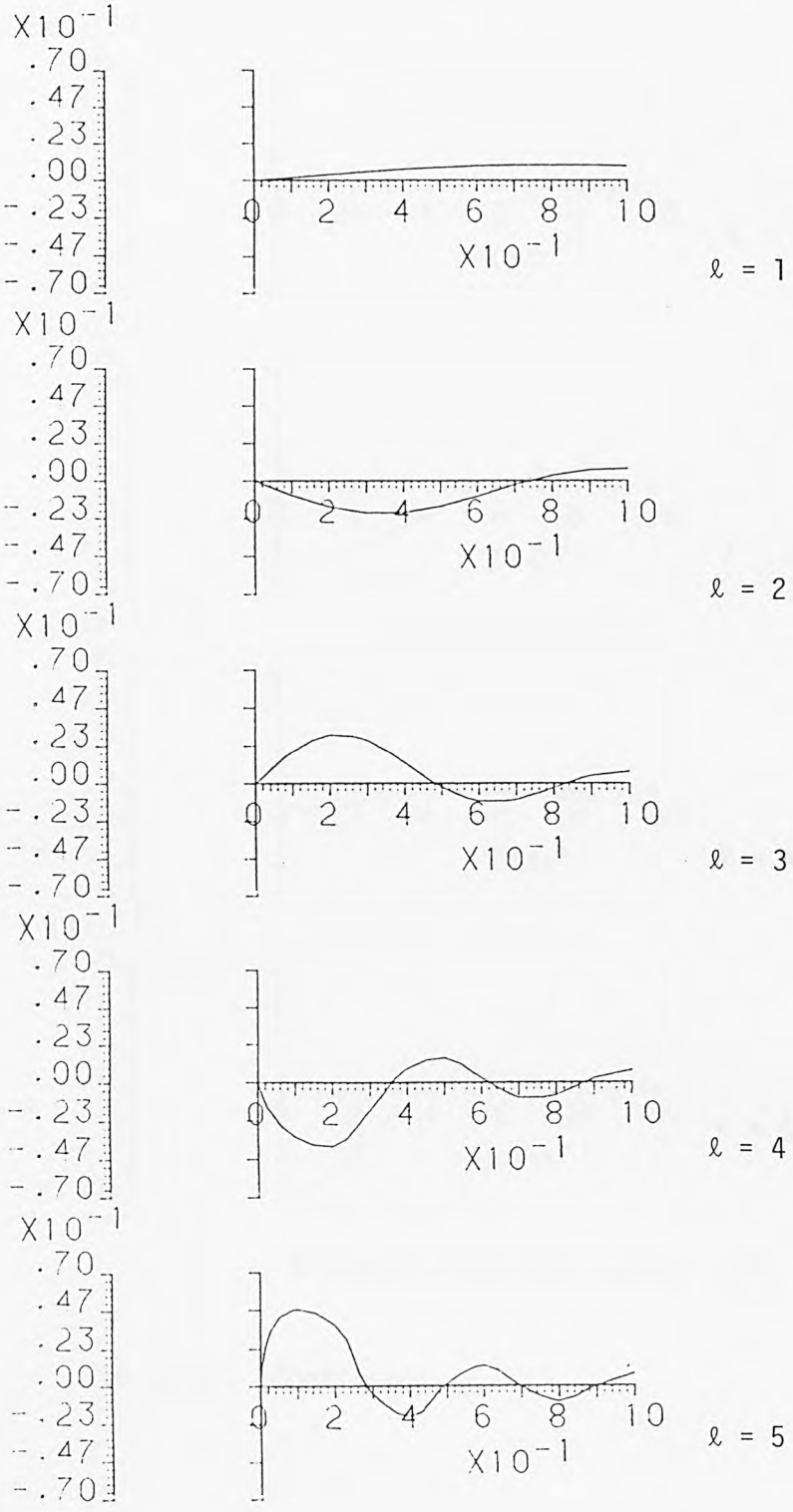

FIG.6.3. Variation of normalised displacement (u_r) of spheroidal vibration along the radius. (Poisson ratio = 0.29, n = 0).

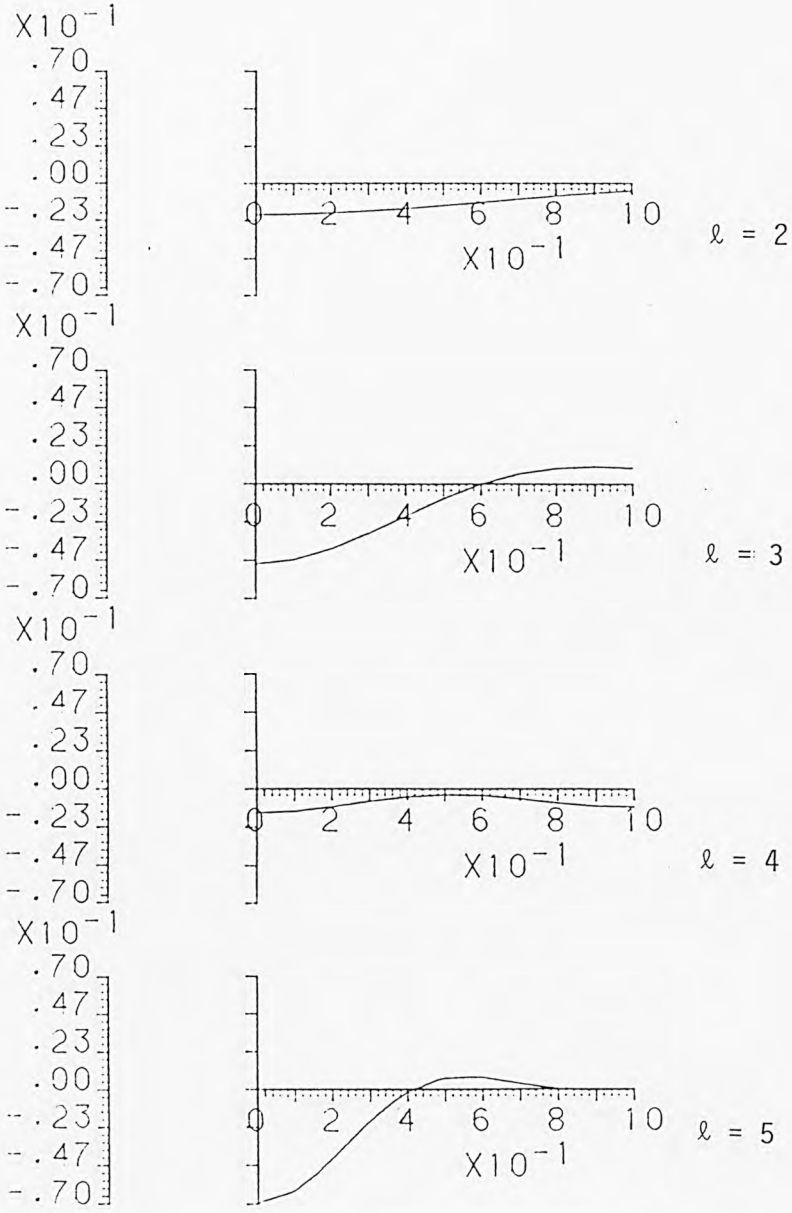

FIG. 6.3. (Continued) n = 1

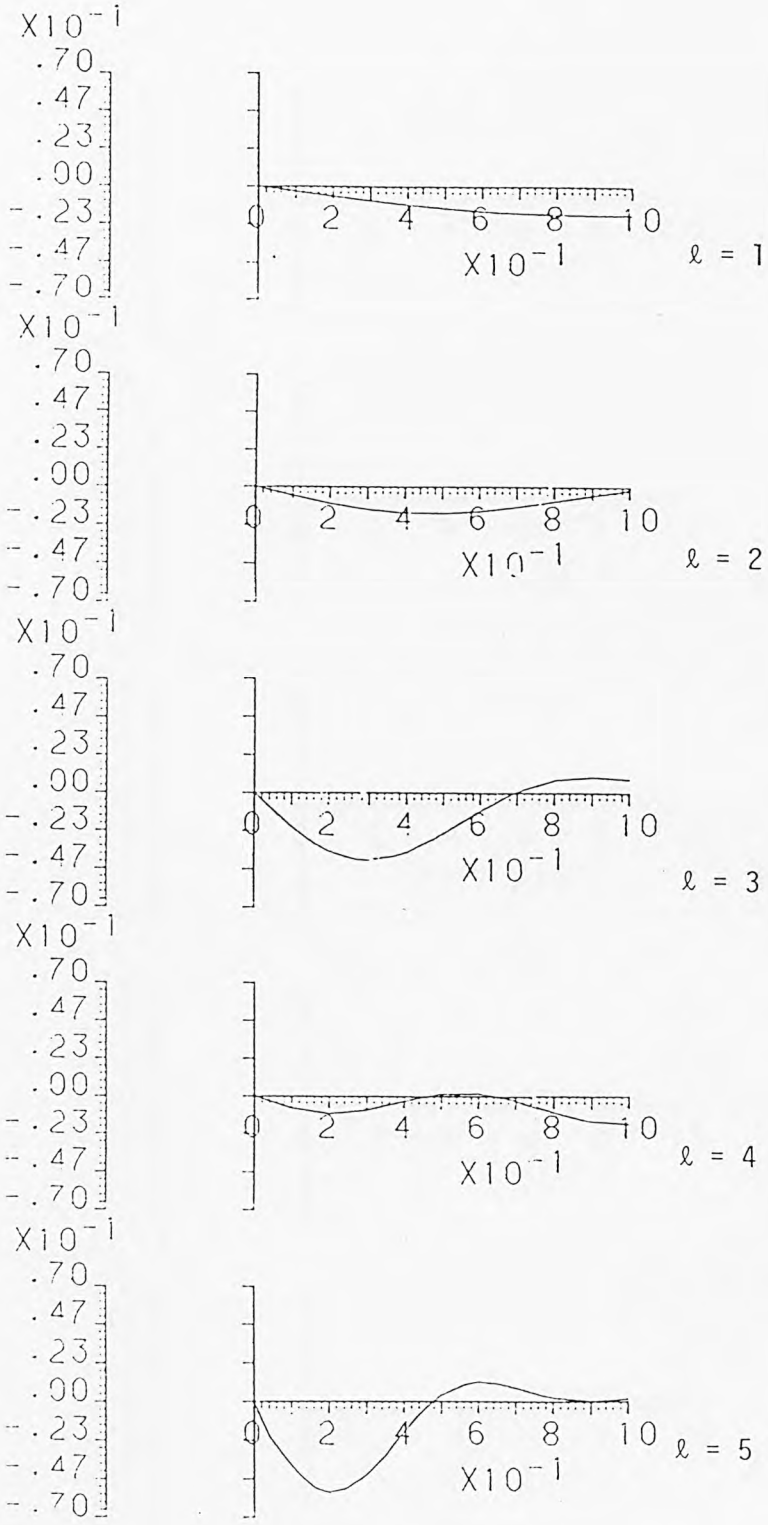

FIG.6.3. (Continued) n = 2

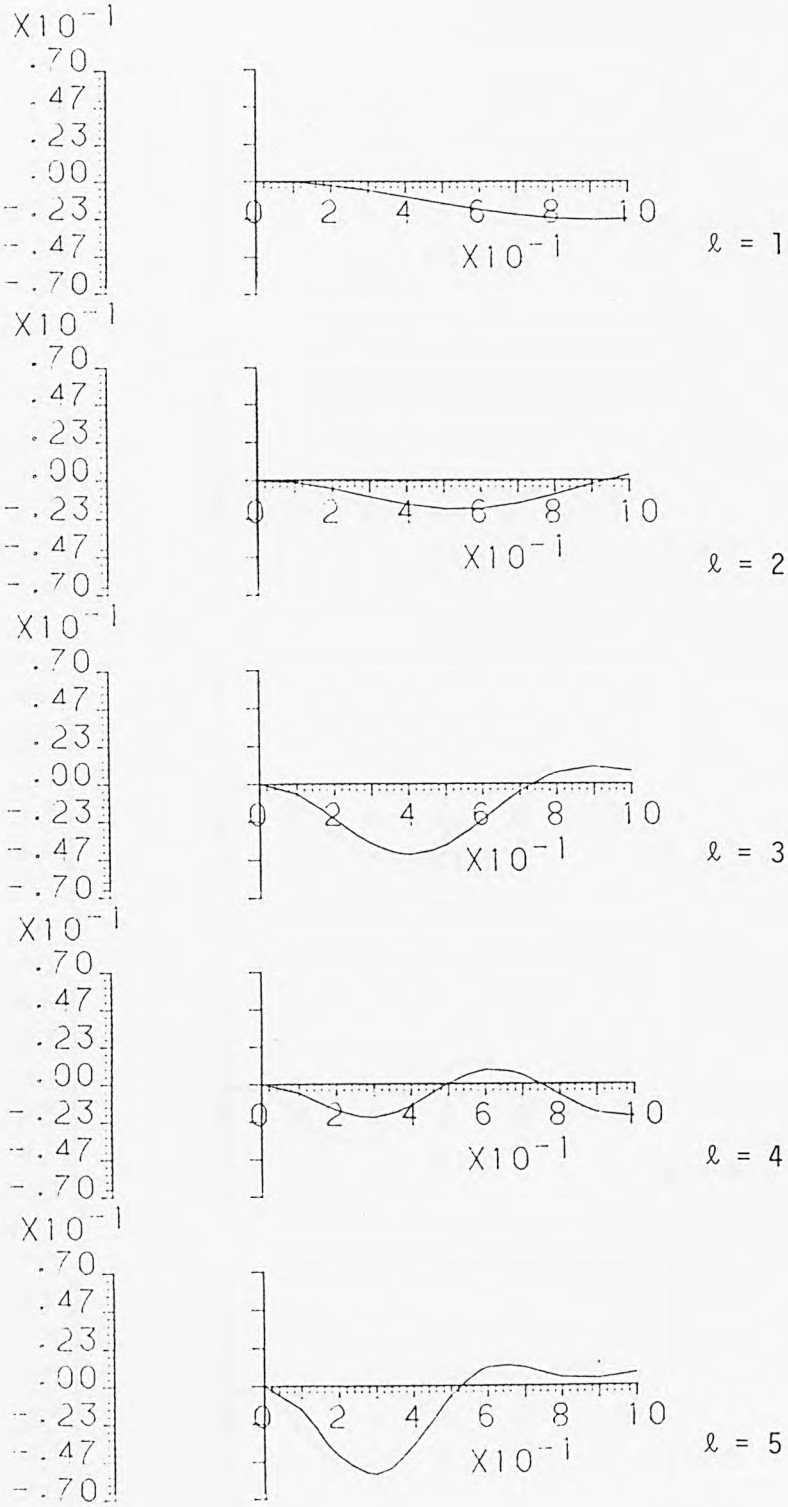

FIG.6.3. (Continued) n = 3

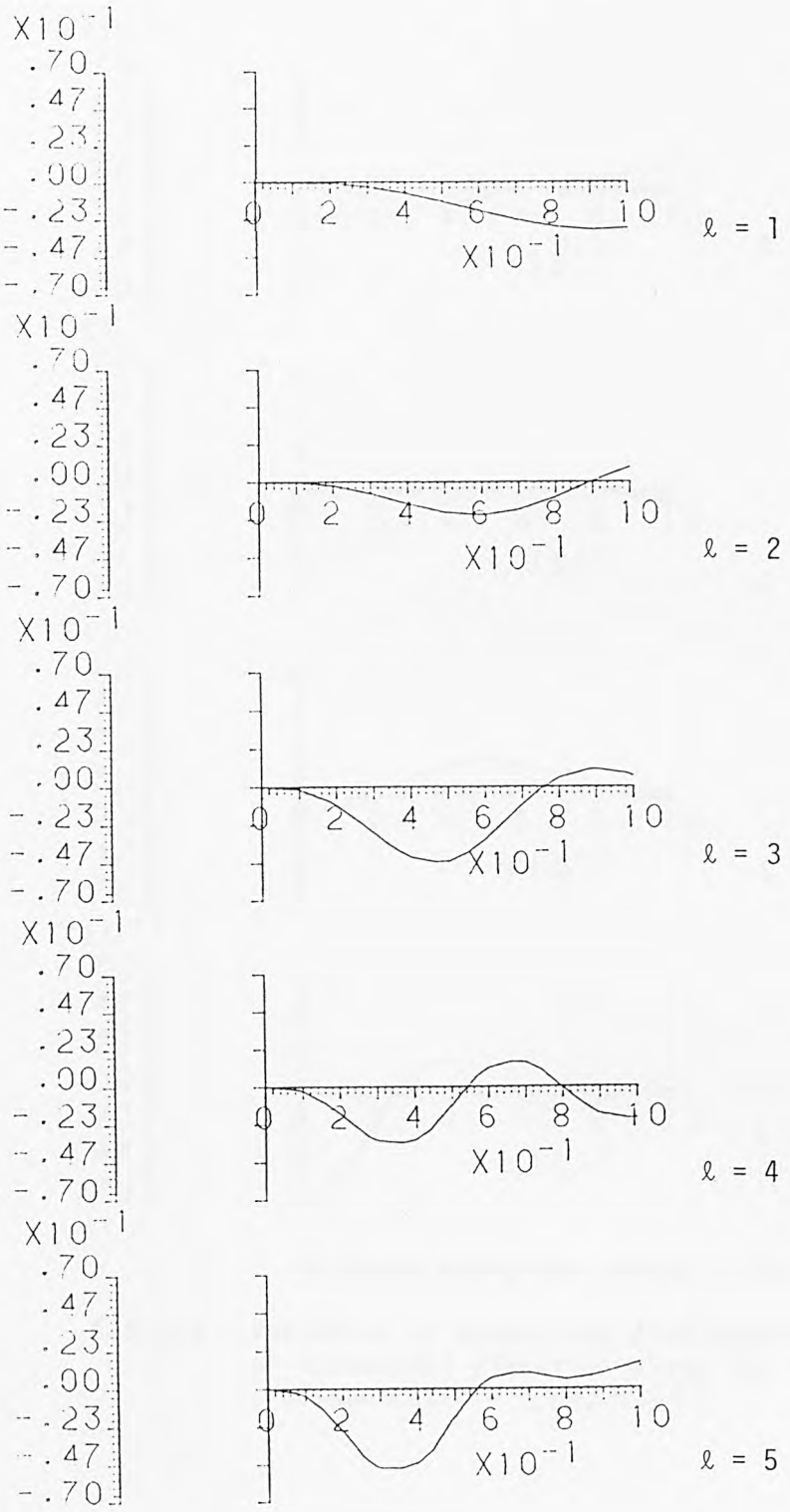

Distance along the radius = r/a.

FIG.6.3. (Continued) n = 4

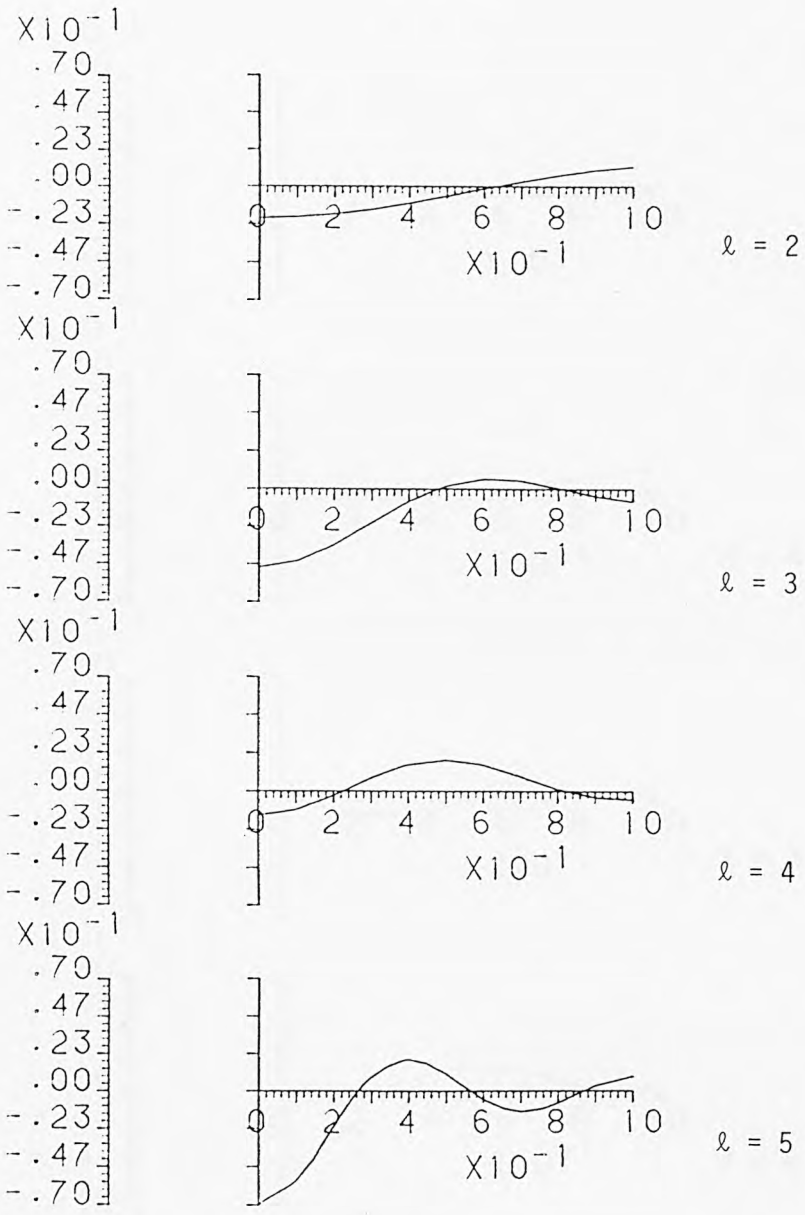

Distance along the radius = r/a.

FIG.6.4. Variation of normalised displacement (u_θ) of spheroidal vibration along the radius. (Poisson ratio = 0.29, n = 1)

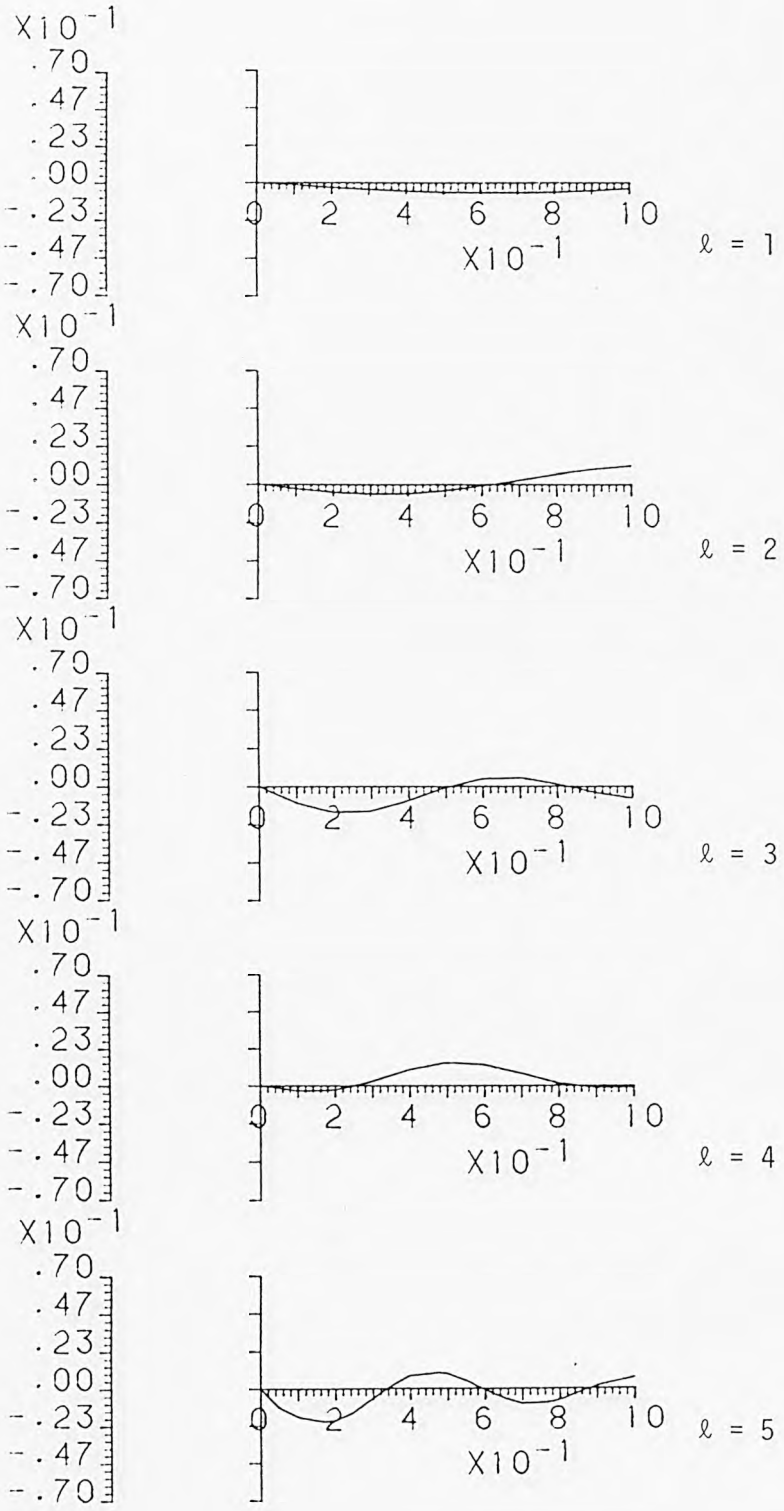

Distance along the radius = r/a.

FIG.6.4. (Continued) n = 2

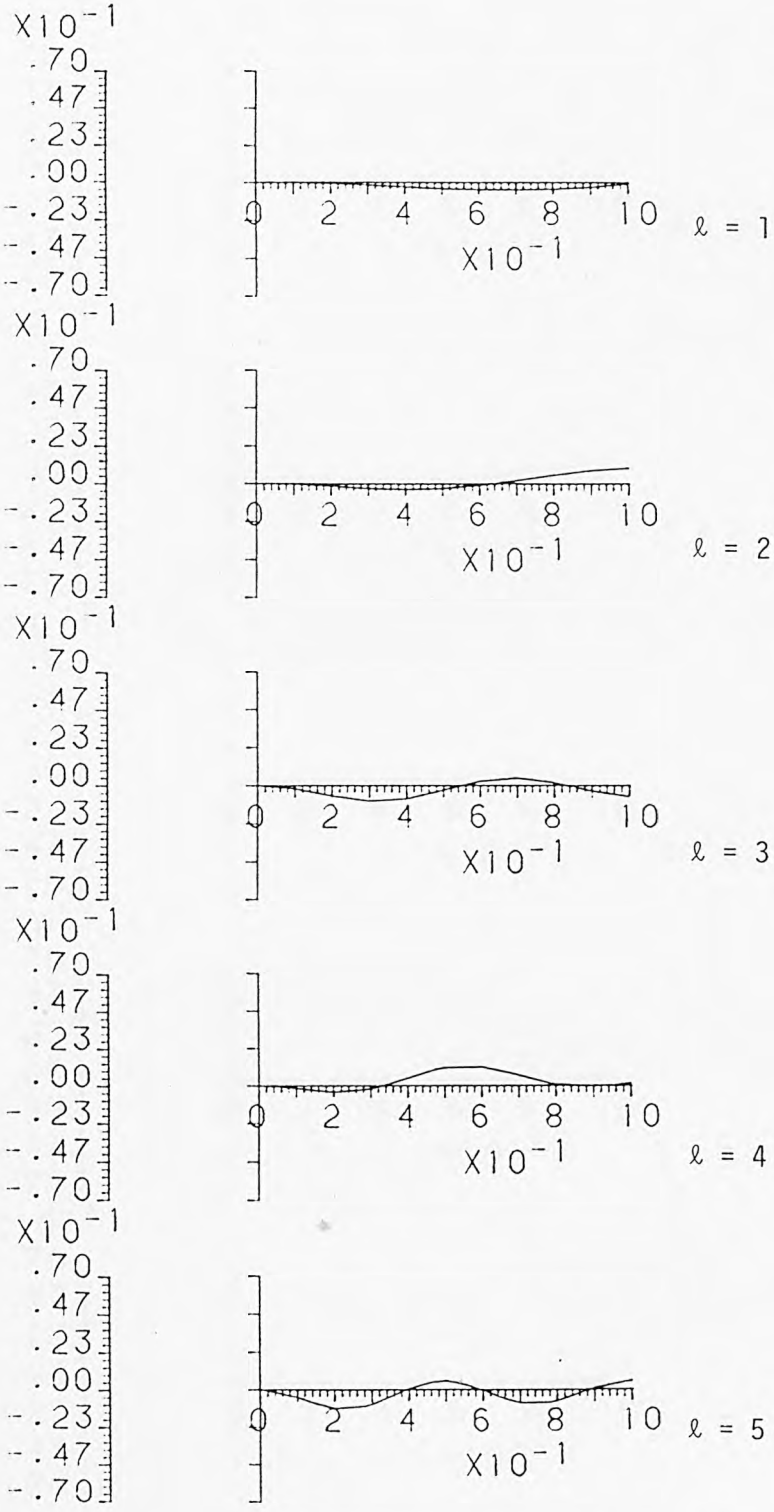

FIG.6.4. (Continued) n = 3

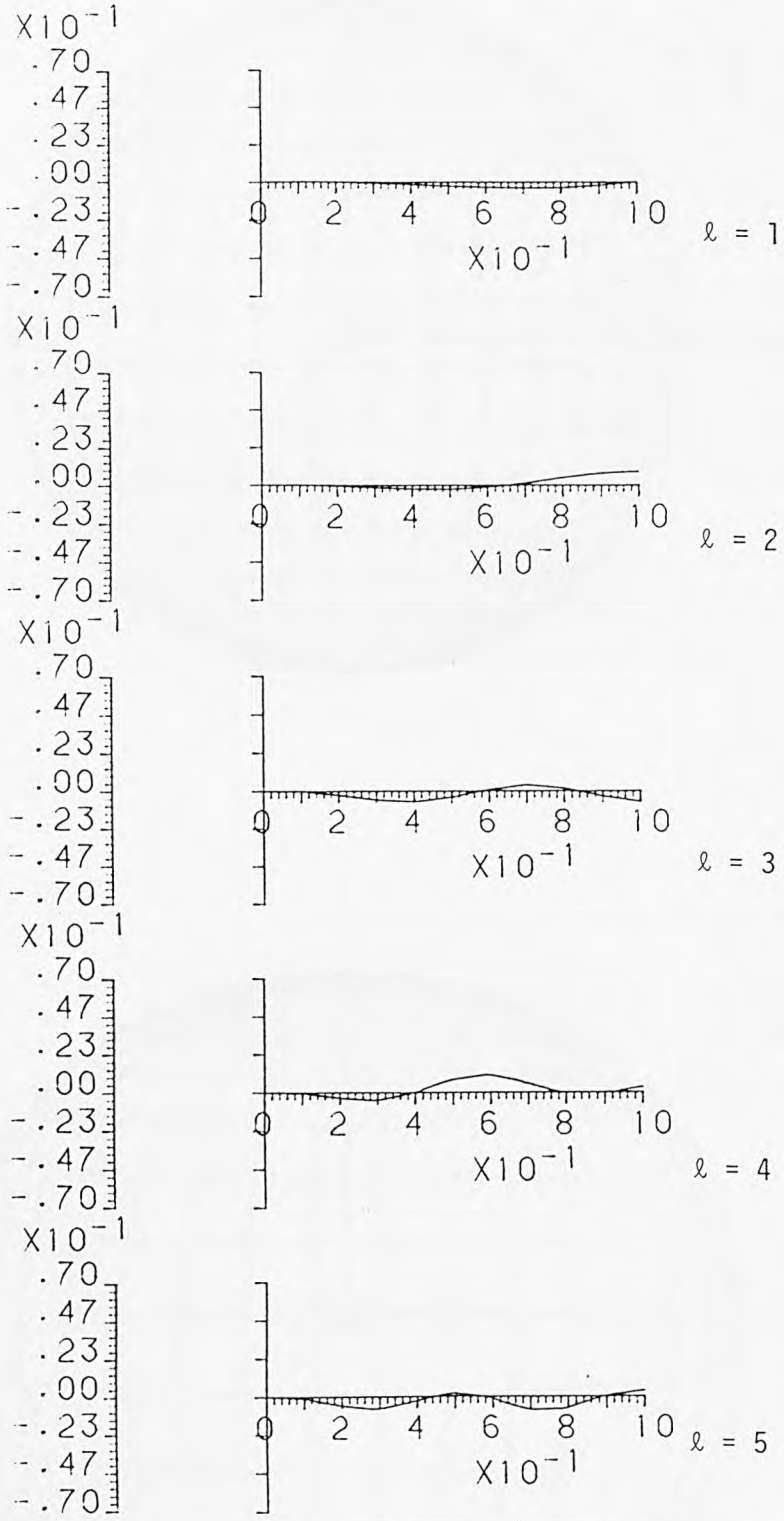

FIG. 6.4. (Continued) n = 4

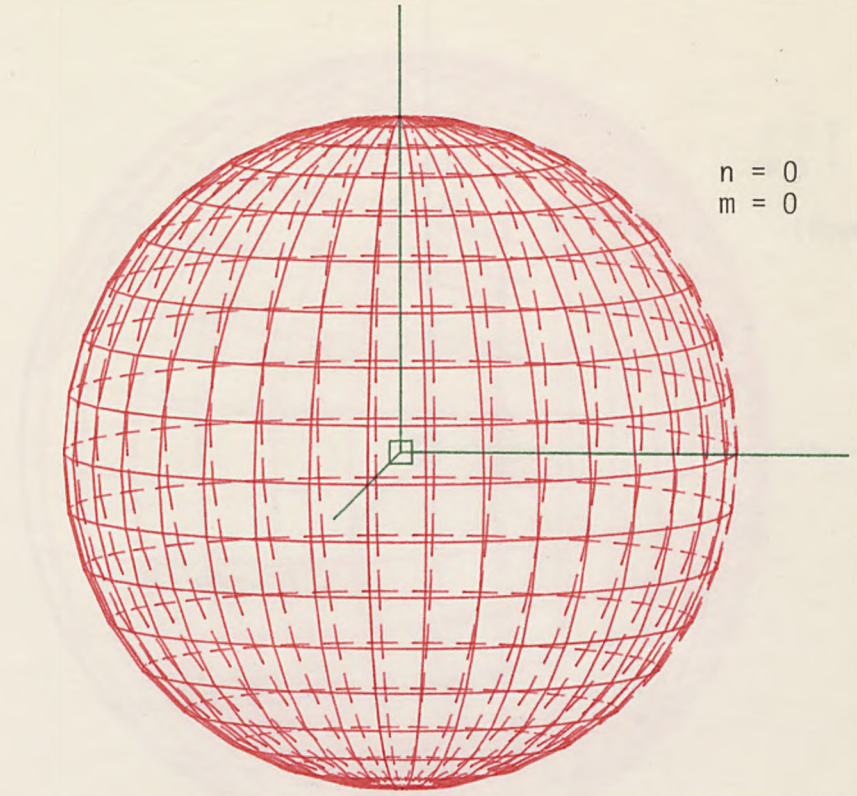

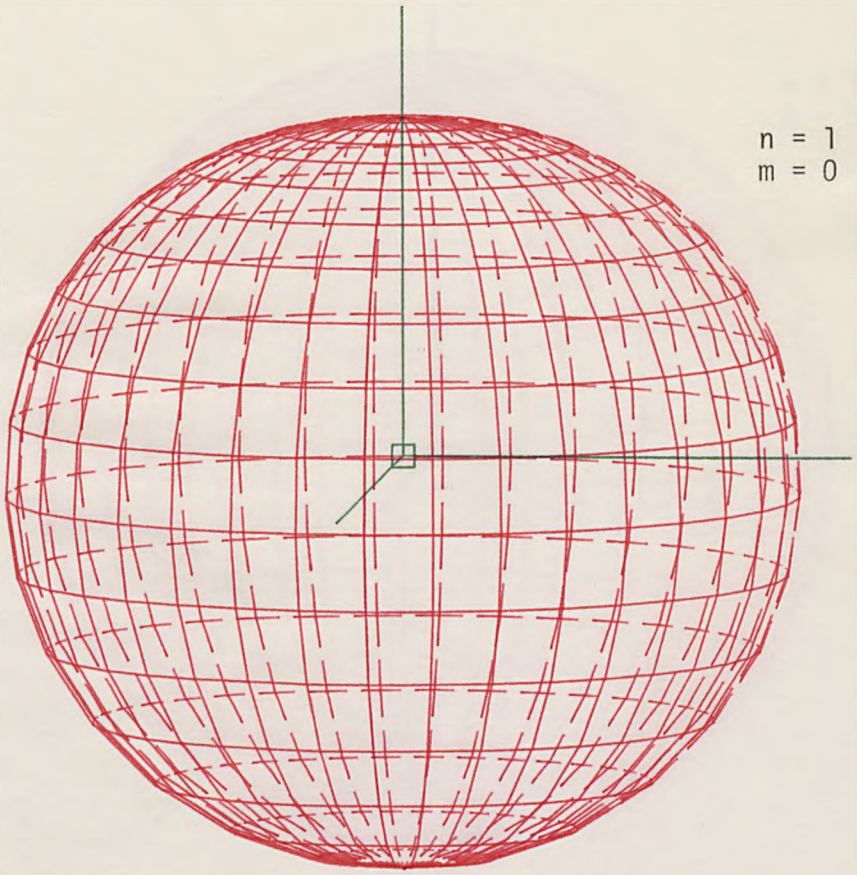

FIG.6.5. Diagrams of the surface mode shapes of spheroidal vibration

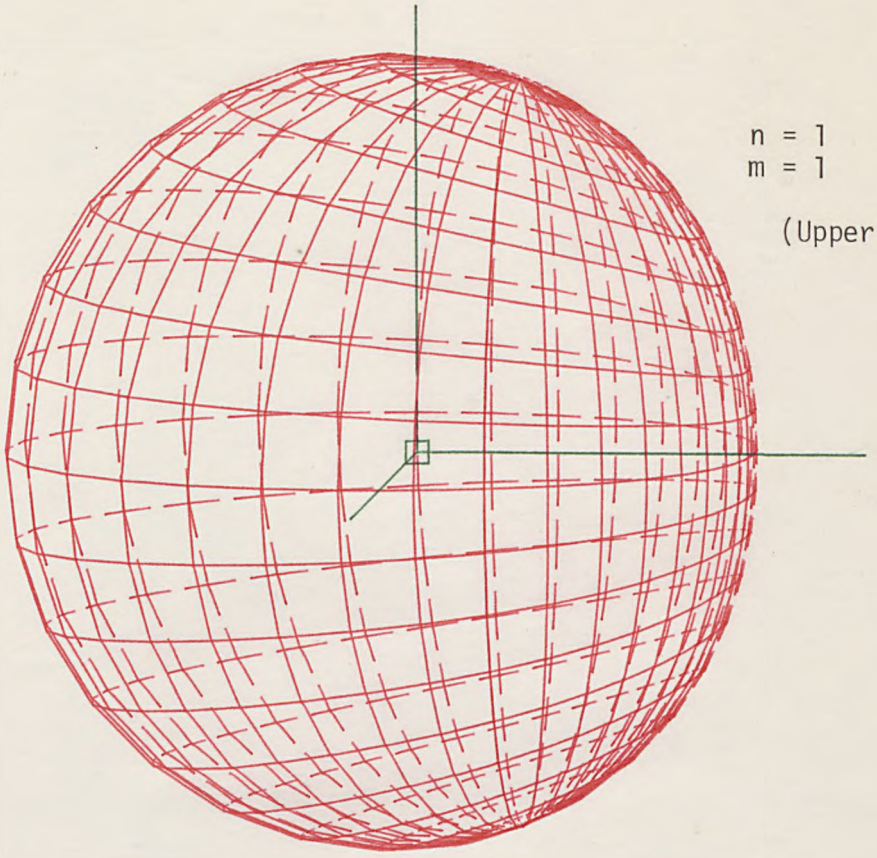

n = 1
m = 1

(Upper function)

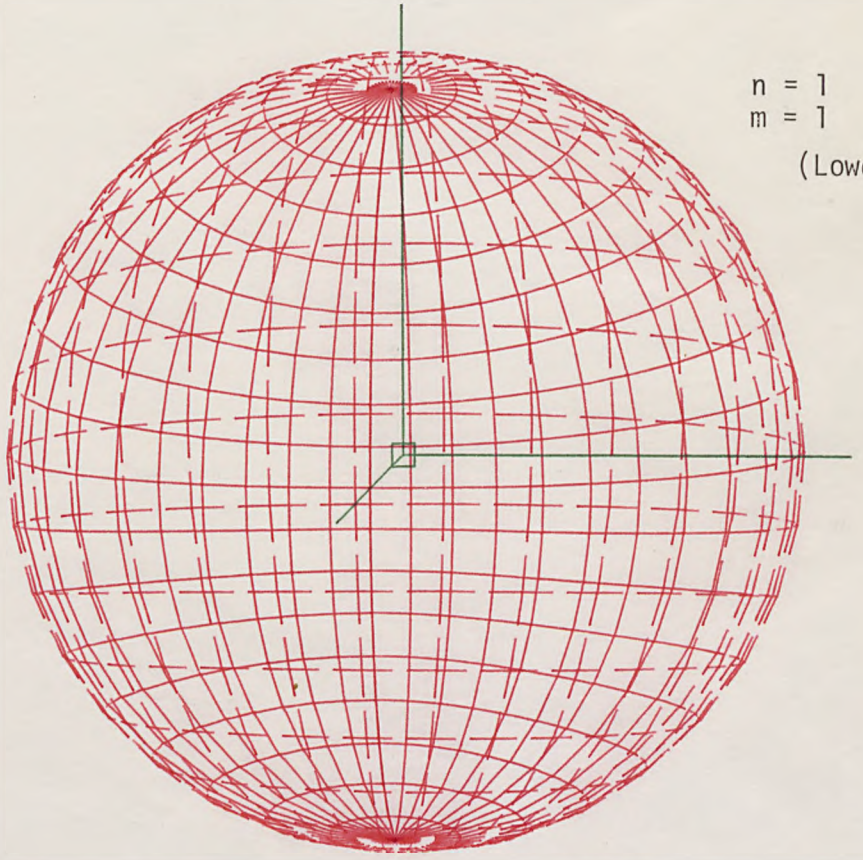

n = 1
m = 1

(Lower function)

FIG.6.5. (Continued)

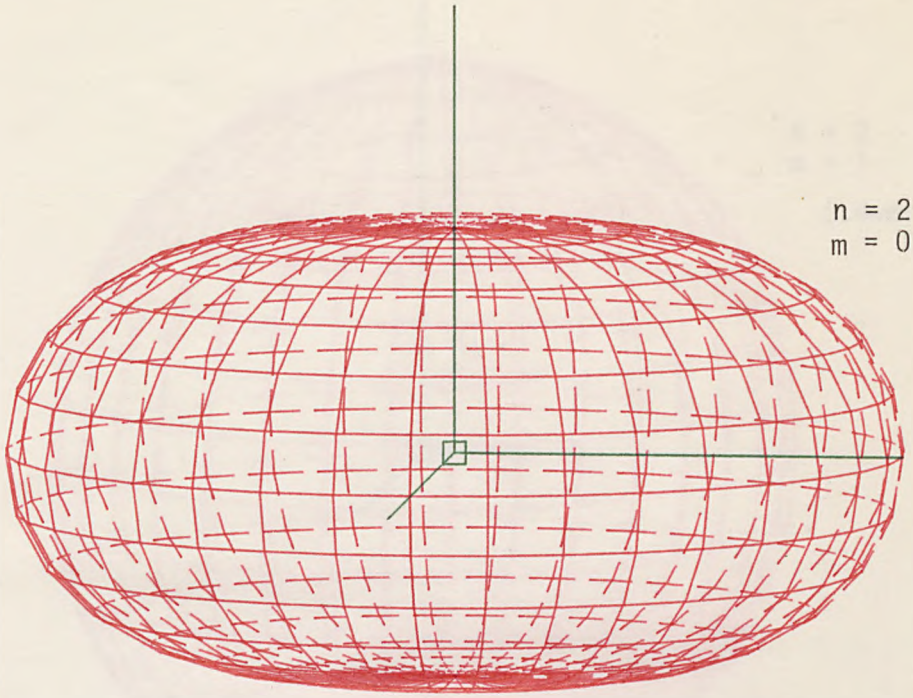

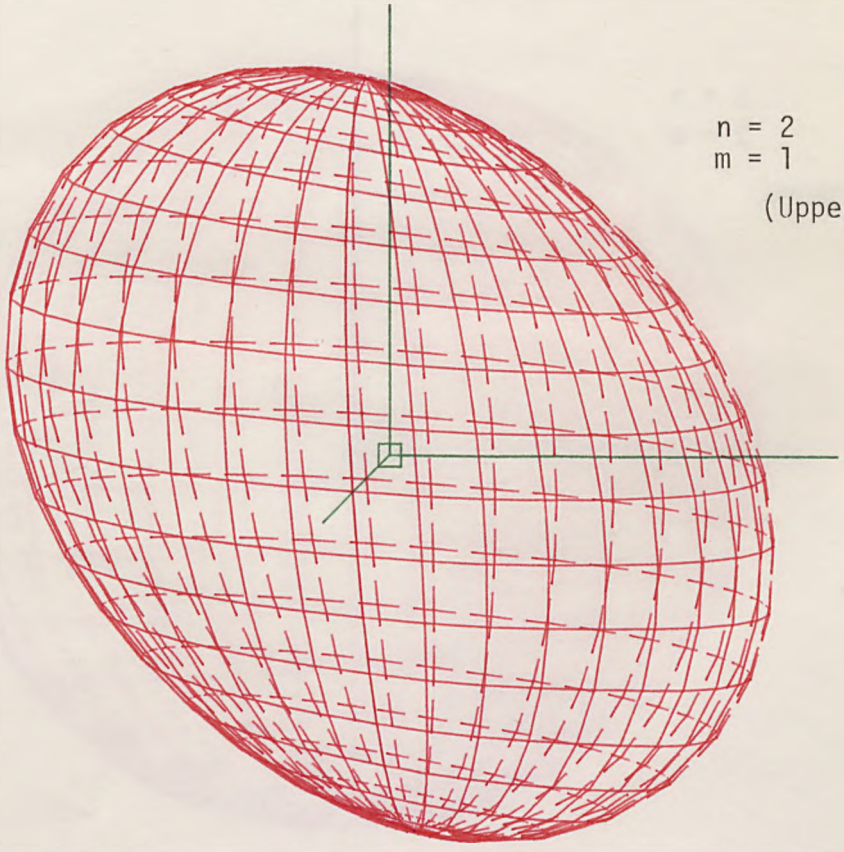

FIG.6.5. (Continued)

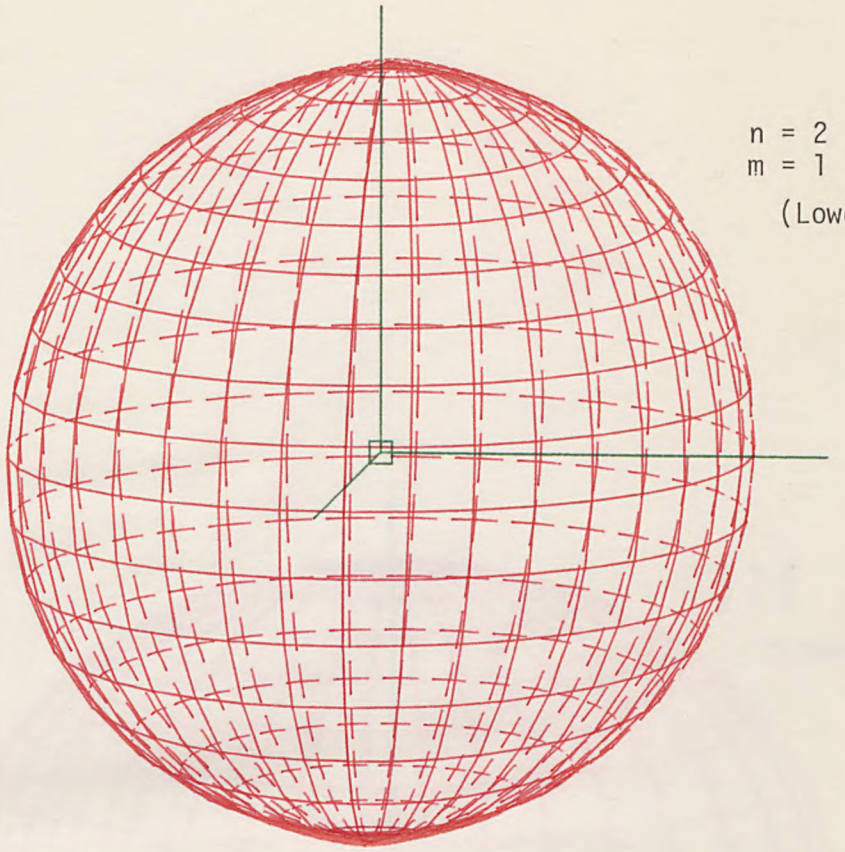

n = 2
m = 1

(Lower function)

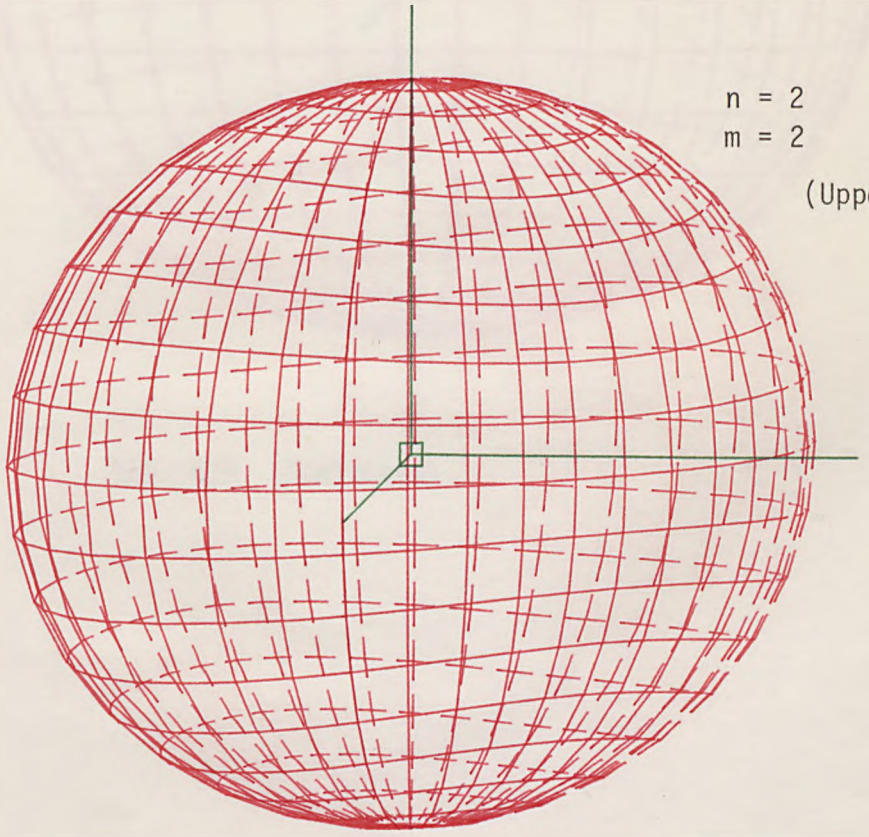

n = 2
m = 2

(Upper function)

FIG.6.5. (Continued)

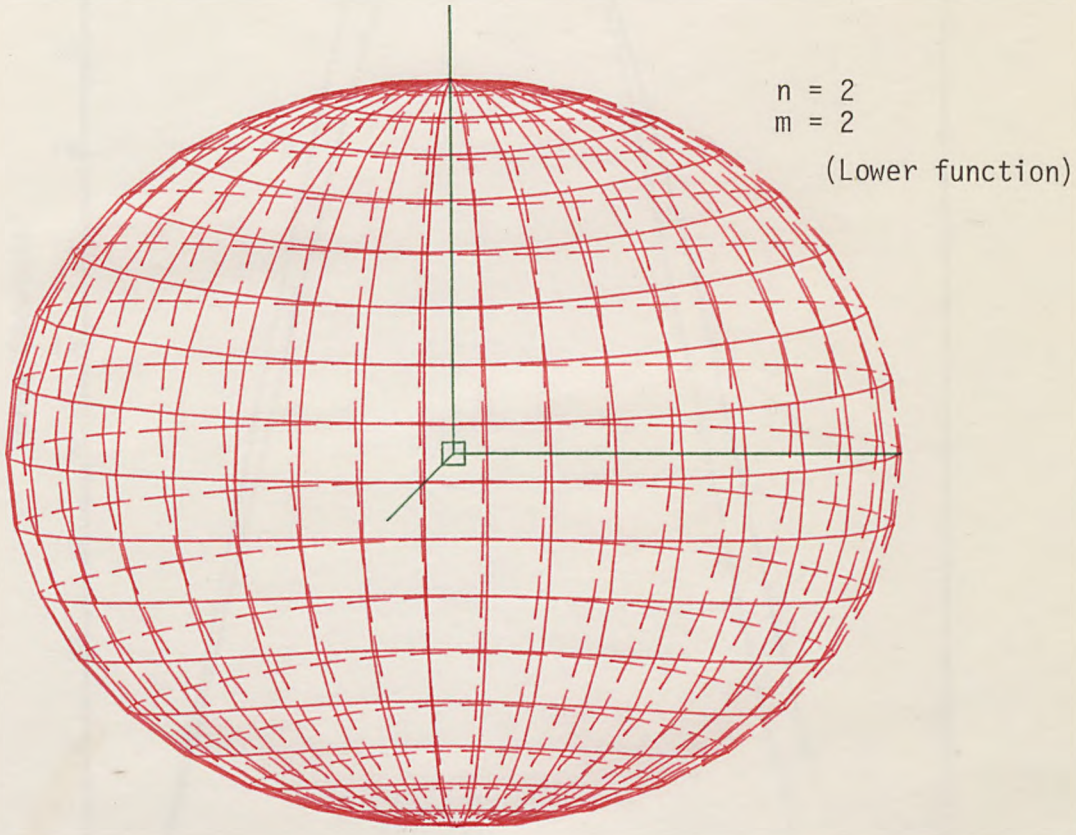

FIG. 6.5. (Continued)

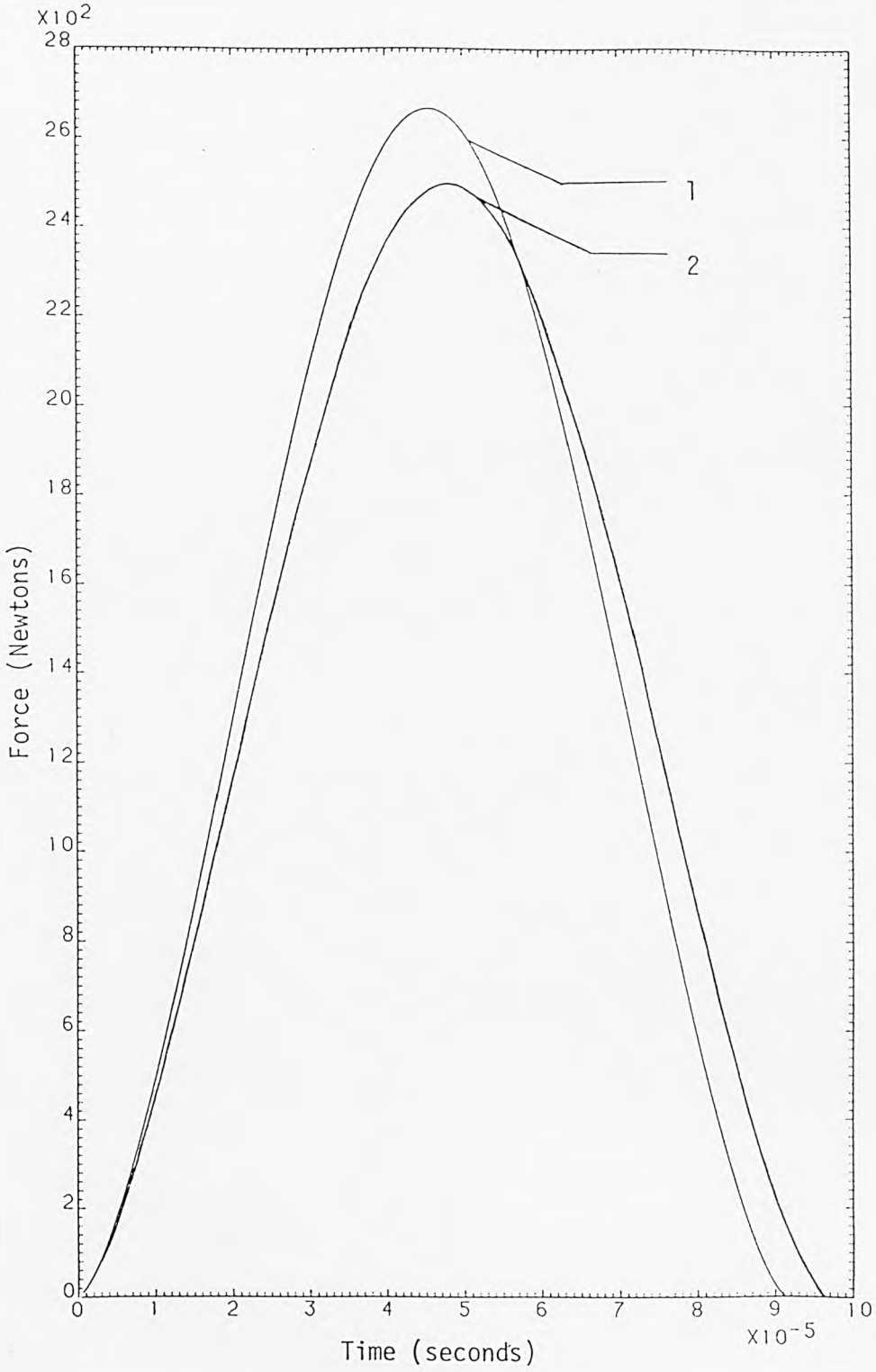

FIGURE 6.6. FORCE-TIME CURVES FOR A PAIR OF COLLIDING SPHERES OF RADII 1.27 cm and 7.112 cm (Eq.(6.161), n= 0, and ℓ = 1,5)

1 = Vibration terms excluded

2 = Vibration terms included

7. SOUND RADIATION FROM TRANSIENT VIBRATIONS OF HOLLOW SPHERES

The transient vibration of hollow spheres, together with the sound generated from this vibration, receives attention in this chapter. This study is very similar to that given for solid spheres except that spherical Bessel functions of the second kind, which played no part in the solid sphere investigation, should now be taken into account. In order to satisfy the object of this chapter, the following studies are carried out:

(a) The frequency equations for both torsional and spheroidal vibrations are derived and their successive roots for different order and different ratio of inner to outer radii are tabulated.

(b) Orthogonality is examined and diagrams showing variations of the normalised displacement across the thickness of hollow spheres are given.

(c) Finally, the sound pressure caused by transient vibration of a hollow sphere is considered.

7.1. Vibration of Hollow Sphere

Vibrations of a hollow sphere can be easily studied by following similar procedures as given for a solid sphere. In order to carry out this study, let us consider a hollow sphere of inner and outer radii of a* and a, respectively. Unlike the solid sphere the Bessel functions of the second kind with the non-zero coefficients should be introduced into the formula representing displacement, since their presentation yield to

the finite solution at both r=a and r=a*. Thus displacements due to torsional and spheroidal vibrations of hollow spheres are respectively:

$$u_r = 0 \tag{7.1a}$$

$$u_\theta = \mp \left[\bar{A}_n j_n(K_2 r) + \bar{\bar{A}}_n y_n(K_2 r)\right] \frac{m}{\sin\theta} P_n^m(\cos\theta) \begin{matrix}\cos m\psi \\ \sin m\psi\end{matrix} \tag{7.1b}$$

$$u_\psi = \left[\bar{A}_n j_n(K_2 r) + \bar{\bar{A}}_n y_n(K_2 r)\right] \frac{d}{d\theta} P_n^m(\cos\theta) \begin{matrix}\sin m\psi \\ \cos m\psi\end{matrix} \tag{7.1c}$$

$$\begin{aligned} u_r = -\{&\bar{B}_n \left[n j_{n-1}(K_1 r) - (n+1) j_{n+1}(K_1 r)\right] \frac{K_1}{2n+1} \\ &+ \bar{\bar{B}}_n \left[n y_{n-1}(K_1 r) - (n+1) y_{n+1}(K_1 r)\right] \frac{K_1}{2n+1} \\ &- \frac{n(n+1)}{r} \left[\bar{D}_n j_n(K_2 r) + \bar{\bar{D}}_n y_n(K_2 r)\right]\} P_n^m(\cos\theta) \begin{matrix}\sin m\psi \\ \cos m\psi\end{matrix} \end{aligned} \tag{7.2a}$$

$$\begin{aligned} u_\theta = -\{&\frac{1}{r}\left[\bar{B}_n j_n(K_1 r) + \bar{\bar{B}}_n y_n(K_1 r)\right] - \frac{1}{r}\left[\bar{D}_n j_n(K_2 r) + \bar{\bar{D}}_n y_n(K_2 r)\right] \\ &- \bar{D}_n \left[n j_{n-1}(K_2 r) - (n+1) j_{n+1}(K_2 r)\right] \frac{K_2}{2n+1} \\ &- \bar{\bar{D}}_n \left[n y_{n-1}(K_2 r) - (n+1) y_{n+1}(K_2 r)\right] \frac{K_2}{2n+1}\} x \frac{d}{d\theta} P_n^m(\cos\theta) \begin{matrix}\sin m\psi \\ \cos m\psi\end{matrix} \end{aligned} \tag{7.2b}$$

$$u_\psi = \mp \{\frac{1}{r}\left[\bar{B}_n j_n(K_1 r) + \bar{\bar{B}}_n y_n(K_1 r)\right] - \frac{1}{r}\left[\bar{D}_n j_n(K_2 r) + \bar{\bar{D}}_n y_n(K_2 r)\right]$$

$$- \bar{D}_n\left[n j_{n-1}(K_2 r) - (n+1) j_{n+1}(K_2 r)\right]\frac{K_2}{2n+1}$$

$$- \bar{\bar{D}}_n\left[n y_{n-1}(K_2 r) - (n+1) y_{n+1}(K_2 r)\right]\frac{K_2}{2n+1}\} \times \frac{m}{\sin\theta} P_n^m(\cos\theta)\begin{matrix}\cos m\psi \\ \sin m\psi\end{matrix}$$

(7.2c)

7.2. Frequency equation

The stress-strain relation given by equations (6.30a) to (6.30c) and (6.31a) to (6.31c) may be used for the derivation of the frequency equations for both torsional and spheroidal vibrations of a hollow sphere. The boundary conditions which should be satisfied at both r=a and r=a* can be written as:

$$\sigma_{rr} = \sigma_{r\theta} = \sigma_{r\psi} = 0 \qquad (7.3)$$

For torsional vibration the above boundary conditions can be satisfied if:

$$f'_\theta\Big|_{r=a} - \frac{1}{a} f_\theta\Big|_{r=a} = 0 \qquad (7.3a)$$

$$f'_\theta\Big|_{r=a^*} - \frac{1}{a^*} f_\theta\Big|_{r=a^*} = 0 \qquad (7.3b)$$

Thus the frequency equation of torsional vibrations of hollow spheres may be written as:

$$\left[(n-1)y_n(K_2a) - K_2a y_{n+1}(K_2a)\right]\left[(n-1)j_n(K_2a^*) - K_2a^* j_{n+1}(K_2a^*)\right]$$

$$= \left[(n-1)y_n(K_2a^*) - K_2a^* y_{n+1}(K_2a^*)\right]\left[(n-1)j_n(K_2a) - K_2a j_{n+1}(K_2a)\right]$$

(7.4)

The ratio $\bar{A}_n/\bar{\bar{A}}_n$ may also be given by:

$$\frac{\bar{A}_n}{\bar{\bar{A}}_n} = -\frac{(n-1)y_n(K_2a) - K_2a y_{n+1}(K_2a)}{(n-1)j_n(K_2a) - K_2a j_{n+1}(K_2a)} \qquad (7.5)$$

The successive roots of equation (7.4) for different ratios $\frac{a^*}{a}$ and n are tabulated in Tables (7.1) to (7.4). To derive the frequency equation of spheroidal vibration the boundary conditions given by expression (7.3) may be written as:

$$-\lambda K_1^2 R\Big|_{r=a} + 2u\left[R''\Big|_{r=a} - \frac{n(n+1)}{a}\left(f'_\psi\Big|_{r=a} - \frac{1}{a} f_\psi\Big|_{r=a}\right)\right] = 0$$

(7.6a)

$$\frac{2}{a}\left(R'\Big|_{r=a} - \frac{1}{a}R\Big|_{r=a}\right) + \frac{2}{a^2} f_\psi\Big|_{r=a} - \frac{n(n+1)}{a^2} f_\psi\Big|_{r=a} - f''_\psi\Big|_{r=a} = 0$$

(7.6b)

$$\pm\frac{2}{a}\left(R'\Big|_{r=a} - \frac{1}{a}R\Big|_{r=a}\right) + \frac{2}{a^2} f_\theta\Big|_{r=a} \mp \frac{n(n+1)}{a^2} f_\psi\Big|_{r=a} - f''_\theta\Big|_{r=a} = 0$$

(7.6c)

$$- \lambda K_1^2 \, R\Big|_{r=a^*} + 2\mu \left[R''\Big|_{r=a} - \frac{n(n+1)}{a^*} \left(f'_\psi\Big|_{r=a^*} - \frac{1}{a^*} f_\psi\Big|_{r=a^*} \right) \right] = 0 \tag{7.6d}$$

$$\frac{2}{a^*} \left(R'\Big|_{r=a^*} - \frac{1}{a^*} R\Big|_{r=a^*} \right) + \frac{2}{a^{*2}} f_\psi\Big|_{r=a^*} - \frac{n(n+1)}{a^{*2}} f_\psi\Big|_{r=a^*} - f''_\psi\Big|_{r=a^*} = 0 \tag{7.6e}$$

$$\pm \frac{2}{a^*} \left(R'\Big|_{r=a^*} - \frac{1}{a^*} R\Big|_{r=a} \right) + \frac{2}{a^{*2}} f_\theta\Big|_{r=a^*} \mp \frac{n(n+1)}{a^{*2}} f_\psi\Big|_{r=a^*} - f''_\theta\Big|_{r=a^*} = 0 \tag{7.6f}$$

Substituting for R, f_θ and f_ψ from equations (6.23a) to (6.23c) gives:

$$\begin{bmatrix} \bar{a}_{11} & \bar{a}_{12} & \bar{a}_{13} & \bar{a}_{14} \\ \bar{a}_{21} & \bar{a}_{22} & \bar{a}_{23} & \bar{a}_{24} \\ \bar{a}_{31} & \bar{a}_{32} & \bar{a}_{33} & \bar{a}_{34} \\ \bar{a}_{41} & \bar{a}_{42} & \bar{a}_{43} & \bar{a}_{44} \end{bmatrix} \begin{bmatrix} \bar{B}_n \\ \bar{\bar{B}}_n \\ \bar{D}_n \\ \bar{\bar{D}}_n \end{bmatrix} = \begin{bmatrix} 0 \\ 0 \\ 0 \\ 0 \end{bmatrix} \tag{7.8}$$

where:

$$\bar{a}_{11} = K_2^2 a^2 j_n(K_1 a) - 2n(n-1) j_n(K_1 a) - 4K_1 a j_{n+1}(K_1 a) \tag{7.9a}$$

$$\bar{a}_{12} = K_2^2 a^2 y_n(K_1 a) - 2n(n-1) y_n(K_1 a) - 4K_1 a y_{n+1}(K_1 a) \tag{7.9b}$$

$$\bar{a}_{13} = 2n(n+1) \left[(n-1) j_n(K_2 a) - k_2 a j_{n+1}(K_2 a) \right] \tag{7.9c}$$

$$\bar{a}_{14} = 2n(n+1) \left[(n-1) y_n(K_2 a) - K_2 a y_{n+1}(K_2 a) \right] \tag{7.9d}$$

$$\bar{a}_{21} = 2(n-1)j_n(K_1a)-2K_1aj_{n+1}(K_1a) \qquad (7.9e)$$

$$\bar{a}_{22} = 2(n-1)y_n(K_1a)-2K_1ay_{n+1}(K_1a) \qquad (7.9f)$$

$$\bar{a}_{23} = 2(1-n^2)j_n(K_2a)-2K_2aj_{n+1}(K_2a)+K_2^2a^2j_n(K_2a) \qquad (7.9g)$$

$$\bar{a}_{24} = 2(1-n^2)y_n(K_2a)-2K_2ay_{n+1}(K_2a)+K_2^2a^2y_n(K_2a) \qquad (7.9h)$$

The remaining two rows can be obtained from the first two by substitution of a* for a. In order to find a nontrivial solution of equation (7.8) determinant $\bar{a}_{kj}$ must be equated to zero. Thus:

$$\bar{a}_{22}\bar{a}_{32}\Big[(\bar{a}_{13}\bar{a}_{31}-\bar{a}_{11}\bar{a}_{33})(\bar{a}_{42}\bar{a}_{24}-\bar{a}_{22}\bar{a}_{44})+(\bar{a}_{21}\bar{a}_{33}-\bar{a}_{23}\bar{a}_{31})$$

$$\times\,(\bar{a}_{42}\bar{a}_{14}-\bar{a}_{12}\bar{a}_{44})+(\bar{a}_{23}\bar{a}_{41}-\bar{a}_{21}\bar{a}_{43})(\bar{a}_{14}\bar{a}_{32}-\bar{a}_{12}\bar{a}_{34})$$

$$-\,(\bar{a}_{13}\bar{a}_{41}-\bar{a}_{11}\bar{a}_{43})(\bar{a}_{24}\bar{a}_{32}-\bar{a}_{34}\bar{a}_{22})+(\bar{a}_{11}\bar{a}_{23}-\bar{a}_{13}\bar{a}_{21})$$

$$(\bar{a}_{34}\bar{a}_{42}-\bar{a}_{44}\bar{a}_{32})+(\bar{a}_{31}\bar{a}_{43}-\bar{a}_{33}\bar{a}_{41})(\bar{a}_{14}\bar{a}_{22}-\bar{a}_{24}\bar{a}_{12})\Big] = 0 \qquad (7.10)$$

The ratios $\frac{\bar{\bar{B}}_n}{\bar{B}_n}$, $\frac{\bar{\bar{D}}_n}{\bar{B}_n}$ and $\frac{\bar{D}_n}{\bar{B}_n}$ may be found to be:

$$\frac{\bar{\bar{B}}_n}{\bar{B}_n} = \frac{\bar{a}_{11}(\bar{a}_{24}\bar{a}_{33}-\bar{a}_{23}\bar{a}_{34})+\bar{a}_{21}(\bar{a}_{13}\bar{a}_{34}-\bar{a}_{14}\bar{a}_{33})+\bar{a}_{31}(\bar{a}_{14}\bar{a}_{23}-\bar{a}_{13}\bar{a}_{24})}{\bar{a}_{12}(\bar{a}_{23}\bar{a}_{34}-\bar{a}_{24}\bar{a}_{33})+\bar{a}_{22}(\bar{a}_{14}\bar{a}_{33}-\bar{a}_{13}\bar{a}_{34})+\bar{a}_{32}(\bar{a}_{13}\bar{a}_{24}-\bar{a}_{14}\bar{a}_{23})} \qquad (7.11a)$$

$$\frac{\bar{\bar{D}}_n}{\bar{B}_n} = \frac{\bar{a}_{11}(\bar{a}_{22}\bar{a}_{33}-\bar{a}_{23}\bar{a}_{32})+\bar{a}_{21}(\bar{a}_{13}\bar{a}_{32}-\bar{a}_{12}\bar{a}_{33})+\bar{a}_{31}(\bar{a}_{12}\bar{a}_{23}-\bar{a}_{13}\bar{a}_{22})}{\bar{a}_{14}(\bar{a}_{23}\bar{a}_{32}-\bar{a}_{22}\bar{a}_{33})+\bar{a}_{24}(\bar{a}_{12}\bar{a}_{33}-\bar{a}_{13}\bar{a}_{32})+\bar{a}_{34}(\bar{a}_{13}\bar{a}_{22}-\bar{a}_{12}\bar{a}_{23})}$$

(7.11b)

$$\frac{\bar{D}_n}{\bar{B}_n} = \frac{\bar{a}_{11}(\bar{a}_{22}\bar{a}_{34}-\bar{a}_{24}\bar{a}_{32})+\bar{a}_{21}(\bar{a}_{14}\bar{a}_{32}-\bar{a}_{12}\bar{a}_{34})+\bar{a}_{31}(\bar{a}_{12}\bar{a}_{24}-\bar{a}_{14}\bar{a}_{22})}{\bar{a}_{13}(\bar{a}_{24}\bar{a}_{32}-\bar{a}_{22}\bar{a}_{34})+\bar{a}_{23}(\bar{a}_{12}\bar{a}_{34}-\bar{a}_{14}\bar{a}_{32})+\bar{a}_{33}(\bar{a}_{14}\bar{a}_{22}-\bar{a}_{12}\bar{a}_{24})}$$

(7.11c)

The successive roots of equation (7.10) for different ratios $\frac{a^*}{a}$ and n are tabulated in Tables (7.5) to (7.8).

7.3. Orthogonality and normalisation of torsional modes

The natural modes of torsional vibration of hollow spheres can be given by equations (7.1a) to (7.1c) in the form:

$$u_{r,nm\ell} = 0 \qquad (7.12a)$$

$$u_{\theta,nm\ell} = \mp \left[\bar{A}_{nm\ell} j_n(\omega_{n\ell}\frac{r}{c_2}) + \bar{\bar{A}}_{nm\ell} y_n(\omega_{n\ell}\frac{r}{c_2})\right] \frac{m}{\sin\theta} P_n^m(\cos\theta) \begin{matrix}\cos m\psi \\ \sin m\psi\end{matrix}$$

(7.12b)

$$u_{\psi,nm\ell} = \left[\bar{A}_{nm\ell} j_n(\omega_{n\ell}\frac{r}{c_2}) + \bar{\bar{A}}_{nm\ell} y_n(\omega_{n\ell}\frac{r}{c_2})\right] \frac{d}{d\theta} P_n^m(\cos\theta) \begin{matrix}\sin m\psi \\ \cos m\psi\end{matrix}$$

(7.12c)

Multiplying equations (7.12b) and (7.12c) by $u_{\theta,psq}$ and $u_{\psi,psq}$ respectively, and following the same procedure as given in section (6.4) gives:

$$\int_D \left[u_{\theta,nm\ell} \cdot u_{\theta,psq} + u_{\psi,nm\ell} \cdot u_{\psi,psq} \right] dD$$

$$= \frac{4\pi n(n+1)}{\varepsilon_m (2n+1)} \frac{(n+m)!}{(n-m)!} \delta_{ms} \delta_{pn} \int_{a^*}^{a} z_1 \cdot z_2 r^2 dr \qquad (7.13)$$

where

$$z_1 = \bar{A}_{nm\ell} j_n(\omega_{n\ell} \frac{r}{c_2}) + \bar{\bar{A}}_{nm\ell} y_n(\omega_{n\ell} \frac{r}{c_2}) \qquad (7.14a)$$

$$z_2 = \bar{A}_{psq} j_p(\omega_{pq} \frac{r}{c_2}) + \bar{\bar{A}}_{psq} y_p(\omega_{pq} \frac{r}{c_2}) \qquad (7.14b)$$

Since equations (7.14a) and (7.14b) satisfy the Bessel differential equations one easily obtains:

$$\frac{\omega_{nq}^2 - \omega_{n\ell}^2}{c_2^2} \int_b^a r^2 z_1 \cdot z_2 dr = \{ r^2 \left[z_2 \cdot z'_1 - z_1 \cdot z'_1 \right] \}_{r=b}^{r=a} \qquad (7.15)$$

Upon using equations (7.3a) and (7.3b) the orthogonality to torsional modes can be given by:

$$\int_D \left[u_{\theta,nm\ell} \cdot u_{\theta,psq} + u_{\psi,nm\ell} \cdot u_{\psi,psq} \right] dD = 0 \qquad (7.16)$$

which is valid whenever unequality between any pair of corresponding indices exist. To normalise the modal functions one requires to solve the integral (7.16) for the case of n=p, m=s and ℓ=q. Thus:

$$\int_D \rho \left[u^2_{\theta,nm\ell} + u^2_{\theta,nm\ell}\right] dD = \frac{2\rho\pi n(n+1)(n+m)!}{\varepsilon_m(2n+1)(n-m)!} \bar{A}^2_{nm\ell} a^3$$

$$\left[\left[j_n\left(\frac{\omega_{n\ell}}{c_2}a\right) + \frac{\bar{\bar{A}}_{nm\ell}}{\bar{A}_{nm\ell}} y_n\left(\frac{\omega_{n\ell}}{c_2}a\right)\right]^2 - \left[j_{n-1}\left(\frac{\omega_{n\ell}}{c_2}a\right) + \frac{\bar{\bar{A}}_{nm\ell}}{\bar{A}_{nm\ell}} y_{n-1}\left(\frac{\omega_{n\ell}}{c_2}a\right)\right]\right.$$

$$\left[j_{n+1}\left(\frac{\omega_{n\ell}}{c_2}a\right) + \frac{\bar{\bar{A}}_{nm\ell}}{\bar{A}_{nm\ell}} y_{n+1}\left(\frac{\omega_{n\ell}}{c_2}a\right)\right] - \frac{a^{*3}}{a^3}\left[j_n\left(\frac{\omega_{n\ell}}{c_2}a^*\right) + \frac{\bar{\bar{A}}_{nm\ell}}{\bar{A}_{nm\ell}} y_n\left(\frac{\omega_{n\ell}}{c_2}a^*\right)\right]^2$$

$$\left. + \frac{a^{*3}}{a^3}\left[j_{n-1}\left(\frac{\omega_{n\ell}}{c_2}a^*\right) + \frac{\bar{\bar{A}}_{nm\ell}}{\bar{A}_{nm\ell}} y_{n-1}\left(\frac{\omega_{n\ell}}{c_2}a\right)\right]\left[j_{n+1}\left(\frac{\omega_{n\ell}}{c_2}a\right) + \frac{\bar{\bar{A}}_{nm\ell}}{\bar{A}_{nm\ell}} y_{n+1}\left(\frac{\omega_{n\ell}}{c_2}a^*\right)\right]\right] \tag{7.17}$$

The normal modes of torsional vibration may now be written as:

$$u_{\theta,nm\ell} = \mp \bar{A}_{nm\ell}\left[j_n\left(\omega_{n\ell}\frac{r}{c_2}\right) + \frac{\bar{\bar{A}}_{nm\ell}}{\bar{A}_{nm\ell}} y_n\left(\omega_{n\ell}\frac{r}{c_2}\right)\right] \frac{m}{\sin\theta} P_n^m(\cos\theta) \begin{matrix}\cos m\psi \\ \sin m\psi\end{matrix} \tag{7.18a}$$

$$u_{\psi,nm\ell} = \bar{A}_{nm\ell}\left[j_n\left(\omega_{n\ell}\frac{r}{c_2}\right) + \frac{\bar{\bar{A}}_{nm\ell}}{\bar{A}_{nm\ell}} y_n\left(\omega_{n\ell}\frac{r}{c_2}\right)\right] \frac{d}{d\theta} P_n^m(\cos\theta) \begin{matrix}\sin m\psi \\ \cos m\psi\end{matrix} \tag{7.18b}$$

where:

$$\bar{A}^2_{nm\ell} = \frac{\varepsilon_m(2n+1)(n-m)!}{2\rho\pi n(n+1)(n+m)!} \times \frac{1}{a^3}\left[\left[j_n\left(\frac{\omega_{n\ell}}{c_2}a\right) + \frac{\bar{\bar{A}}_{nm\ell}}{\bar{A}_{nm\ell}} y_n\left(\frac{\omega_{n\ell}}{c_2}a\right)\right]^2\right.$$

$$- \left[j_{n-1}\left(\frac{\omega_{n\ell}}{c_2}a\right) + \frac{\bar{\bar{A}}_{nm\ell}}{\bar{A}_{nm\ell}} y_{n-1}\left(\frac{\omega_{n\ell}}{c_2}a\right)\right]\left[j_{n+1}\left(\frac{\omega_{n\ell}}{c_2}a\right) + \frac{\bar{\bar{A}}_{nm\ell}}{\bar{A}_{nm\ell}} y_{n+1}\left(\frac{\omega_{n\ell}}{c_2}a\right)\right]$$

$$- \frac{a^{*3}}{a^3}\left[j_n\left(\frac{\omega_{n\ell}}{c_2}a^*\right) + \frac{\bar{\bar{A}}_{nm\ell}}{\bar{A}_{nm\ell}} y_n\left(\frac{\omega_{n\ell}}{c_2}a^*\right)\right]^2 + \frac{a^{*3}}{a^3}\left[j_{n-1}\left(\frac{\omega_{n\ell}}{c_2}a^*\right)\right.$$

$$\left.\left. + \frac{\bar{\bar{A}}_{nm\ell}}{\bar{A}_{nm\ell}} y_{n+1}\left(\frac{\omega_{n\ell}}{c_2}a^*\right)\right]\right]^{-1} \tag{7.19}$$

Plots showing variations of the normalised displacement along the thickness of hollow spheres are given in Fig.(7.1).

7.4. Orthogonality and normalisation of spheroidal modes

The natural modes of spheroidal vibrations of a hollow sphere can be given by equations (7.2a) to (7.2c) in the form:

$$u_{r,nm\ell} = -F(r)_{nm\ell} . P_n^m(\cos\theta) \begin{matrix}\sin m\psi \\ \cos m\psi\end{matrix} \qquad (7.20a)$$

$$u_{\theta,nm\ell} = -G(r)_{nm\ell} \cdot \frac{d}{d\theta} P_n^m(\cos\theta) \begin{matrix}\sin m\psi \\ \cos m\psi\end{matrix} \qquad (7.20b)$$

$$u_{\psi,nm\ell} = \mp G(r)_{nm\ell} \cdot \frac{m}{\sin\theta} P_n^m(\cos\theta) \begin{matrix}\cos m\psi \\ \sin m\psi\end{matrix} \qquad (7.20c)$$

where

$$F(r)_{nm\ell} = \bar{B}_{nm\ell} j_n'(\omega_{n\ell} \frac{r}{c_1}) + \bar{\bar{B}}_n y_n'(\omega_{n\ell} \frac{r}{c_1}) - \frac{n(n+1)}{r} \left[\bar{D}_{nm\ell} j_n(\omega_{n\ell} \frac{r}{c_2}) + \bar{\bar{D}}_{nm\ell} y_n(\omega_{n\ell} \frac{r}{c_2})\right] \qquad (7.21a)$$

$$G(r)_{nm\ell} = \frac{1}{r}\left[\bar{B}_{nm\ell} j_n(\omega_{n\ell} \frac{r}{c_1}) + \bar{\bar{B}}_{nm\ell} y_n(\omega_{n\ell} \frac{r}{c_1})\right] - \frac{1}{r}\left[\bar{D}_{nm\ell} j_n(\omega_{n\ell} \frac{r}{c_2}) + \bar{\bar{D}}_{nm\ell} y_n(\omega_{n\ell} \frac{r}{c_2})\right] - \bar{D}_{nm\ell} j_n'(\omega_{n\ell} \frac{r}{c_2}) - \bar{\bar{D}}_{nm\ell} y_n'(\omega_{n\ell} \frac{r}{c_2}) \qquad (7.21b)$$

By following similar procedure as given in section (6.6) one obtains:

$$\int_D \rho \left[u_{r,nm\ell} \cdot u_{r,psq} + u_{\theta,nm\ell} \cdot u_{\theta,psq} + u_{\psi,nm\ell} \cdot u_{\psi,psq} \right] dD$$

$$= \frac{4\pi\rho(n+m)!}{\varepsilon_m (2n+1)(n-m)!} \delta_{ms} \delta_{np} \times \int_{a^*}^{a} \left[F(r)_{nm\ell} \cdot F(r)_{psq} + n(n+1) G(r)_{nm\ell} \cdot G(r)_{psq} \right] r^2 dr \qquad (7.22)$$

The integral on the right hand side of equation (7.22) when m=s and n=p may be found to be:

$$\int_b^a \left[F(r)_{nm\ell} \cdot F(r)_{nmq} + n(n+1) G(r)_{nm\ell} \cdot G(r)_{nmq} \right] r^2 dr$$

$$= \int_{a^*}^{a} \left[r^2 R'_1 R'_2 + n(n+1) R_1 R_2 \right] dr - n(n+1) \int_{a^*}^{a} (R_1 Y_2 + r R'_1 Y_2 + r R_1 Y'_2) dr$$

$$- n(n+1) \int_{a^*}^{a} (R_2 Y_1 + r R'_2 Y_1 + r R_2 Y'_1) dr + n(n+1) \int_{a^*}^{a} (Y_1 Y_2 + r Y'_1 Y'_2 + r Y_1 Y'_2) dr + n(n+1) \int_{a^*}^{a} \left[r^2 Y'_1 Y'_2 + n(n+1) Y_1 Y_2 \right] dr \qquad (7.23)$$

where

$$R_1 = \bar{B}_{nm\ell} j_n(\omega_{n\ell} \frac{r}{c_1}) + \bar{\bar{B}}_{nm\ell} y_n(\omega_{n\ell} \frac{r}{c_1}) \qquad (7.24a)$$

$$Y_1 = \bar{D}_{nm\ell} j_n(\omega_{n\ell} \frac{r}{c_2}) + \bar{\bar{D}}_{nm\ell} y_n(\omega_{n\ell} \frac{r}{c_2}) \qquad (7.24b)$$

$$R_2 = \bar{B}_{nmq} j_n(\omega_{nq} \frac{r}{c_1}) + \bar{\bar{B}}_{nmq} y_n(\omega_{nq} \frac{r}{c_1}) \qquad (7.24c)$$

and

$$Y_2 = \bar{D}_{nmq} j_n(\omega_{nq} \frac{r}{c_2}) + \bar{\bar{D}}_{nmq} y_n(\omega_{nq} \frac{r}{c_2}) \qquad (7.24d)$$

Since equations (7.24a) to (7.24d) satisfy the Bessel differential equation, it can be easily shown that:

$$\int_{a^*}^{a} \left[F(r)_{nm\ell}.F(r)_{nmq}+n(n+1)G(r)_{nm\ell}.G(r)_{nmq}\right]r^2dr$$

$$= \frac{1}{\omega^2_{nq}-\omega^2_{n\ell}} \left[\omega^2_{nq}\left[r^2R'_1R_2\right]_{a^*}^{a} - \omega^2_{n\ell}\left[r^2R'_2R_1\right]_{a^*}^{a} \right.$$

$$- n(n+1)(\omega^2_{nq} - \omega^2_{n\ell})\left[rR_1Y_2\right]_{a^*}^{a} -n(n+1)(\omega^2_{nq}- \omega^2_{n\ell})\left[rR_2Y_1\right]_{a^*}^{a}$$

$$+ n(n+1)(\omega^2_{nq}- \omega^2_{n\ell})\left[rY_1Y_2\right]_{a^*}^{a} +n(n+1)\omega^2_{nq}\left[r^2Y'_1Y_2\right]_{a^*}^{a}$$

$$\left. - n(n+1)\omega^2_{n\ell}\left[r^2Y'_2Y_1\right]_{a^*}^{a}\right] \qquad (7.25)$$

Using the boundary conditions given in section (7.2) and substituting for R and f_ψ from (7.24a) and (7.24b) gives:

$$\frac{\omega^2_{n\ell}}{c_2^2}\, a^2R_1\Big|_{r=a} -2n(n+1)R_1\Big|_{r=a} +4aR'_1\Big|_{r=a} -2n(n+1)(Y_1\Big|_{r=a}$$

$$- aY'_1\Big|_{r=a}) = 0 \quad (7.26a)$$

$$- 2(R_1\Big|_{r=a} -aR'_1\Big|_{r=a})+ 2Y_1\Big|_{r=a} -2n(n+1)Y_1\Big|_{r=a}$$

$$+2aY'_1\Big|_{r=a} + \frac{\omega^2_{n\ell}}{c_2^2}\, a^2\, Y_1\Big|_{r=a} = 0 \quad (7.26b)$$

$$\frac{\omega^2_{n\ell}}{c_2^2}\, a^{*2} R_1\Big|_{r=a^*} - 2n(n+1) R_1\Big|_{r=a^*} + 4a^* R'_1\Big|_{r=a^*}$$

$$- 2n(n+1)\left(Y_1\Big|_{r=a^*} - a^* Y'_1\Big|_{r=a^*}\right) = 0 \qquad (7.26c)$$

$$-2\left(R_1\Big|_{r=a^*} - a^* R'_1\Big|_{r=a^*}\right) + 2Y_1\Big|_{r=a^*} - 2n(n+1) Y_1\Big|_{r=a^*}$$

$$+ 2a^* Y'_1\Big|_{r=a^*} + \frac{\omega^2_{n\ell}}{c_2^2}\, a^{*2} Y_1\Big|_{r=a^*} = 0 \qquad (7.26d)$$

By following similar procedures as given in section (6.6) one obtains:

$$\omega^2_{nq}\, a\left[R'_1 R_2\right]_{r=a} - \omega^2_{n\ell}\, a\left[R'_2 R_1\right]_{r=a} - n(n+1)\left(\omega^2_{nq} - \omega^2_{n\ell}\right)$$

$$\left[R_1 Y_2 + R_2 Y_1\right]_{r=a} + n(n+1)\left(\omega^2_{nq} - \omega^2_{n\ell}\right)\left[Y_1 Y_2\right]_{r=a}$$

$$+ n(n+1)\omega^2_{nq}\, a\left[Y'_1 Y_2\right]_{r=a} - n(n+1)\omega^2_{n\ell}\, a\left(Y_1 Y'_2\right)_{r=a} = 0 \qquad (7.27a)$$

$$\omega^2_{nq} a^*\left[R'_1 R_2\right]_{r=a^*} - \omega^2_{n\ell} a^*\left[R'_2 R_1\right]_{r=a^*} - n(n+1)\left(\omega^2_{nq} - \omega^2_{n\ell}\right)$$

$$\left[R_1 Y_2 + R_2 Y_1\right]_{r=a^*} + n(n+1)\left(\omega^2_{nq} - \omega^2_{n\ell}\right)\left[Y_1 Y_2\right]_{r=a^*}$$

$$+ n(n+1)\omega^2_{nq} a^*\left[Y'_1 Y_2\right]_{r=a} - n(n+1)\omega^2_{n\ell} a^*\left[Y_1 Y'_2\right]_{r=a^*} = 0 \qquad (7.27b)$$

Thus:

$$\int_{a^*}^{a}\left[F(r)_{nm\ell}.F(r)_{nmq}+n(n+1)G(r)_{nm\ell}.G(r)_{nmq}\right]r^2dr = 0$$

$$\ell \neq q \qquad (7.28)$$

Also from (7.23),

$$\int_{a^*}^{a}\left[F^2(r)_{nm\ell}+n(n+1)G^2(r)_{nm\ell}\right]r^2dr = \int_{a^*}^{a}\left[r^2R'^2_1+n(n+1)R_1^2\right]dr$$

$$-2n(n+1)\left[rR_1Y_1\right]_{a^*}^{a} + n(n+1)\left[rY_1^2\right]_{a^*}^{a}$$

$$+ n(n+1)\int_{a^*}^{a}\left[r^2Y'^2_1+n(n+1)Y_1^2\right]dr \qquad (7.29)$$

The Bessel differential equation in the form of equation (6.87a) may now be used for simplifying the integrals on the right hand side of equation (7.29). Thus one obtains:

$$\int_{a^*}^{a}\left[F^2(r)_{nm\ell}+n(n+1)G^2(r)_{nm\ell}\right]r^2dr$$

$$= \frac{\omega^2_{n\ell}}{c_1^2}\int_{a^*}^{a} r^2R_1^2dr + \left[r^2R'_1R_1\right]_{a^*}^{a} -2n(n+1)\left[rR_1Y_1\right]_{a^*}^{a}$$

$$+ n(n+1)\left[rY_1^2\right]_{a^*}^{a} +n(n+1)\frac{\omega^2_{n\ell}}{c_2^2}\int_{a^*}^{a} r^2Y_1^2dr + \left[r^2Y'_1Y_1\right]_{a^*}^{a}$$

(7.30)

or

$$\int_{a^*}^{a}\left[F^2(r)_{nm\ell}+n(n+1)G^2(r)_{nm\ell}\right]r^2dr$$

$$=\frac{1}{2}\frac{\omega^2_{n\ell}}{c_1^2}\left[r^3R_1^2\right]_{a^*}^{a}-\frac{1}{2}\left[n(n+1)R_1^2r-3R_1R'_1r^2\right.$$

$$\left.-R'^2_1r^3\right]_{a^*}^{a}-2n(n+1)\left[rR_1Y_1\right]_{a^*}^{a}+n(n+1)\left[rY_1^2\right]_{a^*}^{a}$$

$$+\frac{n(n+1)}{2}\frac{\omega^2_{n\ell}}{c_2^2}\left[r^3Y_1^2\right]_{a^*}^{a}-\frac{n(n+1)}{2}\left[n(n+1)Y_1^2r\right.$$

$$\left.-3Y_1Y'_1r^2-Y'^2_1r^3\right]_{a^*}^{a}=\bar{B}^2_{nm\ell}\bar{\xi}_{n\ell} \qquad (7.31)$$

where

$$R'_1=\bar{B}_{nm\ell}\left[\left[\frac{n}{r}j_n(\omega_{n\ell}\frac{r}{c_1})-\frac{\omega_{n\ell}}{c_1}j_{n+1}(\omega_{n\ell}\frac{r}{c_1})\right]\right.$$

$$\left.+\left[\frac{n}{r}y_n(\omega_{n\ell}\frac{r}{c_1})-\frac{\omega_{n\ell}}{c_1}y_{n+1}(\omega_{n\ell}\frac{r}{c_1})\right]\frac{\bar{\bar{B}}_{nm\ell}}{\bar{B}_{nm\ell}}\right] \qquad (7.32a)$$

$$Y'_1=\bar{B}_{nm\ell}\left[\left[\frac{n}{r}j_n(\omega_{n\ell}\frac{r}{c_2})-\frac{\omega_{n\ell}}{c_2}j_{n+1}(\omega_{n\ell}\frac{r}{c_2})\right]\frac{\bar{D}_{nm\ell}}{\bar{B}_{nm\ell}}\right.$$

$$\left.+\left[\frac{n}{r}y_n(\omega_{n\ell}\frac{r}{c_2})-\frac{\omega_{n\ell}}{c_2}y_{n+1}(\omega_{n\ell}\frac{r}{c_2})\right]\frac{\bar{\bar{D}}_{nm\ell}}{\bar{B}_{nm\ell}}\right] \qquad (7.32b)$$

Upon using (7.28) and (7.31) equation (7.22) can be written as:

$$\int_D\left[u_{r,nm\ell}.u_{r.psq}+u_{\theta,nm\ell}.u_{\theta psq}+u_{\psi,nm\ell}.u_{\psi,psq}\right]dD$$

$$=\frac{4\pi\rho(n+m)!}{\varepsilon_m(2n+1)(n-m)!}\bar{B}^2_{nm\ell}\bar{\xi}_{n\ell}x\ \delta_{ms}.\delta_{np}.\delta_{\ell q} \qquad (7.33)$$

The orthogonality of the spheroidal modes may now be given by:

$$\int_D \rho \left[u_{r,nm\ell} \cdot u_{r,psq} + u_{\theta,nm\ell} \cdot u_{\theta,psq} + u_{\psi,nm\ell} \cdot u_{\theta,psq} \right] dD = 0 \qquad ((7.34)$$

which is true whenever inequality between any pair of corresponding indices exist. The normal modes of spheroidal vibration may be found to be:

$$u^*_{r,nm\ell} = -\bar{B}_{nm\ell} \left[\left[n j_{n-1}(\omega_{n\ell} \frac{r}{c_1}) - (n+1) j_{n+1}(\omega_{n\ell} \frac{r}{c_1}) \right] \frac{\omega_{n\ell}}{c_1(2n+1)} \right.$$

$$+ \frac{\bar{\bar{B}}_{nm\ell}}{\bar{B}_{nm\ell}} \left[n y_{n-1}(\omega_{n\ell} \frac{r}{c_1}) - (n+1) y_{n+1}(\omega_{n\ell} \frac{r}{c_1}) \right] \frac{\omega_{n\ell}}{c_1(2n+1)}$$

$$\left. - \frac{n(n+1)}{r} \left[\frac{\bar{D}_{nm\ell}}{\bar{B}_{nm\ell}} j_n(\omega_{n\ell} \frac{r}{c_2}) + \frac{\bar{\bar{D}}_{nm\ell}}{\bar{B}_{nm\ell}} y_n(\omega_{n\ell} \frac{r}{c_2}) \right] \right] P_n^m(\cos\theta) \begin{matrix} \sin m\psi \\ \cos m\psi \end{matrix}$$

(7.35a)

$$u^*_{\theta,nm\ell} = -\bar{B}_{nm\ell} \left[\frac{1}{r} \left[j_n(\omega_{n\ell} \frac{r}{c_1}) + \frac{\bar{\bar{B}}_{nm\ell}}{\bar{B}_{nm\ell}} y_n(\omega_{n\ell} \frac{r}{c_1}) \right] \right.$$

$$- \frac{1}{r} \left[\frac{\bar{D}_{nm\ell}}{\bar{B}_{nm\ell}} j_n(\omega_{n\ell} \frac{r}{c_2}) + \frac{\bar{\bar{D}}_{nm\ell}}{\bar{B}_{nm\ell}} y_n(\omega_{n\ell} \frac{r}{c_2}) \right] - \frac{\bar{D}_{nm\ell}}{\bar{B}_{nm\ell}} \left[n j_{n-1}(\omega_{n\ell} \frac{r}{c_2}) \right.$$

$$\left. - (n+1) j_{n+1}(\omega_{n\ell} \frac{r}{c_2}) \right] \frac{\omega_{n\ell}}{c_2(2n+1)} - \frac{\bar{\bar{D}}_{nm\ell}}{\bar{B}_{nm\ell}} \left[n y_{n-1}(\omega_{n\ell} \frac{r}{c_2}) \right.$$

$$\left. \left. - (n+1) y_{n+1}(\omega_{n\ell} \frac{r}{c_2}) \right] \right] \frac{\omega_{n\ell}}{c_2(2n+1)} \frac{d}{d\theta} P_n^m(\cos\theta) \begin{matrix} \sin m\psi \\ \cos m\psi \end{matrix}$$

(7.35b)

$$u^*_{\psi,nm\ell} = \mp \bar{B}_{nm\ell}\left[\frac{1}{r}\left[j_n(\omega_{n\ell}\frac{r}{c_1}) + \frac{\bar{\bar{B}}_{nm\ell}}{\bar{B}_{nm\ell}} y_n(\omega_{n\ell}\frac{r}{c_1})\right]\right.$$

$$- \frac{1}{r}\left[\frac{\bar{D}_{nm\ell}}{\bar{B}_{nm\ell}} j_n(\omega_{n\ell}\frac{r}{c_2}) + \frac{\bar{\bar{D}}_{nm\ell}}{\bar{B}_{nm\ell}} y_n(\omega_{n\ell}\frac{r}{c_2})\right] - \frac{\bar{D}_{nm\ell}}{\bar{B}_{nm\ell}}\left[n j_{n-1}(\omega_{n\ell}\frac{r}{c_2})\right.$$

$$\left.-(n+1) j_{n+1}(\omega_{n\ell}\frac{r}{c_2})\right]\frac{\omega_{n\ell}}{c_2(2n+1)} - \frac{\bar{\bar{D}}_{nm\ell}}{\bar{B}_{nm\ell}}\left[n y_{n-1}(\omega_{n\ell}\frac{r}{c_2})\right.$$

$$\left.\left. - (n+1) y_{n+1}(\omega_{n\ell}\frac{r}{c_2})\right]\frac{\omega_{n\ell}}{c_2(2n+1)}\right] \times \frac{m}{\sin\theta} P_n^m(\cos\theta)\begin{matrix}\cos m\psi \\ \sin m\psi\end{matrix} \qquad (7.35c)$$

where

$$\bar{B}^2_{nm\ell} = \frac{\varepsilon_m(2n+1)(n-m)!}{4\pi\rho(n+m)!} \times \frac{1}{\bar{\bar{\xi}}_{n\ell}} \qquad (7.36)$$

Graphs showing variations of the normalised u_r and u_θ along the thickness of hollow spheres are given in Figs.(7.2) and (7.3) respectively.

7.5. Sound generated by transient vibration of hollow spheres

The general equations (6.141a) to (6.141c) given in chapter 6 can be used for finding the response of a hollow sphere to any type of radial concentrated force. As an illustration, let us examine a force in the form of half sine pulse acting at the position r=a and $\theta = \pi$. By following similar procedures as given for solid sphere the response at position r=a and $\theta = 0$ can be easily found to be:

$$u_r(r=0,\theta=0,t) = \sum_{n=0}^{\infty}\sum_{\ell=1}^{\infty} \frac{(-1)^n F_{max} u^{*2}_{r,n\ell}(r=a,\theta=\pi)}{\omega_{n\ell}(b^2 - \omega^2_{n\ell})}$$

$$(b\sin\omega_{n\ell}t - \omega_{n\ell}\sin bt) \qquad t< d \qquad (7.37a)$$

$$u_r(r=a,\theta=0,t) = \sum_{n=0}^{\infty}\sum_{\ell=1}^{\infty} \frac{(-1)^n F_{max} u^{*2}_{r,n\ell}(r=a,\theta=\pi)}{\omega_{n\ell}(b^2 - \omega^2_{n\ell})}$$

$$\left[b\sin\omega_{n\ell}(t-d) + b\sin\omega_{n\ell}t\right] \qquad t> d \qquad (7.37b)$$

where $u^*_{r,n\ell}$ is given by equation (7.35a) after substituting m=0. By taking into account the effect of viscous damping the acceleration in frequency domain may be expressed as:

$$\ddot{u}_r(r=a,\theta=0,\omega) = -\frac{\omega^2 b F_{max}}{(b^2 - \omega^2)}(1+e^{i\omega d})$$

$$\sum_{n=0}^{\infty}\sum_{\ell=1}^{\infty} \frac{(-1)^n u^{*2}_{r,n\ell}(r=a,\theta=\pi)}{\omega^2_{n\ell} - \omega^2 + 2i\beta_{n\ell}\omega_{n\ell}\omega} \qquad (7.38)$$

By following similar procedure as given for solid sphere the sound pressure can be found to be:

$$p(r,\theta,\omega) = \rho_o i\omega \sum_{n=0}^{\infty} \frac{\left[(-1)^n G^*_n - B^*_n\right] h_n^{(2)}(K_r)}{\frac{n}{a} h_n^{(2)}(K_a) - K h_{n+1}^{(2)}(K_a)} P_n(\cos\theta)$$

$$= \sum_{n=0}^{\infty} P_n(r,\theta,\omega) \qquad (7.39)$$

where

$$B^*_n = \frac{\alpha^*}{M} \qquad n = 1 \qquad (7.40a)$$

$$= 0 \quad \text{otherwise}$$

$$\alpha^* = \frac{bF_{max}}{i\omega(b^2-\omega^2)}\,(1+e^{-i\omega d}) \qquad (7.40b)$$

$$G^*_n = \sum_{\ell=1}^{\infty} \frac{\alpha^* u^{*2}_{r,n\ell}(r=a,\theta=\pi)\cdot\omega^2}{\omega^2_{n\ell}-\omega^2+2i\beta_{n\ell}\omega_{n\ell}\omega} \qquad (7.40c)$$

The sound pressure in the time domain may be obtained by means of the inverse discrete Fourier transform.

Value of n	ℓ = 1	ℓ = 2	ℓ = 3	ℓ = 4	ℓ = 5
1	*	5.799	9.310	12.902	16.598
2	2.5	7.118	10.479	13.827	17.310
3	3.864	8.438	11.843	15.094	18.371
4	5.094	9.711	13.197	16.490	19.696
5	6.266	10.950	14.507	17.866	21.114
6	7.403	12.166	15.787	19.199	22.505
7	8.520	13.364	17.045	20.502	23.853
8	9.621	14.548	18.287	21.786	25.172
9	10.711	15.720	19.515	23.054	26.473
10	11.792	16.882	20.731	24.310	27.760

TABLE 7.1. Non-dimensional frequency of torsional vibration of hollow sphere (b/a = 0.2)

Value of n	ℓ =1	ℓ = 2	ℓ = 3	ℓ = 4	ℓ = 5
1	*	6.357	11.141	16.171	21.296
2	2.475	7.237	11.639	16.499	21.540
3	3.850	8.358	12.363	16.986	21.902
4	5.088	9.593	13.288	17.625	22.381
5	6.263	10.859	14.380	18.411	22.974
6	7.403	12.111	15.589	19.355	23.676
7	8.519	13.335	16.863	20.389	24.486
8	9.621	14.534	18.153	21.554	25.403
9	10.711	15.714	19.431	22.801	26.423
10	11.792	16.879	20.683	24.093	27.542

TABLE 7.2. Non-dimensional frequency of torsional vibration of hollow sphere. (b/a = 0.4)

Value of n	$\ell = 1$	$\ell = 2$	$\ell = 3$	$\ell = 4$	$\ell = 5$
1	*	8.443	16.020	23.772	31.574
2	2.373	8.872	16.235	23.915	31.681
3	3.736	9.484	16.552	24.127	31.840
4	4.986	10.248	16.968	24.407	32.051
5	6.182	11.134	17.476	24.754	32.313
6	7.342	12.116	18.070	25.164	32.625
7	8.477	13.169	18.744	25.636	32.986
8	9.592	14.275	19.492	26.166	33.394
9	10.691	15.416	20.307	26.752	33.849
10	11.779	16.580	21.185	27.392	34.347

TABLE 7.3. Non-dimensional frequency of torsional vibration of hollow sphere. (b/a = 0.6).

Value of n	$\ell = 1$	$\ell = 2$	$\ell = 3$	$\ell = 4$	$\ell = 5$
1	*	15.943	31.535	47.203	62.891
2	2.199	16.103	31.614	47.256	62.931
3	3.477	16.341	31.734	47.336	62.991
4	4.663	16.652	31.892	47.442	63.070
5	5.814	17.034	32.089	47.574	63.170
6	6.946	17.482	32.323	47.732	63.288
7	8.066	17.991	32.595	47.915	63.427
8	9.178	18.556	32.903	48.124	63.585
9	10.284	19.173	33.246	48.358	63.762
10	11.384	19.838	33.623	48.617	63.958

TABLE 7.4. Non-dimensional frequency of torsional vibration of hollow sphere. (b/a =0.8)

Value of n	ℓ = 1	ℓ = 2	ℓ = 3	ℓ = 4	ℓ = 5
0	4.725	10.260	16.095	22.746	29.713
1	*	3.565	7.541	8.021	11.583
2	2.556	4.870	8.007	10.245	12.014
3	3.914	6.543	9.430	12.143	13.170
4	5.038	8.181	11.052	13.802	15.090
5	6.075	9.754	12.511	15.465	17.145
6	7.076	11.259	13.900	16.967	19.093
7	8.058	12.696	15.288	18.358	20.878
8	9.028	14.066	16.690	19.707	22.503
9	9.990	15.380	18.100	21.046	24.000
10	10.946	16.645	19.505	22.385	25.415

TABLE 7.5. Non-dimensional frequencyof spheroidal vibration of hollow sphere.
(b/a = 0.2 and Poisson's ratio = 0.29)

Value of n	ℓ = 1	ℓ = 2	ℓ = 3	ℓ = 4	ℓ = 5
0	4.070	10.781	19.855	29.332	38.903
1	*	3.763	7.868	9.626	12.690
2	2.165	4.832	9.298	10.116	14.115
3	3.534	6.327	9.557	12.294	15.081
4	4.820	7.864	10.327	14.184	15.919
5	5.981	9.408	11.489	15.441	17.303
6	7.042	10.957	12.888	16.383	18.990
7	8.047	12.477	14.418	17.387	20.550
8	9.025	13.931	16.015	18.541	21.859
9	9.989	15.305	17.628	19.854	23.025
10	10.946	16.608	19.209	21.310	24.184

TABLE 7.6. Non-dimensional frequency of spheroidal vibration of hollow sphere.
(b/a = 0.4 and Poisson's ratio = 0.29)

Value of n	ℓ = 1	ℓ = 2	ℓ = 3	ℓ = 4	ℓ = 5
0	3.453	14.963	29.213	43.626	58.078
1	*	3.846	9.083	14.333	16.852
2	1.710	5.049	10.461	13.882	17.930
3	2.693	6.588	12.054	13.719	19.091
4	3.812	8.127	13.228	14.382	20.288
5	5.004	9.556	13.713	16.094	21.462
6	6.213	10.820	14.373	17.943	22.550
7	7.405	11.925	15.314	19.703	23.582
8	8.562	12.945	16.460	21.240	24.725
9	9.675	13.966	17.703	22.491	26.096
10	10.744	15.038	18.964	23.554	27.603

TABLE 7.7. Non-dimensional frequency of spheroidal vibration of hollow sphere.
(b/a = 0.6 and Poisson's ratio = 0.29)

Value of n	ℓ = 1	ℓ = 2	ℓ = 3	ℓ = 4	ℓ = 5
0	3.016	29.155	58.049	87.002	115.969
1	*	3.631	16.146	28.856	31.914
2	1.369	4.961	16.689	28.445	32.566
3	1.850	6.599	17.450	28.034	33.340
4	1.424	8.310	18.386	27.672	34.191
5	3.169	10.026	19.456	27.384	35.098
6	4.023	11.720	20.628	27.107	36.052
7	4.943	13.374	21.870	27.107	37.044
8	5.925	14.971	23.149	27.171	38.068
9	6.945	16.492	24.416	27.429	39.118
10	8.139	17.914	25.592	27.971	40.191

TABLE 7.8. Non-dimensional frequency of spheroidal vibration of hollow sphere.
(b/a = 0.8 and Poisson's ratio = 0.29)

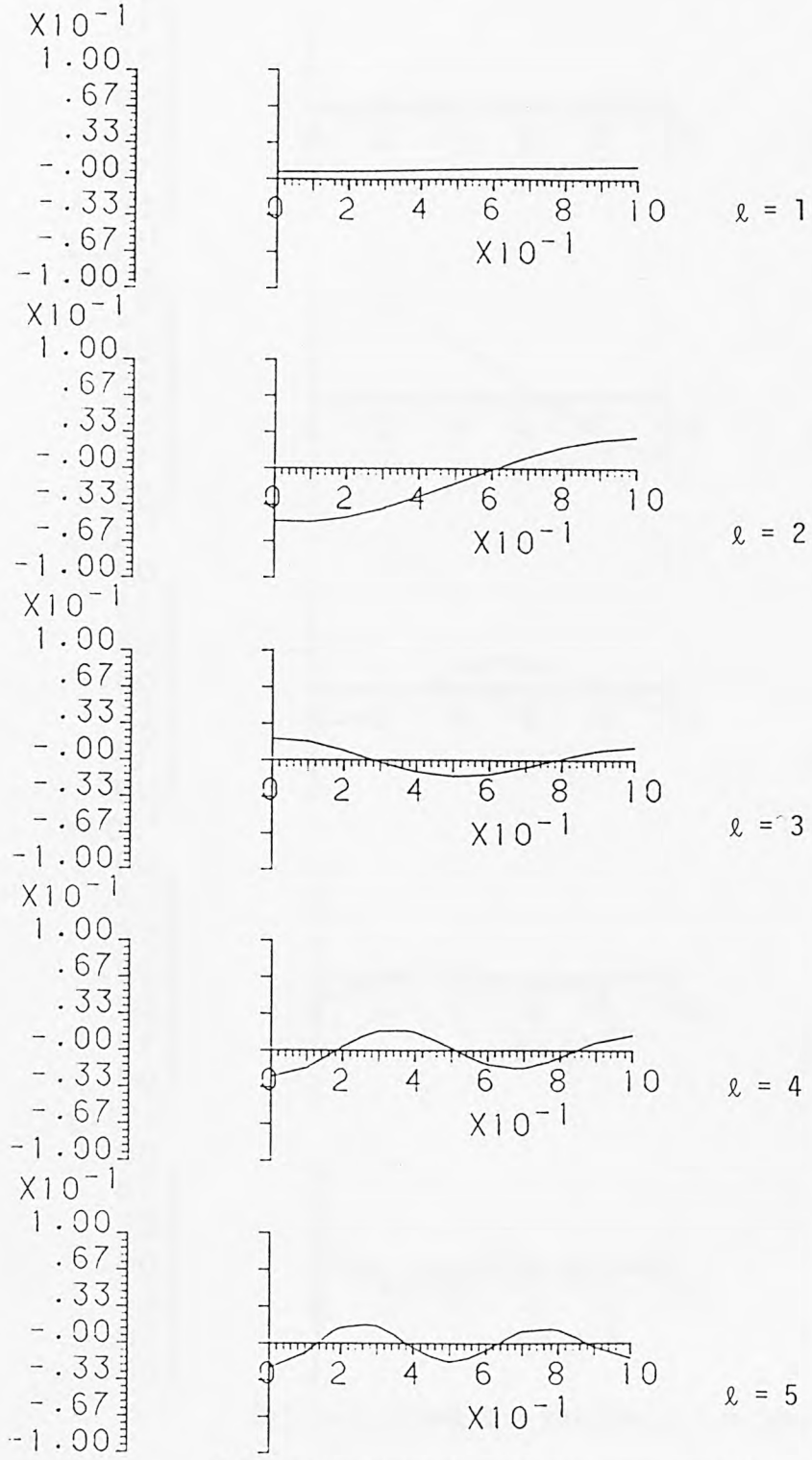

FIGURE 7.1. VARIATION OF NORMALISED DISPLACEMENT OF TORSIONAL VIBRATION OF HOLLOW SPHERE ALONG THE THICKNESS (n = 2, and b/a = 0.6)

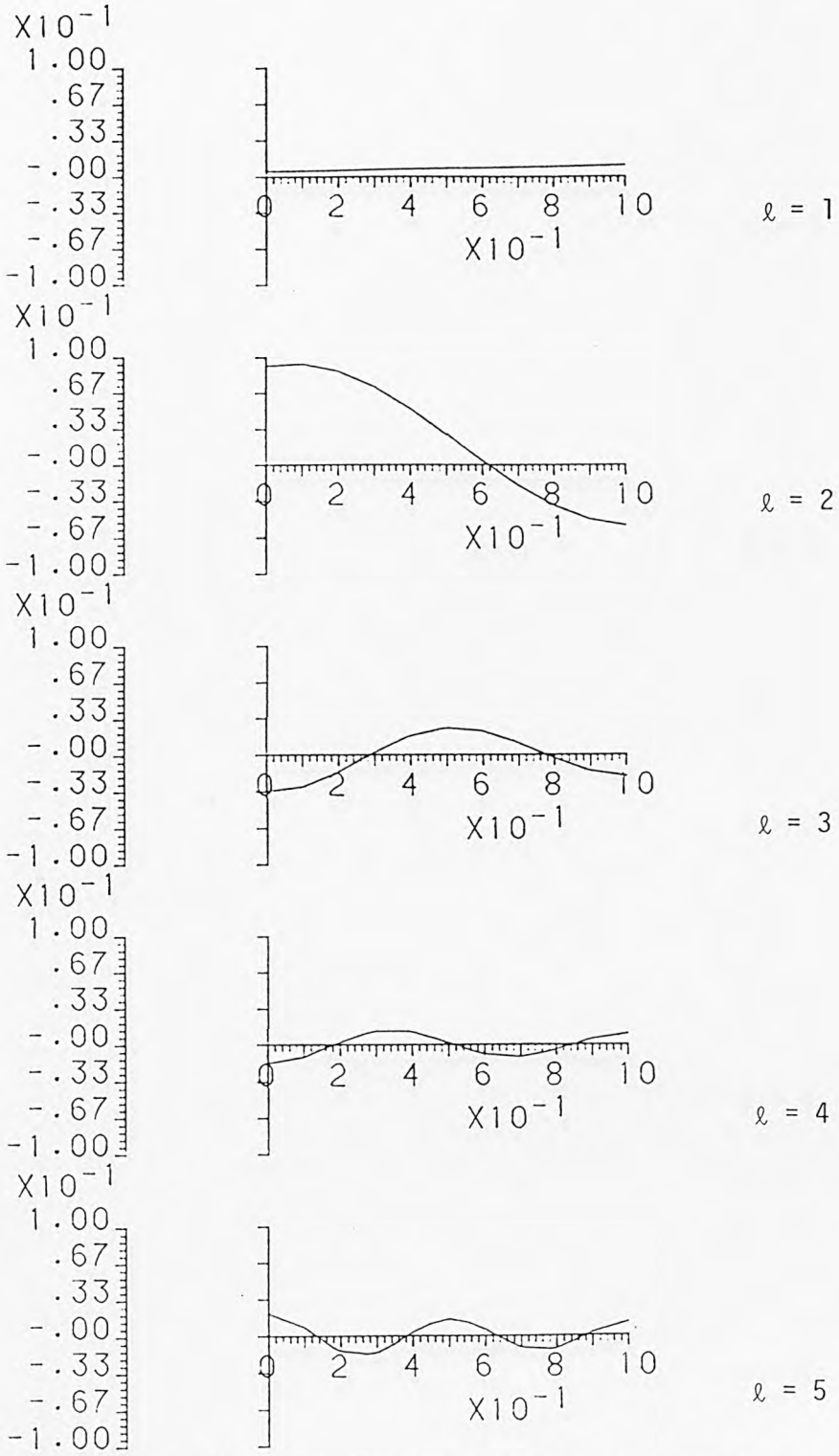

FIGURE 7.1. (Continued) n = 3

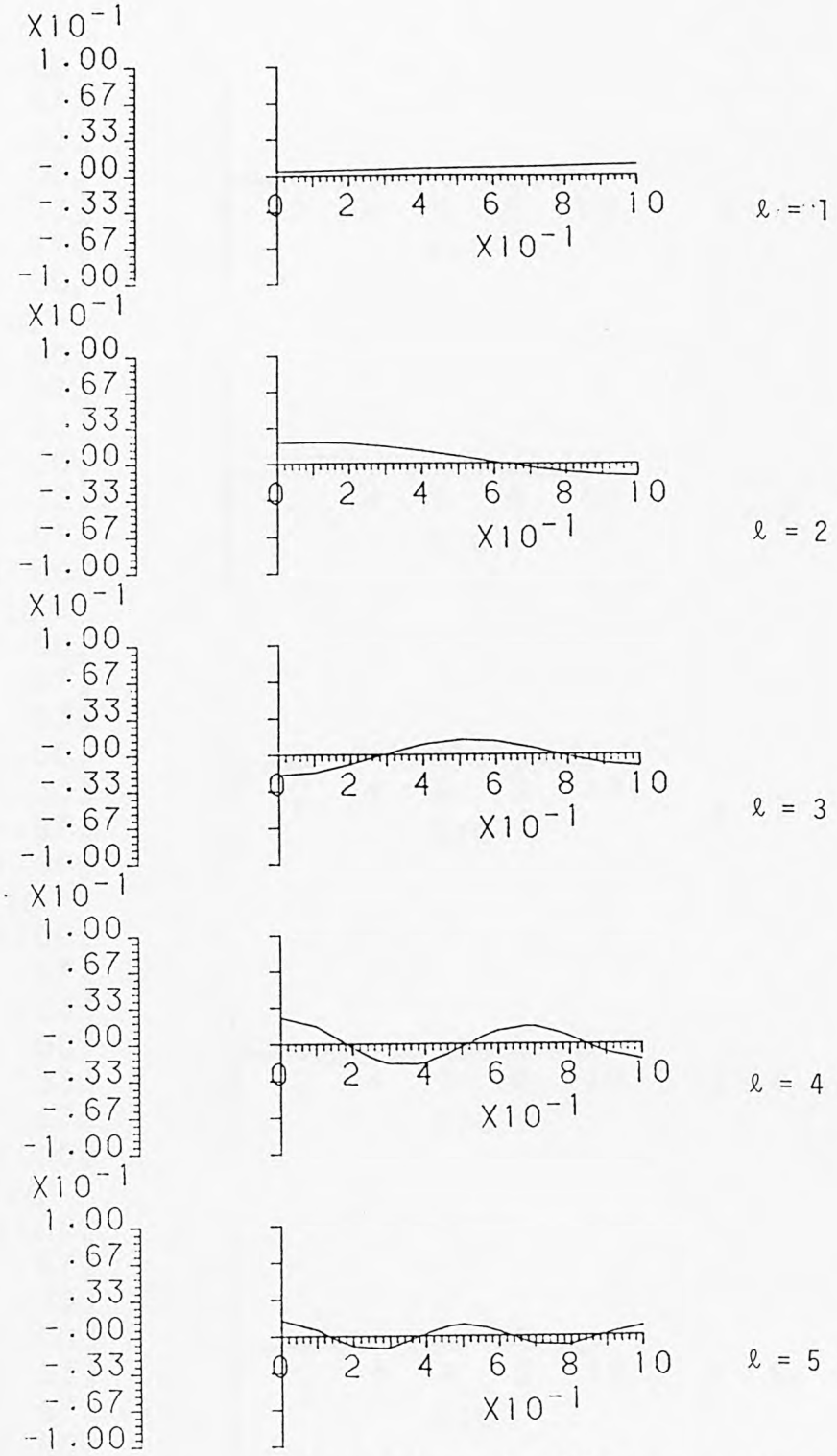

FIGURE 7.1. (Continued) n = 4

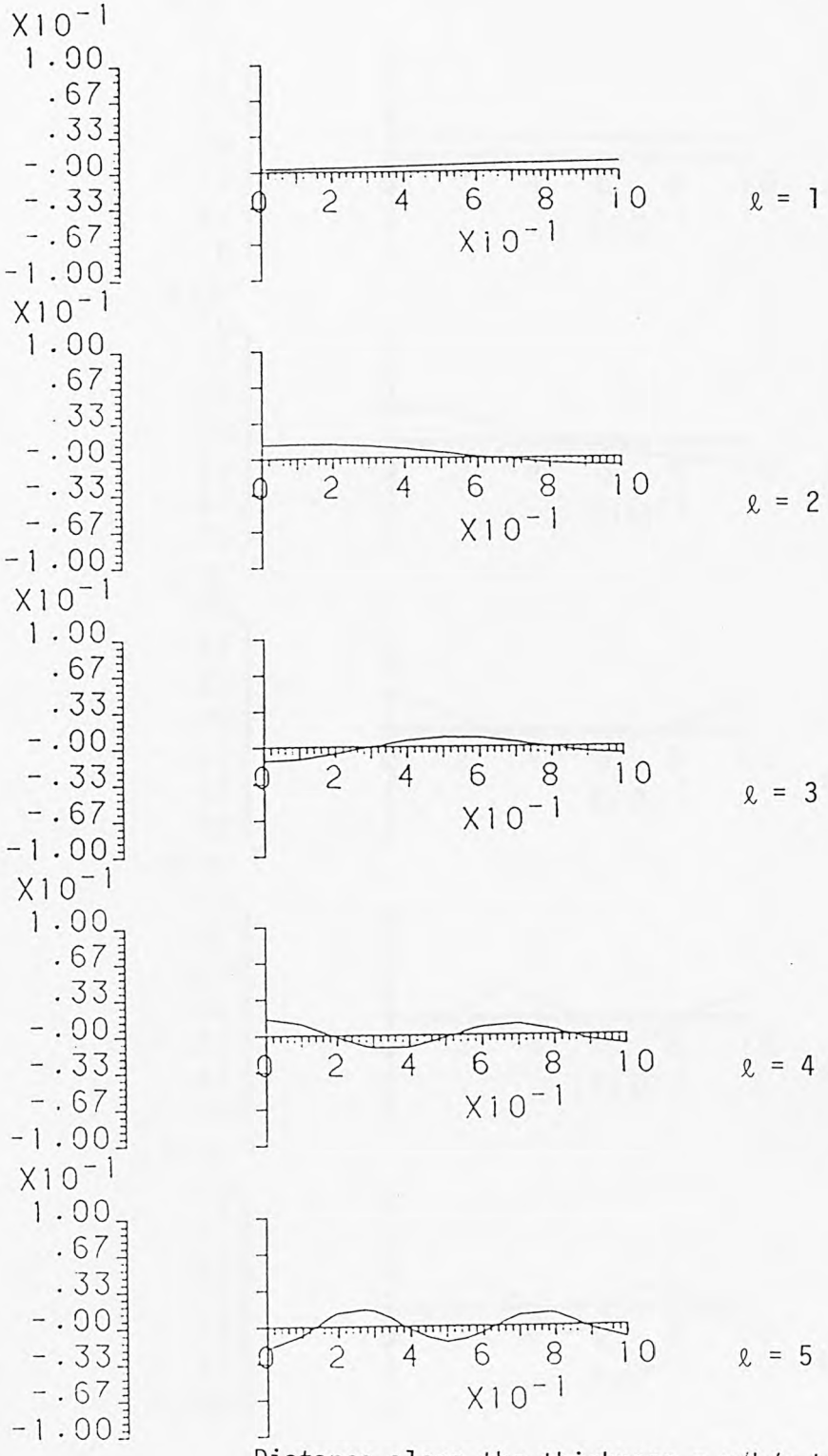

FIGURE 7.1. (Continued) n= 5

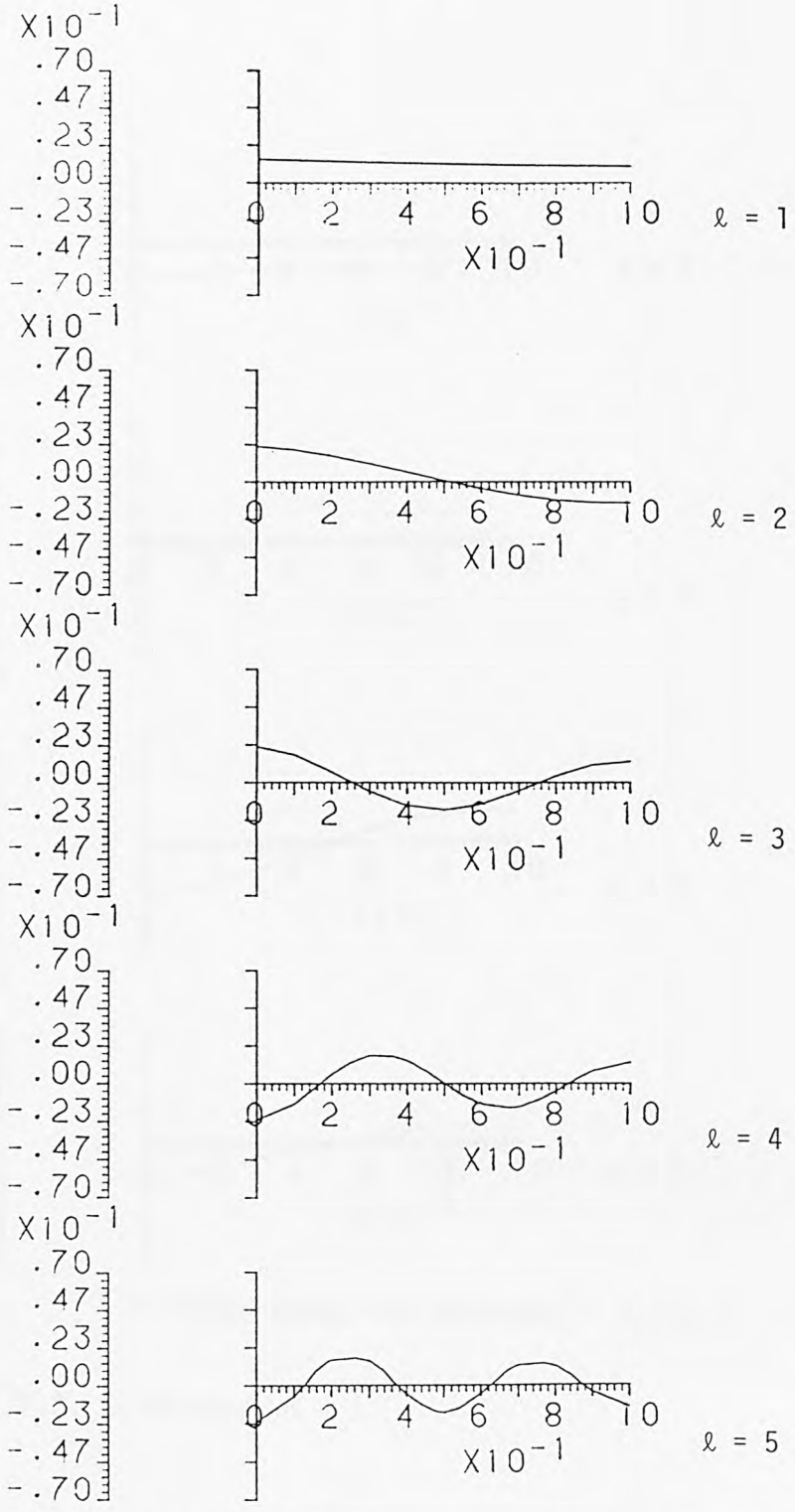

FIGURE 7.2. VARIATION OF NORMALISED DISPLACEMENT (u_r) OF SPHEROIDAL VIBRATION OF HOLLOW SPHERE ALONG THE THICKNESS.
(Poisson's ratio = 0.29, n = 0, and b/a = 0.6)

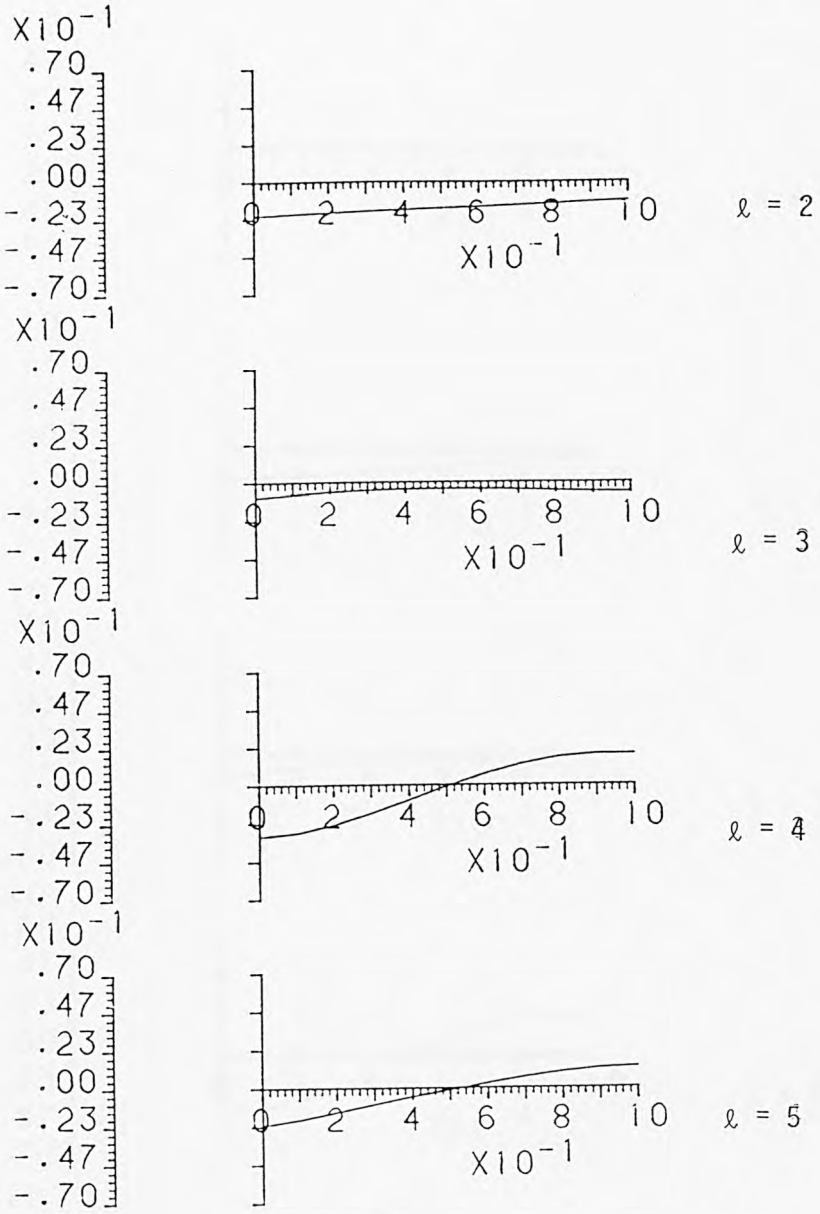

FIGURE 7.2. (Continued) n = 1

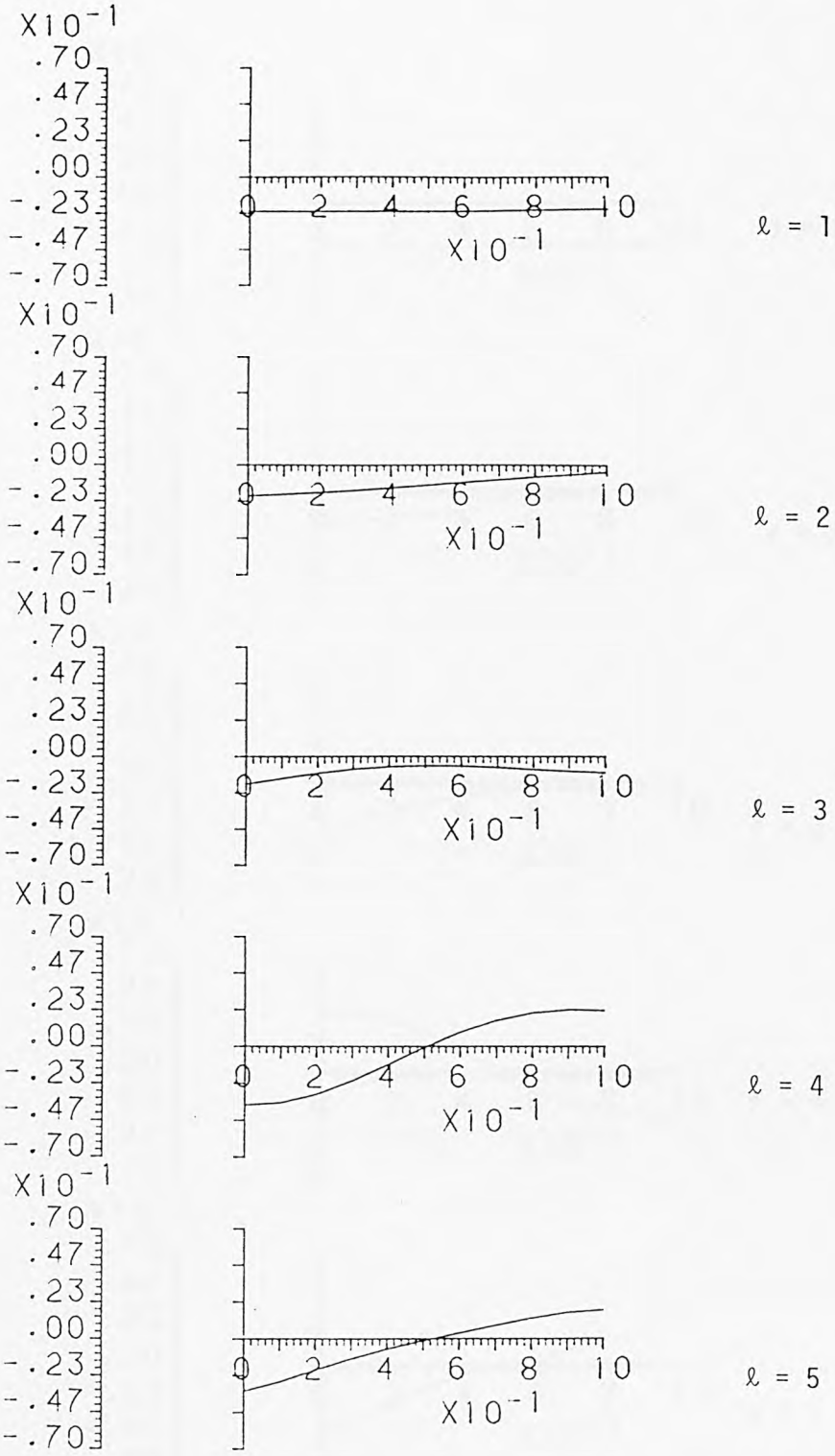

FIGURE 7.2. (Continued) n = 2

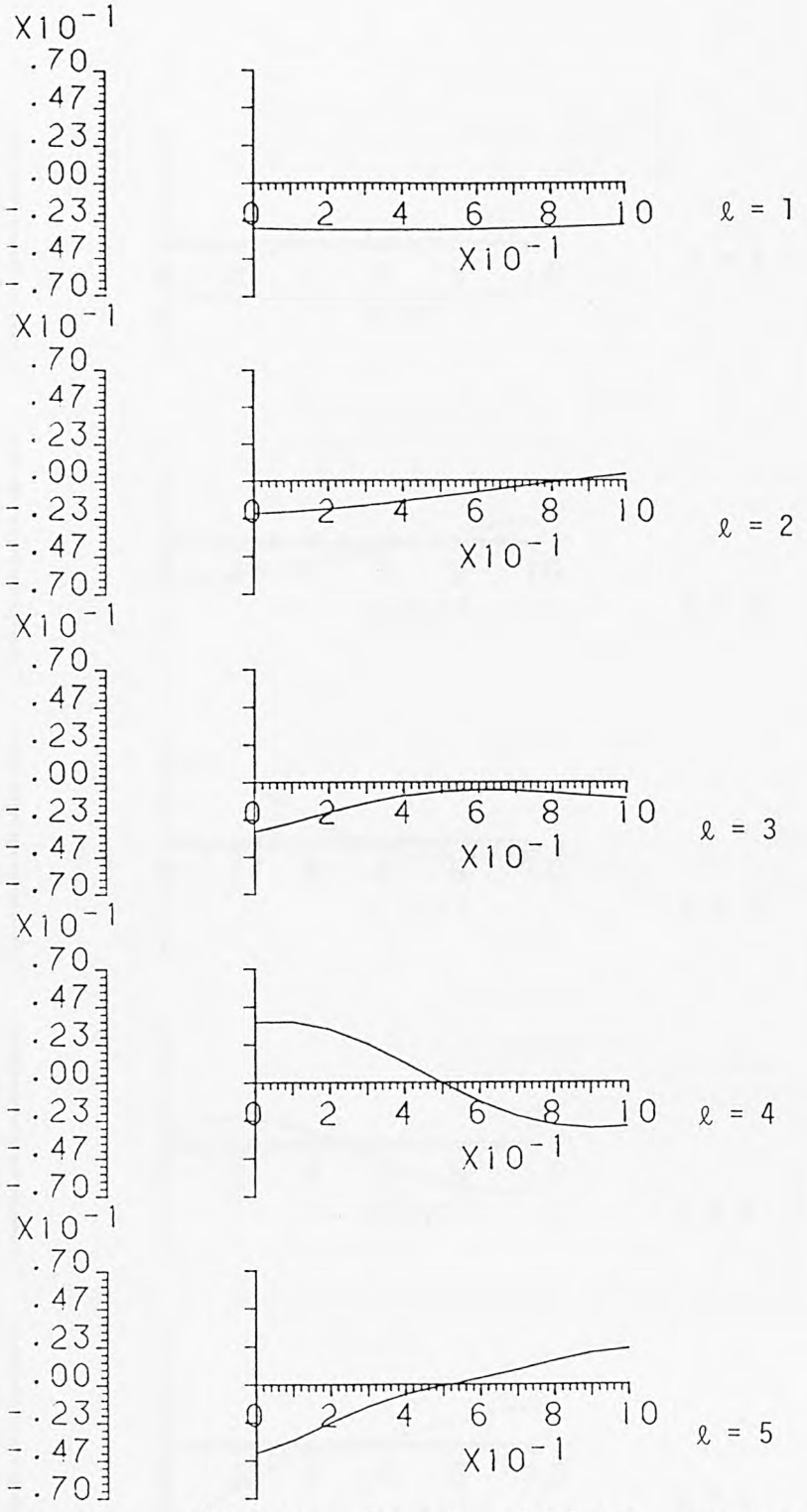

FIGURE 7.2. (Continued) n = 3

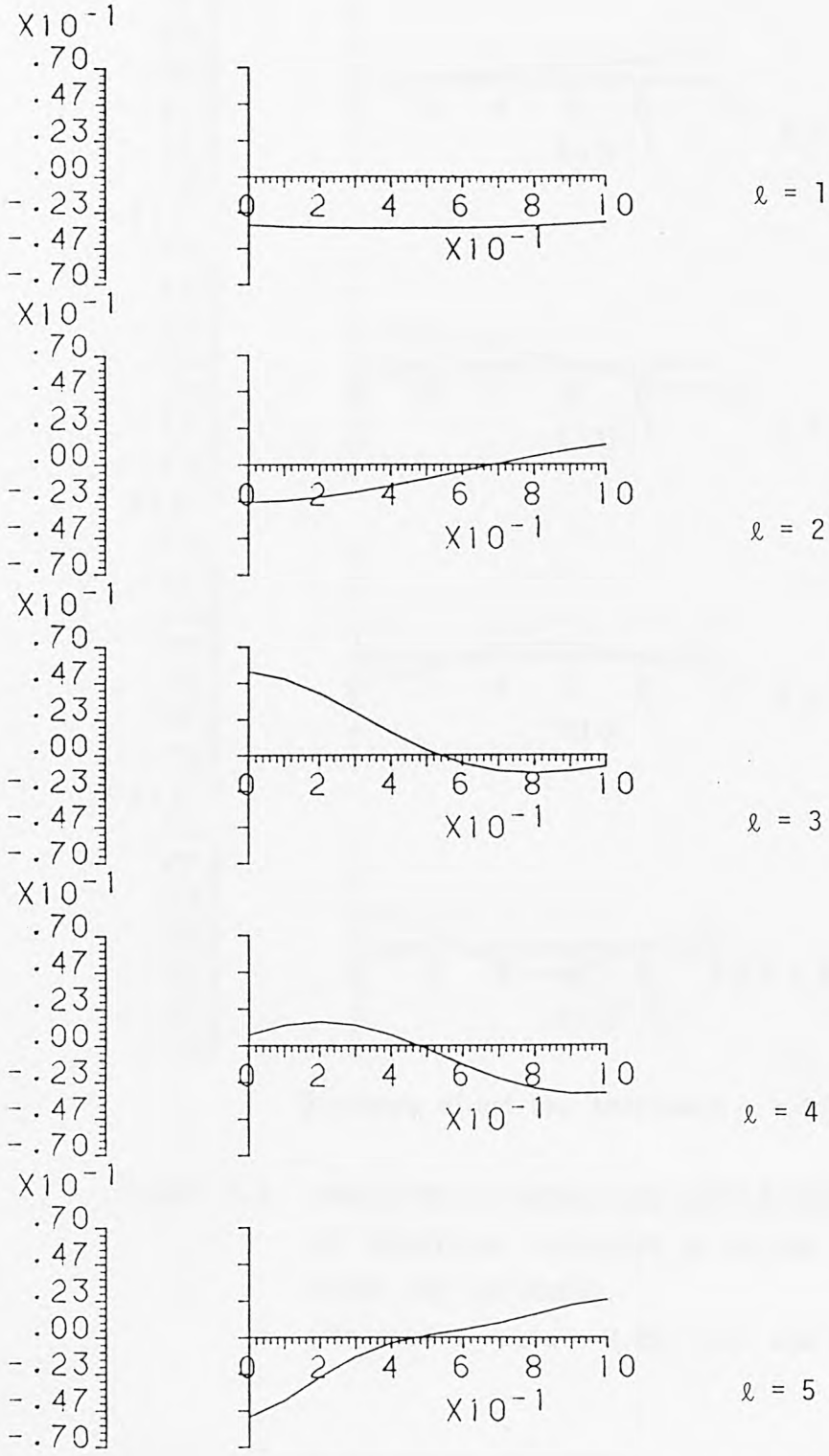

FIGURE 7.2.(Continued) n = 4

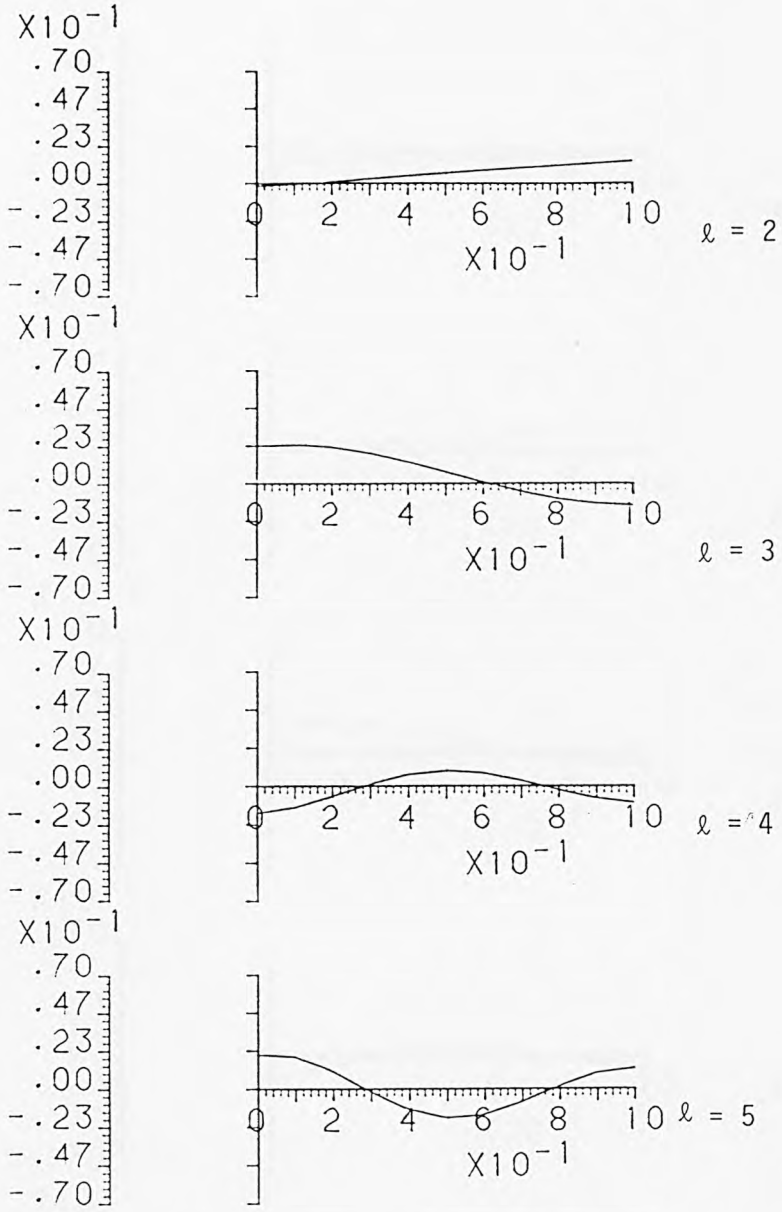

FIGURE 7.3. VARIATION OF NORMALISED DISPLACEMENT (u_θ) OF SPHEROIDAL VIBRATION OF HOLLOW SPHERE ALONG THE THICKNESS.
(Poisson's ratio = 0.29, n=1, and b/a = 0.6)

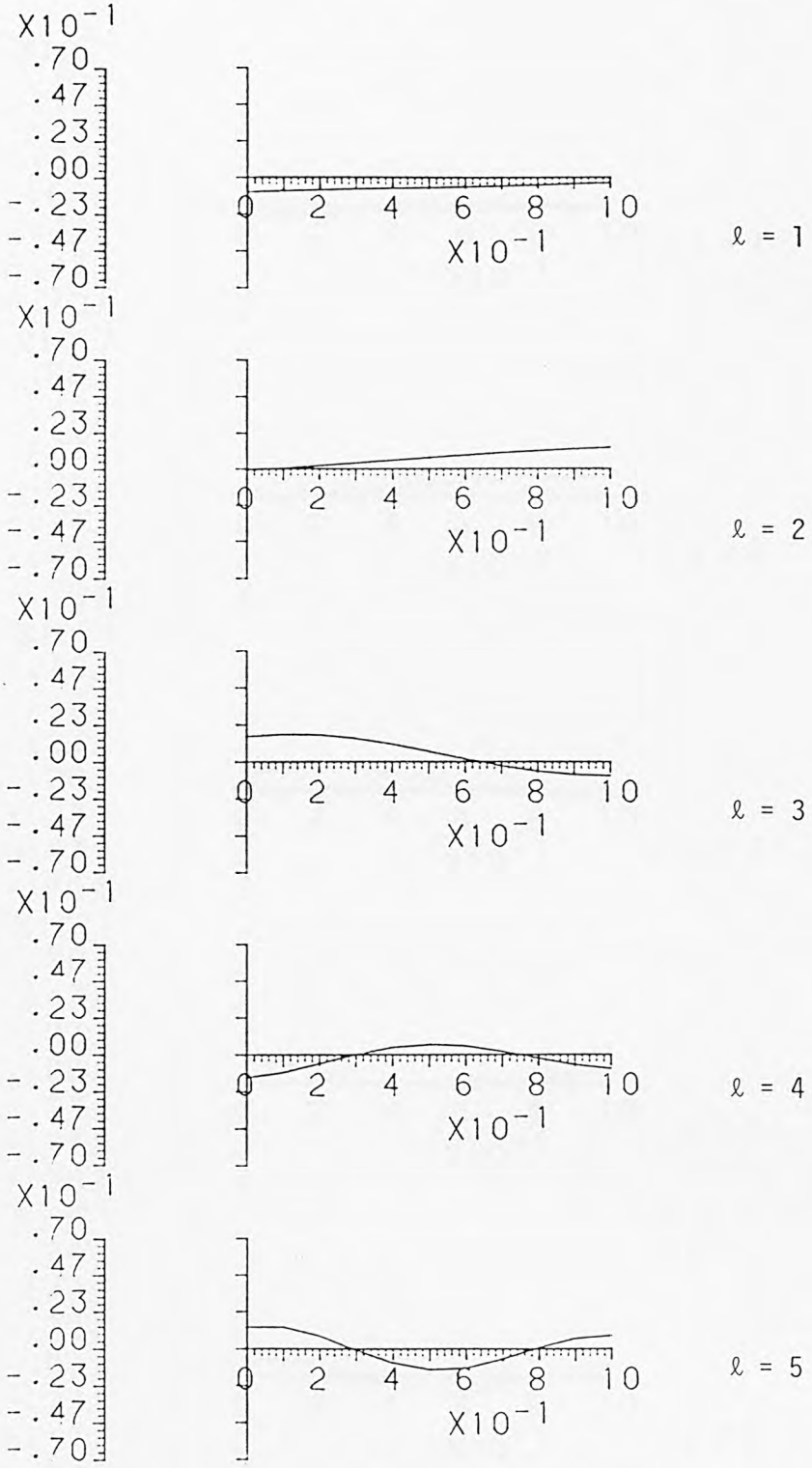

FIGURE 7.3. (Continued) n = 2

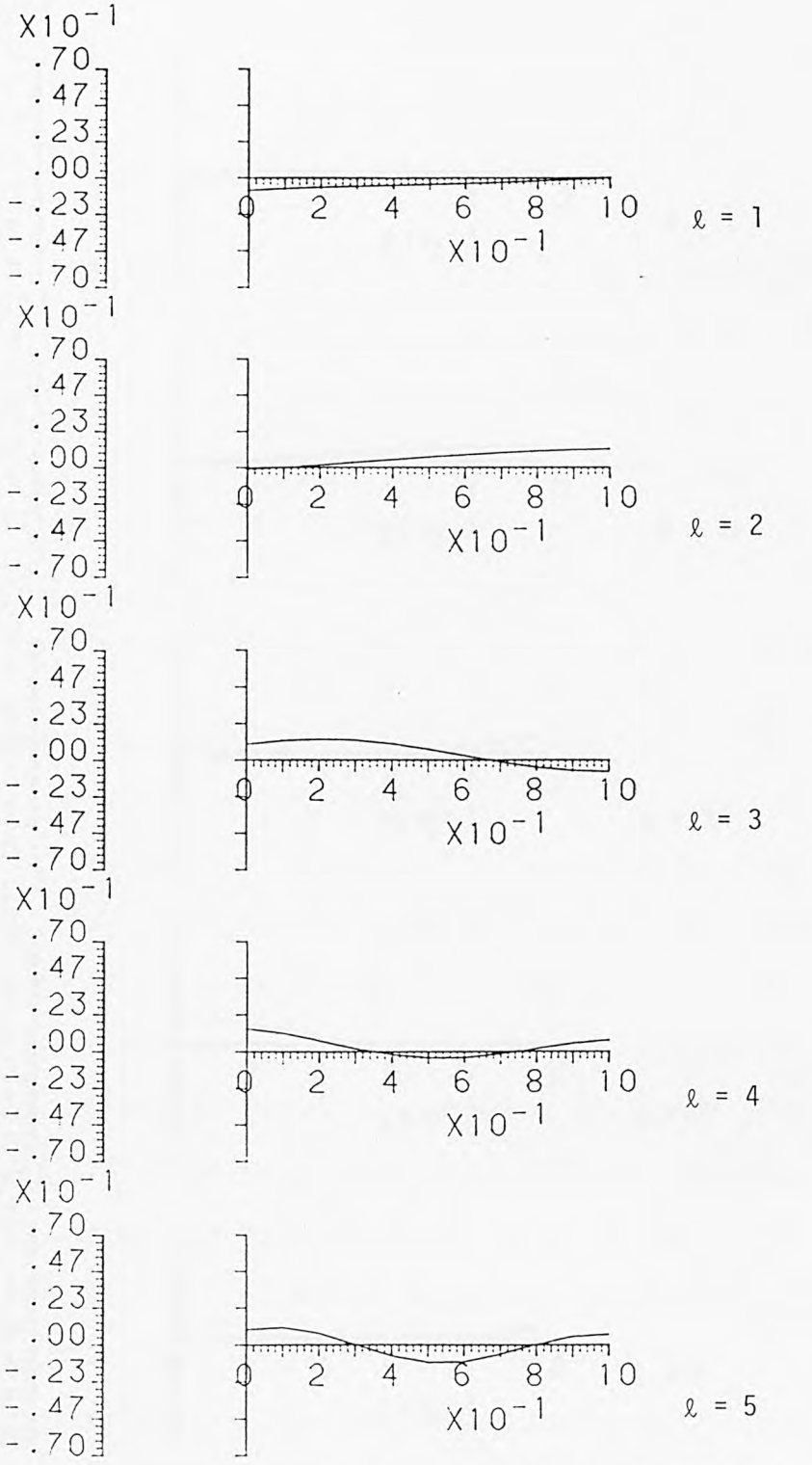

FIGURE 7.3. (Continued) n = 3

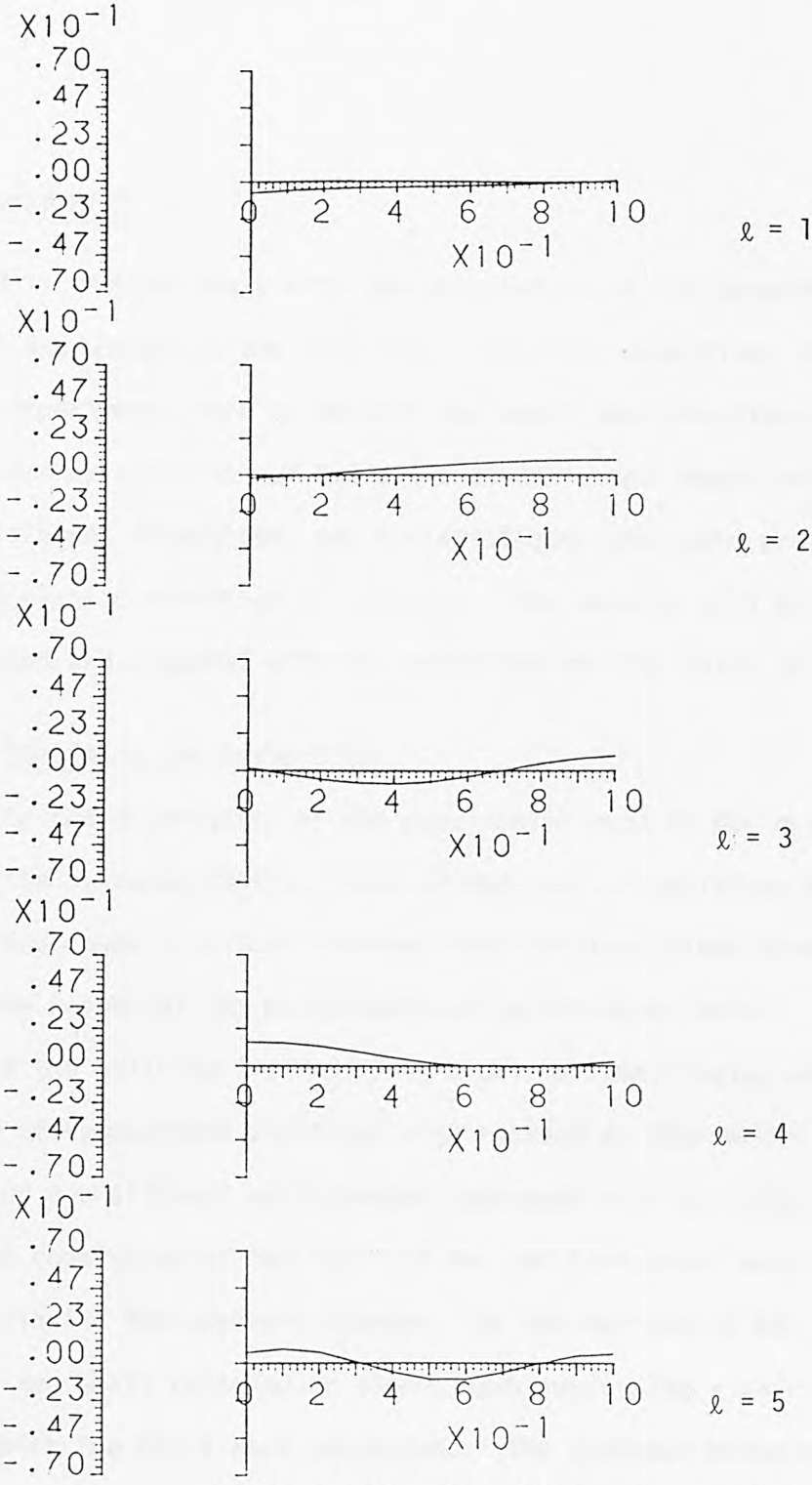

FIGURE 7.3. (Continued) n = 4

8. EXPERIMENT

This chapter deals with the description of the experimental set up and design of the test rig. The main objectives of these experiments were to measure the sound pressure-time histories generated by collision of two balls at different impact velocities and different directions, and to investigate the sound pressure due to elastic vibration of spheres. The results will be discussed and compared with the predicted results later in Chapter 9.

8.1. Specimens and Suspension

The characteristics of the steel balls used in the experiments are given in Table (8.1). Each of the pair of colliding balls were suspended by either fishing lines or steel wires depending upon the weight of the balls used during the experiments. To suspend the balls by fishing lines a pair of small holes were spark eroded at symmetrical positions with respect to the centre of each ball and a small hook was cemented into each hole by using araldite. A frame consisting of two vertical and one horizontal bars was placed inside the anechoic chamber. On the horizontal bar was fitted two small rectangular pieces each possessing a pair of hooks from which the balls were suspended. The distance between the hooks could be adjusted according to the size of the selected pair of colliding balls. To suspend the forged steel balls by steel wires a pair of holes were made at symmetrical positions with respect to the centre of each ball and a $\frac{3}{8}$" bolt was screwed into each hole. A schematic diagram of balls suspension is given in Fig.(8.1).

8.2. Design of the Test Rig

In order to measure the sound pressure in different directions about the contact point it was required to rotate the microphone on the imaginary circle centred at the impact point. To carry out this task a test rig as shown in Fig.(8.2) was designed.

This structure consisted of a base plate 1 on which the horizontal arms 2 and 3 were mounted. Located within the base are ball races which enable the arms to rotate freely about the fixed axis zz. The impact point of the balls is also arranged to lie on the axis zz. The pointers 4 and 5 attached to the horizontal arms could be positioned in any of 360 holes drilled in two concentric circles on the face of a circular plate 6 which was connected to the base 1 through ½" bolts. The vertical stand 7 carrying the microphone holder 8 was assembled on the horizontal arm 2 through sliding base 9 which could be clamped at any position. The whole structure enabled the position of the microphone with respect to the impact point to be estimated with the aid of scales mounted on both the horizontal arm and vertical stands. It should be emphasised that the direction of the swing of the balls was chosen as a reference for estimating the angular coordinate of the microphone position. To maintain the same distance from the contact point during rotation of the horizontal arm the axis of shaft 10 zz, passing through the centre of base 2 was checked by a plumb-line to ensure that the impact point of the spheres was lying on the axis zz.

To reduce the interference of the sound reflecting back from the microphone holder a conical shape of microphone holder was found suitable. To release the balls an electromagnetic holder 11 was attached by sliding part 12 to the vertical stand 13, along which it could slide and be clamped. A scale graduated in mm was mounted on the vertical stand 13 to measure the drop height of the balls.

8.3. Fourier analyzer/54SIC Hewlett Packard

Since the Fourier analyzer played the main role in displaying and analysing the experimental results a brief note about how it works may be found to be useful.

The instrument transforms data from the time domain to the frequency domain by means of the discrete finite transform (D.F.T.). This transformation is carried out quickly by means of a special algorithm, the fast Fourier transform (F.F.T). For example, 1024 data points in the time domain are transformed into the frequency domain in 55 ms. The resolution Δf between lines in the frequency spectrum is related to the total time of the record T by:

$$\Delta f = \frac{1}{T}$$

The time T, the sampling time Δt and the number of data points N are related by:

$$T = N \Delta t$$

The highest frequency in the spectrum F_{max} is given by:

$$F_{max} = \frac{N}{2} \Delta f$$

The highest possible value of F_{max} with the Fourier analyzer is 100 kHz.

In using the Fourier analyzer it is important to ensure that that there are no aliasing errors. This is achieved by passing the analog time data through a low pass filter before the data is sampled by the analog to digital converter. The cut-off of the low pass filter was selected to be F_{max} or less.

A main feature of the Fourier analyzer is a keyboard on which the user can punch keys for a variety of mathematical functions to be performed on the frequency data. More information about this may be found in the manufacture application note (see ref.(65)).

8.4. Anechoic chamber

The anechoic chamber used during the experiment was designed by Anderson 66 and is situated on level 1 in the Department of Mechanical Engineering. The chamber is a 50 mm thick concrete box mounted on rubber pads which act as vibration isolators. Polyurethane foam wedges (Dunlop DP103) of length 600 mm line the chamber leaving a maximum working space of 4.5 m x 3 m by 3.87 m high. The background noise in the chamber is 30 dB(A) and is mainly structure-borne sound of low frequency. A good anechoic chamber should, by definition, be echo-free. The walls need to be perfectly absorbing, so that free-field conditions are achieved. For a point source of sound in a free-field the intensity of sound is inversely proportional to the square of the distance from the source. Thus the inverse square law test is the most sensitive test of the quality of an anechoic chamber, and a good room should exhibit very small deviations from the inverse square law. Details

about the inverse square law test carried out by Anderson can be found in ref. 66 . Service ducts for electricity, water pipes, air tubes, microphone cables, etc., are underneath the chamber. A control cabin is adjacent to the chamber and contains standard B8K analysis equipment and the Hewlett Packard Fourier analyzer.

8.5. Acoustic measurements

The sound measuring system consisted of a Bruel and Kjaer ¼ inch condenser microphone (type 4135) and a type 2608 measuring amplifier. The output of the measuring amplifier was connected to the input of the Fourier analyzer. After each collision the pressure-time pulse could be displayed on the oscilloscope of the Fourier analyzer and stored on a magnetic disc. A Bruel and Kjaer ½ inch condenser microphone (type 4133) was used to trigger the scope. This was necessary because of the fast transient nature of the pulse. The triggering microphone was attached to another measuring amplifier, whose output was connected to the external trigger of the Fourier analyzer. To prevent reflections of the sound pulse off the triggering microphone from reaching the measuring microphone the triggering microphone was positioned at a suitable distance away from the measuring microphone.

A schematic diagram of the apparatus used for the acoustic test is given in Fig.(8.3). To calibrate the measuring system, a Bruel and Kjaer type 4220 pistonphone was used. This produces a sound level of 124 dB re 20 μpa, plus or minus a correction factor which depends upon the barometric pressure. The apparatus

was set up as shown in Fig.(8.3) except for the trigger circuit which was not required. The pistonphone was then placed over the ¼ inch microphone and the range setting of the measuring amplifier was set on the 0.3V full scale deflection. A sine wave form signal generated by the pistonphone was displayed on the oscilloscope and the peak amplitude was noted. For every collision the impactor was held back against the electromagnet and its circuit was broken through the switch placed in the control room. The impact velocity v_o is determined from the drop height of the ball, h_D, by using the relation, $v_o = (2g_G h_D)^{\frac{1}{2}}$ where g_G is the gravitational acceleration.

8.6. Acceleration measurement

Surface acceleration of the impactee was measured by means of a Bruel and Kjaer accelerometer type 8309 with a calibration constant of 0.0184 mV/ms^{-2}. The accelerometer was screwed into a hole which had been prepared on the side opposite to the impact point. The accelerometer was connected to a Bruel and Kjaer precision sound level meter. The output of the sound level meter was connected to the Fourier analyzer so that the acceleration time histories can be displayed. A Bruel and Kjaer ½ inch condenser microphone (type 4133) was used to trigger the scope. The triggering microphone connected via a measuring amplifier to the external trigger of the Fourier analyzer. A schematic diagram of the apparatus used for the acceleration measurement is given in Fig.(8.4). To calibrate the measuring system a function generator type (TWG 501) was used and its input was measured by a voltmeter. The function generator was connected

to sound level meter, whose output was connected to the input of the Fourier analyzer. It was found that with the sound level meter on 110 dB an input of 99 mV gave an output of 2.68 Volts on the Fourier analyzer. Thus a simple calculation shows that the calibration constant for the system is given by 1V = 2007.6 m/s^2.

Diameter (")	1	2	$\frac{357}{64}$
Diameter (cm)	2.54	5.08	14.17*
Type	Non-corrodable	non-corrodable	Forged
Hardness (Rockwell)	55 - 56	55 - 56	-
Weight (g)	66	528	11800
Density (g/cm^3)	7.8	7.8	

TABLE 8.1. CHARACTERISTICS OF THE BALLS USED FOR THE TESTS.

* Average Diameter

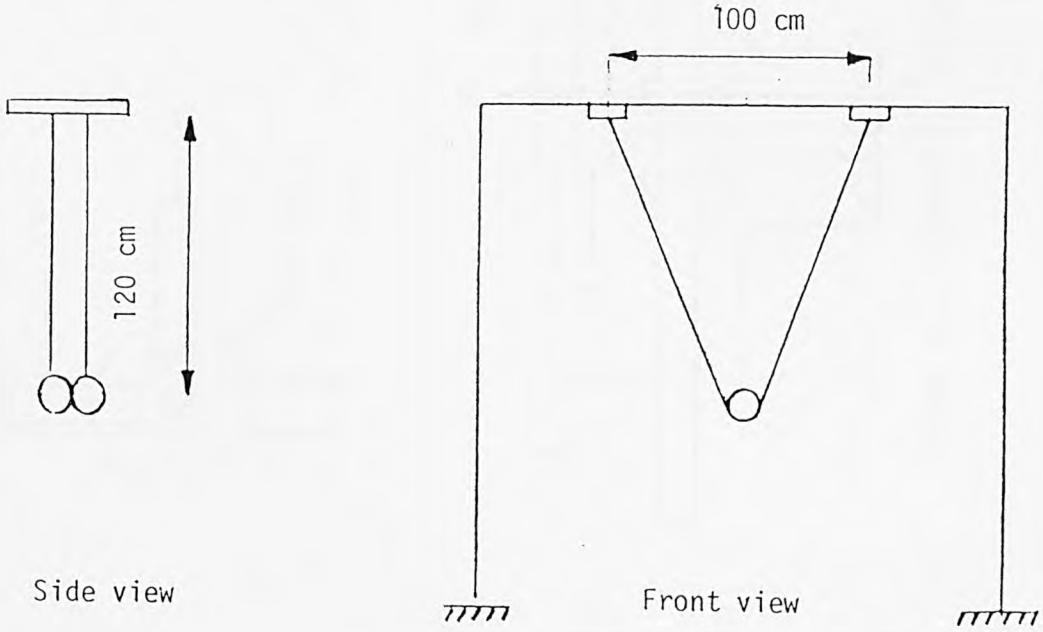

FIGURE 8.1. SCHEMATIC OF BALL SUSPENSION

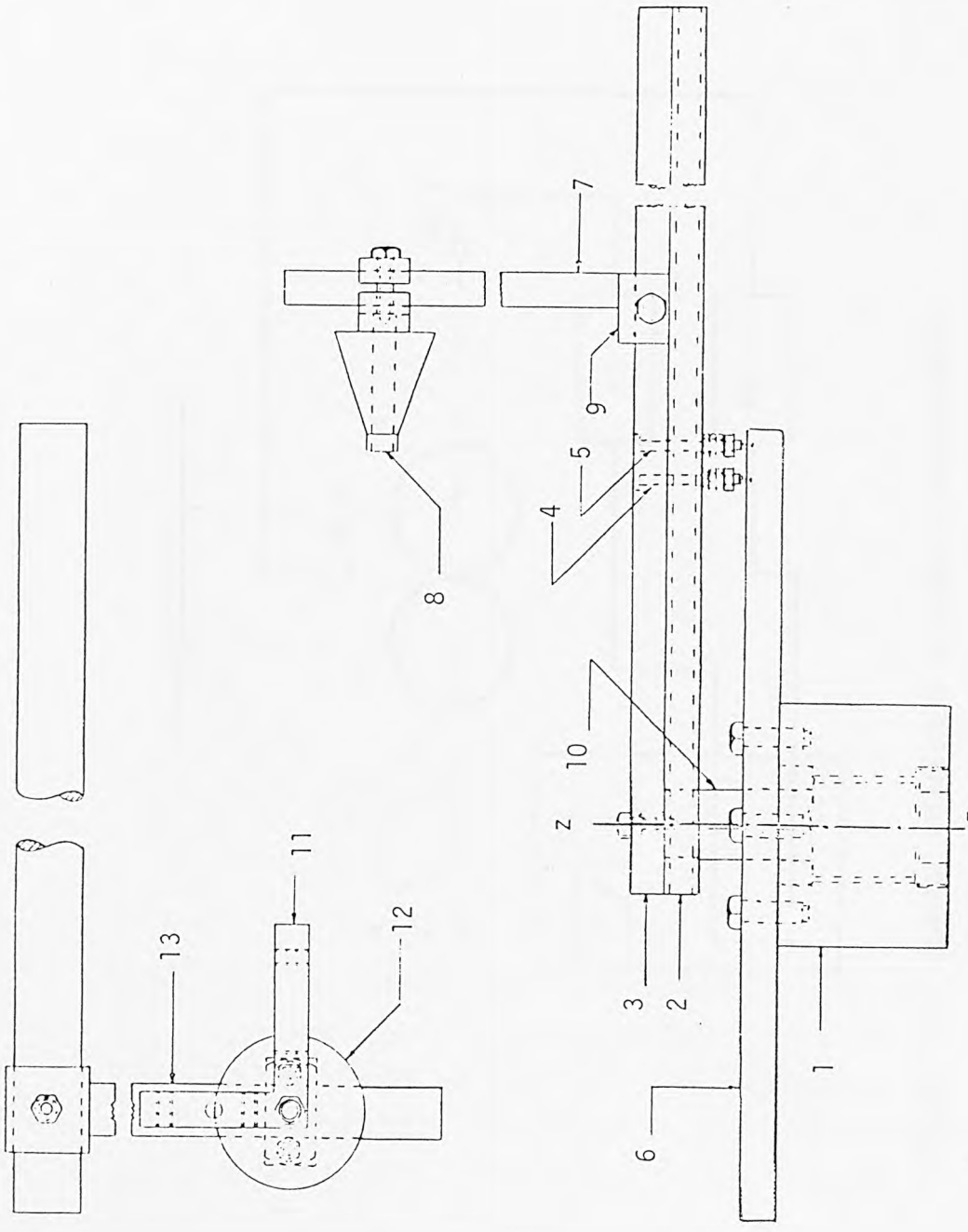

FIGURE 8.2. SCHEMATIC DIAGRAM OF THE TEST RIG.

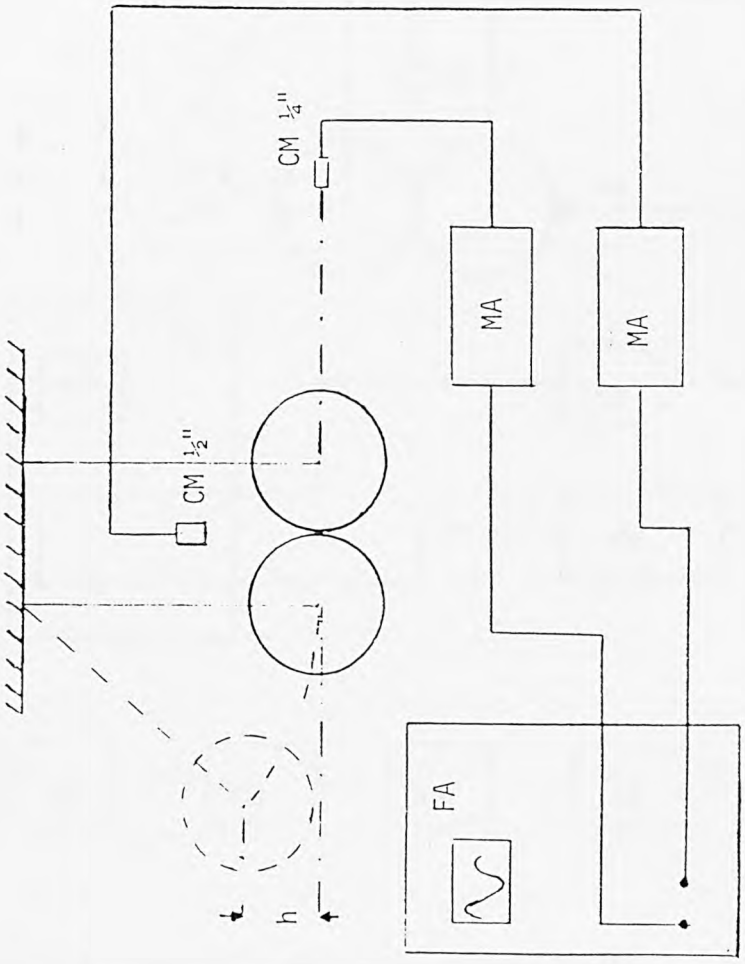

FIGURE 8.3. GENERAL ARRANGEMENT OF ACOUSTIC MEASUREMENTS.
CM: Condenser Microphone, MA: Measuring amplifier,
FA: Fourier analyser

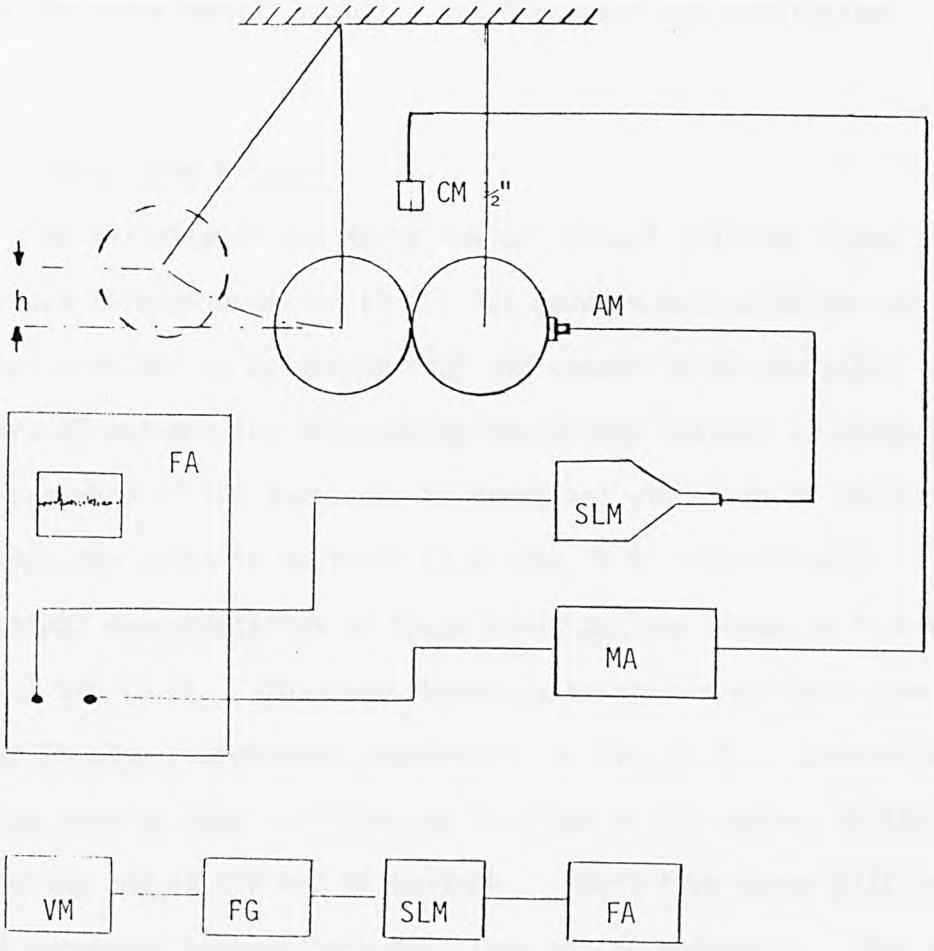

FIGURE 8.4. GENERAL ARRANGEMENT OF ACCELERATION MEASUREMENT AND APPARATUS USED IN CALIBRATION. CM: Condenser Microphone, MA: Measuring amplifier, AM: Accelerometer, SLM: Sound Level meter, FA: Fourier analyser, VM: Voltmeter, FG: Function generator.

9. DISCUSSION AND CONCLUSIONS

Predicted results obtained in previous chapters, together with the experimental results, are discussed and conclusions drawn.

9.1. Force-time history

The validity of the Hertz law of contact relating force and approach through equation (2.60) has been investigated for many impact problems by Goldsmith [43] and proved to be adequate. The numerical methods for calculating force-time history in absence and presence of the terms due to transient vibration of colliding spheres are given in sections (2.6) and (6.9) respectively. Graphical representation of these solutions are shown in Figures (2.2.) and (6.6). Solutions based on assumption of half sine pulse is also represented graphically in Fig.(2.2). Comparison of the results show a difference in slope of the curves at the beginning and at the end of contact. Apart from these differences good agreement between both solutions may be observed. Thus one may conclude that analytical representation of force-time history as a half sine pulse is a good approximation.

9.2. Impulsively accelerated and pulsating spheres

Graphs representing pressure-time histories at $\theta = 0^{o}$ and 60^{o} for an impulsively accelerated sphere is given in Fig.(3.1). At the wave front i.e. $\tau = 0$, pressures are maximum and their peak values may be given by $P = P_{M}\cos\theta$. As θ increases from 0^{o} to 90^{o} the peak value at the wave front decreases and this is the same

also for the rarefactive peak which is forming later in time.

Pressure-time curve of impulsively pulsating sphere as shown in Fig.(3.2) has the same switch on value as the impulsively accelerated one given for $\theta = 0^{o}$. Unlike the impulsively accelerated sphere the sound pressure radiated by an impulsively pulsating sphere decays exponentially with time and forms no rarefactive peak. It is also independent of θ.

In Fig.(3.7) both the exact solution of the sound radiated by an impulsively accelerated sphere and approximate evaluation of that sound obtained by the aerodynamic approach are compared. Both pressure decay rates and switch-on values agree very closely.

9.3. Sphere undergoing a Hertzian acceleration

The logarithmic plot of dimensionless peak pressure amplitude against non-dimensional contact time β is given in Fig.(3.3). Observation of this graph suggests that the variation of peak amplitude with respect to β can be approximated by the straight lines shown at the same Figure. Thus one finds:

$$\frac{P_{max}}{P_N \cos\theta} = 0.525\beta^{-0.45} \qquad \text{for} \quad \beta < 0.3,$$

$$\frac{P_{max}}{P_N \cos\theta} = 0.28\beta^{-0.98} \qquad \text{for} \quad 0.3 < \beta < 1$$

and

$$\frac{P_{max}}{P_N \cos\theta} = 0.28\beta^{-1.73} \qquad \text{for} \quad \beta > 1$$

The non-dimensional contact time β can be related to the impact velocity through equation (3.41b) and it is not difficult to show that:

$$\beta_1 = 555.37\ \rho_1^{0.4}\left(\frac{1+\bar{M}}{\bar{M}}\right)^{-0.4}\left(\frac{1-\nu_1^2}{E_1}+\frac{1-\nu_2^2}{E_2}\right)^{0.4}\left(\frac{a_2}{a_1+a_2}\right)^{-0.2} v_o^{-0.2}$$

where units are all in the SI system. This equation together with the approximate relations given for peak amplitude may be used for predicting the peak pressure when one or some of the variables such as size of colliding spheres, modules of elasticity, and etc. change. Since the non-dimensional contact time β varies with the inverse of impact velocity to the power 0.2 the proportionality of the peak pressure amplitude and impact velocity can be written as:

$$P_{max} \alpha v_o^{1.09} \qquad \text{for} \quad \beta < 0.3$$

$$P_{max} \alpha v_o^{1.2} \qquad \text{for} \quad 0.3 < \beta < 1$$

and

$$P_{max} \alpha v_o^{1.35} \qquad \text{for} \quad \beta > 1$$

The dimensionless time $\hat{n}$ for which the peak occurs is also plotted logarithmically versus β and is shown in Fig.(3.4). Approximation based on representation of this graph with the straight lines for different regions of β suggests that:

$$\hat{n}_{max} = 0.61\beta^{-0.17} \qquad \text{for } \beta < 0.3$$

$$\hat{n}_{max} = 0.48\beta^{-0.36} \qquad \text{for } 0.3 < \beta < 1$$

and

$$\hat{n}_{max} = 0.48\beta^{-0.72} \qquad \text{for } \beta > 1$$

Thus for all values of β within the range of $0.1 < \beta < 10$ the value of $\hat{n}$ never exceeds unity.

Due to max the dependency of the peak pressure on $\cos\theta$ its directional distribution is symmetrical about $\theta = 90^{o}$ and depending upon whether $0 < \theta < \frac{\pi}{2}$ a compressive peak or $\frac{\pi}{2} < \theta < \pi$ a rarefactive peak can be generated.

The logarithmic plot of dimensionless peak of transform against non-dimensional contact time β is given in Fig.(3.5) and can be approximated by straight lines for different regions of β. Thus one may write:

$$\left|\frac{p_{max}}{P_L}\right| = 0.49 \qquad \text{for } \beta < 0.3$$

$$\left|\frac{p_{max}}{P_L}\right| = 0.35\beta^{-0.26} \qquad \text{for } 0.3 < \beta < 1$$

and

$$\left|\frac{p_{max}}{P_L}\right| = 0.35\,\beta^{-0.91} \qquad \text{for } \beta > 1$$

The value of dimensionless frequency n* for which the transform peak occurs is also plotted logarithmically against β and is shown in Fig.(3.6). It can be easily shown that these values can be approximately given by:

$$n^*_{max} = 0.63\beta \qquad \text{for } \beta < 0.7$$

$$n^*_{max} = 0.5\beta^{0.34} \qquad \text{for } 0.7 < \beta < 2.5$$

and

$$n^*_{max} = 0.683 \qquad \text{for } \beta > 2.5$$

Dimensionless pressure time curves for a pair of colliding spheres are given in Fig.(3.11) to (3.14). There are seven dimensionless parameters $\beta_1, \beta_2, \bar{M}, \xi_1, \xi_2, \theta$ and $\hat{n}$ which take part in predicting the resultant dimensionless pressure. The dimensionless time delay n' may be expressed in terms of β_1 and β_2 as:

$$n' = \left(\frac{1}{\beta_1} + \frac{1}{\beta_2}\right)\frac{\cos\theta}{\pi}$$

The pressure generated by the impactor reaches the microphone after the above dimensionless time delay has elapsed. Thus the value of the first compressive peak would be unaffected by the pressure contribution of the second sphere if the dimensionless time $\hat{n}_{max}$ for which the compressive peak occurs is less than n'. It can be easily shown that the value of n' at $\theta = 0^o$ for colliding spheres of equal and unequal sizes never could be less than $\frac{2}{\pi\beta_1}$ and $\frac{1}{\pi\beta_1}$ respectively. By examining different values of β_1 and observing the time for which the peak occurs one would be able to find an upper bound value of β below which $\hat{n}_{max} < n'$. Thus for a pair of colliding spheres of equal and unequal sizes an upper bound value of β below which $\hat{n}_{max} < n'$ may be given by $\beta_1 = 2.79$ and $\beta_1 = 0.53$ respectively. For any pair of colliding spheres

the first compressive peak would reamin unaffected by arrival of sound pressure from the second sphere, if the dimensionless contact time β_1 has a lower value than the corresponding upper bound value. This can also be confirmed by comparing the values of the first compressive peak in Figs.(3.11) to (3.14), with those which could be estimated by using expressions given previously for a single sphere. In order to study the effect of the replacement of the impactee by another impactee of the same size but different material one may write:

$$\beta = 637.95\ \rho^{0.4}\left(\frac{1-\nu^2}{E}\right)^{0.4}\ v_o^{-0.2}$$

and

$$\beta_x = 637.95\ \rho^{0.4}\left(\frac{1}{1+\rho/\rho_x}\right)^{0.4}\left(\frac{1-\nu^2}{E}\right)^{0.4}\left(1+\frac{1-\nu_x^2}{1-\nu^2}\times\frac{E}{E_x}\right)^{0.4} v_o^{-0.2}$$

where β and β_x are dimensionless contact times before and after replacement of the impactee respectively. The ratio of β_x to β may now be written as:

$$\frac{\beta_x}{\beta} = \left[\frac{1+\dfrac{1-\nu_x^2}{1-\nu^2}\times\dfrac{E}{E_x}}{1+\dfrac{\rho}{\rho_x}}\right]^{0.4}$$

Depending upon the value of the right hand side of above expression one would be able to predict the outcome of this replacement. As an example let the impactee of a pair of colliding steel spheres in Fig.(3.11) be replaced by a copper sphere of the same size. As a result of this replacement one

obtains $\frac{\beta_x}{\beta} = 1.15$. Since $\beta_x > \beta$ and the fact that p_{max}/P_N decreases as β increased, one should expect to obtain a lower value of p_{max}/P_N in case of the new arrangement. This can also be confirmed by comparing the values of first p_{max}/P_N in Figs.(3.11) and (3.13). To consider the effect of the replacement of the impactee by another impactee of the same material but different size, a similar procedure yields:

$$\frac{\beta_x}{\beta} = 1.148 \frac{(1+\frac{a_x}{a})^{0.2}}{(1+\frac{a_x^3}{a^3})^{0.4}}$$

If the size of impactee of colliding steel spheres in Fig.(3.11) increases by a factor 2, one obtains $\beta_x/\beta = 0.594$. Thus as a result of this replacement a greater value of p_{max}/P_N should be expected. Comparisons of the first p_{max}/P_N in Figs.(3.11) and (3.12) justifies this prediction. (Note that: $\frac{p_{max}}{P_N} = \frac{p_{max}}{\rho_o c v_o} \times \frac{1+\bar{M}}{1.17\bar{M}} \times \frac{r}{a}$).

For a pair of similar spheres of equal sizes the pressure profiles are functions of five parameters only. These parameters are $\beta, \xi_1, \xi_2, \theta$ and $\hat{n}$. By substituting $\xi_1 = \frac{r_1}{a}$, $\xi_2 = \frac{r_2}{a}$, $\theta = 0^o$, and $n' = \frac{2}{\pi\beta}$ in equations (3.60a) to (3.60d) and neglecting the difference between r, r_1 and r_2 in the denominator of the result, one would be able to express the resultant pressure in terms of β and $\hat{n}$ only. The logarithmic plot of dimensionless rarefactive peak amplitude against β is given in Fig.(3.19). Approximations

based on representation of this graph with the straight lines for different regions of β suggests that:

$$\frac{p_{max}}{P_M} = 0.547\beta^{-0.52} \qquad \text{for } \beta < 1$$

$$\frac{p_{max}}{P_M} = 0.547\beta^{-1.78} \qquad \text{for } 1 < \beta < 1.5$$

and

$$\frac{p_{max}}{P_M} = 1.14\beta^{-3} \qquad \text{for } \beta > 1.5$$

The proportionality of the rarefactive peak amplitude and impact velocity may be given by:

$$p_{max} \alpha\ v_o^{1.1} \qquad \text{for } \beta < 1$$

$$p_{max} \alpha\ v_o^{1.35} \qquad \text{for } 1 < \beta < 1.5$$

and

$$p_{max} \alpha\ v_o^{1.6} \qquad \text{for } \beta > 1.5$$

The dimensionless time $\hat{n}$ for which the rarefactive peak occurs is also plotted logarithmically against β and is shown in Fig.(3.20). It can be easily shown that these values can be approximately given by:

$$\hat{n}_{max} = 1.14\beta^{-0.8} \qquad \beta < 1$$

$$\hat{n}_{max} = 1.14\beta^{-0.46} \qquad 1 < \beta < 3$$

and

$$\hat{n}_{max} = 0.8\beta^{-0.16} \qquad 3 < \beta < 10$$

The directional distribution of the sound radiated by a pair of similar spheres of equal and unequal sizes are given in Figs.(3.15) and (3.16), respectively. The sound distribution for colliding spheres of equal sizes in symmetrical about a line joining the centres of the spheres and about a line perpendicular to this line through the contact point. The minimum pressure occurs at angle $\theta = 90^{o}$. The sound distribution for colliding spheres of unequal sizes is also symmetrical about a line joining the centres of the spheres and no symmetry about the perpendicular direction exists. The sound pressure is minimum at angles of $\theta = 90^{o}$ and 270^{o}. The directional distributions of the sound radiated by a pair of dissimilar spheres of equal and unequal sizes are also given in Figs.(3.17) and (3.18) respectively. The same behaviour as mentioned for the pair of similar spheres can be observed in Figs.(3.17) and (3.18).

In Figs.(3.21) to (3.24) are shown the transforms for the pressure-time results given in Figs.(3.11) to (3.14). The levels of transforms are constant for a limited bank of low frequencies and peak in the region of $n^* = 0.3\text{-}0.4$. For a pair of similar spheres of equal sizes the dimensionless pressure transforms are functions of five dimensionless parameters. These parameters are $\beta, \xi_1, \xi_2, \theta$ and n^*. By substituting $\xi_1 = \frac{r_1}{a}$, $\xi_2 = \frac{r_2}{a}$, and $\theta = 0^{o}$ in equation (3.64) and neglecting the difference between r, r_1 and r_2 in the denominator of the result, the dimensionless pressure transforms can be expressed in terms of β and n^* only. The logarithmic plot of dimensionless frequency n^* for which the

transform peak occurs against β is given in Fig.(3.25). It can be easily shown that:

$$n^*_{max} = 0.7\beta \qquad \text{for } \beta < 0.7$$

$$n^*_{max} = 0.58\ \beta^{0.45} \qquad \text{for } 0.7 < \beta < 2.5$$

and

$$n^*_{max} = 0.89 \qquad \text{for } \beta > 2.5$$

Thus for all values of β within the range $0.1 < \beta < 10$ the value of n^*_{max} never exceeds unity. The value of $n^*=1$ can be interpreted as the frequency associated with the duration of the contact. The value of f_{max} for which the transform peak occurs may also be given by:

$$f_{max} = \frac{76.4}{a} \qquad \text{for } \beta < 0.7$$

$$f_{max} = \frac{63.3}{a}\ \beta^{-0.55} \qquad \text{for } 0.7 < \beta < 2.5$$

and

$$f_{max} = \frac{97.2}{a}\ \beta^{-1} \qquad \text{for } \beta > 2.5$$

It may be interesting to note that for a pair of colliding spheres at radii $a_1 = a_2 < 0.38$ cm and $\beta < 0.7$ the Fourier transform of pressure time history peaks above the audible frequency region and the audible sound will be due to lower amplitude portions of the transform.

The sound pressure-time history calculated both analytically and numerically are compared in Fig.(3.26). No significant

difference between the results can be observed. Thus the half sine pulse approximation is adequate in most calculations.

In Fig.(3.8) both the exact solution for the sound radiated by a sphere undergoing a Hertzian acceleration and approximate evaluation of that sound obtained by aeroacoustic approach are compared. Both curves are identical for a certain period of time and agree very closely afterward. The only advantage of the aerodynamic approach is that the final formula are slightly simpler.

9.4. Radiation due to change of Volume of Sphere

The dimensionless pressure-time trace due to change of volume of 2.54 cm diameter colliding spheres is shown in Fig.(3.28). If the values of velocity and distance are chosen to be the same as those given in Fig.(3.26) it can be calculated that the maximum sound pressure is 0.53×10^{-2} Pa. Pressure of this magnitude may be neglected in comparison with the rigid body sound pressure radiated by colliding spheres of the same size, for which results are shown in Fig.(3.26).

9.5. Acoustic Energy

The acoustic energy radiated by an impulsively accelerated sphere in the far field is given by equation (3.90) and may be written in terms of velocity and mass of air displaced by the sphere as:

$$\hat{E} = \frac{1}{4} \bar{\bar{m}} v_o^2$$

Thus energy radiated by an impulsively accelerated sphere is equal to half the kinetic energy of air displaced by the sphere. It can be easily shown from equation (3.87) that at the surface of the sphere

$$\hat{E}_{IS} = \frac{1}{2} \bar{\bar{m}} v_o^2 = \frac{1}{2} \frac{\rho_o}{\rho} M v_o^2$$

where M is the mass of sphere. In Fig.(3.29) is shown the logarithmic plot of dimensionless energy against β for a sphere undergoing a Hertzian acceleration. Approximation based on representation of this graph with the straight lines in different regions of β suggests that:

$$\frac{\hat{E}}{E^*} = 0.26\beta^{-0.36} \qquad \text{for } \beta < 0.4$$

$$\frac{\hat{E}}{E^*} = 0.13\beta^{-1.14} \qquad \text{for } 0.4 < \beta < 1$$

and

$$\frac{\hat{E}}{E^*} = 0.13\beta^{-2.67} \qquad \text{for } \beta > 1$$

where $E^* = \frac{2\bar{M}^2}{(1+\bar{M})^2} \bar{\bar{m}} v_o^2$. When the impactor is a similar sphere of the same size as the impactee ($E^* = \hat{E}_{IS}$) one may conclude that energy never exceeds the kinetic energy of air displaced by the impactee. The proportionality of the energy and impact velocity may be written as:

$$\hat{E} \alpha v_o^{2.1} \qquad \text{for } \beta < 0.4$$

$$\hat{E} \alpha v_o^{2.23} \qquad \text{for } 0.4 < \beta < 1$$

and

$$\hat{E} \alpha\ v_o^{2.53} \qquad \text{for } \beta > 1$$

In order to calculate the total energy radiated by a pair of similar spheres of equal size it is assumed that $\theta_1 = \theta_2 = \theta$ and $r_1 = r_2 = r$. Such assumptions allow the total dimensionless pressure to be expressed in terms of β, $\hat{n}$ and θ. The logarithmic plot of total dimensionless energy against β is given in Fig.(3.30). and it can be easily shown that:

$$\frac{\hat{E}_T}{\hat{E}_{IS}} = 0.7\beta^{-0.3} \qquad \text{for } \beta < 0.4$$

$$\frac{\hat{E}_T}{\hat{E}_{IS}} = 0.41\beta^{-0.9} \qquad \text{for } 0.4 < \beta < 0.8$$

$$\frac{\hat{E}_T}{\hat{E}_{IS}} = 0.32\ \beta^{-2.4} \qquad \text{for } 0.8 < \beta < 1.5$$

and

$$\frac{\hat{E}_T}{\hat{E}_{IS}} = 0.76\ \beta^{-4.12} \qquad \text{for } \beta > 1.5$$

Once again one may conclude that the total energy radiated by a pair of colliding spheres is less than kinetic energy of air displaced by the impactee. It may also be interesting to note that since for a pair of colliding steel spheres the ratio ($\rho_o/\rho = 1.5 \times 10^{-4}$), therefore the total radiated energy will never be greater than 1.5×10^{-4} times the kinetic energy of the impactee. This in turn means that only about less than one-six thousandth of the kinetic energy of the impactee may be

radiated as acoustic energy.

9.6. Radiation of sound due to inelastic collision of spheres

A typical force time history for the collision of a 2.54 cm diameter lead sphere is given in Fig.(4.1). Observation of this graph shows that the force increases slowly during the elastic-plastic loading and decays rapidly during the elastic unloading period. The duration of the elastic-plastic period is much greater than the duration of the elastic loading and elastic unloading periods. Thus the major part of the duration of the contact is allocated to the elastic-plastic loading period . For the lead spheres considered in Fig.(4.1) the duration of the contact and duration of the elastic-plastic loading period are 353.7 μs and 331.8 μs, respectively. The analytical and numerical solutions of pressure time history radiated by the impactee are compared in Fig.(4.2). There is a slight difference between both solutions in the region of rarefactive peak and that should be due to the difference of the analytical and numerical estimation of the duration of the elastic-plastic period. Consideration of these graphs also show that a low sound can be radiated until the elastic unloading period is started. This is because of the fact that the accerlation increases slowly. It can also be noticed that because of the abrupt slope of the acceleration more sound can be generated during the elastic unloading period. In Fig.(4.3) is shown the sound presssure radiated by a pair of colliding lead spheres. Unlike the pressure time history of a pair of colliding steel spheres of

the same sizes the amplitude of the second compressive peak is higher than the first one. This is due to slow rate of deceleration of the impactor which prevents a high sound pressure being radiated before the time equal to the time delay plus the time taken for both first and second periods to be completed. The Fourier transform of total pressure time history is shown in Fig.(4.4). The transform peaks at frequencies 2.3 and 4.7 kHz. The transforms of dimensionless pressure time history and acceleration for the impactee are given in Figs.(4.5) and (4.6) respectively. Comparison of these Figures shows that the lesser amplitude peaks in pressure transform are associated with the transform of the acceleration.

9.7. Radiation of sound due to collision of viscoelastic spheres

Typical examples of pressure time history for viscoelastic spheres with the properties described in Table 5.1. are given in Figs.(5.1) to (5.3). The force time history due to collision of viscoelastic and steel spheres for each example are also given in Fig.(5.4). Observation of these graphs indicate that the amplitude of the peak pressure increase as the amplitude of the force increase and shorter contact durations register shorter pressure time traces. In Fig.(5.5) is shown the transform for the pressure time result given in Fig.(5.3). The position of the main peak and lesser amplitude peaks may be approximately given by $\frac{63.3}{a}\beta^{-0.55}$, 2/d, 3/d and etc. respectively.

9.8. Vibration of solid and hollow spheres

The radial displacement for torsional vibration is zero. Thus the motion except case of zonal harmonic (m = 0) is a combination

of two displacements, namely u_θ and u_ψ . The radial dependent function appearing in both u_θ and u_ψ expressions are identical. Distribution of normalised radial dependent functions along the radius of spheres for different values of n and ℓ are given in Figs.(6.1) and (7.1). The nodal points give the position of spherical surfaces across which there is no displacement. The number of these surfaces depend on ℓ and may be expressed as ℓ-1. The fundamental mode for given n is that with ℓ = 1. If n >2 distribution of radial dependent function of displacement for fundamental mode registers no node. Thus by analogy for n = 1 there is no fundamental mode. In Fig.(6.2) the surface mode shapes are given for different values of n and m. If n = 1, m must be either zero or one and the surface motion corresponding to these values of n and m are simply rotation about one of the axis. In case n = 2 and m = 0, the upper and lower hemispheres of surface rotate in opposite directions and a nodal circle can be formed.

For spheroidal vibrations the motion, except for case of zonal harmonic (m = 0) is a combination of three displacements, namely u_r, u_θ and u_ψ. The radial dependent function in both u_θ and u_ψ expressions are identical. Distribution of radial dependent functions appearing in u_r and u_θ expressions for different values of n and are given in Figs.(6.3),(6.4), (7.2) and (7.3). The number of spherical surfaces across which there is no displacement, apart from the case n = 0, can no longer be given by ℓ-1. As well as torsional vibration there should be

no fundamental mode corresponding to case n = 1. Regardless of value of m (m = 0, or m = 1) the motion in case n = 1 is merely translation in direction of one of the axis. Such motion is not a free oscillation and needs an external force to be sustained. Thus the frequency equation has no root corresponding to $\ell = 1$. This in turn explains why there is no fundamental mode corresponding to case n = 1. In Fig.(6.5) the surface mode shapes are given for different values of n and m. All the points undergo oscillation and no nodal point exists.

9.9. Experimental Results

As the theory indicates the pressure-time history generated by a pair of colliding spheres is a function of angle θ. Thus the agreement between theoretical and experimental results should be examined for different angles. The agreement also depends on how accurately results could be predicted by the ray theory assumption. The theoretical and measured pressure-time traces are compared in Figs.(9.1) to (9.4). The results agree well for $\theta = 0^{o}$, 40^{o}, and 60^{o}. For $\theta = 90^{o}$ discrepancy can be observed and this might be due to reflection of sound wave between colliding spheres.

The theoretical and measured Fourier transform of pressure time histories as a function of angle (θ) are compared in Figs.(9.5) to (9.8). The predicted result was obtained by using D.F.T. method; and the resolution was chosen to be the same as the one selected on the Fourier analyser. Once again the experimental results verify the theoretical ones for all angles except for $\theta = 90^{o}$.

The value of f_{max} for which the transform peak occurs confirms the relation $f_{max} = \frac{76.4}{a}$, suggested previously. In Fig.(9.9) the measured transforms for various sizes of spheres are shown. The transforms peak at frequencies 6, 3 and 1.1 kHz, which are inversely proportional with the radii of spheres. Observation of Fig.(9.10) showing measured transforms as a function of angle θ also indicates that the position of transform peak is independent of θ. The pressure transform for a 5.08 cm diameter colliding sphere is shown in Fig.(9.11). Peaks at frequencies 55 and 82 kHz respectively correspond to the first and second lowest fundamental frequencies of spheroidal vibration of a sphere. The theoretical and experimental polar distribution of both compressive and rarefactive peaks compared in Fig.(9.12) and (9.13). Measured and predicted compressive peaks agree well for all except $\theta = 80^{o}$ and 90^{o}. Once again the reflection of the sound wave between colliding spheres could be the cause of the discrepancy. For the rarefactive peak the agreement also very much depends on the accuracy with which one can predict the time delay between arrival of the sound from impactee and the impactor. In Fig.(9.14) both predicted and measured energy integrations are compared and good agreement can be observed. The compressive and rarefactive peaks are respectively plotted logarithmically in Figs.(9.15) and (9.16) as a function of velocity for $\theta = 0^{o}$. The graphs are straight lines with slope 1.2.

The logarithmic plots of measured and predicted energy integration as a function of velocity for $\theta = 0^{o}$ and $\theta = 40^{o}$ are

compared in Figs.(9.17) and (9.18). These logarithmic plots suggest that the energy integration is proportional to the impact velocity to the power 2.4.

The measured and predicted Fourier transform of acceleration are compared in Figs.(9.20) to (9.23). Predicted results are obtained by using equation (6.169) with no damping. Thus the finite peak values, as ω tends to $\omega_{n\ell}$, are due to the selection of resolution frequency and can be varied by variation of the resolution frequency. All modes up to frequency of 70 kHz are included in predicted results. For the lower modes there is a reasonable degree of agreement between the theoretical and experimental results. However discrepancy appearing in higher modes is rather peculiar. In the comparison of the predicted and measured results the resolution in the D.F.T. is the same, and hence any leakage losses should be the same. Thus a direct comparison may be made between theory and experiment in Figs. (9.24) and (9.25). In both theoretical and experimental curves no absolute values can be assumed. The results can only be regarded as a guide to actual response levels.

9.10. Conclusions

Conclusions with regard to rigid body sound are:

1) The force-time history for the case of elastic collision of spheres can be approximately given by a half sine pulse even when vibratory terms are included.

2) Both compressive and rarefactive peaks for an impulsively accelerated sphere decrease as θ increases.

3) The pressure-time curve of a pulsating sphere forms no rarefactive peak and it is also independent of θ.

4) The aerodynamic approach for predicting the sound of an impulsively accelerated sphere has been compared with the exact solution and found to agree very closely.

5) Empirical formula relating peak pressure and dimensionless contact time have been found for a single sphere undergoing a Hertzian acceleration.

6) The equation involving the dimensionless contact time and the impact velocity together with the empirical formula enables one to predict the peak pressure when one or some of the characteristics of colliding spheres, such as size, modulus of elasticity, etc., are known.

7) For the collision of the metallic spheres the peak pressure generated by a single sphere occurs after a time less than the duration of the contact of that particular collision.

8) Empirical formulae relating peak of Fourier transform and dimensionless contact time have been found for a single sphere undergoing a Hertzian acceleration.

9) Empirical formulae relating frequency associated with the peak of transform and dimensionless contact time have been found for a single sphere undergoing a Hertzian acceleration.

10) A typical sound pressure-time trace for a pair of colliding spheres is like a damped sine wave. The initial peak might be compressive or rarefactive followed by a secondary peak normally higher than the initial one.

11) Depending upon whether the initial peak is compressive or rarefactive the secondary peak is either rarefactive or compressive respectively.

12) For most of the duration of the collision of equal radii metallic spheres the first compressive peak at $\theta = 0^{o}$ would be unaffected by the pressure contribution of the second sphere.

13) Empirical formulae relating the dimensionless rarefactive peak amplitude and dimensionless contact time have been found for a pair of similar spheres of equal sizes. The dimensionless time for which the rarefactive peak occurs is also investigated and expressed empirically in terms of dimensionless contact time.

14) The directional distribution of the sound radiated by a pair of colliding spheres of equal sizes is symmetrical about a line joining the centres of the spheres and about a line perpendicular to this line through the contact point. The directional distribution of the sound for a pair of colliding spheres of unequal sizes is also symmetrical about a line joining the centres of the spheres and no symmetry about the perpendicular direction exists.

15) Empirical formula relating frequency at which the peak of transform occurs and dimensionless contact time have been found for a pair of colliding spheres.

16) Energy radiated by an impulsively accelerated sphere is equal to half the kinetic energy of air displaced by the sphere.

17) Empirical formula relating energy and dimensionless contact time are given for a sphere undergoing a Hertzian acceleration.

18) For spheres of the same size energy never exceeds the kinetic energy of air displaced by the impactee.

19) The total energy radiated by a pair of colliding steel spheres will never be greater than 1.5×10^{-4} times the kinetic energy of the impactee.

20) The sound pressure in the far field has been calculated for plastic and visco-elastic spheres.

21) The sound pressure due to collision of a pair of visco-elastic spheres of the same material may be found by assuming each sphere individually colliding with a rigid massive metallic plane with an initial relative velocity equal to half the relative velocity of the spheres.

22) Materials which are similar when judged by their static rigidity may behave differently as radiators of sound if their visco-elastic functions are not the same.

23) Numerical methods given for the visco-elastic case may also be applied for elastic case by simply assuming $\tau_i = \infty$.

Conclusions with respect to transient vibration sound are:-

1) Orthogonality conditions have been shown to be satisfied for both torsional and spheroidal modes.
2) The response of spheres to any excitation could be calculated and has been calculated for step acceleration functions and Hertzian acceleration function.
3) Modal shapes have been established and illustrated graphically.
4) The sound pressure due to transient vibration of spheres has been calculated.
5) Theoretical and experimental results are compared and their compatibility has been discussed.

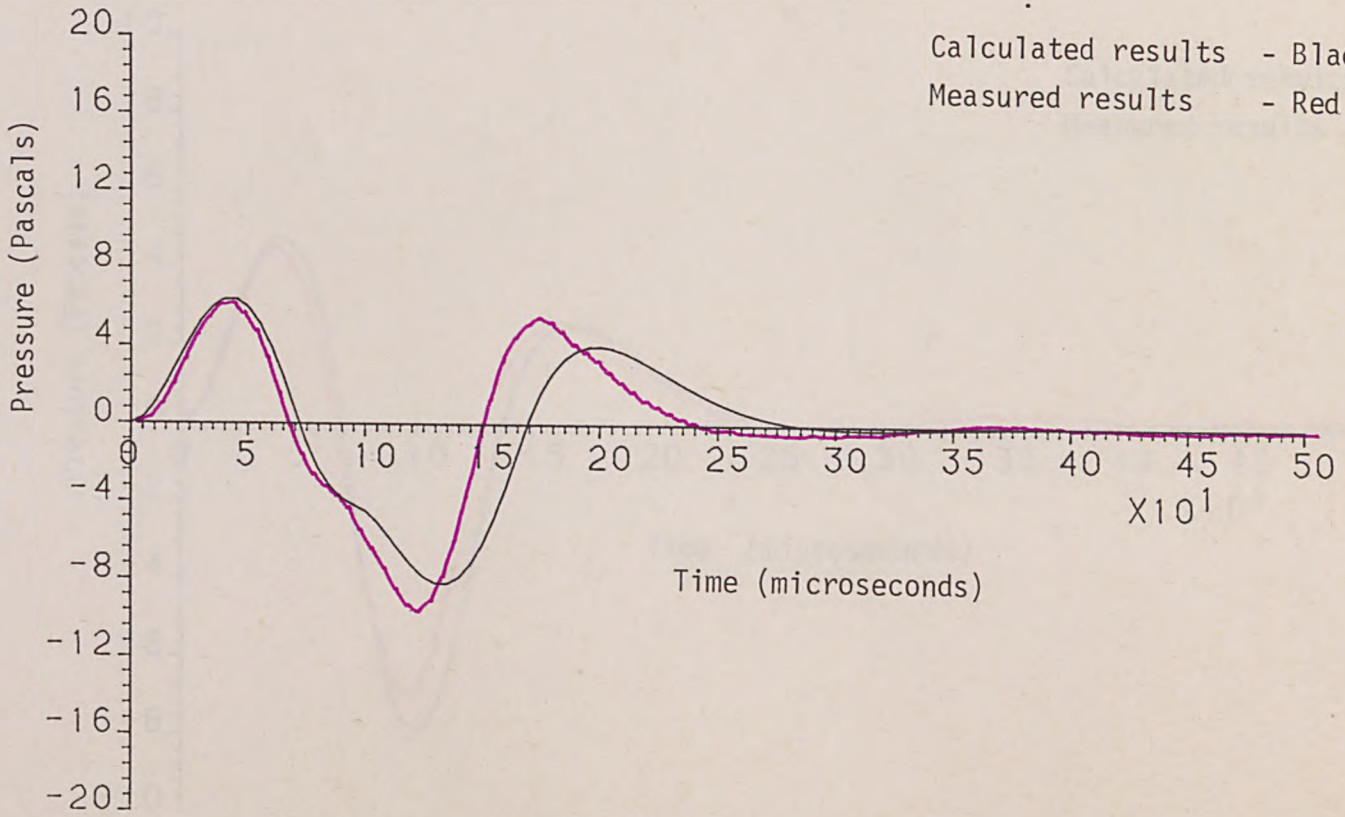

FIGURE 9.1. COMPARISON OF MEASURED PRESSURE TIME RESULTS AND CALCULATED RESULTS FOR 2.54 cm DIAMETER SPHERES. (v_o = 1.5 m/s, $\theta = 0^o$, r = 0.375 m)

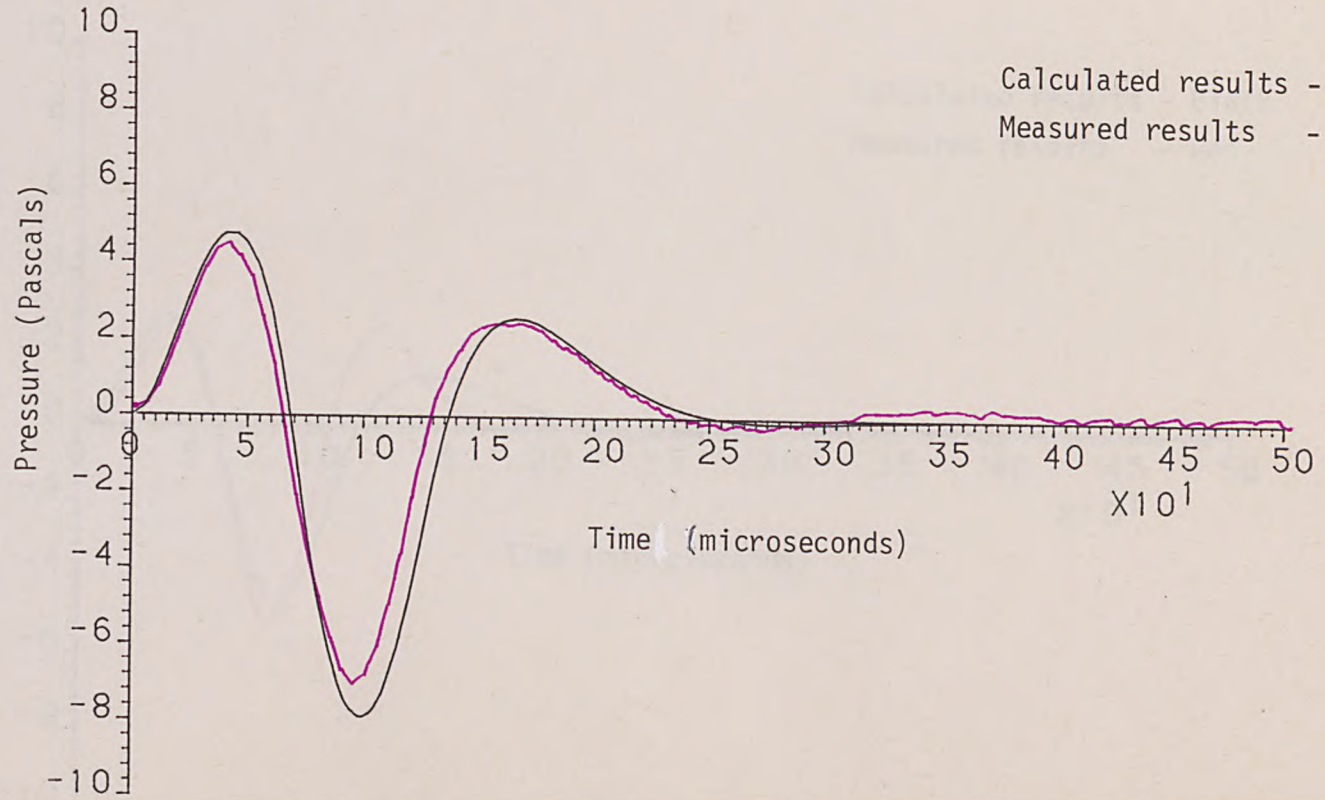

FIGURE 9.2. COMPARISON OF MEASURED PRESSURE TIME RESULTS AND CALCULATED RESULTS FOR 2.54 cm DIAMETER SPHERES. (v_o = 1.5 m/s, θ = 40°, r = 0.375 m)

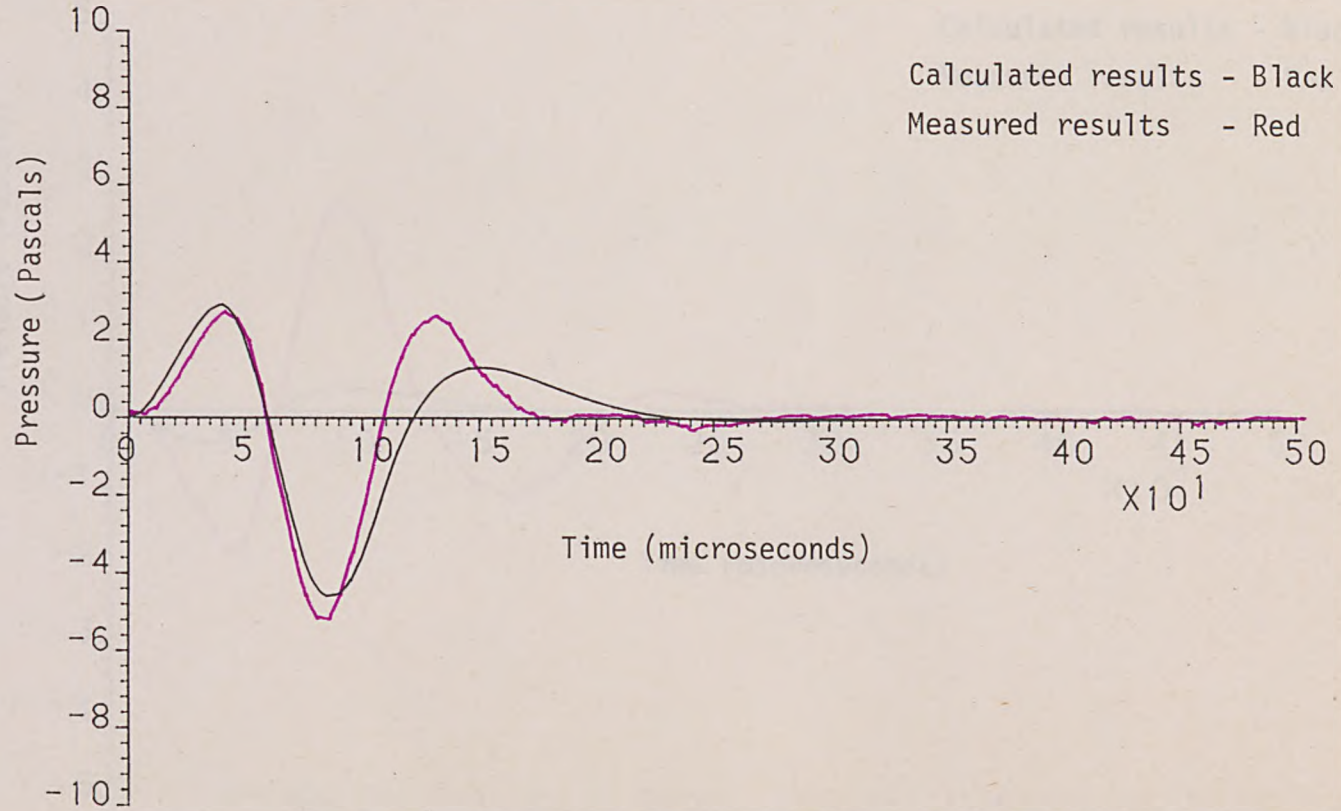

FIGURE 9.3. COMPARISON OF MEASURED PRESSURE TIME RESULTS AND CALCULATED RESULTS FOR 2.54 cm DIAMETER SPHERES. (v_o = 1.5 m/s, $\theta = 60^o$, r = 0.375 m)

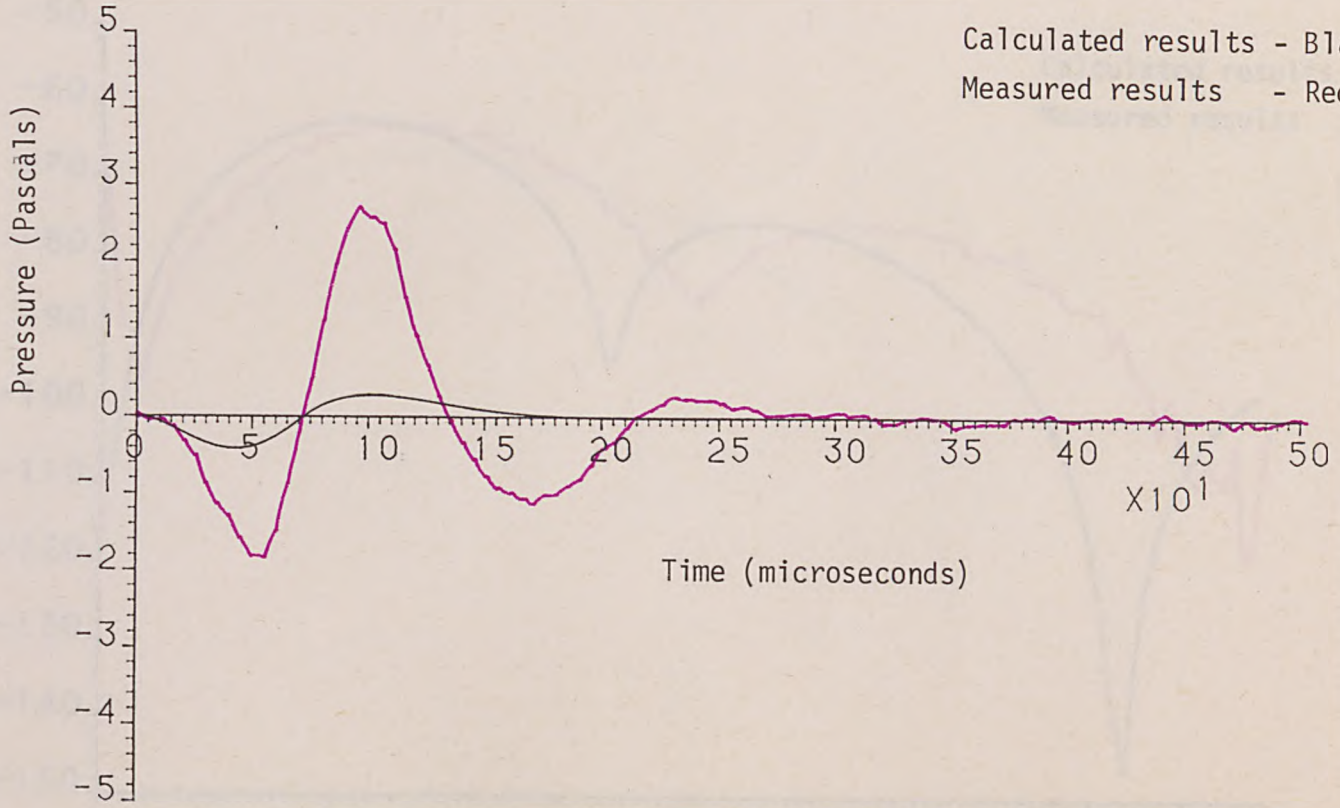

FIGURE 9.4. COMPARISON OF MEASURED PRESSURE TIME RESULTS AND CALCULATED RESULTS FOR 2.54 cm DIAMETER SPHERES. (v_o = 1.5 m/s, $\theta = 90^o$, r = 0.375 m)

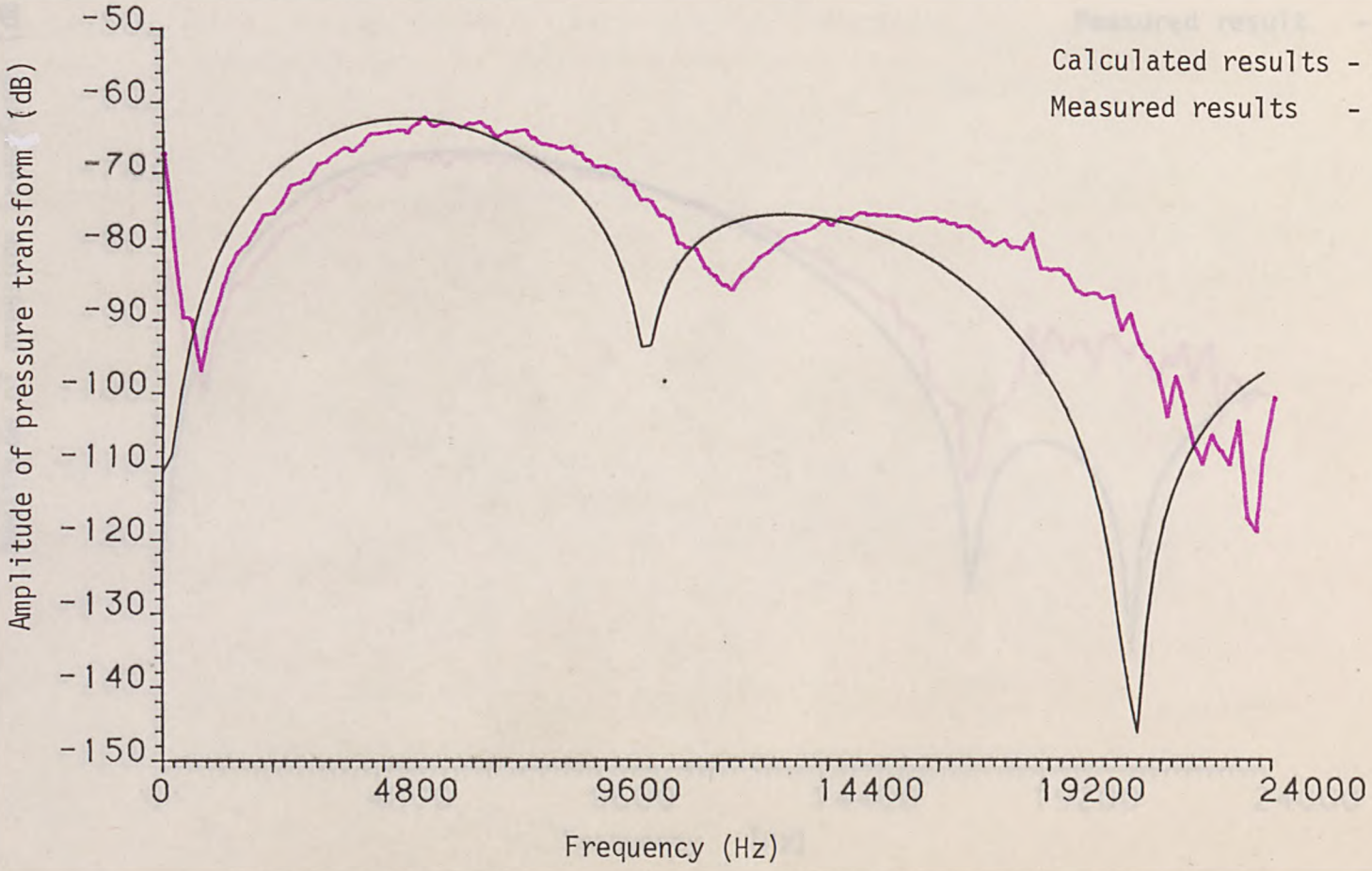

FIGURE 9.5. COMPARISON OF MEASURED FOURIER TRANSFORM PRESSURE RESULT AND CALCULATED RESULT FOR 2.54 cm DIAMETER SPHERES. (v_o = 1.5 m/s, $\theta = 0^o$, r = 0.375 m)

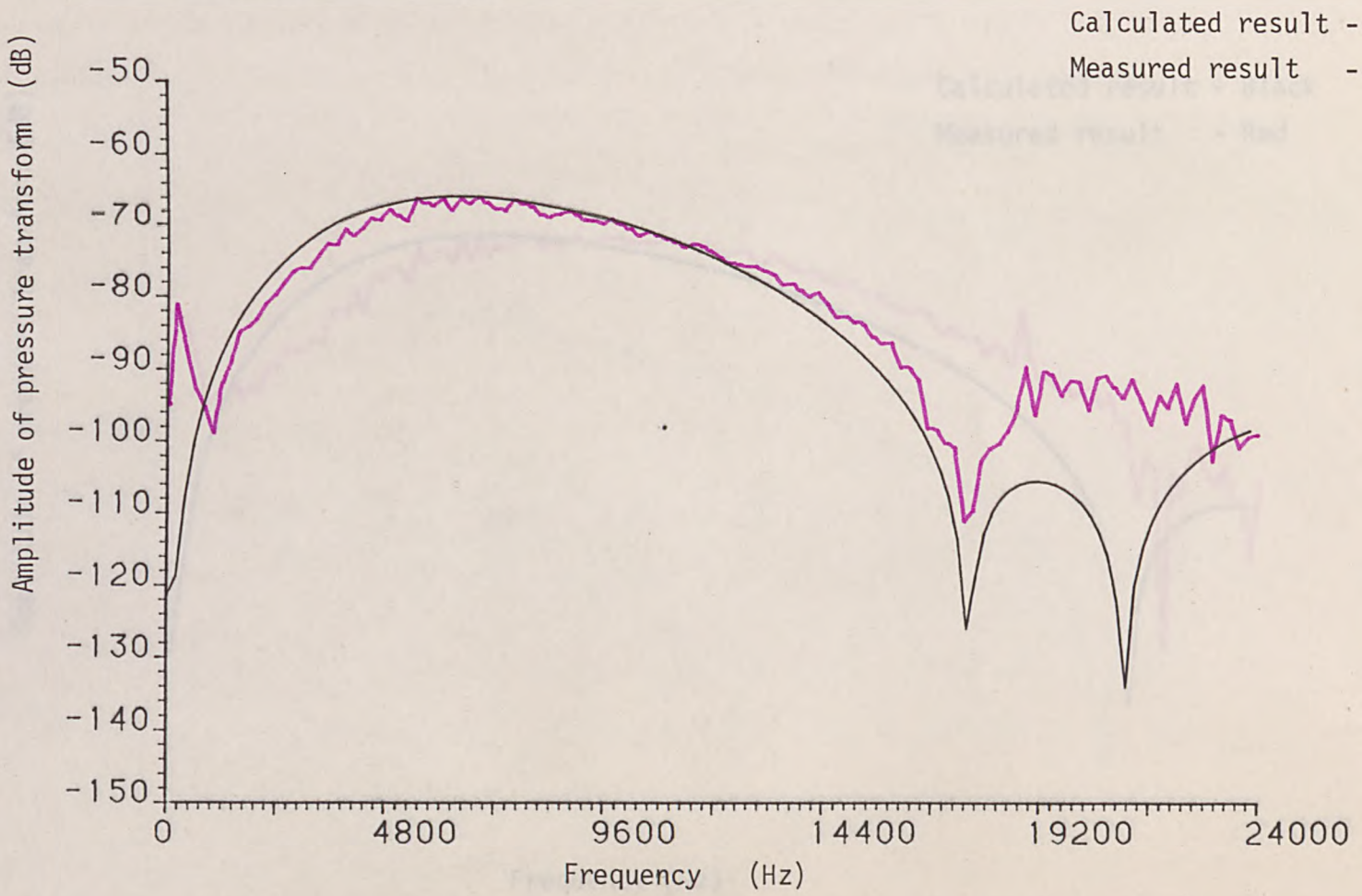

FIGURE 9.6. COMPARISON OF MEASURED FOURIER TRANSFORM PRESSURE RESULT AND CALCULATED RESULT FOR 2.54 cm DIAMETER SPHERES. (v_o = 1.5 m/s, $\theta = 40^o$, r = 0.375 m)

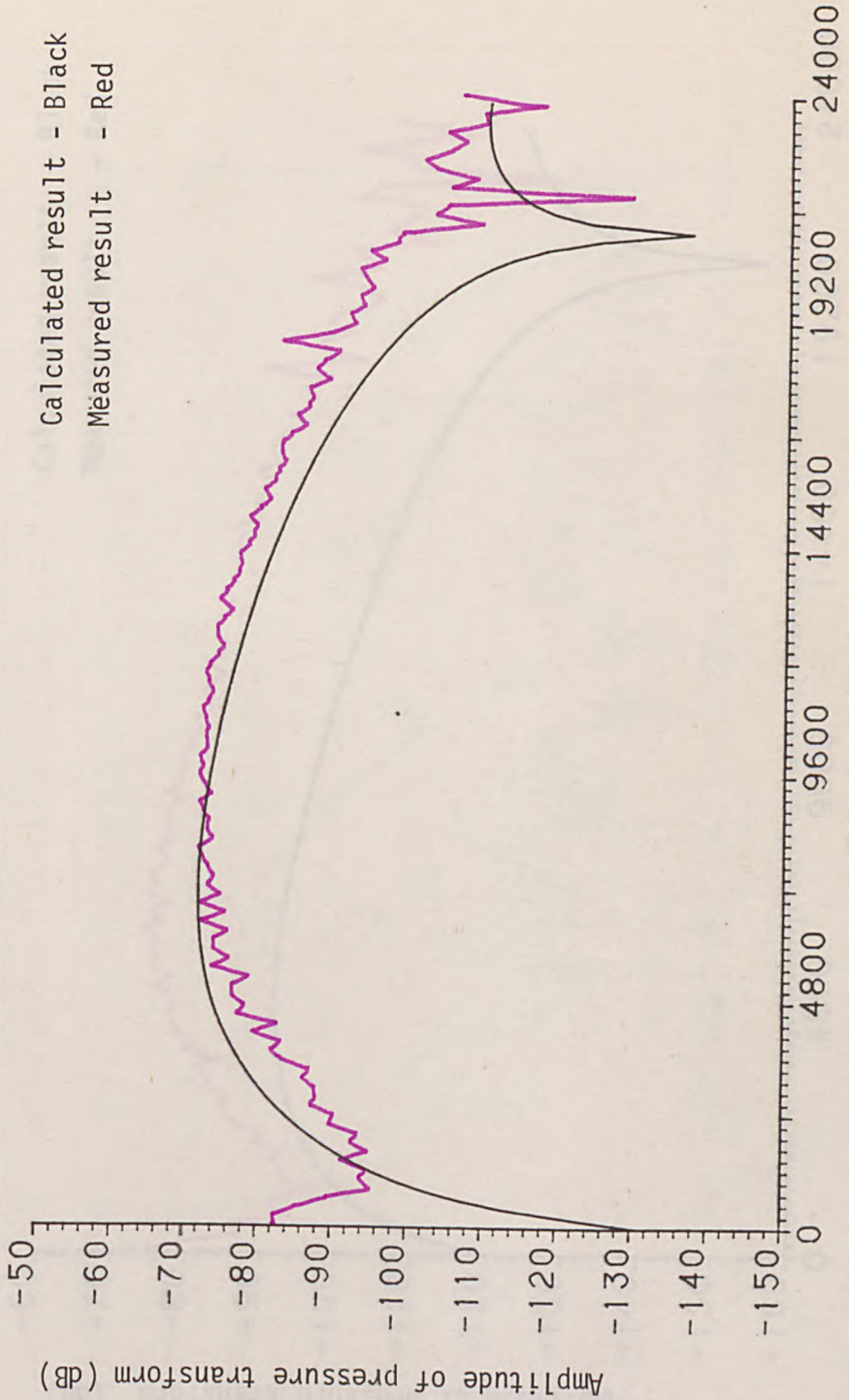

FIGURE 9.7. COMPARISON OF MEASURED FOURIER TRANSFORM PRESSURE RESULT AND CALCULATED RESULT FOR 2.54 cm DIAMETER SPHERES. ($\dot{y}_o$ = 1.5 m/s, $\theta = 60^o$, r = 0.375 m)

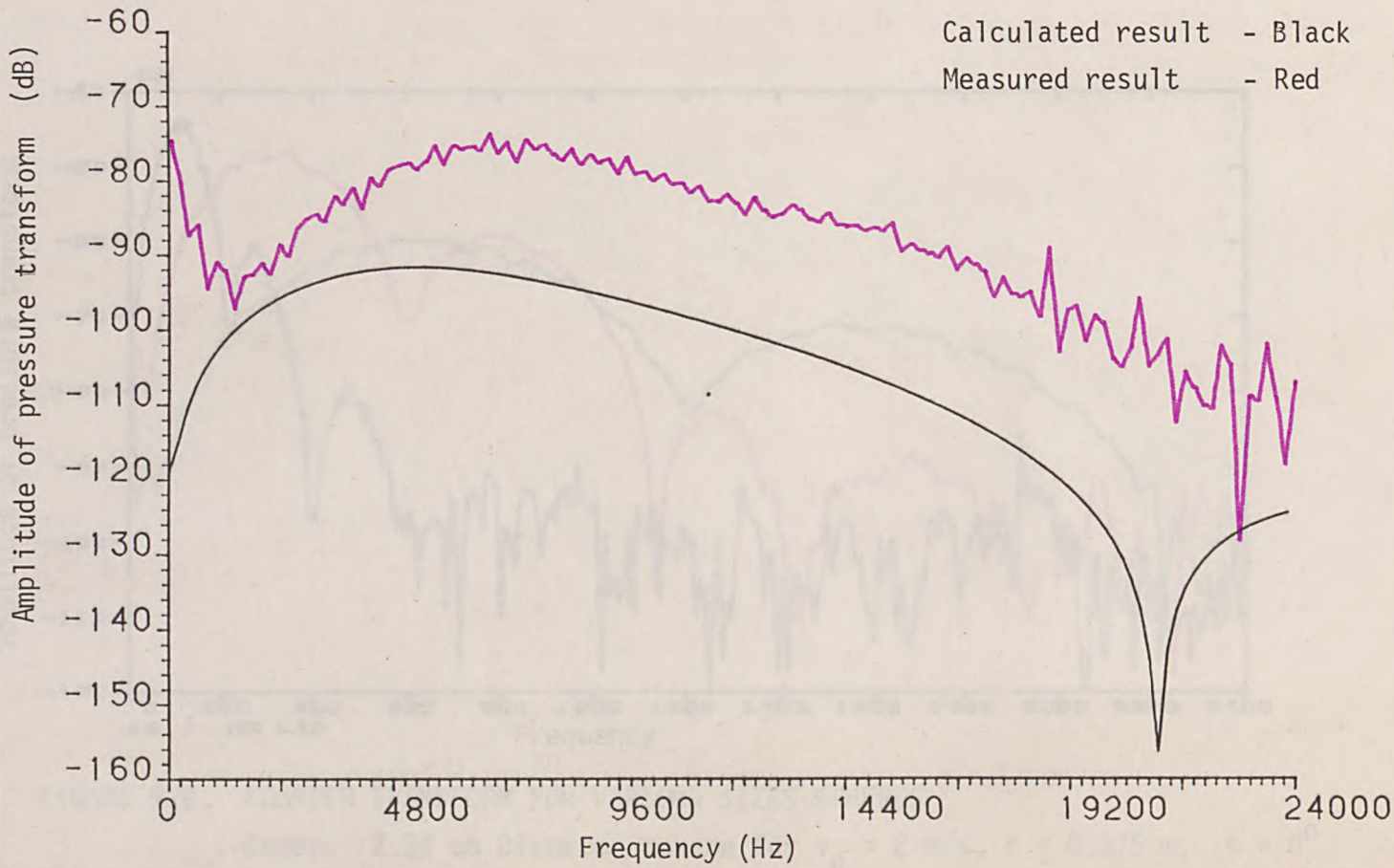

FIGURE 9.8. COMPARISON OF MEASURED FOURIER TRANSFORM PRESSURE RESULT AND CALCULATED RESULT FOR 2.54 cm DIAMETER SPHERES. (v_o = 1.5 m/s, $\theta = 90^o$, r = 0.375 m)

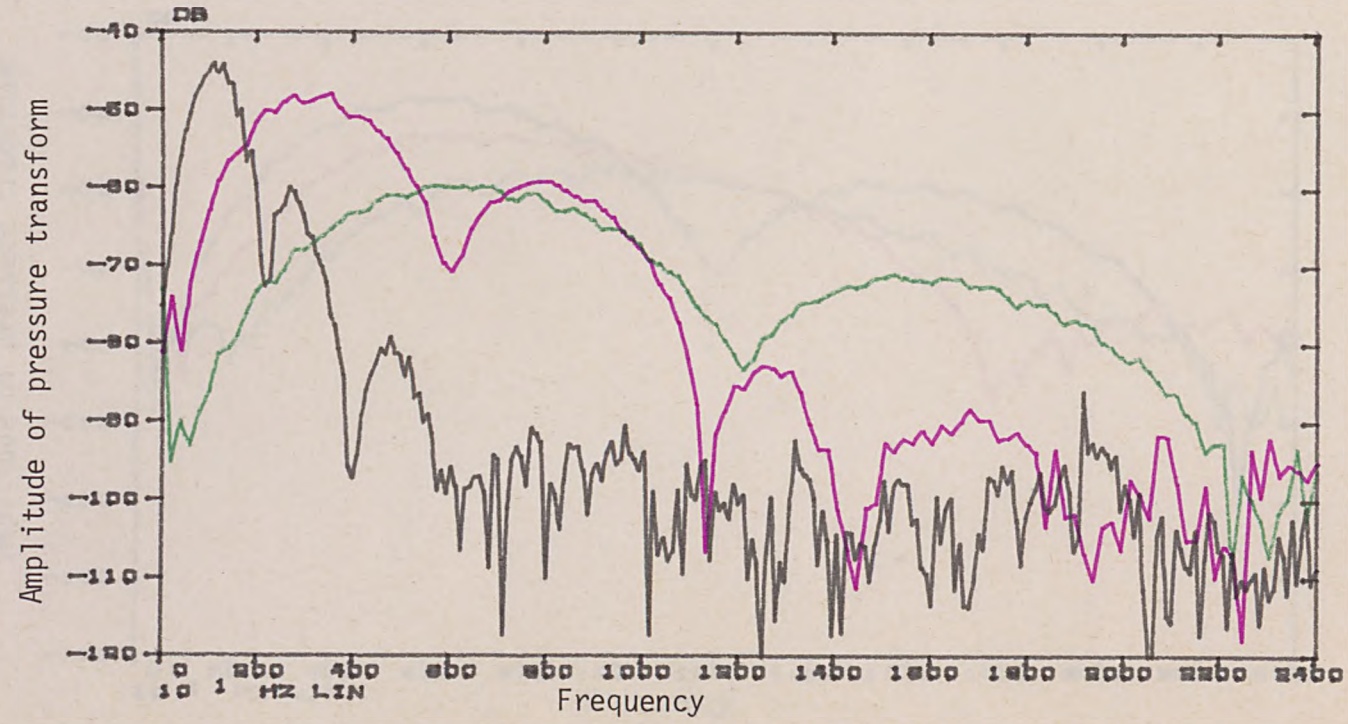

FIGURE 9.9. FOURIER TRANSFORM FOR VARIOUS SIZES SPHERES

Green: 2.54 cm Diameter sphere for v_o = 2 m/s, r = 0.375 m, $\theta = 0^o$

Red: 5.08 cm Diameter sphere for v_o = 2 m/s, r = 0.415 m, $\theta = 0^o$

Black: 14.0 cm Diameter sphere for v_o = 1 m/s, r = 0.8 m, $\theta = 0^o$

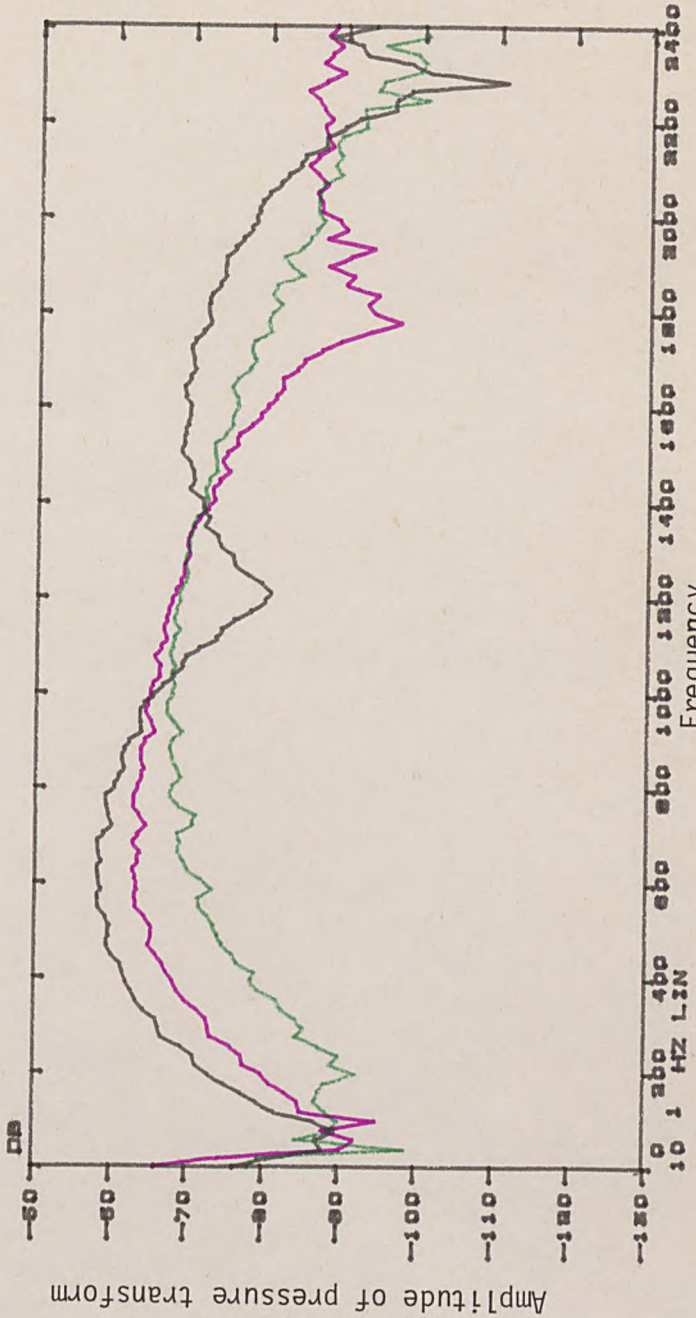

FIGURE 9.10. FOURIER TRANSFORM COMPARISON FOR 2.54 cm DIAMETER SPHERES AS A FUNCTION OF THE ANGLE θ FOR v_o = 2.5 m/s, r = 0.375 m, Black: $\theta = 0^o$, Red: $\theta = 40^o$, Green: $\theta = 60^o$

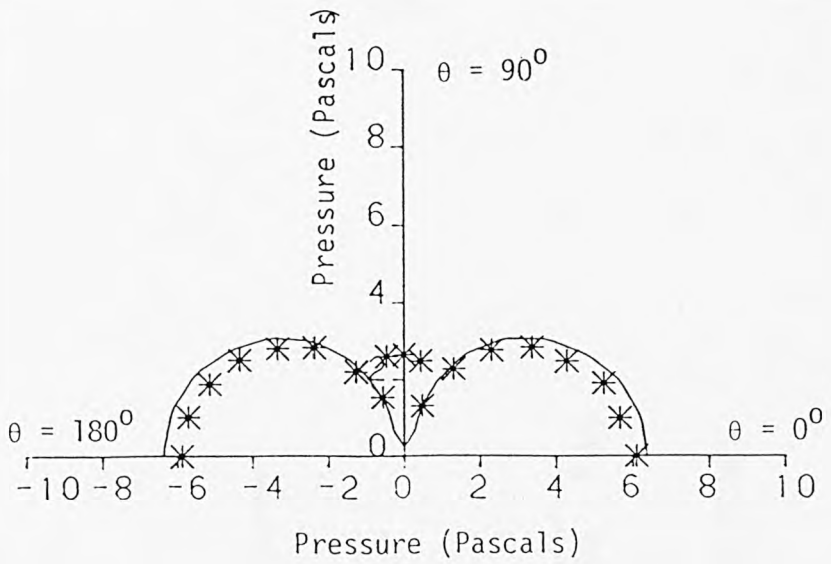

FIGURE 9.12. POLAR DISTRIBUTION OF POSITIVE PEAK PRESSURE FOR 2.54 cm DIAMETER SPHERES.
(v_o = 1.5 m/s, r = 0.375 m)
* Measured; __ Calculated.

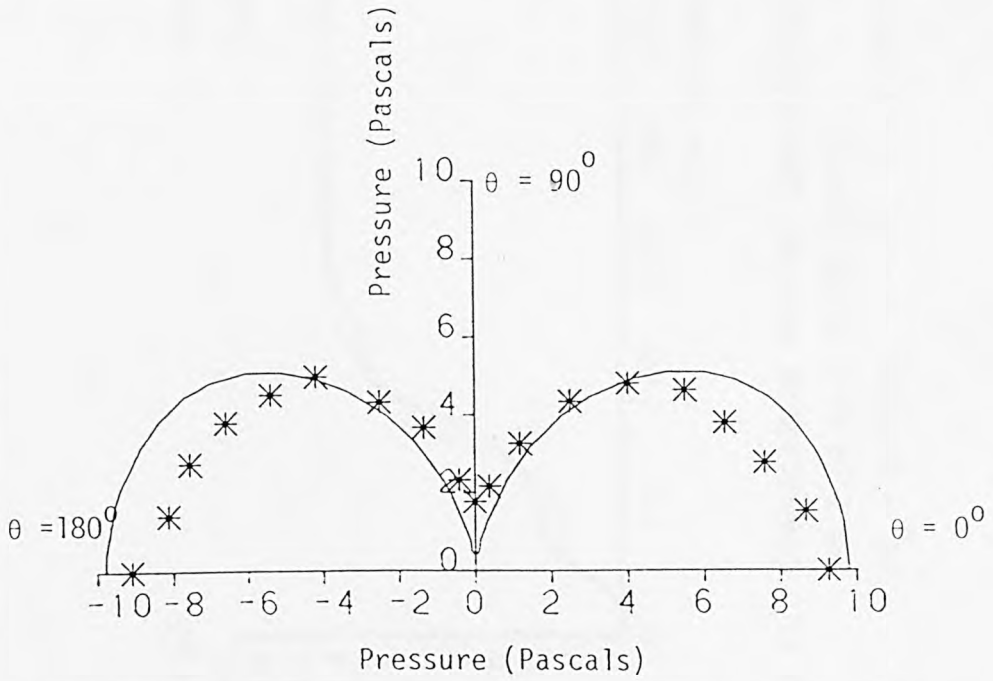

FIGURE 9.13. POLAR DISTRIBUTION OF NEGATIVE PEAK PRESSURE FOR 2.54 cm DIAMETER SPHERES.
(v_o = 1.5 m/s, r = 0.375 m)
* Measured; _____ Calculated.

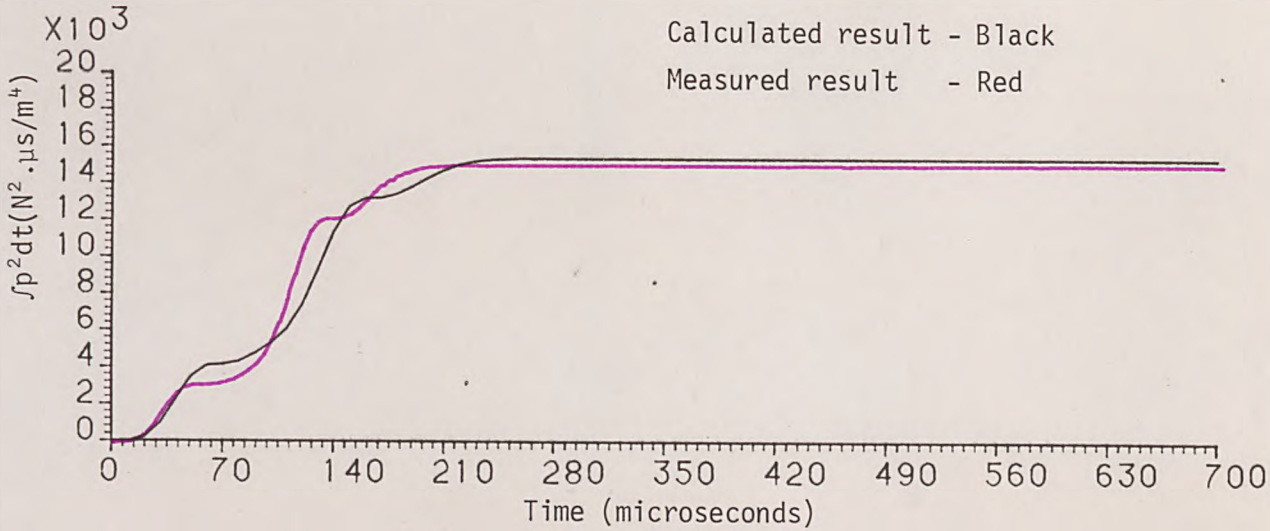

FIGURE 9.14. COMPARISON OF MEASURED ENERGY INTEGRATION RESULT AND CALCULATED RESULT FOR 2.54 cm DIAMETER SPHERES.
(v_o = 2.5 m/s, $\theta = 0^o$, r = 0.375 m)

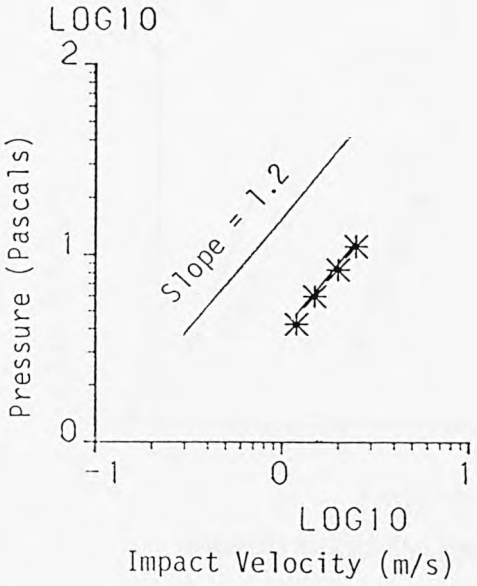

FIGURE 9.15. POSITIVE PEAK PRESSURE VS IMPACT VELOCITY FOR 2.54 cm DIAMETER SPHERES.
($r \fallingdotseq 0.375$, $\theta = 0^{o}$)
* Measured; _____Calculated.

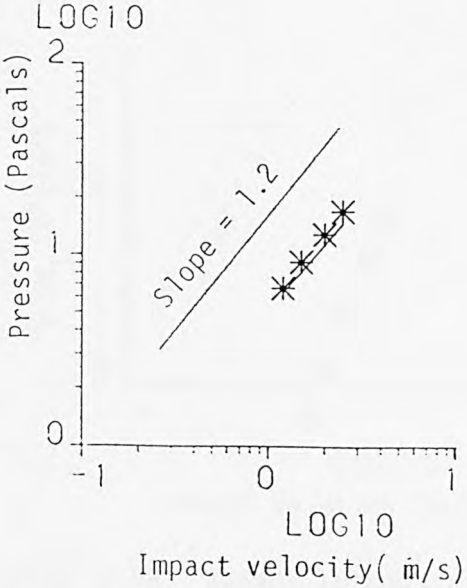

FIGURE 9.16. NEGATIVE PEAK PRESSURE VS IMPACT VELOCITY FOR 2.54 cm DIAMETER SPHERES.
($r = 0.375$ m, $\theta = 0^{o}$)
* Measured; ____ Calculated.

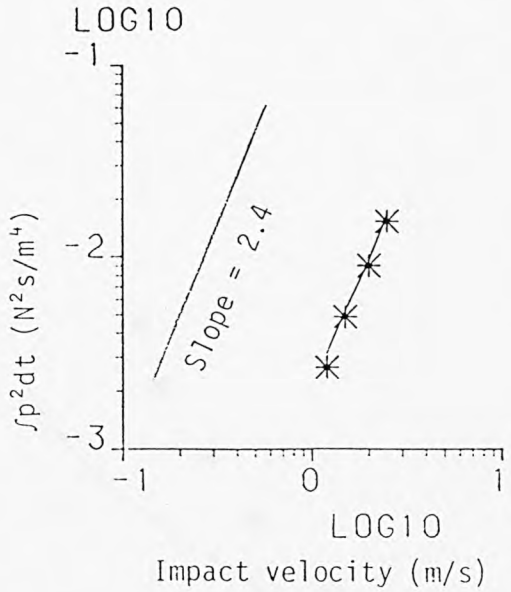

FIGURE 9.17. ENERGY INTEGRATION VS IMPACT VELOCITY FOR 2.54 cm DIAMETER SPHERES.
(r = 0.375 m, $\theta = 0^o$)
* Measured; ____ Calculated.

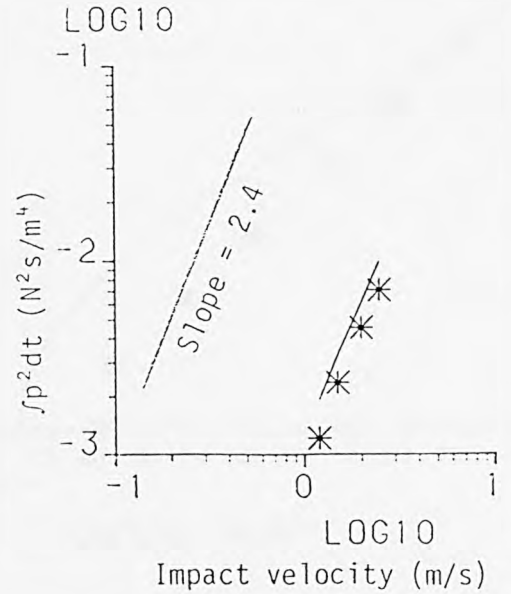

FIGURE 9.18. ENERGY INTEGRATION VS IMPACT VELOCITY FOR 2.54 cm DIAMETER SPHERES.
(r = 0.375 m, $\theta = 40^o$)
* Measured; ____ Calculated.

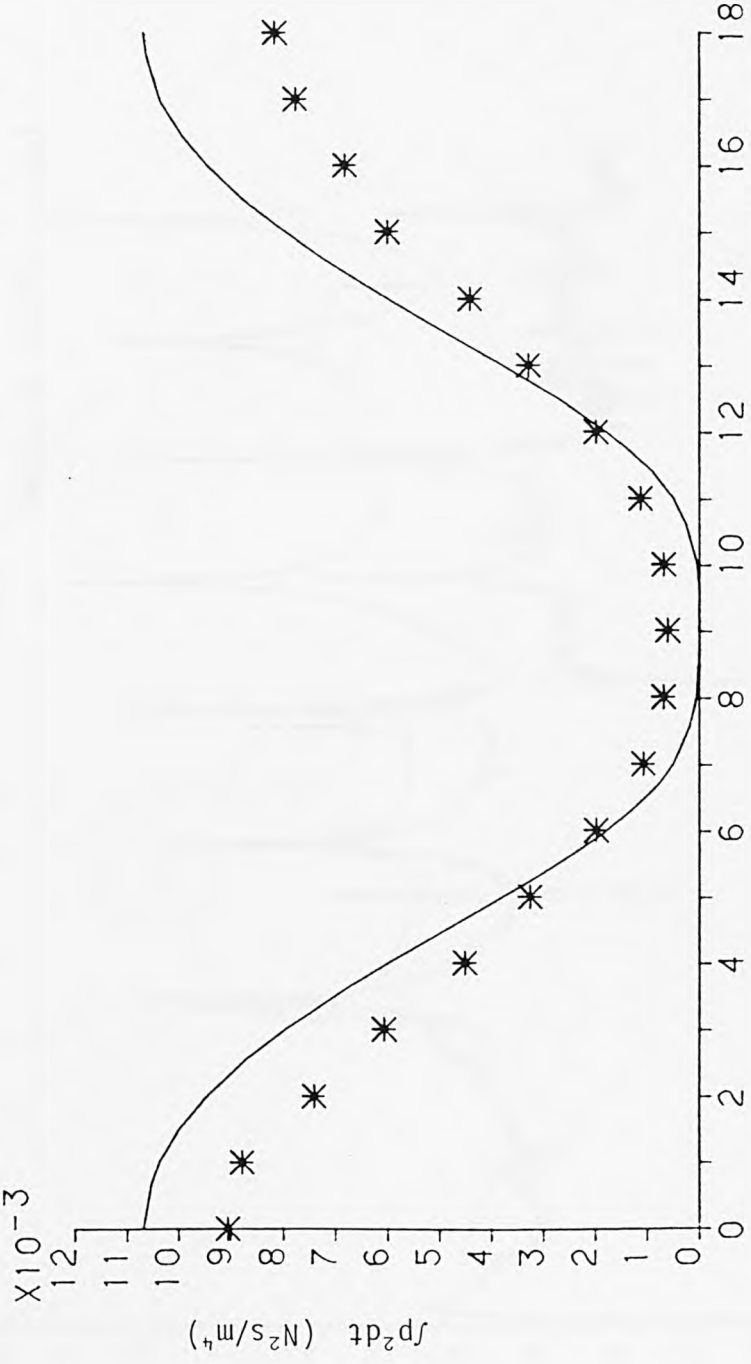

FIGURE 9.19. DISTRIBUTION OF ENERGY INTERGRATION FOR 2.54 cm DIAMETER SPHERES
($r = 0.375$ m, $v_o = 2$ m/s)
* Measured; _____ Calculated.

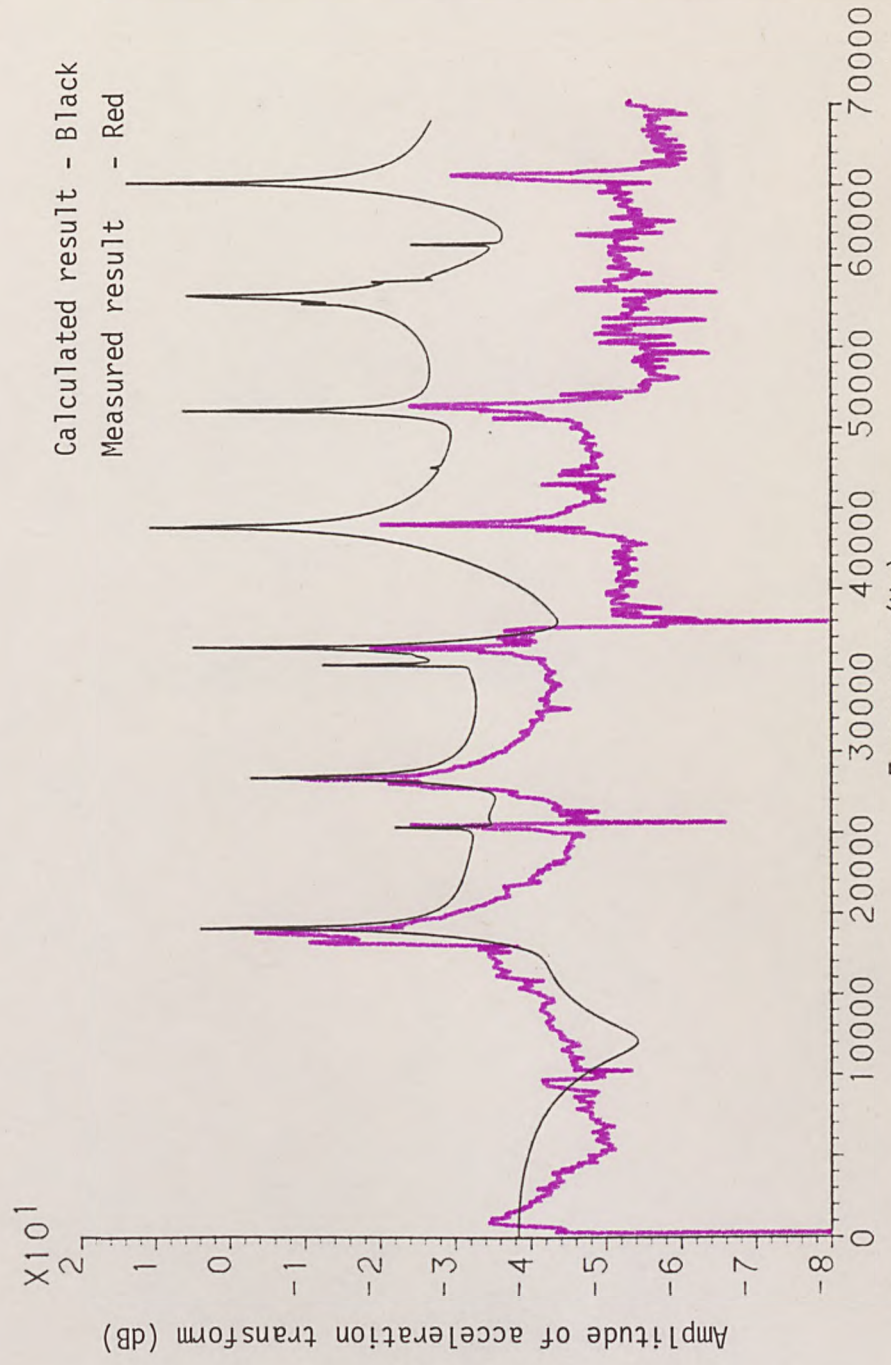

FIGURE 9.20. COMPARISON OF MEASURED FOURIER TRANSFORM ACCELERATION RESULT AND CALCULATED RESULT FOR IMPACTEE OF RADIUS 7.1 cm AT POSITION r = 7.1 cm and $\theta = 0^{o}$. (Impactor radius = 1.27 cm, initial velocity = 100 cm/s)

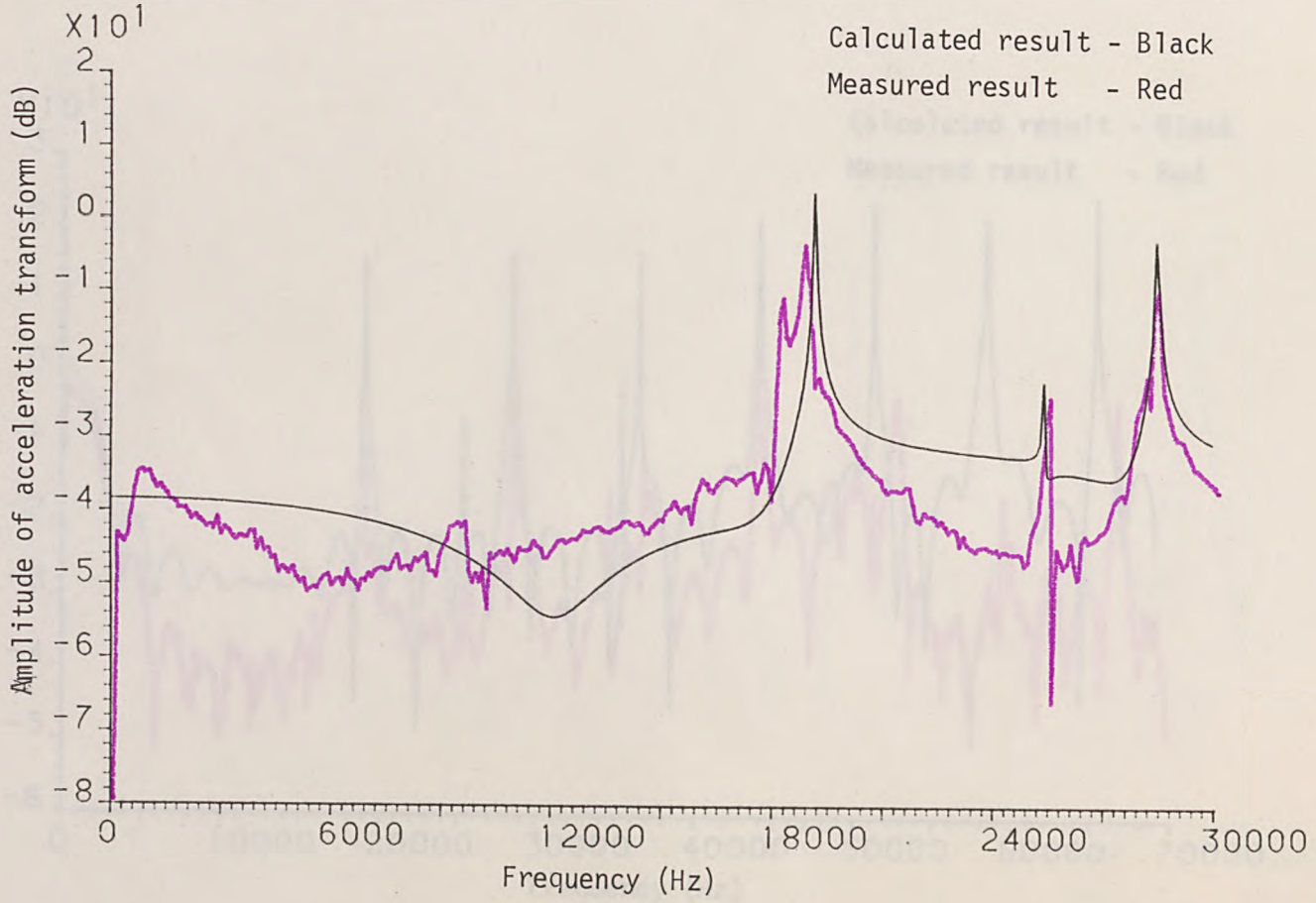

FIGURE 9.21. COMPARISON OF MEASURED FOURIER TRANSFORM ACCELERATION RESULT AND CALCULATED RESULT FOR IMPACTEE OF RADIUS 7.1 cm AT POSITION r = 7.1 cm and $\theta = 0^{o}$.
(Impactor radius = 1.27 cm, initial velocity = 100 cm/s)

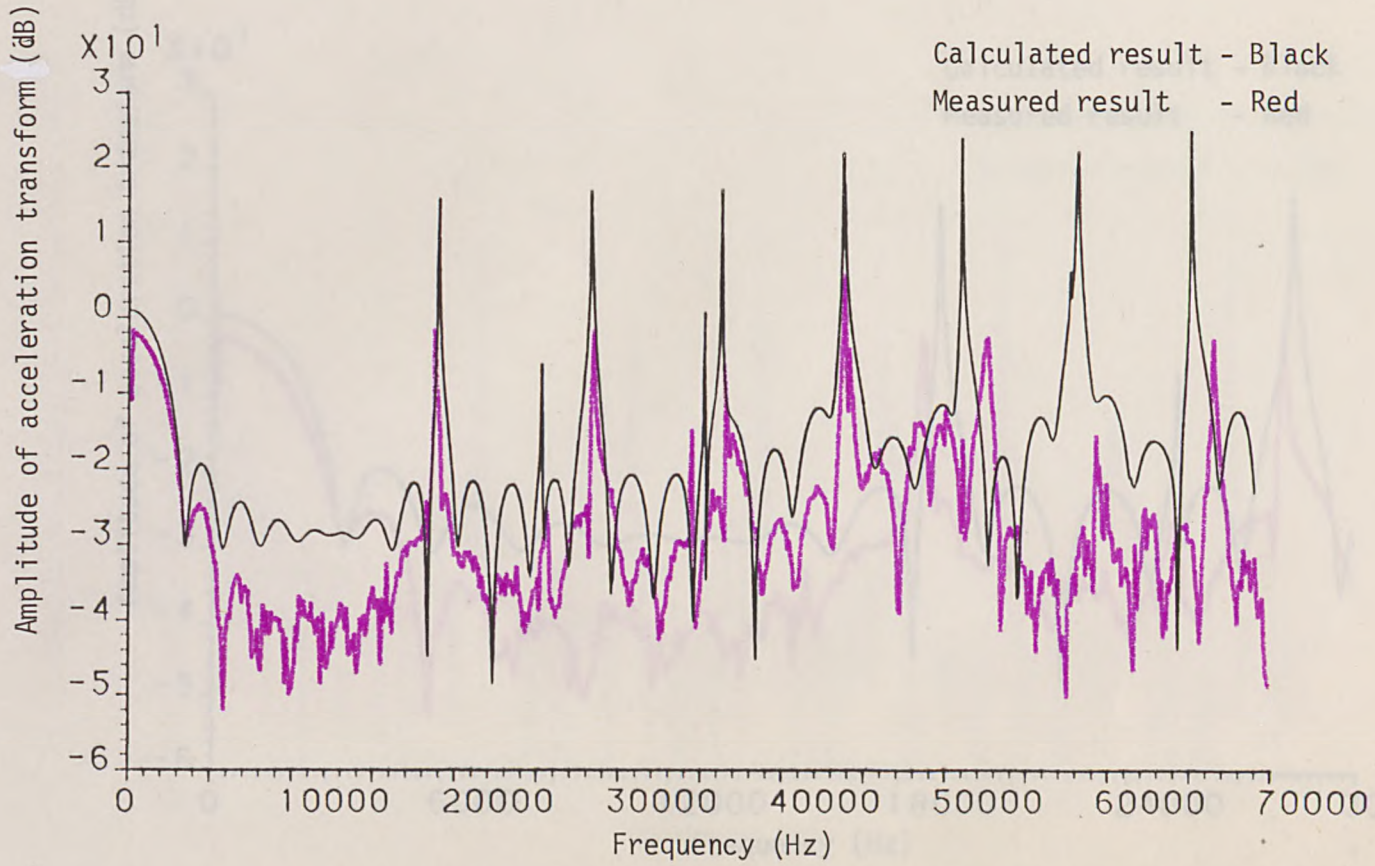

FIGURE 9.22. COMPARISON OF MEASURED FOURIER TRANSFORM ACCELERATION RESULT AND CALCULATED RESULT FOR IMPACTEE OF RADIUS 7.1 cm AT POSITION r = 7.1 cm and $\theta = 0^{o}$. (Impactor radius = 7.1 cm, initial velocity = 100 cm/s)

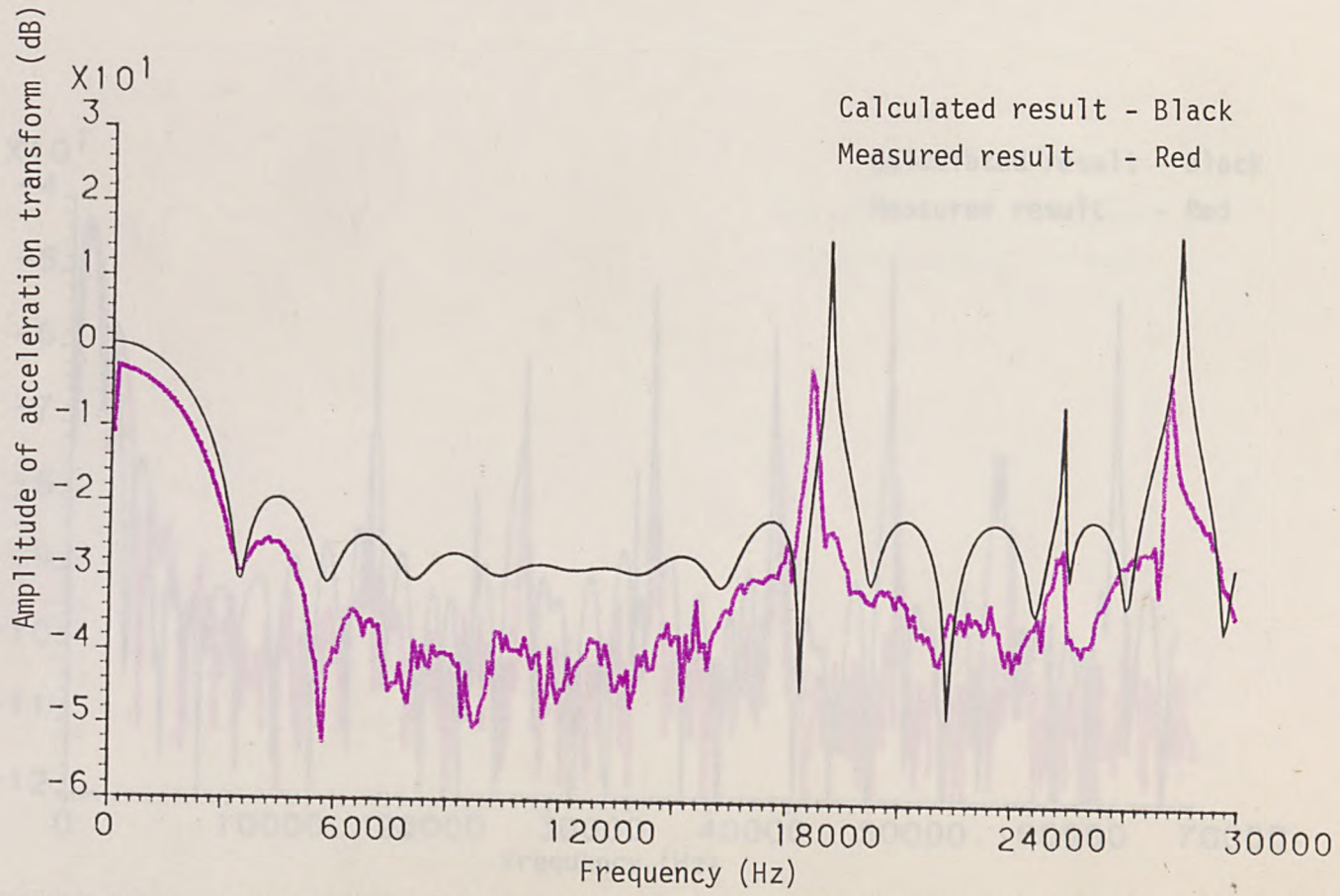

FIGURE 9.23. COMPARISON OF MEASURED FOURIER TRANSFORM ACCELERATION RESULT AND CALCULATED RESULT FOR IMPACTEE OF RADIUS 7.1 cm AT POSITION r = 7.1 cm and $\theta = 0^{o}$.
(Impactor radius = 7.1 cm, initial velocity = 100 cm/s)

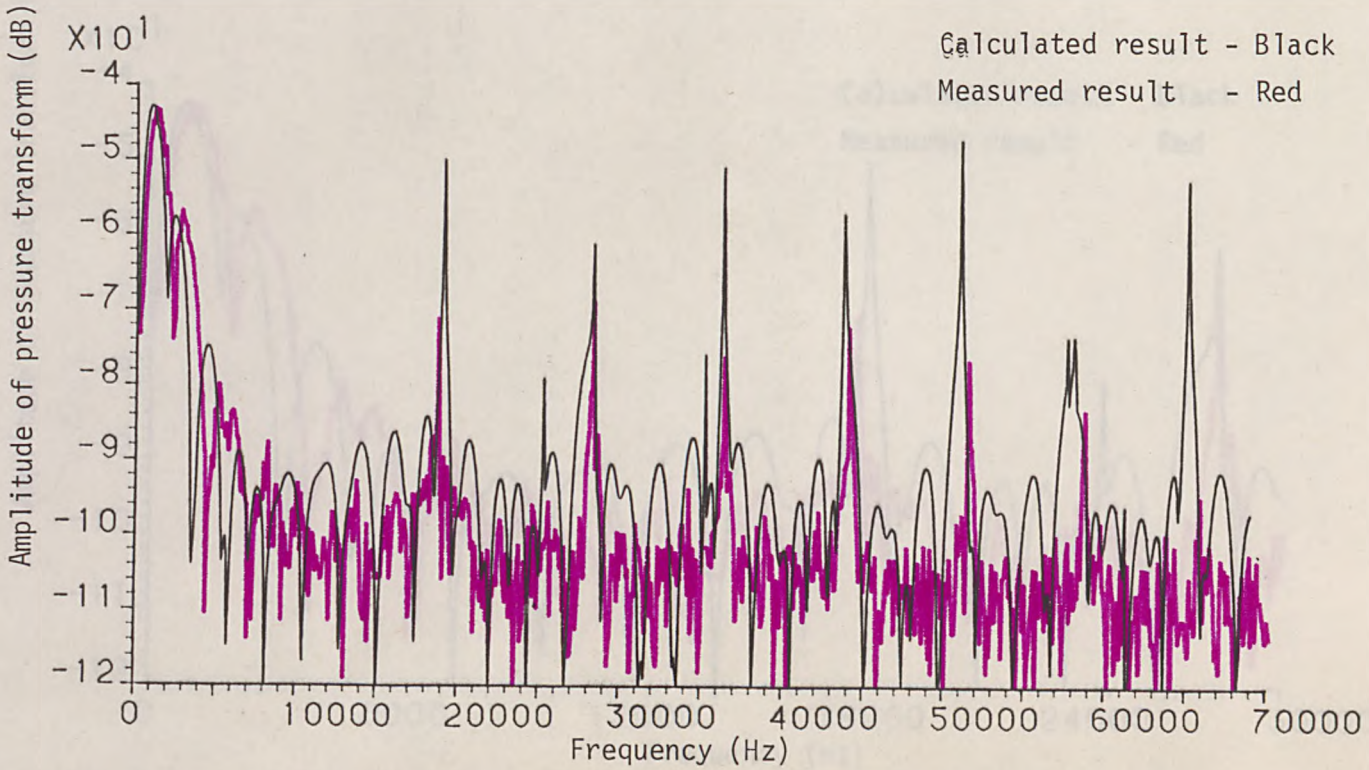

FIGURE 9.24. COMPARISON OF MEASURED FOURIER TRANSFORM PRESSURE RESULT AND CALCULATED RESULT FOR 7.1 cm RADIUS SPHERES. (v_o = 1 m/s, $\theta = 0^o$, r = 0.8 m)

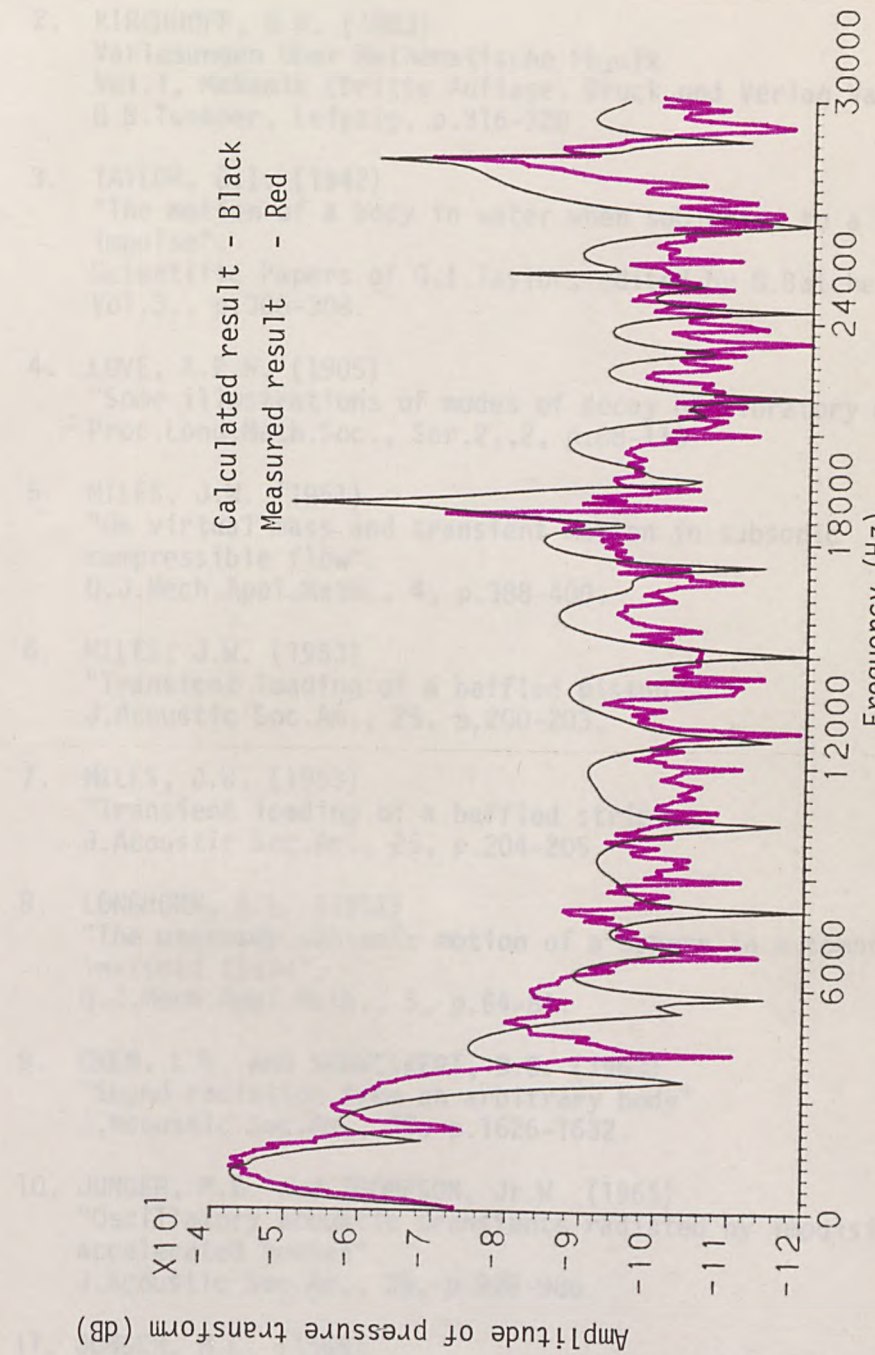

FIGURE 9.25. COMPARISON OF MEASURED FOURIER TRANSFORM PRESSURE RESULT AND CALCULATED RESULT FOR 7.1 cm RADIUS SPHERES. (v_o = 1 m/s, $\theta = 0^o$, r = 0.8 m)

REFERENCES

1. AKAY, A. (1978)
"A Review of Impact Noise"
J.Acoustic Soc.Am., Vol.64, No.4, p.977-987.

2. KIRCHHOFF, G.R. (1883)
Varlesungen Uber Mathematische Physik
Vol.1, Mekanik (Dritte Auflage, Druck und Verlag Van.
G.B.Tuebner, Leipzig, p.316-320.

3. TAYLOR, G.I. (1942)
"The motion of a body in water when subjected to a sudden impulse".
Scientific Papers of G.I.Taylor, edited by G.Batchelor,
Vol.3., p.306-308.

4. LOVE, A.E.H. (1905)
"Some illustrations of modes of decay of vibratory motions".
Proc.Lond.Math.Soc., Ser.2.,2, p.88-113.

5. MILES, J.W. (1951)
"On virtual mass and transient motion in subsonic compressible flow".
Q.J.Mech.Appl.Math., 4, p.388-400.

6. MILES, J.W. (1953)
"Transient loading of a baffled piston".
J.Acoustic Soc.Am., 25, p.200-203.

7. MILES, J.W. (1953)
"Transient loading of a baffled strip"
J.Acoustic Soc.Am., 25, p.204-205.

8. LONGHORN, A.L. (1952)
"The unsteady subsonic motion of a sphere in a compressible inviscid fluid".
Q.J.Mech.Appl.Math., 5, p.64-81.

9. CHEN, L.H. and SCHWEIKERT, D.G. (1963)
"Sound radiation from an arbitrary body"
J.Acoustic Soc.Am., 35, p.1626-1632.

10. JUNGER, M.C. and THOMPSON, Jr.W. (1965)
"Oscillatory acoustic transients radiated by impulsively accelerated bodies".
J.Acoustic Soc.Am., 38, p.978-986.

11. JUNGER, M.C. (1966)
"Energy exchange between incompressible near and acoustic farfield for transient sources".
J.Acoustic Soc.Am., 49, p.1025-1030.

12. FARN, C.L.S. and HUANG (1968)
"Transient acoustic fields generated by a body of arbitrary shape".
J.Acoustic Soc.Am., 43, p.252-257.

13. JUNGER, M.C. (1968)
"Comments on transient acoustic fields generated by a body of arbitrary shape".
J.Acoustic Soc.Am., 44, p.825-826.

14. FARRASSAT, F. and SEARS, W.R. (1973)
"The far field sound of rigid bodies in arbitary motion".
In Procs.of the Interagency Symposium on University research in Transportation Noise (Stanford Univ.U.S.A.)

15. FFOWCS WILLIAMS, J.E. and LOVELY, D.J. (1977)
"An approximate method for evaluating the sound of impulsively accelerated bodies".
J.Sound Vib., 50, p.333-343.

16. AKAY, A. and HODGSON, T.H. (1978)
"Sound radiation from an accelerated or decelerated sphere".
J.Acoustic Soc.Am., 63 (2), p.313-318.

17. BANERJI, S. (1916)
"On aerial waves generated by impact".
Philos.Mag., Ser.632, p.96-111.

18. BANERJI, S. (1918)
"On aerial waves generated by impact - Part II".
Philos.Mag., Ser.635, p.97-111.

19. NISHIMURA, G. and TAKAHASHI, K. (1962)
"Impact sound of steel ball collision".
J.Soc.Precision Mech., Jpn, 4, p.220-230.

20. NISHIMURA, G. and TAKAHASHI, K. (1963)
"Impact sound by mutual collision of two steel balls".
Bull.Japan Soc. Precision Eng. 1(2), p.47-51.

21. KOSS, L.L. and ALFREDSON, R.J. (1973)
"Transient sound radiated by spheres undergoing an elastic collision".
J.Sound Vib., 27, p.59-75.

22. KOSS, L.L. (1974)
"Transient sound from colliding spheres -normalised results".
J.Sound Vib., 36, p.541-553.

23. KOSS, L.L. (1974)
"Transient sound from colliding spheres - inelastic collisions".
J.Sound Vib., 36, p.555-562.

24. HUDSON, R.R. and COPLEY, J.C. (1974)
"Sound radiation by impacting solid spheres".
Eighth Intl.Congress on Acoustics, London.
Contributed papers, Vol.II, p.497.

25. ANDERSON J.S. (1975)
"Impulsive noise with particular reference to pile drivers".
Paper presented to Spring Meeting of the Inst.of Acoustics,
Nottingham Univ.

26. HODGSON, D.C. (1976)
"Platen deceleration as a mechanism of noise production
in impact forming machines".
J.Mech. Eng.Sci., 18, p.126-130.

27. HOLMES, D.G. (1976)
"Impact sounds due to sudden acceleration".
J.Sound Vib., 44, p.63-73.

28. HOLMES, A.T., RICHARDS, E.J. and WESTCOTT, M.E. (1977)
"Some comments on impact sound".
J.Sound Vib., 51, p.139-142 (L)

29. RICHARDS, E.J., WESTCOTT, M.E. and JEYAPALAN, R.K. (1974)
"On the prediction of impact noise (I), acceleration noise".
J.Sound Vib., 62(4), p.547-575.

30. RICHARDS, E.J. (1965-1966)
"Noise considerations in the design of machines and factories"
Inst.Mech.Eng., London, Proc., 180, p.1099-1128.

31. LORD RAYLEIGH (1906)
"On the production of vibrations by forces of relatively
long duration, with application to the theory of collisions".
Philos.Mag., Ser.611, p.283-291.

32. LAMB, H. (1982)
"On the vibration of an elastic sphere".
Proc.Lond.Math.Soc., p.189-212.

33. TAKITA, Y. (1961)
"Vibration of a plate and sound radiation generated by an
impulsive force".
J.Phys.Soc., Jpn, 16, p.1008-1019.

34. TAKITA, Y. (1960)
"Vibration and sound radiation of a plate generated by an
impulsive force (I)"
J.Acoustic Soc.Jpn, 16(3), p.170-177 (Japanese-English abstract).

35. TAKITA, Y. (1961)
"Vibration and sound radiation of a plate generated by an
impulsive force (II)"
J.Acoustic Soc.Jpn, 17(2), p.116-122 (Japanese-English abstract).

36. MAGRAB, E.B. and READER, W.T. (1968)
"Far field radiation from an infinite elastic plate excited by a transient point loading".
J.Acoustic Soc.Am., 44, p.1623-1627.

37. AKAY, A., HODGSON, T.H. and BAILEY, J.R. (1975)
"Sound radiation from the impact of a sphere on an elastic plate".
ASME paper No.75-DET-51.

38. MATSUMOTO, G.Y. and SIMPSON, W.J. (1976)
"Acoustadynamics of the longitudinal collinear impact of finite elastic cylinders".
ASME paper No.76-WA/DE-19.

39. AKAY, A., and HODGSON, T.H. (1978)
"Acoustic radiation from the elastic impact of a sphere with a slab".
Appl. Acoustics, 11, p.285-303.

40. RICHARDS, E.J., WESTCOTT, M.E. and JEYAPALAN, R.K. (1979)
"On the prediction of impact noise, II: Ringing noise".
J.Sound Vib., 65(3), p.419-451.

41. BENEDETTO, G., SPAGNOLO, R.and MARINGELLI, M. (1980)
"Transient sound from the impact of a sphere on a thin square plate".
J.Sound Vib., 69(1), p.157-161.

42. ENDO, M., NISHI, S., NAKAGAWA, M., and SAKATA, M. (1981)
"Sound radiation from a circular cylinder subjected to elastic collision by a sphere".
J.Sound Vib., 75(2), p.285-302.

43. GOLDSMITH, W. (1960)
Impact,
London: Edward Arnold, Chapt.IV.

44. LAMB, H. (1881)
"On the oscillations of a viscous spheroid".
Proc.Lond.Math.Soc., p.51-66.

45. MALECKI, I. (1969)
Physical Foundations of Technical Acoustics.
Oxford: Pergamon Press Ltd., p.18.

46. JUNGER, M.C. (1972)
"Sound structures and their interaction."
The MIT Press Cambridge, Mass., and London, p.21,p.191,p.197.

47. JONES, E.H. (1961)
Audio Frequency Engineering.
Chatto and Windus Ltd., p.16.

48. HUNTER, J.L. (1962)
Acoustics.
2nd Ed., Prentice-Hall, Inc. p.133.

49. SKUDRZYK, E. (1971)
The Fundamentals of Acoustics.
Spring-Verlag, New York, p.378,381.

50. MORSE, P.M. (1936)
Vibration and Sound.
2nd Ed., McGraw-Hill Book Co.Inc., p.246.

51. STRATTON, J.A. (1941)
Electromagnetic Theory.
McGraw-Hill Book Co.Inc.

52. HUNTER, S.C. (1957)
"Energy absorbed by elastic waves during impact".
J.Mech.Phys.Solids, 5, p.162.

53. KOLSKY, H. (1963)
Stress Waves in Solids.
Dover Publications,Inc., p.11,9

54. LAMB, H. (1932)
Hydrodynamics.
6th Ed., Cambridge, p.110.

55. MORSE, P.M. and FESHBACH, H. (1953)
Methods of Theoretical Physics (Part II).
Mc-Graw-Hill Book Co.Inc., p.1264.

56. CHAMPENEY, D.C. (1973)
Fourier transforms and their physical applications.
Academic Press, London and New York, p.34.

57. McLACHLAN, N.W. (1934)
Bessel functions for engineers.
Oxford University Press, p.29.

58. ANDREWS, J.P. (1931)
"Experiments on impact".
Proc.Phys.Soc.Lond., 43, p.8.

59. ANDREWS, J.P. (1930)
"Theory of Collision of spheres of soft metal".
Phil.Mag., Ser.7, 9, p.593.

60. CARNAHAN, B., LUTHER, H.A. and WILKES, J.O. (1969)
Applied Numerical Methods.
John Wiley & Sons. Inc., p.361-366, p.343.

61. SCHEID, F. (1968)
Theory and problems of numerical analysis.
Mc-Graw-Hill Book Co.Inc., p.224.

62. PAO, Y.H. (1955)
"Extension of the Hertz theory of impact to the visco-elastic case".
J.Appl.Phys., 26, p.1083-1088.

63. SCHREIBER, E., ANDERSON, O.L. and SAGA, N. (1973)
Elastic constants and their measurement.
Mc-Graw-Hill Book Co.Inc., p.127-132.

64. MEIROVITCH, L. (1967)
Analytical methods in vibrations.
The Macmillan Publ.Co., p.398.

65. "Fourier analyser training manual".
Application note 140-0, Hewlett hp Packard.

66. ANDERSON, J.S. (1977)
"The design, construction and operation of the anechoic chamber in the Department of Mechanical Engineering."
Memorandum ML96, The City University.